Aleksandra Zdanowicz, MSc.

Testing of cation carriers as prospective therapeutic agents for the treatment of B-cell-derived malignancies

Dissertation for the degree of Doctor of Medicine and health sciences in the discipline of pharmaceutical sciences

Supervisor: prof. Marta Struga

Co-supervisor: Beata Pyrzyńska, Ph.D

Chair and Department of Biochemistry

Medical University of Warsaw

Defense of the doctoral dissertation to the Pharmaceutical Sciences Council,

Medical University of Warsaw

Warsaw, 2025

Mgr. Aleksandra Zdanowicz

Testowanie nośników kationowych jako potencjalnych terapeutyków w leczeniu nowotworów wywodzących się od limfocytów B

Rozprawa na stopień doktora nauk medycznych i nauk o zdrowiu

w dyscyplinie nauki farmaceutyczne

Promotor: prof. dr hab. Marta Struga

Promotor pomocniczy: dr n. biol. Beata Pyrzyńska

Katedra i Zakład Biochemii

Warszawski Uniwersytet Medyczny

Obrona rozprawy doktorskiej przed Radą Dyscypliny Nauk Farmaceutycznych

Warszawskiego Uniwersytetu Medycznego

Warszawa, 2025

I dedicate this work to my beloved Mother.

Я прысвячаю гэту працу маёй любімай Маме.

Я посвящаю эту работу моей любимой Маме.

Tę pracę dedykuję mojej ukochanej Mamie.

Acknowledgments

Writing these words, I am acutely aware that I cannot possibly thank everyone who has contributed to this work and supported me throughout my four years of Ph.D. studies. However, it would be insincere not to acknowledge at least a few individuals to whom I am especially grateful.

First and foremost, I owe a great debt of gratitude to **Athar Amar**, Ph.D., for being the first to recognize my research potential and for his invaluable support and assistance during my admission to the Ph.D. program.

I wish to express my heartfelt gratitude to my co-supervisor, **Beata Pyrzyńska**, Ph.D., for her dedication, hard work, and invaluable assistance throughout my journey.

I would also like to extend my sincere thanks to the staff of the Chair and Department of Biochemistry at the Medical University of Warsaw for their supportive words and encouragement during challenging times.

Additionally, I am profoundly thankful to the inspiring scientists in London, whose warmth and steadfast support made me feel at home throughout my internship. Their kindness and motivation were truly invaluable.

I sincerely thank **Malwina Jędrysik**, M.Sc., and **Alicja Głuszko**, Ph.D., for always being an invaluable source of psychological and intellectual support, offering both encouragement and insightful guidance. Their kindness and unwavering belief in me have been instrumental throughout my journey.

I am also deeply grateful to **Emilia Grosicka-Maciąg**, Ph.D., **Magdalena Mielczarek-Puta**, Ph.D., and **Barbara Żyżyńska-Granica**, Ph.D. for their kindness, open hearts, and immeasurable help during my most challenging days. Their unwavering support, generosity, and willingness to lend a helping hand, whether through thoughtful advice or simply their reassuring presence, have made an incredible difference in my journey.

I sincerely thank my fellow Ph.D. students—**Natalia Melnyk**, **Dominika Grzelak**, **Bhaskar Pradhan**, **Miłosz Ludwinek**, and **Miłosz Majka**—for their daily assistance, valuable advice, and unwavering support in managing laboratory schedules and maintaining equipment.

I would like to express my deepest gratitude to my beloved family and closest friends for always being by my side with unwavering support and encouragement—it has meant more to me than words can ever convey. I am truly thankful for your patience, the time you've devoted to me, for listening, supporting, cooking for me, offering wise advice, and for sharing in both my tears and my joys.

Additionally, I am profoundly grateful to my mentors from the House of St. Ignatius of Loyola in Jastrzębia Góra, Chapel of St. Joseph, and the Church of St. Andrew Bobola in Warsaw, whose wisdom and guidance have been a source of strength throughout my journey.

Funding

This research was funded by the National Science Centre (NCN, Poland) grant no 2019/35/B/NZ5/01445 (to B.P.)

1. List of publications constituting the doctoral dissertation

1. Torun A.*, **Zdanowicz A**.*, Miazek-Zapala N., Zapala P., Pradhan B., Jedrzejczyk M., Ciechanowicz A., Pilch Z., Skorzynski M., Słabicki M., Rymkiewicz G., Barankiewicz J., Martines C., Laurenti L., Struga M., Winiarska M., Golab J., Kucia M., Ratajczak M.Z., Huczynski A., Calado D.P., Efremov D.G., Zerrouqi A., Pyrzynska B. Potassium /sodium cation carriers robustly up-regulate CD20 antigen by targeting MYC, and synergize with anti-CD20 immunotherapies to eliminate malignant B cells. Haematologica Early view Dec 19, 2024; https://doi.org/10.3324/haematol.2024.285826 (IF=8.2; MEiN: 140)
   *- AT and AZ contributed equally as co-first authors.

2. **Zdanowicz A**., Grosicka-Maciąg E. The Interplay between Autophagy and Mitochondria in Cancer. Int. J. Mol. Sci. 2024, 25(17), 9143; https://doi.org/10.3390/ijms25179143 (IF=4.9; MEiN=140)

3. **Zdanowicz A**., Ilchenko O., Ciechanowicz A., Chi H., Struga M., Pyrzynska B., Low-Dose Salinomycin Alters Mitochondrial Function and Reprograms Metabolism in Burkitt Lymphoma. Int. J. Mol. Sci. 2025, 26(11), 5125; https://doi.org/10.3390/ijms26115125 (IF=4.9; MEiN:140)

2. Table of contents

1. List of publications constituting the doctoral dissertation 7
2. Table of contents 8
3. List of figures 9
4. List of abbreviations 10
5. Abstracts and keywords 11
6. Background and justification of study research 13
6.1 B-cell Derived Cancer Immunotherapy 13
6.2 Cation carriers 15
6.3 Mechanisms of SAL's Anticancer Action 16
6.4 Safety Profile and Toxicity of SAL 17
7. Aim of the thesis 19
8. Reprint of publications constituting the doctoral dissertation 21
8.1. Publication No.1 21
8.2 Publication No. 2 239
8.3 Publication No. 3 273
9. Summary and Conclusions 297
9.1 Publication No. 1: Enhancing anti-CD20 immunotherapy in B-cell malignancies cells... 297
9.2 Publication No. 2: A literature review focused on mitochondrial functionality in cancer. 299
9.3 Publication No. 3: The impact of SAL on mitochondrial function and the metabolomic profile of Burkitt lymphoma. 300
9.4 Conclusions 301
10. Approval of the Bioethics and Ethics Committee 303
11. Co-authors' statements 306
11. 1 Publication No. 1 306
11.2 Publication No. 2 330
11.3 Publication No. 3 332
12. References 344

3. List of figures

Figure 1. The most prominent mechanisms by which the anti-CD20 antibody Rituximab exerts its effects.……14

Figure 2. Chemical structure of salinomycin.……16

4. List of abbreviations

ACD	autophagy-dependent cell death
ADCC	antibody-dependent cellular cytotoxicity
ADCP	antibody-dependent cellular phagocytosis
ATP	adenosine triphosphate
B-NHL	B cell–derived non-Hodgkin lymphoma
BR	combination bendamustine with rituximab
CAR	chimeric antigen receptor
CDC	complement-dependent cytotoxicity
ChIP	chromatin immunoprecipitation
CHOP regimen	cyclophosphamide, doxorubicin, vincristine, and prednisone
CLL	chronic lymphocytic leukemia
CSCs	cancer stem cells
DLBCL	diffuse large B-cell lymphoma
ECAR	extracellular acidification rate
EMA	the European Medicines Agency
ER	endoplasmic reticulum
ETC	electron transport chain
FCR	fludarabine with cyclophosphamide and rituximab
FDA	the U.S. Food and Drug Administration
FL	Burkitt lymphoma
LC3B	microtubule-associated protein 1 light chain 3β
mAb	monoclonal antibody
MCL	mantle cell lymphoma
MDR	multidrug resistance
MMP	mitochondrial membrane potential
mtROS	mitochondrial reactive oxygen species
NF-κB	activator of nuclear factor-kappa B
NK	natural killer
OXPHOS	oxidative phosphorylation
R-GemOx regimen	combination with rituximab and oxaliplatin
ROS	reactive oxygen species
RTX	rituximab
SAL	salinomycin
TCA	tricarboxylic acid

5. Abstracts and keywords

Streszczenie

Tytuł: Testowanie nośników kationowych jako potencjalnych terapeutyków w leczeniu nowotworów wywodzących się od limfocytów B

Leczenie nowotworów hematologicznych wywodzących się z limfocytów B polega m.in. na zastosowaniu monoklonalnych przeciwciał anty-CD20 z chemioterapią. Jednakże u niektórych pacjentów rozwija się oporność na takie podejście terapeutyczne. Jedną z dobrze poznanych przyczyn tej oporności lub ograniczonej skuteczności terapii jest zmniejszona ekspresja białka CD20 na powierzchni komórek nowotworowych. W związku z tym istnieje pilna potrzeba opracowania nowych podejść terapeutycznych, które pozwolą przezwyciężyć tę oporność i poprawić wyniki leczenia u tych pacjentów.

W niniejszej rozprawie doktorskiej przebadano grupę nośników kationowych, do której należy salinomycyna (SAL), pod kątem ich zdolności do zwiększania ekspresji białka CD20 na powierzchni komórek nowotworowych oraz poprawy skuteczności istniejącej terapii anty-CD20 w modelach *in vitro* i *in vivo*. Dodatkowo, z wykorzystaniem technik biologii molekularnej, takich jak ilościowy RT-PCR i Western blotting, szczegółowo przeanalizowano molekularny mechanizm prowadzący do zwiększonej ekspresji CD20 po zastosowaniu SAL. Ponadto, kompleksowo oceniono wpływ SAL na funkcjonowanie mitochondriów oraz związane z tym zmiany w profilu metabolicznym komórek nowotworowych.

Wyniki przedstawione w niniejszej rozprawie doktorskiej zostały opublikowane w trzech artykułach naukowych. W oryginalnym artykule, opublikowanym w czasopiśmie „Haematologica", wykazano, że nośniki kationowe zwiększają ekspresję CD20, wyjaśniono molekularny mechanizm tego zjawiska oraz potwierdzono poprawę skuteczności terapii z wykorzystaniem monoklonalnych przeciwciał anty-CD20. Artykuł o charakterze przeglądowym oraz kolejny artykuł będący oryginalną pracą badawczą (opublikowano w czasopiśmie „International Journal of Molecular Science"), podkreśliły kluczową rolę mitochondriów w molekularnym mechanizmie działania SAL. Badania te ujawniły wpływ SAL na oddychanie mitochondrialne, zmianę metabolizmu w kierunku glikolizy oraz jej rolę w obniżeniu poziomu L-argininy w komórkach nowotworowych. Uzyskane wyniki mogą mieć istotne znaczenie dla przyszłych strategii terapeutycznych.

Słowa kluczowe: nowotwory wywodzące się z limfocytów B, CD20, nośniki kationowe, salinomycyna, immunoterapia, mitochondria.

Abstract

Title: Testing of cation carriers as prospective therapeutic agents for the treatment of B-cell-derived malignancies

The first-line treatment for many types of B-cell-derived hematological malignancies includes anti-CD20 immunotherapy, frequently administered in combination with chemotherapy. However, some patients develop resistance to this therapeutic approach. A well-recognized cause of such resistance is the variable expression of CD20 on the surface of malignant B cells, with many cases showing low CD20 levels. This variability significantly limits the effectiveness of anti-CD20 therapies. Therefore, there is an urgent need to develop new strategies to overcome resistance and improve treatment outcomes for these patients.

This PhD dissertation investigated the potential of cation carriers, such as salinomycin (SAL), to increase CD20 expression on the surface of malignant B cells and thereby enhance the efficacy of anti-CD20 immunotherapy in both *in vitro* and *in vivo* models. A secondary focus of the dissertation was to elucidate the molecular mechanisms of SAL-induced CD20 upregulation, using molecular biology techniques such as qRT-PCR and Western blotting. Additionally, the effects of SAL on mitochondrial function and the metabolic profile of treated cells were comprehensively assessed.

The results of this PhD dissertation were published in three scientific articles. The original article, published in the journal *Haematologica*, demonstrated the ability of cation carriers to upregulate CD20 expression, explained the molecular mechanism behind this phenomenon, and confirmed the improved efficacy of therapy using anti-CD20 monoclonal antibodies. A review article and a subsequent original research paper (published in *International Journal of Molecular Sciences*) highlighted the key role of mitochondria in the molecular mechanism of SAL action. These studies revealed SAL's impact on mitochondrial respiration, induction of a metabolic shift toward glycolysis, and its role in depleting L-arginine levels in malignant B cells. The obtained results may have significant implications for future therapeutic strategies.

Keywords: B-cell malignancies, CD20, cation carriers, salinomycin, immunotherapy, mitochondria

6. Background and justification of study research

6.1 B-cell Derived Cancer Immunotherapy

The CD20 antigen, expressed on the surface of B cells, is a well-established therapeutic target in B cell–derived hematologic malignancies. Immunotherapeutic strategies, including monoclonal and bispecific antibodies, as well as chimeric antigen receptor (CAR)-based cellular therapies, have demonstrated efficacy in targeting CD20 [1]. These approaches specifically recognize surface CD20 and eliminate only B cells, with minimal off-target effects on other cells.

Immunotherapy targeting CD20 is often combined with the CHOP chemotherapy regimen (cyclophosphamide, doxorubicin, vincristine, and prednisone). This treatment approach is widely employed for malignancies originating from B cells, including chronic lymphocytic leukemia (CLL) and various B cell–derived non-Hodgkin lymphomas (B-NHL), including follicular lymphoma (FL), Burkitt lymphoma, diffuse large B-cell lymphoma (DLBCL) [2] and mantle cell lymphoma (MCL) [1].

The first anti-CD20 monoclonal antibody (mAb) introduced into clinical practice was rituximab (RTX), a chimeric mouse-human antibody approved in 1997 [3]. It is characterized by a high safety profile, a well-understood mechanism of action, and relatively mild and manageable side effects. RTX is a key component of many effective therapeutic regimens, including the BR combination (bendamustine with RTX) and FCR (fludarabine with cyclophosphamide and RTX). These combinations are widely used as standard first-choice therapy in selected groups of patients with CLL and B-NHL [1]. Obinutuzumab, a fully human mAb, is employed in combination with chemotherapy as a first-line treatment for certain patients with CLL and [1]. The mechanism of action of RTX involves several parallel processes (Fig. 1), including complement-dependent cytotoxicity (CDC), antibody-dependent cellular cytotoxicity (ADCC), antibody-dependent cellular phagocytosis (ADCP), as well as the direct induction of apoptosis [4].

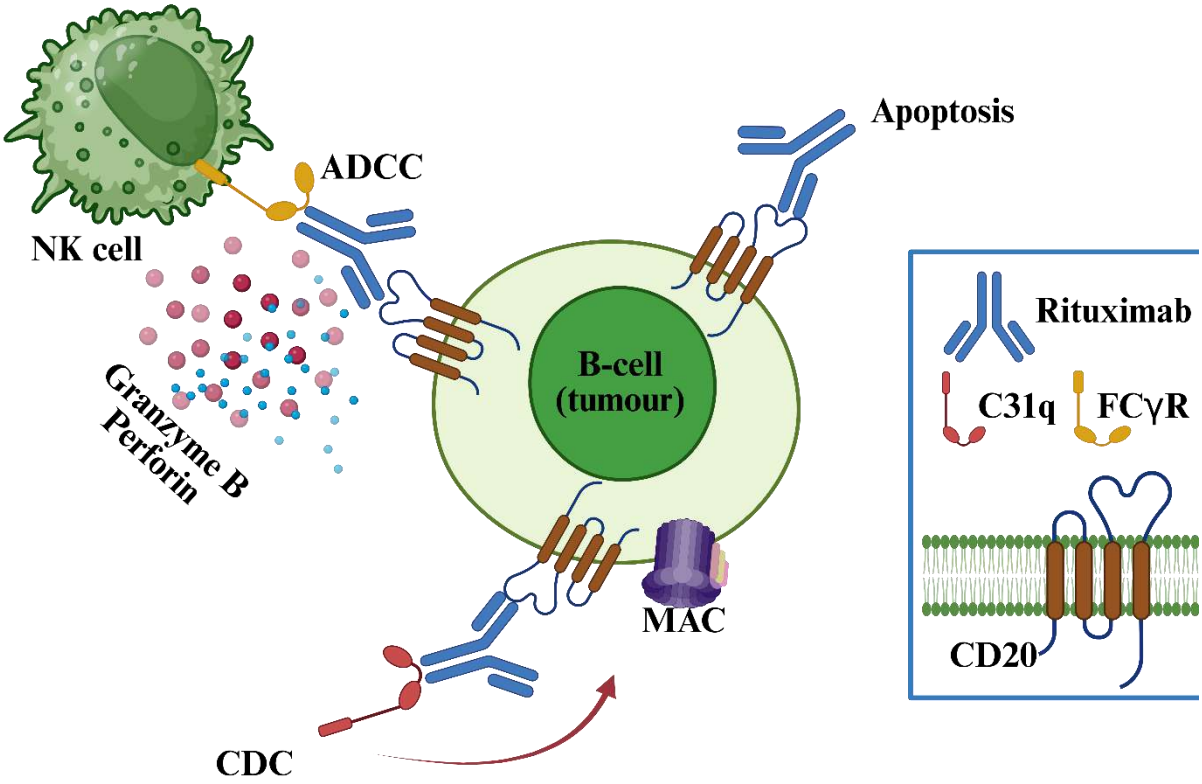

Figure 1: The most prominent mechanisms by which the anti-CD20 antibody RTX exerts its effects.

RTX acts through several pathways, including complement-dependent cytotoxicity (CDC), antibody-dependent cellular cytotoxicity (ADCC), and the induction of direct apoptosis. MAC – membrane attack complex.

In patients with resistance to first-line therapy or disease relapse, innovative bispecific antibodies have emerged as a promising therapeutic option. These antibodies have the ability to simultaneously bind to the CD20 antigen on cancer cells and activate cytotoxic T lymphocytes [5]. Bispecific antibodies such as epcoritamab, glofitamab, and mosunetuzumab have been clinically approved for the treatment of B-cell malignancies [1]. Such antibodies are specifically designed to simultaneously target CD20 on B cells and CD3 on T cell surface [6].

Despite the high level of advancement in anti-CD20–targeted immunotherapies, various mechanisms of resistance to these regimens have been identified. One of the primary causes of resistance is the variable expression of CD20 on the surface of B cells. In B cell–derived malignancies, CD20 expression can vary significantly—not only among patients with the same cancer type but also among different subpopulations of malignant cells within an individual patient [7]. A diminished level of CD20 expression, especially in the context of CLL, represents a major

obstacle to the success of anti-CD20 mAb treatments [8]. This situation underscores the urgent necessity for novel therapies that can overcome resistance to anti-CD20 mAbs. Current strategies to address this challenge involve combining anti-CD20 antibodies with agents that enhance CD20 expression on cancer cell surfaces. Numerous clinical trials are currently underway to evaluate the effectiveness of modulators that influence CD20 expression, including both epigenetic and transcriptional factors [7]. Valproic acid, a histone deacetylase inhibitor, is one such compound that has been used in combination with mAbs and the CHOP regimen for the treatment of patients with DLBCL. The VALFRID study demonstrated that administration of valproic acid prior to therapy leads to histone acetylation and an increase in CD20 expression— at both the transcriptional and protein levels [9]. Moreover, gemcitabine, which acts as an activator of nuclear factor-kappa B (NF-κB), has shown high efficacy and a favorable safety profile in combination with RTX and oxaliplatin (the R-GemOx regimen) in patients with DLBCL in a phase II clinical trial [10]. However, none of the agents that increase CD20 expression have been approved by the FDA (the U.S. Food and Drug Administration) or EMA (the European Medicines Agency) yet, highlighting the need for new therapeutic strategies [7].

6.2 Cation carriers

Our recent studies [11] have demonstrated that one of the most effective natural compound groups capable of enhancing CD20 expression are polyether ionophores (cation carriers), which selectively bind and transport cations across cellular lipid membranes [12]. Their ionophoric activity stems from their molecular structure, which includes carboxylic, ketone, and hydroxyl groups, as well as tetrahydropyran and tetrahydrofuran rings. Moreover, cation carriers possess numerous inward-oriented oxygen atoms that create a hydrophilic interior, facilitating selective cation binding, while their lipophilic exterior enables them to cross cellular membranes [13] [14].

Among cation carriers, the best-known compound is salinomycin (SAL) (Fig. 2), which was initially isolated from *Streptomyces albus*. SAL has been widely used in veterinary medicine as a treatment for coccidiosis (a disease caused by protozoa of the genus *Coccidia*) and as an agent against Gram-positive bacteria [15, 16].

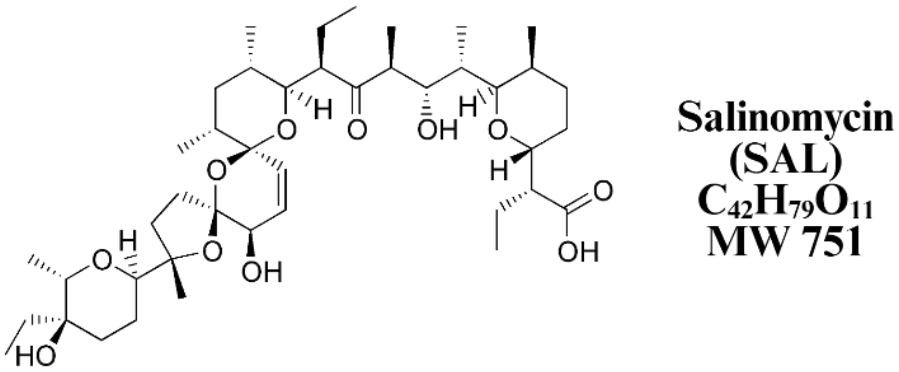

Figure 2: Chemical structure of salinomycin.

SAL functions by binding to a range of cations with a notable preference for K^+ (potassium) and Na^+ (sodium), enabling their movement in both directions across cellular membranes [17]. Consequently, SAL alters the cellular balance of these ions, affecting intracellular pH, osmotic pressure, and mitochondrial homeostasis [14].

6.3 Mechanisms of SAL's Anticancer Action

In 2009, Gupta's team was the first to describe the anticancer activity of SAL, demonstrating its 100-fold greater efficacy and selectivity against breast cancer stem cells (CSCs) compared to conventional chemotherapeutic agents [18]. Various studies have next shown that SAL exerts potent anticancer effects across diverse tumor models. Specifically, in the PC-3 prostate cancer cell line, it triggers apoptosis in a dose- and time-dependent fashion [19]. In models of cisplatin-resistant ovarian cancer, SAL effectively eradicates both chemosensitive and multidrug-resistant (MDR) cancer cell populations [20]. In osteosarcoma (U2OS) and glioma (U87MG) cells, SAL promotes both autophagy and apoptosis by inducing caspase-3 cleavage, increasing the expression of autophagy-related proteins such as LC3B (microtubule-associated protein 1 light chain 3β), and reducing the acidity of vesicular organelles [21, 22].

Autophagy is an intracellular catabolic degradation process that enables the maintenance of cellular homeostasis under conditions of metabolic stress. However, its excessive activation can lead to autophagy-dependent cell death (ACD) [23]. Some studies have shown that SAL induces autophagy as a survival mechanism and suppresses apoptosis, for instance, in human non-small cell lung cancer cell lines (A549, Calu-1, and H157) by triggering endoplasmic reticulum (ER) stress [24]. In prostate cancer (PC-3) and breast cancer (SKBR3 and MDA-MB-468) cell lines, SAL similarly triggers a protective autophagic response, including the activation of mitophagy [25]. In contrast, in the melanoma cell line SK-Mel-19, SAL disrupted the fusion of autophagosomes with lysosomes, leading to ACD [26].

Owing to its ionophoric properties, SAL is expected to disrupt mitochondrial homeostasis by altering the mitochondrial membrane potential (MMP), changing mitochondrial reactive oxygen species (mtROS) levels, and affecting oxidative phosphorylation (OXPHOS). SAL treatment in human osteosarcoma HOS cells led to mitochondrial fragmentation and morphological changes [27]. In the Raji cancer cell model, SAL decreases MMP, elevates mtROS production, and induces oxidative stress [28]. Similarly, in the RB383 cancer cell line, SAL reduces both OXPHOS and MMP [29]. Furthermore, SAL affects iron homeostasis through iron sequestration in lysosomes, causing lysosomal membrane peroxidation and initiating ferroptosis [30].

6.4 Safety Profile and Toxicity of SAL

The ionophoric activity of SAL contributes to its potential toxicity. Accidental inhalation by a 35-year-old patient led to nausea, tachycardia, and muscle pain [31]. Most toxicological research on SAL has been carried out in animal models. In broiler chickens, SAL toxic dose affects the spleen and pancreas [32], whereas the recommended non-toxic dose is 60 ppm. Doses in the range of 120–180 ppm are associated with an increased risk of adverse effects. In ruminants, high dose SAL (above 15 mg/kg) administration can lead to side effects like anorexia, muscle weakness, and an increased heart rate [33]. In mice, weight loss and sensory polyneuropathy were observed at doses exceeding 5 mg/kg [34].

Despite the toxicity of SAL at higher doses, there have been attempts to use the lower doses of SAL therapeutically, and the results are very promising. In a preliminary clinical study with patients suffering from ovarian, head and neck, and metastatic breast cancers, intravenous SAL given at 200–250 µg/kg every other day over a three-week period induced a reduction of metastasis. Acute side effects were infrequent, with no serious long-term side effects documented [35].

To minimize further the potential adverse effects associated with SAL, numerous derivatives with improved anticancer properties have been synthesized [14] [36] and are currently being tested in various preclinical models alongside other cation carriers, such as monensin.

In summary, this PhD thesis explores strategies to overcome resistance to anti-CD20 immunotherapy, which is often caused by reduced CD20 expression on the surface of malignant B cells. Our recent findings demonstrate that cation carriers effectively increase CD20 levels. Beyond upregulating CD20, these carriers exhibit diverse anticancer activities that vary by

cancer type. Notably, their ion-transporting ability across lipid bilayers influences mitochondrial function.

7. Aim of the thesis

The primary objective of this dissertation is to investigate strategies for enhancing anti-CD20 immunotherapy with potential new therapeutics for the treatment of B-cell malignancies. Specifically, the research focuses on evaluating whether cation carriers can upregulate surface expression of the CD20 antigen and enhance the efficacy of anti-CD20 therapeutic antibodies *in vitro*, *ex vivo*, and *in vivo*. The evaluation includes:

1. Screening cation carriers for their ability to increase surface CD20 expression in cells derived from B-cell malignancies, including established cell lines as well as primary CLL and DLBCL cells. CD20 surface levels were evaluated by staining cells with fluorochrome-conjugated monoclonal anti-CD20 antibodies, in conjunction with Zombie-NIR dye to exclude non-viable cells. Quantification of CD20 expression was performed using flow cytometry.
2. Investigating the molecular mechanisms behind CD20 upregulation induced by cation carriers, with emphasis on changes in gene expression, transcription factor activity, and signaling pathways. This involves quantifying *MS4A1* mRNA (encoding CD20) using RT-qPCR and assessing protein levels via Western blotting. Additionally, the binding of transcription factors to *MS4A1* promoter regions is analyzed through chromatin immunoprecipitation (ChIP) assays.
3. Confirmation of the involvement of specific transcription factors and their related signaling pathways in the regulation of CD20 expression. This task was implemented by performing targeted knockdown of numerous genes encoding signaling molecules, using CRISPR/Cas9 gene editing technology.
4. Evaluation of the efficacy of selected compounds in enhancing the *in vitro* killing of cells derived from B-cell malignancies by using them in combination with the therapeutic anti-CD20 antibody RTX. This covers assessing the impact of cation carriers on CDC.
5. Assessment of the efficacy of selected compounds combined with the therapeutic anti-CD20 antibody using an *in vivo* model. This involves inoculating SCID mice with Raji cells and monitoring tumor growth reduction following treatment with the combination of cation carriers and RTX.

A secondary objective is to elucidate the molecular mechanisms underlying the effects of cation carriers, with particular focus on the well-characterized cation carrier SAL and its impact on mitochondrial function and the metabolic profile in Raji cells. This investigation aimed to

evaluate the potential for future clinical application in patients with B-cell malignancies. The specific assessments included:

1. A critical examination of the current knowledge regarding the impact of cation carriers on mitochondrial homeostasis.
2. Assessment of cation carrier impact on MMP using MitoPT JC-1 and TMRM assay kits.
3. Evaluation of mitochondrial superoxide levels and oxidative stress induced by cation carriers using MitoSOX and CellRox assay kits.
4. Analysis of cellular bioenergetics through measurements of cellular respiration and glycolysis using the Seahorse XFe96 extracellular flux analyzer.
5. Profiling of metabolomic changes following cation carrier treatment via Solarix 2xR 7T FT-ICR MS (ultra-high-resolution Fourier-transform ion cyclotron resonance mass spectrometer).

8. Reprint of publications constituting the doctoral dissertation

8.1. Publication No.1

haematologica
Journal of the Ferrata Storti Foundation

Potassium/sodium cation carriers robustly up-regulate CD20 antigen by targeting MYC, and synergize with anti-CD20 immunotherapies to eliminate malignant B cells

by Anna Torun, Aleksandra Zdanowicz, Nina Miazek-Zapala, Piotr Zapala, Bhaskar Pradhan, Marta Jedrzejczyk, Andrzej Ciechanowicz, Zofia Pilch, Marcin Skorzynski, Mikołaj Słabicki, Grzegorz Rymkiewicz, Joanna Barankiewicz, Claudio Martines, Luca Laurenti, Marta Struga, Magdalena Winiarska, Jakub Golab, Magdalena Kucia, Mariusz Z. Ratajczak, Adam Huczynski, Dinis P. Calado, Dimitar G. Efremov, Abdessamad Zerrouqi, and Beata Pyrzynska

Received: May 13, 2024.
Accepted: December 10, 2024.

Citation: Anna Torun, Aleksandra Zdanowicz, Nina Miazek-Zapala, Piotr Zapala, Bhaskar Pradhan, Marta Jedrzejczyk, Andrzej Ciechanowicz, Zofia Pilch, Marcin Skorzynski, Mikołaj Słabicki, Grzegorz Rymkiewicz, Joanna Barankiewicz, Claudio Martines, Luca Laurenti, Marta Struga, Magdalena Winiarska, Jakub Golab, Magdalena Kucia, Mariusz Z. Ratajczak, Adam Huczynski, Dinis P. Calado, Dimitar G. Efremov, Abdessamad Zerrouqi, and Beata Pyrzynska. Potassium/sodium cation carriers robustly up-regulate CD20 antigen by targeting MYC, and synergize with anti-CD20 immunotherapies to eliminate malignant B cells. Haematologica. 2024 Dec 19. doi: 10.3324/haematol.2024.285826 [Epub ahead of print]

Potassium/sodium cation carriers robustly up-regulate CD20 antigen by targeting MYC, and synergize with anti-CD20 immunotherapies to eliminate malignant B cells.

Cation carriers synergize with anti-CD20 therapies.

* Anna Torun[1], * Aleksandra Zdanowicz[1,2], Nina Miazek-Zapala[1], Piotr Zapala[1], Bhaskar Pradhan[1,2], Marta Jedrzejczyk[3], Andrzej Ciechanowicz[1], Zofia Pilch[1], Marcin Skorzynski[1], Mikołaj Słabicki[4], Grzegorz Rymkiewicz[5], Joanna Barankiewicz[6], Claudio Martines[7], Luca Laurenti[8], Marta Struga[1], Magdalena Winiarska[1], Jakub Golab[1], Magdalena Kucia[1], Mariusz Z. Ratajczak[1], Adam Huczynski[3], Dinis P. Calado[9], Dimitar G. Efremov[7], Abdessamad Zerrouqi[1,10], Beata Pyrzynska[1,10,11]

* AT and AZ contributed equally as co-first authors;
1 Medical University of Warsaw, Warsaw, Poland;
2 Doctoral School, Medical University of Warsaw, Warsaw, Poland;
3 Adam Mickiewicz University, Poznan, Poland;
4 Broad Institute of MIT and Harvard, Cambridge, MA, USA; Dana-Farber Cancer Institute, Boston, MA, USA;
5 Maria Sklodowska-Curie National Research Institute of Oncology, Warsaw, Poland;
6 Institute of Hematology and Transfusion Medicine, Warsaw, Poland;
7 Molecular Hematology Unit, International Centre for Genetic Engineering and Biotechnology, Trieste, Italy;
8 Hematology Unit, Fundazione Policlinico Universitario A Gemelli IRCCS, Rome, Italy;
9 The Francis Crick Institute, London, United Kingdom;
10 Senior authors;
11 Corresponding author (e-mail address: beata.pyrzynska@wum.edu.pl)

Funding agencies

This work is supported by the National Science Centre (NCN, Poland) grant OPUS18 (2019/35/B/NZ5/01445 to B. Pyrzynska). The CAR-T cells- and the NK cells-related experiments were supported by the grants OPUS12 (NCN, 2016/23/B/NZ5/02622 to B. Pyrzynska) and OPUS20 (NCN, 2020/39/B/NZ6/03513 to A. Zerrouqi), respectively. The RNAseq experiments were funded by the Ministry of Science and Higher Education (Poland), Diamond grant (DI2014007344 to N. Miazek-Zapala).

Acknowledgments

We acknowledge the patients and healthy donors who donated blood and biopsy samples. We also thank Mrs. Elzbieta Gutowska and Mrs. Iwona Rosa for helping isolate PBMCs, the laboratories of Professor Grazyna Sygitowicz and Professor Malgorzata Lewandowska-Szumiel for access to the RT-PCR and CytoFLEX machines, respectively, and Dr. Wojciech Eliasz (Thermo Fisher Scientific) for the demonstration and access to the Neon NxT electroporation system.

Author contributions

BP conceptualized the manuscript and prepared the original draft. AT, AZ, BP, Aze, NMZ, PZ, AC, ZP, BPr, MSk, and CM contributed to biological experiments and data visualization. MJ and AH performed the chemical synthesis and contributed to data visualization. GR, LL, and JB provided and/or diagnosed the patient's samples. Aze, DGE, DPC, AH, MW, JG, MSł, MS, MR, and MK contributed to the conceptual ideas and methodology.

Declaration of interests

MSł has received research funding from Calico Life Sciences LLC.

Materials availability

Further information and requests for resources and reagents should be directed to and will be fulfilled by the lead contact, Beata Pyrzynska. Chemicals generated in this study will be made available on request. Still, if there is potential for commercial application, we may require a payment and/or a completed materials transfer agreement.

Abstract

Our investigation uncovers that nanomolar concentrations of salinomycin, monensin, nigericin, and narasin (a group of potassium/sodium cation carriers) robustly enhance surface expression of CD20 antigen in B-cell-derived tumor cells, including primary malignant cells of chronic lymphocytic leukemia and diffuse large B-cell lymphoma. Experiments in vitro, ex vivo, and animal model reveal a novel approach of combining salinomycin or monensin with therapeutic anti-CD20 monoclonal antibodies or anti-CD20 CAR-T cells, significantly improving nonHodgkin lymphoma (NHL) therapy. The results of RNA-seq, genetic editing, and chemical inhibition

delineate the molecular mechanism of CD20 upregulation, at least partially, to the downregulation of MYC, the transcriptional repressor of the MS4A1 gene encoding CD20. Our findings propose the cation carriers as compounds targeting MYC oncogene, which can be combined with anti-CD20 antibodies or adoptive cellular therapies to treat NHL and mitigate resistance, which frequently depends on the CD20 antigen loss, offering new solutions to improve patient outcomes.

Article summary

We found that a group of cation carriers induces a robust upregulation of CD20 antigen in NHL cells *via* downregulation of MYC, the repressor of *MS4A1*, and synergizes with anti-CD20 immunotherapies. This discovery provides a rationale for the clinical evaluation of cation carriers to obtain better therapeutical responses in patients with NHL.

Introduction

The CD20 antigen, a membrane-spanning protein prevalent in over 90% of B-cell lymphomas, serves as a primary target for therapeutic monoclonal antibodies (mAbs), bispecific antibodies, and chimeric antigen receptor (CAR)-based therapies (1-3). Standard care for patients suffering from B cell-derived malignancies, such as diffuse large B-cell lymphoma (DLBCL), Burkitt lymphoma, follicular lymphoma, and high-grade B-cell lymphoma involves anti-CD20 monoclonal antibodies (4, 5), e.g., rituximab, combined with a cocktail of chemotherapeutics (1). While chemoimmunotherapy yields long-term benefits, the emergence of relapsed or refractory malignancies post-treatment necessitates further investigation into resistance mechanisms, notably altered antigen expression and CD20 antigen escape (6-8).

The expression of CD20 is highly variable between different tumor types. For example, in conditions like chronic lymphocytic leukemia (CLL), characterized by low CD20 levels (9), the efficacy of anti-CD20 mAbs is constrained (10, 11). Therefore, new therapeutic approaches combining the compounds augmenting CD20 surface expression with the anti-CD20 mAbs or adoptive cellular therapies emerge as potential strategies for optimizing anticancer therapies. To address these challenges, specific agents enhancing the expression and/or the levels of surface CD20 have already been reported, with some currently being evaluated in clinical trials (1); however, they have yet to be included in the standard therapeutic regimens.

Our previous studies underlined the role of the AKT signaling axis as a critical player in the transcriptional regulation of the *MS4A1* gene encoding CD20 (12, 13). Therefore, we further explored the anticancer agents capable of stimulating AKT, with a particular focus on Salinomycin (SAL) (14), initially recognized for its efficacy in eradicating breast cancer stem cells (CSCs) (15) and later reported as a compound with a variety of anticancer properties (1618), and ability to suppress numerous cancer- or CSCs-associated signaling pathways (19). SAL is also a cation carrier that can transport monovalent cations (mainly K^+ and Na^+ ions) through lipid bilayers, such as cellular membranes. SAL may perform the cation transport in at least two ways: i) exchange of cations for protons across the membrane in an electrically silent way (nonelectrogenic cation/H^+ exchange), often leading to alterations in the intracellular and mitochondrial pH gradient or ii) transport of cations in an electrogenic manner (without transport of protons), leading to changes in electrical potential on cellular membranes (20). However, the prospective link between the cation carrier and anticancer properties of salinomycin is currently unclear. Of note, extensive research efforts toward introducing new drug delivery systems (21) are ongoing worldwide to reduce the potential toxicity of SAL, partially related to dysregulation of ion concentration followed by

inhibition of oxidative phosphorylation (22). Additionally, to make the cation carriers clinically applicable, various SAL analogs with different chemical modifications have been synthesized and reported to improve the anticancer properties of the original SAL (20).
Presenting novel insights, we demonstrate for the first time that SAL upregulates CD20 antigen, enhancing the efficacy of anti-CD20 immunotherapies both *in vitro* and *in vivo*. Furthermore, our study identifies a whole group of potassium/sodium cation carriers as inducers of CD20 upregulation and attributes their mechanism of action to the simultaneous inhibition of two repressors of *MS4A1* expression, namely FOXO1 and MYC oncogene. Although the direct association between cation carrier and cellular signaling-modifying properties of SAL has not been delineated, these findings underscore a fundamental basis for repurposing SAL and advancing other cation carriers as future pharmaceuticals for augmenting the surface levels of CD20 and enhancing the efficacy of current lymphoma treatments.

Methods

NK cell-mediated cytotoxicity (ADCC) and CAR-T cell-mediated killing assays.

Target Burkitt lymphoma or DLBCL cell lines (1×10^6 cells) were pretreated with SAL or MON for 24 h, labeled with CFSE (carboxyfluorescein succinimidyl ester), according to the manufacturer's recommendations, followed by further treatment with SAL or MON for the next 24 h. NK and T effector cells were isolated from healthy donors' peripheral blood mononuclear cells with EasySep Human NK Cell Enrichment Kit (STEMCELL Technologies, cat. # 19055) and Human T Cell Enrichment Kit (STEMCELL Technologies, cat. # 19051), respectively. CFSE-labeled target cells were seeded in 96-well plates (3×10^4) together with effector NK cells (1.2×10^5) for 3 h in the presence or absence of RTX (0.03 μg/ml) and subsequently stained with PI. The viability of the CFSE-positive population (target cells) was analyzed using flow cytometry and presented as a percentage of controls (target cells treated with cation carriers but not incubated with NK cells).
For the generation of CAR-T, the isolated human T cells were cultured in RPMI medium supplemented with 5% human serum (Sigma-Aldrich, cat. # H3667) and interleukin-2 (IL-2; 100 U/ml; Peprotech, cat. # 200-02), and were activated with anti-CD3/CD28 Dynabeads (bead-tocell ratio of 1:1; Thermo Fisher Scientific, cat. # 11161D) for three days. The expanded T cells were transduced with the lentivirus (10 TU/cell) encoding the 2nd generation anti-CD20 CAR (BPS Bioscience, cat. # 78606) in the presence of Polybrene (5 μg/ml; Sigma-Aldrich, cat. # TR1003-G). During the following 1-3 weeks, the CAR-T cell activities were tested in the killing assays by co-incubation with the SAL- or MON-pretreated and CFSE-labeled Raji cells at the effector-to-target ratio of 4:1 for 24 h. The viability of Raji cells was presented as a percentage of controls (Raji cells pretreated with cation carriers but not incubated with T cells).

Genome editing using CRISPR/Cas9 technology

For the stable knock-out of CD20, the sgMS4A1 was generated with the following oligonucleotide pair (CACCGCAGCAACGGAGAAAAACTCC and AAACGGAGTTTTTCTCCGTTGCTGC) and cloned into pLenti-CRISPRv2 (CRISPR/Cas9 system, gift from Feng Zhang; Addgene plasmid # 52961; RRID: Addgene_52961). The presence of the cloned sequence was confirmed by sequencing using the CRISPR-seq primer (GTACAAAATACGTGACG). HEK 293T cells (3×10^6) seeded into 10 cm plates were used to

produce a replication-incompetent lentivirus. Cells were first co-transfected with 8.6 μg of pLenti-CRISPRv2 and components of 2nd generation of packaging vectors, namely 8.6 μg of psPAX2 and 5.5 μg of pMD2.G, using standard calcium chloride method. 48-72 hours posttransfection, the lentiviruses-containing medium was collected and added to target Raji cells at the volume ratio 1:1. Two days later, puromycin (2 μg/ml) was added to Raji cells for the following week. Single clones were obtained from resistant cell pools by limiting dilution. Three clones with a confirmed lack of CD20 expression were mixed for the animal study.

For the generation of transient knock-out in Raji cells, the Cas9 nuclease (cat. # 1081058), tracrRNA (cat. # 1072533), and the following Alt-R CRISPR-Cas9 crRNAs were purchased from Integrated DNA Technologies: MYC.1.AC, MYC.1.AB, SGK1.1.AC, and SGK1.1.AT. The single guide RNA (sgRNA) for the ablation of each gene was generated separately by annealing crRNA and tracrRNA at an equimolar ratio (0.15 nmol each). Next, the ribonucleoprotein (RNP) complexes were prepared by adding Cas9 nuclease (12.5 μg) and incubating for 20 min at room temperature. The electroporation enhancer (0.15 nmol), purchased from Integrated DNA Technologies, was added to the RNP complexes, followed by mixing with 1×10^6 Raji cells suspended in 100 μl of the Resuspension Genome Editing Buffer (Thermo Fisher Scientific, cat. # N10025). Cells were electroporated using the Neon NxT machine (Thermo Fisher Scientific, cat. # NEON1S2YR), set at 1500V, 30 ms, 1 pulse.

Surfaceome analysis

Raji cells were treated with either SAL (0.25 μM) or vehicle for 48 h, followed by isolation of membrane fractions using the Mem-PER™ Plus Membrane Protein Extraction Kit (Thermo Fisher Scientific, cat. # 89842) according to the manufacturer's recommendations. Five μg of protein per sample were trypsinized, followed by chromatographic separation using nanoUHPLC (nanoElute, Bruker) coupled with the CaptiveSpray ion source of the ESI-Q-TOF mass spectrometer (Compact, Bruker). The collected spectra were analyzed and calibrated in DataAnalysis (Bruker), followed by ProteinScape 4.2 (Bruker) identification using the MASCOT server. Proteins were identified using the online SwissProt and NCBI_prot databases.

Human CLL and DLBCL patient samples

The primary chronic lymphocytic leukemia (CLL) cells were isolated from whole blood, while the primary diffuse large B cell lymphoma (DLBCL) cells were isolated from lymph nodes of patients using Histopaque 1077, according to manufacturer's recommendations (Sigma-Aldrich). Approvals for the study were obtained from the Institutional Review Boards of the Medical University of Warsaw, Poland (no KB/65/2023) and the Catholic University Hospital, Rome, Italy (no 14563/15), and conducted according to the Declaration of Helsinki. Each patient signed an informed consent for the procedures. The primary cells (2×10^5/well) were maintained in 96well plates in IMDM medium (supplemented with 10% FBS), treated with either SAL, MON, or vehicle for 48 h, and stained with a mix of anti-CD19, anti-CD20 antibodies, and Zombie-NIR. The MFI of CD20 was estimated in the CD19-positive/ Zombie-NIR-negative cell population.

Results

Sodium/potassium cation carriers strongly upregulate CD20 levels.

We found that 48 h-long incubation of Raji cells with subtoxic doses of sodium/potassium cation carriers (group of polyether ionophores; Fig. 1A), namely salinomycin (SAL), monensin (MON), nigericin (NIG), and narasin (NAR) significantly increased the levels of surface antigen CD20 (2.2-4-fold increase; Fig. 1B and Suppl. Fig. 1A). The maximum upregulation of both the surface and the total CD20 protein levels were achieved with cation carrier concentrations as low as 0.25-0.5 μM in the case of SAL, NIG, NAR, and 0.01-0.05 μM in the case of MON (Fig. 1B and Suppl. Fig. 1A, B). At the same time, the viability of Raji cells was affected at much higher concentrations, 2.49, 2.6, 2.77, and 0.73 μM, respectively (Fig. 1C). Other cation carriers were less efficient in CD20 antigen upregulation (Suppl. Fig. 2), with lasalocid and A23187 exhibiting maximum CD20 upregulation at concentrations as high as 1-2.5 μM. At the same time, ionomycin, the selective calcium carrier, upregulated CD20 to a much lesser extent. Therefore, we concluded that sodium/potassium cation carriers are the most efficient stimulators of CD20 antigen upregulation. Notably, 48 h-long exposure to the subtoxic doses of either SAL (0.25-1 μM) or MON (0.025-0.25 μM) significantly and dose-dependently upregulated CD20 antigen also in human B cell-derived primary tumor cells, such as CLL cells (cohort treated with SAL, n = 24, and cohort treated with MON, n = 13; Fig. 1D, Suppl. Fig. 3 and Suppl. Table 5) and DLBCL cells (cohort treated with SAL, n = 10; Fig. 1E, Suppl. Fig. 3A and Suppl. Table 3) cultured *ex vivo*.

Salinomycin and monensin increase the efficacy of anti-CD20 mAbs and CAR-T cells.

Since the CD20 antigen is an essential therapeutic target in B cell-derived malignancies, we further studied the therapeutic outcomes and the molecular mechanisms of CD20 upregulation. We found that both SAL and MON potentiated the cytotoxic efficacy of the therapeutic antiCD20 antibody, rituximab (RTX), in the presence of human complement (Fig. 2A). Since the effectiveness of therapeutic mAbs in the complement-dependent cytotoxicity (CDC) assays also depends on the level of membrane-bound complement-regulatory proteins (mCRPs) (23, 24), we assessed surface levels of CD46 and CD55 in Raji cells incubated with selected cation carriers. We found that both SAL and MON significantly downregulated CD55 (Suppl. Fig. 4A) and, to a lesser extent also CD46 (Suppl. Fig. 4B). Collectively, our results suggested that cation carriers sensitize cancer cells to complement-dependent killing by both upregulation of CD20, the target antigen for RTX, and downregulation of complement-inhibitory mCRPs, particularly CD55. Besides CDC, many therapeutic anti-CD20 mAbs eliminate cancer cells by activating NK celldependent cytotoxicity. We found that the cation carriers significantly increased the cytotoxicity of human NK cells toward SAL- or MON-pretreated target Raji cells and increased the efficacy of RTX in antibody-dependent cell-mediated cytotoxicity assays (ADCC; Fig. 2B). We noticed that the improvement of NK cells cytotoxicity toward SAL- or MON-pretreated target cells was not only the result of CD20 upregulation in Raji cells since the effect was evident even in the absence of anti-CD20 mAb, RTX (Fig. 2B; bars "Raji+NK"). We, therefore, performed a global analysis of surface proteins of target Raji cells upon 48 h-long exposure to SAL. In addition to CD20, numerous surface proteins were upregulated, including the proteins known to interact with activating or inhibitory receptors on NK cells (Fig. 2C). Using the specific antibodies and flow cytometry analysis, we confirmed that SAL and MON upregulated the proteins known to positively regulate

the immune effector cell's function, such as the costimulatory molecules TNF5 (CD40) and ICAM1 (Suppl. Fig. 4C-D) as well as numerous HLA molecules. Surprisingly, the CD47 antigen ("do not eat me" molecule) was also upregulated, however, only by the lower concentrations of SAL and MON (Suppl. Fig. 4E). Numerous other cell surface proteins have been previously reported to stimulate NK cell's activity (25). We found that SAL and MON upregulated CD80, CD155, ULBP2/5/6, and to a lesser extent also CD86 (Suppl. Fig. 4F). Collectively, these results suggest that the treatment of cancer cells with cation carriers results in upregulation of numerous surface antigens, which may allow target cells to be recognized and killed by NK cells more efficiently.

Since adoptive cellular therapies based on T cells engineered to express the chimeric antigen receptors (CAR-T cells) have recently been used in the treatment of B cell-derived malignancies, we tested the cytotoxic activity of anti-CD20 CAR-T cells towards SAL- and MON-treated target cells (Fig. 2D). We found that in suboptimal conditions the CAR-T cells exhibited significantly higher efficacy towards Raji cells with cation carrier-mediated upregulation of the target antigen CD20 when compared to control cells.

As most of the results presented above were obtained using the Raji model cell line, we next confirmed our findings in a broad panel of established tumor cell lines of B-cell origin. For each cell line, including Burkitt lymphoma (CA46, Daudi, Ramos, and BL41; Suppl. Fig. 5) and DLBCL cell lines, both GCB subtype (OCI-Ly1 and OCI-Ly7; Fig. 3A) and ABC subtype (HBL-1 and U2932; Fig. 3B) we determined concentrations of SAL and MON able to induce significant upregulation of CD20 (left panels), and confirmed that these cation carriers potentiate the efficacy of RTX in CDC assays (right panels).

Additionally, we confirmed that another therapeutic anti-CD20 antibody, ofatumumab (OFA), exhibited significantly higher efficacy toward SAL- or MON-treated cells in the presence of complement (Fig. 3C). Moreover, the improvement of NK cells cytotoxicity toward SALpretreated target cells (demonstrated for Raji in Fig. 2B) was additionally confirmed in the case of other Burkitt lymphoma (CA46 and Ramos) and DLBCL (OCI-Ly1 and HBL1) cell lines (Fig. 3D). Collectively, these data confirm that sodium/potassium cation carriers exhibit numerous beneficial effects on the therapeutic efficacy of both anti-CD20 mAbs and CAR-T cells when studied *in vitro*.

Salinomycin and monensin improve the anti-tumor activity of rituximab in vivo.

Since the cation carriers improve RTX-mediated CDC and ADCC in cell culture studies, we further aimed to assess the anti-tumor efficacy of the combination treatment (RTX plus cation carrier) *in vivo* (Fig. 4). We used a model of SCID mice, inoculated s.c. with Raji cells. In this model, eliminating tumor cells with the therapeutic RTX relies on both the NK cells and the complement, as both components are present in the SCID mouse strain (Charles River Laboratories). RTX as a single agent only partially delayed Raji lymphoma cells' growth as tumors. Noteworthy, the combined therapy of RTX with either SAL or MON remarkably limited tumor growth, as estimated by both the tumor measurement over 27 days upon inoculation of cells (Fig. 4A) and tumor weight at the end of experiments (Fig. 4B). In parallel experiments we also monitored the tumor growth upon inoculation of either control Raji cells (mix of clones transduced with empty vector) or cells with depletion of CD20 (mix of Raji clones with disrupted *MS4A1* locus; Suppl. Fig. 6A). The Raji cells with depletion of CD20 were remarkably resistant to RTX treatment in CDC assays, except for the highest RTX concentration (Suppl. Fig. 6B) and entirely resistant for RTX in ADCC assays (Suppl. Fig. 6C), retaining however, the SAL-induced sensitization to NK cell-mediated lysis. In

the experiments *in vivo*, the lack of CD20 abolished the beneficial effect of SAL on tumor growth as documented by the photos of isolated tumors or by the measurement of tumor weight (Fig. 4C). Together, these results provide strong support for the conclusion about the improvement of anti-tumor activity of RTX by sodium/potassium cation carriers *in vivo*.

Cation carriers stimulate the transcription of the MS4A1 gene encoding CD20

To get insight into the molecular mechanisms of CD20 upregulation, we first tested whether it might result from inflammasome activation since some cation carriers, particularly nigericin, are known activators of NLRP3 signaling. We found, however, that preincubation of Raji cells with MCC950 (NLRP3 inhibitor) did not affect the CD20 upregulation induced by NIG, SAL, or MON (Suppl. Fig. 7).

Next, we tested SAL and MON for their influence on the expression of the *MS4A1* gene encoding CD20. Quantitative RT-PCR revealed a significant increase in *MS4A1* mRNA levels, first detected at 12 h upon the treatment with either SAL or MON and reaching a 2-fold increase at 18 h upon the treatment (Fig. 5A). As the existence of different *MS4A1* mRNA variants has been documented (8), we tested the variants 1 and 3, most commonly expressed by Raji cells. We found that both variants were upregulated by SAL and MON (Suppl. Fig. 8). A conventional inhibitor of transcription, actinomycin D, incubated with cells for up to 24 h (more prolonged exposure was toxic), revealed that in the context of the transcriptional blockade, SAL does not upregulate either *MS4A1* mRNA (Fig. 5B, left panel) nor surface CD20 (Fig. 5B, right panel). Therefore, we concluded that the observed cation carrier-induced upregulation of CD20 occurs mainly at the transcriptional level.

Transcriptional profiling of Raji cells incubated for 18 h with either 0.5 μM SAL or 0.1 μM MON was carried out to characterize molecular changes induced by the cation carriers. The differential expression analysis of RNA-seq (*q* value cut-off <0.05) revealed 65 significantly changed genes in cells incubated with SAL (Fig. 5C and Suppl. Table 6) and 896 genes in cells treated with MON (Fig. 5C and record GSE282862 deposited in the Gene Expression Omnibus repository). Overall, the magnitude of changes in gene expression (log2 Fold change (FC) varied between +1.63 and -1.33 or between +2.46 and -1.61 in the case of SAL- and MON-regulated genes, respectively. Noteworthy, all 17 genes downregulated and 48 upregulated by SAL were also down- and upregulated by MON, respectively, confirming the reproducibility of acquired data. Since cation carriers upregulate CD20 transcriptionally, we sought transcription factors/miRNAs responsible for this effect. We ran the Gene Set Enrichment Analysis (GSEA; based on gene target predictions) and identified 6 and 101 transcription factors/miRNAs altered by SAL and MON, respectively (Fig. 5D). The activity of four of them, namely Forkhead family (FOXO), MYC, NF-Y, and mir181 appeared to be commonly altered by both cation carriers.

Downregulation of MYC is sufficient to upregulate CD20 in response to cation carriers' treatment.

The transcriptional profiling of Raji cells revealed that *SGK1* mRNA, encoding a kinase known to inhibit both FOXO and MYC transcription factors (26), was remarkably increased by the treatment with either SAL or MON (log2 FC = 1.37 and 1.87, respectively). Additionally, the transcriptional target of FOXO, *IL7R* mRNA was among the most strongly downregulated transcripts by SAL and MON (log2 FC = -1.33 and -1.59, respectively), suggesting that the cation carriers may affect the

activity of FOXO transcription factors. Therefore, we validated the changes in mRNAs encoding SGK1 and IL7R using qRT-PCR (Fig. 6A) and further studied the FOXO signaling using Western blotting. Indeed, we found that both SAL and MON increased the levels of two upstream negative regulators of FOXO, namely the active phosphorylated AKT (27) and SGK1 (28), leading ultimately to the increase in phosphorylated FOXO1 at Ser256 (Fig. 6B). The phosphorylation of FOXO1 implicates its exclusion from the nucleus and block of its activity as a transcription factor (29, 30).

Besides the changes in FOXO signaling, we also noticed the downregulation of *MYC* mRNA upon the treatment with MON (log2 FC = -0.53) in RNA-seq data. Indeed, using qRT-PCR, we confirmed the significant drop in the expression of *MYC* mRNA (Fig. 7A) and MYC protein levels (Fig. 7B and Suppl. Fig. 9A) upon the treatment with the cation carriers. The GSEA analysis of RNA-seq data revealed numerous MYC target genes among MON-downregulated genes (Fig. 7C; hallmarks – MYC targets, version 1 and version 2; *p*-value = 2.1 e^{-10} and 5.88 e^{-9}, respectively). The significant downregulation of the MYC-dependent gene, *PLK1*, was additionally confirmed with qRT-PCR (Fig. 7D, left panel). At the same time, *TNFAIP3*, known to be repressed by MYC (31), was significantly upregulated by the treatment with SAL and MON (Fig. 7D, middle panel). Among known MYC transcriptional targets in Burkitt lymphoma (32), *PTPN6* mRNA was one of the most strongly upregulated genes in our RNA-seq data by both SAL and MON (log2 FC = 1.63 and 2.04, respectively), suggesting that *PTPN6* is probably a transcript repressed by MYC. Indeed, we confirmed the remarkable upregulation of *PTPN6* mRNA upon the treatment with the cation carriers (Fig. 7D, right panel). Using the ELISA assay, detecting specific binding of MYC to its consensus DNA binding motif E-box, we confirmed that the treatment with either SAL or MON leads to a significant drop in the levels of MYC transcription factor bound to DNA (Suppl. Fig. 9B).

Consistently with the known role of MYC in regulating the cell cycle, the GSEA analysis of RNA-seq data revealed the MON-induced downregulation of numerous G2/M checkpoint genes (Suppl. Fig. 9C; *p*-value = 2.31 e^{-21}). Indeed, the incubation with either SAL or MON for 48 h decreased the percentage of Raji cells in the G1 phase (from 58-60% to 41-44%) while increasing the rate of cells in the G2/M phase (from 20-23% to 30-32%; Suppl. Fig. 9D). To get insight into the relationship between the expression of MYC and CD20, we employed the P493-6 lymphoblastoid cell line with the MYC Tet-OFF system, where treatment with tetracycline or doxycycline (DOX) switches off the expression of MYC (33). Using the flow cytometry, we confirmed that the expression of MYC protein was repressed during 24 h of incubation with DOX, and it was also remarkably downregulated by the treatment with SAL (Fig. 7E, left panel). Confirming the hypothesis about MYC being a negative regulator of CD20 expression, the DOX-induced repression of MYC led to an almost double increase in the level of surface CD20 during a 48 h-long treatment (from 55.5 x 10^3 to 99.2 x 10^3 CD20 molecules/cell; Fig. 7E, right panel). Of note is that the lower the expression of MYC, the higher the level of surface CD20, with the highest levels achieved by the treatment with DOX plus either SAL or MON (Fig. 7E and Suppl. Fig. 10). On the other hand, the treatment with SAL alone induced higher CD20 upregulation than the one observed upon the DOX-initiated repression of MYC alone (from 55.5 x 10^3 to 150.5 x 10^3 CD20 molecules/cell; Fig. 7E, right panel). This fact suggests that the overall effect of SAL and MON on the regulators of CD20 expression is broader than just the repression of MYC levels.

In summary, these results indicated that cation carriers inhibit the activity of the FOXO1 transcription factor and downregulate the levels of MYC, which correlates with the upregulation of CD20. This suggests that these transcription factors may be the *MS4A1* repressors. To further

validate this hypothesis, we synthesized five derivatives of SAL, which lack the CD20upregulating ability despite exhibiting a high similarity in the chemical structure to the original SAL (Fig. 8A and Suppl. Fig. 11A, B). The changes in the chemical structures of SAL included modifications in positions C1 or C20 (Suppl. Fig. 11A; positions marked in red and blue, respectively). Knowing that these modifications lead to a complete loss of CD20-upregulating ability, we hypothesized that the derivatives of SAL also lost the ability to increase the phosphorylated AKT and FOXO1 and downregulate the MYC transcription factor. Surprisingly, we discovered that SAL derivatives 1, 2, 4, and 5 retained the ability to stimulate either phosphorylation of AKT, FOXO1, or both (Suppl. Fig. 11C). In contrast, MYC was downregulated exclusively by the original SAL but not by the derivatives (Fig. 8B). Similarly, the kinase SGK1, a potential upstream negative regulator of MYC (26, 34), was upregulated exclusively by the original SAL but not by the SAL derivatives (Fig. 8B). We, therefore, hypothesized that the signaling axis SGK1-MYC might be the key regulator of CD20 expression in response to cation carriers treatment.

Using the CRISPR/Cas9 genome editing, we transiently ablated either *MYC* or *SGK1*. We measured the basal level of CD20 two days after the nucleofection (Fig. 8C), followed by the treatment with cation carriers and the measurement of CD20 levels again 48 h later (Suppl. Fig. 12B-D). The basal levels of CD20 were increased exclusively upon the knockout of *MYC* with two tested sgRNA sequences (Fig. 8C, right panel; sgMYC #1 and sgMYC #2), even though the ablation was just partial (Fig. 8C, left panel; Suppl. Fig. 12A). The lowest levels of MYC obtained upon the ablation of *MYC* plus the treatment with cation carriers correlated with the highest levels of CD20 antigen (Suppl. Fig. 12B), confirming again that MYC is a negative regulator of CD20 expression. Similarly, MYC inhibitor, 10058-F4, induced an equally significant upregulation of CD20 as the incubation with SAL (Fig. 8D). Additionally, using the CUT&RUN protein-DNA interaction assays, we found that MYC was bound to *MS4A1* promoter in control cells, but the binding was significantly reduced by the treatment with SAL (Fig. 8E).

In contrast to MYC, the ablation of *SGK1* did not change the basal levels of either CD20 (Fig. 8C, right panel) or MYC (Fig. 8C, left panel). Ablation of SGK1 did not affect the SAL- or MON-induced upregulation of CD20 (Suppl. Fig. 12C, D), nor the downregulation of MYC by cation carriers (Fig. 8C, left panel), suggesting a lack of signaling connection between SGK1 and MYC as well as SGK1 and CD20. Moreover, an inhibitor of SGK1, EMD638683, did not affect the SAL- or MON-induced upregulation of CD20 antigen (Suppl. Fig. 12E). Together, our results uncover the role of MYC as the key player and the negative transcriptional regulator of CD20 antigen expression.

Discussion

The understanding of molecular mechanisms leading to the CD20 antigen escape in the therapies with either mAbs or CARs is crucial for refining treatment strategies, fostering the development of new combinatorial therapeutic approaches, and ultimately enhancing the efficacy of antiCD20 therapies in overcoming resistance and improving the clinical outcomes for patients suffering from B-NHL. We and others have previously reported that upregulation of surface CD20 leads to more effective treatments in preclinical lymphoma models (13, 35, 36) and clinical cases of leukemia (37). Here, we provide a new combinatorial strategy for fully exploiting the therapeutic potential of anti-CD20 mAbs and CAR-T cells.

In this study, we initially explored the potential of SAL to upregulate CD20 antigen, as this particular anticancer compound has been reported to activate AKT signaling (14), one of the

critical pathways controlling the expression of CD20 (12, 13). Indeed, we found that SAL strongly upregulated CD20 antigen in numerous B-NHL cell lines and patients-derived malignant cells. The cation carriers are natural products with antimicrobial and anticancer properties. Importantly, SAL and another functionally similar compound, monensin (MON), with potassium/sodium cation carrier properties, have previously been revealed in unbiased screens as compounds explicitly targeting CSCs (15, 38) and chemo-resistant cancer cells (39). Therefore, this group of compounds is worth exploring as potential therapeutic agents. The anticancer efficacy of SAL and MON toward certain types of leukemia has been reported (4042); however, their ability to upregulate CD20 antigen at low doses and serve as potential drug candidates combined with anti-CD20 mAbs or CAR-T therapies is a novel concept.

In this study, we tested many members of the cation carrier group of compounds. We concluded that the monovalent cation carriers specific for transporting potassium and sodium, namely SAL, MON, narasin, and nigericin, are most efficient in upregulating the CD20 antigen. We also delineated the molecular mechanisms of the cation carrier's action on CD20 to the transcriptional regulation of its gene, *MS4A1*. Based on the initial expectations, SAL and MON appeared to activate the AKT pathway, leading to the phosphorylation of the FOXO1 transcription factor. The phosphorylation of FOXOs implicates their exclusion from the nucleus and blocks their activity as transcription factors (29). We have previously reported that FOXO1 (activated by the BCR signaling inhibitors) acts as a negative regulator of the *MS4A1* expression (13). Importantly, our RNA-seq data revealed additional molecular targets of cation carriers. We demonstrate that besides activation of the AKT kinase, SAL and MON remarkably increase the expression of SGK1, the alternative kinase previously reported to inhibit FOXO transcription factors *via* phosphorylation (28). Thus, we demonstrate that cation carriers simultaneously activate two negative regulators of FOXOs, kinases AKT and SGK1.

Of particular interest is, however, our finding that the treatment with SAL and MON leads to a significant drop in the levels of MYC and a reduction in the binding to its consensus DNA motif, E-box, which inversely correlates with the expression of *MS4A1*. Indeed, we and others confirmed that MYC can bind to the promoter of *MS4A1,* where it represses the expression of CD20 (31, 36, 43). For example, the PIM kinase inhibitors, which decreased levels of MYC, could upregulate CD20 antigen in a MYC-dependent fashion (36). Murine primary lymphomas and immortalized human lymphocytes upregulated CD20 upon inactivation of MYC (43). Here, using the CUT&RUN protein-DNA binding assay, we show that MYC binds to the *MS4A1* promoter, and this binding is significantly reduced upon incubation with SAL. The RT-PCRamplified fragment of the *MS4A1* promoter contains the E-box-like motif sequence CACCTG (244 to -239 bp), which might be responsible for the MYC binding.

We also present additional evidence of the signaling connection between MYC and CD20. We found that the derivatives of SAL, which cannot upregulate CD20, can also not downregulate MYC. However, the link between MYC's downregulation and salinomycin's or monensin's cation carrier function is unclear. The sodium/potassium cation carriers can perform either nonelectrogenic exchange of K^+ or Na^+ ions for protons or serve as an electrogenic ion carrier. The chemical modification of SAL by synthesizing ester or amide derivatives can eliminate the possibility of protonation/deprotonation of the C1 carboxylic group (COOH) (44). Although some of the SAL derivatives used in this study retain the ability to form complexes with monovalent cations, similar to the original SAL (data not shown), they are expected to have a reduced ability to induce cation/H^+ exchange and non-electrogenic fluxes on lipid bilayers. For example, the ester

derivative of MON can transport cations mainly in an electrogenic manner (45), and the amide derivative of SAL can also bind some divalent cations (20). Therefore, we cannot exclude the possibility that the non-electrogenic transport (cation/ H^+ exchange) or binding to monovalent cations specifically might be necessary to initiate the SAL- and MONinduced downregulation of MYC followed by the upregulation of CD20 antigen.
In this study, we also provided genetic evidence for MYC-dependent regulation of CD20, showing that only partial knockout of *MYC* is sufficient to increase the surface levels of CD20 in Raji cells. Moreover, in the engineered P493-6 cells with Tet-OFF system for MYC regulation, CD20 antigen can be significantly upregulated by either the treatment with SAL and MON or by the tetracycline/doxycycline-induced elimination of MYC expression. However, the fact that SAL or MON upregulates CD20 to a higher level than the MYC removal alone (initiated by DOX treatment) favors the hypothesis that MYC is not the only factor responsible for cation carrier-induced upregulation of CD20.

Overall, we reveal here that cation carriers have a unique ability to simultaneously inhibit the activity of two essential repressors of *MS4A1* expression, namely FOXO1 and MYC. Besides MYC and FOXO1, our RNA-seq data suggested that SAL and MON induce changes in the activity of two other transcription regulators, namely NF-Y and mir-181. However, their involvement in the regulation of *MS4A1* expression requires further investigation. This study documented the upregulation of CD20 antigen by sodium/potassium-specific cation carriers in both lymphoma cell lines and patient-derived primary CLL and DLBCL cells. The low level of CD20 antigen on malignant cells, such as CLL cells, is a common problem in anti-CD20 immunotherapy. Therefore, the employment of compounds that increase the levels of CD20 in the therapeutic regimen could be beneficial for the outcome of anti-CD20 mAbs and CAR-T therapy. Here, we validated the RTX plus cation carrier combination in the preclinical model and reported its superior efficiency in reducing the growth of Burkitt lymphoma *in vivo*. Since the therapeutic mAbs act *via* different molecular mechanisms (46), we also tested the efficacy of RTX plus cation carriers in various *in vitro* assays. The two main mechanisms of tumor cell eradication by RTX, namely CDC, and ADCC, are known to depend on the CD20 expression level (47). We demonstrate here that SAL and MON increase the efficacy of RTX *via* both mechanisms. New anti-CD20 mAbs, such as ofatumumab (OFA) or obinutuzumab (48), and bispecific antibodies, such as mosunetuzumab, epcoritamab, or glofitamab have been introduced to the clinic. Therefore, in addition to RTX, we also tested OFA and provided evidence for its increased cytotoxicity toward SAL- or MON-treated tumor cells in CDC assays. However, in our hands, the cation carrier-mediated improvement of mAb efficacy was more evident in the case of RTX than OFA.

Additionally, we found that the beneficial effects of cation carriers are not limited only to the increase of surface CD20. Based on the previous reports demonstrating that the mechanisms of resistance to anti-CD20 mAbs include the increased expression of CRPs, namely CD55, CD46, and CD59, which impair the efficacy of RTX by inhibiting CDC (49, 50), we tested the levels of surface CD55 and CD46 (while CD59 was not expressed in Raji). Importantly, we found that SAL and MON consistently and significantly decreased surface CD55, which can be considered an additional therapeutic benefit of the cation carrier's action. In addition, our unbiased proteome profiling of surfaceome revealed the cation carrier-mediated upregulation of many HLA molecules, ICAM1 and CD40, which play an essential role in antigen presentation and recognition of cancer cells by T or NK cells. Overall, we concluded that cation carriers can potentially induce a more robust immunogenicity in B cell-derived malignancies *via* upregulation of HLA molecules

(51) and improve the cytotoxic activity of immune cells *via* better recognition of cancer cells with upregulated levels of ICAM1 or CD40. As the cytotoxic NK cells are the executors in the ADCC mechanism of the therapeutic mAbs, we also tested other surface molecules of cancer cells known to influence the activity of NK cells (25). Numerous proteins known to interact with activating receptors of NK cells (52) were upregulated, namely CD80, CD155, ULBP2/5/6, and CD86. This may also explain why, in our ADCC assays, the SAL- or MON-pretreated cells, compared to control Raji cells, were more efficiently eliminated by NK cells, even in the absence of RTX.

In summary, due to the broad spectrum of interesting biological and pharmacological properties exhibited by SAL and other cation carriers, nanotechnology has recently been employed to provide salinomycin-based nanocarriers with increased accumulation in tumor tissue and reduced toxicity toward healthy cells (21). Additionally, the natural research direction is a chemical modification of cation carriers, which can lead to the synthesis of unique derivatives with significantly better biological activity and lower toxicity than those of unmodified antibiotics (20, 44). With the ultimate goal of bringing these compounds to the clinic, the derivatives of SAL with chemical modifications in positions C-1, C-20, and a few others have already been synthesized and tested for their selective toxicity towards malignant cells and CSC (16, 20, 44). However, these compounds still need to be tested for CD20-upregulating activity, and their safety needs to be thoroughly evaluated in preclinical and clinical models.

References

1. Pavlasova G, Mraz M. The regulation and function of CD20: an "enigma" of B-cell biology and targeted therapy. Haematologica. 2020;105(6):1494-1506.

2. Wang V, Gauthier M, Decot V, Reppel L, Bensoussan D. Systematic Review on CAR-T Cell Clinical Trials Up to 2022: Academic Center Input. Cancers (Basel). 2023;15(4):1003.

3. Lopedote P, Shadman M. Targeted Treatment of Relapsed or Refractory Follicular Lymphoma: Focus on the Therapeutic Potential of Mosunetuzumab. Cancer Manag Res. 2023;15:257-264.

4. Luo C, Wu G, Huang X, et al. Efficacy and safety of new anti-CD20 monoclonal antibodies versus rituximab for induction therapy of CD20(+) B-cell non-Hodgkin lymphomas: a systematic review and meta-analysis. Sci Rep. 2021;11(1):3255.

5. Casan JML, Wong J, Northcott MJ, Opat S. Anti-CD20 monoclonal antibodies: reviewing a revolution. Hum Vaccin Immunother. 2018;14(12):2820-2841.

6. Pierpont TM, Limper CB, Richards KL. Past, Present, and Future of Rituximab-The World's First Oncology Monoclonal Antibody Therapy. Front Oncol. 2018;8:163.

7. Tomita A. Genetic and Epigenetic Modulation of CD20 Expression in B-Cell Malignancies: Molecular Mechanisms and Significance to Rituximab Resistance. J Clin Exp Hematop. 2016;56(2):89-99.

8. Ang Z, Paruzzo L, Hayer KE, et al. Alternative splicing of its 5'-UTR limits CD20 mRNA translation and enables resistance to CD20-directed immunotherapies. Blood. 2023;142(20):1724-1739.

9. Prevodnik VK, Lavrencak J, Horvat M, Novakovic BJ. The predictive significance of CD20 expression in B-cell lymphomas. Diagn Pathol. 2011;6:33.

10. Shadman M. Diagnosis and Treatment of Chronic Lymphocytic Leukemia: A Review. JAMA. 2023;329(11):918-932.

11. Burger JA, Sivina M, Jain N, et al. Randomized trial of ibrutinib vs ibrutinib plus rituximab in patients with chronic lymphocytic leukemia. Blood. 2019;133(10):1011-1019.

12. Bojarczuk K, Siernicka M, Dwojak M, et al. B-cell receptor pathway inhibitors affect CD20 levels and impair antitumor activity of anti-CD20 monoclonal antibodies. Leukemia. 2014;28(5):1163-1167.

13. Pyrzynska B, Dwojak M, Zerrouqi A, et al. FOXO1 promotes resistance of non-Hodgkin lymphomas to anti-CD20-based therapy. Oncoimmunology. 2018;7(5):e1423183.

14. Kim JH, Choi AR, Kim YK, Kim HS, Yoon S. Low amount of salinomycin greatly increases Akt activation, but reduces activated p70S6K levels. Int J Mol Sci. 2013;14(9):17304-17318.

15. Gupta PB, Onder TT, Jiang G, et al. Identification of selective inhibitors of cancer stem cells by highthroughput screening. Cell. 2009;138(4):645-659.

16. Qi D, Liu Y, Li J, Huang JH, Hu X, Wu E. Salinomycin as a potent anticancer stem cell agent: State of the art and future directions. Med Res Rev. 2022;42(3):1037-1063.

17. Mai TT, Hamai A, Hienzsch A, et al. Salinomycin kills cancer stem cells by sequestering iron in lysosomes. Nat Chem. 2017;9(10):1025-1033.

18. Arfaoui A, Rioualen C, Azzoni V, et al. A genome-wide RNAi screen reveals essential therapeutic targets of breast cancer stem cells. EMBO Mol Med. 2019;11(10):e9930.

19. Wang H, Zhang H, Zhu Y, Wu Z, Cui C, Cai F. Anticancer Mechanisms of Salinomycin in Breast Cancer and Its Clinical Applications. Front Oncol. 2021;11:654428.

20. Antoszczak M, Huczynski A. Salinomycin and its derivatives - A new class of multiple-targeted "magic bullets". Eur J Med Chem. 2019;176:208-227.

21. Tefas LR, Barbalata C, Tefas C, Tomuta I. Salinomycin-Based Drug Delivery Systems: Overcoming the Hurdles in Cancer Therapy. Pharmaceutics. 2021;13(8):1120.

22. Ekinci IB, Chlodowska A, Olejnik M. Ionophore Toxicity in Animals: A Review of Clinical and Molecular Aspects. Int J Mol Sci. 2023;24(2):1696.

23. Bologna L, Gotti E, Da Roit F, et al. Ofatumumab is more efficient than rituximab in lysing B chronic lymphocytic leukemia cells in whole blood and in combination with chemotherapy. J Immunol. 2013;190(1):231-239.

24. Dwojak M, Bobrowicz M, Bil J, et al. Sorafenib improves rituximab and ofatumumab efficacy by decreasing the expression of complement regulatory proteins. Blood Cancer J. 2015;5(4):e300.

25. Tremblay-McLean A, Coenraads S, Kiani Z, Dupuy FP, Bernard NF. Expression of ligands for activating natural killer cell receptors on cell lines commonly used to assess natural killer cell function. BMC Immunol. 2019;20(1):8.

26. Sang Y, Kong P, Zhang S, et al. SGK1 in Human Cancer: Emerging Roles and Mechanisms. Front Oncol. 2020;10:608722.

27. Tang ED, Nunez G, Barr FG, Guan KL. Negative regulation of the forkhead transcription factor FKHR by Akt. J Biol Chem. 1999;274(24):16741-16746.

28. Di Pietro N, Panel V, Hayes S, et al. Serum- and glucocorticoid-inducible kinase 1 (SGK1) regulates adipocyte differentiation via forkhead box O1. Mol Endocrinol. 2010;24(2):370-380.

29. Brunet A, Bonni A, Zigmond MJ, et al. Akt promotes cell survival by phosphorylating and inhibiting a Forkhead transcription factor. Cell. 1999;96(6):857-868.

30. Zhang X, Gan L, Pan H, et al. Phosphorylation of serine 256 suppresses transactivation by FKHR (FOXO1) by multiple mechanisms. Direct and indirect effects on nuclear/cytoplasmic shuttling and DNA binding. J Biol Chem. 2002;277(47):45276-45284.

31. Seitz V, Butzhammer P, Hirsch B, et al. Deep sequencing of MYC DNA-binding sites in Burkitt lymphoma. PLoS One. 2011;6(11):e26837.

32. Li Z, Van Calcar S, Qu C, Cavenee WK, Zhang MQ, Ren B. A global transcriptional regulatory role for cMyc in Burkitt's lymphoma cells. Proc Natl Acad Sci U S A. 2003;100(14):8164-8169.

33. Pajic A, Spitkovsky D, Christoph B, et al. Cell cycle activation by c-myc in a burkitt lymphoma model cell line. Int J Cancer. 2000;87(6):787-793.

34. Lee LYW, Woolley C, Starkey T, et al. Serum- and Glucocorticoid-induced Kinase Sgk1 Directly Promotes the Differentiation of Colorectal Cancer Cells and Restrains Metastasis. Clin Cancer Res. 2019;25(2):629-640.

35. Bobrowicz M, Dwojak M, Pyrzynska B, et al. HDAC6 inhibition upregulates CD20 levels and increases the efficacy of anti-CD20 monoclonal antibodies. Blood. 2017;130(14):1628-1638.

36. Szydlowski M, Garbicz F, Jablonska E, et al. Inhibition of PIM Kinases in DLBCL Targets MYC Transcriptional Program and Augments the Efficacy of Anti-CD20 Antibodies. Cancer Res. 2021;81(23):6029-6043.

37. Dworzak MN, Schumich A, Printz D, et al. CD20 up-regulation in pediatric B-cell precursor acute lymphoblastic leukemia during induction treatment: setting the stage for anti-CD20 directed immunotherapy. Blood. 2008;112(10):3982-3988.

38. Vanneste M, Huang Q, Li M, et al. High content screening identifies monensin as an EMT-selective cytotoxic compound. Sci Rep. 2019;9(1):1200.

39. Wang X, Wu X, Zhang Z, et al. Monensin inhibits cell proliferation and tumor growth of chemoresistant pancreatic cancer cells by targeting the EGFR signaling pathway. Sci Rep. 2018;8(1):17914.

40. Roulston GD, Burt CL, Kettyle LM, et al. Low-dose salinomycin induces anti-leukemic responses in AML and MLL. Oncotarget. 2016;7(45):73448-73461.

41. Urbaniak A, Delgado M, Antoszczak M, Huczynski A, Chambers TC. Salinomycin derivatives exhibit activity against primary acute lymphoblastic leukemia (ALL) cells in vitro. Biomed Pharmacother. 2018;99:384-390.

42. Yusenko MV, Trentmann A, Andersson MK, et al. Monensin, a novel potent MYB inhibitor, suppresses proliferation of acute myeloid leukemia and adenoid cystic carcinoma cells. Cancer Lett. 2020;479:61-70.

43. Yu D, Dews M, Park A, Tobias JW, Thomas-Tikhonenko A. Inactivation of Myc in murine two-hit B lymphomas causes dormancy with elevated levels of interleukin 10 receptor and CD20: implications for adjuvant therapies. Cancer Res. 2005;65(12):5454-5461.

44. Antoszczak M. A comprehensive review of salinomycin derivatives as potent anticancer and antiCSCs agents. Eur J Med Chem. 2019;166:48-64.

45. Antonenko YN, Rokitskaya TI, Huczynski A. Electrogenic and nonelectrogenic ion fluxes across lipid and mitochondrial membranes mediated by monensin and monensin ethyl ester. Biochim Biophys Acta. 2015;1848(4):995-1004.

46. Boross P, Leusen JH. Mechanisms of action of CD20 antibodies. Am J Cancer Res. 2012;2(6):676-690.

47. van Meerten T, van Rijn RS, Hol S, Hagenbeek A, Ebeling SB. Complement-induced cell death by rituximab depends on CD20 expression level and acts complementary to antibody-dependent cellular cytotoxicity. Clin Cancer Res. 2006;12(13):4027-4035.

48. Klein C, Jamois C, Nielsen T. Anti-CD20 treatment for B-cell malignancies: current status and future directions. Expert Opin Biol Ther. 2021;21(2):161-181.

49. Terui Y, Sakurai T, Mishima Y, et al. Blockade of bulky lymphoma-associated CD55 expression by RNA interference overcomes resistance to complement-dependent cytotoxicity with rituximab. Cancer Sci. 2006;97(1):72-79.

50. Hu W, Ge X, You T, et al. Human CD59 inhibitor sensitizes rituximab-resistant lymphoma cells to complement-mediated cytolysis. Cancer Res. 2011;71(6):2298-2307.

51. God JM, Haque A. Burkitt lymphoma: pathogenesis and immune evasion. J Oncol. 2010;2010:516047.

52. Paul S, Lal G. The Molecular Mechanism of Natural Killer Cells Function and Its Importance in Cancer Immunotherapy. Front Immunol. 2017;8:1124.

Figure legends

Figure 1. Monovalent cation carriers markedly increase CD20 on the surface of lymphoma and leukemia cells. (A) The chemical structures of selected cation carriers, namely salinomycin (SAL; left), monensin (MON; middle), nigericin (NIG; middle), and narasin (NAR; right), were visualized using ChemDraw Ultra 12.0. **(B)** Flow cytometry analysis of surface levels of CD20 antigen (quantification of MFI values) and **(C)** viability of propidium iodide-stained Raji cells, pretreated for 48 h with corresponding cation carriers (concentration range 0.01-2.5 μM). **(D, E)** Flow cytometry analysis of cell surface levels of CD20 antigen in 3 cohorts of primary tumor cells (CD19-positive). In the cohorts of chronic lymphocytic leukemia samples **(D)**, the cells were pretreated *ex vivo* with increasing concentrations of either SAL (left graph, n = 24) or MON (right graph, n = 13), while in the cohort of 10 samples of diffuse large B-cell lymphoma, DLBCL **(E)**, the cells were pretreated *ex vivo* with SAL for 48 h. MFI values of anti-CD20-FITC staining in cation-carrier-treated cells were normalized to the MFI values in vehicle-treated cells and presented as fold change.

Figure 2. Salinomycin and monensin enhance the complement-dependent and NK celldependent cytotoxicity of rituximab and the anti-CD20 CAR-T cell cytotoxic activity. (A) CDC (complement-dependent cytotoxicity) assays showing the improved killing of Raji cells pretreated with either SAL (0.25-0.5 μM; left graph) or MON (0.05-0.1 μM; right graph) for 48 h followed by treatment with rituximab (RTX; 1-100 μg/ml) for 1 h, in the presence of human serum as a source of complement. The viability of cells was assessed with PI iodide (PI) staining followed by flow cytometry analysis. The results were presented as a percentage of alive control cells (untreated with RTX). **(B)** ADCC (antibody-dependent cellular cytotoxicity) assays showing improved cytotoxicity of NK cells towards Raji cells pretreated with either SAL (0.25 μM; left panel) or MON (0.05 μM; right panel) for 48 h, followed by staining of Raji cells with CFSE and co-incubation with unstained donor-derived NK cells for 3 h, in the absence or presence of RTX (0.03 μg/ml). The survival of CFSE-positive Raji cells was assessed with PI, as above, and presented as a percentage of control cells (Raji not incubated with NK cells). Graphs show data from 3 experiments (NK cells isolated from 3 donors). **(C)** The heat map presents the log2 fold change in the levels of surface proteins in Raji cells treated with either SAL (0.25 μM) or vehicle for 48 h (six samples of each treatment were analyzed). The list includes only the proteins potentially implicated in regulating NK cell activity. The changes in CD20 were also included to serve as a positive control. **(D)** Anti-CD20 CAR-T-mediated killing assays showing improved cytotoxicity of CAR-T cells towards CFSE-stained Raji cells pretreated with either SAL (left panel) or MON (right panel) for 48 h. For these cytotoxicity assays, Raji cells were co-incubated with the unstained effector cells, either T cells or CAR-T cells, for 24 h. Survival of Raji cells was assessed with PI staining followed by flow cytometry analysis of CFSE-positive cells. Results were presented as a percentage of control cells (Raji not incubated with T cells). Graphs summarize data from 3 experiments.

Figure 3. Salinomycin and monensin increase CD20 levels and rituximab efficacy in a panel of B-cell tumor cell lines. (A-B) The left panels present flow cytometry analysis of surface levels of CD20 antigen (MFI of anti-CD20-FITC antibody) in DLBCL cell lines pretreated with either SAL (0.1-0.5 μM), MON (0.01-0.1 μM) or corresponding vehicles for 48 h. The right panels present their response to rituximab in CDC assays upon preincubation with either SAL or vehicle

(at two selected concentrations); **(A**) GCB subtype (OCI-Ly1 and OCI-Ly7 cells), **(B)** ABC subtype (HBL-1 and U2932 cells). **(C)** CDC assays show the improved killing of Raji cells pretreated with either SAL, MON, or vehicle for 48 h, followed by treatment with ofatumumab (OFA; 1-100 μg/ml) for 1 h, in the presence of human serum as a source of complement. The survival of cells was determined with flow cytometry and was presented as a percentage of alive control cells (untreated with OFA). **(D)** Assays showing improved cytotoxicity of NK cells towards B-cell tumor cell lines, such as CA46 (left panel), Ramos (middle panel), OCI-Ly1 (middle panel), and HBL-1 (right panel) pretreated with SAL (0.1-0.25 μM) for 48 h, followed by staining of these cells with CFSE and co-incubation with unstained donor-derived NK cells for 3 h. The survival of CFSE-positive tumor cells was assessed with PI and presented as a percentage of control cells (not incubated with NK cells). Graphs show data from at least 3 experiments (NK cells isolated from 3 donors).

Figure 4. Salinomycin and monensin potentiate the antitumor activity of rituximab *in vivo*. SCID mice (CB17/Icr-Prkdc^{scid}/IcrIcoCrl) were inoculated subcutaneously (sc.) with Raji cells. Mice were then injected intraperitoneally (ip.) with either SAL (2.5 mg/kg), MON (1 mg/kg), or vehicle on days 5 and 7. The ip. administration of RTX (10 mg/kg) started on day 9 and has been applied every second day, together with injections of SAL, MON, or vehicle. **(A)** The graph presents the volume of tumors measured every 3-4 days. **(B)** The tumors were post-mortally isolated on day 30 and weighed (n = 6-11 tumors/group). **(C)** The SCID mice were inoculated sc. with a mix of three clones (in proportion 1:1:1) of Raji cells transduced with either empty vector or sgMS4A1. Mice were then injected ip. with either SAL or vehicle, followed by injections of RTX, as described above. The photos (left panel) and the weight (right panel) of tumors (isolated post-mortally on day 32) were documented (n = 5-6 tumors/group).

Figure 5. Salinomycin and monensin regulate the *MS4A1* gene transcription. (A) Analysis of mRNA levels of *MS4A1* (estimated by qRT-PCR; 2 minus delta CT method) in Raji cells treated with either SAL (0.5 μM), MON (0.1 μM), or corresponding vehicles for 12-18 h. **(B)** The analysis was performed like in (A), using Raji cells pretreated with transcription inhibitor Actinomycin D (ActD; 5 μg/ml) for 2 hours. SAL (0.5 μM) or vehicle (Veh.) was then added for the next 18 h (estimation of *MS4A1* mRNA level; left panel) or 24 h (analysis of the surface level of CD20; right panel). **(C)** The differential expression heatmap (left panel) shows the comparison of gene expression profiles (estimated by RNA-seq; log2 fold change; *q* value cut-off <0.05) in Raji cells treated with either vehicle (Veh.), SAL (0.5 μM), or MON (0.1 μM) for 18 h (in two biological replicates). The volcano plot (right panel) depicts the number of significantly upregulated (red dots) and downregulated (green dots) mRNAs upon the treatment of Raji cells with SAL. **(D)** The Venn diagram represents the prediction of transcription factor/miRNA binding sites in the regulatory elements of the differentially expressed target genes (analyzed with GSEA/MSigDB website v6.3). SAL and MON affected six (the small dark blue circle) and 101 (the big bright blue circle) transcription factors/miRNAs, respectively. The activity of four transcription factors/miRNAs **(**FOXO, MYC, NF-Y, and mir181) appeared to be commonly affected by both SAL and MON.

Figure 6. The cation carriers affect FOXO signaling pathways. (A) qRT-PCR (2 minus delta CT method) validation of changes in mRNA levels of selected genes, namely *SGK1* (left panel)

and *IL7R* (right panel), upon treatment with either SAL or MON for 12-18 h. **(B)** Western blotting analysis of both phosphorylated and total protein levels of AKT and FOXO1, as well as the total level of SGK1 kinase in Raji cells, pretreated with either SAL (0.25 and 0.5 μM), MON (0.05 and 0.1 μM) or vehicle (-) for 18 h. The level of GAPDH was used as a loading control. Western blotting images are presented in the top panel, while the quantification of phosphorylated AKT (p-AKT; Ser473 residue), phosphorylated FOXO1 (p-FOXO1; Ser256 residue) and SGK1 from 3-4 images are presented in the bottom panel.

Figure 7. The cation carriers affect MYC levels. (A) Downregulation of *MYC* mRNA upon 12 h of treatment with either SAL or MON, estimated by qRT-PCR (2 minus delta CT method). **(B)** Estimation of MYC protein levels by Western blotting analysis in both Raji cells and P493-6 lymphoblastoid cell line, pretreated with either SAL, MON, or vehicle (-) for 18 h. The level of GAPDH was used as a loading control. **(C)** The differential expression heatmap with RNA-seq data listing the genes regulated by MYC (according to GSEA analysis; hallmarks – MYC targets v1 and v2) and presents the fold change of their expression in Raji cells treated for 18 h with either SAL (0.5 μM) or MON (0.1 μM). The treatment with MON downregulated all the listed genes with statistical significance (q value <0.05), while the treatment with SAL decreased their expression, with the statistical significance reached for the *RPS10* gene only. **(D)** qRT-PCR validation of changes in the expression of known MYC target genes, namely *PLK1* (left panel), *TNFAIP3* (middle panel), and *PTPN6* (right panel) upon 18 h of treatment with either SAL, MON, or corresponding vehicle (Veh.). **(E)** Flow cytometry analysis of either intracellular level of MYC (left panel) or surface level of CD20 (right panel) in P493-6 cells expressing MYC under the control of Tet-off system. P493-6 cells were treated with either SAL, doxycycline (DOX, 0.1 μg/ml), or both for either 24 or 48 h (left and right panel, respectively). Additionally, the number of CD20 molecules per cell was quantified by comparison of anti-CD20-PE MFI to the fluorescence intensity of quantibrite beads labeled with the known number of PE molecules.

Figure 8. Derivatives of SAL unable to downregulate MYC are also unable to upregulate CD20. (A) Comparison of the changes in surface CD20 induced by increasing concentrations of either SAL or selected SAL derivatives (derivatives 1 and 5). Raji cells were treated with either vehicle (Veh.) at low (L), medium (M), or high (H) concentrations or SAL derivatives (conc. range 0.01-2.5 μM). The MFI values of anti-CD20-PE detected in the case of SAL derivativetreated cells were normalized to the MFI values corresponding to vehicle-treated cells and were presented as fold change. The chemical structures of SAL derivatives 1 and 5 are shown in the corresponding graphs, with modifications of the SAL structure marked in red and blue, respectively. **(B)** Western blotting analysis of MYC and SGK1 in Raji cells, pretreated with either SAL, its derivatives, or vehicle (-) for 18 h. Levels of MYC (graph in the middle) and SGK1 (right graph) were quantified from 3 experiments and presented as a fold change of protein levels in SAL- or derivatives-treated cells *versus* levels in vehicle-treated cells. **(C)** Western blotting analysis of MYC and SGK1 (left panel) in Raji cells nucleofected with RNP complexes consisting of sgRNA targeting either *MYC* (sgMYC) or *SGK1* (sgSGK1) and Cas9 nuclease followed by treatment with MON for 18 h. For the mock nucleofection, the RNPs lacked sgRNA. Forty-eight hours upon nucleofection, the MFI of CD20-PE (right panel) was quantified in Raji cells nucleofected with RNPs consisting of sgRNA targeting either *MYC* (sgMYC #1 and sgMYC #2) or *SGK1* (sgSGK1 #1 and sgSGK1 #2) and was normalized to MFI in mock-nucleofected cells. **(D)** Comparison of the upregulation of surface CD20 in Raji cells pretreated with either SAL, MYC inhibitor (10058-F4; 100-150 μM) or

corresponding vehicles for 48 h. **(E)** Results of the CUT&RUN protein-DNA binding assay show the binding of MYC to the *MS4A1* promoter in either vehicle- or SAL-treated Raji cells (18 h of the treatment). The RTPCR-amplified fragment of the *MS4A1* promoter (from -313 to -198).

Figure 1.

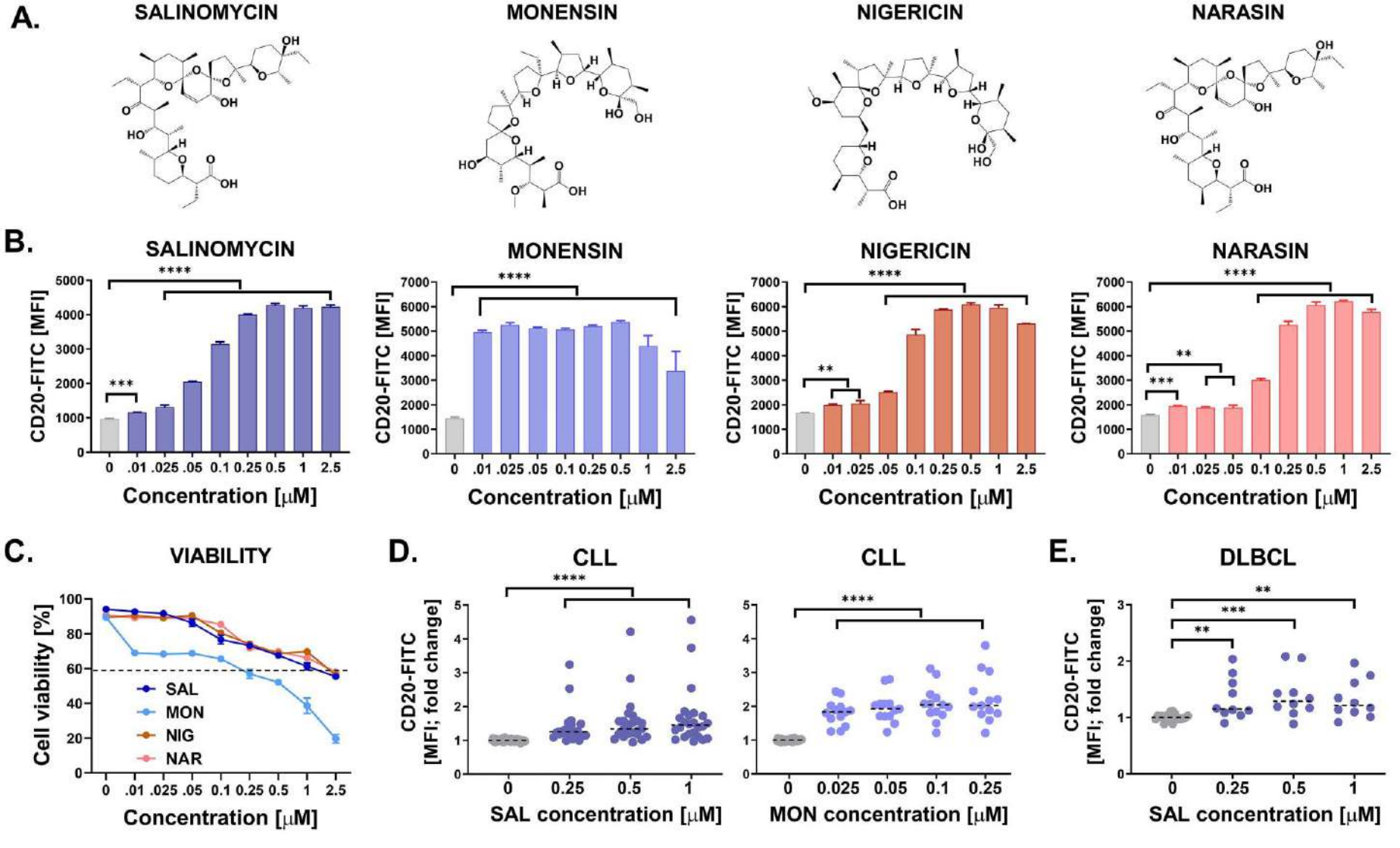
A.
SALINOMYCIN
MONENSIN
NIGERICIN
NARASIN
B.
SALINOMYCIN
MONENSIN
NIGERICIN
NARASIN
CD20-FITC [MFI]
Concentration [μM]
0 .01 .025 .05 0.1 0.25 0.5 1 2.5
C.
VIABILITY
Cell viability [%]
SAL
MON
NIG
NAR
Concentration [μM]
D.
CLL
CLL
CD20-FITC [MFI; fold change]
SAL concentration [μM]
MON concentration [μM]
E.
DLBCL
CD20-FITC [MFI; fold change]
SAL concentration [μM]

Figure 2.

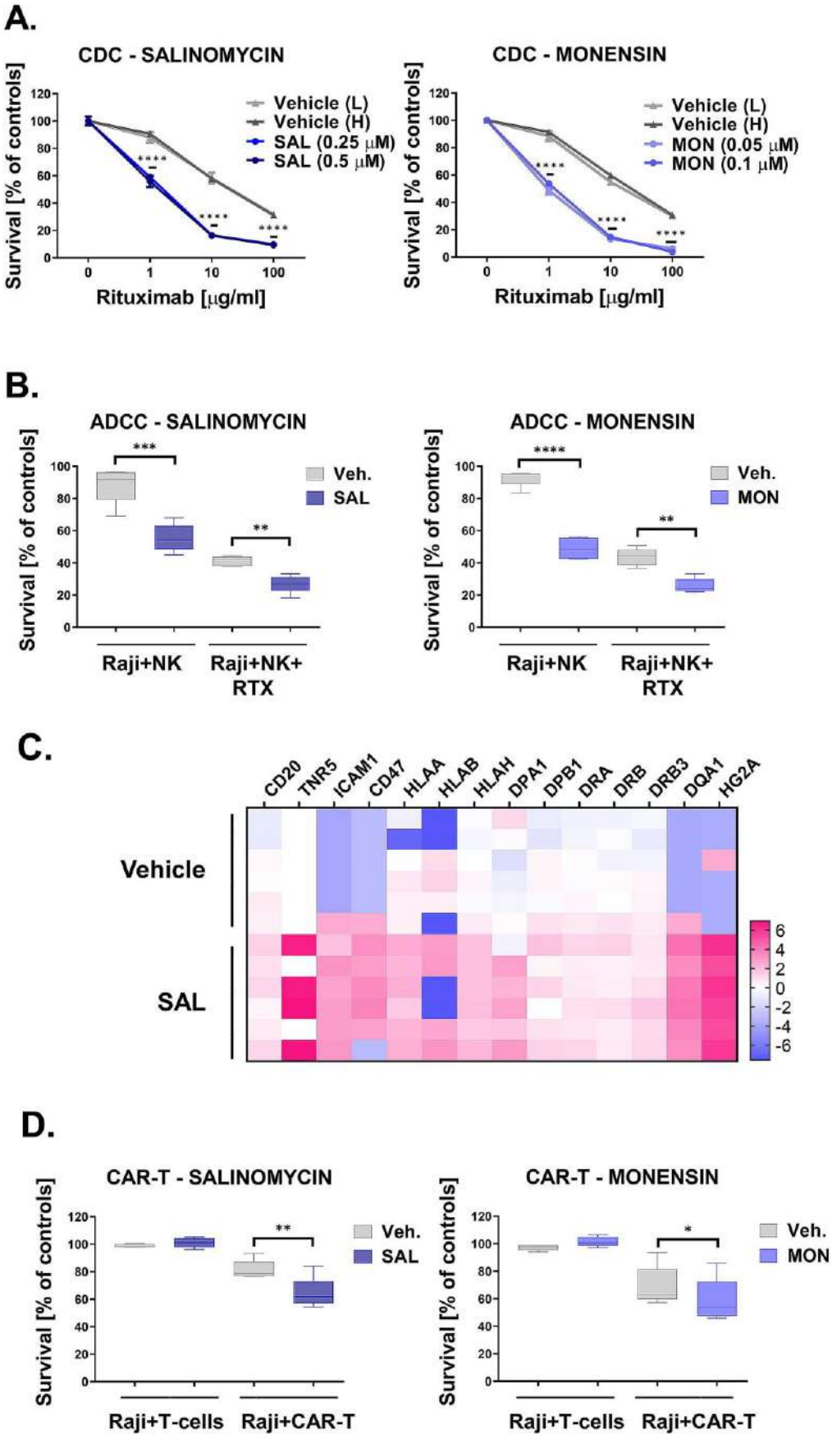
A.
CDC - SALINOMYCIN
Survival [% of controls]
Rituximab [μg/ml]
Vehicle (L)
Vehicle (H)
SAL (0.25 μM)
SAL (0.5 μM)
CDC - MONENSIN
MON (0.05 μM)
MON (0.1 μM)
B.
ADCC - SALINOMYCIN
Veh.
SAL
Raji+NK
Raji+NK+ RTX
ADCC - MONENSIN
MON
C.
CD20
TNR5
ICAM1
CD47
HLAA
HLAB
HLAH
DPA1
DPB1
DRA
DRB
DRB3
DQA1
HG2A
Vehicle
SAL
D.
CAR-T - SALINOMYCIN
Raji+T-cells
Raji+CAR-T
CAR-T - MONENSIN

Figure 3.

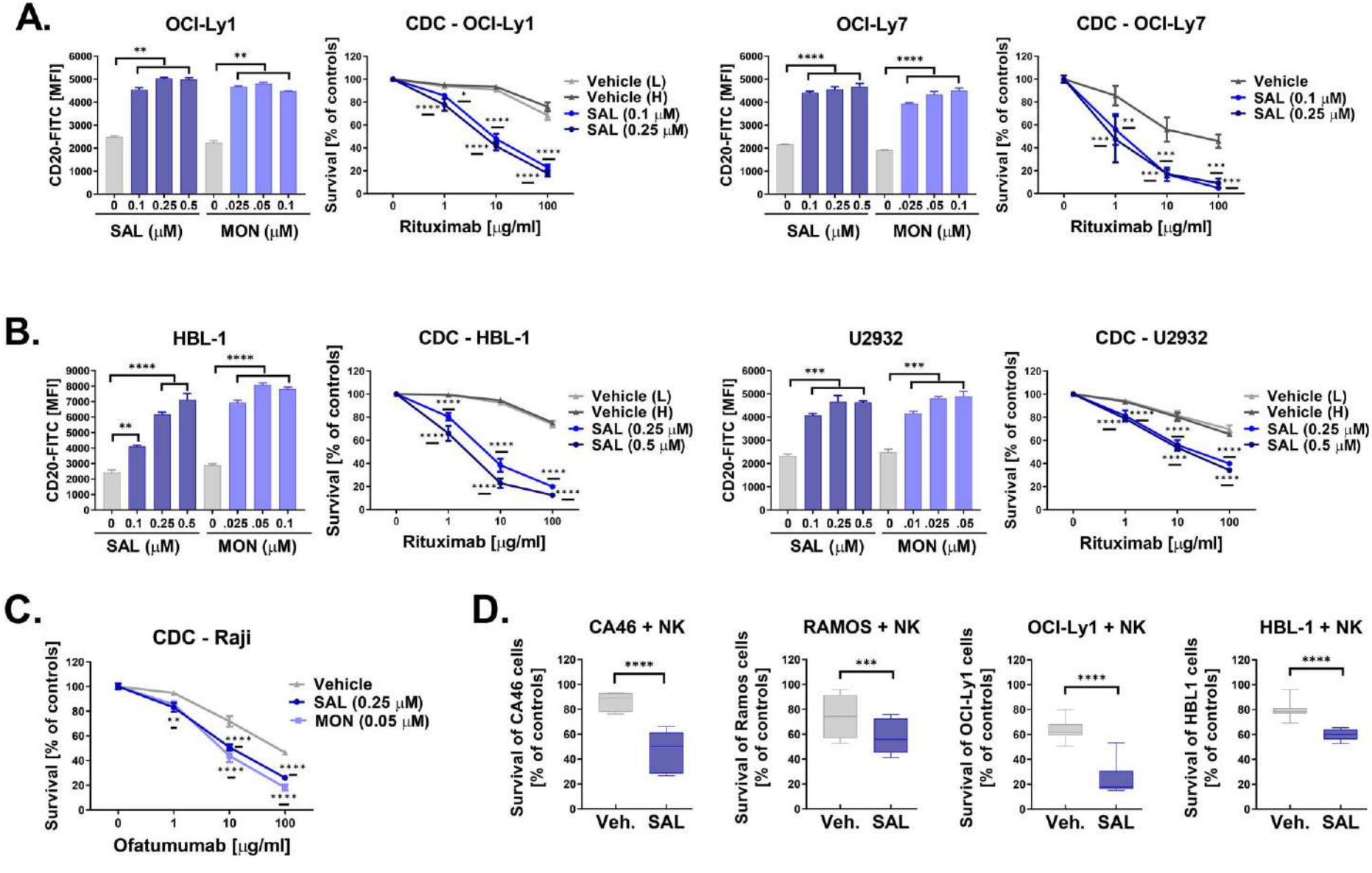
A.
OCI-Ly1
CD20-FITC [MFI]
SAL (μM)
MON (μM)
CDC - OCI-Ly1
Survival [% of controls]
Rituximab [μg/ml]
Vehicle (L)
Vehicle (H)
SAL (0.1 μM)
SAL (0.25 μM)
OCI-Ly7
CDC - OCI-Ly7
Vehicle
SAL (0.1 μM)
SAL (0.25 μM)
B.
HBL-1
CDC - HBL-1
SAL (0.25 μM)
SAL (0.5 μM)
U2932
CDC - U2932
C.
CDC - Raji
MON (0.05 μM)
Ofatumumab [μg/ml]
D.
CA46 + NK
Survival of CA46 cells [% of controls]
RAMOS + NK
Survival of Ramos cells [% of controls]
OCI-Ly1 + NK
Survival of OCI-Ly1 cells [% of controls]
HBL-1 + NK
Survival of HBL1 cells [% of controls]
Veh.
SAL

Figure 4.

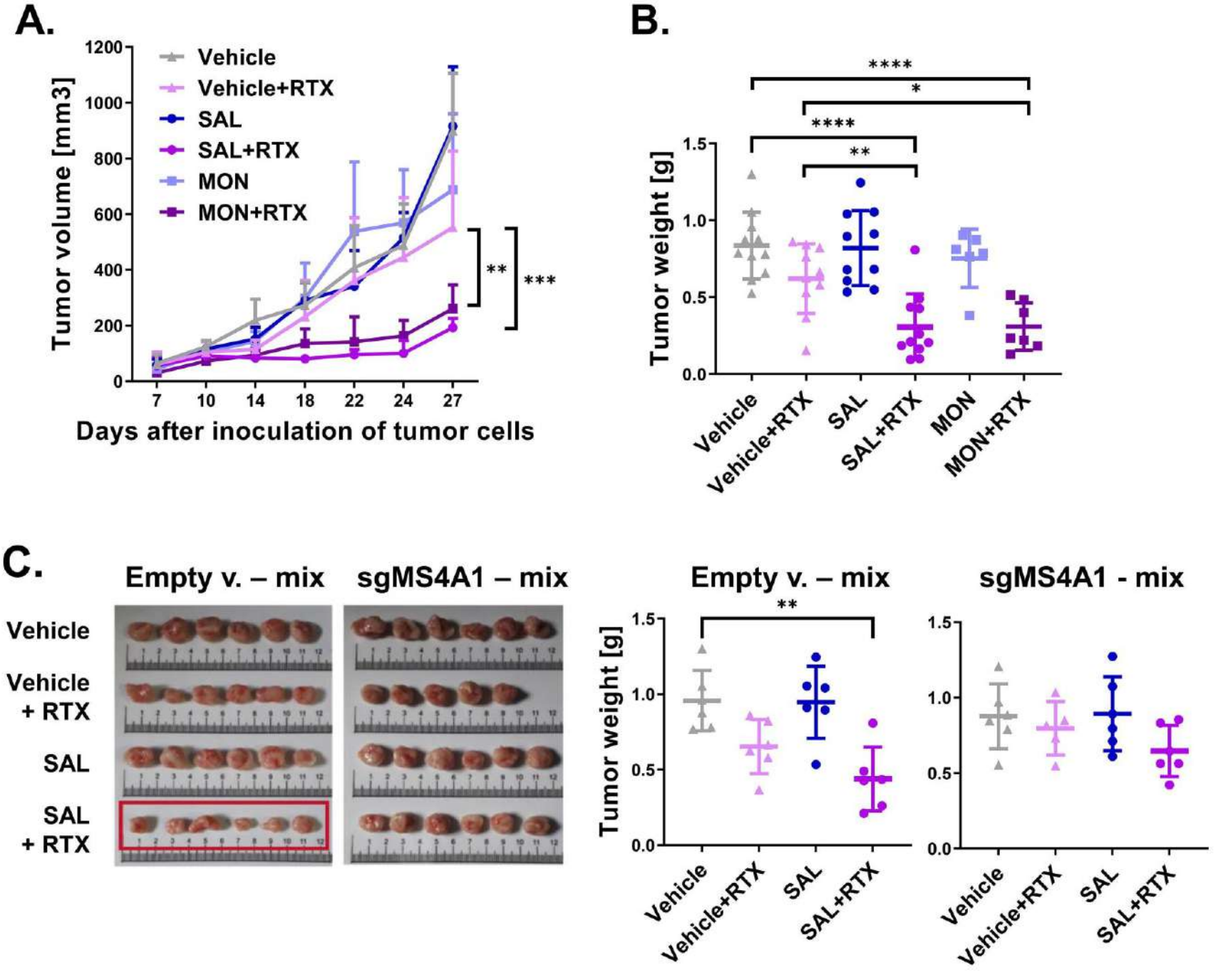
A.
Tumor volume [mm3]
1200
1000
800
600
400
200
0
Vehicle
Vehicle+RTX
SAL
SAL+RTX
MON
MON+RTX
**
***
7
10
14
18
22
24
27
Days after inoculation of tumor cells
B.
Tumor weight [g]
1.5
1.0
0.5
0.0
****
*
****
**
Vehicle
Vehicle+RTX
SAL
SAL+RTX
MON
MON+RTX
C.
Empty v. – mix
sgMS4A1 – mix
Vehicle
Vehicle + RTX
SAL
SAL + RTX
Empty v. – mix
sgMS4A1 - mix
Tumor weight [g]
**
Vehicle
Vehicle+RTX
SAL
SAL+RTX

Figure 5.

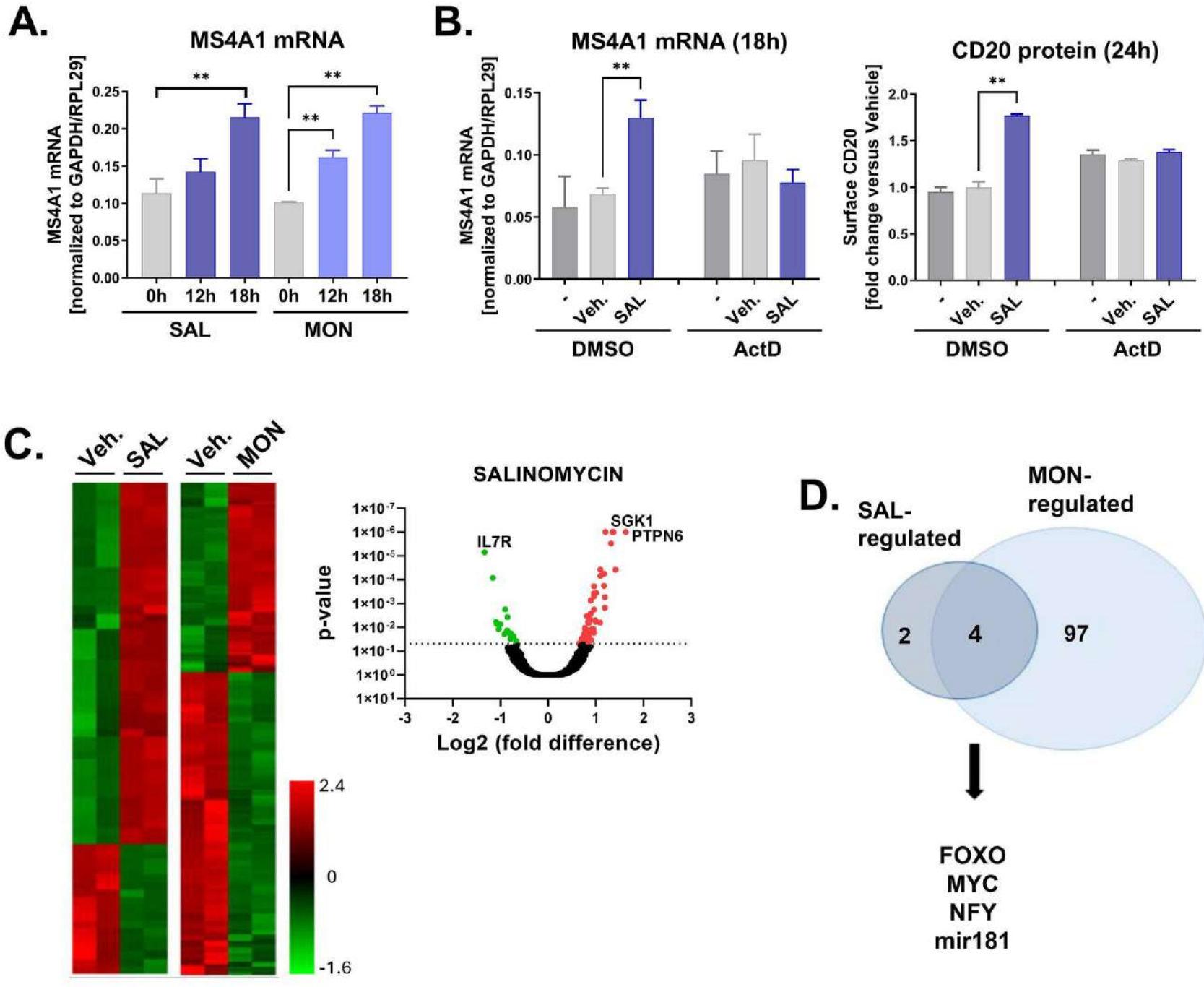
A.
MS4A1 mRNA
MS4A1 mRNA [normalized to GAPDH/RPL29]
0.25
0.20
0.15
0.10
0.05
0.00
**
**
**
0h 12h 18h 0h 12h 18h
SAL
MON
B.
MS4A1 mRNA (18h)
MS4A1 mRNA [normalized to GAPDH/RPL29]
0.15
0.10
0.05
0.00
**
-
Veh.
SAL
DMSO
ActD
CD20 protein (24h)
Surface CD20 [fold change versus Vehicle]
2.0
1.5
1.0
0.5
0.0
**
C.
Veh.
SAL
Veh.
MON
2.4
0
-1.6
SALINOMYCIN
p-value
1×10-7
1×10-6
1×10-5
1×10-4
1×10-3
1×10-2
1×10-1
1×100
1×101
IL7R
SGK1
PTPN6
-3 -2 -1 0 1 2 3
Log2 (fold difference)
D.
SAL-regulated
MON-regulated
2
4
97
FOXO
MYC
NFY
mir181

Figure 6.

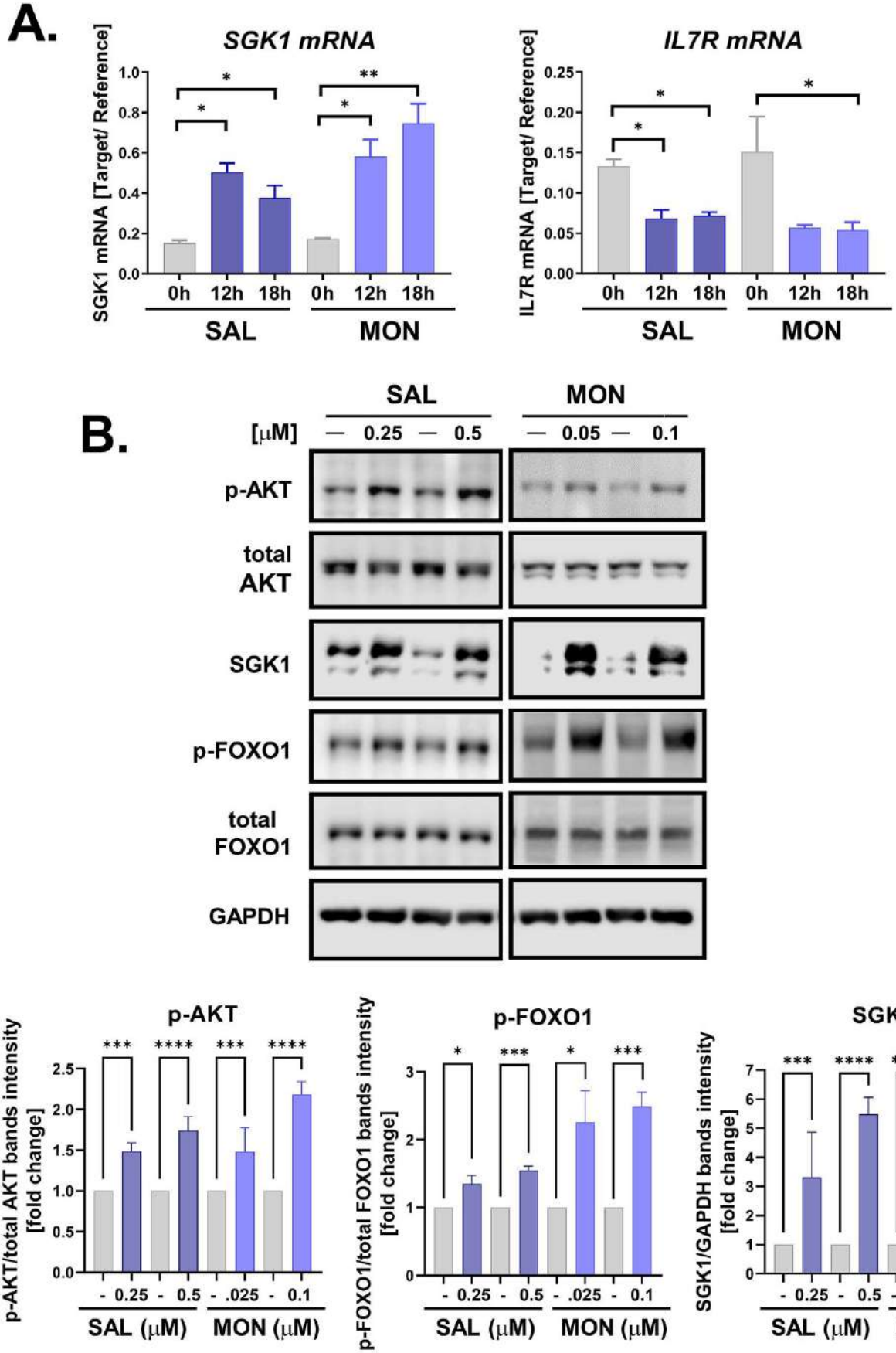
A.
SGK1 mRNA
SGK1 mRNA [Target/ Reference]
0h 12h 18h 0h 12h 18h
SAL MON
IL7R mRNA
IL7R mRNA [Target/ Reference]
0h 12h 18h 0h 12h 18h
SAL MON
B.
SAL MON
[μM] — 0.25 — 0.5 — 0.05 — 0.1
p-AKT
total AKT
SGK1
p-FOXO1
total FOXO1
GAPDH
p-AKT
p-AKT/total AKT bands intensity [fold change]
- 0.25 - 0.5 - .025 - 0.1
SAL (μM) MON (μM)
p-FOXO1
p-FOXO1/total FOXO1 bands intensity [fold change]
- 0.25 - 0.5 - .025 - 0.1
SAL (μM) MON (μM)
SGK1
SGK1/GAPDH bands intensity [fold change]
- 0.25 - 0.5 - .025 - 0.1
SAL (μM) MON (μM)

Figure 7.

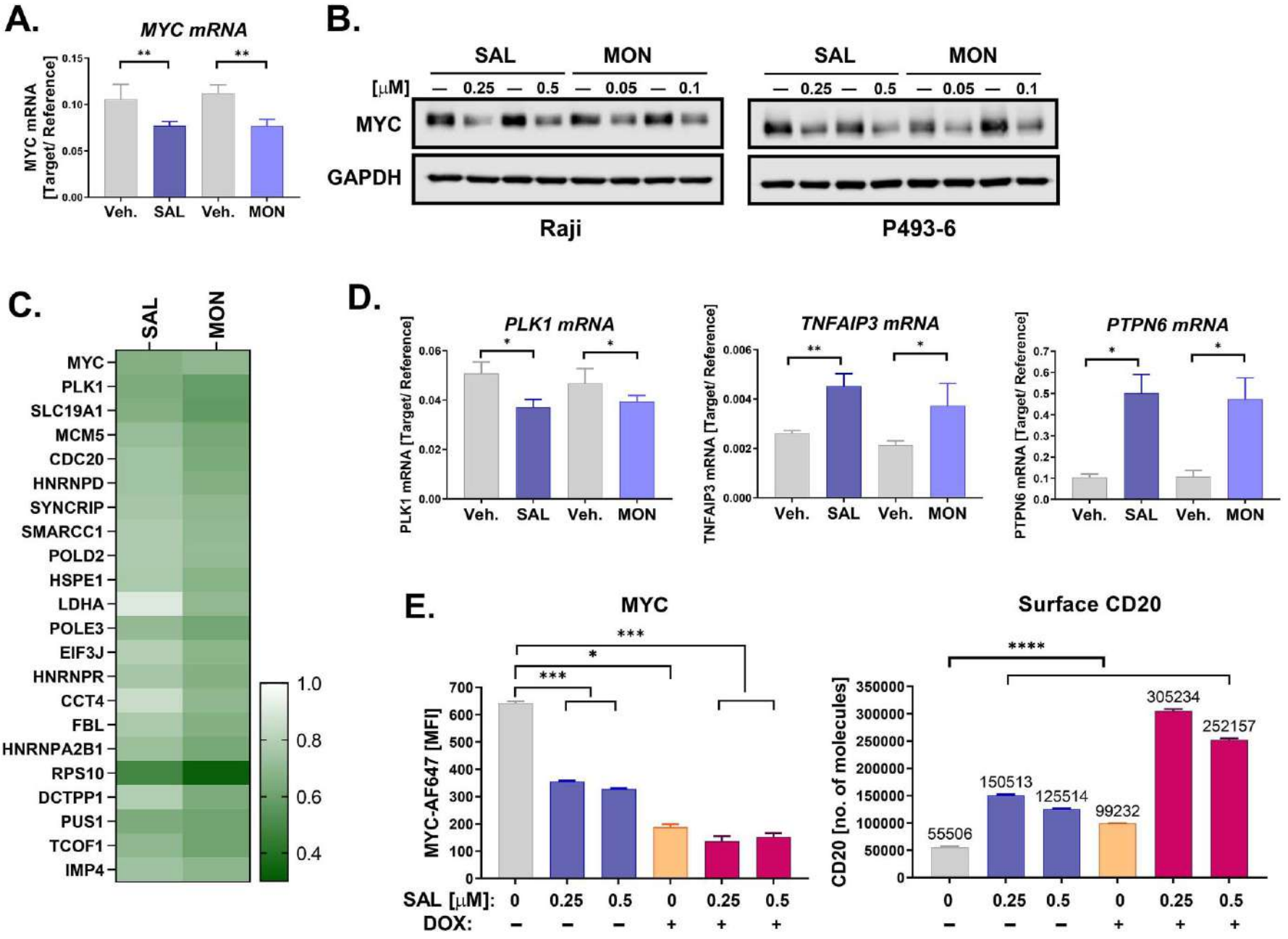
A.
MYC mRNA
MYC mRNA [Target/ Reference]
Veh.
SAL
Veh.
MON
B.
SAL
MON
[μM]
0.25
0.5
0.05
0.1
MYC
GAPDH
Raji
P493-6
C.
SAL
MON
MYC
PLK1
SLC19A1
MCM5
CDC20
HNRNPD
SYNCRIP
SMARCC1
POLD2
HSPE1
LDHA
POLE3
EIF3J
HNRNPR
CCT4
FBL
HNRNPA2B1
RPS10
DCTPP1
PUS1
TCOF1
IMP4
D.
PLK1 mRNA
PLK1 mRNA [Target/ Reference]
TNFAIP3 mRNA
TNFAIP3 mRNA [Target/ Reference]
PTPN6 mRNA
PTPN6 mRNA [Target/ Reference]
E.
MYC
MYC-AF647 [MFI]
SAL [μM]:
DOX:
Surface CD20
CD20 [no. of molecules]
55506
150513
125514
99232
305234
252157

Figure 8.

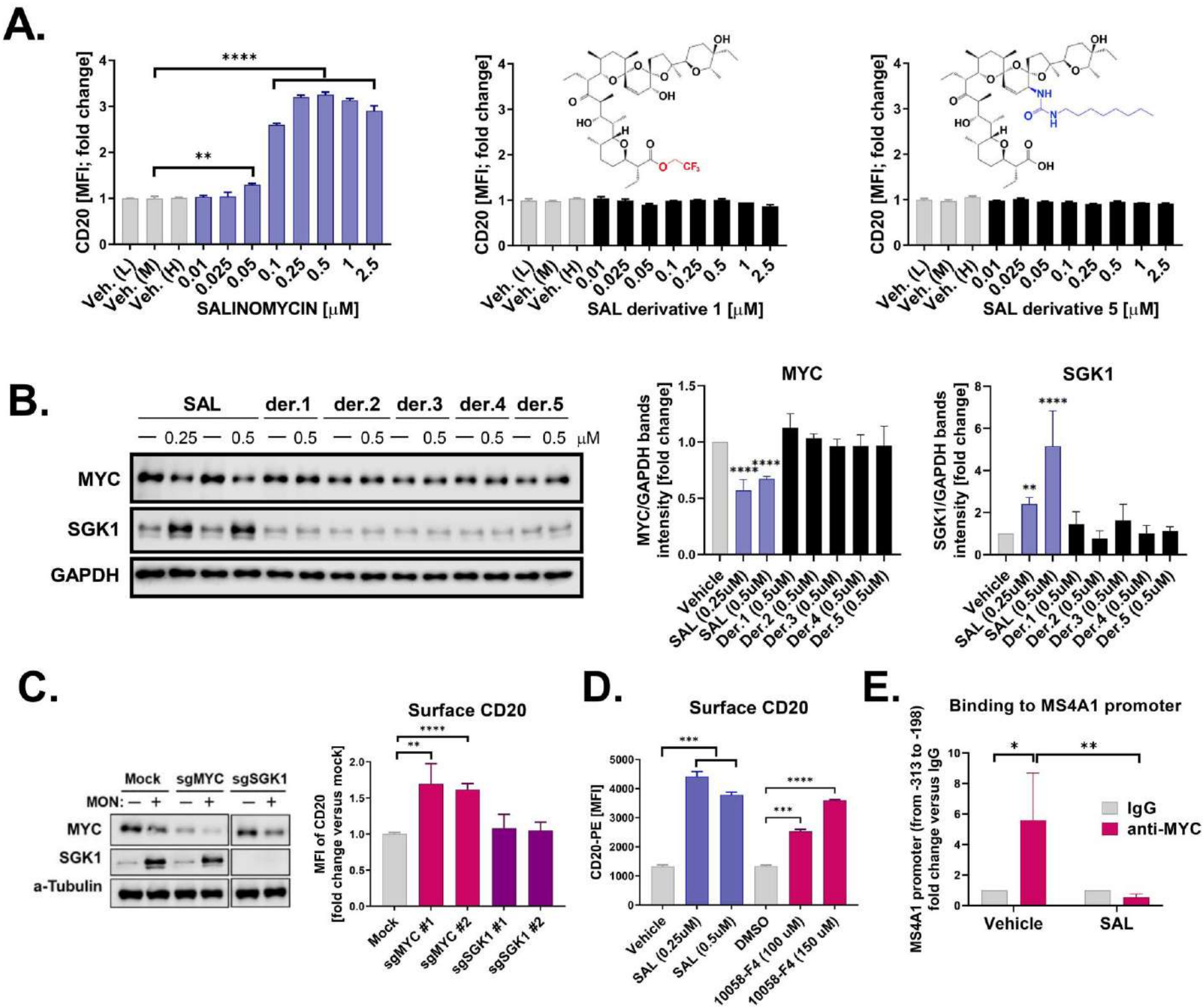
A.
CD20 [MFI; fold change]
SALINOMYCIN [μM]
SAL derivative 1 [μM]
SAL derivative 5 [μM]
Veh. (L)
Veh. (M)
Veh. (H)
0.01
0.025
0.05
0.1
0.25
0.5
1
2.5
B.
SAL
der.1
der.2
der.3
der.4
der.5
0.25
0.5
μM
MYC
SGK1
GAPDH
MYC/GAPDH bands intensity [fold change]
SGK1/GAPDH bands intensity [fold change]
Vehicle
SAL (0.25uM)
SAL (0.5uM)
Der.1 (0.5uM)
Der.2 (0.5uM)
Der.3 (0.5uM)
Der.4 (0.5uM)
Der.5 (0.5uM)
C.
Mock
sgMYC
sgSGK1
MON:
a-Tubulin
Surface CD20
MFI of CD20 [fold change versus mock]
sgMYC #1
sgMYC #2
sgSGK1 #1
sgSGK1 #2
D.
Surface CD20
CD20-PE [MFI]
DMSO
10058-F4 (100 uM)
10058-F4 (150 uM)
E.
Binding to MS4A1 promoter
MS4A1 promoter (from -313 to -198) fold change versus IgG
IgG
anti-MYC

Supplementary Methods

B-cell lymphoma cell lines and chemicals

The cell lines and media used in the study are listed in Suppl. Table 1 below. Appropriate media were supplemented with 10% fetal bovine serum (Fisher Scientific, cat. # SH3007203), penicillin (100 units/ml), and streptomycin (100 µg/ml). All cell lines were regularly tested negative for mycoplasma contamination.

Suppl. Table 1. Cell lines used in the study.

Cell line	**Medium**
Burkitt lymphoma cell lines: Raji (RRID:CVCL_0511), CA46 (RRID:CVCL_1101), Daudi (RRID:CVCL_0008), Ramos (RRID:CVCL_0597), and BL41 (RRID:CVCL_1087)	RPMI 1640 (Corning, cat. # 10-040-CVR) with 10% FBS
DLBCL cell lines: OCI-Ly1 (RRID:CVCL_1879), OCILy7 (RRID:CVCL_1881), HBL-1 (RRID:CVCL_4213), and U2932 (RRID:CVCL_1896) (kindly provided by Prof. M.A. Shipp)	IMDM (Thermo Fisher Scientific, cat # 31980030) with 10% FBS
P493-6 lymphoblastoid cell line (RRID:CVCL_6783)	RPMI-1640 with 10% tetsystem approved FBS (Thermo Fisher Scientific, cat. # A4736201)
HEK 293T (RRID:CVCL_0063)	DMEM (Corning, cat. # 10013-CVR) with 10% FBS

The *MYC* translocation status in the Burkitt lymphoma and DLBCL cell lines used in this study is presented in Suppl. Table 2 below.

Suppl. Table 2. *MYC* gene rearrangement status in cell lines used in the study.

Cell line	**MYC rearrangement**	**Source**
Raji	Yes/ t(8;14)	Taub et al., 1982 [1]; Li et al., 2019 [2]
CA46	Yes/ t(8;14)	Showe et al., 1985 [3]; Khaira et al., 1998 [4]
Daudi	Yes/ t(8;14)	Veronese et al., 1995 [5]
Ramos	Yes/ t(8;14)	Wiman et al., 1984 [6]; Li et al., 2019 [2]
BL41	Yes/ t(8;14)	Torsteinsdottir et al., 1989 [7]
OCI-Ly1	Gene amplification	Mehra et al., 2002 [8]; Li et al., 2019 [2]

OCI-Ly7	Rearrangement 8q24.21	Chang et al., 1995 [9]; Mehra et al., 2002 [8]; Dharanipragada & Parekh, 2023 [10]
HBL-1	No	Li et al., 2019 [2]
U2932	No	Li et al., 2019 [2]

Cation carriers were purchased from Sigma-Aldrich as sodium salts. Salinomycin (SAL; cat. # S4526), monensin (MON; cat. # M5273), narasin (NAR; cat. # N1271), nigericin (NIG; cat. # N7143), and lasalocid A (cat. # 73996) were dissolved either in methanol or ethanol, while A23187 (cat. # C7522) and ionomycin calcium salt (cat. # I0634) were dissolved in DMSO. MYC inhibitor (10058-F4; cat. # S7153), SGK1 inhibitor (EMD638683; cat. # S8824) and NLRP3 inhibitor (MCC950; cat. # S8930) were purchased from Selleckchem and dissolved in DMSO. Rituximab (RTX) was purchased from Roche, while Ofatumumab (OFA; cat. # ICH4027) was purchased from Ichorbio. Propidium iodide (PI; Sigma-Aldrich, cat. # P4170) and puromycin dihydrochloride (Thermo Fisher Scientific, cat. # A111380) were dissolved in water. Carboxyfluorescein succinimidyl ester (CFSE; eBioscience, cat. # 65-0850-84) and actinomycin D (Sigma-Aldrich, cat. # A9415) were dissolved in DMSO.

Staining of cells for flow cytometry

For flow cytometry analysis of cell surface antigens, 2-3×10^5 cells were incubated with saturating amounts of the following antibodies recognizing human antigens: anti-CD20 (BD Biosciences, clone L27, cat. # 345792 and 345793), anti-CD19-APC (BD Pharmingen, cat. # 555415), antiCD40-PE (Thermo Fisher Scientific, cat. # MA1-19776), anti-CD46-FITC (BD Biosciences, cat. # 555949), anti-CD47-PE/Cy7 (eBioscience, cat. # 25-0479-42), anti-CD54-PE (BD Pharmingen, cat. # 555511), anti-CD55-FITC (BD Biosciences, cat. # 555693), anti-CD80-PE/Cy5 (BioLegend, cat. # 305209), anti-CD86-PE (BioLegend, cat. # 305405), anti-CD155-APC (BioLegend, cat. # 337617), anti-HLA-ABC-PE (eBioscience, cat. # 12-9983-42), antiULBP2/5/6-BV421 (BD OptiBuild, cat. # 748128). The corresponding fluorochrome-conjugated IgG1 (Becton Dickinson) was used as isotype control. After 30 min incubation at 4°C, washing with PBS, and staining with either propidium iodide (PI, 4 µg/ml) or Zombie-NIR Dye (BioLegend, cat. # 423106), the cells were acquired using either FACS Canto II, FACS Verse (Becton Dickinson), CytoFLEX (Beckman Coulter) or CellStream (Cytek Biosciences) cytometers. The mean fluorescence intensity (MFI) of Zombie-NIR-negative or PI-negative cells served as a measure for Ab binding on a per-cell basis. To quantify the number of CD20 molecules on Raji and P493-6 cells, the beads labeled with the known number of PE molecules (BD Quantibrite PE Phycoerythrin Fluorescence Quantitation Kit; BD Biosciences, cat. # 340495) were acquired in the same experiments as anti-CD20-PE-stained cells, and the number of CD20 molecules was calculated according to the manufacturer's recommendations. For flow cytometry data visualization, some plots were generated using the FlowJo software (BD, FlowJo v10.7.1). The intracellular staining of MYC was performed with an anti-MYC-AF647 antibody (Abcam, cat. # 190560), using the True-Nuclear™ Transcription Factor Buffer Set (BioLegend, cat. # 424401), according to the manufacturer's recommendations.

The anti-CD20 CAR expression was detected by the staining of transduced T cells with the recombinant biotinylated Protein L (2 µg/ml; Thermo Fisher Scientific, cat. # 29997) followed by

incubation with Streptavidin-PE (1 μg/ml; eBioscience, cat. # 12-4317-87) and analysis of the percentage of PE-positive cells.

Human DLBCL patient samples

The diffuse large B cell lymphoma (DLBCL) cases were routinely diagnosed at the Maria Sklodowska-Curie National Research Institute of Oncology in Warsaw, Poland. The diagnosis of DLBCL, NOS, FL G3B and DLBCL/HGBL/DH-BCL2+ were established according to the WHOHAEM5, based on histopathologic/immunohistochemical examination, with flow-cytometry analysis (FCM), classical cytogenetics (CC), including karyotyping and fluorescence in situ hybridization (FISH), material obtained by fine needle aspiration biopsy (FNAB). DLBCL samples, verified by FCM and CC, were also obtained by FNAB of lymph nodes or extranodal lesions as previously described [11]. The diagnostic algorithm for detecting *MYC* gene rearrangement by FCM (CD38 overexpression on lymphoma cells), classical cytogenetic methods, and material obtained using FNAB have been described previously [11]. Suppl. Table 3 presents the status of MYC translocations in primary DLBCL cells.

Suppl. Table 3. MYC translocation status in DLBCL samples used in the study.

Diagnosis Nodal (N) vs. extranodal (E)	**GCB vs. Non-GCB**	**Site of FNAB/FCM/ CC**	***MYC*R by CD38 FCM overexpression**	***MYC*R by CC (FISH and karyotyping)**
(N) DLBCL, NOS/FL G3B	GCB	cLN	yes	yes
(N) DLBCL, NOS	GCB	ingLN	no	no
(E) DLBCL, NOS	GCB	TG	no	no
(N) DLBCL, NOS	non-GCB	abLN	no	no
(N) DLBCL, NOS	non-GCB	cLN	no	no
(N) DLBCL, NOS	GCB and non-GCB	axLN	no	no
(N/E) DLBCL, NOS	GCB	cLN	no	no
(N) DLBCL, NOS	non-GCB	axLN	no	no
(N) DLBCL, NOS	GCB	cLN	no	no
(N) DLBCL/HGBL/DH-BCL2+	GCB	cLN	yes	yes

Diagnosis: DLBCL, NOS – Diffuse Large B-cell Lymphoma, not otherwise specified, FL G3B, – Follicular lymphoma, high-grade G3B, DLBCL/HGBL/DH-BCL2+ – Diffuse large B-cell Lymphoma / High-grade B-cell lymphoma with *MYC* and *BCL2* double hit rearrangements. The cell of origin: GCB – Germinal Center B-cell-like; non-GCB – non-Germinal Center B-celllike; GCB and non-GCB – intermediate between GCB and non-GCB.
Site of FANB/FCM/CC – site of fine needle aspiration biopsy (FNAB) for flow cytometry (FCM) and classical cytogenetic (CC) analysis, LN – Lymph Node: c, cervical, ing, inguinal, ax, axillary; ab – abdominal; TG – thyroid gland.
*MYC*R – *MYC* gene rearrangement; FISH – Fluorescence In Situ Hybridization.

Complement-dependent cytotoxicity (CDC) assays

CDC assays were performed with therapeutic anti-CD20 antibodies, either RTX or OFA. Cells (1×10^5) were seeded into a 96-well plate in FBS-free RPMI 1640 medium. RTX or OFA (working concentration range 1-100 μg/ml) and human AB serum (as a source of complement; 10% final conc.) were added to cells. After a 1-h incubation, PI (final conc. 4 μg/ml) was added, and cell viability was analyzed using the flow cytometry and presented as a percentage of controls (cells treated with cation carriers but not incubated with the therapeutic antibody).

Western blotting

The whole-cell protein extracts were prepared by lysing cells with a buffer containing 1% Triton X-100, 50 mM HEPES (pH 7.4), 150 mM NaCl, 5 mM EDTA, and 10% glycerol supplemented freshly with phosphatase and protease inhibitor cocktails. Protein concentration was measured with Pierce BCA Protein Assay Kit (Thermo Fisher Scientific). Samples of 1-25 μg total protein were subjected to SDS-PAGE. Resolved proteins were transferred to nitrocellulose membrane (Whatman), probed with specific antibodies, and detected with the Odyssey imaging system (LICOR Biosciences). The following primary antibodies were used: anti-AKT (pan, clone 40D4), anti-phospho-AKT (Ser473, clone D9E), anti-FOXO1 (clone C29H4), anti-phospho-FOXO1 (Ser256, polyclonal), anti-MYC (clone D84C12), and anti-SGK1 (clone D27C11), all from Cell Signaling Technology. Anti-CD20 (polyclonal) Ab was purchased from Abcam. For equal loading control, the blots were re-probed with either anti-□-tubulin (clone 11H10, Cell Signaling Technology), anti-β-tubulin (clone D-10), or anti-GAPDH (clone 0411), both from Santa Cruz Biotechnology. After the overnight incubation at 4°C either in the presence of 5% BSA or 5% nonfat dry milk, the secondary HRP-conjugated anti-mouse or anti-rabbit IgG antibodies (Jackson ImmunoResearch) were applied for 1 h. The chemiluminescence reaction for HRP was developed using the luminol-based chemiluminescence reagent Super Signal West Femto Substrate (Thermo Fisher Scientific, cat. # 34095) and visualized with Odyssey Fc (Li-COR). Densitometric analysis of CD20, phospho-AKT, phospho-FOXO1, MYC, and SGK1 was performed using the Image Studio Software.

RNA-seq and bioinformatics analysis

RNA was isolated from Raji cells pretreated with SAL (0.5 μM), MON (0.1 μM), or corresponding vehicle (in two biological replicates each) for 18 h using a High Pure RNA Isolation Kit (Roche). The quality of samples was initially checked on 1% agarose gel. Further sample quantity, purity and integrity assessment with the Agilent TapeStation system, RNA-seq library preparation with TruSeq Stranded mRNA Library kit (Illumina), library normalization, sequencing with HiSeq XTen platform in a PE 2x150bp format, with at least 10 million reads and bioinformatics analysis (mapping, alignment, differential expression) were commercially provided by Omega Bioservices. The reference genome UCSC hg19, the BamStats summary method, Isis analysis software (version 2.6.25.19), BEDTools (version 2.17.0), Picard (version 1.128), and DESeq2 (version 1.6.3) were used. The annotation gene count was 26,364, while the assessed gene count was 10,280. The differential expression analysis (with q value cut-off <0.05) was accessed through Illumina's Basespace webportal (https://basespace.illumina.com/). Additionally, the prediction of transcription factor/miRNA binding sites in the regulatory elements of the differentially expressed target genes has been performed to select these

transcription factors and miRNAs, whose activity was commonly changed by both SAL and MON (GSEA/MSigDB website v6.3).

Quantitative Real-time PCR

Total RNA was isolated with a High Pure Isolation Kit (Roche, cat. # 11828665001). For cDNA synthesis, random nonamers (cat. # R7647), oligo(dT)$_{23}$ primers (cat. # O4387), and M-MLV reverse transcriptase (cat. # M1302) were purchased from Sigma-Aldrich and used according to the manufacturer's instructions. LightCycler 480 II thermocycler (Roche) was used to run quantitative PCR with LightCycler® Fast Start DNA Master PLUS SYBRGreen I (Roche, cat. # 03515869001) and specific intron-spanning primers (Suppl. Table 4 below).

Suppl. Table 4. Primers used in qRT-PCR

Target	**Forward primer**	**Reverse primer**
MS4A1	GAATGGGCTCTTCCACATTGCC	TCTCCGTTGCTGCCAGGAGT
MS4A1 (variant 1specific)	GGCCTTGGAGACTCAGATCC	TGTCAGTCTCTTCCCCACAGA
MS4A1 (variant 3specific)	CCTTGGAGACTCAGGAGTTTTG	AGGGCCTTTCATTGGCTCTG
PTPN6	TTGACCACAGCCGAGTGATCCT	CTGGCGATGTAGGTCTTAGCGT
IL7R	ATCGCAGCACTCACTGACCTGT	TCAGGCACTTTACCTCCACGAG
SGK1	GGGAGCTGTCTTGTATGAGATG	TGGAGAGGCTTGTTCAGAATG
PLK1	TTCCTGAATGAAGATCTGGAG	AACAAGGTATACATGATACACC
TNFAIP3	GCGAGCGAGCCCGAC	TTGTGCTCTCCAACACCTCTC
GAPDH	GTCTCCTCTGACTTCAACAGCG	ACCACCCTGTTGCTGTAGCCAA
RPL29	CAGCTCAGGCTCCCAAAC	GCACCAGTCCTTCTGTCCTC

Analysis was performed using the relative quantification (RQ) method and normalization *versus* endogenous controls: *GAPDH* and *RPL29* (2 minus delta CT method).
The FAM-labelled TaqMan gene expression assays (Thermo Fisher Scientific, cat. # 4331182) were used for quantification of the following mRNAs: *MS4A1* (assay ID: Hs00544819_m1), *MYC* (assay ID: Hs00905030_m1), *GAPDH* (assay ID: Hs02786624_g), and *RPL29* (assay ID: Hs00988959_g). The qRT-PCR reactions were performed according to the manufacturer's recommendations using the TaqMan Fast Advanced Master Mix (Thermo Fisher Scientific, cat. # 4444557).

Quantification of DNA binding of MYC

The nuclear lysates were isolated from Raji cells treated for 12-18 h with either SAL, MON, or corresponding vehicles using the Nuclear Extract Kit (Active Motif, cat. # 40010). Five μg of proteins from the nuclear extract were then applied to TransAM c-Myc ELISA (Active Motif, cat. # 43396) to estimate the binding of MYC to its target DNA motif, according to the manufacturer's recommendations. The results were quantified by measuring the optical density (OD) at 450 nm.

CUT&RUN MYC-DNA interaction assay

Raji cells (2.5×10^5/sample) were treated with either SAL (0.25 μM) or the corresponding vehicle for 18 h. Cells were fixed with 0.1% formaldehyde and immobilized on Concanavalin A-coated magnetic beads according to the manufacturer's recommendations (CUT&RUN Assay Kit; Cell Signaling, cat. # 86652). Next, digitonin-permeabilized cells were incubated with either ChIPgrade anti-MYC antibody (Abcam, cat. # ab32072; clone Y69) or control rabbit IgG overnight at 4°C with rotation. The chromatin fragmented by the MNase enzyme was then purified with DNA Purification Spin Columns (Cell Signaling, cat. # 14209). The qRT-PCR was next run with the pair of the following primers specific to the sequence in MS4A1 promoter: forward – 5'AGTGAAGCCAGAAGGTAAAAGT-3'; reverse – 5'-GCTACCTTAATTAGAAGAACTTC-3' to quantify the MYC binding.

Analysis of cell cycle

For cell cycle analysis, Raji cells were plated in a 24-well plate (1.5×10^5 cells/well) and treated with either SAL (0.25 or 0.5 μM), MON (0.05 or 0.1 μM), or the corresponding vehicles. At 24 or 48 h after the treatment, cells were centrifuged and resuspended in ice-cold 70% ethanol. After the overnight fixation at 4°C, the cells were treated with PI/RNase Staining Buffer (BD Pharmingen, cat. # 550825) for 30 min. The DNA content was evaluated by flow cytometry according to the manufacturer's recommendations.

Animal studies

For all experiments, 6-8 week-old Fox Chase SCID females (CB17/Icr-Prkdc^{scid}/IcrIcoCrl) were obtained from Charles River Laboratories. Mice were inoculated subcutaneously with 3×10^6 Raji cells in 50% Matrigel (Corning, cat. # 356231) and randomly assigned to experimental groups. Mice were intraperitoneally (i.p.) treated with either SAL (2.5 mg/kg), MON (1 mg/kg), or a corresponding volume of DMSO every second day starting on day 5, while rituximab (10 mg/kg) was applied every second day starting on day 9 after inoculation of tumor cells. Tumor volume was calculated using the formula (L×W×W)/2, where L corresponds to tumor length while W corresponds to tumor width. Mice were sacrificed on days 30-32, and the tumors were isolated and weighed. All *in vivo* experiments followed the guidelines and were approved by the local Ethics Committee.

Synthesis of SAL derivatives

General procedures

All reagents and solvents used to synthesize SAL derivatives were obtained from Merck or Trimen Chemicals. CD_3CN, CD_2Cl_2, and CD_6 spectral grades solvents were stored over 3Å molecular sieves for several days. Reaction mixtures were stirred using Teflon-coated magnetic stir bars and were monitored by thin-layer chromatography (TLC) using aluminum-backed plates (Merck $60F_{254}$). TLC plates were visualized by UV light (254 nm), followed by treatment with phosphomolybdic acid (PMA, 5% in absolute EtOH) and gentle heating. Products of the reactions were purified using CombiFlash®Rf+ Lumen Flash Chromatography System (Teledyne Isco) with integrated ELS and UV detectors and Electrospray Ionization (ESI) mass spectroscopy. All solvents used in flash chromatography were of HPLC grade. Solvents were removed using a rotary evaporator.

NMR spectra were recorded on a Varian 400 (^{1}H NMR at 403 MHz, ^{13}C NMR at 101 MHz, ^{19}F 379 MHz) magnetic resonance spectrometer. ^{1}H NMR spectra are reported in chemical shifts downfield from TMS using the respective residual solvent peak as internal standard (C_6D_6 δ 7.15 ppm; CD_2Cl_2 δ 5.32 ppm; $CDCl_3$ δ 7.26 ppm) ^{1}H NMR spectra are reported as follows: chemical shift (δ, ppm), multiplicity (s = singlet, d = doublet, q = quartet, dd = doublet of doublets, dt = doublet of triplets, dq = doublet of quartets, ddd = doublet of doublet of doublets, ddt = doublet of doublet of triplets, dddd = doublet of doublet of doublet of doublets, m = multiplet), coupling constant(s) in Hz, and integration. Significant peaks are reported within the overlapping ~2.00–0.50 ppm region of the ^{1}H NMR spectra. The ^{13}C NMR spectra are reported in chemical shifts downfield from TMS using the respective residual solvent peak as internal standard (C_6D_6 δ 128.62 ppm; CD_2Cl_2 δ 53.84 ppm; $CDCl_3$ δ 77.36 ppm). Line broadening parameters were 0.5 or 1.0 Hz, while the error of chemical shift value was 0.1 ppm. The ^{31}P NMR spectra are reported in chemical shifts. The electrospray ionization (ESI) high-resolution mass spectra were recorded on a QTOF (Impact HD, Bruker Daltonics) mass spectrometer in the positive ion detection mode. Samples were prepared in dry acetonitrile. The mass range for ESI experiments was from m/z = 400 to m/z = 1300.

SAL was isolated as sodium salt from commercially available veterinary premix SACOX®, using the procedure described previously [12]. After that, the isolated sodium salt of **SAL** was dissolved in CH_2Cl_2 and vigorously extracted with a layer of aqueous sulphuric acid (pH 1.0). Then, the organic layer containing SAL was washed with distilled water, and CH2Cl2 was evaporated under reduced pressure to dryness, giving **SAL** as clear oil. After the 3-times repeated evaporation with n-pentane, this oil was transformed into a white amorphous solid. The spectral properties of **SAL** were in agreement with the previously published data.

Five analogs of **SAL** have been synthesized by chemical modification at the C1 or C20 position **(Scheme 1)**.

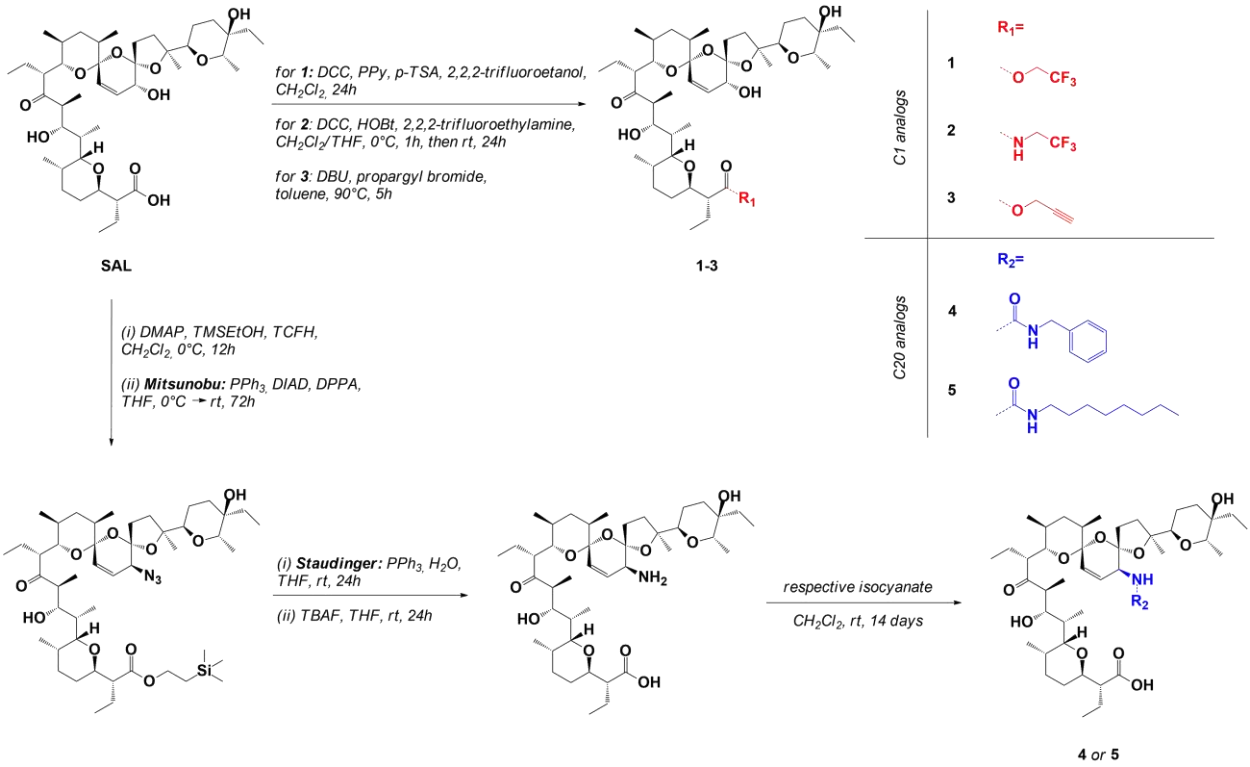

Scheme 1. Synthesis of **SAL** derivatives.

By modifying the carboxyl group of **SAL**, we have obtained SAL derivatives **1**, **2**, and **3**. These derivatives are already known in the literature, and their synthetic procedures were described elsewhere [13-15]. SAL derivatives **4** and **5** have been obtained as a result of multi-step synthesis, according to methods described by Li et al., 2018 [16] and then by Antoszczak et al., 2023 [17]. To obtain these derivatives, it was mandatory to block the carboxyl group at the C1 position and then conduct the Mitsunobu reaction. This led to the conversion of the hydroxyl group at the C20 position to the azide group with an inverted absolute configuration. The procedures for both reactions were described previously in detail [18]. The next step was reducing the azide group to an amine group using the Staudinger reaction [16]. Then, the reaction between the respective isocyanate and the amine group led to corresponding urea analogs, the SAL derivatives **4** and **5** [17].

To confirm the structures of synthesized products, we used spectroscopic (NMR) and spectrometric (ESI-MS) methods (data not shown).

Detailed procedures

*Synthesis of 2,2,2-trifluoroethyl ester of salinomycin - **derivative 1***

To a stirred solution of **SAL** (1.0 eq.) in anhydrous CH_2Cl_2, the following reagents were added at intervals of 15 minutes: 1,3-dicyclohexylcarbodiimide (DCC) (1.5 eq.), 4-(piperidine-4yl) pyridine (PPy) (0.5 eq.), 2,2,2- trifluoroethanol (7.5 eq.) and catalytic *p*-toluenesulfonic acid (pTSA). The reaction mixture was stirred at 0 °C for 6 h, then for 18 h at room temperature. The formed by-

product 1,3-dicyclohexylurea (DCU), which was insoluble in CH_2Cl_2, was filtered off. The filtrate was concentrated in vacuo and purified chromatographically on silica gel using the CombiFlash®Rf+ system (ethyl acetate/chloroform 0→50%) to give the pure product **1** as a clear oil. After repeated evaporation with n-pentane three times, the oily product was completely converted into a white amorphous solid. Yield: 71%. ^{1}H NMR (400 MHz, C_6D_6) δ 6.12 (dd, *J* = 10.7, 1.5Hz, 1H), 5.78 (dd, *J* = 10.7, 2.3 Hz, 1H), 5.25 (dq, *J* = 13.1, 8.9 Hz, 1H), 4.96 (dq, *J* = 13.1, 8.8 Hz, 1H), 4.31 (dd, *J* = 10.0, 5.7 Hz, 1H), 4.21 (dt, *J* = 9.1, 1.9 Hz, 1H), 4.14 (d, *J* = 9.1 Hz, 1H), 4.06 (dd, *J* = 10.9, 5.9 Hz, 1H), 3.85–3.72 (m, 2H), 3.69 (dd, *J* = 9.7, 2.3 Hz, 1H), 3.58 (dd, *J* = 10.3, 2.4 Hz, 1H), 3.12 (dq, *J* = 10.0, 7.2 Hz, 1H), 2.94 (td, *J* = 11.1, 4.0 Hz, 1H), 2.75 (d, *J* = 5.9 Hz, 1H), 2.62 (dt, *J* = 9.8, 2.6 Hz, 1H), 2.48 (dt, *J* = 13.4, 9.8 Hz, 1H), 2.35 (s, 1H), 2.24 (ddq, *J* = 14.4, 9.7, 7.2 Hz, 1H), 2.11–1.95 (m, 2H), 1.89 (ddd, *J* = 13.1, 6.7, 4.0 Hz, 1H), 1.80–0.50 (m, 49H) ppm; ^{13}C NMR (101 MHz, C_6D_6) δ 212.9, 172.9, 133.5, 120.5, 106.6, 98.9, 88.1, 79.3, 77.0, 74.05, 74.01, 71.8, 70.3, 69.1, 67.5, 60.8, 60.5, 55.3, 48.6, 47.0, 40.4, 38.4, 36.8, 36.6, 34.1, 32.8, 30.9, 30.3, 29.1, 28.1, 26.1, 25.8, 22.5, 22.4, 22.1, 19.6, 18.2, 17.2, 15.6, 14.3, 14.1, 13.9, 13.4, 11.4, 10.9, 7.7, 6.3 ppm, one signal overlapped; ESI MS (*m/z*): $[M+Na]^+$ Calcd for $C_{44}H_{71}F_3NaO_{11}^+$ 855.5; Found 855.

Synthesis of 2,2,2-trifluoroethyl amide of salinomycin - ***derivative 2***

A solution of **SAL** (1.0 eq.), 1,3-dicyclohexylcarbodiimide (DCC) (1.2 eq.), and 2,2,2trifluoroethylamine (2.5 eq.) in 40 mL of CH_2Cl_2, as well as 1-hydroxy benzotriazole hydrate (HOBt) (0.5 eq.) dissolved in 5 mL of THF were mixed and stirred at 0 °C for 1h. Then, the reaction mixture was stirred at room temperature for 24 hours. Next, the reaction mixture was concentrated under reduced pressure to produce yellow oil. Purification on silica gel using the CombiFlash®Rf+ system (EtOAc/$CHCl_3$ 0→50%) gave the pure product **2** as a colorless oil. After thrice evaporation to dryness with n-pentane, the oil was transformed into a white amorphous solid.

Yield: 80%. ^{1}H NMR (403 MHz, CD_2Cl_2) δ 7.05 (dd, J = 6.8, 6.0 Hz, 1H), 6.12 (dd, J = 10.7, 2.2 Hz, 1H), 5.97 (dd, J = 10.7, 1.6 Hz, 1H), 4.47 (dddd, J = 19.4, 15.2, 9.7, 7.8 Hz, 1H), 4.21–4.07 (m, 2H), 4.04–3.99 (m, 1H), 3.98–3.91 (m, 1H), 3.86 (d, J = 7.5 Hz, 1H), 3.80 (q, J = 6.8 Hz, 1H), 3.75 (dd, J = 10.1, 2.5 Hz, 1H), 3.68 (dd, J = 9.9, 2.5 Hz, 1H), 3.63 (dd, J = 11.0, 3.2 Hz, 1H), 2.98 (dq, J = 9.4, 7.3 Hz, 1H), 2.71–2.63 (m, 1H), 2.53 (dt, J = 8.5, 2.7 Hz, 1H), 2.44 (s, 1H), 2.40 (d, J = 8.5 Hz, 1H), 2.33 (dt, J = 12.6, 10.1 Hz, 1H), 2.18 (ddd, J = 12.5, 9.8, 2.7 Hz, 1H), 1.95 (ddd, J = 12.5, 8.9, 2.6 Hz, 1H), 1.91–0.82 (m, 45H), 0.77 (d, J = 7.0 Hz, 3H), 0.72 (d, J = 6.7 Hz, 3H) ppm; ^{13}C NMR (101 MHz, CD_2Cl_2) δ 213.5, 176.4, 134.1, 126.7, 124.0, 120.4, 106.8, 99.1, 89.2, 80.2, 77.3, 75.9, 74.8, 71.2, 70.9, 69.5, 67.3, 53.6, 48.6, 46.8, 40.8, 40.4, 40.1, 39.8, 38.6, 37.3, 36.6, 32.9, 31.0, 30.4, 29.5, 28.6, 27.1, 26.0, 22.3, 22.2, 20.7, 17.9, 17.3, 15.8, 15.0, 14.7, 14.4, 11.7, 11.5, 8.6, 6.5. One signal overlapping; ^{19}F NMR (379 MHz, CD_2Cl_2) δ –73.01, –73.04, –73.07 ppm; ESI MS (m/z): $[M+Na]^+$ Calcd for $C_{44}H_{72}F_3NNaO_{10}$ 855; Found 855.

Synthesis of propargyl ester of salinomycin - ***derivative 3***

To a solution of **SAL** (1.0 eq.) in anhydrous toluene, DBU (1.7 eq.) was added, and the mixture was stirred and heated at 90°C for 20 minutes. Then, propargyl bromide (2.2 eq.) was added, and the reaction mixture was stirred at 90°C for 5h. After cooling, the mixture was concentrated in vacuo and purified chromatographically on silica gel using the CombiFlash®Rf+ system to give the pure product **3** as a clear oil. After thrice evaporation to dryness with n-pentane, the oily product was wholly converted into a white amorphous solid. Yield: 88%. ^{1}H NMR (400 MHz, C_6D_6) δ

6.13 (dd, *J* = 10.7, 1.3 Hz, 1H), 5.83 (dd, *J* = 10.8, 2.2 Hz, 1H), 5.36–5.20 (m, 2H), 4.41– 4.32 (m, 1H), 4.26–4.12 (m, 2H), 4.08 (dd, *J* = 11.1, 6.0 Hz, 1H), 3.84–3.75 (m, 2H), 3.72 (dd, *J* = 9.7, 2.3 Hz, 1H), 3.64 (dd, *J* = 10.4, 2.4 Hz, 1H), 3.14 (dq, *J* = 10.1, 7.2 Hz, 1H), 3.00 (d, *J* = 5.4 Hz, 1H), 2.94 (td, *J* = 11.2, 4.1 Hz, 1H), 2.66 (dt, *J* = 9.7, 2.7 Hz, 1H), 2.55–2.43 (m, 1H), 2.28 (ddq, *J* = 14.4, 9.8, 7.2 Hz, 1H), 2.08 (d, *J* = 3.1 Hz, 1H), 2.05 (t, *J* = 2.5 Hz, 1H), 1.90 (dtd, *J* = 13.5, 6.7, 4.0 Hz, 1H), 1.80– 0.50 (m, 51H) ppm; ^{13}C NMR (101 MHz, C_6D_6) δ 212.7, 173.9, 133.3, 120.7, 106.5, 99.0, 87.9, 79.0, 78.5, 77.0, 74.7, 74.3, 74.0, 71.7, 70.3, 69.2, 67.7, 55.9, 52.5, 48.5, 47.3, 40.5, 38.6, 36.8, 36.7, 33.1, 30.9, 30.3, 29.3, 28.1, 26.1, 25.8, 22.7, 22.1, 19.6, 18.4, 17.3, 15.6, 14.3, 14.1, 13.3, 11.6, 10.9, 7.6, 6.3 ppm; ESI MS (*m/z*): $[M+Na]^+$ Calcd for $C_{45}H_{72}NaO_{11}^+$ 811.5; Found 811.

Synthesis of C20-benzylurea of C20-epi-aminosalinomycin - ***derivative 4***

To a solution of C20-epi-aminosalinomycin (1.0 eq.) in anhydrous CH_2Cl_2, benzyl isocyanate (3.0 eq.) was added dropwise under stirring at room temperature. The reaction was stirred overnight, then washed with Na_2CO_3 (0.1 M aq.), and the organic layers were concentrated in vacuo. Purification on silica gel using the CombiFlash®Rf+ system (0 → 40% acetone/chloroform) gave the pure urea **4** as a clear oil. After evaporation to dryness with n-pentane three times, the oily product was wholly converted into a white amorphous solid. Yield: 86%. ^{1}H NMR (401 MHz, $CDCl_3$) δ 7.41 – 7.26 (m, 5H), 6.29 (dd, *J* = 9.5, 7.0 Hz, 1H), 5.81 (d, *J* = 9.5 Hz, 1H), 5.56 (d, *J* = 9.8 Hz, 1H), 4.60 (dd, *J* = 14.3, 7.6 Hz, 1H), 4.34 (dd, *J* = 9.8, 7.0 Hz, 1H), 4.16 – 4.09 (m, 2H), 4.01 (dd, *J* = 10.9, 5.2 Hz, 1H), 3.91 (d, *J* = 10.4 Hz, 1H), 3.75 (dt, *J* = 11.0, 4.4 Hz, 3H), 3.39 (t, *J* = 6.8 Hz, 1H), 3.04 (td, *J* = 11.3, 3.9 Hz, 1H), 2.71 (ddd, *J* = 13.3, 12.3, 5.0 Hz, 2H), 2.65 – 2.55 (m, 1H), 2.17 – 2.02 (m, 2H), 1.97 – 0.63 (m, 53H); ^{13}C NMR (101 MHz, $CDCl_3$) δ 219.18, 176.86, 160.10, 139.31, 133.09, 131.02, 128.29 (2C), 128.10 (2C), 126.91, 109.86, 95.70, 86.18, 75.06, 72.56, 71.94, 71.16, 71.04, 68.15, 55.04, 51.05, 48.74, 47.03, 44.61, 39.40, 36.59, 35.59, 35.34, 33.90, 32.48, 30.33, 29.66, 29.35, 27.99, 25.75, 22.12, 21.52, 20.97, 19.92, 18.10, 17.77, 16.08, 14.10, 13.23, 12.55, 11.93, 11.83, 7.29, 6.38 ppm; ESI MS (m/z): $[M+H]^+$ Calcd for $C_{50}H_{78}N_2NaO_{11}^+$ 905.5; Found 906.

Synthesis of C20-n-octyl urea of salinomycin - ***derivative 5***

To a solution of C20-epi-aminosalinomycin (1.0 eq.) in anhydrous CH_2Cl_2, octyl isocyanate (3.0 eq.) was added dropwise under stirring at room temperature. The reaction was stirred overnight, then washed with Na_2CO_3 (0.1 M aq.), and the organic layers were concentrated in vacuo. Purification on silica gel using the CombiFlash®Rf+ system (0 → 40% acetone/chloroform) gave the pure urea **5** as a clear oil. Then, the oily product was wholly converted into a white amorphous solid by three times evaporation with n-pentane. Yield: 95%. ^{1}H NMR (401 MHz, $CDCl_3$) δ 6.29 (dd, J = 9.5, 6.9 Hz, 1H), 5.80 (d, J = 9.5 Hz, 1H), 5.37 (d, J = 10.0 Hz, 1H), 4.30 (dd, J = 9.9, 6.9 Hz, 1H), 4.11 (d, J = 7.5 Hz, 1H), 3.93 – 3.87 (m, J = 10.6, 6.1 Hz, 2H), 3.73 (qu, J = 14.7, 7.6 Hz, 2H), 3.63 (d, J = 4.4 Hz, 1H), 3.40 – 3.35 (m, J = 10.2 Hz, 1H), 3.31 (qu, J = 13.0, 6.6 Hz, 1H), 3.13 (t, 2H), 3.06 – 2.96 (m, J = 11.2, 3.8 Hz, 2H), 2.77 – 2.68 (m, 2H), 2.61 – 2.51 (m, 1H), 2.18 – 0.71 (m, 65H) ppm; ^{13}C NMR (101 MHz, $CDCl_3$) δ 218.69, 176.83, 160.26, 132.91, 131.25, 109.91, 95.74, 86.16, 75.02, 72.57, 71.97, 71.08, 71.05, 67.78, 55.06, 51.03, 48.63, 47.01, 40.73, 40.47, 39.44, 36.65, 35.48, 35.36, 33.96, 32.59, 31.91, 31.85, 31.77, 29.67, 27.94, 27.05, 26.88,

25.71, 22.64, 22.61, 22.19, 21.57, 20.95, 19.94, 18.15, 17.63, 16.10, 14.10, 14.06, 13.24, 12.74, 11.94, 11.87, 7.31, 6.39 ppm; ESI MS (m/z): $[M+H]^+$ Calcd for $C_{51}H_{88}N_2NaO_{11}^+$ 927.6; Found 928.

Statistics

Results were plotted with GraphPad Prism, and statistical significance was assessed by appropriate tests provided in Figure legends. The *p-values* were marked with the asterisks on the charts (*p<0.05, **p<0.01, ***p<0.001, ****p<0.0001).

References

1. Taub, R., et al., *Translocation of the c-myc gene into the immunoglobulin heavy chain locus in human Burkitt lymphoma and murine plasmacytoma cells.* Proc Natl Acad Sci U S A, 1982. **79**(24): p. 7837-41.
2. Li, W., et al., *Targeting MYC activity in double-hit lymphoma with MYC and BCL2 and/or BCL6 rearrangements with epigenetic bromodomain inhibitors.* J Hematol Oncol, 2019. **12**(1): p. 73.
3. Showe, L.C., et al., *Cloning and sequencing of a c-myc oncogene in a Burkitt's lymphoma cell line that is translocated to a germ line alpha switch region.* Mol Cell Biol, 1985. **5**(3): p. 501-9.
4. Khaira, P., C.D. James, and M. Leffak, *Amplification of the translocated c-myc genes in three Burkitt lymphoma cell lines.* Gene, 1998. **211**(1): p. 101-8.
5. Veronese, M.L., et al., *Detection of myc translocations in lymphoma cells by fluorescence in situ hybridization with yeast artificial chromosomes.* Blood, 1995. **85**(8): p. 2132-8.
6. Wiman, K.G., et al., *Activation of a translocated c-myc gene: role of structural alterations in the upstream region.* Proc Natl Acad Sci U S A, 1984. **81**(21): p. 6798-802.
7. Torsteinsdottir, S., et al., *Reversion of tumorigenicity and decreased agarose clonability after EBV conversion of an IgH/myc translocation-carrying BL line.* Int J Cancer, 1989. **43**(2): p. 273-8.
8. Mehra, S., et al., *Molecular cytogenetic characterization of non-Hodgkin lymphoma cell lines.* Genes Chromosomes Cancer, 2002. **33**(3): p. 225-34.
9. Chang, H., et al., *p53 mutations, c-myc and bcl-2 rearrangements in human non-Hodgkin's lymphoma cell lines.* Leuk Lymphoma, 1995. **19**(1-2): p. 165-71.
10. Dharanipragada, P. and N. Parekh, *In Silico Identification and Functional Characterization of Genetic Variations across DLBCL Cell Lines.* Cells, 2023. **12**(4).
11. Rymkiewicz, G., et al., *A comprehensive flow-cytometry-based immunophenotypic characterization of Burkitt-like lymphoma with 11q aberration.* Mod Pathol, 2018. **31**(5): p. 732743.
12. Huczynski, A., et al., *Synthesis and antimicrobial activity of amide derivatives of polyether antibiotic-salinomycin.* Bioorg Med Chem Lett, 2012. **22**(14): p. 4697-702.
13. Kuran, D., et al., *Ester derivatives of salinomycin efficiently eliminate breast cancer cells via ERstress-induced apoptosis.* Eur J Pharmacol, 2021. **893**: p. 173824.
14. Sulik, M., et al., *Antibacterial activity of singly and doubly modified salinomycin derivatives.* Bioorg Med Chem Lett, 2020. **30**(9): p. 127062.
15. Sulik, M., et al., *Synthesis and Anticancer Activity of Dimeric Polyether Ionophores.* Biomolecules, 2020. **10**(7).

16. Li, Y., et al., *Synthesis and biological evaluation of 20-epi-amino-20-deoxysalinomycin derivatives.* Eur J Med Chem, 2018. **148**: p. 279-290.
17. Antoszczak, M., et al., *Synthesis of urea and thiourea derivatives of C20-epi-aminosalinomycin and their activity against Trypanosoma brucei.* Eur J Med Chem, 2023. **250**: p. 115241.
18. Shi, Q., et al., *Discovery of a (19)F MRI sensitive salinomycin derivative with high cytotoxicity towards cancer cells.* Chem Commun (Camb), 2016. **52**(29): p. 5136-9.

8.1.1 Supplementary Legends for Figures and Tables

Suppl. Figure 1. Effects of selected cation carriers on both surface and total levels of CD20 antigen.
(A) Analysis of levels of surface CD20 upon treatment of Raji cells with selected concentrations of either salinomycin (SAL), monensin (MON), narasin (NAR), nigericin (NIG), or corresponding vehicles (-). The number of CD20 molecules present on the surface of cells was quantified with flow cytometry in alive cells (Zombie-NIR-negative events), stained with anti-CD20-PE antibody. The beads labeled with the known number of PE molecules (BD Quantibrite PE Phycoerythrin Fluorescence Quantitation Kit) were acquired in the same experiments, allowing the calculation of CD20 molecule numbers according to the manufacturer's recommendations. **(B)** Total levels of CD20 protein were analyzed by Western blotting in extracts from Raji cells treated as in (A). GAPDH levels were used as a loading control. Results from 3 experiments were quantified, calculated as fold change increase (+/-SD) upon treatment with ionophores *versus* treatment with corresponding vehicles, and presented below the Western blotting images.

Suppl. Figure 2. Effects of lasalocid, A23187, and ionomycin on the levels of surface CD20 and cell viability.
Chemical structures **(A),** levels of surface CD20 **(B)**, and viability **(C)** of Raji cells treated with increasing concentrations of either lasalocid (upper panels), A23187 (middle panels), or ionomycin (lower panels). The surface CD20 and viability of cells were estimated as in Fig. 1.

Suppl. Figure 3. Upregulation of surface CD20 by salinomycin and monensin in primary CLL and DLBCL cells.
(A) Viability of DLBCL (left panel) and CLL (right panel) cells treated *ex vivo* for 48 hours with increasing concentrations of either SAL (0.25-1 μM) or MON (0.025-0.25 μM), respectively. The percentage of viable cells (Zombie-NIR-negative events) was normalized to the percentage of viable cells in samples treated with the corresponding vehicle. **(B)** Examples of graphs generated using the FlowJo software depicting the flow cytometry analysis of surface levels of CD20 antigen in primary CLL cells upon the treatment with either SAL (0.5 μM; in dark blue), MON (0.1 μM; in bright blue) or corresponding vehicles (in grey) for 48 hours. CLL samples were stained with a mix of anti-CD19-APC and anti-CD20-FITC antibodies. Zombie-NIR was used to stain the dead cells. The plots in the left panels visualize the gating of the CD19-positive population, followed by analysis for the CD20 levels (right panels). **(C)** Changes in cell surface levels of CD20 antigen in primary CLL cells (samples from Fig. 1D, n=13) pretreated *ex vivo* for 48 hours with MON (0.05 and 0.1 μM). The MFI values of anti-CD20-FITC were transformed to log2 values to visualize each sample on the same axis.

Suppl. Figure 4. Salinomycin and monensin influence the levels of tumor cell antigens involved in regulating complement's and NK cell activity. (A, B) The flow cytometry analysis of complement inhibitors, namely CD55 **(A)** and CD46 **(B),** on the surface of Raji cells treated with either SAL (0.25 and 0.5 μM; left panels) or MON (0.05 and 0.1 μM; right panels) for 48 h. **(C-E)** The validation of changes in the levels of selected surface antigens detected in Raji cells by proteomics analysis. Cells pretreated with either SAL (left panels) or MON (right panels) were incubated with the following antibodies: anti-CD40 (TNR5) **(C)**, anti-ICAM1 **(D)**, and anti-CD47 **(E)**. In addition, other surface antigens known to influence NK cell activity were analyzed **(F)** upon the treatment of Raji with either SAL (0.25 μM) or MON (0.05 μM) for 48h, including CD80 (left panel), CD155 and ULBP-2/5/6 (middle panels), and CD86 (right panel).

Suppl. Figure 5. Salinomycin and monensin increase CD20 levels and rituximab efficacy in a panel of Burkitt lymphoma cell lines. The left panels present flow cytometry analysis of surface levels of CD20 antigen (MFI of anti-CD20-FITC antibody) in Burkitt lymphoma cell lines, such as CA46 **(A)**, Daudi **(B)**, Ramos **(C)**, and BL41 **(D)** pretreated with either SAL (0.05-1 μM), MON (0.01-0.1 μM) or corresponding vehicles for 48 h. The right panels present the response of Burkitt lymphoma cell lines to rituximab in CDC assays upon pretreatment of cells with either SAL or vehicle (at two selected concentrations).

Suppl. Figure 6. The effect of stable knockout of the *MS4A1* gene on complement- and NK cells-dependent elimination of tumor cells by rituximab.
(A) Generation of clones of Raji cells with a stable knockout of the *MS4A1* gene. Raji cells were stably transduced with sgRNA targeting the *MS4A1* gene (encoding CD20) using the CRISPR/Cas9 genome editing technology. The left panel presents the Western blotting detection of CD20 in the extracts from clones of Raji cells genetically modified with either empty vector (clones 1-3) or sgMS4A1 (clones 2, 4, and 10). These clones were also mixed (1:1:1) and called either "Empty v.-mix" or "sgMS4A1-mix", respectively. The right panel presents the surface level of CD20 antigen estimated with flow cytometry in Raji cell clones and their mixes (as above), transduced with either empty vector or sgMS4A1 and treated with SAL for 48 h. **(B)** Complementdependent cytotoxicity (CDC) assays were performed with Raji cells, either Empty vector - mix (left panel) or sgMS4A1 – mix (right panel) pretreated with SAL (0.25 μM or 0.5 μM) for 48 h followed by the treatment with increasing concentrations of rituximab. **(C)** Antibody-dependent cellular cytotoxicity (ADCC) assays testing the cytotoxicity of NK cells towards Raji cells pretreated with either SAL (dark blue bars) or vehicle (grey bars) for 48 h, followed by staining of Raji cells with CFSE and co-incubation with unstained donor-derived NK cells for 3 h, in the absence or presence of rituximab (RTX; 0.03 μg/ml). The survival of CFSE-positive Raji cells was assessed with PI, and presented as a percentage of control cells (Raji not incubated with NK cells). The ADCC assays were performed with either Empty vector-mix or sgMS4A1-mix Raji cells. Graphs show data from 3 experiments (NK cells isolated from 3 donors).

Suppl. **Figure 7. Inhibition of NLRP3 inflammasome does not affect the cation carrierinduced upregulation of CD20 antigen.** Raji cells were pretreated for 30 min with NLRP3 inhibitor (MCC950) at a concentration of either 10 μM (left panel) or 20 μM (right panel), followed by 48 h-long treatment with cation carriers, namely nigericin (NIG; 1 μM; brown bars), SAL (0.5

μM; dark blue bars) or MON (0.1 μM; bright blue bars). Surface CD20 was estimated by flow cytometry. MFIs of anti-CD20-PE or anti-CD20-FITC were calculated as fold change *versus* MFI values of control cells (treated with DMSO and vehicle).

Suppl. **Figure 8. Upregulation of different variants of *MS4A1* mRNA by salinomycin and monensin.** Raji cells were pretreated with either SAL (0.25 μM), MON (0.05 μM) or corresponding vehicle for 18 h, followed by RNA isolation, cDNA synthesis and RT-PCR analysis of *MS4A1* mRNA using pairs of primers specific for either transcript variant 1 (MS4A1-V1; NM_152866.3; left panel), variant 3 (MS4A1-V3; NM_021950.4; middle panel) or pair of primers recognizing all transcript variants (right panel).

Suppl. Figure 9. The effects of cation carriers on the MYC-dependent cellular functions. (A) The quantification of MYC protein levels by Western blotting analysis in both Raji cells (left graph) and P493-6 cell line (right graph), pretreated with either SAL, MON, or vehicle (-) for 18 h. The graphs summarize the quantification from 4 Western blotting images (including the images presented in Fig. 7B). **(B)** Quantification of the binding of MYC to its target E-box DNA motif using the TransAM MYC ELISA. The nuclear extracts obtained from Raji cells treated with either SAL (0.25 μM), MON (0.1 μM), or vehicle for 12-18 h were applied on the ELISA plate. The values corresponding to the binding of MYC in SAL- or MON-treated cells are normalized to the values corresponding to the vehicle-treated cells and are presented as fold change. **(C)** The differential expression heatmap with RNA-seq data listing the genes involved in the G2/M checkpoint (according to GSEA analysis; Hallmark – G2M checkpoint) and presents the fold change of their expression in Raji cells treated for 18 h with either SAL (0.5 μM) or MON (0.1 μM). The downregulation of all listed genes reached statistical significance (q value <0.05) upon the treatment with MON and exhibited a downregulation tendency (without statistical significance) upon the treatment with SAL. **(D)** The cell cycle pie charts depicting changes in cell cycle phases upon treating Raji cells with either SAL (0.25 and 0.5 μM; top panel) or MON (0.05 and 0.1 μM) for 48 h. The numbers represent the percentage of cells in a particular cell cycle phase.

Suppl. Figure 10. The effect of salinomycin and monensin on the level of surface CD20 depends on the status of MYC expression. (A) Examples of histograms generated using the FlowJo software depicting the flow cytometry analysis of surface levels of CD20 antigen in the P493-6 cell line with MYC Tet-OFF system. The histograms on the left present CD20 levels in cells treated with either SAL (0.25 μM; in dark blue), doxycycline (DOX, 0.1 μg/ml; in orange), or both (in dark red) for 48 h and stained with anti-CD20-PE antibody. The analogous histograms on the right present results from cells treated with either MON (0.05 μM; in blue), DOX (in orange), or both (in red). **(B)** The bars show the number of CD20 molecules present on the surface of P493-6 cells (treated as in (A), right panel) and quantified based on the comparison to the fluorescence intensity of the beads labeled with the known number of PE molecules (BD Quantibrite PE Phycoerythrin Fluorescence Quantitation Kit), according to the manufacturer's recommendations.

Suppl. Figure 11. Effect of selected derivatives of salinomycin on the level of surface CD20 antigen and AKT/FOXO1 signaling. (A) Chemical structures of salinomycin and its selected derivatives 2, 3, and 4, with position C1 marked in red and position C20 marked in blue, were

visualized using ChemDraw Ultra 12.0. **(B)** Flow cytometry analysis of surface levels of CD20 antigen in Raji cells treated with the increasing concentrations of SAL derivatives (range 0.01-2.5 μM). The graphs represent the fold change of MFI values, normalized to the average values from cells treated with the vehicle at low (L), medium (M), and high (H) concentrations. **(C)** Western blotting analysis of both phosphorylated and total protein levels of AKT and FOXO1 in Raji cells, pretreated with either SAL, its derivatives (der. 1, 2, 3, 4, or 5), or vehicle (-) for 18 h. The level of GAPDH was used as a loading control. The quantification of the levels of p-AKT (graph in the middle) and p-FOXO1 (right graph) in SAL- or derivatives-treated cells is presented as a fold change *versus* levels in vehicle-treated cells (quantification from 3 experiments).

Suppl. Figure 12. Effect of selected signaling pathways on the expression of CD20. (A-B) Transient ablation of *MYC* in Raji cells. **(A)** Western blotting analysis of MYC in extracts from Raji cells mock-nucleofected or genome-edited with sgMYC, followed by treatment with either SAL (0.25 μM) or vehicle (Veh.) for 18 h. GAPDH was used as a loading control. **(B)** Flow cytometry analysis of surface CD20 on Raji cells mock-nucleofected or genome-edited with sgMYC, followed by treatment with either SAL (0.25 μM), MON (0.05 μM), or corresponding vehicles for 48 h. Data was presented as a fold change of MFI, normalized to the mocknucleofected, vehicle-treated cells. **(C-D)** Transient ablation of *SGK1* in Raji cells. The experiments were performed, and the results were presented analogously to A and B. **(E)** Flow cytometry analysis of surface CD20 on Raji cells pretreated with either EMD638683 (EMD; 2550 μM) or DMSO for 1 h, followed by the treatment with either SAL (0.25 μM) or vehicle for next 48 h. The cell culture medium with fresh compounds was exchanged after 24 h. Data was presented as a fold change of MFI, normalized to the DMSO plus vehicle-treated cells.

Suppl. Table 5. The MFI values for CD20 antigen staining in CLL samples treated with increasing concentrations of monensin. The primary CLL cells (samples from Fig. 1D, n=13) were pretreated *ex vivo* for 48 hours with MON (concentration range 0.025-0.25 μM). The cells stained with a mix of anti-CD19-APC Ab, anti-CD20-FITC Ab, and Zombie-NIR were analyzed with flow cytometry. The raw MFI values corresponding to anti-CD20-FITC signals in the Zombie-NIR-negative/ CD19-positive cell populations are presented for each sample.

Suppl. Table 6. The differential expression analysis of genes expressed in Raji cells pretreated with either salinomycin or the control vehicle. The table lists the genes identified by RNA-seq analysis of 0.5 μM SAL- and control vehicle-treated Raji cells (two biological replicates for each treatment), followed by the differential expression analysis (SAL *versus* control). The "log2 (fold change)" values represent the magnitude of SAL-induced changes in the expression of genes, while the *q* values represent the statistical significance of these changes.

Suppl. Figure 1.

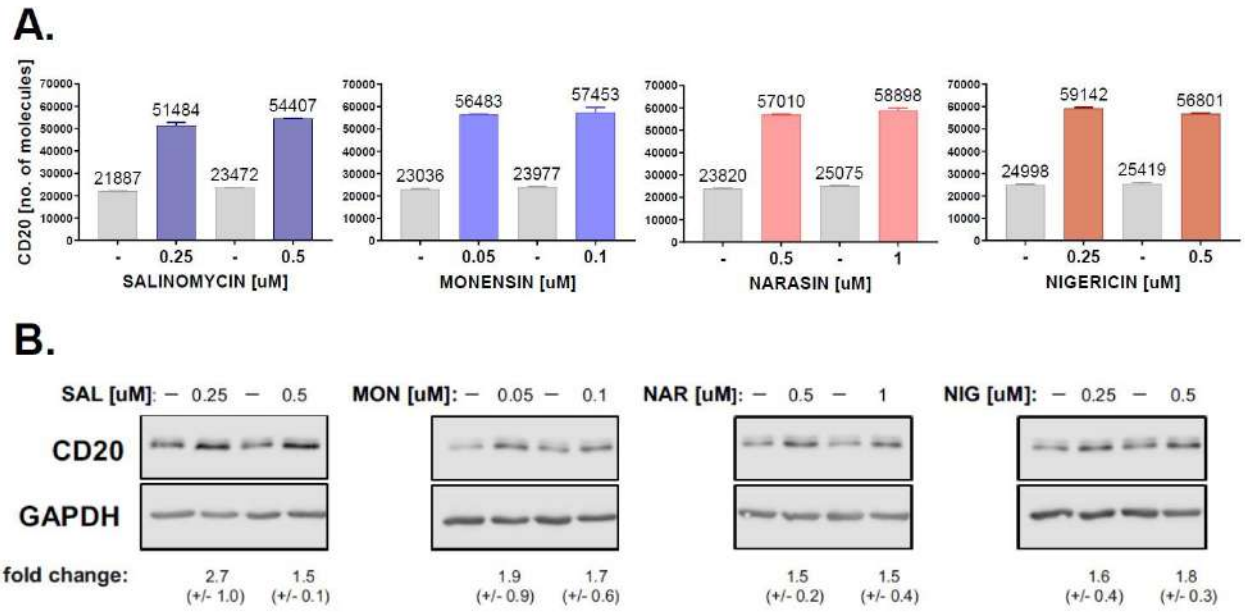

Suppl. Figure 2.

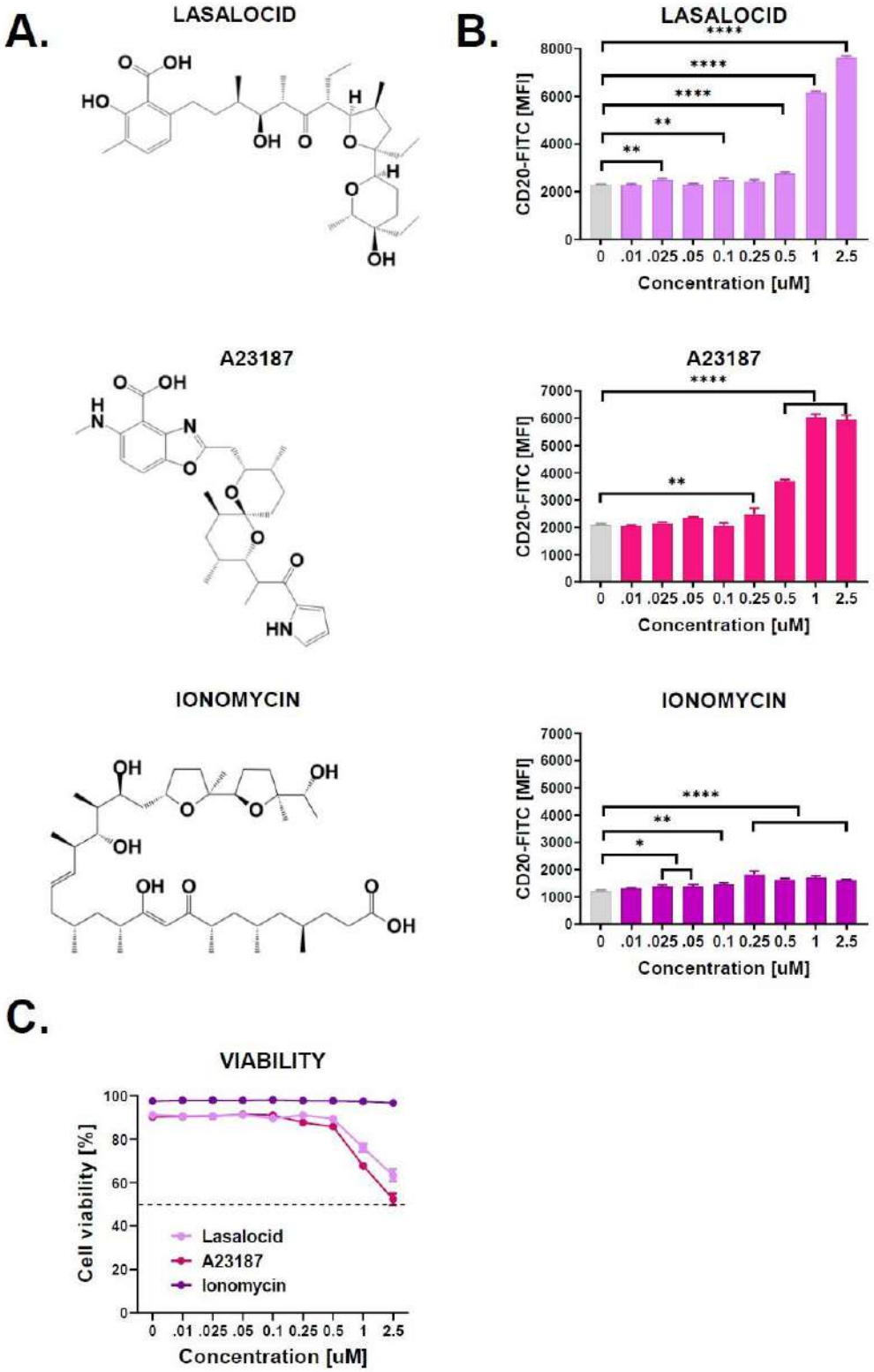

Suppl. Figure 3.

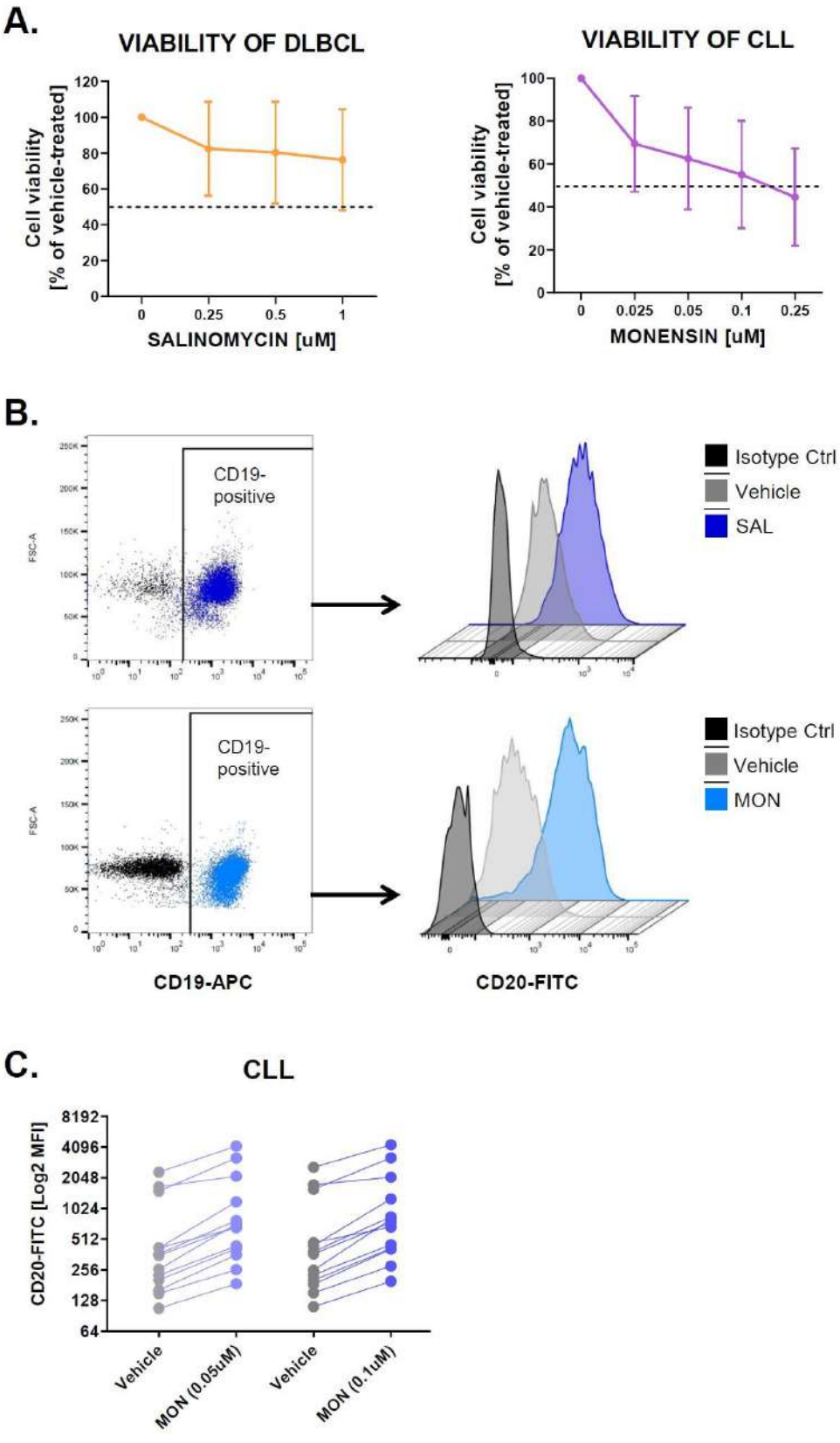

Suppl. Figure 4.

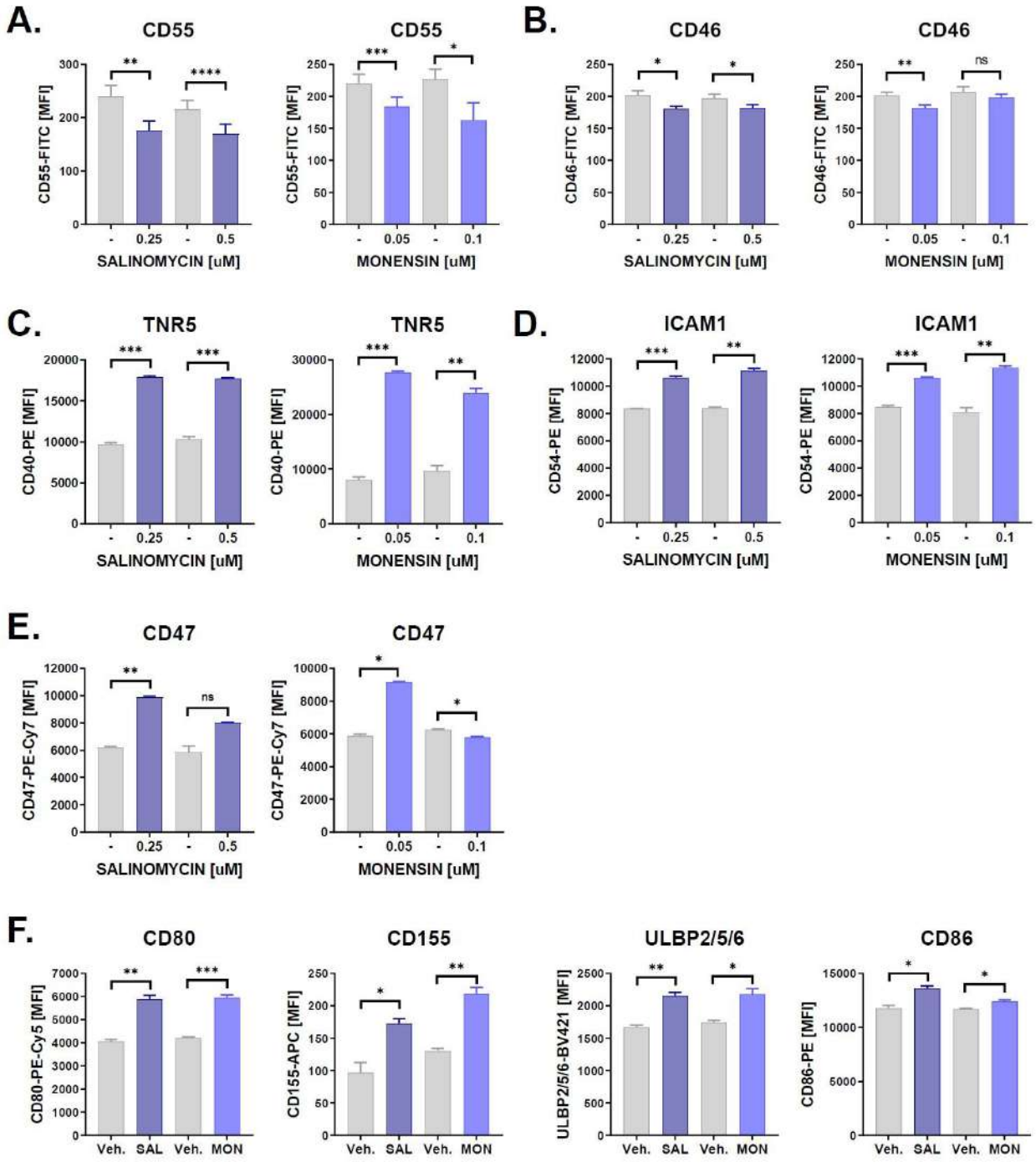

Suppl. Figure 5.

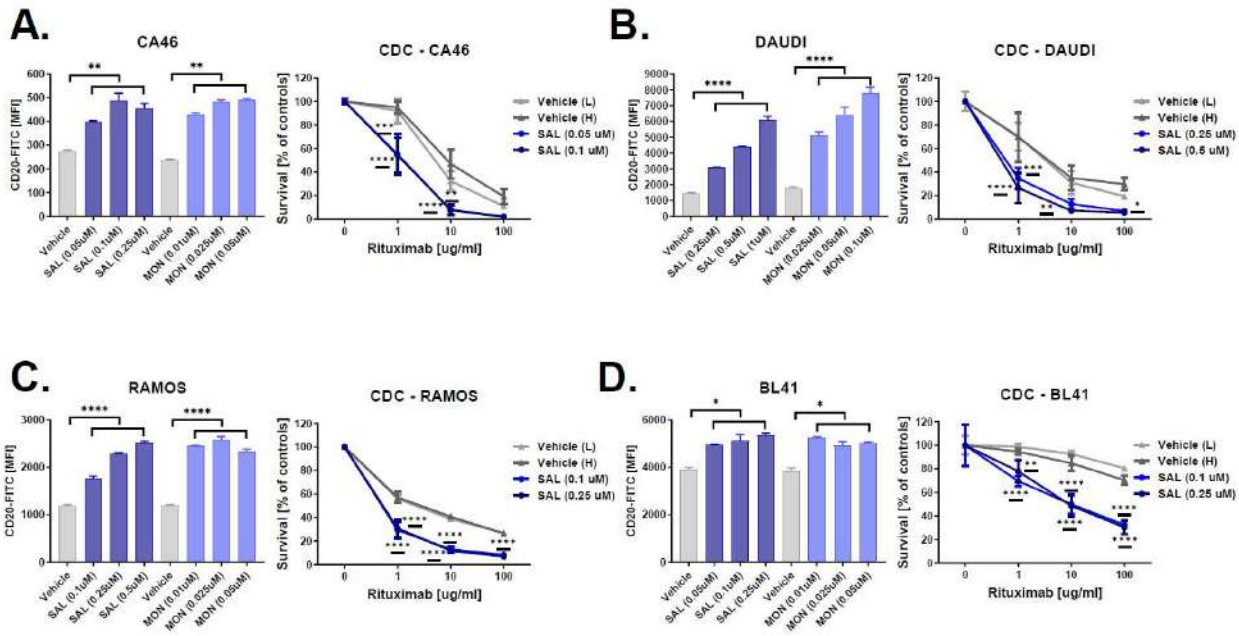

Suppl. Figure 6.

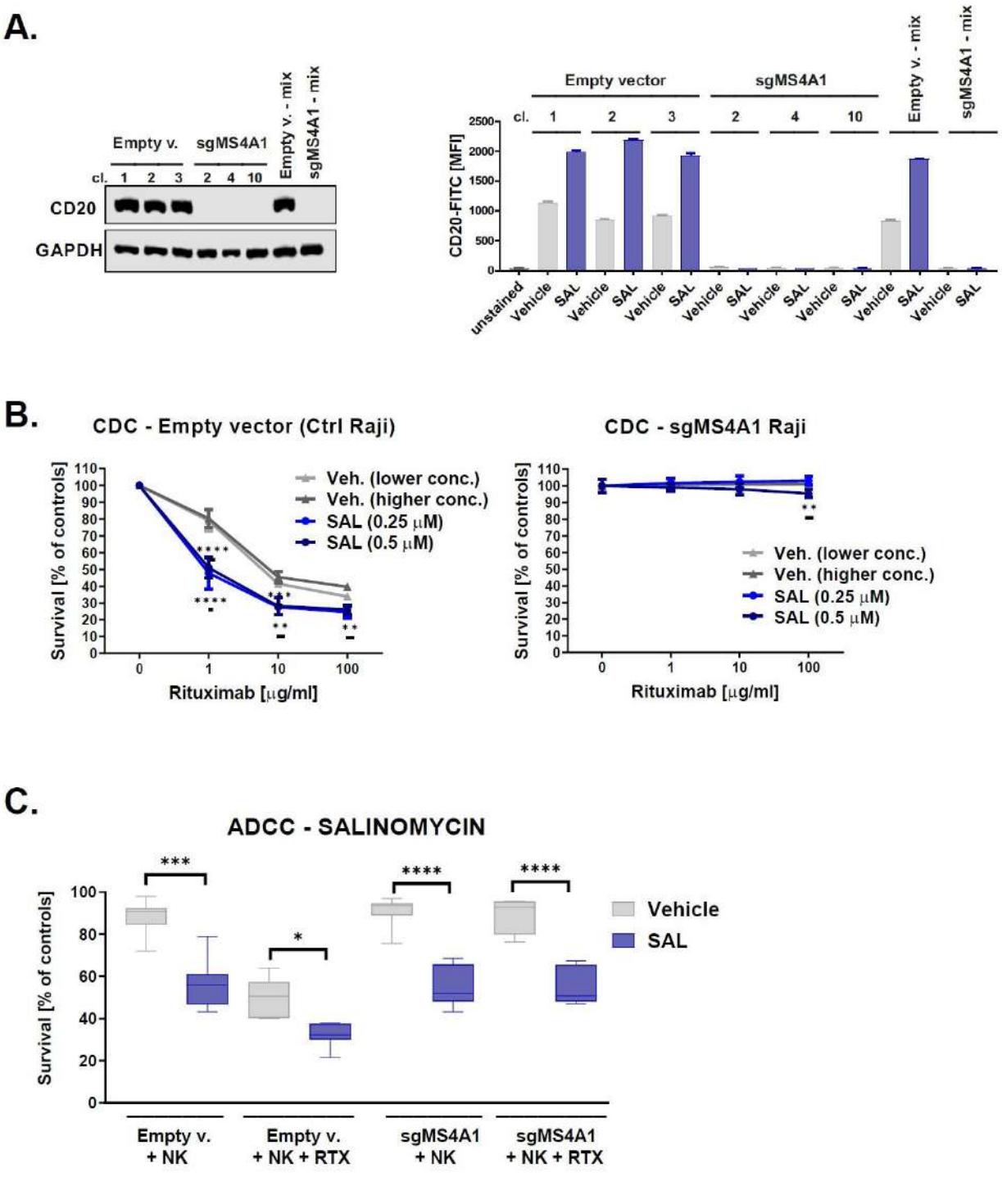

Suppl. Figure 7.

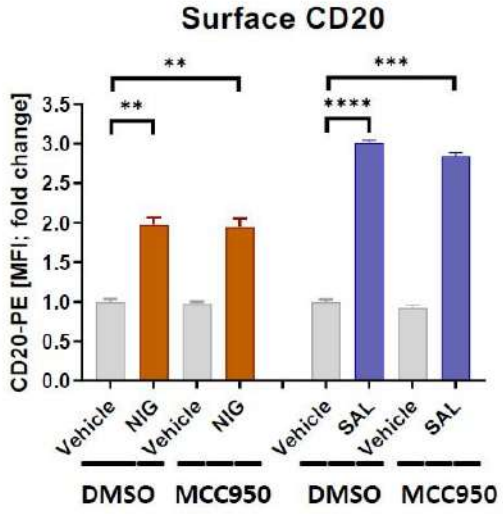

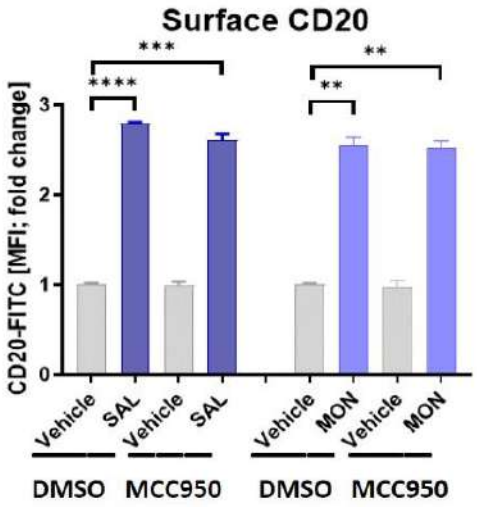

Suppl. Figure 8.

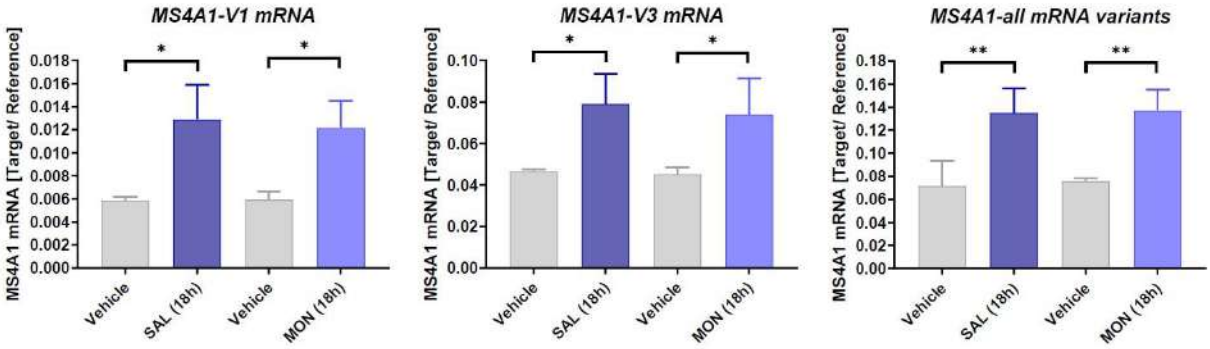

Suppl. Figure 9.

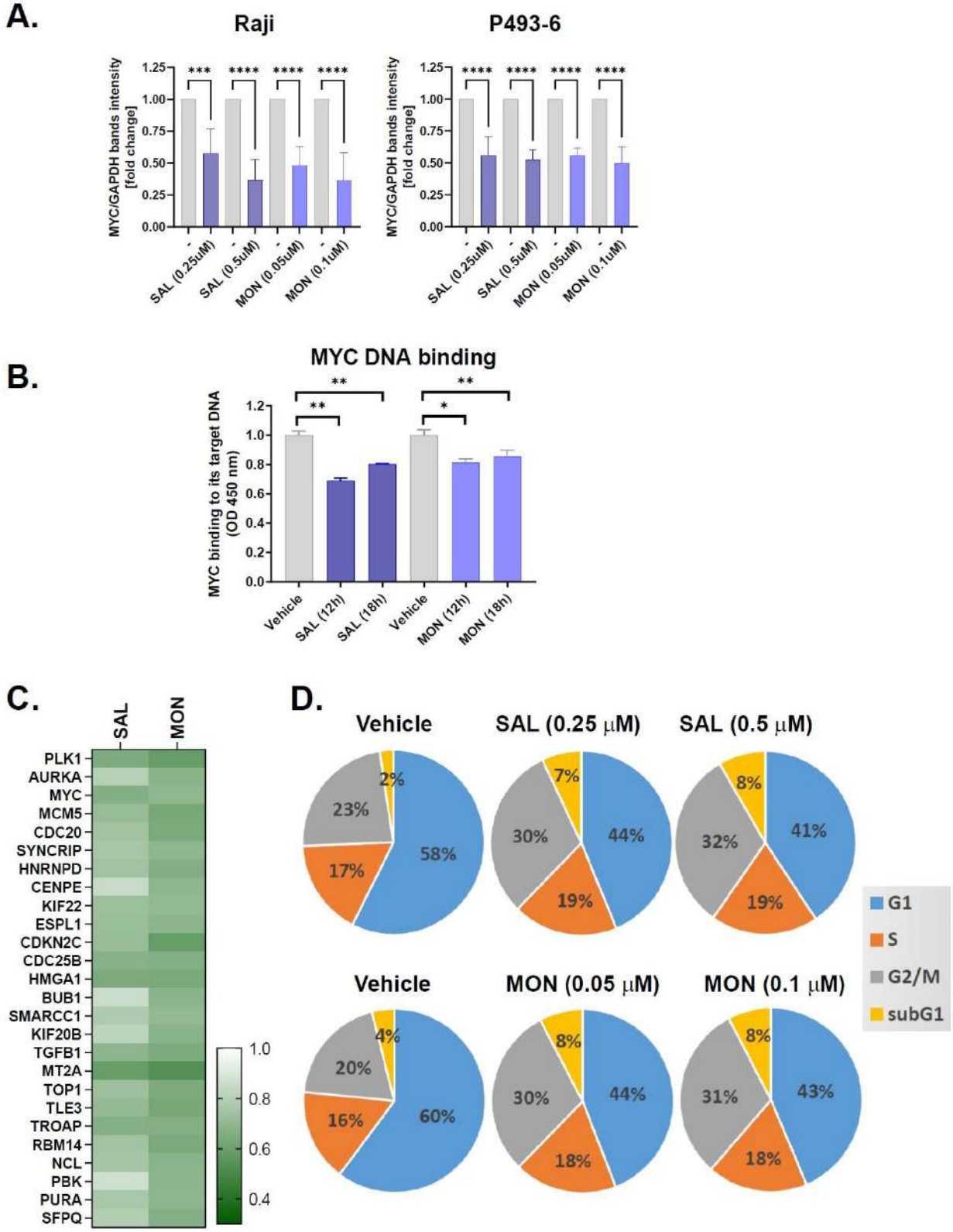

Suppl. Figure 10.

A.

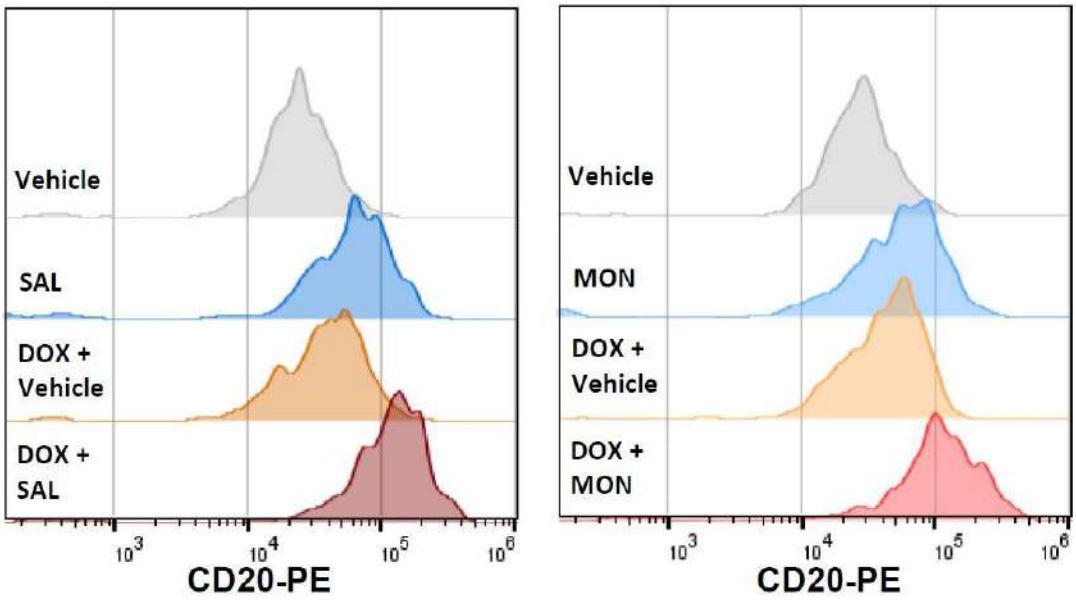

B.

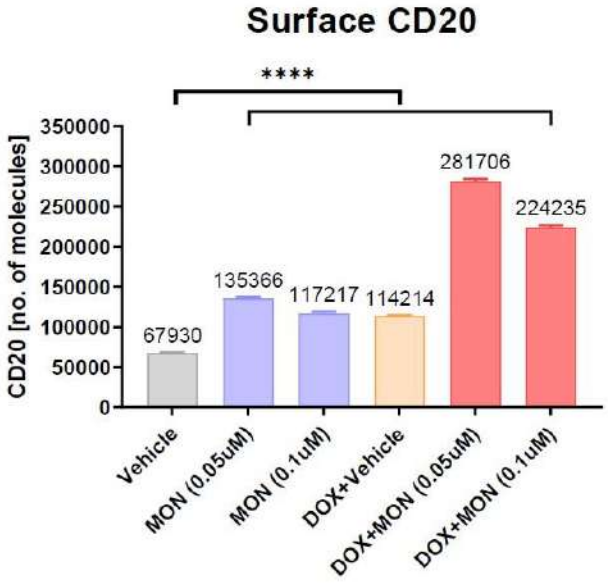

Suppl. Figure 11.

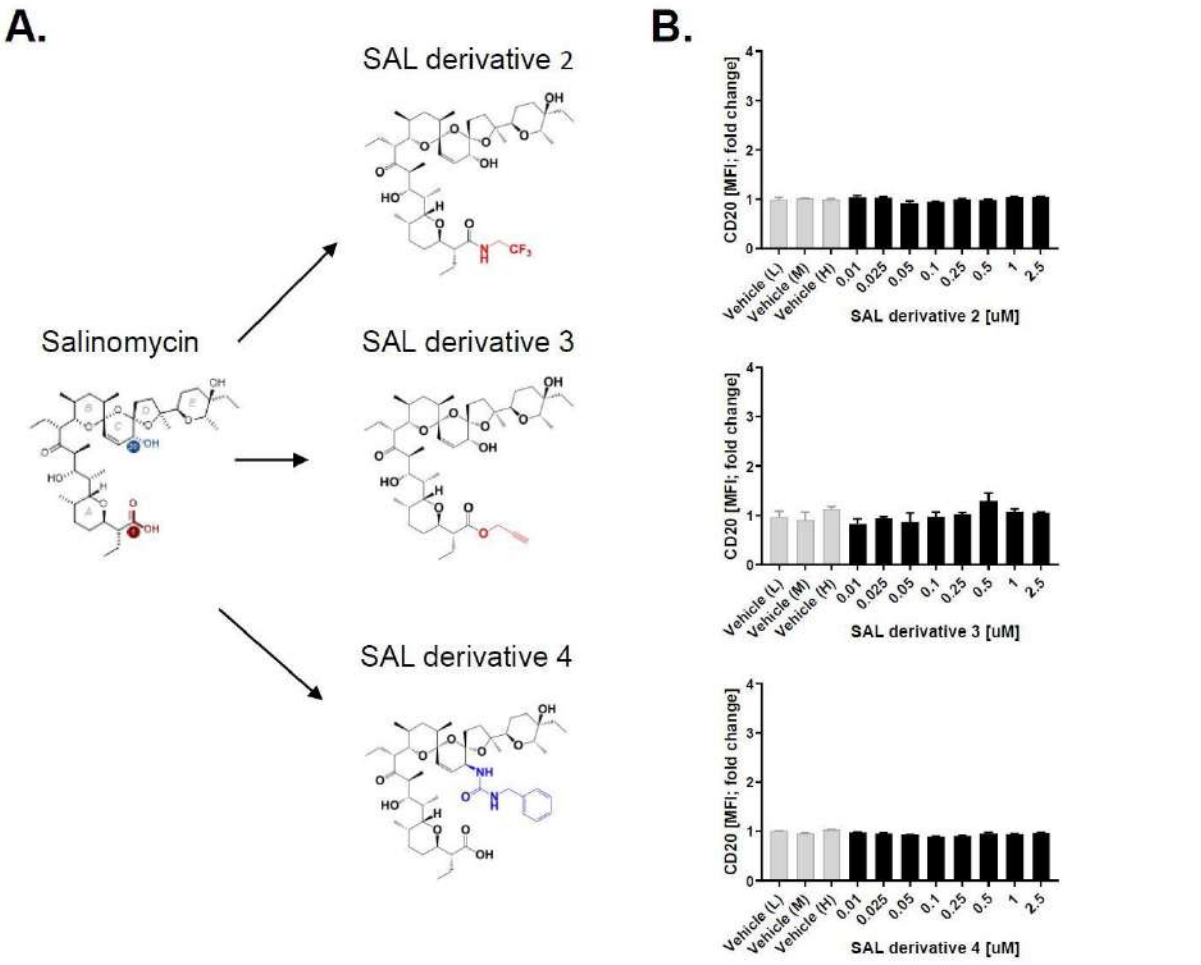

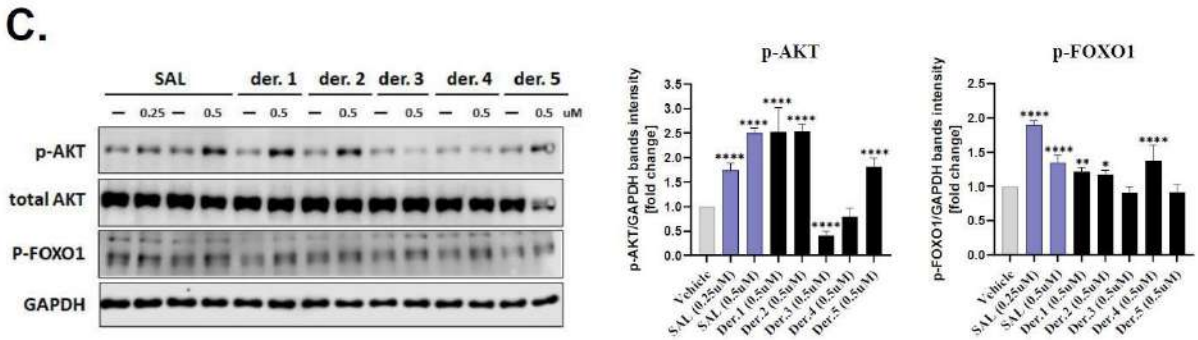

Suppl. Figure 12.

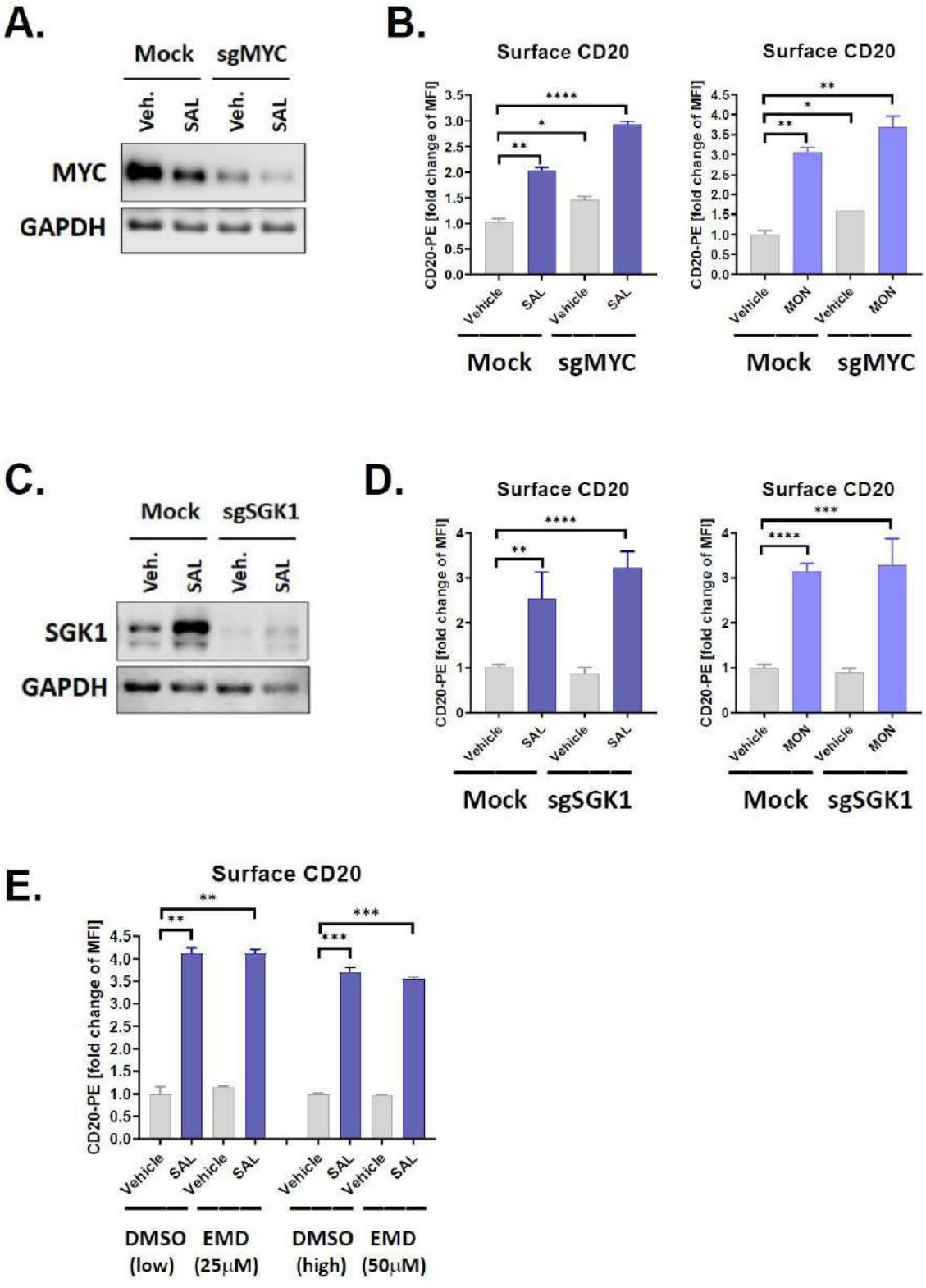

Suppl. Table 5. The MFI values for CD20 antigen staining in CLL samples treated with increasing concentrations of MON.

Sample code	Vehicle	MON (0.025 □M)	MON (0.05 □M)	MON (0.1 □M)	MON (0.25 □M)
G101	151	271	257	278	284
G160	227	425	437	450	406
G364	1544	3126	3196	3209	3127
G365	257	626	719	799	975
G374	2458	3450	4182	4309	4353
G401	173	327	359	407	526
G429	447	564	665	672	710
G441	376	746	779	846	922
G449	203	372	412	414	439
G450	1707	2146	2118	2074	2065
G453	360	609	674	743	795
G454	429	1022	1187	1267	1351
GD1	109	179	187	198	217

Suppl. Table 6. The differential expression analysis of genes expressed in Raji cells pretreated with either salinomycin or the control vehicle.

Gene	Mean Count	log2(Fold Change)	Std. Err. log2(Fold Change)	q Value
A1BG-AS1	10.04	0.14	0.2	9.89e-1
A4GALT	411.98	-0.09	0.23	9.90e-1
AAAS	610.65	-0.11	0.22	9.90e-1
AACS	100.3	0.03	0.24	9.93e-1
AAGAB	410.92	0.03	0.21	9.93e-1
AAK1	96.5	-0.4	0.24	8.23e-1
AAMP	878.54	-0.08	0.21	9.90e-1
AAR2	366.39	-0.22	0.22	9.54e-1
AARS	2019.48	0.48	0.18	3.49e-1
AARS2	289.06	-0.24	0.22	9.49e-1
AASDH	116.89	0.37	0.24	8.52e-1
AASDHPPT	654.98	0.18	0.21	9.78e-1
AATF	1469.83	-0.27	0.19	8.74e-1
ABAT	45.18	0.01	0.25	9.97e-1
ABCA1	241.27	0.34	0.22	8.49e-1
ABCA11P	52.16	0.2	0.25	9.86e-1
ABCA5	19.28	0.26	0.24	9.47e-1
ABCA6	10.89	0.02	0.21	9.95e-1
ABCA7	510.94	0.09	0.22	9.90e-1
ABCB10	369.16	0.2	0.22	9.68e-1
ABCB6	20.41	-0.09	0.23	9.90e-1
ABCB7	149.01	0.3	0.23	9.20e-1
ABCB8	338.42	-0.32	0.25	9.21e-1
ABCB9	42.99	-0.35	0.25	8.91e-1
ABCC1	1076.02	-0.18	0.19	9.72e-1
ABCC10	72.83	-0.21	0.25	9.81e-1
ABCC4	271.64	0.16	0.23	9.87e-1
ABCC5	330.1	0.17	0.21	9.81e-1
ABCD1	21.88	0.01	0.24	9.96e-1
ABCD3	413.17	0.2	0.22	9.66e-1
ABCD4	214.84	0.13	0.22	9.90e-1
ABCE1	2681.08	-0.11	0.19	9.90e-1
ABCF1	1816.71	-0.4	0.19	6.03e-1
ABCF2	1759.61	-0.18	0.18	9.61e-1
ABCF3	397.09	0	0.21	9.98e-1
ABHD11	124.69	0.13	0.24	9.90e-1
ABHD12	143.2	0.36	0.23	8.49e-1
ABHD13	98.17	0.22	0.25	9.72e-1
ABHD14B	204.13	-0.35	0.23	8.47e-1
ABHD15	89.57	0.11	0.25	9.90e-1
ABHD16A	126.63	0.07	0.24	9.93e-1
ABHD17A	196.7	0.01	0.24	9.97e-1
ABHD17B	136.68	0.28	0.24	9.47e-1
ABHD17C	75.13	0.3	0.25	9.47e-1
ABHD2	350.21	-0.04	0.21	9.93e-1
ABHD3	209.42	0.2	0.22	9.73e-1
ABHD4	90.04	0.17	0.25	9.88e-1
ABHD5	87.22	0.08	0.25	9.91e-1
ABHD6	142.54	0.54	0.23	5.33e-1
ABI1	774.71	0.23	0.2	9.47e-1
ABI2	519.32	-0.17	0.2	9.80e-1
ABI3	502.13	-0.37	0.23	8.40e-1
ABL1	528.73	-0.26	0.21	9.33e-1
ABL2	451.34	-0.17	0.21	9.81e-1
ABLIM1	259.21	-0.03	0.22	9.93e-1
ABR	1384.41	-0.26	0.19	8.94e-1
ABRACL	96.74	0.58	0.24	4.84e-1
ABT1	270.78	-0.16	0.23	9.87e-1
ABTB1	18.55	0.1	0.23	9.90e-1
ABTB2	38.43	-0.19	0.25	9.87e-1
ACAA1	171.98	0.04	0.23	9.93e-1
ACAA2	158.58	0.49	0.23	6.03e-1
ACACA	1300.97	0.06	0.19	9.92e-1

ACACB	250.17	**0.18**	0.22	**9.83e-1**
ACAD10	100.84	**0.04**	0.24	**9.93e-1**
ACAD11	10.55	**-0.13**	0.21	**9.90e-1**
ACAD8	122.65	**0.11**	0.24	**9.90e-1**
ACAD9	587.4	**-0.39**	0.2	**7.03e-1**
ACADM	1214.95	**0.29**	0.19	**8.61e-1**
ACADS	18.98	**-0.22**	0.23	**9.59e-1**
ACADSB	376.74	**-0.15**	0.21	**9.87e-1**
ACADVL	1368.96	**-0.01**	0.2	**9.96e-1**
ACAP1	399.6	**-0.13**	0.23	**9.90e-1**
ACAP2	544.71	**0.22**	0.21	**9.49e-1**
ACAP3	185.3	**-0.32**	0.24	**9.12e-1**
ACAT1	446.79	**0.12**	0.21	**9.90e-1**
ACAT2	293	**-0.17**	0.21	**9.86e-1**
ACBD3	445.44	**0.32**	0.21	**8.52e-1**
ACBD4	70.06	**-0.23**	0.25	**9.72e-1**
ACBD5	165.46	**0.17**	0.23	**9.87e-1**
ACBD6	227.33	**0.12**	0.22	**9.90e-1**
ACBD7	22.65	**-0.19**	0.24	**9.86e-1**
ACD	209.68	**-0.27**	0.24	**9.49e-1**
ACER3	138.89	**0.11**	0.24	**9.90e-1**
ACIN1	2653.82	**-0.37**	0.2	**7.04e-1**
ACKR3	103.7	**-0.09**	0.24	**9.90e-1**
ACKR4	51.41	**-0.49**	0.25	**6.87e-1**
ACLY	3997.44	**-0.39**	0.19	**6.07e-1**
ACO1	157.51	**0.14**	0.23	**9.90e-1**
ACO2	1658.11	**-0.04**	0.19	**9.93e-1**
ACOT13	76.09	**0.24**	0.25	**9.60e-1**
ACOT7	648.88	**0.12**	0.2	**9.90e-1**
ACOT8	76.32	**-0.15**	0.25	**9.90e-1**
ACOT9	137.52	**-0.04**	0.23	**9.93e-1**
ACOX1	168.53	**0.06**	0.23	**9.93e-1**
ACOX3	77.99	**0.11**	0.25	**9.90e-1**
ACP1	491.87	**0.14**	0.2	**9.88e-1**
ACP2	34.36	**-0.42**	0.25	**8.17e-1**
ACPP	13.93	**-0.21**	0.22	**9.66e-1**
ACRC	26.42	**0.13**	0.25	**9.90e-1**
ACSF2	50.22	**-0.19**	0.25	**9.87e-1**
ACSF3	259.05	**0.06**	0.23	**9.93e-1**
ACSL1	670.74	**0.1**	0.2	**9.90e-1**
ACSL3	562.33	**-0.21**	0.2	**9.54e-1**
ACSL4	1208.39	**-0.02**	0.2	**9.95e-1**
ACSL5	587.14	**0.19**	0.2	**9.60e-1**
ACSS1	524.89	**-0.14**	0.21	**9.90e-1**
ACTA2	30.28	**0.02**	0.25	**9.96e-1**
ACTB	21086.2	**-0.08**	0.18	**9.90e-1**
ACTG1	5576.93	**-0.37**	0.19	**7.04e-1**
ACTL6A	678.98	**0.06**	0.2	**9.92e-1**
ACTN4	2590.08	**-0.49**	0.2	**4.40e-1**
ACTR10	198.75	**0.5**	0.23	**5.86e-1**
ACTR1A	639.6	**-0.11**	0.2	**9.90e-1**
ACTR1B	200.3	**0.1**	0.23	**9.90e-1**
ACTR2	3787.51	**0.04**	0.19	**9.93e-1**
ACTR3	1687.64	**0.25**	0.19	**9.12e-1**
ACTR3B	246.74	**0.05**	0.22	**9.93e-1**
ACTR5	161.91	**0.08**	0.23	**9.90e-1**
ACTR6	160.79	**0.24**	0.23	**9.54e-1**
ACTR8	249.61	**-0.07**	0.22	**9.90e-1**
ACVR1B	80.82	**0.06**	0.25	**9.93e-1**
ACVR2B	30.73	**-0.01**	0.25	**9.97e-1**
ACY3	40.16	**-0.15**	0.25	**9.90e-1**
ACYP1	42.9	**0.29**	0.25	**9.47e-1**
ACYP2	18.87	**0.23**	0.23	**9.60e-1**
ADA	292	**0.44**	0.21	**6.14e-1**
ADAL	125.76	**0.07**	0.24	**9.93e-1**

ADAM10	515.48	**0.12**	0.21	**9.90e-1**
ADAM11	14.89	**-0.08**	0.22	**9.90e-1**
ADAM15	678.58	**-0.4**	0.24	**8.03e-1**
ADAM17	452.27	**0.21**	0.21	**9.58e-1**
ADAM19	362.88	**0.09**	0.21	**9.90e-1**
ADAM1A	45.18	**0.03**	0.25	**9.93e-1**
ADAM22	208.12	**0.11**	0.23	**9.90e-1**
ADAM23	115.82	**-0.17**	0.24	**9.87e-1**
ADAM28	87.08	**-0.32**	0.25	**9.20e-1**
ADAM8	12.74	**-0.11**	0.21	**9.90e-1**
ADAM9	542.7	**0.39**	0.21	**7.22e-1**
ADAMDEC1	43.11	**0.31**	0.25	**9.42e-1**
ADAR	3749.25	**-0.2**	0.18	**9.47e-1**
ADAT1	177.79	**0.07**	0.23	**9.91e-1**
ADAT2	236.2	**0.25**	0.22	**9.47e-1**
ADAT3	11.36	**-0.08**	0.21	**9.90e-1**
ADCK1	104.98	**-0.16**	0.24	**9.89e-1**
ADCK2	268.55	**0.03**	0.23	**9.93e-1**
ADCK3	238.62	**0.1**	0.23	**9.90e-1**
ADCK4	196.79	**-0.4**	0.24	**8.17e-1**
ADCK5	54.24	**-0.05**	0.25	**9.93e-1**
ADCY3	842.89	**-0.21**	0.21	**9.57e-1**
ADCY7	203.08	**0.09**	0.23	**9.90e-1**
ADD1	613.9	**-0.18**	0.2	**9.73e-1**
ADD3	1064.84	**0.31**	0.2	**8.41e-1**
ADGRE5	114.54	**-0.14**	0.24	**9.90e-1**
ADGRF3	26.41	**0.06**	0.25	**9.93e-1**
ADGRG5	27.22	**-0.6**	0.25	**4.62e-1**
ADGRL1	282.47	**-0.43**	0.23	**7.41e-1**
ADH5	521.69	**0.34**	0.2	**8.11e-1**
ADI1	457.32	**0.4**	0.2	**6.80e-1**
ADIPOR1	912.9	**-0.16**	0.19	**9.80e-1**
ADIPOR2	657.87	**0.09**	0.19	**9.90e-1**
ADK	329.64	**0.33**	0.22	**8.52e-1**
ADM5	105.9	**-0.19**	0.25	**9.87e-1**
ADNP	1746.19	**0.15**	0.2	**9.87e-1**
ADNP2	255.9	**-0.24**	0.22	**9.49e-1**
ADO	248.94	**0.06**	0.22	**9.93e-1**
ADORA2A	11.06	**-0.09**	0.21	**9.90e-1**
ADORA2B	36.72	**-0.06**	0.25	**9.93e-1**
ADPGK	425.15	**-0.02**	0.2	**9.95e-1**
ADPRHL1	38.57	**-0.01**	0.25	**9.96e-1**
ADPRHL2	202.65	**-0.07**	0.23	**9.93e-1**
ADPRM	25.8	**0.06**	0.25	**9.93e-1**
ADRBK1	1160.04	**-0.27**	0.21	**9.30e-1**
ADRBK2	646.82	**0.05**	0.2	**9.93e-1**
ADRM1	1134.46	**-0.5**	0.23	**5.86e-1**
ADSL	896.33	**0.18**	0.19	**9.68e-1**
ADSS	564.6	**0.13**	0.2	**9.90e-1**
AEBP2	447.69	**-0.11**	0.21	**9.90e-1**
AEN	507.82	**-0.37**	0.22	**7.99e-1**
AES	912.58	**-0.16**	0.21	**9.87e-1**
AFAP1	14.13	**0.56**	0.22	**4.14e-1**
AFAP1-AS1	139.51	**-0.11**	0.23	**9.90e-1**
AFF1	325.61	**-0.47**	0.22	**5.91e-1**
AFF2	387.83	**-0.5**	0.21	**4.68e-1**
AFF3	665.27	**-0.38**	0.19	**6.79e-1**
AFF4	612.22	**0.08**	0.21	**9.90e-1**
AFG3L1P	357.25	**0.05**	0.21	**9.93e-1**
AFG3L2	1350.74	**0.15**	0.19	**9.81e-1**
AFMID	427.91	**-0.06**	0.2	**9.93e-1**
AFTPH	413.53	**0.06**	0.21	**9.93e-1**
AGA	69.61	**0.47**	0.25	**7.13e-1**
AGAP2	291.31	**-0.26**	0.23	**9.47e-1**
AGAP3	432.21	**-0.32**	0.23	**8.78e-1**

AGAP4	33.21	**-0.07**	0.25	**9.93e-1**
AGAP5	34.46	**-0.05**	0.25	**9.93e-1**
AGAP6	199.04	**-0.12**	0.22	**9.90e-1**
AGBL5	495.13	**-0.28**	0.21	**9.10e-1**
AGER	58.18	**-0.01**	0.25	**9.96e-1**
AGFG1	819.44	**-0.04**	0.21	**9.93e-1**
AGFG2	83.01	**-0.35**	0.25	**8.91e-1**
AGK	309.19	**0.04**	0.22	**9.93e-1**
AGL	424.25	**-0.04**	0.21	**9.93e-1**
AGO1	1409.21	**-0.01**	0.19	**9.96e-1**
AGO2	485.79	**-0.19**	0.2	**9.65e-1**
AGO3	244.02	**0.08**	0.22	**9.90e-1**
AGPAT1	339.16	**-0.26**	0.23	**9.47e-1**
AGPAT2	139.32	**0.04**	0.24	**9.93e-1**
AGPAT3	857.48	**-0.04**	0.2	**9.93e-1**
AGPAT4	71	**0.08**	0.25	**9.92e-1**
AGPAT5	734.3	**0.27**	0.2	**9.10e-1**
AGPAT6	802.32	**0.2**	0.19	**9.53e-1**
AGPS	389.28	**-0.05**	0.21	**9.93e-1**
AGRN	12.06	**-0.03**	0.21	**9.93e-1**
AGTPBP1	407.69	**0.34**	0.22	**8.41e-1**
AGTRAP	87.59	**-0.28**	0.25	**9.47e-1**
AHCTF1	1899.45	**-0.09**	0.2	**9.90e-1**
AHCTF1P1	33.27	**0**	0.25	**9.99e-1**
AHCY	4221.98	**-0.18**	0.2	**9.68e-1**
AHCYL1	761.15	**0.08**	0.19	**9.90e-1**
AHCYL2	170.1	**0.1**	0.23	**9.90e-1**
AHDC1	116.84	**-0.29**	0.25	**9.47e-1**
AHI1	220.56	**-0.01**	0.23	**9.96e-1**
AHRR	26.26	**-0.11**	0.25	**9.90e-1**
AHSA1	2100.92	**-0.28**	0.18	**8.53e-1**
AHSA2	209.56	**-0.04**	0.22	**9.93e-1**
AICDA	152	**-0.74**	0.23	**1.20e-1**
AIDA	286.19	**-0.09**	0.22	**9.90e-1**
AIFM1	715.44	**0.2**	0.19	**9.56e-1**
AIFM2	24.11	**-0.13**	0.25	**9.90e-1**
AIG1	13.78	**0.02**	0.22	**9.93e-1**
AIM1	1388.73	**0.06**	0.19	**9.91e-1**
AIM2	249.78	**0.09**	0.22	**9.90e-1**
AIMP1	453.92	**-0.09**	0.21	**9.90e-1**
AIMP2	549.21	**-0.03**	0.2	**9.93e-1**
AIP	277.95	**0.12**	0.22	**9.90e-1**
AK2	4623.63	**-0.35**	0.18	**6.87e-1**
AK3	617.7	**-0.04**	0.21	**9.93e-1**
AK4	4125.54	**-0.1**	0.18	**9.90e-1**
AK6	199.37	**0.33**	0.23	**8.76e-1**
AK9	34.58	**0.13**	0.25	**9.90e-1**
AKAP1	1479.49	**-0.31**	0.19	**8.14e-1**
AKAP10	211.59	**0.05**	0.23	**9.93e-1**
AKAP11	667.44	**0.24**	0.21	**9.47e-1**
AKAP13	1164.56	**-0.04**	0.19	**9.93e-1**
AKAP17A	584.76	**-0.03**	0.22	**9.93e-1**
AKAP8	431.03	**-0.17**	0.2	**9.81e-1**
AKAP8L	412.74	**-0.1**	0.21	**9.90e-1**
AKAP9	561.76	**-0.06**	0.21	**9.91e-1**
AKIP1	24.27	**0.12**	0.25	**9.90e-1**
AKIRIN1	521.62	**0.07**	0.2	**9.91e-1**
AKIRIN2	557.87	**0.36**	0.2	**7.57e-1**
AKNA	1469.31	**-0.55**	0.22	**4.11e-1**
AKR1A1	845.6	**0.34**	0.2	**8.03e-1**
AKR1B1	838.39	**0.21**	0.19	**9.49e-1**
AKR7A2	254.2	**0.15**	0.22	**9.87e-1**
AKT1	1091.4	**-0.21**	0.21	**9.56e-1**
AKT1S1	553.81	**-0.26**	0.22	**9.42e-1**

AKT2	1279.08	**-0.54**	0.22	**4.40e-1**
AKTIP	36.47	**0.12**	0.25	**9.90e-1**
ALAD	179.6	**-0.1**	0.23	**9.90e-1**
ALAS1	381.49	**0.1**	0.21	**9.90e-1**
ALCAM	258.82	**0.34**	0.22	**8.53e-1**
ALDH16A1	374.23	**-0.11**	0.25	**9.90e-1**
ALDH18A1	1635.08	**-0.11**	0.18	**9.90e-1**
ALDH1B1	205.17	**-0.32**	0.22	**8.69e-1**
ALDH1L1	70.31	**0.27**	0.25	**9.49e-1**
ALDH4A1	32.1	**0.01**	0.25	**9.97e-1**
ALDH5A1	1552.62	**0.48**	0.18	**3.52e-1**
ALDH6A1	138.44	**0.37**	0.23	**8.41e-1**
ALDH9A1	373.25	**0.36**	0.21	**8.04e-1**
ALDOA	7839.85	**-0.14**	0.19	**9.87e-1**
ALDOC	244.79	**-0.06**	0.22	**9.93e-1**
ALG1	271.57	**0.12**	0.21	**9.90e-1**
ALG10	76.55	**-0.1**	0.25	**9.90e-1**
ALG10B	150.28	**0.21**	0.23	**9.74e-1**
ALG11	30.95	**0.04**	0.25	**9.93e-1**
ALG12	104.09	**-0.05**	0.25	**9.93e-1**
ALG13	281.1	**0.15**	0.22	**9.88e-1**
ALG14	32.21	**0.37**	0.25	**8.64e-1**
ALG2	224.66	**0.08**	0.22	**9.90e-1**
ALG3	562.95	**-0.22**	0.21	**9.54e-1**
ALG5	138.3	**0.23**	0.24	**9.61e-1**
ALG6	218.67	**0.04**	0.23	**9.93e-1**
ALG8	392.99	**0.34**	0.22	**8.38e-1**
ALG9	177.46	**0.13**	0.23	**9.90e-1**
ALKBH1	134.96	**0.06**	0.23	**9.93e-1**
ALKBH2	132.93	**-0.01**	0.23	**9.97e-1**
ALKBH3	92.89	**0.1**	0.25	**9.90e-1**
ALKBH4	81.04	**-0.31**	0.25	**9.33e-1**
ALKBH5	661.97	**0.13**	0.2	**9.89e-1**
ALKBH6	81.3	**-0.54**	0.25	**5.94e-1**
ALKBH7	54.58	**0.1**	0.25	**9.90e-1**
ALKBH8	148.16	**0.15**	0.24	**9.90e-1**
ALMS1	706.79	**-0.22**	0.21	**9.49e-1**
ALMS1-IT1	12.73	**-0.33**	0.22	**8.53e-1**
ALOX12-AS1	11.1	**0.07**	0.21	**9.91e-1**
ALOX12B	28.05	**-0.23**	0.25	**9.66e-1**
ALOX5	847	**-0.45**	0.2	**5.79e-1**
ALOX5AP	390.96	**0.15**	0.21	**9.87e-1**
ALPK1	142.05	**0.12**	0.24	**9.90e-1**
ALS2	145.83	**0.06**	0.23	**9.93e-1**
ALYREF	800.88	**0.57**	0.2	**2.45e-1**
AMBRA1	330.35	**-0.3**	0.23	**9.12e-1**
AMD1	1901.85	**-0.1**	0.2	**9.90e-1**
AMDHD2	141.56	**-0.41**	0.25	**8.17e-1**
AMFR	1120.54	**0.7**	0.19	**3.33e-2**
AMH	98.21	**-0.25**	0.25	**9.58e-1**
AMIGO3	53.53	**-0.2**	0.25	**9.86e-1**
AMMECR1	222.66	**0**	0.22	**9.98e-1**
AMMECR1L	151.85	**-0.07**	0.23	**9.91e-1**
AMN1	32.77	**-0.11**	0.25	**9.90e-1**
AMPD2	492.15	**-0.27**	0.22	**9.39e-1**
AMPD3	45.58	**-0.24**	0.25	**9.66e-1**
AMT	17.65	**0.19**	0.23	**9.82e-1**
AMZ1	26.87	**0.03**	0.25	**9.93e-1**
AMZ2	368.45	**-0.09**	0.21	**9.90e-1**
AMZ2P1	84.56	**0.16**	0.25	**9.90e-1**
ANAPC1	1022.79	**-0.06**	0.19	**9.91e-1**
ANAPC10	67.43	**0.2**	0.25	**9.86e-1**
ANAPC11	54.9	**0.14**	0.25	**9.90e-1**
ANAPC13	365.82	**0.41**	0.21	**6.87e-1**
ANAPC15	233.65	**-0.12**	0.23	**9.90e-1**

ANAPC16	318.13	**0.46**	0.21	**5.91e-1**
ANAPC2	270.32	**-0.14**	0.23	**9.90e-1**
ANAPC4	341.69	**0.17**	0.21	**9.83e-1**
ANAPC5	1524.68	**0.32**	0.19	**8.21e-1**
ANAPC7	653.17	**0.04**	0.2	**9.93e-1**
ANGEL1	325.01	**-0.23**	0.21	**9.49e-1**
ANGEL2	225.4	**0.09**	0.22	**9.90e-1**
ANGPTL6	25.03	**0.06**	0.25	**9.93e-1**
ANK1	26.55	**0.07**	0.25	**9.93e-1**
ANK2	137.99	**0.38**	0.23	**8.29e-1**
ANKFY1	730.76	**0.05**	0.19	**9.93e-1**
ANKH	263.87	**0.01**	0.21	**9.96e-1**
ANKHD1	12.08	**0.04**	0.21	**9.93e-1**
ANKHD1-EIF4EBP3	32.77	**-0.26**	0.25	**9.54e-1**
ANKIB1	504.4	**0.09**	0.21	**9.90e-1**
ANKLE1	825.39	**-0.29**	0.21	**9.04e-1**
ANKLE2	590.53	**0.2**	0.2	**9.58e-1**
ANKMY1	130.09	**-0.07**	0.24	**9.92e-1**
ANKMY2	45.35	**-0.15**	0.25	**9.90e-1**
ANKRA2	36.27	**0.21**	0.25	**9.80e-1**
ANKRD10	176.55	**0.48**	0.23	**6.37e-1**
ANKRD11	1165.08	**-0.21**	0.2	**9.50e-1**
ANKRD12	392.36	**-0.12**	0.22	**9.90e-1**
ANKRD13A	1333.32	**0.25**	0.19	**9.14e-1**
ANKRD13B	394.26	**-0.43**	0.22	**6.87e-1**
ANKRD13C	234.86	**0.02**	0.22	**9.93e-1**
ANKRD13D	139.5	**-0.25**	0.24	**9.49e-1**
ANKRD16	81.63	**0.08**	0.25	**9.91e-1**
ANKRD17	2484.5	**-0.31**	0.18	**8.09e-1**
ANKRD23	27.3	**-0.02**	0.25	**9.96e-1**
ANKRD26	322.03	**0**	0.21	**9.99e-1**
ANKRD27	1009.35	**0.07**	0.19	**9.90e-1**
ANKRD28	937.41	**0.29**	0.2	**8.64e-1**
ANKRD32	166.59	**-0.06**	0.23	**9.93e-1**
ANKRD33B	596.02	**0.48**	0.2	**4.62e-1**
ANKRD34A	36.35	**-0.29**	0.25	**9.47e-1**
ANKRD36	80.93	**-0.29**	0.25	**9.47e-1**
ANKRD36B	50.25	**-0.06**	0.25	**9.93e-1**
ANKRD36BP2	241.48	**0.02**	0.22	**9.93e-1**
ANKRD36C	52.05	**-0.43**	0.25	**8.08e-1**
ANKRD39	64.95	**0.03**	0.25	**9.93e-1**
ANKRD40	751.49	**-0.08**	0.2	**9.90e-1**
ANKRD42	37.98	**-0.14**	0.25	**9.90e-1**
ANKRD44	199.38	**0**	0.23	**9.99e-1**
ANKRD46	129.81	**-0.01**	0.24	**9.98e-1**
ANKRD49	132.67	**0.08**	0.23	**9.90e-1**
ANKRD52	1059.6	**-0.62**	0.22	**2.52e-1**
ANKRD54	197.75	**-0.15**	0.23	**9.90e-1**
ANKS1A	274.13	**-0.36**	0.22	**8.12e-1**
ANKS3	45.03	**-0.26**	0.25	**9.52e-1**
ANKS6	415.11	**-0.03**	0.2	**9.93e-1**
ANKZF1	201.2	**-0.05**	0.22	**9.93e-1**
ANLN	577.57	**-0.08**	0.2	**9.90e-1**
ANO10	21.8	**0.11**	0.24	**9.90e-1**
ANO6	220.85	**-0.06**	0.22	**9.93e-1**
ANO8	102.82	**0.04**	0.24	**9.93e-1**
ANP32A	3759.79	**-0.32**	0.18	**7.56e-1**
ANP32B	3721.91	**0.2**	0.18	**9.47e-1**
ANP32E	2927.07	**-0.03**	0.19	**9.93e-1**
ANXA11	465.17	**-0.15**	0.21	**9.88e-1**
ANXA2	48.6	**0.04**	0.25	**9.93e-1**
ANXA4	222.94	**-0.08**	0.22	**9.90e-1**
ANXA5	319.63	**0.07**	0.21	**9.91e-1**
ANXA6	456.92	**0.33**	0.2	**8.30e-1**

ANXA7	703.32	**0.14**	0.2	**9.88e-1**
AOC2	14.32	**-0.07**	0.23	**9.92e-1**
AP1AR	282.11	**0.51**	0.22	**5.42e-1**
AP1B1	1284.81	**-0.37**	0.22	**7.99e-1**
AP1G1	1252.76	**-0.11**	0.19	**9.90e-1**
AP1G2	703.72	**-0.18**	0.21	**9.74e-1**
AP1M1	418.6	**-0.23**	0.22	**9.52e-1**
AP1S1	267.67	**0.04**	0.21	**9.93e-1**
AP1S2	192.02	**0.33**	0.24	**8.82e-1**
AP1S3	223.23	**-0.13**	0.22	**9.90e-1**
AP2A1	756.98	**-0.32**	0.22	**8.66e-1**
AP2A2	361.96	**0.12**	0.21	**9.90e-1**
AP2B1	1255.07	**0.1**	0.19	**9.90e-1**
AP2M1	1169.54	**-0.2**	0.19	**9.51e-1**
AP2S1	170.5	**0.11**	0.23	**9.90e-1**
AP3B1	470.52	**0.13**	0.2	**9.90e-1**
AP3D1	1518.76	**-0.11**	0.19	**9.90e-1**
AP3M1	811.38	**-0.08**	0.2	**9.90e-1**
AP3M2	105.34	**0.2**	0.24	**9.81e-1**
AP3S1	267.5	**0.47**	0.23	**6.07e-1**
AP4B1	228.07	**0.25**	0.22	**9.47e-1**
AP4E1	100.77	**0.19**	0.24	**9.87e-1**
AP4M1	66.59	**-0.11**	0.25	**9.90e-1**
AP4S1	43.89	**-0.18**	0.25	**9.87e-1**
AP5B1	413.93	**-0.4**	0.22	**7.57e-1**
AP5M1	392.88	**0.23**	0.22	**9.49e-1**
AP5S1	67.52	**-0.11**	0.25	**9.90e-1**
AP5Z1	290.3	**-0.28**	0.24	**9.47e-1**
APAF1	92.9	**0.11**	0.25	**9.90e-1**
APBA3	134.96	**-0.03**	0.25	**9.93e-1**
APBB1IP	847.83	**-0.4**	0.19	**6.07e-1**
APBB2	155.26	**-0.07**	0.23	**9.91e-1**
APC	509.39	**-0.17**	0.21	**9.80e-1**
APEH	1131.97	**-0.1**	0.21	**9.90e-1**
APEX1	2857.51	**-0.05**	0.18	**9.93e-1**
APEX2	331.69	**0.02**	0.21	**9.95e-1**
APH1A	809.06	**-0.01**	0.21	**9.96e-1**
API5	1188.6	**-0.14**	0.2	**9.87e-1**
APIP	268.76	**0.51**	0.22	**5.32e-1**
APLF	49.36	**0.39**	0.25	**8.51e-1**
APLP2	1442.58	**0.09**	0.19	**9.90e-1**
APMAP	342.75	**0.12**	0.21	**9.90e-1**
APOA1BP	232.48	**-0.36**	0.23	**8.38e-1**
APOBEC3B	62.74	**1.19**	0.25	**1.51e-3**
APOBEC3C	220.58	**-0.06**	0.23	**9.93e-1**
APOBEC3D	42.47	**0.3**	0.25	**9.47e-1**
APOBEC3F	123.36	**0.43**	0.24	**7.57e-1**
APOBEC3G	325.71	**0.65**	0.21	**1.54e-1**
APOBR	109.85	**-0.39**	0.25	**8.45e-1**
APOL1	10.84	**-0.11**	0.21	**9.90e-1**
APOL2	160.25	**-0.09**	0.23	**9.90e-1**
APOL3	287.13	**0.04**	0.22	**9.93e-1**
APOL6	141.31	**-0.08**	0.24	**9.91e-1**
APOLD1	40.39	**0.29**	0.25	**9.47e-1**
APOM	11.72	**0.09**	0.21	**9.90e-1**
APOO	93.89	**0.13**	0.24	**9.90e-1**
APOOL	268.31	**0.05**	0.22	**9.93e-1**
APOPT1	100.38	**0.1**	0.24	**9.90e-1**
APPBP2	215.98	**0.2**	0.22	**9.74e-1**
APPL1	910.39	**0.01**	0.2	**9.96e-1**
APPL2	72.16	**0.29**	0.25	**9.47e-1**
APRT	217.46	**-0.29**	0.25	**9.47e-1**
APTR	73.62	**0.08**	0.25	**9.91e-1**
APTX	341.5	**0.08**	0.21	**9.90e-1**
AQR	725.53	**0.05**	0.2	**9.93e-1**

ARAF	477.01	**-0.16**	0.21	**9.87e-1**
ARAP1	880.14	**-0.32**	0.23	**8.91e-1**
ARAP2	164.93	**-0.05**	0.23	**9.93e-1**
ARCN1	1215.26	**0.16**	0.19	**9.81e-1**
AREL1	375.48	**-0.02**	0.21	**9.95e-1**
ARF1	2249.28	**-0.29**	0.19	**8.53e-1**
ARF3	1718.54	**-0.32**	0.19	**8.10e-1**
ARF4	717.3	**-0.07**	0.19	**9.90e-1**
ARF5	475.27	**0.07**	0.22	**9.90e-1**
ARF6	914.27	**0.01**	0.19	**9.96e-1**
ARFGAP1	554.73	**-0.25**	0.23	**9.49e-1**
ARFGAP2	594.48	**-0.06**	0.21	**9.93e-1**
ARFGAP3	186.72	**0.52**	0.23	**5.37e-1**
ARFGEF1	561.35	**0.22**	0.21	**9.49e-1**
ARFGEF2	1539.78	**0.21**	0.19	**9.49e-1**
ARFIP1	135.47	**0.11**	0.24	**9.90e-1**
ARFIP2	364.13	**-0.14**	0.21	**9.88e-1**
ARFRP1	408.87	**0.11**	0.22	**9.90e-1**
ARG2	50.56	**0.16**	0.25	**9.90e-1**
ARGLU1	774.93	**-0.13**	0.2	**9.90e-1**
ARHGAP1	516.1	**-0.27**	0.21	**9.12e-1**
ARHGAP10	116.05	**-0.3**	0.24	**9.36e-1**
ARHGAP11A	1434.17	**-0.26**	0.19	**8.80e-1**
ARHGAP11B	77.39	**-0.08**	0.25	**9.91e-1**
ARHGAP12	179.44	**0.17**	0.23	**9.87e-1**
ARHGAP15	81.63	**-0.17**	0.25	**9.89e-1**
ARHGAP17	724.85	**0.33**	0.2	**8.04e-1**
ARHGAP18	36.22	**0.04**	0.25	**9.93e-1**
ARHGAP19	357.95	**0.06**	0.21	**9.92e-1**
ARHGAP21	414.77	**-0.26**	0.21	**9.30e-1**
ARHGAP24	57.2	**-0.06**	0.25	**9.93e-1**
ARHGAP25	220.32	**-0.05**	0.22	**9.93e-1**
ARHGAP26	210.74	**-0.12**	0.22	**9.90e-1**
ARHGAP27	232.96	**-0.39**	0.24	**8.12e-1**
ARHGAP30	2087.67	**-0.4**	0.22	**7.57e-1**
ARHGAP32	14.15	**-0.08**	0.23	**9.90e-1**
ARHGAP33	122.1	**-0.46**	0.25	**7.49e-1**
ARHGAP35	1102.68	**-0.4**	0.19	**6.22e-1**
ARHGAP39	50.52	**-0.01**	0.25	**9.97e-1**
ARHGAP4	558.08	**-0.08**	0.23	**9.90e-1**
ARHGAP44	74.29	**0.01**	0.25	**9.96e-1**
ARHGAP5	304.36	**-0.2**	0.22	**9.66e-1**
ARHGAP9	39.07	**0.17**	0.25	**9.89e-1**
ARHGDIA	2344.86	**-0.24**	0.24	**9.56e-1**
ARHGDIB	2741.18	**-0.35**	0.18	**6.87e-1**
ARHGEF1	897.53	**-0.19**	0.21	**9.72e-1**
ARHGEF12	188.4	**0.33**	0.23	**8.68e-1**
ARHGEF18	1272.45	**-0.22**	0.21	**9.49e-1**
ARHGEF2	1216.44	**-0.3**	0.2	**8.53e-1**
ARHGEF26	57.71	**-0.1**	0.25	**9.90e-1**
ARHGEF3	14.68	**-0.22**	0.23	**9.59e-1**
ARHGEF39	135.53	**-0.14**	0.23	**9.90e-1**
ARHGEF6	436.44	**-0.28**	0.2	**9.04e-1**
ARHGEF7	565.76	**0.18**	0.2	**9.66e-1**
ARHGEF9	121.6	**0.07**	0.24	**9.93e-1**
ARID1A	2308.95	**-0.48**	0.19	**3.77e-1**
ARID1B	811.18	**-0.09**	0.19	**9.90e-1**
ARID2	414.88	**-0.13**	0.21	**9.90e-1**
ARID3A	34.47	**0.01**	0.25	**9.96e-1**
ARID3B	20.11	**-0.28**	0.24	**9.47e-1**
ARID4A	309.68	**-0.24**	0.21	**9.47e-1**
ARID4B	543.87	**0.07**	0.2	**9.90e-1**
ARID5A	77.14	**-0.31**	0.25	**9.42e-1**
ARID5B	13.21	**0.28**	0.21	**9.12e-1**
ARIH1	621.48	**0.18**	0.21	**9.74e-1**

ARIH2	1308.34	**-0.02**	0.19	**9.94e-1**
ARL1	183.97	**-0.02**	0.23	**9.93e-1**
ARL11	101.86	**0.05**	0.24	**9.93e-1**
ARL13B	114.37	**-0.06**	0.24	**9.93e-1**
ARL14EP	338.76	**0.13**	0.22	**9.90e-1**
ARL15	139.89	**-0.33**	0.24	**8.91e-1**
ARL16	106.14	**0.01**	0.24	**9.96e-1**
ARL17A	37.79	**-0.12**	0.25	**9.90e-1**
ARL2	89.15	**-0.08**	0.25	**9.90e-1**
ARL2BP	414.18	**-0.12**	0.2	**9.90e-1**
ARL3	127.33	**-0.26**	0.24	**9.49e-1**
ARL4A	45.06	**0.03**	0.25	**9.93e-1**
ARL5A	897.86	**0.02**	0.21	**9.96e-1**
ARL5B	177.22	**0.4**	0.23	**7.87e-1**
ARL6	36	**-0.22**	0.25	**9.77e-1**
ARL6IP1	1162.36	**0.36**	0.2	**7.35e-1**
ARL6IP4	466.81	**-0.12**	0.23	**9.90e-1**
ARL6IP5	204.43	**0.14**	0.22	**9.90e-1**
ARL6IP6	177.86	**0.5**	0.23	**5.84e-1**
ARL8A	167.38	**0.1**	0.24	**9.90e-1**
ARL8B	587.05	**0.31**	0.21	**8.64e-1**
ARMC1	610.22	**0.18**	0.21	**9.79e-1**
ARMC10	787.73	**0.43**	0.21	**6.49e-1**
ARMC2	34.27	**0.13**	0.25	**9.90e-1**
ARMC5	89.4	**-0.15**	0.25	**9.90e-1**
ARMC6	591.37	**-0.15**	0.23	**9.88e-1**
ARMC7	64.03	**-0.35**	0.25	**8.92e-1**
ARMC8	318.03	**0**	0.22	**9.98e-1**
ARMC9	65.53	**0.25**	0.25	**9.59e-1**
ARMCX6	26.08	**-0.28**	0.25	**9.47e-1**
ARMT1	213.55	**-0.15**	0.22	**9.88e-1**
ARNT	250.58	**-0.09**	0.22	**9.90e-1**
ARPC1A	1030.42	**-0.07**	0.19	**9.90e-1**
ARPC1B	2146.49	**0.15**	0.2	**9.86e-1**
ARPC2	2420.22	**0.1**	0.18	**9.90e-1**
ARPC3	963.13	**0.33**	0.2	**7.97e-1**
ARPC4	196.51	**-0.02**	0.23	**9.96e-1**
ARPC5	789.36	**0.02**	0.2	**9.95e-1**
ARPC5L	233.43	**0.42**	0.22	**6.87e-1**
ARPP19	1886.3	**-0.03**	0.2	**9.93e-1**
ARRB2	303.18	**-0.3**	0.22	**8.80e-1**
ARRDC1	149.31	**-0.26**	0.25	**9.54e-1**
ARRDC1-AS1	122.87	**-0.26**	0.25	**9.49e-1**
ARRDC2	150	**-0.04**	0.24	**9.93e-1**
ARRDC3	60.49	**-0.37**	0.25	**8.64e-1**
ARSA	133.52	**-0.4**	0.25	**8.40e-1**
ARSB	114.32	**0.08**	0.24	**9.90e-1**
ARSG	44.01	**0.08**	0.25	**9.91e-1**
ARSK	49.19	**0.09**	0.25	**9.90e-1**
ARV1	75.08	**0.28**	0.25	**9.47e-1**
ARVCF	26.07	**-0.1**	0.24	**9.90e-1**
ASAH1	659.46	**0.7**	0.21	**8.70e-2**
ASAP1	640.88	**-0.09**	0.2	**9.90e-1**
ASAP3	75.73	**-0.32**	0.25	**9.16e-1**
ASB1	320.82	**-0.05**	0.21	**9.93e-1**
ASB13	444.97	**-0.1**	0.21	**9.90e-1**
ASB16-AS1	83.38	**-0.38**	0.25	**8.45e-1**
ASB6	164.02	**-0.32**	0.23	**8.92e-1**
ASB7	148.2	**0.18**	0.23	**9.86e-1**
ASB8	156.45	**-0.09**	0.23	**9.90e-1**
ASCC1	259.8	**0.09**	0.22	**9.90e-1**
ASCC2	526.35	**-0.02**	0.2	**9.93e-1**
ASCC3	1497.27	**0.04**	0.2	**9.93e-1**
ASF1A	416.76	**-0.04**	0.22	**9.93e-1**

ASF1B	481.74	**0.16**	0.21	**9.87e-1**
ASH1L	489.9	**0.05**	0.2	**9.93e-1**
ASH1L-AS1	14.05	**0.1**	0.22	**9.90e-1**
ASH2L	332.27	**0.25**	0.21	**9.45e-1**
ASL	119.08	**-0.03**	0.24	**9.93e-1**
ASMTL	536.94	**-0.19**	0.21	**9.77e-1**
ASMTL-AS1	36.01	**-0.18**	0.25	**9.87e-1**
ASNA1	359.87	**-0.04**	0.21	**9.93e-1**
ASNS	1119.68	**1.35**	0.2	**0.00e+0**
ASNSD1	581.65	**-0.11**	0.2	**9.90e-1**
ASPH	216.36	**0.01**	0.23	**9.96e-1**
ASPHD2	105.07	**0.14**	0.24	**9.90e-1**
ASPM	1195.86	**-0.06**	0.21	**9.91e-1**
ASPSCR1	146.88	**0.09**	0.24	**9.90e-1**
ASTE1	67.01	**-0.03**	0.25	**9.93e-1**
ASTN2	18.49	**0.07**	0.24	**9.93e-1**
ASUN	948.3	**-0.05**	0.19	**9.93e-1**
ASXL1	1441.95	**-0.14**	0.19	**9.87e-1**
ASXL2	570.15	**-0.16**	0.2	**9.81e-1**
ASZ1	10.04	**0.13**	0.21	**9.90e-1**
ATAD1	512.44	**0.18**	0.21	**9.80e-1**
ATAD2	1454.34	**0.09**	0.2	**9.90e-1**
ATAD2B	278.3	**-0.21**	0.22	**9.63e-1**
ATAD3A	749.52	**-0.43**	0.24	**7.41e-1**
ATAD3B	539.46	**-0.45**	0.23	**6.79e-1**
ATAD5	386.98	**-0.04**	0.22	**9.93e-1**
ATAT1	109.03	**-0.14**	0.24	**9.90e-1**
ATE1	485.87	**0.27**	0.21	**9.10e-1**
ATF1	266.41	**0.22**	0.22	**9.58e-1**
ATF2	353.69	**-0.02**	0.22	**9.95e-1**
ATF4	2190.87	**0.34**	0.18	**7.36e-1**
ATF5	277.07	**0.63**	0.24	**3.33e-1**
ATF6	492.55	**0.14**	0.2	**9.87e-1**
ATF6B	985.52	**-0.32**	0.21	**8.48e-1**
ATF7	301.79	**-0.2**	0.21	**9.67e-1**
ATF7IP	815.32	**-0.27**	0.19	**8.91e-1**
ATG101	204.96	**-0.22**	0.24	**9.66e-1**
ATG12	194.76	**0.19**	0.23	**9.80e-1**
ATG13	550.03	**0.22**	0.2	**9.49e-1**
ATG14	104.26	**0.05**	0.24	**9.93e-1**
ATG16L1	191.62	**0.13**	0.22	**9.90e-1**
ATG16L2	115.26	**-0.16**	0.24	**9.90e-1**
ATG2A	331.23	**-0.34**	0.23	**8.56e-1**
ATG2B	558.9	**0.11**	0.21	**9.90e-1**
ATG3	732.15	**0.31**	0.2	**8.52e-1**
ATG4A	93.16	**-0.03**	0.24	**9.93e-1**
ATG4B	423.18	**-0.1**	0.21	**9.90e-1**
ATG4C	196.66	**0.15**	0.23	**9.90e-1**
ATG4D	114.65	**-0.09**	0.25	**9.90e-1**
ATG5	311.88	**0.15**	0.22	**9.88e-1**
ATG7	87.4	**0.14**	0.25	**9.90e-1**
ATG9A	369.25	**-0.3**	0.22	**8.92e-1**
ATG9B	11.21	**-0.32**	0.21	**8.56e-1**
ATHL1	425.58	**-0.25**	0.24	**9.49e-1**
ATIC	1660.58	**0.02**	0.19	**9.93e-1**
ATL2	497.4	**0.24**	0.21	**9.47e-1**
ATL3	295.77	**0.02**	0.21	**9.93e-1**
ATM	575.83	**0.21**	0.21	**9.58e-1**
ATMIN	690.75	**0.32**	0.21	**8.50e-1**
ATN1	701.08	**-0.62**	0.24	**3.64e-1**
ATOX1	162.9	**-0.08**	0.24	**9.90e-1**
ATP10D	232.93	**-0.07**	0.22	**9.91e-1**
ATP11A	373.04	**-0.07**	0.21	**9.90e-1**
ATP11B	507.05	**0.27**	0.21	**9.12e-1**
ATP11C	513.58	**0.12**	0.21	**9.90e-1**

ATP13A1	987.96	**-0.24**	0.21	**9.47e-1**
ATP13A2	93.86	**0.23**	0.25	**9.66e-1**
ATP13A3	1809.88	**0.17**	0.2	**9.80e-1**
ATP1A1	2854.62	**0.02**	0.18	**9.94e-1**
ATP1A1-AS1	10.67	**0.11**	0.21	**9.90e-1**
ATP1A3	994.03	**-0.44**	0.21	**6.07e-1**
ATP1B1	37.82	**0.18**	0.25	**9.87e-1**
ATP1B3	608.38	**0.28**	0.2	**8.68e-1**
ATP2A1	10.25	**-0.08**	0.21	**9.90e-1**
ATP2A1-AS1	37.77	**-0.3**	0.25	**9.45e-1**
ATP2A2	3822.78	**0.13**	0.18	**9.88e-1**
ATP2A3	3485.85	**-0.09**	0.21	**9.90e-1**
ATP2B1	940.39	**-0.01**	0.2	**9.98e-1**
ATP2B4	714.95	**-0.07**	0.19	**9.90e-1**
ATP2C1	391.72	**0.4**	0.22	**7.38e-1**
ATP5A1	3971.74	**0.29**	0.18	**8.39e-1**
ATP5B	5737.77	**0.22**	0.18	**9.25e-1**
ATP5C1	1061.43	**0.1**	0.2	**9.90e-1**
ATP5D	319.58	**0.15**	0.23	**9.90e-1**
ATP5E	16.45	**0.08**	0.23	**9.90e-1**
ATP5F1	1276.44	**0.25**	0.19	**9.12e-1**
ATP5G1	604.54	**-0.23**	0.2	**9.47e-1**
ATP5G2	678.54	**-0.12**	0.21	**9.90e-1**
ATP5G3	857.56	**0.08**	0.19	**9.90e-1**
ATP5H	389.29	**0.14**	0.2	**9.89e-1**
ATP5I	211.2	**0**	0.22	**9.98e-1**
ATP5J	706.36	**-0.3**	0.19	**8.41e-1**
ATP5J2	570.45	**-0.46**	0.2	**5.45e-1**
ATP5L	649.17	**-0.04**	0.19	**9.93e-1**
ATP5O	774.84	**0.33**	0.19	**7.97e-1**
ATP5S	43.32	**-0.09**	0.25	**9.90e-1**
ATP5SL	283.64	**-0.17**	0.23	**9.87e-1**
ATP6AP1	358.29	**0.05**	0.21	**9.93e-1**
ATP6AP2	339.98	**0.37**	0.21	**7.85e-1**
ATP6V0A1	1035.74	**0.11**	0.2	**9.90e-1**
ATP6V0A2	639.42	**0.04**	0.2	**9.93e-1**
ATP6V0B	621.61	**-0.11**	0.22	**9.90e-1**
ATP6V0C	614.93	**0.04**	0.22	**9.93e-1**
ATP6V0D1	300.59	**0.18**	0.21	**9.80e-1**
ATP6V0E1	322.36	**-0.21**	0.21	**9.59e-1**
ATP6V0E2	154.98	**-0.27**	0.24	**9.47e-1**
ATP6V1A	1091.55	**-0.08**	0.19	**9.90e-1**
ATP6V1B1-AS1	23.44	**-0.28**	0.25	**9.47e-1**
ATP6V1B2	532.92	**0.19**	0.2	**9.61e-1**
ATP6V1C1	713.79	**0.14**	0.2	**9.87e-1**
ATP6V1D	143.86	**0.22**	0.24	**9.66e-1**
ATP6V1E1	377.11	**0.27**	0.21	**9.12e-1**
ATP6V1E2	10.82	**0.24**	0.21	**9.47e-1**
ATP6V1F	541.32	**-0.34**	0.23	**8.56e-1**
ATP6V1G1	422.01	**0.03**	0.2	**9.93e-1**
ATP6V1G2	16.39	**0.31**	0.23	**9.08e-1**
ATP6V1H	181.04	**0.41**	0.23	**7.56e-1**
ATP7A	90.2	**0.11**	0.25	**9.90e-1**
ATP8A1	972.19	**0.74**	0.21	**6.62e-2**
ATP8B3	22.85	**-0.1**	0.24	**9.90e-1**
ATP9B	77	**0.22**	0.25	**9.77e-1**
ATPAF1	133.61	**0.13**	0.24	**9.90e-1**
ATPAF2	188.09	**-0.19**	0.23	**9.80e-1**
ATPIF1	434.04	**-0.36**	0.21	**7.80e-1**
ATR	825.15	**0.05**	0.2	**9.93e-1**
ATRAID	283.78	**0.06**	0.22	**9.93e-1**
ATRIP	148.83	**-0.03**	0.23	**9.93e-1**
ATRX	799.76	**-0.06**	0.2	**9.93e-1**
ATXN10	925.22	**0.28**	0.19	**8.73e-1**

ATXN1L	402.76	**-0.35**	0.21	**8.23e-1**
ATXN2	657.96	**-0.5**	0.19	**3.77e-1**
ATXN2L	3031.91	**-0.21**	0.21	**9.58e-1**
ATXN3	164.47	**0.19**	0.23	**9.83e-1**
ATXN7	370	**0.04**	0.21	**9.93e-1**
ATXN7L2	117.98	**-0.2**	0.25	**9.86e-1**
ATXN7L3	514.22	**-0.18**	0.22	**9.80e-1**
ATXN7L3B	532.4	**0.08**	0.2	**9.90e-1**
AUH	71.96	**0.39**	0.25	**8.41e-1**
AUNIP	117.42	**-0.16**	0.24	**9.88e-1**
AUP1	1297.1	**-0.24**	0.21	**9.47e-1**
AURKA	361.17	**-0.32**	0.21	**8.44e-1**
AURKAIP1	266.73	**-0.11**	0.21	**9.90e-1**
AURKB	560.81	**-0.13**	0.2	**9.90e-1**
AUTS2	607.34	**-0.21**	0.2	**9.54e-1**
AVEN	98.09	**0.32**	0.24	**9.12e-1**
AVIL	10.8	**0.18**	0.21	**9.80e-1**
AVL9	710.81	**0.27**	0.2	**9.04e-1**
AXIN1	641.74	**-0.18**	0.22	**9.81e-1**
AXIN2	15.69	**0.13**	0.23	**9.90e-1**
AZI2	136.79	**0.31**	0.24	**9.12e-1**
AZIN1	1817.96	**0.06**	0.19	**9.90e-1**
B2M	2746.07	**0.34**	0.19	**7.23e-1**
B3GALNT2	219.66	**0.01**	0.23	**9.96e-1**
B3GALT6	177.65	**0.24**	0.23	**9.49e-1**
B3GAT3	195.31	**-0.15**	0.24	**9.90e-1**
B3GLCT	123.03	**-0.17**	0.24	**9.87e-1**
B3GNT2	166.09	**0.06**	0.24	**9.93e-1**
B3GNTL1	49.86	**0.26**	0.25	**9.56e-1**
B4GALNT1	111.6	**-0.48**	0.25	**6.83e-1**
B4GALT1	696.84	**-0.2**	0.19	**9.49e-1**
B4GALT2	666.56	**-0.39**	0.22	**7.57e-1**
B4GALT3	333.3	**-0.1**	0.22	**9.90e-1**
B4GALT4	78.91	**0.24**	0.25	**9.60e-1**
B4GALT5	817.62	**0.32**	0.19	**8.07e-1**
B4GALT7	105.57	**-0.09**	0.25	**9.90e-1**
B4GAT1	84.27	**-0.25**	0.25	**9.57e-1**
B9D1	58	**-0.08**	0.25	**9.91e-1**
B9D2	11.9	**0.02**	0.22	**9.96e-1**
BABAM1	613.14	**-0.05**	0.21	**9.93e-1**
BACE2	16.66	**0.27**	0.23	**9.47e-1**
BACH1	167.91	**0.52**	0.24	**5.76e-1**
BACH2	47.17	**-0.23**	0.25	**9.66e-1**
BAD	58.22	**-0.33**	0.25	**9.23e-1**
BAG1	815.37	**0.45**	0.19	**5.27e-1**
BAG2	299.93	**-0.08**	0.21	**9.90e-1**
BAG3	13.76	**-0.27**	0.22	**9.42e-1**
BAG4	259.68	**-0.09**	0.22	**9.90e-1**
BAG5	720.5	**-0.05**	0.19	**9.93e-1**
BAG6	2455.14	**-0.46**	0.23	**6.54e-1**
BAHD1	509.78	**-0.52**	0.22	**5.29e-1**
BAK1	176.58	**-0.43**	0.24	**7.49e-1**
BANF1	804.08	**-0.05**	0.19	**9.93e-1**
BANK1	129.62	**-0.08**	0.24	**9.90e-1**
BANP	123.3	**-0.04**	0.24	**9.93e-1**
BAP1	589.39	**-0.08**	0.21	**9.90e-1**
BARD1	320.41	**0.1**	0.22	**9.90e-1**
BASP1	921.43	**0.26**	0.19	**9.08e-1**
BATF	15.97	**-0.03**	0.23	**9.93e-1**
BAX	285	**-0.1**	0.24	**9.90e-1**
BAZ1A	1942.32	**-0.44**	0.18	**4.78e-1**
BAZ1B	2646.27	**-0.11**	0.18	**9.90e-1**
BAZ2A	2234.46	**-0.56**	0.19	**2.15e-1**
BAZ2B	59.38	**-0.11**	0.25	**9.90e-1**
BBC3	40.14	**0.23**	0.25	**9.72e-1**

BBIP1	67.11	**0.01**	0.25	**9.96e-1**
BBS1	43.93	**-0.03**	0.25	**9.93e-1**
BBS10	80.15	**0.12**	0.25	**9.90e-1**
BBS12	20.17	**0.21**	0.24	**9.74e-1**
BBS2	106.59	**0.34**	0.24	**8.73e-1**
BBS4	77.51	**0.19**	0.25	**9.86e-1**
BBS5	21.98	**-0.14**	0.24	**9.90e-1**
BBS7	133.48	**0.26**	0.24	**9.47e-1**
BBS9	40.13	**0.28**	0.25	**9.49e-1**
BBX	526.89	**-0.1**	0.21	**9.90e-1**
BCAP29	166.19	**0.16**	0.24	**9.89e-1**
BCAP31	440.44	**0.03**	0.22	**9.93e-1**
BCAR3	32.08	**0.1**	0.25	**9.90e-1**
BCAS2	274.2	**0.13**	0.22	**9.90e-1**
BCAS3	26.44	**0.16**	0.25	**9.90e-1**
BCAS4	253.83	**-0.2**	0.23	**9.80e-1**
BCAT1	2489.84	**0.38**	0.19	**6.59e-1**
BCAT2	270	**-0.13**	0.23	**9.90e-1**
BCCIP	807.72	**-0.01**	0.2	**9.96e-1**
BCDIN3D	37.73	**0.14**	0.25	**9.90e-1**
BCKDHA	328.43	**-0.03**	0.22	**9.93e-1**
BCKDHB	284.44	**0.09**	0.22	**9.90e-1**
BCKDK	306.82	**-0.23**	0.23	**9.58e-1**
BCL10	126.08	**0.11**	0.24	**9.90e-1**
BCL11A	488.73	**-0.01**	0.2	**9.96e-1**
BCL2	161.87	**0.72**	0.23	**1.34e-1**
BCL2A1	76.67	**0.54**	0.25	**5.91e-1**
BCL2L1	521.44	**-0.4**	0.22	**7.41e-1**
BCL2L11	871.11	**0.16**	0.19	**9.81e-1**
BCL2L12	209.42	**-0.45**	0.24	**7.31e-1**
BCL2L13	499.96	**0.13**	0.2	**9.90e-1**
BCL3	146.1	**0.08**	0.25	**9.91e-1**
BCL6	2157.64	**-0.22**	0.2	**9.49e-1**
BCL7A	1015.31	**-0.28**	0.19	**8.69e-1**
BCL7B	422.15	**-0.17**	0.22	**9.87e-1**
BCL9	335.08	**-0.56**	0.23	**4.15e-1**
BCL9L	694.41	**-0.63**	0.24	**3.41e-1**
BCLAF1	2887.65	**-0.12**	0.19	**9.90e-1**
BCOR	961.71	**-0.16**	0.2	**9.81e-1**
BCORL1	97.58	**-0.41**	0.25	**8.20e-1**
BCR	258.8	**-0.19**	0.23	**9.81e-1**
BCS1L	374.34	**-0.07**	0.21	**9.90e-1**
BDH1	440.05	**0**	0.22	**9.99e-1**
BDH2	48.54	**0.14**	0.25	**9.90e-1**
BDP1	1238.87	**-0.18**	0.2	**9.68e-1**
BECN1	531.71	**0.04**	0.2	**9.93e-1**
BEND3	296.48	**-0.28**	0.21	**9.12e-1**
BEND4	580.98	**-0.14**	0.21	**9.88e-1**
BET1	166.52	**0.49**	0.23	**6.14e-1**
BET1L	603.86	**-0.14**	0.21	**9.90e-1**
BFAR	505.05	**-0.1**	0.2	**9.90e-1**
BFSP2	32.63	**0.45**	0.25	**7.57e-1**
BHLHE40	43.15	**0.53**	0.25	**6.07e-1**
BICC1	106.61	**-0.38**	0.24	**8.40e-1**
BICD1	219.92	**-0.09**	0.22	**9.90e-1**
BICD2	445.93	**-0.23**	0.2	**9.47e-1**
BID	249.8	**0.1**	0.22	**9.90e-1**
BIK	115.48	**-0.36**	0.25	**8.66e-1**
BIN3	163.87	**-0.07**	0.23	**9.91e-1**
BIRC2	231.11	**0.33**	0.23	**8.73e-1**
BIRC3	7335.76	**0.07**	0.19	**9.90e-1**
BIRC5	785.72	**-0.03**	0.19	**9.93e-1**
BIRC6	1262.18	**0.04**	0.2	**9.93e-1**
BISPR	94.76	**0.01**	0.25	**9.96e-1**
BLCAP	578.03	**0.13**	0.2	**9.90e-1**

BLK	1523.09	**-0.25**	0.2	**9.25e-1**
BLM	382.49	**-0.18**	0.21	**9.77e-1**
BLMH	829.16	**0.01**	0.19	**9.96e-1**
BLNK	416.07	**0.32**	0.2	**8.41e-1**
BLOC1S1	16.13	**-0.05**	0.23	**9.93e-1**
BLOC1S2	144.77	**0.37**	0.24	**8.41e-1**
BLOC1S3	73.34	**-0.04**	0.25	**9.93e-1**
BLOC1S4	24.78	**0.09**	0.25	**9.90e-1**
BLOC1S6	608.88	**0.03**	0.21	**9.93e-1**
BLVRB	63.99	**0.09**	0.25	**9.90e-1**
BLZF1	62.78	**0.07**	0.25	**9.93e-1**
BMF	95.02	**0.49**	0.24	**6.59e-1**
BMI1	18.5	**-0.15**	0.23	**9.90e-1**
BMP1	68.73	**-0.1**	0.25	**9.90e-1**
BMP2K	1197.37	**0.3**	0.2	**8.52e-1**
BMP7	1614.5	**-0.35**	0.19	**7.13e-1**
BMPR1A	131.84	**0.24**	0.24	**9.59e-1**
BMPR2	157.71	**-0.2**	0.23	**9.80e-1**
BMS1	1220.99	**-0.19**	0.19	**9.54e-1**
BMS1P20	255.9	**-0.1**	0.22	**9.90e-1**
BMS1P4	33.24	**-0.02**	0.25	**9.95e-1**
BNC2	26.18	**-0.61**	0.25	**4.44e-1**
BNIP1	59.79	**0.17**	0.25	**9.90e-1**
BNIP2	503.37	**0.06**	0.2	**9.92e-1**
BNIP3L	422.75	**0.54**	0.21	**4.11e-1**
BOD1	217.32	**0.22**	0.22	**9.58e-1**
BOD1L1	792.14	**0.04**	0.2	**9.93e-1**
BOLA3	115.36	**-0.22**	0.24	**9.66e-1**
BOP1	616.7	**-0.46**	0.22	**6.14e-1**
BORA	221.54	**-0.04**	0.22	**9.93e-1**
BPGM	77.99	**0**	0.25	**9.99e-1**
BPHL	89.14	**-0.04**	0.25	**9.93e-1**
BPNT1	580.98	**0.12**	0.2	**9.90e-1**
BPTF	3273.36	**-0.24**	0.19	**9.23e-1**
BRAF	236.28	**0.01**	0.22	**9.96e-1**
BRAP	308.44	**0.02**	0.21	**9.96e-1**
BRAT1	477.9	**-0.23**	0.24	**9.59e-1**
BRCA1	1409.15	**0.04**	0.19	**9.93e-1**
BRCA2	447.03	**-0.09**	0.21	**9.90e-1**
BRCC3	408.49	**-0.07**	0.21	**9.91e-1**
BRD1	287.34	**0.1**	0.21	**9.90e-1**
BRD2	2905.88	**-0.32**	0.2	**8.28e-1**
BRD3	339.65	**-0.07**	0.21	**9.90e-1**
BRD4	1476.81	**-0.31**	0.2	**8.41e-1**
BRD7	1246.98	**-0.01**	0.19	**9.96e-1**
BRD8	610.68	**-0.23**	0.2	**9.47e-1**
BRD9	348.07	**-0.09**	0.21	**9.90e-1**
BRE	126.5	**0.08**	0.24	**9.90e-1**
BRF1	155.96	**-0.34**	0.24	**8.68e-1**
BRF2	49.35	**-0.02**	0.25	**9.95e-1**
BRI3	57.66	**0.69**	0.25	**3.05e-1**
BRI3BP	392.54	**-0.28**	0.21	**9.10e-1**
BRICD5	11.63	**-0.29**	0.21	**9.03e-1**
BRIP1	229.04	**0.04**	0.23	**9.93e-1**
BRIX1	591.25	**-0.03**	0.2	**9.93e-1**
BRK1	443.73	**0.22**	0.2	**9.49e-1**
BRMS1	345.41	**-0.13**	0.22	**9.90e-1**
BRMS1L	120.22	**0.11**	0.24	**9.90e-1**
BROX	244.27	**0.11**	0.22	**9.90e-1**
BRPF1	229.42	**-0.11**	0.23	**9.90e-1**
BRPF3	468.36	**-0.22**	0.21	**9.50e-1**
BRWD1	715.07	**0.22**	0.21	**9.56e-1**
BRWD3	275.57	**-0.14**	0.22	**9.90e-1**
BSCL2	28.37	**-0.32**	0.25	**9.23e-1**

BSDC1	451.97	**0**	0.22	**9.98e-1**
BSG	1296.25	**-0.24**	0.2	**9.42e-1**
BSN	126.43	**0.04**	0.25	**9.93e-1**
BST2	368.97	**-0.19**	0.22	**9.74e-1**
BTAF1	976.62	**0.14**	0.2	**9.88e-1**
BTBD1	1698.73	**0.27**	0.19	**8.80e-1**
BTBD10	163.31	**0.18**	0.23	**9.86e-1**
BTBD2	820.23	**-0.14**	0.22	**9.90e-1**
BTBD6	118.2	**-0.03**	0.24	**9.93e-1**
BTBD7	304.3	**0.16**	0.21	**9.87e-1**
BTBD9	48.65	**-0.11**	0.25	**9.90e-1**
BTF3	2658.59	**0.06**	0.18	**9.91e-1**
BTF3L4	554.08	**0.28**	0.21	**8.97e-1**
BTG1	160.13	**0.53**	0.23	**5.37e-1**
BTG2	1006.71	**-0.41**	0.2	**6.07e-1**
BTG3	116.42	**0.32**	0.24	**9.05e-1**
BTK	1479.16	**-0.12**	0.18	**9.90e-1**
BTN2A1	138.31	**-0.14**	0.23	**9.90e-1**
BTN2A2	299.18	**0.29**	0.22	**9.08e-1**
BTN3A1	166.56	**-0.04**	0.23	**9.93e-1**
BTN3A2	285.43	**-0.06**	0.21	**9.93e-1**
BTN3A3	100.67	**0.06**	0.24	**9.93e-1**
BTRC	239.31	**0**	0.22	**9.98e-1**
BUB1	797.39	**-0.23**	0.2	**9.49e-1**
BUB1B	1478.21	**-0.19**	0.19	**9.54e-1**
BUB3	1025.56	**0.37**	0.2	**7.06e-1**
BUD13	327.88	**-0.34**	0.21	**8.30e-1**
BUD31	528.51	**0.26**	0.2	**9.19e-1**
BYSL	365.66	**-0.27**	0.22	**9.39e-1**
BZRAP1	27.62	**-0.3**	0.24	**9.25e-1**
BZRAP1-AS1	253.05	**-0.22**	0.22	**9.58e-1**
BZW1	1412.68	**0.02**	0.19	**9.93e-1**
BZW2	977.89	**0.22**	0.19	**9.47e-1**
C10orf12	129.2	**-0.14**	0.24	**9.90e-1**
C10orf2	915.32	**-0.44**	0.2	**5.91e-1**
C10orf25	15.32	**0.02**	0.23	**9.96e-1**
C10orf32	28.51	**0.13**	0.25	**9.90e-1**
C10orf76	260.83	**-0.07**	0.21	**9.91e-1**
C10orf88	52.83	**-0.17**	0.25	**9.89e-1**
C10orf91	23.28	**-0.04**	0.24	**9.93e-1**
C11orf1	147.14	**-0.11**	0.23	**9.90e-1**
C11orf24	266.47	**-0.09**	0.22	**9.90e-1**
C11orf30	286.15	**-0.14**	0.21	**9.90e-1**
C11orf31	70.61	**-0.14**	0.25	**9.90e-1**
C11orf49	131.38	**-0.22**	0.23	**9.66e-1**
C11orf54	148.24	**0.21**	0.24	**9.73e-1**
C11orf57	450.96	**-0.38**	0.2	**7.27e-1**
C11orf58	1144.66	**0.1**	0.19	**9.90e-1**
C11orf68	100.48	**-0.04**	0.25	**9.93e-1**
C11orf71	54.57	**0.12**	0.25	**9.90e-1**
C11orf73	113.38	**0**	0.24	**9.98e-1**
C11orf80	27.36	**-0.14**	0.25	**9.90e-1**
C11orf84	245.41	**-0.34**	0.24	**8.73e-1**
C11orf95	204.2	**-0.13**	0.23	**9.90e-1**
C12orf10	231	**0.01**	0.22	**9.96e-1**
C12orf29	296.92	**-0.23**	0.22	**9.49e-1**
C12orf4	186.34	**0.23**	0.23	**9.58e-1**
C12orf43	207.76	**-0.24**	0.22	**9.49e-1**
C12orf45	118.81	**0.02**	0.24	**9.96e-1**
C12orf49	879.31	**-0.22**	0.19	**9.47e-1**
C12orf57	52.28	**0.27**	0.25	**9.49e-1**
C12orf65	121.75	**-0.01**	0.24	**9.96e-1**
C12orf66	131.99	**0.05**	0.23	**9.93e-1**
C12orf73	57.18	**-0.06**	0.25	**9.93e-1**
C12orf75	145.37	**0.51**	0.24	**5.91e-1**

C12orf76	14.53	**0.51**	0.23	**5.47e-1**
C12orf77	44.83	**0.72**	0.25	**2.59e-1**
C14orf1	258.14	**-0.12**	0.21	**9.90e-1**
C14orf119	121.69	**0.09**	0.24	**9.90e-1**
C14orf132	12.48	**-0.13**	0.22	**9.90e-1**
C14orf142	165.7	**0.11**	0.23	**9.90e-1**
C14orf159	479.68	**0.02**	0.2	**9.94e-1**
C14orf166	955.73	**0.16**	0.19	**9.81e-1**
C14orf169	203.54	**-0.17**	0.23	**9.87e-1**
C14orf2	270.2	**0.03**	0.22	**9.93e-1**
C14orf79	11.44	**0.15**	0.22	**9.87e-1**
C14orf80	149.08	**-0.14**	0.25	**9.90e-1**
C14orf93	65.81	**0.02**	0.25	**9.94e-1**
C15orf39	1222.71	**-0.48**	0.23	**6.07e-1**
C15orf40	50.48	**0.12**	0.25	**9.90e-1**
C15orf41	25.13	**-0.17**	0.25	**9.88e-1**
C15orf57	60.44	**-0.06**	0.25	**9.93e-1**
C15orf61	18.19	**0.25**	0.24	**9.49e-1**
C16orf13	227.55	**-0.19**	0.24	**9.85e-1**
C16orf46	29.83	**0.07**	0.25	**9.93e-1**
C16orf52	52.77	**0**	0.25	**9.98e-1**
C16orf54	57.83	**-0.28**	0.25	**9.47e-1**
C16orf58	307.11	**-0.05**	0.23	**9.93e-1**
C16orf59	157.69	**-0.41**	0.25	**8.25e-1**
C16orf62	201.45	**0.3**	0.23	**9.08e-1**
C16orf70	245.66	**-0.03**	0.22	**9.93e-1**
C16orf72	335.3	**0.24**	0.21	**9.47e-1**
C16orf87	160.48	**0.25**	0.23	**9.49e-1**
C16orf91	81.17	**-0.21**	0.25	**9.80e-1**
C16orf93	23.09	**0.12**	0.25	**9.90e-1**
C16orf95	10.49	**0**	0.21	**1.00e+0**
C17orf51	139.6	**-0.27**	0.24	**9.47e-1**
C17orf53	120.2	**-0.02**	0.24	**9.93e-1**
C17orf58	85.56	**0.22**	0.25	**9.72e-1**
C17orf59	26.59	**-0.01**	0.25	**9.96e-1**
C17orf62	414.72	**0.13**	0.22	**9.90e-1**
C17orf75	144.45	**0.19**	0.24	**9.82e-1**
C17orf80	292.47	**-0.01**	0.21	**9.96e-1**
C17orf85	574.89	**0.08**	0.2	**9.90e-1**
C17orf89	79.76	**0.61**	0.25	**4.44e-1**
C17orf96	270.32	**-0.27**	0.24	**9.48e-1**
C17orf97	145.47	**-0.56**	0.24	**5.32e-1**
C18orf21	107.52	**0.2**	0.24	**9.80e-1**
C18orf25	246.6	**0.16**	0.23	**9.87e-1**
C18orf54	75.66	**0.26**	0.25	**9.54e-1**
C18orf8	277.71	**0.27**	0.22	**9.42e-1**
C19orf12	68.78	**0.03**	0.25	**9.93e-1**
C19orf24	168.24	**-0.34**	0.23	**8.66e-1**
C19orf25	131.37	**-0.38**	0.25	**8.64e-1**
C19orf38	11.4	**-0.05**	0.21	**9.93e-1**
C19orf43	603.91	**-0.01**	0.22	**9.96e-1**
C19orf44	63.59	**0.03**	0.25	**9.93e-1**
C19orf47	192.02	**-0.34**	0.24	**8.80e-1**
C19orf48	1025.16	**-0.19**	0.23	**9.81e-1**
C19orf52	45.65	**0.03**	0.25	**9.93e-1**
C19orf53	257.62	**-0.26**	0.23	**9.47e-1**
C19orf54	220.03	**-0.07**	0.24	**9.93e-1**
C19orf57	51.69	**-0.13**	0.25	**9.90e-1**
C19orf60	71.67	**0.04**	0.25	**9.93e-1**
C19orf66	116.31	**-0.28**	0.24	**9.47e-1**
C19orf68	69.1	**-0.63**	0.25	**4.17e-1**
C19orf70	58.47	**-0.21**	0.25	**9.82e-1**
C1D	181.43	**0.05**	0.24	**9.93e-1**
C1GALT1	206.19	**0.04**	0.23	**9.93e-1**
C1GALT1C1	68.38	**0.04**	0.25	**9.93e-1**

C1orf109	229.01	**-0.13**	0.22	**9.90e-1**
C1orf112	143.08	**0.14**	0.23	**9.90e-1**
C1orf122	57.7	**0.07**	0.25	**9.93e-1**
C1orf123	212.52	**0.27**	0.22	**9.42e-1**
C1orf131	193.36	**-0.28**	0.23	**9.34e-1**
C1orf159	102.01	**-0.36**	0.25	**8.73e-1**
C1orf174	183.24	**0.24**	0.23	**9.49e-1**
C1orf186	62.5	**0.2**	0.25	**9.83e-1**
C1orf198	96.36	**-0.15**	0.24	**9.90e-1**
C1orf21	65.77	**-0.26**	0.25	**9.49e-1**
C1orf216	68.52	**0.2**	0.25	**9.81e-1**
C1orf220	11.21	**-0.02**	0.21	**9.93e-1**
C1orf27	125.49	**-0.03**	0.25	**9.93e-1**
C1orf35	48.16	**-0.11**	0.25	**9.90e-1**
C1orf43	1113.4	**0.12**	0.19	**9.90e-1**
C1orf50	65.29	**-0.14**	0.25	**9.90e-1**
C1orf52	115.57	**0.19**	0.24	**9.82e-1**
C1orf74	63.73	**0.06**	0.25	**9.93e-1**
C1QBP	1995.58	**0.41**	0.19	**5.83e-1**
C1QTNF9B-AS1	23.06	**-0.27**	0.25	**9.49e-1**
C20orf196	63.22	**0.3**	0.25	**9.47e-1**
C20orf24	69.53	**-0.47**	0.25	**7.21e-1**
C20orf27	498.77	**-0.44**	0.24	**7.29e-1**
C20orf96	21.07	**-0.16**	0.24	**9.89e-1**
C21orf2	36.51	**0.18**	0.25	**9.87e-1**
C21orf33	650.1	**0.44**	0.2	**5.86e-1**
C21orf58	171.19	**-0.36**	0.25	**8.69e-1**
C21orf59	570.22	**0.19**	0.2	**9.63e-1**
C21orf91	567.46	**0.12**	0.2	**9.90e-1**
C22orf29	283.9	**-0.22**	0.22	**9.56e-1**
C22orf34	126.55	**-0.07**	0.24	**9.92e-1**
C22orf39	122.57	**0.24**	0.24	**9.54e-1**
C22orf46	134.76	**-0.35**	0.24	**8.73e-1**
C2CD2L	117.59	**-0.11**	0.24	**9.90e-1**
C2CD3	433.37	**-0.13**	0.2	**9.90e-1**
C2CD5	341.66	**0.27**	0.21	**9.23e-1**
C2orf15	16.57	**0.03**	0.23	**9.93e-1**
C2orf42	64.92	**0.07**	0.25	**9.93e-1**
C2orf44	434.07	**-0.2**	0.21	**9.66e-1**
C2orf47	100.81	**0.05**	0.24	**9.93e-1**
C2orf49	224.92	**-0.18**	0.22	**9.86e-1**
C2orf68	158.36	**-0.07**	0.23	**9.93e-1**
C2orf69	212.73	**0.15**	0.23	**9.89e-1**
C2orf74	89.58	**0.05**	0.25	**9.93e-1**
C2orf76	22.1	**-0.11**	0.24	**9.90e-1**
C2orf81	58.91	**0.22**	0.25	**9.74e-1**
C3orf17	321.02	**0.46**	0.22	**6.03e-1**
C3orf18	28.92	**-0.01**	0.25	**9.96e-1**
C3orf20	56.28	**0.09**	0.25	**9.90e-1**
C3orf38	134.25	**-0.02**	0.23	**9.95e-1**
C3orf58	204.51	**0.07**	0.23	**9.92e-1**
C3orf62	45.39	**0.05**	0.25	**9.93e-1**
C3orf67	14.64	**-0.11**	0.23	**9.90e-1**
C4orf27	112.68	**0.08**	0.24	**9.91e-1**
C4orf29	138.96	**0.17**	0.24	**9.88e-1**
C4orf3	213.96	**0.03**	0.22	**9.93e-1**
C4orf32	693.78	**-0.5**	0.21	**5.09e-1**
C4orf33	29.79	**0.23**	0.25	**9.68e-1**
C4orf46	349.21	**0.26**	0.22	**9.47e-1**
C5	25.6	**-0.07**	0.25	**9.93e-1**
C5orf15	262.44	**-0.32**	0.22	**8.64e-1**
C5orf22	223.49	**0.03**	0.22	**9.93e-1**
C5orf24	339.3	**0.26**	0.22	**9.47e-1**
C5orf28	57.03	**0.34**	0.25	**9.07e-1**

C5orf30	218.27	**0.18**	0.22	**9.86e-1**
C5orf34	81.2	**0.11**	0.25	**9.90e-1**
C5orf42	66.34	**-0.01**	0.25	**9.98e-1**
C5orf45	55.72	**0.06**	0.25	**9.93e-1**
C5orf51	486.91	**0.15**	0.21	**9.87e-1**
C5orf66	11.55	**0.19**	0.21	**9.74e-1**
C6orf1	69.16	**-0.11**	0.25	**9.90e-1**
C6orf106	1284.44	**-0.12**	0.2	**9.90e-1**
C6orf120	208.26	**0.23**	0.23	**9.56e-1**
C6orf136	198.4	**-0.41**	0.24	**7.79e-1**
C6orf203	118.7	**0**	0.24	**9.98e-1**
C6orf223	149.66	**-0.47**	0.25	**7.04e-1**
C6orf47	78.19	**-0.03**	0.25	**9.93e-1**
C6orf48	211.9	**0.24**	0.23	**9.50e-1**
C6orf62	545.11	**0.47**	0.21	**5.86e-1**
C6orf89	517.79	**0.17**	0.2	**9.80e-1**
C7orf13	25.82	**-0.01**	0.25	**9.98e-1**
C7orf25	83.72	**0.16**	0.25	**9.90e-1**
C7orf26	274.38	**0.13**	0.21	**9.90e-1**
C7orf31	88.73	**0.14**	0.25	**9.90e-1**
C7orf43	167.88	**-0.06**	0.24	**9.93e-1**
C7orf49	287.91	**0.18**	0.21	**9.80e-1**
C7orf50	171.56	**-0.21**	0.24	**9.74e-1**
C7orf60	49.2	**0.28**	0.25	**9.49e-1**
C7orf73	456.38	**-0.01**	0.2	**9.96e-1**
C8orf33	420.45	**-0.43**	0.2	**6.03e-1**
C8orf37	67.74	**-0.18**	0.25	**9.88e-1**
C8orf44	13.92	**0**	0.22	**9.98e-1**
C8orf58	10.85	**-0.05**	0.21	**9.93e-1**
C8orf59	76.82	**0.06**	0.25	**9.93e-1**
C8orf82	51.87	**-0.16**	0.25	**9.90e-1**
C9orf114	591.47	**-0.29**	0.23	**9.23e-1**
C9orf116	14.55	**0.22**	0.23	**9.60e-1**
C9orf142	81.44	**-0.25**	0.25	**9.60e-1**
C9orf156	75.73	**0.03**	0.25	**9.93e-1**
C9orf16	121.8	**-0.1**	0.19	**9.90e-1**
C9orf172	22.16	**-0.17**	0.24	**9.87e-1**
C9orf3	21.18	**0.11**	0.24	**9.90e-1**
C9orf40	111.56	**0.18**	0.24	**9.87e-1**
C9orf41	300.6	**-0.02**	0.22	**9.94e-1**
C9orf69	231.86	**-0.32**	0.25	**9.20e-1**
C9orf72	89.77	**0.3**	0.25	**9.42e-1**
C9orf78	1120.6	**-0.5**	0.19	**3.77e-1**
C9orf85	55.86	**0.04**	0.25	**9.93e-1**
C9orf89	24.51	**0.04**	0.24	**9.93e-1**
C9orf9	11.28	**0.02**	0.21	**9.96e-1**
C9orf91	365.71	**0.16**	0.21	**9.86e-1**
CA11	31.09	**-0.28**	0.25	**9.47e-1**
CA5B	29.83	**0.04**	0.25	**9.93e-1**
CA5BP1	54.66	**-0.08**	0.25	**9.91e-1**
CAAP1	230.82	**-0.04**	0.22	**9.93e-1**
CAB39	819.04	**0.43**	0.21	**6.11e-1**
CAB39L	84.59	**-0.29**	0.25	**9.47e-1**
CABIN1	813.16	**-0.42**	0.21	**6.79e-1**
CABLES2	281.73	**-0.14**	0.21	**9.90e-1**
CACFD1	11.57	**0.02**	0.21	**9.94e-1**
CACNB1	186.22	**-0.46**	0.24	**7.06e-1**
CACNB4	42.78	**0.28**	0.25	**9.49e-1**
CACTIN	318.59	**-0.32**	0.23	**8.73e-1**
CACUL1	437.45	**0.08**	0.21	**9.90e-1**
CACYBP	1330.29	**-0.16**	0.19	**9.80e-1**
CAD	1968.94	**-0.29**	0.2	**8.73e-1**
CADPS	190.26	**0.18**	0.22	**9.86e-1**
CALCOCO1	76.27	**0.44**	0.25	**7.66e-1**
CALCOCO2	253.77	**0.42**	0.22	**6.86e-1**

CALM1	1611.18	**0.08**	0.19	**9.90e-1**
CALM2	2164.63	**0.35**	0.2	**7.56e-1**
CALM3	1928.21	**-0.12**	0.19	**9.90e-1**
CALML4	91.21	**-0.18**	0.24	**9.87e-1**
CALR	7513.78	**0.01**	0.18	**9.96e-1**
CALU	1305.85	**-0.03**	0.19	**9.93e-1**
CAMK1D	165.56	**0.16**	0.23	**9.88e-1**
CAMK2D	341.81	**-0.05**	0.21	**9.93e-1**
CAMK2G	300.91	**-0.09**	0.21	**9.90e-1**
CAMKK1	51.86	**-0.46**	0.25	**7.41e-1**
CAMKK2	764.28	**-0.24**	0.19	**9.25e-1**
CAMKMT	54.38	**0.18**	0.25	**9.87e-1**
CAMLG	226.47	**0.49**	0.22	**5.79e-1**
CAMSAP1	782.73	**-0.14**	0.19	**9.87e-1**
CAMSAP2	364.55	**-0.24**	0.21	**9.47e-1**
CAMSAP3	10.28	**-0.04**	0.21	**9.93e-1**
CAMTA1	127.49	**0.25**	0.24	**9.50e-1**
CAMTA2	370.61	**-0.33**	0.24	**8.91e-1**
CAND1	1740.03	**0.2**	0.2	**9.57e-1**
CANT1	236.13	**-0.14**	0.23	**9.90e-1**
CANX	7611.17	**0.17**	0.18	**9.72e-1**
CAP1	3103.94	**-0.13**	0.18	**9.87e-1**
CAPN1	569.74	**-0.27**	0.22	**9.33e-1**
CAPN10	118.75	**-0.29**	0.25	**9.47e-1**
CAPN10-AS1	41.61	**-0.09**	0.25	**9.90e-1**
CAPN15	599.8	**-0.21**	0.24	**9.73e-1**
CAPN7	359.85	**0.2**	0.21	**9.66e-1**
CAPNS1	902.28	**-0.08**	0.19	**9.90e-1**
CAPRIN1	4417.36	**-0.1**	0.19	**9.90e-1**
CAPRIN2	36.66	**0.1**	0.25	**9.90e-1**
CAPZA1	1870.2	**0.28**	0.2	**8.73e-1**
CAPZA2	553.7	**0.25**	0.21	**9.42e-1**
CAPZB	1071.18	**-0.08**	0.19	**9.90e-1**
CARD11	1532.81	**0.15**	0.19	**9.87e-1**
CARD6	30.75	**-0.28**	0.25	**9.47e-1**
CARD8	137.35	**0.34**	0.24	**8.69e-1**
CARD8-AS1	43.12	**0.03**	0.25	**9.93e-1**
CARF	36.75	**0.22**	0.25	**9.80e-1**
CARHSP1	194.27	**0.04**	0.23	**9.93e-1**
CARM1	1884.79	**-0.37**	0.2	**6.90e-1**
CARS	361.56	**0.61**	0.21	**2.15e-1**
CARS2	347.55	**-0.04**	0.21	**9.93e-1**
CASC11	222.4	**0.33**	0.22	**8.64e-1**
CASC3	1275.99	**-0.21**	0.19	**9.49e-1**
CASC4	491.61	**0.3**	0.21	**8.79e-1**
CASC5	607.53	**-0.08**	0.21	**9.90e-1**
CASD1	220.82	**0.28**	0.23	**9.33e-1**
CASK	233.54	**-0.07**	0.22	**9.92e-1**
CASP2	1025.38	**-0.09**	0.19	**9.90e-1**
CASP3	205.32	**0.18**	0.22	**9.81e-1**
CASP4	30.08	**-0.02**	0.25	**9.95e-1**
CASP7	222.3	**0.02**	0.22	**9.93e-1**
CASP8	177.75	**0.01**	0.23	**9.96e-1**
CASP8AP2	558.82	**0.02**	0.2	**9.93e-1**
CASP9	92	**-0.29**	0.25	**9.47e-1**
CAST	695.5	**0.27**	0.21	**9.19e-1**
CASZ1	170.73	**-0.41**	0.23	**7.44e-1**
CAT	457.38	**-0.09**	0.2	**9.90e-1**
CBFA2T2	256.42	**0.01**	0.22	**9.96e-1**
CBFA2T3	15.95	**0.05**	0.23	**9.93e-1**
CBFB	1074.04	**0.19**	0.2	**9.66e-1**
CBL	482.74	**-0.27**	0.2	**9.06e-1**
CBLB	203.04	**0**	0.22	**9.98e-1**
CBLL1	788.54	**-0.21**	0.19	**9.49e-1**

CBLN3	68.69	**0.38**	0.25	**8.52e-1**
CBR4	159.88	**0.06**	0.23	**9.93e-1**
CBS	942.72	**-0.05**	0.21	**9.93e-1**
CBWD1	411.76	**-0.32**	0.2	**8.40e-1**
CBWD2	161.91	**-0.17**	0.23	**9.87e-1**
CBWD3	10.09	**0.04**	0.21	**9.93e-1**
CBWD5	195.55	**-0.52**	0.23	**5.45e-1**
CBWD6	13.6	**0.11**	0.22	**9.90e-1**
CBX1	887.68	**0.05**	0.19	**9.93e-1**
CBX2	452.62	**-0.38**	0.22	**7.97e-1**
CBX3	2647.66	**0.17**	0.19	**9.74e-1**
CBX4	230.16	**-0.12**	0.23	**9.90e-1**
CBX5	2067.32	**0.07**	0.18	**9.90e-1**
CBX6	1522.4	**-0.04**	0.24	**9.93e-1**
CBX7	142.51	**0.07**	0.25	**9.93e-1**
CBX8	71.62	**-0.34**	0.25	**9.10e-1**
CBY1	27.81	**0.07**	0.25	**9.92e-1**
CC2D1A	483.43	**-0.48**	0.22	**5.94e-1**
CC2D1B	266.47	**0.07**	0.22	**9.91e-1**
CCAR1	1757.3	**-0.33**	0.19	**7.49e-1**
CCAR2	1873.82	**-0.36**	0.21	**7.57e-1**
CCBL1	125.39	**-0.33**	0.24	**9.06e-1**
CCBL2	102.21	**0.33**	0.25	**9.10e-1**
CCDC101	171.1	**0.12**	0.23	**9.90e-1**
CCDC102A	62.18	**-0.14**	0.25	**9.90e-1**
CCDC106	150.1	**-0.1**	0.25	**9.90e-1**
CCDC107	41.95	**-0.02**	0.25	**9.96e-1**
CCDC109B	361.36	**0.54**	0.22	**4.46e-1**
CCDC112	72.54	**-0.21**	0.25	**9.80e-1**
CCDC115	103.79	**-0.52**	0.25	**6.03e-1**
CCDC117	716.93	**-0.09**	0.21	**9.90e-1**
CCDC12	317.47	**-0.24**	0.24	**9.58e-1**
CCDC122	43.86	**-0.11**	0.25	**9.90e-1**
CCDC124	512.09	**-0.19**	0.23	**9.81e-1**
CCDC125	156.05	**0.02**	0.23	**9.95e-1**
CCDC126	39.18	**0.23**	0.25	**9.71e-1**
CCDC127	76.55	**0.32**	0.25	**9.23e-1**
CCDC130	113.24	**-0.22**	0.25	**9.74e-1**
CCDC134	37.88	**-0.23**	0.25	**9.73e-1**
CCDC136	15.08	**0.1**	0.22	**9.90e-1**
CCDC137	309.73	**-0.16**	0.23	**9.88e-1**
CCDC138	119.48	**0.4**	0.24	**8.10e-1**
CCDC14	485.21	**0.2**	0.2	**9.58e-1**
CCDC142	81.43	**-0.19**	0.25	**9.87e-1**
CCDC146	18.37	**0.31**	0.24	**9.12e-1**
CCDC15	68.74	**-0.2**	0.25	**9.86e-1**
CCDC150	54.31	**0.37**	0.25	**8.68e-1**
CCDC157	12.26	**-0.03**	0.22	**9.93e-1**
CCDC159	13.11	**0.13**	0.22	**9.90e-1**
CCDC163P	45.57	**-0.06**	0.25	**9.93e-1**
CCDC167	168.4	**-0.08**	0.23	**9.90e-1**
CCDC17	18.24	**0.06**	0.24	**9.93e-1**
CCDC171	48.82	**0.08**	0.25	**9.91e-1**
CCDC174	194.89	**-0.14**	0.22	**9.90e-1**
CCDC176	17.66	**0.07**	0.23	**9.91e-1**
CCDC18	331.52	**0.07**	0.22	**9.90e-1**
CCDC183-AS1	158.31	**-0.74**	0.24	**1.79e-1**
CCDC186	227.4	**0.16**	0.23	**9.88e-1**
CCDC22	115.02	**-0.17**	0.25	**9.88e-1**
CCDC24	22.83	**-0.27**	0.24	**9.47e-1**
CCDC25	512.79	**0.06**	0.2	**9.91e-1**
CCDC28A	74.75	**0.19**	0.25	**9.87e-1**
CCDC28B	342.51	**0.17**	0.23	**9.87e-1**
CCDC34	162.34	**-0.16**	0.23	**9.88e-1**
CCDC43	423.2	**0.03**	0.2	**9.93e-1**

CCDC47	1179.43	**-0.1**	0.19	**9.90e-1**
CCDC50	141.58	**0.25**	0.24	**9.49e-1**
CCDC51	259.03	**-0.11**	0.22	**9.90e-1**
CCDC53	48.55	**0.23**	0.25	**9.73e-1**
CCDC57	73.91	**0.02**	0.25	**9.95e-1**
CCDC58	295.39	**-0.14**	0.21	**9.90e-1**
CCDC59	325.56	**-0.29**	0.21	**8.80e-1**
CCDC6	1079.72	**-0.25**	0.2	**9.31e-1**
CCDC61	62.18	**-0.38**	0.25	**8.56e-1**
CCDC62	10.16	**0.11**	0.21	**9.90e-1**
CCDC64	345.52	**-0.05**	0.22	**9.93e-1**
CCDC66	163.01	**-0.05**	0.24	**9.93e-1**
CCDC69	1642.43	**-0.28**	0.19	**8.53e-1**
CCDC71	173.56	**-0.35**	0.23	**8.64e-1**
CCDC71L	38.8	**0.1**	0.25	**9.90e-1**
CCDC74A	150.55	**-0.08**	0.24	**9.90e-1**
CCDC74B	38.14	**0.25**	0.25	**9.59e-1**
CCDC77	172.39	**0.11**	0.23	**9.90e-1**
CCDC78	132.6	**-0.02**	0.24	**9.95e-1**
CCDC82	377.2	**0.11**	0.21	**9.90e-1**
CCDC84	25.03	**-0.09**	0.25	**9.90e-1**
CCDC85A	173.8	**-0.22**	0.23	**9.66e-1**
CCDC85B	96.28	**-0.05**	0.25	**9.93e-1**
CCDC86	810.99	**-0.49**	0.2	**4.59e-1**
CCDC88A	1867.69	**-0.1**	0.2	**9.90e-1**
CCDC88B	596.51	**-0.15**	0.24	**9.90e-1**
CCDC88C	1184.12	**-0.27**	0.2	**8.91e-1**
CCDC9	70.09	**-0.01**	0.25	**9.98e-1**
CCDC90B	194.2	**-0.03**	0.23	**9.93e-1**
CCDC91	80.67	**0.09**	0.25	**9.90e-1**
CCDC92	104.05	**0.16**	0.24	**9.89e-1**
CCDC93	176.16	**0.16**	0.23	**9.88e-1**
CCDC94	283.06	**-0.24**	0.23	**9.52e-1**
CCDC97	286.29	**-0.28**	0.23	**9.42e-1**
CCHCR1	160.75	**-0.06**	0.24	**9.93e-1**
CCL22	388.99	**-0.86**	0.21	**1.34e-2**
CCM2	411.61	**0.01**	0.21	**9.96e-1**
CCNA2	1507.01	**-0.02**	0.19	**9.93e-1**
CCNB1	878.2	**0.01**	0.2	**9.96e-1**
CCNB1IP1	341.99	**0.69**	0.21	**1.22e-1**
CCNB2	556.04	**0.1**	0.2	**9.90e-1**
CCNC	1162.61	**0.16**	0.21	**9.87e-1**
CCND1	26.02	**0.02**	0.25	**9.93e-1**
CCND3	1227.81	**-0.16**	0.21	**9.87e-1**
CCNDBP1	148.3	**0.25**	0.23	**9.49e-1**
CCNE1	160.35	**0.05**	0.23	**9.93e-1**
CCNE2	234.19	**-0.06**	0.22	**9.93e-1**
CCNF	616.53	**-0.19**	0.2	**9.64e-1**
CCNG1	610.99	**0.35**	0.21	**8.16e-1**
CCNG2	266.47	**0.48**	0.22	**5.84e-1**
CCNH	222.62	**0.02**	0.23	**9.94e-1**
CCNI	1804.42	**0.15**	0.19	**9.86e-1**
CCNJ	63.5	**-0.14**	0.25	**9.90e-1**
CCNK	532.03	**-0.4**	0.2	**6.69e-1**
CCNL1	417.16	**0.23**	0.21	**9.47e-1**
CCNL2	405.29	**0.04**	0.21	**9.93e-1**
CCNT1	665.55	**0.09**	0.2	**9.90e-1**
CCNT2	220.32	**0.05**	0.23	**9.93e-1**
CCNY	441.62	**0.1**	0.21	**9.90e-1**
CCNYL1	298.05	**0.29**	0.22	**9.10e-1**
CCP110	473.98	**0.11**	0.21	**9.90e-1**
CCPG1	41.67	**0.11**	0.25	**9.90e-1**
CCR7	323.56	**0.29**	0.21	**8.94e-1**
CCS	65.35	**-0.21**	0.25	**9.80e-1**
CCSAP	122.83	**0.22**	0.24	**9.66e-1**

CCSER2	348.33	**-0.13**	0.22	**9.90e-1**
CCT2	2573.14	**-0.05**	0.18	**9.92e-1**
CCT3	3645.56	**-0.15**	0.18	**9.80e-1**
CCT4	2425.41	**-0.24**	0.18	**9.07e-1**
CCT5	4240.72	**-0.17**	0.18	**9.66e-1**
CCT6A	3478.83	**-0.1**	0.19	**9.90e-1**
CCT6B	10.61	**0.24**	0.21	**9.47e-1**
CCT6P1	73.07	**0.13**	0.25	**9.90e-1**
CCT6P3	23.17	**0.15**	0.25	**9.90e-1**
CCT7	4124.2	**-0.1**	0.18	**9.90e-1**
CCT8	2612.03	**0.22**	0.2	**9.47e-1**
CCZ1	247.65	**0.57**	0.22	**3.64e-1**
CCZ1B	213.35	**-0.01**	0.22	**9.96e-1**
CD151	185.18	**-0.33**	0.23	**8.73e-1**
CD164	1388.71	**0.35**	0.2	**7.70e-1**
CD180	752.08	**0.78**	0.19	**1.49e-2**
CD19	1355.16	**-0.25**	0.21	**9.47e-1**
CD22	3411.47	**1.2**	0.19	**0.00e+0**
CD27	1049.52	**-0.33**	0.2	**8.30e-1**
CD2AP	756.99	**-0.18**	0.21	**9.80e-1**
CD2BP2	785.18	**-0.26**	0.22	**9.47e-1**
CD320	411.37	**-0.47**	0.23	**6.14e-1**
CD37	1278.28	**-0.1**	0.21	**9.90e-1**
CD38	552.53	**-0.26**	0.2	**9.23e-1**
CD3EAP	527.38	**-0.74**	0.22	**8.56e-2**
CD40	385.8	**0.17**	0.21	**9.81e-1**
CD46	360.92	**0.29**	0.21	**9.06e-1**
CD47	554.38	**0.36**	0.21	**8.04e-1**
CD48	456.45	**0.76**	0.2	**3.35e-2**
CD52	49.39	**-0.52**	0.25	**6.28e-1**
CD53	1467.35	**0.6**	0.19	**1.25e-1**
CD55	270.37	**0.23**	0.22	**9.49e-1**
CD58	109.21	**0.45**	0.25	**7.41e-1**
CD63	207.02	**0.13**	0.22	**9.90e-1**
CD68	23.33	**-0.05**	0.25	**9.93e-1**
CD69	42.17	**0.72**	0.25	**2.52e-1**
CD70	460.82	**0.12**	0.22	**9.90e-1**
CD72	153.89	**0.78**	0.23	**8.70e-2**
CD74	22623.61	**-0.03**	0.18	**9.93e-1**
CD79A	2589.91	**-0.28**	0.22	**9.30e-1**
CD79B	1871.78	**-0.13**	0.19	**9.88e-1**
CD80	94.65	**0.09**	0.24	**9.90e-1**
CD81	1001.79	**0.03**	0.21	**9.93e-1**
CD82	523.36	**-0.11**	0.23	**9.90e-1**
CD83	871.6	**0.76**	0.19	**1.86e-2**
CD84	625.5	**-0.18**	0.2	**9.72e-1**
CD86	261.26	**0.11**	0.22	**9.90e-1**
CD99	188.74	**0.14**	0.24	**9.90e-1**
CD99L2	192.12	**-0.03**	0.23	**9.93e-1**
CD99P1	43.74	**-0.21**	0.25	**9.81e-1**
CDADC1	34.57	**0.04**	0.25	**9.93e-1**
CDAN1	137.2	**-0.28**	0.24	**9.47e-1**
CDC123	1221.45	**-0.04**	0.19	**9.93e-1**
CDC14A	48.75	**0.19**	0.25	**9.87e-1**
CDC16	569.28	**0.3**	0.2	**8.61e-1**
CDC20	1114.12	**-0.43**	0.19	**5.45e-1**
CDC23	433.74	**-0.01**	0.21	**9.98e-1**
CDC25A	659.67	**-0.1**	0.19	**9.90e-1**
CDC25B	939.55	**-0.58**	0.19	**2.07e-1**
CDC25C	37.76	**0**	0.25	**9.99e-1**
CDC26	118.83	**-0.08**	0.24	**9.90e-1**
CDC27	917.99	**-0.07**	0.2	**9.90e-1**
CDC34	269.51	**0.07**	0.23	**9.93e-1**
CDC37	1751	**-0.21**	0.2	**9.49e-1**

CDC37L1	87.85	**-0.03**	0.25	**9.93e-1**
CDC40	471.17	**0.08**	0.21	**9.90e-1**
CDC42	1252.29	**-0.05**	0.19	**9.93e-1**
CDC42BPG	75.48	**-0.3**	0.25	**9.47e-1**
CDC42EP2	44.13	**-0.44**	0.25	**7.88e-1**
CDC42EP3	176.12	**-0.06**	0.23	**9.93e-1**
CDC42SE1	590.99	**0.13**	0.2	**9.90e-1**
CDC42SE2	805.59	**0.07**	0.2	**9.90e-1**
CDC45	466.07	**0.28**	0.2	**8.76e-1**
CDC5L	867.35	**0.04**	0.19	**9.93e-1**
CDC6	1016.49	**0.18**	0.19	**9.59e-1**
CDC7	507.75	**-0.06**	0.2	**9.93e-1**
CDC73	447.95	**0.09**	0.21	**9.90e-1**
CDCA2	394.05	**-0.08**	0.21	**9.90e-1**
CDCA3	316.65	**-0.24**	0.21	**9.47e-1**
CDCA4	241.21	**0.04**	0.22	**9.93e-1**
CDCA5	782.24	**-0.13**	0.2	**9.90e-1**
CDCA7	1168.17	**0.17**	0.19	**9.72e-1**
CDCA7L	945.05	**0.05**	0.2	**9.93e-1**
CDCA8	1243.5	**-0.36**	0.19	**7.13e-1**
CDIPT	195.26	**0.09**	0.24	**9.90e-1**
CDK1	790.97	**-0.04**	0.2	**9.93e-1**
CDK10	266.8	**-0.26**	0.23	**9.47e-1**
CDK11A	52.47	**-0.03**	0.25	**9.93e-1**
CDK11B	297.15	**-0.07**	0.22	**9.92e-1**
CDK12	2139.48	**-0.38**	0.18	**6.07e-1**
CDK13	816.14	**-0.03**	0.2	**9.93e-1**
CDK14	928.69	**-0.06**	0.2	**9.93e-1**
CDK16	723.92	**-0.31**	0.21	**8.68e-1**
CDK17	221.5	**0.46**	0.23	**6.52e-1**
CDK18	358.64	**-0.33**	0.23	**8.73e-1**
CDK19	378.57	**0.16**	0.21	**9.87e-1**
CDK2	620.73	**-0.08**	0.2	**9.90e-1**
CDK2AP2	431.07	**0.7**	0.2	**7.89e-2**
CDK4	1006.05	**-0.05**	0.19	**9.93e-1**
CDK5	198.16	**0.01**	0.22	**9.96e-1**
CDK5R1	30.66	**-0.03**	0.25	**9.93e-1**
CDK5RAP1	384.26	**-0.07**	0.2	**9.90e-1**
CDK5RAP2	654.13	**-0.07**	0.2	**9.90e-1**
CDK5RAP3	1416	**0.03**	0.19	**9.93e-1**
CDK6	2053.06	**-0.08**	0.19	**9.90e-1**
CDK7	196.51	**0.24**	0.22	**9.49e-1**
CDK8	225.14	**0.09**	0.22	**9.90e-1**
CDK9	462.28	**-0.25**	0.21	**9.39e-1**
CDKAL1	135.39	**0.16**	0.23	**9.89e-1**
CDKL1	43.79	**-0.42**	0.25	**8.29e-1**
CDKL3	14.85	**-0.07**	0.23	**9.91e-1**
CDKL5	24.2	**-0.41**	0.25	**8.10e-1**
CDKN1A	209.2	**0.23**	0.24	**9.61e-1**
CDKN1B	115.44	**0.21**	0.24	**9.74e-1**
CDKN2A	176.3	**-0.16**	0.23	**9.87e-1**
CDKN2AIP	225.51	**0.13**	0.22	**9.90e-1**
CDKN2AIPNL	168.88	**-0.12**	0.23	**9.90e-1**
CDKN2C	404.76	**-0.49**	0.22	**5.45e-1**
CDKN2D	25.29	**-0.03**	0.25	**9.93e-1**
CDKN3	277.87	**-0.15**	0.22	**9.87e-1**
CDON	31.85	**-0.01**	0.25	**9.97e-1**
CDPF1	63.87	**-0.09**	0.25	**9.90e-1**
CDR2	276.42	**0.19**	0.21	**9.75e-1**
CDS2	1072.54	**-0.21**	0.19	**9.47e-1**
CDT1	487.69	**0.08**	0.22	**9.90e-1**
CDV3	3609.47	**0.23**	0.18	**9.20e-1**
CDYL	200.14	**-0.07**	0.22	**9.92e-1**
CEACAM1	20.24	**-0.1**	0.24	**9.90e-1**
CEBPB	38.73	**0.22**	0.25	**9.80e-1**

CEBPB-AS1	14.09	**0.01**	0.23	**9.96e-1**
CEBPG	351.16	**0.6**	0.21	**2.68e-1**
CEBPZ	1301.14	**-0.17**	0.19	**9.77e-1**
CEBPZOS	376.22	**-0.26**	0.22	**9.47e-1**
CECR1	54.45	**0.05**	0.25	**9.93e-1**
CECR5	527.92	**-0.08**	0.23	**9.90e-1**
CECR7	110.81	**-0.32**	0.25	**9.10e-1**
CEL	11.87	**-0.04**	0.22	**9.93e-1**
CELF1	2233.97	**-0.27**	0.18	**8.64e-1**
CELSR1	52.15	**0.27**	0.25	**9.49e-1**
CELSR3	178.31	**-0.22**	0.24	**9.72e-1**
CENPA	98.95	**0.1**	0.24	**9.90e-1**
CENPB	309.49	**-0.23**	0.23	**9.54e-1**
CENPBD1	53	**-0.01**	0.25	**9.96e-1**
CENPBD1P1	150.08	**-0.22**	0.24	**9.66e-1**
CENPC	276.77	**0.05**	0.22	**9.93e-1**
CENPE	1000.46	**-0.24**	0.2	**9.42e-1**
CENPF	2839.59	**-0.16**	0.19	**9.81e-1**
CENPH	299.92	**0.42**	0.22	**6.87e-1**
CENPI	117.28	**-0.04**	0.24	**9.93e-1**
CENPJ	304.28	**-0.04**	0.22	**9.93e-1**
CENPK	174.09	**0.21**	0.24	**9.80e-1**
CENPL	126.29	**-0.11**	0.24	**9.90e-1**
CENPM	220.94	**-0.35**	0.25	**8.90e-1**
CENPN	334.77	**0.19**	0.22	**9.80e-1**
CENPO	384.22	**-0.16**	0.21	**9.86e-1**
CENPP	84.88	**0.15**	0.25	**9.90e-1**
CENPQ	67.68	**0.33**	0.25	**9.20e-1**
CENPT	365.68	**-0.44**	0.23	**6.87e-1**
CENPU	383.65	**0.28**	0.22	**9.17e-1**
CENPV	224.92	**0.38**	0.23	**8.10e-1**
CENPW	77.76	**0.25**	0.25	**9.58e-1**
CEP104	372.74	**0.1**	0.21	**9.90e-1**
CEP112	30.48	**-0.14**	0.25	**9.90e-1**
CEP120	250	**0.37**	0.22	**7.96e-1**
CEP126	64.16	**0.09**	0.25	**9.90e-1**
CEP128	372.11	**-0.59**	0.21	**2.47e-1**
CEP131	149.37	**-0.01**	0.25	**9.97e-1**
CEP135	491.3	**0.13**	0.21	**9.90e-1**
CEP152	521.92	**0.07**	0.21	**9.90e-1**
CEP162	167.44	**0.16**	0.23	**9.89e-1**
CEP164	376.4	**-0.22**	0.22	**9.58e-1**
CEP170	500.49	**0.04**	0.21	**9.93e-1**
CEP19	43.43	**0**	0.25	**9.99e-1**
CEP192	439.35	**0.23**	0.21	**9.49e-1**
CEP250	1016.63	**-0.12**	0.19	**9.90e-1**
CEP290	368.52	**-0.03**	0.22	**9.93e-1**
CEP295	135.43	**-0.15**	0.24	**9.90e-1**
CEP350	617.63	**0.08**	0.21	**9.90e-1**
CEP41	371.58	**-0.03**	0.21	**9.93e-1**
CEP44	100.54	**0.29**	0.25	**9.47e-1**
CEP55	586.02	**-0.05**	0.2	**9.93e-1**
CEP57	416.96	**0.5**	0.22	**5.58e-1**
CEP57L1	135.81	**0.12**	0.24	**9.90e-1**
CEP63	298.11	**-0.09**	0.21	**9.90e-1**
CEP68	385.28	**-0.14**	0.21	**9.88e-1**
CEP70	12.1	**-0.19**	0.22	**9.74e-1**
CEP72	95.27	**-0.02**	0.24	**9.93e-1**
CEP76	107.18	**0.23**	0.24	**9.66e-1**
CEP78	223.45	**0.13**	0.22	**9.90e-1**
CEP83	237.45	**0.18**	0.23	**9.87e-1**
CEP85	479.36	**-0.2**	0.21	**9.61e-1**
CEP85L	94.07	**0.07**	0.24	**9.93e-1**
CEP89	68.32	**0.01**	0.25	**9.98e-1**

CEP95	333.45	**0.05**	0.22	**9.93e-1**
CEP97	216.34	**0.03**	0.23	**9.93e-1**
CEPT1	483.53	**0.42**	0.21	**6.37e-1**
CERCAM	13.71	**-0.04**	0.22	**9.93e-1**
CERK	488.75	**-0.2**	0.2	**9.59e-1**
CERS2	993.37	**0.02**	0.19	**9.94e-1**
CERS4	673.32	**0.39**	0.2	**6.54e-1**
CERS5	160.41	**0.03**	0.23	**9.93e-1**
CES2	275.26	**-0.2**	0.23	**9.74e-1**
CES3	48.44	**-0.18**	0.25	**9.87e-1**
CETN2	180.51	**0.2**	0.23	**9.74e-1**
CETN3	100.06	**0.26**	0.24	**9.49e-1**
CFAP20	320.14	**-0.21**	0.21	**9.58e-1**
CFAP36	115.5	**0.19**	0.24	**9.86e-1**
CFAP44	65.44	**0.09**	0.25	**9.90e-1**
CFAP47	26.16	**0**	0.25	**9.98e-1**
CFAP61	16.45	**0.08**	0.23	**9.90e-1**
CFAP70	13.59	**0.23**	0.22	**9.50e-1**
CFAP97	1068.84	**-0.1**	0.2	**9.90e-1**
CFDP1	480.95	**-0.11**	0.21	**9.90e-1**
CFL1	4474.85	**-0.2**	0.2	**9.54e-1**
CFL2	268.5	**-0.21**	0.22	**9.71e-1**
CFLAR	389.07	**0.17**	0.2	**9.81e-1**
CGGBP1	953.71	**0.31**	0.2	**8.52e-1**
CGN	32.36	**-0.15**	0.25	**9.90e-1**
CGRRF1	27.72	**0.05**	0.25	**9.93e-1**
CHAC1	51.32	**0.85**	0.25	**8.56e-2**
CHAC2	83.75	**0.04**	0.25	**9.93e-1**
CHAF1A	1229.16	**-0.22**	0.19	**9.47e-1**
CHAF1B	512.19	**-0.29**	0.21	**8.90e-1**
CHAMP1	1193.97	**-0.15**	0.19	**9.86e-1**
CHCHD1	86.23	**-0.02**	0.25	**9.95e-1**
CHCHD10	179.3	**0.09**	0.23	**9.90e-1**
CHCHD2	1166.26	**0.11**	0.2	**9.90e-1**
CHCHD3	1286.86	**-0.01**	0.19	**9.96e-1**
CHCHD4	259.55	**0.04**	0.21	**9.93e-1**
CHCHD5	46.79	**-0.32**	0.25	**9.23e-1**
CHCHD6	71.15	**0.06**	0.25	**9.93e-1**
CHCHD7	379.23	**-0.04**	0.21	**9.93e-1**
CHD1	561.77	**-0.11**	0.21	**9.90e-1**
CHD1L	366.15	**0.36**	0.21	**7.87e-1**
CHD2	540.02	**0.18**	0.2	**9.73e-1**
CHD3	2797.13	**-0.45**	0.19	**5.37e-1**
CHD4	4557.51	**-0.06**	0.18	**9.90e-1**
CHD6	443.2	**-0.13**	0.2	**9.90e-1**
CHD7	925.98	**-0.31**	0.19	**8.36e-1**
CHD8	2171.31	**-0.22**	0.18	**9.42e-1**
CHD9	536.02	**-0.14**	0.21	**9.90e-1**
CHEK1	610.45	**0.18**	0.21	**9.74e-1**
CHEK2	304.31	**-0.54**	0.21	**3.91e-1**
CHERP	1653.8	**-0.53**	0.21	**4.41e-1**
CHI3L2	1316.02	**0.13**	0.19	**9.88e-1**
CHIC1	50.5	**0.18**	0.25	**9.87e-1**
CHIC2	32.52	**0.23**	0.25	**9.68e-1**
CHID1	253.93	**-0.18**	0.23	**9.86e-1**
CHKA	197.51	**0.13**	0.22	**9.90e-1**
CHKB-AS1	14.71	**0.1**	0.23	**9.90e-1**
CHM	112.24	**-0.03**	0.24	**9.93e-1**
CHMP1A	429.72	**-0.26**	0.23	**9.49e-1**
CHMP1B	158.74	**0.5**	0.23	**5.90e-1**
CHMP2A	201.11	**0.08**	0.22	**9.90e-1**
CHMP2B	222.88	**0.27**	0.23	**9.42e-1**
CHMP4A	336.48	**-0.14**	0.21	**9.90e-1**
CHMP4B	708.79	**0.11**	0.19	**9.90e-1**
CHMP5	220.12	**0.52**	0.22	**5.28e-1**

CHMP6	76.92	**-0.25**	0.25	**9.58e-1**
CHMP7	755.99	**0.02**	0.19	**9.93e-1**
CHORDC1	948.55	**-0.34**	0.2	**7.87e-1**
CHP1	544.58	**0**	0.2	**9.98e-1**
CHPF	245.78	**0.01**	0.24	**9.96e-1**
CHPF2	217.2	**-0.36**	0.24	**8.53e-1**
CHRAC1	612.14	**-0.01**	0.2	**9.96e-1**
CHRNA5	116.54	**0.21**	0.25	**9.80e-1**
CHRNA6	98.25	**0.11**	0.24	**9.90e-1**
CHRNB1	42.88	**0.04**	0.25	**9.93e-1**
CHST10	101.37	**-0.08**	0.25	**9.91e-1**
CHST11	573.47	**0.03**	0.2	**9.93e-1**
CHST12	81.11	**0.23**	0.25	**9.72e-1**
CHST14	54.89	**0.04**	0.25	**9.93e-1**
CHST2	102.6	**-0.3**	0.24	**9.30e-1**
CHSY1	395.6	**0.06**	0.21	**9.93e-1**
CHTF18	481.85	**-0.23**	0.24	**9.63e-1**
CHTF8	1033.96	**-0.47**	0.22	**6.03e-1**
CHTOP	639.55	**-0.13**	0.2	**9.90e-1**
CHUK	420.69	**0.13**	0.21	**9.90e-1**
CHURC1	269.65	**0.18**	0.22	**9.86e-1**
CIAO1	787.02	**-0.09**	0.19	**9.90e-1**
CIAPIN1	320.16	**-0.21**	0.21	**9.54e-1**
CIB1	297.03	**-0.09**	0.22	**9.90e-1**
CIC	807.87	**-0.27**	0.24	**9.49e-1**
CIDECP	22.3	**0**	0.24	**9.98e-1**
CIITA	1923.59	**-0.1**	0.21	**9.90e-1**
CINP	190.99	**-0.07**	0.22	**9.91e-1**
CIPC	398.83	**-0.22**	0.22	**9.58e-1**
CIR1	40.25	**0**	0.25	**9.98e-1**
CIRBP	992.96	**-0.31**	0.19	**8.39e-1**
CIRH1A	848.41	**0.1**	0.2	**9.90e-1**
CISD1	294.14	**-0.18**	0.22	**9.82e-1**
CISD2	332.37	**0.36**	0.22	**8.20e-1**
CISD3	150.58	**-0.22**	0.25	**9.74e-1**
CIT	561.66	**-0.23**	0.2	**9.47e-1**
CITED2	298.09	**-0.48**	0.21	**5.64e-1**
CIZ1	1282.72	**-0.35**	0.21	**8.15e-1**
CKAP2	1167.26	**0.07**	0.19	**9.90e-1**
CKAP2L	127.75	**-0.28**	0.24	**9.47e-1**
CKAP5	2994.36	**-0.11**	0.18	**9.90e-1**
CKMT2-AS1	24	**-0.02**	0.25	**9.96e-1**
CKS1B	389.37	**-0.13**	0.2	**9.90e-1**
CKS2	436.88	**-0.04**	0.21	**9.93e-1**
CLASP1	343.55	**-0.08**	0.21	**9.90e-1**
CLASP2	626.46	**0.21**	0.21	**9.58e-1**
CLASRP	532.27	**-0.22**	0.21	**9.49e-1**
CLCC1	151.49	**0**	0.23	**1.00e+0**
CLCF1	50.29	**-0.2**	0.25	**9.86e-1**
CLCN2	76.17	**-0.23**	0.25	**9.66e-1**
CLCN3	729.21	**0.33**	0.2	**8.23e-1**
CLCN4	216.8	**0.07**	0.22	**9.91e-1**
CLCN6	242.55	**-0.04**	0.22	**9.93e-1**
CLCN7	454.74	**-0.03**	0.23	**9.93e-1**
CLDN12	69.59	**0.13**	0.25	**9.90e-1**
CLDN15	175.7	**-0.27**	0.25	**9.49e-1**
CLDND1	259.39	**0.21**	0.22	**9.61e-1**
CLEC11A	14.13	**0.04**	0.22	**9.93e-1**
CLEC16A	902.03	**-0.16**	0.2	**9.81e-1**
CLEC17A	98.45	**-0.06**	0.25	**9.93e-1**
CLEC2B	26.44	**0.11**	0.25	**9.90e-1**
CLEC2D	763.95	**0.24**	0.21	**9.47e-1**
CLEC7A	81.46	**0.2**	0.25	**9.81e-1**
CLECL1	220.36	**-0.45**	0.22	**6.49e-1**
CLHC1	28.66	**0.21**	0.25	**9.81e-1**

CLIC1	1045.75	**0.11**	0.19	**9.90e-1**
CLIC4	2834.72	**0.05**	0.19	**9.93e-1**
CLINT1	1283.6	**-0.3**	0.19	**8.41e-1**
CLIP1	768.73	**0.07**	0.19	**9.90e-1**
CLIP2	356.36	**0.22**	0.23	**9.59e-1**
CLIP4	33.01	**-0.41**	0.25	**8.30e-1**
CLK1	317.28	**0.45**	0.22	**6.28e-1**
CLK2	561.48	**0**	0.2	**9.98e-1**
CLK3	454.39	**-0.2**	0.21	**9.66e-1**
CLK4	111.85	**0.4**	0.25	**8.30e-1**
CLN3	219.33	**0.13**	0.23	**9.90e-1**
CLN5	54.66	**0.06**	0.25	**9.93e-1**
CLN6	480.73	**-0.11**	0.22	**9.90e-1**
CLN8	59.29	**-0.1**	0.25	**9.90e-1**
CLNS1A	983.64	**0.14**	0.2	**9.87e-1**
CLOCK	103.97	**-0.11**	0.25	**9.90e-1**
CLP1	123.91	**-0.09**	0.24	**9.90e-1**
CLPB	277.06	**-0.05**	0.21	**9.93e-1**
CLPP	489.53	**-0.36**	0.23	**8.38e-1**
CLPTM1	1309.05	**-0.27**	0.2	**8.89e-1**
CLPTM1L	779.07	**0.17**	0.19	**9.76e-1**
CLPX	674.58	**0.11**	0.2	**9.90e-1**
CLSPN	1280.18	**-0.33**	0.19	**7.57e-1**
CLSTN1	1985.59	**-0.13**	0.2	**9.90e-1**
CLSTN3	113.29	**-0.09**	0.24	**9.90e-1**
CLTA	689.77	**0.65**	0.2	**1.03e-1**
CLTB	16.95	**0.16**	0.23	**9.88e-1**
CLTC	3077.39	**0.08**	0.19	**9.90e-1**
CLTCL1	16.05	**-0.17**	0.23	**9.87e-1**
CLUAP1	130.45	**0.23**	0.24	**9.60e-1**
CLUH	3515.91	**-0.6**	0.22	**3.04e-1**
CLUHP3	62.15	**-0.24**	0.25	**9.64e-1**
CLYBL	30.43	**0.3**	0.25	**9.42e-1**
CMAHP	49.82	**-0.17**	0.25	**9.89e-1**
CMAS	281.34	**0.31**	0.22	**8.69e-1**
CMC1	63.84	**-0.04**	0.25	**9.93e-1**
CMC2	90.89	**0.02**	0.24	**9.96e-1**
CMC4	26.42	**0.28**	0.25	**9.47e-1**
CMIP	508.31	**-0.05**	0.2	**9.93e-1**
CMPK1	1888.94	**0.37**	0.2	**7.03e-1**
CMSS1	270.27	**-0.16**	0.21	**9.87e-1**
CMTM1	10.25	**0.09**	0.21	**9.90e-1**
CMTM4	48.1	**0.08**	0.25	**9.91e-1**
CMTM6	414.29	**0.39**	0.21	**6.99e-1**
CMTM8	25.51	**0.39**	0.25	**8.38e-1**
CMTR1	569.68	**-0.14**	0.2	**9.87e-1**
CMTR2	169.17	**0.2**	0.23	**9.78e-1**
CNBP	2158.89	**0.05**	0.18	**9.93e-1**
CNDP2	864.13	**-0.15**	0.2	**9.87e-1**
CNEP1R1	57.74	**0.32**	0.25	**9.23e-1**
CNIH1	468.22	**0.51**	0.21	**4.40e-1**
CNIH4	69.88	**0.3**	0.25	**9.46e-1**
CNKSR1	24.91	**-0.27**	0.25	**9.47e-1**
CNN2	1947.69	**-0.37**	0.22	**7.99e-1**
CNNM2	46.78	**0.2**	0.25	**9.86e-1**
CNNM3	264.07	**0.15**	0.22	**9.88e-1**
CNNM4	430.11	**0.01**	0.2	**9.96e-1**
CNOT1	4914.69	**-0.01**	0.19	**9.96e-1**
CNOT10	427.27	**0.18**	0.21	**9.75e-1**
CNOT11	688.01	**-0.04**	0.2	**9.93e-1**
CNOT2	716.96	**-0.24**	0.19	**9.25e-1**
CNOT3	746.83	**-0.33**	0.2	**8.30e-1**
CNOT4	451.05	**-0.36**	0.2	**7.56e-1**
CNOT6	494.96	**0.17**	0.21	**9.81e-1**

CNOT6L	461.25	**0.11**	0.21	**9.90e-1**
CNOT7	1245.11	**0.09**	0.2	**9.90e-1**
CNOT8	325.57	**0.4**	0.22	**7.22e-1**
CNP	559.85	**-0.49**	0.22	**5.84e-1**
CNPPD1	360.5	**-0.07**	0.23	**9.91e-1**
CNPY2	266.57	**0.09**	0.22	**9.90e-1**
CNPY3	326.2	**0.16**	0.22	**9.87e-1**
CNPY4	53.5	**0.05**	0.25	**9.93e-1**
CNR1	11.63	**0.33**	0.22	**8.51e-1**
CNR2	113.7	**0.34**	0.24	**8.78e-1**
CNST	357.57	**0.03**	0.22	**9.93e-1**
CNTLN	190.67	**0.04**	0.23	**9.93e-1**
CNTRL	1052.2	**0.04**	0.2	**9.93e-1**
CNTROB	577.8	**-0.29**	0.22	**9.06e-1**
COA1	295.25	**-0.04**	0.21	**9.93e-1**
COA3	89.44	**0.09**	0.25	**9.90e-1**
COA4	236.54	**-0.11**	0.22	**9.90e-1**
COA5	61.18	**0.39**	0.25	**8.41e-1**
COA6	90.95	**0**	0.24	**1.00e+0**
COA7	643.78	**-0.07**	0.19	**9.90e-1**
COASY	647.31	**-0.46**	0.22	**6.14e-1**
COBLL1	651.84	**-0.32**	0.21	**8.52e-1**
COG1	150.28	**0.27**	0.23	**9.47e-1**
COG2	350.03	**0.1**	0.21	**9.90e-1**
COG3	188.79	**0.2**	0.23	**9.80e-1**
COG4	252.2	**0.24**	0.22	**9.47e-1**
COG5	380.75	**0.21**	0.21	**9.61e-1**
COG6	148.57	**0.14**	0.23	**9.90e-1**
COG7	70.98	**0**	0.25	**9.99e-1**
COG8	139.13	**0.02**	0.23	**9.96e-1**
COIL	271.45	**-0.03**	0.22	**9.93e-1**
COL11A2	44.91	**-0.25**	0.25	**9.59e-1**
COL1A1	92.83	**0.42**	0.25	**8.02e-1**
COL24A1	129.08	**-0.74**	0.24	**1.50e-1**
COL4A3	86.77	**0.18**	0.25	**9.87e-1**
COL4A3BP	338.09	**0.71**	0.22	**1.14e-1**
COL4A4	24.17	**-0.16**	0.24	**9.89e-1**
COL7A1	12.25	**-0.08**	0.21	**9.90e-1**
COL9A2	463.3	**-0.22**	0.22	**9.60e-1**
COLGALT1	1013.34	**-0.12**	0.19	**9.90e-1**
COMMD1	49.37	**0**	0.25	**9.99e-1**
COMMD10	67.99	**0.22**	0.25	**9.80e-1**
COMMD2	158.84	**0.11**	0.23	**9.90e-1**
COMMD3	17.66	**0.17**	0.23	**9.87e-1**
COMMD4	148.16	**0.13**	0.24	**9.90e-1**
COMMD5	84.87	**-0.01**	0.25	**9.98e-1**
COMMD6	76.78	**0.24**	0.25	**9.64e-1**
COMMD7	194.29	**-0.12**	0.23	**9.90e-1**
COMMD8	109.07	**0.26**	0.24	**9.49e-1**
COMMD9	228.25	**-0.22**	0.22	**9.54e-1**
COMT	171.21	**0.08**	0.24	**9.91e-1**
COMTD1	76.87	**0.11**	0.25	**9.90e-1**
COPA	1326.56	**0.2**	0.19	**9.49e-1**
COPB1	778.43	**0.4**	0.2	**6.52e-1**
COPB2	1041.72	**0.05**	0.19	**9.93e-1**
COPE	483.42	**-0.04**	0.22	**9.93e-1**
COPG1	935.74	**0.06**	0.19	**9.93e-1**
COPG2	165.23	**0.12**	0.23	**9.90e-1**
COPRS	173.99	**0.45**	0.23	**6.54e-1**
COPS2	889.45	**0.06**	0.2	**9.92e-1**
COPS3	802.62	**0.42**	0.2	**6.14e-1**
COPS4	248.05	**0.05**	0.22	**9.93e-1**
COPS5	351.4	**0.25**	0.21	**9.47e-1**
COPS6	349.18	**-0.02**	0.21	**9.93e-1**
COPS7A	309.27	**-0.02**	0.22	**9.96e-1**

COPS7B	411.77	**-0.34**	0.22	**8.51e-1**
COPS8	531.07	**0.13**	0.2	**9.90e-1**
COPZ1	709.5	**0.12**	0.19	**9.90e-1**
COQ10A	63.69	**0.27**	0.25	**9.49e-1**
COQ10B	84.97	**0.15**	0.25	**9.90e-1**
COQ2	176.85	**0.6**	0.23	**3.52e-1**
COQ3	46.6	**-0.27**	0.25	**9.49e-1**
COQ4	242.34	**-0.13**	0.23	**9.90e-1**
COQ5	109.65	**-0.07**	0.24	**9.91e-1**
COQ6	71.87	**0.06**	0.25	**9.93e-1**
COQ7	189.65	**0.14**	0.22	**9.90e-1**
COQ9	395.39	**0.35**	0.21	**8.10e-1**
CORO1A	1951.48	**-0.18**	0.22	**9.82e-1**
CORO1B	27.33	**-0.18**	0.25	**9.87e-1**
CORO1C	813.24	**0.32**	0.2	**8.40e-1**
CORO7	44.01	**-0.54**	0.25	**5.87e-1**
COTL1	2593	**-0.24**	0.2	**9.31e-1**
COX10	321.22	**0.05**	0.21	**9.93e-1**
COX10-AS1	60.38	**0.2**	0.25	**9.82e-1**
COX11	287.53	**-0.09**	0.21	**9.90e-1**
COX14	53.81	**0.04**	0.25	**9.93e-1**
COX15	479.59	**0.02**	0.2	**9.95e-1**
COX16	10.09	**-0.06**	0.21	**9.93e-1**
COX17	113.54	**0.07**	0.24	**9.91e-1**
COX18	122.08	**0.2**	0.25	**9.81e-1**
COX19	142.97	**-0.14**	0.23	**9.90e-1**
COX20	216.15	**-0.25**	0.22	**9.47e-1**
COX4I1	1301.83	**0.39**	0.19	**6.06e-1**
COX5A	558.98	**0.74**	0.2	**4.51e-2**
COX5B	362.59	**0.12**	0.21	**9.90e-1**
COX6A1	880.12	**-0.03**	0.2	**9.93e-1**
COX6B1	408.97	**-0.13**	0.23	**9.90e-1**
COX6C	364.37	**0.37**	0.21	**7.57e-1**
COX7A2	1009.46	**0.31**	0.19	**8.38e-1**
COX7A2L	595.37	**0.18**	0.2	**9.69e-1**
COX7B	360.34	**0.15**	0.21	**9.87e-1**
COX7C	419.92	**0.3**	0.21	**8.64e-1**
COX8A	337.05	**-0.11**	0.24	**9.90e-1**
CPA6	26.64	**0.42**	0.25	**8.11e-1**
CPD	86.16	**0.2**	0.25	**9.81e-1**
CPEB2	42.81	**0.06**	0.25	**9.93e-1**
CPEB3	35.04	**0.2**	0.25	**9.86e-1**
CPEB4	379.88	**-0.09**	0.21	**9.90e-1**
CPLX3	11.46	**0.05**	0.21	**9.93e-1**
CPNE1	712.37	**-0.14**	0.2	**9.87e-1**
CPNE5	1416.04	**0.08**	0.23	**9.90e-1**
CPOX	48.05	**-0.03**	0.25	**9.93e-1**
CPPED1	76.55	**0.13**	0.25	**9.90e-1**
CPSF1	987.85	**-0.28**	0.21	**9.12e-1**
CPSF2	1024.02	**-0.06**	0.19	**9.91e-1**
CPSF3	765.5	**0.34**	0.2	**8.07e-1**
CPSF3L	716.12	**-0.36**	0.21	**7.99e-1**
CPSF4	330.61	**-0.05**	0.22	**9.93e-1**
CPSF6	1620.44	**-0.02**	0.19	**9.93e-1**
CPSF7	1850.39	**-0.55**	0.19	**2.62e-1**
CPT1A	129.6	**0.23**	0.24	**9.58e-1**
CPT2	468.07	**0.02**	0.2	**9.94e-1**
CPTP	125.62	**-0.4**	0.25	**8.40e-1**
CR2	1345.99	**0.58**	0.2	**2.15e-1**
CRACR2A	232.35	**-0.14**	0.22	**9.90e-1**
CRADD	16.58	**-0.06**	0.23	**9.93e-1**
CRAMP1L	243.69	**-0.22**	0.22	**9.58e-1**
CRBN	117.23	**0.15**	0.24	**9.90e-1**
CRCP	511.7	**-0.38**	0.2	**7.06e-1**

CREB1	474.73	**-0.1**	0.2	**9.90e-1**
CREB3	115.51	**-0.27**	0.24	**9.47e-1**
CREB3L2	73.71	**0.18**	0.25	**9.87e-1**
CREB3L4	22	**0.05**	0.24	**9.93e-1**
CREB5	155.5	**-0.47**	0.23	**6.36e-1**
CREBBP	1025.59	**-0.38**	0.2	**6.87e-1**
CREBL2	144.61	**0.16**	0.24	**9.89e-1**
CREBRF	45.83	**0.48**	0.25	**7.06e-1**
CREBZF	772.16	**0.07**	0.19	**9.90e-1**
CREG1	481.05	**0.65**	0.21	**1.84e-1**
CRELD1	115.34	**0.04**	0.24	**9.93e-1**
CRELD2	112.99	**0.74**	0.24	**1.48e-1**
CREM	109.71	**0.11**	0.24	**9.90e-1**
CRHR1-IT1	18.9	**-0.19**	0.24	**9.83e-1**
CRIP1	136.7	**-0.17**	0.24	**9.87e-1**
CRIP3	19.9	**0.01**	0.24	**9.98e-1**
CRIPAK	32.99	**0.14**	0.25	**9.90e-1**
CRIPT	62.8	**0.13**	0.25	**9.90e-1**
CRK	344.84	**-0.08**	0.21	**9.90e-1**
CRKL	805.79	**-0.07**	0.19	**9.90e-1**
CRLF3	317.87	**0.14**	0.22	**9.90e-1**
CRLS1	471.5	**0.53**	0.22	**4.44e-1**
CRNDE	21.73	**0.16**	0.24	**9.90e-1**
CRNKL1	432.51	**0**	0.21	**9.98e-1**
CROCC	13.04	**0.04**	0.22	**9.93e-1**
CROCCP2	98.43	**0.1**	0.24	**9.90e-1**
CROT	57.39	**0.04**	0.25	**9.93e-1**
CRTAP	623.91	**0.34**	0.2	**7.99e-1**
CRTC1	154.05	**-0.18**	0.24	**9.87e-1**
CRTC2	638.08	**-0.49**	0.23	**5.86e-1**
CRTC3	48.19	**-0.49**	0.25	**6.90e-1**
CRY2	210.18	**-0.18**	0.23	**9.86e-1**
CRYBB2P1	152.72	**-0.25**	0.24	**9.52e-1**
CRYBG3	102.53	**-0.17**	0.24	**9.87e-1**
CRYM-AS1	11.15	**0.04**	0.21	**9.93e-1**
CRYZ	477.33	**0.24**	0.21	**9.47e-1**
CRYZL1	54.27	**0.29**	0.25	**9.47e-1**
CS	4882.97	**-0.19**	0.18	**9.49e-1**
CSAD	57.53	**-0.01**	0.25	**9.97e-1**
CSDE1	5406.96	**0.02**	0.18	**9.93e-1**
CSE1L	4096.66	**-0.09**	0.2	**9.90e-1**
CSF2RB	281.39	**-0.42**	0.24	**7.57e-1**
CSGALNACT2	182.8	**0.52**	0.23	**5.45e-1**
CSK	2222.83	**-0.17**	0.21	**9.81e-1**
CSNK1A1	597.7	**0.12**	0.2	**9.90e-1**
CSNK1D	638.27	**0.05**	0.21	**9.93e-1**
CSNK1G1	259.46	**-0.13**	0.22	**9.90e-1**
CSNK1G2	950.05	**-0.34**	0.22	**8.53e-1**
CSNK1G3	335.05	**0.13**	0.22	**9.90e-1**
CSNK2A1	2054.36	**-0.2**	0.18	**9.49e-1**
CSNK2A2	566.62	**-0.03**	0.2	**9.93e-1**
CSNK2A3	22.6	**-0.24**	0.25	**9.58e-1**
CSNK2B	1308.41	**-0.01**	0.19	**9.96e-1**
CSPP1	281.59	**-0.13**	0.22	**9.90e-1**
CSRNP1	137.82	**-0.27**	0.24	**9.49e-1**
CSRNP2	144.44	**0.28**	0.23	**9.40e-1**
CSRP1	813.4	**-0.34**	0.21	**8.29e-1**
CSRP2BP	322.09	**0.02**	0.21	**9.93e-1**
CSTB	357.4	**-0.15**	0.21	**9.87e-1**
CSTF1	464.5	**0.01**	0.2	**9.97e-1**
CSTF2	266.69	**0.05**	0.21	**9.93e-1**
CSTF2T	346.19	**-0.2**	0.21	**9.61e-1**
CSTF3	380.15	**0.23**	0.21	**9.47e-1**
CTAGE5	307.55	**0.4**	0.21	**7.04e-1**
CTBP1	629.17	**0.01**	0.21	**9.96e-1**

CTBP1-AS2	125.67	**0.08**	0.24	**9.90e-1**
CTBS	55.81	**0.12**	0.25	**9.90e-1**
CTC1	277.19	**-0.19**	0.22	**9.73e-1**
CTCF	1605.56	**-0.13**	0.18	**9.88e-1**
CTDNEP1	912.78	**-0.02**	0.2	**9.93e-1**
CTDP1	358	**-0.03**	0.22	**9.93e-1**
CTDSP1	528.07	**-0.09**	0.23	**9.90e-1**
CTDSP2	1213.48	**0.03**	0.19	**9.93e-1**
CTDSPL2	479.22	**-0.04**	0.21	**9.93e-1**
CTH	33.5	**0.05**	0.25	**9.93e-1**
CTNNA1	140.91	**0.12**	0.24	**9.90e-1**
CTNNAL1	320.54	**0.17**	0.22	**9.86e-1**
CTNNB1	923.61	**0.1**	0.19	**9.90e-1**
CTNNBIP1	63.98	**0.16**	0.25	**9.90e-1**
CTNNBL1	501.94	**-0.13**	0.2	**9.90e-1**
CTNS	163.26	**-0.14**	0.23	**9.90e-1**
CTPS1	2236.09	**-0.22**	0.18	**9.45e-1**
CTPS2	284.09	**-0.16**	0.22	**9.87e-1**
CTR9	617.58	**-0.2**	0.2	**9.53e-1**
CTRL	22.88	**-0.16**	0.24	**9.89e-1**
CTSA	525.15	**0.01**	0.2	**9.96e-1**
CTSB	57.49	**0.34**	0.25	**9.06e-1**
CTSC	523.18	**-0.05**	0.2	**9.93e-1**
CTSD	581.03	**-0.02**	0.23	**9.95e-1**
CTSH	970.79	**0.02**	0.19	**9.94e-1**
CTSS	449.63	**0.23**	0.21	**9.49e-1**
CTSV	10.05	**-0.13**	0.21	**9.90e-1**
CTSZ	1222.99	**0.12**	0.2	**9.90e-1**
CTTNBP2NL	21.66	**-0.29**	0.24	**9.42e-1**
CTU1	17.88	**0.1**	0.23	**9.90e-1**
CTU2	127.63	**-0.26**	0.25	**9.49e-1**
CUEDC1	22.01	**-0.21**	0.24	**9.75e-1**
CUEDC2	188.85	**-0.08**	0.24	**9.91e-1**
CUL1	1610.33	**-0.03**	0.2	**9.93e-1**
CUL2	377.27	**0.12**	0.21	**9.90e-1**
CUL3	1274.8	**0.09**	0.2	**9.90e-1**
CUL4A	1267.85	**0.06**	0.19	**9.91e-1**
CUL4B	674.67	**0.07**	0.2	**9.90e-1**
CUL5	442.33	**0.05**	0.21	**9.93e-1**
CUL7	82.4	**-0.06**	0.25	**9.93e-1**
CUL9	141.05	**-0.08**	0.24	**9.90e-1**
CUTA	280.43	**0.14**	0.22	**9.90e-1**
CUTC	301.47	**0.15**	0.21	**9.87e-1**
CUX1	1626.64	**-0.27**	0.19	**8.64e-1**
CUX2	62.3	**0.54**	0.25	**5.99e-1**
CWC15	270.96	**0.11**	0.21	**9.90e-1**
CWC22	413.56	**0**	0.22	**9.98e-1**
CWC25	286.28	**0.04**	0.22	**9.93e-1**
CWC27	335.02	**-0.24**	0.21	**9.47e-1**
CWF19L1	210.89	**0.2**	0.22	**9.72e-1**
CWF19L2	155.42	**-0.12**	0.23	**9.90e-1**
CXADR	90.66	**-0.07**	0.25	**9.91e-1**
CXCL10	18.28	**-0.08**	0.24	**9.90e-1**
CXCL9	10.5	**-0.32**	0.21	**8.40e-1**
CXCR4	891.68	**-0.16**	0.19	**9.81e-1**
CXCR5	702.98	**-0.06**	0.23	**9.93e-1**
CXorf21	65.33	**-0.28**	0.25	**9.47e-1**
CXorf23	77.61	**0.26**	0.25	**9.50e-1**
CXorf38	125.19	**0.33**	0.24	**8.74e-1**
CXorf40A	63.57	**0.15**	0.25	**9.90e-1**
CXorf40B	109.51	**0.06**	0.24	**9.93e-1**
CXorf56	220.63	**0.1**	0.22	**9.90e-1**
CXorf57	200.43	**0.11**	0.23	**9.90e-1**
CXXC1	468.22	**-0.16**	0.22	**9.87e-1**
CXXC5	265.13	**0.07**	0.22	**9.91e-1**

CYB561A3	545.02	**0.19**	0.23	**9.81e-1**
CYB561D1	95.7	**-0.02**	0.24	**9.96e-1**
CYB561D2	43.04	**0**	0.25	**9.99e-1**
CYB5A	132.17	**-0.09**	0.23	**9.90e-1**
CYB5B	793.55	**0.02**	0.2	**9.93e-1**
CYB5D1	297.76	**-0.16**	0.21	**9.87e-1**
CYB5D2	32.77	**0.13**	0.25	**9.90e-1**
CYB5R1	106.24	**-0.13**	0.25	**9.90e-1**
CYB5R3	1181.2	**-0.27**	0.22	**9.36e-1**
CYB5R4	412.77	**0.13**	0.21	**9.90e-1**
CYB5RL	123.98	**-0.19**	0.24	**9.83e-1**
CYBA	642.38	**-0.13**	0.24	**9.90e-1**
CYBB	277.66	**-0.31**	0.22	**8.76e-1**
CYC1	907.33	**0.21**	0.2	**9.49e-1**
CYCS	1747.09	**-0.1**	0.19	**9.90e-1**
CYFIP2	3103.33	**0.26**	0.18	**8.68e-1**
CYHR1	105.57	**0.17**	0.24	**9.87e-1**
CYLD	318.83	**0.54**	0.21	**4.11e-1**
CYP20A1	30.72	**0.07**	0.25	**9.93e-1**
CYP27B1	50.73	**0.17**	0.25	**9.89e-1**
CYP2E1	37.72	**-0.12**	0.25	**9.90e-1**
CYP2R1	23.91	**0.31**	0.24	**9.25e-1**
CYP2U1	16.88	**0.13**	0.23	**9.90e-1**
CYP39A1	47.67	**-0.11**	0.25	**9.90e-1**
CYP4V2	158.54	**0.34**	0.23	**8.66e-1**
CYP51A1	278.81	**-0.12**	0.22	**9.90e-1**
CYSTM1	202.27	**-0.12**	0.22	**9.90e-1**
CYTH1	509.24	**0.11**	0.2	**9.90e-1**
CYTH2	238.2	**0.04**	0.23	**9.93e-1**
CYTH3	510.6	**-0.7**	0.2	**6.62e-2**
CYTH4	26.59	**0**	0.25	**9.98e-1**
CYTIP	289.27	**-0.19**	0.22	**9.74e-1**
D2HGDH	97.03	**-0.14**	0.25	**9.90e-1**
DAAM1	295.05	**-0.1**	0.22	**9.90e-1**
DAB2IP	11.62	**-0.23**	0.21	**9.47e-1**
DAD1	296.16	**0.26**	0.21	**9.32e-1**
DAG1	612.26	**-0.43**	0.21	**6.07e-1**
DAGLB	198.02	**-0.34**	0.22	**8.62e-1**
DALRD3	66.58	**0.07**	0.25	**9.93e-1**
DANCR	304.79	**0.28**	0.21	**9.12e-1**
DAP	403.42	**0.14**	0.2	**9.89e-1**
DAP3	1145.65	**0.17**	0.19	**9.76e-1**
DAPK3	177.2	**-0.16**	0.23	**9.87e-1**
DAPP1	231.49	**0.08**	0.22	**9.90e-1**
DARS	461.42	**0.15**	0.21	**9.87e-1**
DARS2	891.23	**0.03**	0.2	**9.93e-1**
DAXX	924.7	**-0.17**	0.2	**9.74e-1**
DAZAP1	2268.4	**-0.21**	0.19	**9.49e-1**
DAZAP2	1509.59	**-0.25**	0.19	**9.20e-1**
DBF4	983.48	**-0.24**	0.2	**9.42e-1**
DBF4B	348.17	**-0.48**	0.22	**5.91e-1**
DBI	466.49	**-0.11**	0.2	**9.90e-1**
DBIL5P	12.9	**-0.08**	0.22	**9.90e-1**
DBNL	902.2	**-0.3**	0.22	**8.92e-1**
DBP	43.71	**0.02**	0.25	**9.96e-1**
DBR1	164.24	**0.17**	0.23	**9.87e-1**
DBT	240.99	**0.22**	0.23	**9.59e-1**
DCAF10	329.44	**0.15**	0.22	**9.87e-1**
DCAF11	596.52	**-0.05**	0.2	**9.93e-1**
DCAF12	1862.95	**0.02**	0.18	**9.93e-1**
DCAF13	650.06	**0.07**	0.2	**9.90e-1**
DCAF15	289.24	**-0.23**	0.23	**9.53e-1**
DCAF16	580.81	**-0.18**	0.2	**9.74e-1**
DCAF17	364.95	**0.14**	0.21	**9.90e-1**

DCAF4	210.76	**-0.18**	0.22	**9.81e-1**
DCAF5	586.1	**-0.15**	0.2	**9.87e-1**
DCAF6	590.35	**-0.12**	0.2	**9.90e-1**
DCAF7	1057.33	**-0.13**	0.19	**9.88e-1**
DCAF8	759.85	**0.09**	0.19	**9.90e-1**
DCAKD	274.32	**-0.27**	0.22	**9.42e-1**
DCBLD2	37.33	**-0.12**	0.25	**9.90e-1**
DCHS1	11.89	**-0.08**	0.22	**9.90e-1**
DCK	1156.11	**-0.11**	0.2	**9.90e-1**
DCLRE1A	166.42	**0.32**	0.24	**8.94e-1**
DCLRE1B	337.34	**-0.29**	0.21	**8.93e-1**
DCLRE1C	197.2	**-0.15**	0.23	**9.89e-1**
DCP1A	311.3	**-0.24**	0.21	**9.47e-1**
DCP1B	186.65	**-0.13**	0.23	**9.90e-1**
DCP2	577.22	**0.26**	0.21	**9.25e-1**
DCPS	257.04	**-0.1**	0.21	**9.90e-1**
DCTD	371.24	**0.33**	0.21	**8.41e-1**
DCTN1	1579.39	**-0.18**	0.2	**9.73e-1**
DCTN2	449.55	**-0.13**	0.2	**9.90e-1**
DCTN3	107.53	**0.18**	0.24	**9.87e-1**
DCTN4	447.11	**0.29**	0.21	**8.87e-1**
DCTN5	609.6	**-0.06**	0.2	**9.91e-1**
DCTN6	197.22	**-0.05**	0.23	**9.93e-1**
DCTPP1	379.81	**-0.35**	0.21	**8.30e-1**
DCUN1D1	559.1	**0.11**	0.21	**9.90e-1**
DCUN1D2	108.02	**0.07**	0.24	**9.93e-1**
DCUN1D3	15.23	**0.07**	0.23	**9.91e-1**
DCUN1D4	190.35	**0.21**	0.23	**9.73e-1**
DCUN1D5	323.67	**-0.01**	0.21	**9.97e-1**
DCXR	160.01	**0.07**	0.23	**9.92e-1**
DDA1	323.83	**-0.33**	0.22	**8.64e-1**
DDAH2	45.75	**0.04**	0.25	**9.93e-1**
DDB1	3436.71	**-0.15**	0.18	**9.81e-1**
DDB2	326.92	**0.04**	0.21	**9.93e-1**
DDHD1	446.87	**-0.03**	0.21	**9.93e-1**
DDHD2	192.05	**0.14**	0.23	**9.90e-1**
DDI2	161.29	**-0.18**	0.23	**9.84e-1**
DDIAS	188.48	**0.15**	0.23	**9.90e-1**
DDIT3	63.48	**0.74**	0.25	**2.19e-1**
DDIT4	206.38	**0.69**	0.23	**2.11e-1**
DDN	33.99	**-0.15**	0.25	**9.90e-1**
DDOST	1075.68	**0.13**	0.19	**9.88e-1**
DDR1	307.78	**-0.39**	0.24	**8.30e-1**
DDRGK1	387.76	**-0.05**	0.22	**9.93e-1**
DDT	117.12	**0.28**	0.24	**9.47e-1**
DDTL	24.49	**0.1**	0.25	**9.90e-1**
DDX1	1544.96	**0.03**	0.19	**9.93e-1**
DDX10	671.79	**-0.21**	0.19	**9.49e-1**
DDX11	784.45	**-0.08**	0.2	**9.90e-1**
DDX12P	286.99	**-0.26**	0.22	**9.47e-1**
DDX17	3933.87	**-0.08**	0.18	**9.90e-1**
DDX18	754.92	**-0.08**	0.19	**9.90e-1**
DDX19A	625.11	**-0.24**	0.19	**9.39e-1**
DDX19B	193.97	**0.12**	0.22	**9.90e-1**
DDX20	545.39	**-0.02**	0.2	**9.93e-1**
DDX21	5966.54	**-0.27**	0.18	**8.53e-1**
DDX23	1493.34	**-0.37**	0.19	**6.84e-1**
DDX24	1780.58	**-0.24**	0.18	**9.11e-1**
DDX26B	156.73	**-0.02**	0.23	**9.93e-1**
DDX27	1153.77	**-0.18**	0.19	**9.61e-1**
DDX28	189.72	**0.07**	0.23	**9.91e-1**
DDX31	405.98	**0.24**	0.21	**9.47e-1**
DDX39A	941.35	**-0.1**	0.2	**9.90e-1**
DDX3X	4347.17	**-0.08**	0.19	**9.90e-1**
DDX3Y	1731.97	**-0.06**	0.19	**9.91e-1**

DDX41	895.9	**-0.34**	0.21	**8.27e-1**
DDX42	1706.6	**-0.06**	0.19	**9.90e-1**
DDX46	1584.95	**-0.48**	0.18	**3.64e-1**
DDX47	458	**0.07**	0.2	**9.90e-1**
DDX49	341.11	**0**	0.21	**9.99e-1**
DDX5	3788.45	**-0.12**	0.18	**9.89e-1**
DDX50	382.58	**0.2**	0.21	**9.60e-1**
DDX51	440.42	**-0.18**	0.21	**9.77e-1**
DDX52	554.44	**-0.01**	0.21	**9.98e-1**
DDX54	1982.69	**-0.41**	0.21	**7.04e-1**
DDX55	368.53	**-0.15**	0.21	**9.87e-1**
DDX56	671.98	**-0.12**	0.19	**9.90e-1**
DDX58	44.16	**-0.15**	0.25	**9.90e-1**
DDX59	120.32	**0.45**	0.24	**7.04e-1**
DDX6	1781.46	**-0.02**	0.18	**9.93e-1**
DEAF1	221.93	**-0.14**	0.23	**9.90e-1**
DECR1	103.22	**0.28**	0.24	**9.47e-1**
DECR2	105.71	**-0.18**	0.25	**9.88e-1**
DEDD	190.01	**-0.03**	0.23	**9.93e-1**
DEDD2	141.22	**-0.15**	0.25	**9.90e-1**
DEF6	107.44	**-0.14**	0.24	**9.90e-1**
DEF8	706.82	**-0.48**	0.22	**5.89e-1**
DEGS1	306.94	**0.19**	0.22	**9.80e-1**
DEK	3310.09	**-0.11**	0.18	**9.90e-1**
DENND1A	369.85	**-0.03**	0.21	**9.93e-1**
DENND1B	145.54	**0.06**	0.24	**9.93e-1**
DENND1C	303.96	**-0.18**	0.23	**9.86e-1**
DENND3	224.24	**0.27**	0.23	**9.42e-1**
DENND4A	1604.73	**0.13**	0.2	**9.90e-1**
DENND4B	880.67	**-0.18**	0.22	**9.81e-1**
DENND4C	463.83	**0.2**	0.21	**9.66e-1**
DENND5B	146.87	**-0.03**	0.24	**9.93e-1**
DENND6A	261.87	**0.15**	0.22	**9.88e-1**
DENND6B	87.42	**-0.53**	0.25	**6.01e-1**
DENR	858.15	**0.01**	0.2	**9.96e-1**
DEPDC1	605.97	**-0.13**	0.21	**9.90e-1**
DEPDC1B	165.08	**-0.21**	0.23	**9.66e-1**
DEPDC5	398.35	**-0.19**	0.2	**9.66e-1**
DEPTOR	212.45	**0.05**	0.22	**9.93e-1**
DERA	64.82	**0.06**	0.25	**9.93e-1**
DERL1	617.75	**0.07**	0.2	**9.90e-1**
DERL2	198.7	**0.32**	0.23	**8.89e-1**
DERL3	223.84	**-0.13**	0.25	**9.90e-1**
DESI1	1320.87	**-0.51**	0.21	**4.30e-1**
DESI2	1004.59	**0.28**	0.2	**9.03e-1**
DET1	32.49	**0.16**	0.25	**9.90e-1**
DEXI	61.32	**-0.05**	0.25	**9.93e-1**
DFFA	559.9	**-0.31**	0.2	**8.52e-1**
DFFB	42.67	**0.02**	0.25	**9.96e-1**
DGAT1	119.36	**-0.21**	0.25	**9.80e-1**
DGAT2	164.32	**0.01**	0.23	**9.98e-1**
DGCR11	12.1	**-0.22**	0.22	**9.54e-1**
DGCR14	155.52	**-0.34**	0.24	**8.73e-1**
DGCR2	400.16	**-0.07**	0.23	**9.91e-1**
DGCR6L	76.39	**-0.04**	0.25	**9.93e-1**
DGCR8	341.71	**-0.15**	0.21	**9.87e-1**
DGKA	76.3	**-0.31**	0.25	**9.33e-1**
DGKD	612.41	**-0.08**	0.2	**9.90e-1**
DGKE	60.87	**0.01**	0.25	**9.96e-1**
DGKH	186.47	**-0.18**	0.23	**9.87e-1**
DGKQ	47.12	**-0.06**	0.25	**9.93e-1**
DGKZ	931.43	**-0.4**	0.21	**7.04e-1**
DGUOK	228.59	**0.12**	0.22	**9.90e-1**
DHCR24	1323.59	**0.01**	0.19	**9.96e-1**
DHCR7	908.11	**-0.6**	0.21	**2.45e-1**

DHDDS	342.13	**-0.27**	0.21	**9.20e-1**
DHFR	1233.94	**-0.18**	0.19	**9.60e-1**
DHFRL1	34.51	**-0.17**	0.25	**9.90e-1**
DHODH	168.42	**-0.39**	0.23	**8.10e-1**
DHPS	291.94	**-0.06**	0.22	**9.93e-1**
DHRS1	12.64	**0.02**	0.21	**9.93e-1**
DHRS11	96.74	**-0.02**	0.24	**9.95e-1**
DHRS13	96.64	**0.21**	0.24	**9.80e-1**
DHRS7B	54.32	**0.1**	0.25	**9.90e-1**
DHRSX	74.93	**0.32**	0.25	**9.25e-1**
DHTKD1	486.13	**0.03**	0.2	**9.93e-1**
DHX15	2123.54	**-0.02**	0.19	**9.95e-1**
DHX16	547	**-0.26**	0.21	**9.35e-1**
DHX29	467.01	**-0.07**	0.2	**9.90e-1**
DHX30	1302.5	**-0.46**	0.2	**5.70e-1**
DHX33	1098.62	**-0.12**	0.19	**9.90e-1**
DHX34	624.38	**-0.33**	0.22	**8.51e-1**
DHX35	178.04	**0.12**	0.23	**9.90e-1**
DHX36	614.38	**0.19**	0.21	**9.73e-1**
DHX37	764.99	**-0.34**	0.23	**8.53e-1**
DHX38	1224.36	**-0.26**	0.2	**9.12e-1**
DHX40	539	**0.32**	0.2	**8.40e-1**
DHX57	88.65	**-0.06**	0.25	**9.93e-1**
DHX8	468.33	**-0.08**	0.2	**9.90e-1**
DHX9	4289.26	**-0.07**	0.18	**9.90e-1**
DIABLO	373.53	**0.03**	0.21	**9.93e-1**
DIAPH1	1739.01	**-0.05**	0.18	**9.93e-1**
DIAPH2	80.7	**-0.28**	0.25	**9.47e-1**
DIAPH3	158.53	**0.09**	0.23	**9.90e-1**
DICER1	715.93	**0.03**	0.21	**9.93e-1**
DIDO1	1420.31	**-0.26**	0.19	**8.94e-1**
DIEXF	371.6	**-0.14**	0.21	**9.90e-1**
DIMT1	412.18	**0.02**	0.21	**9.93e-1**
DIP2A	153.29	**0.1**	0.23	**9.90e-1**
DIP2B	530.65	**-0.17**	0.21	**9.81e-1**
DIP2C	23.05	**0.6**	0.24	**4.46e-1**
DIS3	1141.39	**0.1**	0.2	**9.90e-1**
DIS3L	583.2	**0.08**	0.2	**9.90e-1**
DIS3L2	208.58	**-0.27**	0.22	**9.42e-1**
DISP1	22.65	**0.04**	0.24	**9.93e-1**
DIXDC1	10.4	**-0.1**	0.21	**9.90e-1**
DKC1	1777.71	**-0.12**	0.18	**9.90e-1**
DKFZP434I0714	67.21	**0.23**	0.25	**9.68e-1**
DKFZP586I1420	53.33	**-0.03**	0.25	**9.93e-1**
DLAT	1776.35	**-0.12**	0.19	**9.89e-1**
DLD	1791.1	**0.17**	0.19	**9.73e-1**
DLEU1	152.69	**-0.22**	0.23	**9.66e-1**
DLEU2	51.43	**0.04**	0.25	**9.93e-1**
DLG1	623.57	**0.06**	0.21	**9.93e-1**
DLG3	115.39	**-0.07**	0.24	**9.92e-1**
DLG4	104.96	**-0.37**	0.25	**8.53e-1**
DLGAP4	606.03	**-0.37**	0.22	**8.10e-1**
DLGAP5	709.88	**-0.14**	0.21	**9.88e-1**
DLST	905.83	**-0.18**	0.19	**9.66e-1**
DMAP1	238.64	**-0.12**	0.22	**9.90e-1**
DMC1	46.41	**-0.13**	0.25	**9.90e-1**
DMD	40.09	**0.02**	0.25	**9.94e-1**
DMPK	229.1	**0.22**	0.24	**9.72e-1**
DMTF1	531.8	**0.05**	0.22	**9.93e-1**
DMWD	299.13	**-0.1**	0.25	**9.90e-1**
DMXL1	368.96	**0.05**	0.21	**9.93e-1**
DMXL2	43.78	**0.18**	0.25	**9.87e-1**
DNA2	341.86	**0.16**	0.22	**9.87e-1**
DNAAF2	214.78	**0.18**	0.22	**9.81e-1**

DNAAF3	16.25	**-0.04**	0.23	**9.93e-1**
DNAAF5	945.73	**-0.18**	0.19	**9.73e-1**
DNAH1	10.15	**0.14**	0.2	**9.87e-1**
DNAJA1	2883.38	**-0.24**	0.18	**9.10e-1**
DNAJA2	1058.15	**0**	0.19	**1.00e+0**
DNAJA3	1070.38	**0.09**	0.19	**9.90e-1**
DNAJB1	968.65	**-0.41**	0.19	**5.91e-1**
DNAJB11	560.13	**0.42**	0.2	**6.03e-1**
DNAJB12	360.16	**-0.01**	0.21	**9.96e-1**
DNAJB14	179.29	**0.41**	0.23	**7.76e-1**
DNAJB2	303.87	**-0.23**	0.24	**9.61e-1**
DNAJB4	377.89	**-1.16**	0.22	**8.40e-5**
DNAJB5	40.55	**-0.05**	0.25	**9.93e-1**
DNAJB6	797.46	**-0.13**	0.2	**9.90e-1**
DNAJB9	98.95	**0.35**	0.25	**8.69e-1**
DNAJC1	124.04	**0.25**	0.24	**9.52e-1**
DNAJC10	1371.09	**0.35**	0.2	**7.57e-1**
DNAJC11	1365.23	**-0.23**	0.19	**9.42e-1**
DNAJC12	103.12	**0.13**	0.25	**9.90e-1**
DNAJC13	664.83	**0.1**	0.2	**9.90e-1**
DNAJC14	396.29	**-0.29**	0.21	**9.04e-1**
DNAJC15	74.86	**-0.06**	0.25	**9.93e-1**
DNAJC16	235.29	**0.13**	0.22	**9.90e-1**
DNAJC17	91.53	**-0.12**	0.25	**9.90e-1**
DNAJC18	31.12	**0.09**	0.25	**9.90e-1**
DNAJC19	120.85	**0.14**	0.24	**9.90e-1**
DNAJC2	1197.77	**-0.24**	0.19	**9.25e-1**
DNAJC21	607.06	**0.14**	0.2	**9.89e-1**
DNAJC24	126.43	**0.01**	0.24	**9.96e-1**
DNAJC25	74.85	**0.2**	0.25	**9.81e-1**
DNAJC27	58.15	**0.04**	0.25	**9.93e-1**
DNAJC3	340.02	**0.32**	0.22	**8.64e-1**
DNAJC30	60.41	**-0.21**	0.25	**9.80e-1**
DNAJC3-AS1	15.67	**0.09**	0.23	**9.90e-1**
DNAJC4	68.29	**-0.12**	0.25	**9.90e-1**
DNAJC5	542.41	**0.01**	0.21	**9.96e-1**
DNAJC6	680.96	**-0.16**	0.19	**9.80e-1**
DNAJC7	801.18	**0.21**	0.2	**9.49e-1**
DNAJC8	1461.2	**-0.1**	0.19	**9.90e-1**
DNAJC9	498.37	**0.17**	0.2	**9.80e-1**
DNAL1	51.97	**0.16**	0.25	**9.90e-1**
DNAL4	27.19	**0.04**	0.25	**9.93e-1**
DNASE1	59.78	**0**	0.25	**9.98e-1**
DNASE1L1	86	**-0.02**	0.25	**9.96e-1**
DNASE2	125.93	**0.29**	0.24	**9.39e-1**
DND1	10.67	**-0.06**	0.21	**9.93e-1**
DNHD1	33.32	**-0.04**	0.25	**9.93e-1**
DNLZ	24.82	**0.26**	0.24	**9.49e-1**
DNM1L	1195.17	**0.05**	0.2	**9.93e-1**
DNM2	1155.94	**-0.24**	0.2	**9.42e-1**
DNMBP	882.52	**-0.12**	0.19	**9.90e-1**
DNMT1	6068.1	**-0.28**	0.19	**8.64e-1**
DNMT3B	237.09	**-0.71**	0.22	**1.10e-1**
DNPEP	486.44	**-0.22**	0.22	**9.58e-1**
DNPH1	167.28	**-0.03**	0.24	**9.93e-1**
DNTTIP1	232.8	**0.01**	0.22	**9.96e-1**
DNTTIP2	782.87	**-0.07**	0.2	**9.90e-1**
DOCK10	25.46	**0.11**	0.25	**9.90e-1**
DOCK11	426.78	**0.57**	0.21	**3.32e-1**
DOCK2	1609.51	**0.12**	0.18	**9.90e-1**
DOCK4	72.97	**-0.13**	0.25	**9.90e-1**
DOCK7	269.86	**0.11**	0.22	**9.90e-1**
DOCK8	553.62	**0.15**	0.2	**9.87e-1**

DOCK9	396.75	**0.05**	0.21	**9.93e-1**

DOHH	143.58	**-0.52**	0.25	**6.07e-1**
DOK3	1907.23	**-0.16**	0.22	**9.87e-1**
DOK4	64.03	**-0.05**	0.25	**9.93e-1**
DOLK	80.29	**-0.33**	0.25	**9.10e-1**
DOLPP1	143.73	**-0.1**	0.24	**9.90e-1**
DONSON	327.45	**0.18**	0.21	**9.81e-1**
DOPEY1	199.55	**0.16**	0.22	**9.87e-1**
DOPEY2	109.2	**-0.2**	0.24	**9.83e-1**
DOT1L	1148.44	**-0.26**	0.22	**9.47e-1**
DPAGT1	401.21	**-0.08**	0.21	**9.90e-1**
DPCD	67.6	**0.19**	0.25	**9.87e-1**
DPF1	80.6	**-0.09**	0.25	**9.90e-1**
DPF2	630.21	**-0.31**	0.2	**8.49e-1**
DPH1	312.92	**-0.16**	0.22	**9.87e-1**
DPH2	910.06	**-0.47**	0.21	**5.71e-1**
DPH3	141.25	**0.13**	0.23	**9.90e-1**
DPH5	189.29	**0.11**	0.23	**9.90e-1**
DPH6	48.18	**0.28**	0.25	**9.47e-1**
DPH7	227.7	**-0.08**	0.22	**9.90e-1**
DPM1	422.16	**-0.07**	0.21	**9.91e-1**
DPM2	181.56	**0.09**	0.23	**9.90e-1**
DPP3	668.13	**-0.08**	0.21	**9.90e-1**
DPP7	757.28	**-0.28**	0.23	**9.39e-1**
DPP8	259.86	**0.1**	0.22	**9.90e-1**
DPP9	824	**-0.36**	0.22	**8.11e-1**
DPY19L1	344.22	**0.37**	0.22	**8.10e-1**
DPY19L2P2	24.46	**-0.13**	0.25	**9.90e-1**
DPY19L3	253.11	**0.26**	0.23	**9.47e-1**
DPY19L4	49.26	**0.38**	0.25	**8.62e-1**
DPY30	105.32	**0.18**	0.24	**9.87e-1**
DPYD	73.37	**-0.19**	0.25	**9.87e-1**
DPYSL2	744.93	**0.04**	0.19	**9.93e-1**
DR1	478.53	**0.09**	0.2	**9.90e-1**
DRAM2	206.29	**0.95**	0.23	**1.19e-2**
DRAP1	355.03	**-0.38**	0.22	**7.83e-1**
DRG1	514.12	**-0.05**	0.2	**9.93e-1**
DRG2	288.51	**-0.26**	0.22	**9.47e-1**
DROSHA	865.63	**-0.06**	0.19	**9.91e-1**
DSCC1	349.75	**0.37**	0.22	**8.03e-1**
DSCR3	234.98	**0.05**	0.22	**9.93e-1**
DSN1	313.18	**0.18**	0.22	**9.80e-1**
DST	595.36	**-0.27**	0.2	**9.06e-1**
DSTN	566.08	**0.38**	0.21	**7.22e-1**
DSTYK	142.39	**-0.13**	0.23	**9.90e-1**
DTD1	183.38	**0.3**	0.22	**9.06e-1**
DTD2	172.09	**0.25**	0.23	**9.49e-1**
DTL	770.83	**-0.01**	0.19	**9.96e-1**
DTNB	118.52	**0.19**	0.24	**9.81e-1**
DTNBP1	80.9	**0.28**	0.25	**9.47e-1**
DTWD1	73.53	**0.16**	0.25	**9.90e-1**
DTWD2	46.53	**-0.04**	0.25	**9.93e-1**
DTX1	2824.5	**-0.21**	0.21	**9.53e-1**
DTX2	270.47	**-0.25**	0.24	**9.52e-1**
DTX2P1-UPK3BP1-PMS2P11	31.17	**-0.31**	0.25	**9.32e-1**
DTX3	105.76	**0**	0.24	**9.98e-1**
DTX3L	632.68	**0.15**	0.2	**9.87e-1**
DTX4	644.01	**0.04**	0.21	**9.93e-1**
DTYMK	214.69	**-0.02**	0.22	**9.95e-1**
DUS1L	654.1	**0.02**	0.2	**9.95e-1**
DUS2	221.95	**0.11**	0.22	**9.90e-1**
DUS3L	506.92	**-0.33**	0.22	**8.64e-1**
DUS4L	147.52	**0.19**	0.23	**9.86e-1**
DUSP1	20.71	**-0.12**	0.24	**9.90e-1**
DUSP10	73.27	**0.19**	0.25	**9.87e-1**

DUSP11	278.02	**-0.02**	0.22	**9.94e-1**
DUSP12	201.25	**0.15**	0.22	**9.90e-1**
DUSP14	118.37	**-0.01**	0.24	**9.96e-1**
DUSP16	66.11	**0.22**	0.25	**9.77e-1**
DUSP18	18.7	**-0.09**	0.24	**9.90e-1**
DUSP2	148.6	**0.12**	0.25	**9.90e-1**
DUSP22	479.05	**0.52**	0.2	**4.11e-1**
DUSP28	11.86	**0.14**	0.22	**9.90e-1**
DUSP5	131.58	**0.64**	0.24	**3.16e-1**
DUSP7	573.69	**-0.48**	0.21	**5.45e-1**
DUT	537.67	**0.43**	0.2	**5.91e-1**
DVL1	446.72	**-0.26**	0.24	**9.47e-1**
DVL2	383	**-0.4**	0.23	**7.99e-1**
DVL3	893.84	**-0.37**	0.22	**8.04e-1**
DXO	101.26	**0.07**	0.24	**9.93e-1**
DYM	368.24	**0.08**	0.22	**9.90e-1**
DYNC1H1	3752.16	**-0.03**	0.18	**9.93e-1**
DYNC1I2	448.91	**-0.14**	0.2	**9.88e-1**

DYNC1LI1	426.35	**-0.16**	0.2	**9.87e-1**
DYNC1LI2	670.15	**-0.2**	0.2	**9.58e-1**
DYNC2H1	17.33	**0.15**	0.23	**9.90e-1**
DYNC2LI1	46.8	**0.15**	0.25	**9.90e-1**
DYNLL1	765.17	**0.11**	0.19	**9.90e-1**
DYNLL2	431.77	**0.19**	0.2	**9.66e-1**
DYNLRB1	302.28	**-0.2**	0.21	**9.61e-1**
DYNLT1	60.52	**0.16**	0.25	**9.90e-1**
DYNLT3	128.94	**-0.26**	0.24	**9.49e-1**
DYRK1A	421.96	**0.28**	0.21	**9.07e-1**
DYRK1B	41.29	**0**	0.25	**9.99e-1**
DYRK2	527.63	**-0.11**	0.2	**9.90e-1**
DYRK3	164.58	**0.07**	0.23	**9.92e-1**
DYRK4	34.76	**0.06**	0.25	**9.93e-1**
DZANK1	20.59	**0.16**	0.24	**9.89e-1**
DZIP3	180.23	**0.35**	0.23	**8.53e-1**
E2F1	985.78	**-0.12**	0.21	**9.90e-1**
E2F2	1159.61	**-0.13**	0.21	**9.90e-1**
E2F3	628.16	**0.19**	0.2	**9.59e-1**
E2F4	975.08	**-0.36**	0.22	**8.18e-1**
E2F5	301.42	**0.54**	0.22	**4.29e-1**
E2F6	126.43	**0.12**	0.24	**9.90e-1**
E2F7	147.58	**-0.01**	0.24	**9.96e-1**
E2F8	512.24	**-0.12**	0.2	**9.90e-1**
E4F1	182.66	**0.05**	0.24	**9.93e-1**
EAF1	351.49	**-0.03**	0.21	**9.93e-1**
EAF2	72.1	**0.04**	0.25	**9.93e-1**
EAPP	180.79	**0.22**	0.23	**9.61e-1**
EARS2	501.83	**0.07**	0.2	**9.90e-1**
EBAG9	198.38	**0**	0.23	**9.98e-1**
EBF1	262.26	**-0.24**	0.21	**9.47e-1**
EBI3	103.15	**-0.83**	0.25	**1.02e-1**
EBLN2	11.94	**0.07**	0.22	**9.90e-1**
EBLN3	1667.31	**0.23**	0.19	**9.40e-1**
EBNA1BP2	1859.74	**-0.14**	0.18	**9.86e-1**
EBP	245.29	**-0.12**	0.22	**9.90e-1**
EBPL	105.52	**0.8**	0.25	**1.05e-1**
ECD	296.3	**-0.1**	0.21	**9.90e-1**
ECE1	838.72	**-0.06**	0.2	**9.91e-1**
ECE2	145.13	**-0.04**	0.24	**9.93e-1**
ECH1	276.11	**-0.15**	0.23	**9.89e-1**
ECHDC1	424.17	**-0.07**	0.21	**9.90e-1**
ECHS1	294.51	**0.16**	0.21	**9.87e-1**
ECI1	99.32	**0.13**	0.25	**9.90e-1**
ECI2	660.11	**-0.14**	0.2	**9.87e-1**

ECM1	12.46	**0.02**	0.22	**9.95e-1**
ECSIT	367.06	**0.06**	0.21	**9.92e-1**
ECT2	620.31	**-0.09**	0.21	**9.90e-1**
EDC3	350.12	**-0.41**	0.21	**6.84e-1**
EDC4	1097.92	**-0.39**	0.21	**7.19e-1**
EDEM1	764.54	**0.41**	0.2	**6.07e-1**
EDEM2	145.51	**0.16**	0.23	**9.88e-1**
EDEM3	445.17	**0.1**	0.21	**9.90e-1**
EDF1	721.42	**-0.23**	0.22	**9.49e-1**
EDRF1	274.9	**0**	0.22	**9.98e-1**
EEA1	595.88	**-0.2**	0.21	**9.64e-1**
EED	194.96	**0.06**	0.22	**9.93e-1**
EEF1A1	63278.61	**0.21**	0.18	**9.47e-1**
EEF1B2	2584.37	**0.28**	0.18	**8.51e-1**
EEF1D	1073.76	**-0.05**	0.22	**9.93e-1**
EEF1E1	63.43	**0.1**	0.25	**9.90e-1**
EEF1G	7444.71	**-0.03**	0.19	**9.93e-1**
EEF2	17684.35	**0**	0.2	**9.98e-1**
EEF2K	770.42	**-0.04**	0.19	**9.93e-1**
EEF2KMT	158.43	**0.01**	0.23	**9.96e-1**
EEFSEC	223.6	**-0.19**	0.23	**9.80e-1**
EEPD1	85.37	**0.6**	0.25	**4.46e-1**
EFCAB11	20.61	**0.13**	0.24	**9.90e-1**
EFCAB14	1166.83	**-0.08**	0.19	**9.90e-1**
EFCAB2	53.77	**0.1**	0.25	**9.90e-1**
EFCAB7	103.88	**-0.15**	0.24	**9.90e-1**
EFHC1	33.56	**0.2**	0.25	**9.86e-1**
EFHD2	797.96	**-0.49**	0.23	**6.07e-1**
EFNA3	43	**-0.21**	0.25	**9.80e-1**
EFNA4	38.9	**0.1**	0.25	**9.90e-1**
EFNB1	53.05	**-0.17**	0.25	**9.90e-1**
EFR3A	474.72	**0.18**	0.22	**9.80e-1**
EFTUD1	377.47	**0.08**	0.21	**9.90e-1**
EFTUD2	2011.48	**-0.17**	0.18	**9.66e-1**
EGLN1	152.17	**0.39**	0.23	**8.10e-1**
EGR1	17.26	**0.23**	0.23	**9.58e-1**
EHBP1	235.66	**0.17**	0.23	**9.87e-1**
EHBP1L1	438.12	**-0.52**	0.23	**5.59e-1**

EHD1	2029.61	**-0.26**	0.21	**9.37e-1**
EHD4	238.21	**-0.02**	0.22	**9.95e-1**
EHMT1	1079.11	**-0.24**	0.2	**9.38e-1**
EHMT2	1002.21	**-0.32**	0.2	**8.38e-1**
EI24	1244.51	**0.36**	0.19	**7.13e-1**
EID1	735.59	**0**	0.19	**9.98e-1**
EID2	49.89	**0.75**	0.25	**2.19e-1**
EID2B	12.6	**0.09**	0.22	**9.90e-1**
EIF1	1455	**0.53**	0.19	**2.59e-1**
EIF1AD	318.87	**-0.2**	0.21	**9.66e-1**
EIF1AX	1057.6	**0.1**	0.2	**9.90e-1**
EIF1AY	396.6	**-0.39**	0.2	**7.04e-1**
EIF1B	205.33	**-0.27**	0.22	**9.42e-1**
EIF2A	1496.41	**0.1**	0.2	**9.90e-1**
EIF2AK1	1767.86	**0.16**	0.18	**9.80e-1**
EIF2AK2	167.98	**-0.05**	0.23	**9.93e-1**
EIF2AK3	466.68	**0.23**	0.21	**9.49e-1**
EIF2AK4	242.04	**-0.01**	0.22	**9.96e-1**
EIF2B1	673.66	**-0.1**	0.2	**9.90e-1**
EIF2B2	259.76	**-0.12**	0.21	**9.90e-1**
EIF2B3	389.05	**0**	0.21	**9.99e-1**
EIF2B4	280.33	**-0.36**	0.22	**8.30e-1**
EIF2B5	686.72	**-0.12**	0.19	**9.90e-1**
EIF2D	888.19	**-0.04**	0.19	**9.93e-1**
EIF2S1	966.6	**-0.13**	0.19	**9.90e-1**

EIF2S2	2234.45	**0.09**	0.18	**9.90e-1**
EIF2S3	3227.5	**0.23**	0.19	**9.42e-1**
EIF3A	7436.52	**-0.27**	0.18	**8.53e-1**
EIF3B	3688.36	**-0.02**	0.18	**9.93e-1**
EIF3D	2259.76	**0.06**	0.18	**9.91e-1**
EIF3E	2644.28	**0.18**	0.19	**9.66e-1**
EIF3F	1081.88	**0.49**	0.19	**3.58e-1**
EIF3G	1316.7	**-0.45**	0.21	**5.91e-1**
EIF3H	1605.3	**0.22**	0.19	**9.47e-1**
EIF3I	3546.13	**0**	0.18	**9.98e-1**
EIF3J	1424.23	**-0.34**	0.19	**7.41e-1**
EIF3J-AS1	28.63	**0.01**	0.25	**9.96e-1**
EIF3K	1198.89	**0.03**	0.19	**9.93e-1**
EIF3L	2636.49	**0.31**	0.18	**7.86e-1**
EIF3M	1626.5	**0.31**	0.2	**8.40e-1**
EIF4A2	2097.36	**0.29**	0.19	**8.52e-1**
EIF4A3	733.44	**0.33**	0.2	**8.12e-1**
EIF4B	10197.28	**0.26**	0.18	**8.58e-1**
EIF4E	865.79	**0.04**	0.19	**9.93e-1**
EIF4E2	514.93	**-0.44**	0.2	**5.94e-1**
EIF4EBP1	93.86	**-0.02**	0.25	**9.95e-1**
EIF4EBP2	1744.38	**-0.07**	0.19	**9.90e-1**
EIF4ENIF1	378.05	**-0.12**	0.2	**9.90e-1**
EIF4G1	8737.4	**-0.44**	0.19	**5.37e-1**
EIF4G2	8134.78	**-0.29**	0.18	**8.38e-1**
EIF4G3	1673.32	**-0.19**	0.18	**9.50e-1**
EIF4H	2131.92	**-0.24**	0.19	**9.23e-1**
EIF5	2413.86	**-0.16**	0.19	**9.80e-1**
EIF5A	5313.31	**-0.18**	0.19	**9.66e-1**
EIF5AL1	28.32	**0.47**	0.25	**7.04e-1**
EIF5B	2630.42	**-0.48**	0.18	**3.64e-1**
EIF6	590.26	**-0.08**	0.21	**9.90e-1**
ELAC1	35.27	**-0.07**	0.25	**9.93e-1**
ELAC2	1206.78	**-0.07**	0.19	**9.90e-1**
ELAVL1	1146.25	**-0.06**	0.19	**9.90e-1**
ELF1	1856.36	**-0.03**	0.19	**9.93e-1**
ELF2	259.53	**0.16**	0.22	**9.87e-1**
ELF4	495.2	**-0.24**	0.2	**9.47e-1**
ELK1	374.26	**-0.4**	0.23	**7.59e-1**
ELK3	57.88	**-0.28**	0.25	**9.49e-1**
ELK4	709.07	**-0.01**	0.2	**9.96e-1**
ELL	184.12	**-0.26**	0.25	**9.49e-1**
ELL3	690.04	**-0.05**	0.19	**9.93e-1**
ELMO1	1119.66	**-0.05**	0.19	**9.93e-1**
ELMO2	350.45	**-0.03**	0.21	**9.93e-1**
ELMO3	36.85	**0.12**	0.25	**9.90e-1**
ELMOD2	207.65	**0.23**	0.23	**9.58e-1**
ELMOD3	54.47	**-0.21**	0.25	**9.80e-1**
ELMSAN1	1499.59	**0**	0.2	**1.00e+0**
ELOF1	376.6	**-0.43**	0.22	**7.01e-1**
ELOVL1	635.92	**-0.21**	0.2	**9.53e-1**
ELOVL5	1170.15	**-0.04**	0.19	**9.93e-1**
ELOVL6	257.38	**0.04**	0.22	**9.93e-1**
ELP2	473.05	**0.25**	0.21	**9.37e-1**
ELP3	465.06	**0.11**	0.2	**9.90e-1**
ELP4	103.92	**0.22**	0.24	**9.73e-1**
ELP5	336.33	**0.06**	0.21	**9.91e-1**
ELP6	167.04	**0.09**	0.23	**9.90e-1**

EMB	833.39	**-0.02**	0.21	**9.93e-1**
EMBP1	34.62	**0.09**	0.25	**9.90e-1**
EMC1	535.75	**-0.09**	0.2	**9.90e-1**
EMC10	206.85	**-0.09**	0.24	**9.90e-1**
EMC2	167.69	**0**	0.23	**9.98e-1**

EMC3	167.69	**0.05**	0.23	**9.93e-1**
EMC3-AS1	133.49	**-0.2**	0.23	**9.80e-1**
EMC4	252.39	**0.23**	0.22	**9.49e-1**
EMC6	121.93	**-0.22**	0.25	**9.80e-1**
EMC7	169.21	**0.17**	0.23	**9.87e-1**
EMC8	183.27	**0.31**	0.23	**8.94e-1**
EMC9	75.1	**0.06**	0.25	**9.93e-1**
EMD	362.88	**-0.21**	0.22	**9.63e-1**
EME1	136.04	**0.05**	0.23	**9.93e-1**
EME2	121.92	**-0.28**	0.25	**9.47e-1**
EMG1	243.42	**-0.17**	0.23	**9.87e-1**
EML2	307.29	**0.08**	0.24	**9.90e-1**
EML2-AS1	41.82	**-0.06**	0.25	**9.93e-1**
EML3	308.46	**-0.23**	0.24	**9.61e-1**
EML4	832.08	**-0.11**	0.2	**9.90e-1**
EML5	97.93	**0.06**	0.24	**9.93e-1**
EML6	215.07	**0.1**	0.22	**9.90e-1**
ENAH	249.87	**-0.24**	0.22	**9.49e-1**
ENDOD1	326.31	**-0.05**	0.22	**9.93e-1**
ENDOG	11.62	**0.07**	0.22	**9.91e-1**
ENKD1	49.4	**0.03**	0.25	**9.93e-1**
ENO1	11214.96	**-0.09**	0.18	**9.90e-1**
ENO2	161.59	**0.22**	0.23	**9.64e-1**
ENO3	42.71	**0.1**	0.25	**9.90e-1**
ENOPH1	358.33	**0.25**	0.21	**9.47e-1**
ENOX2	116.11	**0.16**	0.24	**9.89e-1**
ENPP1	35.84	**0.03**	0.25	**9.93e-1**
ENPP4	120.23	**0.15**	0.24	**9.90e-1**
ENPP5	15.57	**0.15**	0.23	**9.90e-1**
ENSA	796.71	**0.04**	0.19	**9.93e-1**
ENTHD2	116.03	**-0.24**	0.25	**9.66e-1**
ENTPD1-AS1	21.72	**0.12**	0.24	**9.90e-1**
ENTPD4	606.01	**0.05**	0.2	**9.93e-1**
ENTPD5	75.71	**0**	0.25	**9.98e-1**
ENTPD6	409.63	**-0.21**	0.22	**9.60e-1**
ENTPD7	146.14	**0.03**	0.23	**9.93e-1**
ENY2	402.59	**0.24**	0.2	**9.43e-1**
EP300	1530.19	**-0.26**	0.18	**8.73e-1**
EP400	981.33	**-0.28**	0.2	**8.85e-1**
EP400NL	41.17	**-0.29**	0.25	**9.47e-1**
EPB41	1860.82	**-0.02**	0.18	**9.93e-1**
EPB41L4A-AS1	86.22	**0.11**	0.25	**9.90e-1**
EPC1	317.97	**0.15**	0.22	**9.87e-1**
EPC2	38.53	**-0.1**	0.25	**9.90e-1**
EPG5	109.01	**0.2**	0.24	**9.81e-1**
EPHB4	118.42	**-0.18**	0.25	**9.87e-1**
EPHX3	18.18	**-0.24**	0.24	**9.58e-1**
EPM2A	94.4	**0.13**	0.24	**9.90e-1**
EPM2AIP1	513.03	**0.02**	0.21	**9.93e-1**
EPN1	1098.61	**-0.41**	0.24	**7.97e-1**
EPN2	46.51	**-0.08**	0.25	**9.91e-1**
EPOR	38.24	**0.06**	0.25	**9.93e-1**
EPRS	3513.65	**0.15**	0.19	**9.86e-1**
EPS15	2141.84	**0.06**	0.19	**9.91e-1**
EPS15L1	529.75	**-0.07**	0.21	**9.91e-1**
EPSTI1	24.71	**-0.01**	0.25	**9.96e-1**
EPT1	1083.63	**0.19**	0.2	**9.60e-1**
ERAL1	478.17	**0.1**	0.2	**9.90e-1**
ERAP1	1075.32	**0.13**	0.19	**9.89e-1**
ERAP2	90.2	**-0.16**	0.25	**9.90e-1**
ERBB2	33.85	**0.23**	0.25	**9.73e-1**
ERBB2IP	724.74	**0.01**	0.2	**9.96e-1**
ERC1	281.22	**-0.24**	0.22	**9.48e-1**
ERCC1	352.27	**-0.16**	0.23	**9.89e-1**
ERCC2	157.35	**-0.13**	0.24	**9.90e-1**

ERCC3	230.63	**0.13**	0.22	**9.90e-1**
ERCC4	145.61	**0.15**	0.24	**9.90e-1**
ERCC5	10.77	**-0.18**	0.21	**9.80e-1**
ERCC6	98.38	**0.02**	0.25	**9.95e-1**
ERCC6L	297.27	**-0.04**	0.22	**9.93e-1**
ERCC6L2	185.05	**0.19**	0.23	**9.82e-1**
ERCC8	61.27	**0.11**	0.25	**9.90e-1**
ERF	618.72	**-0.31**	0.23	**8.92e-1**
ERGIC1	752.59	**-0.31**	0.2	**8.52e-1**
ERGIC2	212.59	**0.3**	0.24	**9.25e-1**
ERGIC3	611.56	**0.24**	0.21	**9.47e-1**
ERH	851.19	**0.31**	0.2	**8.40e-1**
ERI1	321.21	**0.13**	0.21	**9.90e-1**

ERI2	149.67	**0.04**	0.24	**9.93e-1**
ERI3	468.36	**-0.13**	0.21	**9.90e-1**
ERICH1	392.66	**-0.5**	0.23	**5.86e-1**
ERLEC1	246.92	**0.19**	0.22	**9.74e-1**
ERLIN1	301.31	**0.14**	0.21	**9.90e-1**
ERLIN2	318.52	**-0.1**	0.21	**9.90e-1**
ERMAP	64.72	**0.17**	0.25	**9.89e-1**
ERMARD	83.51	**0.25**	0.25	**9.54e-1**
ERMP1	251.88	**-0.13**	0.22	**9.90e-1**
ERN1	116.98	**0.08**	0.24	**9.91e-1**
ERO1A	894.15	**0.03**	0.2	**9.93e-1**
ERO1B	85.62	**0.44**	0.25	**7.57e-1**
ERP29	1007.62	**-0.2**	0.22	**9.74e-1**
ERP44	362.77	**0.32**	0.22	**8.64e-1**
ERV3-1	44.79	**-0.23**	0.25	**9.69e-1**
ERVK13-1	37.39	**-0.09**	0.25	**9.90e-1**
ESCO1	466.6	**0.15**	0.21	**9.87e-1**
ESCO2	265.58	**0.01**	0.23	**9.96e-1**
ESD	125.06	**0.24**	0.24	**9.59e-1**
ESF1	641.49	**-0.36**	0.2	**7.33e-1**
ESPL1	1008.81	**-0.47**	0.22	**5.91e-1**
ESPNL	44.42	**-0.27**	0.25	**9.49e-1**
ESRRA	336.68	**-0.04**	0.24	**9.93e-1**
ESYT1	656.31	**0.01**	0.2	**9.96e-1**
ESYT2	699.53	**0.06**	0.2	**9.91e-1**
ETAA1	173.63	**0.17**	0.23	**9.87e-1**
ETF1	2079.71	**-0.06**	0.19	**9.91e-1**
ETFA	621.64	**0.22**	0.2	**9.49e-1**
ETFB	273.87	**0.31**	0.22	**8.78e-1**
ETFDH	151.27	**0.54**	0.23	**5.36e-1**
ETHE1	19.43	**0.03**	0.24	**9.93e-1**
ETNK1	550.12	**0.22**	0.21	**9.54e-1**
ETS1	2079.13	**-0.07**	0.19	**9.90e-1**
ETS2	124.11	**0.04**	0.24	**9.93e-1**
ETV3	81.25	**-0.24**	0.25	**9.61e-1**
ETV5	27.79	**0.78**	0.25	**1.45e-1**
ETV6	520.45	**-0.12**	0.2	**9.90e-1**
EVC	149.54	**-0.58**	0.24	**4.95e-1**
EVC2	25.6	**0.3**	0.25	**9.42e-1**
EVI2A	94.15	**0.18**	0.24	**9.87e-1**
EVI2B	1181.58	**-0.55**	0.19	**2.21e-1**
EVI5	81.99	**0.31**	0.25	**9.25e-1**
EVI5L	26.64	**0.05**	0.25	**9.93e-1**
EWSR1	3474.82	**-0.22**	0.19	**9.47e-1**
EXD3	65.46	**-0.01**	0.25	**9.96e-1**
EXO1	626.98	**-0.03**	0.2	**9.93e-1**
EXOC1	220.32	**0.17**	0.23	**9.87e-1**
EXOC2	253.29	**0.16**	0.22	**9.87e-1**
EXOC3	262.51	**0.16**	0.22	**9.87e-1**
EXOC4	513.23	**0.18**	0.2	**9.72e-1**

EXOC5	656.39	**0.16**	0.21	**9.86e-1**
EXOC6	267.62	**-0.1**	0.22	**9.90e-1**
EXOC7	686.79	**-0.14**	0.2	**9.87e-1**
EXOC8	159.65	**-0.13**	0.23	**9.90e-1**
EXOG	128.04	**0.14**	0.24	**9.90e-1**
EXOSC1	128.75	**0.07**	0.24	**9.93e-1**
EXOSC10	963.26	**-0.06**	0.19	**9.91e-1**
EXOSC2	538.73	**-0.02**	0.2	**9.95e-1**
EXOSC3	235.8	**0.24**	0.22	**9.49e-1**
EXOSC4	103.35	**0.29**	0.24	**9.45e-1**
EXOSC5	176.41	**-0.11**	0.24	**9.90e-1**
EXOSC6	131.23	**0**	0.23	**9.98e-1**
EXOSC7	266.32	**0.12**	0.21	**9.90e-1**
EXOSC8	295.89	**0.29**	0.22	**9.10e-1**
EXOSC9	404.18	**-0.03**	0.21	**9.93e-1**
EXT1	34.28	**-0.07**	0.25	**9.93e-1**
EXT2	142.73	**0.08**	0.23	**9.90e-1**
EXTL2	43.05	**-0.01**	0.25	**9.98e-1**
EXTL3	204.16	**-0.04**	0.23	**9.93e-1**
EYA3	595.43	**-0.12**	0.2	**9.90e-1**
EZH1	388.11	**-0.01**	0.21	**9.97e-1**
EZH2	1231.41	**-0.02**	0.19	**9.93e-1**
EZR	4781.14	**-0.25**	0.18	**8.92e-1**
F11R	201.63	**0.19**	0.22	**9.80e-1**
F8A1	30.26	**0.2**	0.25	**9.86e-1**
FAAP100	393.27	**-0.34**	0.24	**8.74e-1**
FAAP20	84.26	**-0.07**	0.25	**9.93e-1**
FAAP24	58	**-0.35**	0.25	**8.83e-1**
FABP5	1087.86	**-0.32**	0.19	**8.07e-1**
FADD	153.13	**0.37**	0.23	**8.40e-1**
FADS1	21.74	**-0.18**	0.24	**9.87e-1**
FADS2	38.43	**-0.18**	0.25	**9.88e-1**
FADS3	250.82	**-0.45**	0.24	**6.93e-1**

FAF1	817.97	**0.14**	0.2	**9.87e-1**
FAF2	433.44	**0.06**	0.2	**9.93e-1**
FAHD1	41.01	**0.08**	0.25	**9.91e-1**
FAHD2A	125.26	**0.13**	0.25	**9.90e-1**
FAHD2B	66.91	**0.14**	0.25	**9.90e-1**
FAIM	53.35	**-0.23**	0.25	**9.74e-1**
FAM102A	1187.99	**-0.27**	0.23	**9.45e-1**
FAM102B	151.01	**0.31**	0.24	**9.12e-1**
FAM103A1	45.8	**-0.17**	0.25	**9.89e-1**
FAM104A	236.42	**0**	0.22	**9.99e-1**
FAM104B	33.61	**0.02**	0.25	**9.96e-1**
FAM107B	1873.49	**0.6**	0.19	**1.42e-1**
FAM109A	26.76	**-0.14**	0.23	**9.90e-1**
FAM110A	72.75	**0**	0.25	**9.98e-1**
FAM111A	323.95	**0.03**	0.21	**9.93e-1**
FAM111B	409.98	**0.19**	0.22	**9.74e-1**
FAM114A2	114.35	**0.18**	0.24	**9.87e-1**
FAM117A	820.02	**-0.19**	0.22	**9.74e-1**
FAM117B	331.05	**-0.24**	0.22	**9.49e-1**
FAM118A	124.02	**0.01**	0.24	**9.96e-1**
FAM118B	78.39	**0.09**	0.25	**9.90e-1**
FAM120A	2734.21	**-0.26**	0.18	**8.64e-1**
FAM120AOS	235.39	**-0.03**	0.22	**9.93e-1**
FAM120B	388.05	**-0.02**	0.21	**9.94e-1**
FAM120C	135.11	**0.16**	0.23	**9.90e-1**
FAM122A	202.87	**0.12**	0.23	**9.90e-1**
FAM122B	699.99	**0.28**	0.2	**8.95e-1**
FAM122C	25.97	**-0.05**	0.25	**9.93e-1**
FAM126A	526.16	**-0.05**	0.21	**9.93e-1**
FAM126B	194.55	**-0.09**	0.23	**9.90e-1**

FAM129A	519.65	**0.17**	0.2	**9.80e-1**
FAM129C	164.19	**-0.3**	0.24	**9.33e-1**
FAM134A	540.88	**-0.11**	0.2	**9.90e-1**
FAM134C	265.39	**-0.01**	0.22	**9.96e-1**
FAM135A	406.24	**0.25**	0.22	**9.47e-1**
FAM136A	652.75	**0.05**	0.2	**9.93e-1**
FAM13B	510.85	**0.07**	0.21	**9.90e-1**
FAM149B1	54.77	**0.32**	0.25	**9.32e-1**
FAM156A	13.27	**0.09**	0.22	**9.90e-1**
FAM160A2	167.72	**-0.17**	0.24	**9.87e-1**
FAM160B1	103.83	**0.49**	0.24	**6.44e-1**
FAM160B2	243.25	**-0.48**	0.24	**6.52e-1**
FAM161A	104.04	**-0.05**	0.24	**9.93e-1**
FAM161B	29.76	**0.02**	0.25	**9.95e-1**
FAM162A	259.06	**0.22**	0.22	**9.58e-1**
FAM167A	315.15	**0.08**	0.22	**9.90e-1**
FAM168A	319	**-0.04**	0.21	**9.93e-1**
FAM168B	680.19	**-0.29**	0.2	**8.68e-1**
FAM171A2	26.77	**-0.01**	0.24	**9.96e-1**
FAM172A	90.7	**0.09**	0.25	**9.90e-1**
FAM173A	14.45	**-0.03**	0.23	**9.93e-1**
FAM173B	149.45	**0**	0.23	**9.98e-1**
FAM174A	17.73	**0.23**	0.24	**9.60e-1**
FAM175A	125.1	**0.29**	0.24	**9.42e-1**
FAM175B	267.6	**0.22**	0.21	**9.52e-1**
FAM177A1	85.23	**0.18**	0.25	**9.87e-1**
FAM178A	579.34	**0.02**	0.2	**9.93e-1**
FAM179B	173.65	**0.19**	0.23	**9.81e-1**
FAM188A	87.64	**0.2**	0.25	**9.84e-1**
FAM189B	360.27	**-0.31**	0.24	**9.12e-1**
FAM192A	859.66	**0.04**	0.19	**9.93e-1**
FAM193A	414.29	**-0.11**	0.21	**9.90e-1**
FAM193B	366.03	**-0.3**	0.23	**9.12e-1**
FAM195A	117.28	**-0.24**	0.25	**9.61e-1**
FAM195B	91.22	**-0.25**	0.25	**9.58e-1**
FAM199X	227.28	**0.29**	0.23	**9.25e-1**
FAM200A	65.79	**0.05**	0.25	**9.93e-1**
FAM200B	31.97	**0.11**	0.25	**9.90e-1**
FAM204A	153.14	**0.04**	0.23	**9.93e-1**
FAM206A	178.26	**0.18**	0.23	**9.86e-1**
FAM207A	170.83	**0.01**	0.23	**9.97e-1**
FAM208A	1037.8	**0.08**	0.2	**9.90e-1**
FAM208B	1894.66	**-0.43**	0.19	**5.76e-1**
FAM20B	386.54	**0.23**	0.21	**9.49e-1**
FAM210A	271.25	**0.14**	0.22	**9.90e-1**
FAM212A	19.98	**-0.06**	0.24	**9.93e-1**
FAM212B	39.53	**0.14**	0.25	**9.90e-1**
FAM213A	96.91	**-0.06**	0.25	**9.93e-1**
FAM213B	56.18	**-0.09**	0.25	**9.90e-1**
FAM214A	277.69	**-0.02**	0.22	**9.93e-1**
FAM214B	56.71	**0.13**	0.25	**9.90e-1**
FAM216A	398.94	**0.34**	0.21	**8.21e-1**
FAM217B	291.13	**0.02**	0.21	**9.94e-1**

FAM219A	83.61	**-0.1**	0.25	**9.90e-1**
FAM219B	131.89	**0.25**	0.24	**9.49e-1**
FAM21A	549.73	**-0.07**	0.2	**9.90e-1**
FAM21C	421.07	**0**	0.2	**9.98e-1**
FAM220A	225.17	**0.24**	0.22	**9.49e-1**
FAM222A	15.75	**-0.3**	0.22	**8.91e-1**
FAM222B	301.01	**-0.31**	0.21	**8.64e-1**
FAM229B	16.07	**0.2**	0.23	**9.80e-1**
FAM27E3	15.04	**-0.06**	0.22	**9.93e-1**
FAM32A	393.77	**-0.07**	0.21	**9.90e-1**
FAM35A	670.64	**-0.19**	0.2	**9.66e-1**

FAM3A	107.18	**-0.14**	0.25	**9.90e-1**
FAM3C	704.28	**0.27**	0.19	**8.86e-1**
FAM49A	19.44	**0.25**	0.24	**9.54e-1**
FAM49B	1177.62	**0.34**	0.21	**8.21e-1**
FAM50A	256.5	**0.1**	0.22	**9.90e-1**
FAM53B	803.64	**-0.45**	0.23	**6.54e-1**
FAM53C	647.82	**-0.4**	0.21	**6.87e-1**
FAM57A	114.03	**0.08**	0.24	**9.90e-1**
FAM58A	61.61	**0.21**	0.25	**9.81e-1**
FAM60A	730.47	**0.13**	0.2	**9.90e-1**
FAM63B	46.93	**-0.18**	0.25	**9.87e-1**
FAM65A	39.09	**-0.24**	0.25	**9.61e-1**
FAM65B	1012.39	**-0.31**	0.19	**8.25e-1**
FAM69A	279.04	**0.05**	0.22	**9.93e-1**
FAM72B	421.91	**-0.58**	0.21	**3.01e-1**
FAM73A	51.61	**-0.02**	0.25	**9.95e-1**
FAM73B	263.04	**-0.39**	0.25	**8.41e-1**
FAM76A	78.35	**0.05**	0.25	**9.93e-1**
FAM76B	249.74	**0.23**	0.22	**9.52e-1**
FAM78A	385.46	**-0.42**	0.23	**7.41e-1**
FAM81A	445.19	**0.21**	0.2	**9.49e-1**
FAM83D	322.57	**0.11**	0.21	**9.90e-1**
FAM83G	224.85	**-0.14**	0.24	**9.90e-1**
FAM86B1	57.79	**0.14**	0.25	**9.90e-1**
FAM86B2	22.59	**0.12**	0.24	**9.90e-1**
FAM86B3P	42.68	**-0.36**	0.25	**8.74e-1**
FAM86C1	149.15	**0.1**	0.23	**9.90e-1**
FAM86C2P	55.74	**-0.12**	0.25	**9.90e-1**
FAM86DP	119.22	**-0.11**	0.24	**9.90e-1**
FAM86EP	53.02	**0.06**	0.25	**9.93e-1**
FAM86HP	25.83	**-0.01**	0.25	**9.97e-1**
FAM86JP	27.37	**0.39**	0.25	**8.41e-1**
FAM89B	67	**-0.19**	0.25	**9.87e-1**
FAM8A1	185.34	**-0.02**	0.23	**9.94e-1**
FAM91A1	626.81	**0.3**	0.21	**8.73e-1**
FAM96A	386.68	**0.01**	0.21	**9.96e-1**
FAM96B	101.26	**-0.16**	0.25	**9.90e-1**
FAM98A	1257.99	**-0.34**	0.19	**7.33e-1**
FAM98B	498.25	**-0.27**	0.21	**9.20e-1**
FAM98C	32.31	**-0.08**	0.25	**9.91e-1**
FAN1	86.58	**0.31**	0.25	**9.25e-1**
FANCA	1041.34	**-0.01**	0.19	**9.96e-1**
FANCB	92.62	**-0.34**	0.24	**8.91e-1**
FANCC	105.67	**-0.13**	0.24	**9.90e-1**
FANCD2	887.63	**0.16**	0.2	**9.81e-1**
FANCE	109.71	**-0.09**	0.24	**9.90e-1**
FANCF	64.74	**0.03**	0.25	**9.93e-1**
FANCG	231.41	**-0.22**	0.22	**9.58e-1**
FANCI	1247.13	**0.12**	0.19	**9.90e-1**
FANCL	92.41	**0.41**	0.25	**8.07e-1**
FANCM	170.78	**-0.04**	0.23	**9.93e-1**
FAR1	1096.96	**0.16**	0.21	**9.86e-1**
FARP2	258.37	**-0.16**	0.22	**9.87e-1**
FARS2	79.88	**-0.09**	0.25	**9.90e-1**
FARSA	1536.72	**-0.26**	0.2	**9.20e-1**
FARSB	1044.15	**0.05**	0.2	**9.93e-1**
FAS	419.35	**0.41**	0.21	**6.69e-1**
FASN	6258.44	**-0.41**	0.23	**7.41e-1**
FASTK	387.29	**-0.22**	0.23	**9.63e-1**
FASTKD1	315.35	**0.06**	0.22	**9.93e-1**
FASTKD2	615.31	**0.14**	0.21	**9.90e-1**
FASTKD3	262.64	**-0.01**	0.22	**9.96e-1**
FASTKD5	360.16	**-0.02**	0.21	**9.95e-1**
FAU	1084.06	**0.09**	0.2	**9.90e-1**

FBF1	97.06	**-0.15**	0.25	**9.90e-1**
FBL	1998.8	**-0.38**	0.21	**7.31e-1**
FBRS	1429.32	**-0.18**	0.21	**9.80e-1**
FBRSL1	387.96	**-0.55**	0.25	**5.64e-1**
FBXL12	125.3	**-0.14**	0.24	**9.90e-1**
FBXL13	10.29	**-0.01**	0.21	**9.96e-1**
FBXL14	200.75	**-0.31**	0.23	**8.98e-1**
FBXL15	22.01	**-0.09**	0.23	**9.90e-1**

FBXL17	88.3	**0.04**	0.25	**9.93e-1**
FBXL18	255.73	**-0.4**	0.24	**8.07e-1**
FBXL19	407.81	**-0.3**	0.25	**9.39e-1**
FBXL19-AS1	30.47	**-0.27**	0.25	**9.49e-1**
FBXL20	110.86	**-0.02**	0.24	**9.93e-1**
FBXL3	250.82	**0.3**	0.22	**9.06e-1**
FBXL4	213.14	**0.2**	0.23	**9.80e-1**
FBXL5	134.34	**0.28**	0.24	**9.47e-1**
FBXL6	126.24	**-0.11**	0.25	**9.90e-1**
FBXL8	15.81	**-0.08**	0.21	**9.90e-1**
FBXO10	108.15	**-0.35**	0.24	**8.64e-1**
FBXO11	491.05	**0.1**	0.21	**9.90e-1**
FBXO16	24.16	**0.11**	0.25	**9.90e-1**
FBXO18	525.1	**0.02**	0.2	**9.93e-1**
FBXO21	560.3	**0.17**	0.2	**9.80e-1**
FBXO22	280.42	**0.12**	0.21	**9.90e-1**
FBXO28	205.94	**0.18**	0.23	**9.83e-1**
FBXO3	114.21	**0.11**	0.24	**9.90e-1**
FBXO30	302.9	**-0.1**	0.22	**9.90e-1**
FBXO31	276.49	**-0.15**	0.23	**9.90e-1**
FBXO33	191.1	**0.05**	0.23	**9.93e-1**
FBXO34	220.22	**0.27**	0.22	**9.37e-1**
FBXO38	253.6	**0.13**	0.22	**9.90e-1**
FBXO4	47.58	**0.18**	0.25	**9.87e-1**
FBXO41	1131.38	**-0.43**	0.22	**6.75e-1**
FBXO42	245.65	**-0.05**	0.22	**9.93e-1**
FBXO45	359.42	**0.21**	0.21	**9.58e-1**
FBXO46	223.01	**-0.23**	0.22	**9.54e-1**
FBXO48	19.94	**0.05**	0.24	**9.93e-1**
FBXO5	353.21	**0.02**	0.21	**9.95e-1**
FBXO7	711.81	**0.06**	0.19	**9.91e-1**
FBXO8	54	**0.43**	0.25	**8.10e-1**
FBXO9	223.49	**0.33**	0.22	**8.52e-1**
FBXW11	528.98	**0.14**	0.2	**9.88e-1**
FBXW2	933.51	**-0.01**	0.19	**9.96e-1**
FBXW4	119.67	**-0.19**	0.24	**9.86e-1**
FBXW5	368.86	**-0.22**	0.24	**9.63e-1**
FBXW7	293.11	**-0.04**	0.22	**9.93e-1**
FBXW8	204.3	**-0.33**	0.22	**8.64e-1**
FBXW9	39.38	**-0.14**	0.25	**9.90e-1**
FCER2	63.65	**0.71**	0.25	**2.61e-1**
FCF1	390.14	**-0.19**	0.21	**9.66e-1**
FCGBP	189.33	**-0.03**	0.24	**9.93e-1**
FCGR2B	45.95	**-0.28**	0.25	**9.47e-1**
FCHO1	711.92	**-0.27**	0.23	**9.42e-1**
FCHO2	40.26	**-0.1**	0.25	**9.90e-1**
FCHSD2	604.25	**0.23**	0.2	**9.47e-1**
FCMR	49.37	**0.22**	0.25	**9.76e-1**
FCRL1	66.48	**-0.24**	0.25	**9.66e-1**
FCRL2	184.53	**0.11**	0.22	**9.90e-1**
FCRL3	568.82	**0.28**	0.2	**8.74e-1**
FCRL4	24.46	**0.16**	0.25	**9.89e-1**
FCRLA	1456.09	**-0.04**	0.19	**9.93e-1**
FCRLB	27.91	**0.03**	0.25	**9.93e-1**
FDFT1	1718.81	**-0.11**	0.18	**9.90e-1**
FDPS	1086.38	**-0.26**	0.19	**8.87e-1**

FDX1	116.51	**0.36**	0.24	**8.64e-1**
FDX1L	60.44	**-0.25**	0.25	**9.58e-1**
FDXACB1	67.35	**0.1**	0.25	**9.90e-1**
FDXR	151.87	**-0.07**	0.25	**9.92e-1**
FECH	303.05	**0.24**	0.22	**9.47e-1**
FEM1A	301.66	**-0.13**	0.23	**9.90e-1**
FEM1B	497.68	**0.11**	0.21	**9.90e-1**
FEM1C	143.99	**0.19**	0.24	**9.81e-1**
FEN1	1152.21	**-0.15**	0.2	**9.87e-1**
FER	113.27	**-0.13**	0.24	**9.90e-1**
FERMT3	942.68	**-0.08**	0.23	**9.90e-1**
FEZ2	161.66	**0.32**	0.23	**8.96e-1**
FGD2	219.77	**-0.09**	0.23	**9.90e-1**
FGD3	102.58	**-0.17**	0.24	**9.88e-1**
FGD4	17.49	**0.01**	0.24	**9.96e-1**
FGD5-AS1	600.77	**0.22**	0.21	**9.49e-1**
FGD6	278.87	**0.2**	0.22	**9.66e-1**
FGF11	109.57	**-0.1**	0.24	**9.90e-1**
FGFR1OP	233.04	**0.24**	0.22	**9.49e-1**
FGFR1OP2	202.2	**0.15**	0.23	**9.90e-1**
FGFR4	197.96	**-0.23**	0.25	**9.68e-1**
FGFRL1	34.1	**0.18**	0.25	**9.87e-1**
FGGY	11.3	**0.2**	0.21	**9.62e-1**
FGR	1124.1	**-0.12**	0.22	**9.90e-1**
FH	532.86	**0.32**	0.21	**8.62e-1**
FHOD1	504.94	**-0.12**	0.22	**9.90e-1**
FIBP	269.67	**0.22**	0.21	**9.50e-1**

FICD	16.89	**0.21**	0.23	**9.72e-1**
FIG4	187.99	**0.43**	0.23	**7.15e-1**
FIGNL1	271.98	**0.21**	0.23	**9.66e-1**
FIP1L1	832.49	**-0.26**	0.19	**8.97e-1**
FIS1	544.43	**-0.1**	0.22	**9.90e-1**
FITM2	50.77	**-0.29**	0.25	**9.47e-1**
FIZ1	93.39	**-0.15**	0.25	**9.90e-1**
FKBP11	613.5	**-0.19**	0.2	**9.66e-1**
FKBP14	48.96	**0**	0.25	**9.98e-1**
FKBP15	811.56	**-0.16**	0.19	**9.80e-1**
FKBP1A	1755.16	**0.13**	0.19	**9.89e-1**
FKBP2	211.75	**-0.17**	0.24	**9.88e-1**
FKBP3	322.27	**0.09**	0.22	**9.90e-1**
FKBP4	2482.7	**-0.31**	0.18	**7.99e-1**
FKBP5	2435.39	**-0.5**	0.18	**3.07e-1**
FKBP7	46.74	**-0.14**	0.25	**9.90e-1**
FKBP8	647.25	**-0.12**	0.23	**9.90e-1**
FKBPL	54.03	**0.04**	0.25	**9.93e-1**
FKRP	72.35	**-0.22**	0.25	**9.75e-1**
FKTN	89.06	**0.22**	0.25	**9.73e-1**
FLAD1	258.67	**-0.34**	0.23	**8.64e-1**
FLCN	102.29	**0.28**	0.25	**9.47e-1**
FLI1	751.3	**-0.29**	0.2	**8.68e-1**
FLII	1143.66	**0**	0.19	**9.99e-1**
FLJ10038	55.33	**0.4**	0.25	**8.39e-1**
FLJ37453	22.61	**0**	0.25	**9.98e-1**
FLJ42627	40.48	**-0.19**	0.25	**9.87e-1**
FLNA	4833.24	**-0.18**	0.21	**9.80e-1**
FLNB	1755.64	**-0.09**	0.19	**9.90e-1**
FLOT1	450.56	**0.08**	0.21	**9.90e-1**
FLOT2	702.22	**-0.03**	0.2	**9.93e-1**
FLT3LG	24.89	**-0.23**	0.25	**9.72e-1**
FLVCR1	207.65	**-0.12**	0.22	**9.90e-1**
FLYWCH1	269.06	**-0.3**	0.24	**9.37e-1**
FLYWCH2	97.06	**-0.3**	0.25	**9.47e-1**
FMNL1	769.34	**-0.31**	0.21	**8.68e-1**

FMNL2	133.32	**0.24**	0.24	**9.56e-1**
FMNL3	639.43	**-0.12**	0.2	**9.90e-1**
FMR1	550.55	**0.1**	0.21	**9.90e-1**
FN3KRP	124.56	**-0.19**	0.24	**9.86e-1**
FNBP1	3498.15	**0.03**	0.18	**9.93e-1**
FNBP4	1172.59	**-0.11**	0.19	**9.90e-1**
FNDC3A	293.7	**0.4**	0.22	**7.38e-1**
FNDC3B	81.5	**-0.03**	0.25	**9.93e-1**
FNIP1	166.2	**0.15**	0.23	**9.89e-1**
FNIP2	12.29	**0.52**	0.21	**4.48e-1**
FNTA	465.71	**0.3**	0.21	**8.73e-1**
FNTB	16.45	**-0.43**	0.23	**7.22e-1**
FOCAD	317.63	**-0.04**	0.21	**9.93e-1**
FOPNL	451.12	**-0.01**	0.21	**9.98e-1**
FOSB	27.98	**0.01**	0.25	**9.96e-1**
FOSL2	16.4	**-0.04**	0.23	**9.93e-1**
FOXD2-AS1	84.1	**-0.21**	0.25	**9.81e-1**
FOXJ2	154.01	**-0.29**	0.23	**9.39e-1**
FOXJ3	1236.91	**-0.05**	0.19	**9.93e-1**
FOXK1	1102.58	**-0.21**	0.21	**9.58e-1**
FOXK2	1008.05	**-0.27**	0.19	**8.82e-1**
FOXM1	1706.99	**-0.43**	0.2	**5.96e-1**
FOXN2	350.42	**0.22**	0.22	**9.60e-1**
FOXN3	545.28	**0.53**	0.2	**3.41e-1**
FOXO1	750.31	**-0.05**	0.19	**9.93e-1**
FOXO3	411.39	**0.31**	0.21	**8.61e-1**
FOXO4	54.7	**0.11**	0.25	**9.90e-1**
FOXP1	279.09	**-0.32**	0.22	**8.64e-1**
FOXP4	827.54	**-0.39**	0.23	**7.95e-1**
FOXP4-AS1	15.61	**-0.09**	0.23	**9.90e-1**
FOXRED1	389.84	**-0.2**	0.22	**9.74e-1**
FOXRED2	627.46	**-0.2**	0.2	**9.58e-1**
FPGS	443.93	**-0.19**	0.23	**9.80e-1**
FPGT	35.65	**0.17**	0.25	**9.90e-1**
FRA10AC1	141.71	**-0.17**	0.23	**9.87e-1**
FRAT2	30.17	**0**	0.25	**9.98e-1**
FRG1	290.1	**-0.13**	0.21	**9.90e-1**
FRG1B	93.9	**-0.17**	0.25	**9.87e-1**
FRMD8	333.83	**-0.28**	0.23	**9.37e-1**
FRRS1	50.94	**0.15**	0.25	**9.90e-1**
FRS2	86.82	**-0.02**	0.25	**9.96e-1**
FRS3	34.57	**-0.41**	0.25	**8.31e-1**
FRY	155.3	**-0.08**	0.23	**9.90e-1**
FRYL	485.21	**0.09**	0.22	**9.90e-1**
FSD1	22.56	**0.02**	0.25	**9.96e-1**
FSD1L	349.95	**0.5**	0.22	**5.42e-1**
FSTL3	42.02	**-0.08**	0.25	**9.91e-1**

FTH1	6557.6	**0.29**	0.19	**8.51e-1**
FTL	2903.35	**-0.12**	0.21	**9.90e-1**
FTO	395.63	**-0.06**	0.21	**9.93e-1**
FTSJ1	532.5	**-0.21**	0.2	**9.50e-1**
FTSJ2	345.08	**-0.11**	0.21	**9.90e-1**
FTSJ3	1228.39	**-0.28**	0.19	**8.64e-1**
FUBP1	1553.67	**-0.41**	0.18	**5.70e-1**
FUBP3	910.14	**-0.43**	0.2	**5.91e-1**
FUCA1	148.03	**0.38**	0.23	**8.30e-1**
FUK	47.44	**-0.16**	0.25	**9.90e-1**
FUNDC1	76.31	**0.16**	0.25	**9.90e-1**
FUNDC2	176.67	**0.11**	0.23	**9.90e-1**
FURIN	123.45	**-0.23**	0.25	**9.66e-1**
FUS	4334.18	**-0.38**	0.18	**6.14e-1**
FUT10	42.44	**-0.08**	0.25	**9.91e-1**
FUT11	88.72	**0**	0.25	**9.99e-1**

FUT8	316.68	**0.38**	0.22	**7.89e-1**
FUZ	122.77	**-0.08**	0.24	**9.91e-1**
FXN	131.09	**0.25**	0.23	**9.49e-1**
FXR1	1052.63	**0.1**	0.19	**9.90e-1**
FXR2	426.24	**-0.27**	0.21	**9.29e-1**
FXYD1	10.14	**0.01**	0.2	**9.96e-1**
FXYD5	422.14	**-0.04**	0.22	**9.93e-1**
FYCO1	346.7	**-0.3**	0.21	**8.70e-1**
FYN	375.57	**0.48**	0.21	**5.31e-1**
FYTTD1	615.83	**0.06**	0.2	**9.91e-1**
FZD3	245.48	**-0.02**	0.22	**9.96e-1**
FZD5	42.6	**-0.02**	0.25	**9.94e-1**
FZR1	284.42	**-0.19**	0.22	**9.77e-1**
G2E3	193.22	**0.11**	0.23	**9.90e-1**
G3BP1	2677.66	**-0.13**	0.18	**9.88e-1**
G3BP2	2125.41	**-0.28**	0.19	**8.64e-1**
G6PC3	480.53	**-0.31**	0.23	**9.03e-1**
G6PD	702.93	**-0.44**	0.22	**6.64e-1**
GAA	182.03	**-0.46**	0.25	**7.35e-1**
GAB1	152.57	**-0.12**	0.23	**9.90e-1**
GABARAP	372.34	**-0.23**	0.21	**9.49e-1**
GABARAPL2	260.93	**0.86**	0.22	**2.14e-2**
GABBR1	86.41	**-0.23**	0.25	**9.72e-1**
GABPA	419	**0.31**	0.22	**8.73e-1**
GABPB1	195.59	**0.19**	0.23	**9.81e-1**
GABPB1-AS1	55.34	**0.21**	0.25	**9.81e-1**
GABPB2	39.44	**0.13**	0.25	**9.90e-1**
GABRA5	10.08	**0.1**	0.21	**9.90e-1**
GABRR2	11.67	**-0.03**	0.22	**9.93e-1**
GADD45A	107.18	**-0.4**	0.24	**8.20e-1**
GADD45B	273.21	**-0.13**	0.22	**9.90e-1**
GADD45GIP1	256.72	**0.49**	0.22	**5.37e-1**
GAK	730.34	**-0.32**	0.22	**8.69e-1**
GAL3ST4	10.55	**-0.17**	0.21	**9.83e-1**
GALE	69.88	**0.01**	0.25	**9.97e-1**
GALK2	20.73	**0.11**	0.24	**9.90e-1**
GALNS	52	**0**	0.25	**9.99e-1**
GALNT1	543.69	**0.14**	0.2	**9.88e-1**
GALNT10	281.86	**-0.1**	0.22	**9.90e-1**
GALNT12	55.46	**0.06**	0.25	**9.93e-1**
GALNT14	447.25	**-0.33**	0.2	**8.30e-1**
GALNT18	104.83	**-0.12**	0.24	**9.90e-1**
GALNT2	546.93	**0.05**	0.2	**9.93e-1**
GALNT6	176.15	**0.26**	0.23	**9.47e-1**
GALNT7	436	**-0.17**	0.21	**9.86e-1**
GALT	88.19	**-0.14**	0.25	**9.90e-1**
GAN	33.03	**0.01**	0.25	**9.96e-1**
GANAB	2418.02	**-0.25**	0.2	**9.39e-1**
GANC	97.59	**-0.1**	0.24	**9.90e-1**
GAPDH	21570.46	**-0.4**	0.2	**6.54e-1**
GAPT	11.29	**-0.15**	0.21	**9.87e-1**
GAPVD1	550.44	**0.1**	0.2	**9.90e-1**
GAR1	429.28	**-0.42**	0.2	**6.14e-1**
GAREM	128.45	**-0.33**	0.24	**8.87e-1**
GARS	2974.79	**0.56**	0.19	**1.88e-1**
GART	2210.19	**-0.12**	0.18	**9.90e-1**
GAS5	856.35	**0.53**	0.2	**3.43e-1**
GAS6-AS1	10.69	**0.18**	0.21	**9.80e-1**
GAS7	36.19	**-0.4**	0.25	**8.40e-1**
GATAD1	186.44	**0.09**	0.22	**9.90e-1**
GATAD2A	2270.91	**-0.63**	0.21	**2.15e-1**
GATAD2B	572.57	**-0.09**	0.2	**9.90e-1**
GATB	303.64	**0.14**	0.21	**9.89e-1**
GATC	508.36	**-0.32**	0.2	**8.40e-1**
GATS	30.94	**-0.09**	0.25	**9.90e-1**

GATSL2	13.26	**-0.32**	0.22	**8.68e-1**
GBA	337.95	**-0.41**	0.21	**6.69e-1**

GBA2	396.55	**0.09**	0.21	**9.90e-1**
GBAP1	98.79	**-0.03**	0.24	**9.93e-1**
GBAS	591.52	**0.21**	0.21	**9.59e-1**
GBAT2	30.31	**0.26**	0.25	**9.52e-1**
GBE1	351.11	**-0.11**	0.21	**9.90e-1**
GBF1	942.68	**-0.23**	0.19	**9.45e-1**
GBP1	23.38	**-0.23**	0.25	**9.71e-1**
GCA	25.55	**0.54**	0.24	**5.76e-1**
GCAT	72.53	**-0.26**	0.25	**9.53e-1**
GCC1	258.48	**0.21**	0.22	**9.66e-1**
GCC2	223.11	**-0.14**	0.23	**9.90e-1**
GCDH	201.97	**-0.21**	0.23	**9.74e-1**
GCFC2	139.59	**0.11**	0.24	**9.90e-1**
GCH1	165.37	**0.62**	0.23	**3.33e-1**
GCHFR	43.09	**-0.07**	0.25	**9.93e-1**
GCLC	364.05	**0.43**	0.21	**6.14e-1**
GCLM	434.88	**0.07**	0.22	**9.91e-1**
GCN1	2411.2	**-0.09**	0.19	**9.90e-1**
GCNT1	18.06	**-0.07**	0.24	**9.91e-1**
GCNT2	255.93	**0.06**	0.22	**9.93e-1**
GCSAM	1524.69	**0.08**	0.19	**9.90e-1**
GCSH	325.31	**0.33**	0.23	**8.69e-1**
GCSHP3	25.84	**0.18**	0.25	**9.87e-1**
GDAP1	164.98	**0.04**	0.23	**9.93e-1**
GDAP2	123.54	**0.14**	0.24	**9.90e-1**
GDE1	474.34	**-0.02**	0.21	**9.93e-1**
GDF11	91.81	**-0.38**	0.25	**8.44e-1**
GDI1	607.83	**-0.26**	0.2	**9.12e-1**
GDI2	3102.21	**0.22**	0.19	**9.47e-1**
GDPD1	16.79	**0.04**	0.23	**9.93e-1**
GDPD5	181.21	**0.35**	0.23	**8.54e-1**
GEMIN2	117.09	**0.09**	0.24	**9.90e-1**
GEMIN4	761.46	**-0.18**	0.21	**9.74e-1**
GEMIN5	1469.74	**-0.43**	0.19	**5.37e-1**
GEMIN6	112.74	**0.07**	0.24	**9.93e-1**
GEMIN7	100.37	**-0.14**	0.25	**9.90e-1**
GEMIN8	78.63	**0.43**	0.25	**7.89e-1**
GEMIN8P4	12.62	**0.12**	0.22	**9.90e-1**
GEN1	599.3	**0.09**	0.21	**9.90e-1**
GET4	214.77	**0.26**	0.24	**9.49e-1**
GFER	121.34	**-0.11**	0.25	**9.90e-1**
GFI1B	109.76	**-0.48**	0.24	**6.70e-1**
GFM1	946.09	**0.05**	0.2	**9.93e-1**
GFM2	473.69	**0.02**	0.21	**9.93e-1**
GFOD1	103.69	**-0.41**	0.24	**7.99e-1**
GFOD2	186.6	**-0.12**	0.23	**9.90e-1**
GFPT1	544.61	**0.15**	0.21	**9.87e-1**
GGA1	401.09	**-0.17**	0.23	**9.87e-1**
GGA2	1907.34	**0.12**	0.18	**9.90e-1**
GGA3	730.32	**-0.46**	0.21	**5.79e-1**
GGCT	487.15	**0.05**	0.2	**9.93e-1**
GGCX	95.95	**-0.12**	0.24	**9.90e-1**
GGH	124.31	**0.08**	0.24	**9.90e-1**
GGNBP2	393.12	**0.29**	0.2	**8.76e-1**
GGPS1	133.68	**0.48**	0.24	**6.52e-1**
GGT1	107.42	**0.21**	0.25	**9.80e-1**
GHDC	62.23	**-0.06**	0.25	**9.93e-1**
GHITM	1888.15	**0.12**	0.18	**9.90e-1**
GHRLOS	20.47	**0.03**	0.24	**9.93e-1**
GID4	119.11	**-0.03**	0.24	**9.93e-1**
GID8	738.76	**0.14**	0.2	**9.87e-1**

GIGYF1	1090.34	**-0.44**	0.23	**7.04e-1**
GIGYF2	849.17	**-0.16**	0.19	**9.80e-1**
GIN1	42.03	**0.07**	0.25	**9.93e-1**
GINM1	121.17	**0.39**	0.24	**8.23e-1**
GINS1	448.05	**0.06**	0.21	**9.92e-1**
GINS2	586.68	**-0.07**	0.2	**9.90e-1**
GINS3	395.72	**-0.1**	0.2	**9.90e-1**
GINS4	248.7	**-0.04**	0.22	**9.93e-1**
GIPC2	18.24	**-0.19**	0.24	**9.81e-1**
GIT1	951.08	**-0.47**	0.21	**5.86e-1**
GIT2	788.9	**0.02**	0.19	**9.95e-1**
GJC1	90.47	**-0.14**	0.24	**9.90e-1**
GK	148.63	**0.16**	0.23	**9.88e-1**
GK5	210.06	**-0.09**	0.23	**9.90e-1**
GKAP1	13.87	**0.12**	0.22	**9.90e-1**
GLA	191.04	**0.03**	0.22	**9.93e-1**
GLB1	228.31	**-0.12**	0.22	**9.90e-1**
GLB1L	20.06	**0.02**	0.24	**9.93e-1**
GLCCI1	382.64	**0.26**	0.21	**9.25e-1**
GLCE	143.53	**0.22**	0.24	**9.68e-1**
GLE1	667.26	**-0.02**	0.19	**9.93e-1**
GLG1	880.47	**0.29**	0.19	**8.53e-1**

GLI1	26.44	**-0.05**	0.25	**9.93e-1**
GLI4	55.72	**-0.08**	0.25	**9.91e-1**
GLIDR	78.7	**-0.16**	0.25	**9.90e-1**
GLIPR1	71.58	**-0.71**	0.25	**2.67e-1**
GLMN	109.1	**0.16**	0.25	**9.89e-1**
GLO1	1166.47	**0.13**	0.2	**9.90e-1**
GLOD4	488.15	**0.21**	0.2	**9.49e-1**
GLRX	114.98	**-0.12**	0.24	**9.90e-1**
GLRX2	35.44	**0.2**	0.25	**9.86e-1**
GLRX3	473.13	**0.31**	0.21	**8.53e-1**
GLRX5	330.91	**0.65**	0.21	**1.59e-1**
GLS	1446.5	**0.21**	0.2	**9.54e-1**
GLT8D1	237.27	**-0.06**	0.22	**9.93e-1**
GLTP	251.36	**-0.02**	0.22	**9.93e-1**
GLTSCR1	152.86	**-0.32**	0.24	**9.12e-1**
GLTSCR1L	309.95	**0.12**	0.21	**9.90e-1**
GLTSCR2	1116.29	**0.11**	0.21	**9.90e-1**
GLUD1	1387.72	**0.32**	0.19	**8.12e-1**
GLUD1P3	22.88	**-0.29**	0.24	**9.42e-1**
GLUD2	19.65	**0.42**	0.24	**7.57e-1**
GLYCTK	53.21	**0.16**	0.25	**9.90e-1**
GLYR1	1402.54	**-0.33**	0.19	**7.87e-1**
GM2A	729.17	**0.57**	0.19	**2.15e-1**
GMCL1	284.27	**-0.01**	0.21	**9.96e-1**
GMDS	74.17	**0.12**	0.25	**9.90e-1**
GMEB1	125.4	**-0.02**	0.24	**9.95e-1**
GMEB2	232.25	**-0.21**	0.23	**9.68e-1**
GMFB	639.97	**-0.01**	0.21	**9.96e-1**
GMFG	10.43	**-0.25**	0.21	**9.47e-1**
GMIP	409.98	**-0.27**	0.22	**9.25e-1**
GMNN	313.05	**0.11**	0.21	**9.90e-1**
GMPPA	203.15	**0.06**	0.23	**9.93e-1**
GMPPB	146.64	**-0.21**	0.24	**9.80e-1**
GMPR2	210.9	**0.24**	0.22	**9.49e-1**
GMPS	1538.55	**0.01**	0.19	**9.96e-1**
GNA11	269.71	**-0.4**	0.23	**7.59e-1**
GNA12	405.33	**-0.12**	0.2	**9.90e-1**
GNA13	2008.5	**0.33**	0.2	**8.10e-1**
GNAI2	1310.79	**-0.23**	0.2	**9.47e-1**
GNAI3	543.01	**0.21**	0.21	**9.59e-1**
GNAS	4162.97	**0.51**	0.18	**2.80e-1**

GNAS-AS1	23.15	**-0.14**	0.24	**9.90e-1**
GNAZ	54.16	**0.05**	0.25	**9.93e-1**
GNB1	3091.36	**-0.04**	0.18	**9.93e-1**
GNB1L	33.28	**-0.1**	0.25	**9.90e-1**
GNB2	749.75	**-0.1**	0.21	**9.90e-1**
GNB2L1	5584.53	**0.06**	0.18	**9.91e-1**
GNB3	37.34	**-0.54**	0.25	**5.91e-1**
GNB4	225.99	**-0.36**	0.22	**8.38e-1**
GNB5	92.86	**-0.04**	0.24	**9.93e-1**
GNE	82.77	**0.03**	0.25	**9.93e-1**
GNG5	301.18	**0.32**	0.21	**8.52e-1**
GNG7	517.02	**0.1**	0.22	**9.90e-1**
GNGT2	136.72	**-0.18**	0.24	**9.86e-1**
GNL1	413.3	**-0.18**	0.23	**9.83e-1**
GNL2	1183.13	**-0.13**	0.19	**9.90e-1**
GNL3	1670.06	**0.15**	0.2	**9.86e-1**
GNL3L	787.75	**-0.34**	0.19	**7.87e-1**
GNPAT	392.27	**0.18**	0.21	**9.80e-1**
GNPDA2	74.51	**-0.07**	0.25	**9.92e-1**
GNPNAT1	741.65	**0.01**	0.2	**9.96e-1**
GNPTAB	588.03	**-0.04**	0.21	**9.93e-1**
GNPTG	74.7	**0.32**	0.25	**9.25e-1**
GNRH1	15.53	**0.23**	0.23	**9.58e-1**
GNS	120.96	**0.38**	0.24	**8.37e-1**
GOLGA1	121.29	**0.24**	0.24	**9.54e-1**
GOLGA2	311.21	**0.3**	0.22	**9.01e-1**
GOLGA2P10	27.24	**0.17**	0.25	**9.88e-1**
GOLGA2P5	189.57	**0.2**	0.23	**9.73e-1**
GOLGA2P7	126.99	**-0.46**	0.24	**7.11e-1**
GOLGA3	640.33	**-0.03**	0.2	**9.93e-1**
GOLGA4	709.31	**-0.17**	0.2	**9.81e-1**
GOLGA5	209.64	**0.03**	0.23	**9.93e-1**
GOLGA6L9	21.21	**-0.05**	0.24	**9.93e-1**
GOLGA7	374.69	**0.09**	0.21	**9.90e-1**
GOLGA8A	120.48	**-0.45**	0.24	**7.40e-1**
GOLGA8B	133.86	**0.41**	0.23	**7.64e-1**
GOLGB1	539.44	**0.31**	0.22	**8.69e-1**
GOLIM4	366.27	**0.18**	0.21	**9.80e-1**
GOLPH3	524.37	**0.11**	0.21	**9.90e-1**
GOLPH3L	235.6	**-0.07**	0.22	**9.92e-1**
GOLT1B	183.95	**0.53**	0.23	**5.37e-1**
GON4L	444.01	**-0.15**	0.2	**9.87e-1**

GOPC	840.33	**-0.04**	0.2	**9.93e-1**
GORAB	76.05	**0.4**	0.25	**8.38e-1**
GORASP1	272.43	**-0.58**	0.22	**3.64e-1**
GORASP2	1608.6	**-0.42**	0.19	**5.45e-1**
GOSR1	388.96	**-0.17**	0.2	**9.81e-1**
GOSR2	415.27	**-0.01**	0.2	**9.96e-1**
GOT1	520.61	**0.19**	0.2	**9.61e-1**
GOT2	2628.23	**0.09**	0.18	**9.90e-1**
GPAA1	243.51	**-0.1**	0.24	**9.90e-1**
GPALPP1	125.74	**-0.06**	0.24	**9.93e-1**
GPAM	239.99	**0.15**	0.22	**9.90e-1**
GPANK1	203	**-0.27**	0.23	**9.47e-1**
GPAT2	416.13	**-0.16**	0.24	**9.88e-1**
GPATCH1	128.14	**-0.05**	0.24	**9.93e-1**
GPATCH11	214.63	**-0.15**	0.23	**9.89e-1**
GPATCH2	82.98	**0.1**	0.25	**9.90e-1**
GPATCH2L	230.32	**0.28**	0.22	**9.23e-1**
GPATCH3	119.59	**-0.08**	0.24	**9.91e-1**
GPATCH4	1603.36	**-0.62**	0.22	**2.52e-1**
GPATCH8	1058.75	**-0.37**	0.19	**6.87e-1**
GPBP1	740.3	**0.15**	0.21	**9.87e-1**

GPBP1L1	1729.5	**0.01**	0.19	**9.96e-1**
GPC1	41.59	**0.01**	0.25	**9.98e-1**
GPC2	28.78	**-0.17**	0.25	**9.89e-1**
GPCPD1	709.68	**0.77**	0.2	**2.42e-2**
GPD1L	266.24	**0.01**	0.22	**9.96e-1**
GPD2	42.33	**-1.09**	0.25	**5.93e-3**
GPER1	117.13	**-0.39**	0.25	**8.51e-1**
GPI	4555.44	**-0.11**	0.19	**9.90e-1**
GPKOW	141.36	**-0.11**	0.23	**9.90e-1**
GPLD1	89.64	**0.28**	0.24	**9.47e-1**
GPN1	361.3	**0.02**	0.21	**9.93e-1**
GPN2	120.41	**-0.11**	0.24	**9.90e-1**
GPN3	253.51	**0.16**	0.22	**9.87e-1**
GPNMB	20.22	**0.31**	0.24	**9.20e-1**
GPR107	384.55	**-0.13**	0.2	**9.90e-1**
GPR108	161.81	**-0.06**	0.23	**9.93e-1**
GPR132	108.21	**0.16**	0.25	**9.90e-1**
GPR135	12.47	**-0.14**	0.21	**9.90e-1**
GPR137	301.12	**-0.1**	0.25	**9.90e-1**
GPR137B	34.02	**0.34**	0.25	**8.97e-1**
GPR137C	15.83	**0.1**	0.23	**9.90e-1**
GPR155	33.05	**-0.13**	0.25	**9.90e-1**
GPR158	91.44	**-0.53**	0.25	**5.94e-1**
GPR160	83.4	**0.42**	0.25	**8.12e-1**
GPR18	103.3	**0.36**	0.24	**8.61e-1**
GPR180	257.4	**0.1**	0.22	**9.90e-1**
GPR183	125.4	**-1**	0.24	**7.45e-3**
GPR75	57.7	**-0.29**	0.25	**9.47e-1**
GPR89A	99.74	**-0.22**	0.24	**9.72e-1**
GPR89B	36.23	**-0.26**	0.25	**9.53e-1**
GPRIN1	40.44	**-0.14**	0.25	**9.90e-1**
GPS1	527.62	**-0.18**	0.2	**9.74e-1**
GPS2	489.47	**-0.29**	0.2	**8.76e-1**
GPSM2	182.95	**0.16**	0.23	**9.89e-1**
GPSM3	409.8	**-0.18**	0.22	**9.82e-1**
GPT2	326.99	**0.61**	0.22	**2.53e-1**
GPX1	86.56	**0.05**	0.25	**9.93e-1**
GPX4	641.87	**0.2**	0.21	**9.61e-1**
GRAMD1A	679.86	**-0.08**	0.22	**9.90e-1**
GRAMD1C	21.55	**-0.11**	0.24	**9.90e-1**
GRAMD4	229.76	**-0.04**	0.23	**9.93e-1**
GRAP	589.25	**-0.24**	0.22	**9.49e-1**
GRB2	1502.69	**0.09**	0.19	**9.90e-1**
GREB1	43.72	**0.04**	0.25	**9.93e-1**
GRHL1	31.72	**-0.17**	0.25	**9.88e-1**
GRHPR	1704	**0.1**	0.19	**9.90e-1**
GRIN2D	12.84	**-0.08**	0.21	**9.90e-1**
GRINA	552.57	**0.12**	0.21	**9.90e-1**
GRIPAP1	481.43	**-0.01**	0.21	**9.96e-1**
GRK5	159.73	**0.05**	0.23	**9.93e-1**
GRK6	468.66	**0.16**	0.22	**9.87e-1**
GRN	2961.26	**0.02**	0.22	**9.93e-1**
GRPEL1	602.58	**-0.04**	0.2	**9.93e-1**
GRPEL2	273.21	**0.06**	0.22	**9.93e-1**
GRPR	12.46	**0.05**	0.22	**9.93e-1**
GRSF1	1227.16	**0.27**	0.2	**8.91e-1**
GRWD1	821.68	**-0.41**	0.21	**6.69e-1**
GS1-124K5.11	109.42	**0.12**	0.24	**9.90e-1**
GSAP	36.36	**0.03**	0.25	**9.93e-1**
GSDMB	43.41	**-0.12**	0.25	**9.90e-1**
GSDMD	116.57	**-0.08**	0.25	**9.90e-1**
GSE1	546	**0.17**	0.2	**9.80e-1**
GSG2	331.77	**-0.03**	0.21	**9.93e-1**

GSK3A	732.92	**-0.24**	0.2	**9.47e-1**
GSK3B	515.63	**0.01**	0.2	**9.96e-1**
GSKIP	90.82	**0.27**	0.25	**9.49e-1**
GSN	12.95	**-0.08**	0.22	**9.90e-1**
GSPT1	2930.78	**-0.04**	0.18	**9.93e-1**
GSPT2	158.15	**-0.04**	0.23	**9.93e-1**
GSR	1393.83	**0.3**	0.19	**8.29e-1**
GSS	276.05	**0.1**	0.21	**9.90e-1**
GSTCD	152.59	**0.06**	0.23	**9.93e-1**
GSTK1	427.22	**0.16**	0.2	**9.86e-1**
GSTM4	79.32	**-0.14**	0.25	**9.90e-1**
GSTO1	63.29	**0.17**	0.25	**9.89e-1**
GSTZ1	112.44	**0.21**	0.24	**9.80e-1**
GTDC1	120.25	**0.12**	0.24	**9.90e-1**
GTF2A1	523.74	**0.06**	0.21	**9.93e-1**
GTF2A2	234.98	**-0.16**	0.22	**9.87e-1**
GTF2B	226.44	**-0.2**	0.22	**9.71e-1**
GTF2E1	171.92	**-0.12**	0.23	**9.90e-1**
GTF2E2	553.99	**0.7**	0.21	**8.94e-2**
GTF2F1	776.14	**-0.11**	0.21	**9.90e-1**
GTF2F2	218.21	**0.09**	0.22	**9.90e-1**
GTF2H1	590.19	**0.08**	0.21	**9.90e-1**
GTF2H2	113.71	**0.16**	0.24	**9.90e-1**
GTF2H2B	61.03	**0.04**	0.25	**9.93e-1**
GTF2H3	370.21	**0.06**	0.21	**9.93e-1**
GTF2H4	246.63	**-0.36**	0.23	**8.38e-1**
GTF2H5	92.89	**0.24**	0.25	**9.61e-1**
GTF2I	1388.19	**-0.01**	0.19	**9.96e-1**
GTF2IP20	94.29	**-0.1**	0.25	**9.90e-1**
GTF2IRD2	17.79	**0.36**	0.23	**8.41e-1**
GTF3A	1561.04	**0.3**	0.19	**8.34e-1**
GTF3C1	812.92	**-0.12**	0.19	**9.90e-1**
GTF3C2	1047.08	**-0.34**	0.19	**7.59e-1**
GTF3C3	258.91	**0.22**	0.22	**9.57e-1**
GTF3C4	454.06	**0.01**	0.2	**9.96e-1**
GTF3C5	611.8	**-0.26**	0.21	**9.40e-1**
GTF3C6	688.73	**0.17**	0.2	**9.80e-1**
GTPBP1	525.67	**-0.21**	0.21	**9.59e-1**
GTPBP10	533.5	**0.11**	0.21	**9.90e-1**
GTPBP2	414.2	**-0.03**	0.21	**9.93e-1**
GTPBP3	464.86	**-0.05**	0.23	**9.93e-1**
GTPBP4	1450.3	**0.06**	0.19	**9.93e-1**
GTPBP6	150.02	**0.15**	0.24	**9.90e-1**
GTPBP8	129.15	**-0.24**	0.24	**9.54e-1**
GTSE1	561.74	**-0.39**	0.2	**6.87e-1**
GUCD1	1072.41	**-0.3**	0.21	**8.68e-1**
GUF1	857.81	**-0.15**	0.2	**9.87e-1**
GUK1	353.63	**0**	0.22	**9.98e-1**
GUSB	440.5	**0.11**	0.2	**9.90e-1**
GUSBP1	47.31	**0.22**	0.25	**9.80e-1**
GUSBP11	95.88	**-0.1**	0.24	**9.90e-1**
GUSBP4	38.17	**-0.13**	0.25	**9.90e-1**
GXYLT1	393.47	**0.14**	0.21	**9.90e-1**
GYG1	171.48	**0.2**	0.23	**9.77e-1**
GYS1	477.56	**-0.39**	0.2	**7.01e-1**
GZF1	264.82	**0.06**	0.21	**9.93e-1**
H1FX	11.24	**0.01**	0.21	**9.96e-1**
H2AFV	808.7	**0.12**	0.19	**9.90e-1**
H2AFX	604.26	**-0.21**	0.23	**9.66e-1**
H2AFY	1394.95	**0.06**	0.19	**9.91e-1**
H2AFZ	1790.83	**0.09**	0.18	**9.90e-1**
H3F3B	1691.35	**-0.06**	0.18	**9.90e-1**
H6PD	196.21	**-0.07**	0.23	**9.91e-1**
HABP4	84.95	**0.12**	0.25	**9.90e-1**
HACD2	234.63	**0.1**	0.23	**9.90e-1**

HACD3	1321.19	**-0.22**	0.19	**9.47e-1**
HACE1	102.51	**0.47**	0.24	**6.90e-1**
HACL1	106.76	**0.24**	0.24	**9.59e-1**
HADH	474.85	**0.31**	0.21	**8.53e-1**
HADHA	1408.75	**0.27**	0.19	**8.70e-1**
HADHB	464.43	**0.31**	0.21	**8.62e-1**
HAGH	39.99	**0.1**	0.25	**9.90e-1**
HAGHL	127.65	**-0.13**	0.25	**9.90e-1**
HARBI1	12.9	**0.04**	0.22	**9.93e-1**
HARS	598.98	**0.17**	0.2	**9.80e-1**
HARS2	199.23	**0.13**	0.22	**9.90e-1**
HAT1	649.04	**0.2**	0.2	**9.58e-1**
HAUS1	199.26	**-0.04**	0.22	**9.93e-1**
HAUS2	321.52	**0.06**	0.22	**9.93e-1**
HAUS3	186.02	**0.24**	0.23	**9.52e-1**
HAUS4	225.45	**0.42**	0.22	**7.02e-1**
HAUS5	421.65	**-0.11**	0.22	**9.90e-1**
HAUS6	955.79	**-0.16**	0.2	**9.86e-1**
HAUS7	197.19	**0**	0.23	**9.99e-1**
HAUS8	192.4	**-0.31**	0.22	**8.92e-1**
HAX1	519.78	**0.04**	0.2	**9.93e-1**
HBP1	133.48	**0.91**	0.24	**3.48e-2**
HBS1L	626.7	**0**	0.2	**9.99e-1**
HCCS	169.88	**-0.04**	0.23	**9.93e-1**
HCFC1	4167.28	**-0.72**	0.22	**9.59e-2**
HCFC1R1	179.78	**-0.48**	0.25	**6.90e-1**
HCFC2	67.25	**0.09**	0.25	**9.90e-1**
HCG18	269.44	**-0.02**	0.21	**9.93e-1**
HCG26	11.08	**0**	0.21	**9.98e-1**
HCG27	14.87	**-0.31**	0.23	**8.94e-1**
HCG8	14.92	**-0.19**	0.23	**9.81e-1**
HCLS1	1588.3	**-0.22**	0.2	**9.47e-1**
HCN3	100.09	**-0.28**	0.25	**9.47e-1**
HCP5	157.77	**0.2**	0.23	**9.80e-1**
HDAC1	2938.22	**0.18**	0.18	**9.59e-1**
HDAC10	205.92	**-0.21**	0.24	**9.76e-1**
HDAC2	1953.76	**-0.07**	0.18	**9.90e-1**
HDAC3	381.76	**0.21**	0.21	**9.52e-1**
HDAC4	164.86	**0.04**	0.23	**9.93e-1**
HDAC5	165.42	**0.27**	0.24	**9.47e-1**
HDAC6	253.83	**0.13**	0.23	**9.90e-1**
HDAC7	1482.26	**-0.49**	0.22	**5.62e-1**
HDAC8	75.37	**-0.03**	0.25	**9.93e-1**
HDAC9	19.19	**0.07**	0.24	**9.93e-1**
HDDC2	421.82	**0.21**	0.21	**9.54e-1**
HDDC3	80.97	**-0.17**	0.25	**9.88e-1**
HDGF	3355.57	**-0.3**	0.19	**8.52e-1**
HDGFRP2	522.34	**-0.14**	0.22	**9.90e-1**
HDHD1	204.31	**0.12**	0.22	**9.90e-1**
HDHD2	270.29	**0.16**	0.22	**9.87e-1**
HDHD3	61.86	**-0.07**	0.25	**9.93e-1**
HDLBP	3836.44	**-0.08**	0.18	**9.90e-1**
HEATR1	1335.3	**-0.05**	0.2	**9.93e-1**
HEATR3	233.78	**0.13**	0.22	**9.90e-1**
HEATR5A	225.31	**-0.01**	0.22	**9.96e-1**
HEATR5B	364.28	**0.21**	0.22	**9.63e-1**
HEATR6	108.44	**-0.01**	0.24	**9.98e-1**
HECA	295.3	**0.08**	0.21	**9.90e-1**
HECTD1	1539.65	**0.23**	0.2	**9.47e-1**
HECTD2	46.55	**-0.12**	0.25	**9.90e-1**
HECTD3	526.06	**-0.25**	0.2	**9.40e-1**
HECTD4	369.55	**-0.04**	0.21	**9.93e-1**
HECW2	21.48	**0.02**	0.24	**9.94e-1**

HEG1	508.79	**0.03**	0.2	**9.93e-1**
HEIH	74.72	**0.24**	0.25	**9.61e-1**
HELLS	342.87	**-0.11**	0.22	**9.90e-1**
HELQ	122.3	**0.09**	0.24	**9.90e-1**
HELZ	809.06	**-0.21**	0.2	**9.49e-1**
HELZ2	23.77	**0.09**	0.24	**9.90e-1**
HEMGN	20.19	**0.28**	0.24	**9.47e-1**
HEMK1	95.47	**0.15**	0.25	**9.90e-1**
HERC1	661.93	**-0.12**	0.19	**9.90e-1**
HERC2	753.14	**-0.06**	0.19	**9.93e-1**
HERC2P2	196.47	**0.11**	0.23	**9.90e-1**
HERC2P3	89.18	**0.05**	0.25	**9.93e-1**
HERC2P7	10.93	**-0.05**	0.21	**9.93e-1**
HERC2P9	23.82	**0.15**	0.25	**9.90e-1**
HERC3	229.77	**0.17**	0.22	**9.86e-1**
HERC4	260.61	**0.29**	0.22	**9.19e-1**
HERPUD1	768.95	**0.84**	0.19	**5.92e-3**
HERPUD2	108.56	**0.43**	0.24	**7.57e-1**
HES1	127.51	**0.38**	0.24	**8.30e-1**
HEXA	300.74	**0.18**	0.21	**9.80e-1**
HEXB	79.6	**0.27**	0.25	**9.49e-1**
HEXDC	79.22	**0.16**	0.25	**9.90e-1**
HEXIM1	188.77	**-0.13**	0.24	**9.90e-1**
HEXIM2	27.32	**-0.23**	0.25	**9.72e-1**
HEY1	21.5	**0.09**	0.24	**9.90e-1**
HEY2	10.14	**0.01**	0.21	**9.96e-1**
HGH1	64.51	**0**	0.25	**9.99e-1**
HGS	739.91	**-0.23**	0.22	**9.49e-1**
HGSNAT	137.87	**0**	0.23	**9.98e-1**
HHAT	23.69	**-0.08**	0.24	**9.91e-1**
HHLA3	20.17	**0.13**	0.24	**9.90e-1**
HIAT1	536.63	**0.1**	0.21	**9.90e-1**
HIATL1	1002.18	**0.18**	0.19	**9.66e-1**
HIATL2	13.9	**0.1**	0.22	**9.90e-1**
HIBADH	241.15	**0.08**	0.22	**9.90e-1**
HIBCH	103.16	**-0.04**	0.24	**9.93e-1**
HIC1	19.99	**-0.1**	0.24	**9.90e-1**

HIC2	120.52	**-0.33**	0.25	**9.10e-1**
HIF1A	1685.01	**-0.26**	0.2	**9.23e-1**
HIF1AN	474.55	**0.01**	0.2	**9.97e-1**
HIGD1A	570.35	**-0.04**	0.2	**9.93e-1**
HIGD2A	319.79	**-0.05**	0.23	**9.93e-1**
HILPDA	114.61	**0.01**	0.24	**9.96e-1**
HINFP	91.34	**0.15**	0.24	**9.90e-1**
HINT1	774.05	**0**	0.19	**9.98e-1**
HINT2	29.4	**0.09**	0.25	**9.90e-1**
HINT3	159.05	**0.04**	0.23	**9.93e-1**
HIP1	80.18	**-0.18**	0.25	**9.87e-1**
HIP1R	1211.83	**-0.35**	0.22	**8.40e-1**
HIPK1	710.71	**0.01**	0.2	**9.96e-1**
HIPK3	407.85	**-0.09**	0.21	**9.90e-1**
HIRA	1040.27	**-0.12**	0.19	**9.90e-1**
HIRIP3	374.93	**-0.42**	0.23	**7.20e-1**
HIST1H2BK	106.5	**0.4**	0.24	**8.20e-1**
HIVEP1	455.57	**0.16**	0.2	**9.86e-1**
HIVEP2	415.7	**-0.19**	0.21	**9.71e-1**
HIVEP3	64.31	**0.37**	0.25	**8.64e-1**
HJURP	399.18	**-0.15**	0.21	**9.87e-1**
HK1	47.67	**-0.14**	0.25	**9.90e-1**
HK2	1034.76	**-0.24**	0.19	**9.25e-1**
HKR1	61.27	**-0.25**	0.25	**9.59e-1**
HLA-A	2475.45	**0.11**	0.21	**9.90e-1**
HLA-B	4066.33	**0.09**	0.21	**9.90e-1**

HLA-C	1286.55	**0.21**	0.2	**9.49e-1**
HLA-DMA	1240.66	**-0.01**	0.2	**9.96e-1**
HLA-DMB	854.82	**0.32**	0.19	**8.12e-1**
HLA-DOA	1090.19	**0.01**	0.19	**9.96e-1**
HLA-DOB	457.91	**0.24**	0.2	**9.47e-1**
HLA-DPA1	2226.72	**0.19**	0.18	**9.50e-1**
HLA-DPB1	1648.61	**0.14**	0.19	**9.87e-1**
HLA-DQA1	2008.12	**0.48**	0.18	**3.49e-1**
HLA-DQA2	54.85	**0.7**	0.25	**3.01e-1**
HLA-DQB1	1483.81	**0.71**	0.2	**7.21e-2**
HLA-DQB2	49.52	**0.65**	0.25	**3.88e-1**
HLA-DRA	9290.29	**0.11**	0.18	**9.90e-1**
HLA-DRB1	2412.67	**0.7**	0.19	**2.99e-2**
HLA-DRB5	387.78	**0.96**	0.21	**1.80e-3**
HLA-E	1236.76	**0.3**	0.2	**8.64e-1**
HLA-F	137.61	**0.32**	0.24	**9.08e-1**
HLA-H	44.35	**0.58**	0.25	**5.43e-1**
HLA-L	47.63	**0.15**	0.25	**9.90e-1**
HLCS	140.91	**0.25**	0.23	**9.49e-1**
HLTF	1271.76	**0.03**	0.2	**9.93e-1**
HM13	737.03	**0.11**	0.19	**9.90e-1**
HMBOX1	121.55	**0.06**	0.24	**9.93e-1**
HMBS	335.91	**-0.13**	0.21	**9.90e-1**
HMCES	644.36	**0.23**	0.2	**9.47e-1**
HMCN1	27.21	**0.19**	0.25	**9.86e-1**
HMG20A	534.97	**0.07**	0.2	**9.91e-1**
HMG20B	376.83	**0.03**	0.21	**9.93e-1**
HMGA1	6641.53	**-0.64**	0.23	**3.00e-1**
HMGB1	6310.44	**-0.2**	0.18	**9.49e-1**
HMGB2	2603.34	**0.07**	0.18	**9.90e-1**
HMGB3	442.92	**0.06**	0.2	**9.91e-1**
HMGCL	70.32	**0.22**	0.25	**9.74e-1**
HMGCR	1048.26	**0.15**	0.19	**9.86e-1**
HMGCS1	1452.4	**-0.17**	0.2	**9.80e-1**
HMGN1	1659.73	**0.19**	0.18	**9.54e-1**
HMGN2	2678.34	**0.09**	0.18	**9.90e-1**
HMGN4	264.31	**0.17**	0.23	**9.87e-1**
HMGXB3	746.99	**-0.03**	0.2	**9.93e-1**
HMGXB4	336.73	**-0.05**	0.21	**9.93e-1**
HMHA1	906.22	**-0.24**	0.23	**9.52e-1**
HMMR	1108.34	**-0.02**	0.2	**9.93e-1**
HMOX2	351.67	**-0.26**	0.21	**9.45e-1**
HMSD	11.01	**-0.11**	0.21	**9.90e-1**
HN1	468.25	**-0.17**	0.2	**9.80e-1**
HN1L	1108.12	**-0.24**	0.19	**9.25e-1**
HNRNPA0	1056.39	**-0.32**	0.2	**8.39e-1**
HNRNPA1	298.01	**-0.05**	0.21	**9.93e-1**
HNRNPA1L2	134.06	**0.2**	0.24	**9.81e-1**
HNRNPA2B1	15686.08	**-0.46**	0.18	**3.95e-1**
HNRNPA3	7475.22	**-0.08**	0.18	**9.90e-1**
HNRNPA3P1	24.74	**0.47**	0.25	**6.99e-1**
HNRNPAB	2127.88	**0.11**	0.18	**9.90e-1**
HNRNPC	6843.79	**-0.15**	0.18	**9.80e-1**
HNRNPD	4339.54	**-0.43**	0.19	**5.37e-1**
HNRNPDL	2623.25	**0.08**	0.18	**9.90e-1**
HNRNPF	2918.75	**-0.3**	0.19	**8.31e-1**
HNRNPH1	6305.11	**-0.33**	0.18	**7.05e-1**
HNRNPH3	2281.7	**-0.49**	0.18	**3.41e-1**
HNRNPK	5884.88	**-0.06**	0.18	**9.91e-1**
HNRNPL	2321.27	**-0.1**	0.18	**9.90e-1**
HNRNPM	3240.89	**-0.1**	0.18	**9.90e-1**
HNRNPR	3483.78	**-0.4**	0.18	**5.76e-1**
HNRNPU	7356.8	**-0.17**	0.18	**9.63e-1**
HNRNPU-AS1	342.54	**0.01**	0.22	**9.96e-1**

HNRNPUL1	3926.15	**-0.4**	0.2	**6.84e-1**
HNRNPUL2	484.28	**-0.23**	0.2	**9.47e-1**
HOMEZ	264.51	**-0.26**	0.22	**9.47e-1**
HOOK2	84.04	**0.15**	0.25	**9.90e-1**
HOOK3	341.89	**0.02**	0.22	**9.95e-1**
HOTAIRM1	24.3	**0.04**	0.25	**9.93e-1**
HOXA1	91.7	**-0.08**	0.24	**9.91e-1**
HOXB3	57.24	**-0.21**	0.25	**9.80e-1**
HOXB4	96.91	**-0.25**	0.24	**9.57e-1**
HOXB7	85.94	**-0.2**	0.25	**9.81e-1**
HOXC4	84.59	**-0.39**	0.25	**8.41e-1**
HP1BP3	1383.75	**0.11**	0.19	**9.90e-1**
HPCAL1	88.24	**-0.07**	0.25	**9.93e-1**
HPRT1	587.84	**0.08**	0.21	**9.90e-1**
HPS1	243.23	**-0.09**	0.23	**9.90e-1**
HPS3	230.97	**0.08**	0.23	**9.90e-1**
HPS4	322.56	**0.16**	0.21	**9.86e-1**
HPS5	281.65	**0.18**	0.22	**9.81e-1**
HPS6	108.62	**-0.03**	0.25	**9.93e-1**
HRAS	114.6	**0.36**	0.24	**8.56e-1**
HRK	26.28	**0.2**	0.25	**9.86e-1**
HRSP12	118.91	**-0.24**	0.24	**9.56e-1**
HS1BP3	40.55	**0.03**	0.25	**9.93e-1**
HS2ST1	366.63	**0.24**	0.22	**9.47e-1**
HS3ST3B1	26.86	**0.1**	0.25	**9.90e-1**
HS6ST1	83.55	**-0.3**	0.25	**9.47e-1**
HSBP1	435.77	**0.05**	0.21	**9.93e-1**
HSCB	40.5	**0.06**	0.25	**9.93e-1**
HSD17B10	419.95	**0.02**	0.21	**9.93e-1**
HSD17B11	28.94	**0.35**	0.25	**8.84e-1**
HSD17B12	434.65	**0.24**	0.21	**9.47e-1**
HSD17B4	371.72	**0.27**	0.21	**9.12e-1**
HSD17B6	76.56	**0.55**	0.25	**5.79e-1**
HSD17B7	87.92	**0.4**	0.25	**8.36e-1**
HSD17B7P2	15.95	**0.05**	0.23	**9.93e-1**
HSD17B8	77.84	**0.05**	0.25	**9.93e-1**
HSD3B7	20.17	**-0.09**	0.24	**9.90e-1**
HSDL1	191.1	**0.29**	0.23	**9.21e-1**
HSDL2	234.09	**0.22**	0.22	**9.59e-1**
HSF1	812.32	**-0.36**	0.22	**8.38e-1**
HSF2	245.01	**0.1**	0.22	**9.90e-1**
HSF4	32.72	**-0.14**	0.25	**9.90e-1**
HSH2D	460.7	**-0.04**	0.22	**9.93e-1**
HSP90AA1	17226.61	**-0.56**	0.18	**1.34e-1**
HSP90AB1	20237.69	**-0.21**	0.18	**9.42e-1**
HSP90B1	2249.36	**0.36**	0.19	**7.04e-1**
HSPA13	226.85	**0.47**	0.23	**6.37e-1**
HSPA14	637.07	**0.09**	0.2	**9.90e-1**
HSPA1B	834.3	**-0.69**	0.21	**1.03e-1**
HSPA4	3152.77	**-0.15**	0.19	**9.84e-1**
HSPA5	5830.89	**0.38**	0.18	**6.07e-1**
HSPA8	23249.42	**-0.27**	0.18	**8.53e-1**
HSPA9	6309.67	**0.07**	0.18	**9.90e-1**
HSPB11	191.15	**0.06**	0.22	**9.93e-1**
HSPBAP1	47.38	**0.37**	0.25	**8.73e-1**
HSPBP1	175.54	**0.01**	0.24	**9.98e-1**
HSPD1	12358.67	**-0.01**	0.18	**9.96e-1**
HSPE1	93.44	**-0.38**	0.24	**8.49e-1**
HSPH1	4218.99	**-0.12**	0.19	**9.90e-1**
HTATIP2	161.8	**0.02**	0.23	**9.96e-1**
HTATSF1	997.01	**0.06**	0.19	**9.93e-1**
HTATSF1P2	30.79	**0.07**	0.25	**9.92e-1**
HTRA2	152.07	**0.04**	0.23	**9.93e-1**
HTT	1074.52	**-0.11**	0.19	**9.90e-1**

HUS1	132.02	**0.19**	0.23	**9.81e-1**
HUWE1	4481.52	**-0.03**	0.18	**9.93e-1**
HVCN1	318.19	**0.57**	0.21	**3.01e-1**
HYAL2	69.15	**-0.18**	0.25	**9.88e-1**
HYAL3	59.96	**-0.27**	0.25	**9.50e-1**
HYLS1	10.24	**0.08**	0.21	**9.90e-1**
HYOU1	3225.17	**0.03**	0.19	**9.93e-1**
IARS	3472.95	**0.3**	0.19	**8.38e-1**
IARS2	1351.71	**0.19**	0.19	**9.58e-1**
IBA57	115.2	**-0.11**	0.25	**9.90e-1**
IBTK	715.03	**0.11**	0.2	**9.90e-1**
ICA1	12.21	**0.19**	0.22	**9.74e-1**

ICA1L	11.46	**0.11**	0.21	**9.90e-1**
ICAM1	1339.04	**-0.25**	0.22	**9.47e-1**
ICAM2	107.5	**0.12**	0.24	**9.90e-1**
ICAM5	53.18	**-0.15**	0.25	**9.90e-1**
ICE1	927.3	**-0.09**	0.2	**9.90e-1**
ICE2	500.66	**0.23**	0.21	**9.49e-1**
ICK	196.67	**-0.2**	0.22	**9.76e-1**
ICMT	936.63	**-0.11**	0.19	**9.90e-1**
ICOSLG	723.67	**0.03**	0.22	**9.93e-1**
ICT1	162.98	**0.13**	0.23	**9.90e-1**
ID2	113.29	**-0.04**	0.24	**9.93e-1**
ID3	365.45	**-0.52**	0.24	**5.91e-1**
IDE	704.95	**0.15**	0.21	**9.87e-1**
IDH1	458.75	**-0.15**	0.21	**9.87e-1**
IDH2	407.73	**0.03**	0.21	**9.93e-1**
IDH3A	1535.06	**-0.06**	0.19	**9.91e-1**
IDH3B	1339.58	**0.05**	0.19	**9.93e-1**
IDH3G	362.24	**0.08**	0.21	**9.90e-1**
IDI1	665.46	**-0.06**	0.2	**9.91e-1**
IDS	3143.06	**-0.26**	0.18	**8.69e-1**
IER2	243.93	**0.45**	0.24	**7.04e-1**
IER3IP1	210.02	**0.26**	0.22	**9.47e-1**
IER5	155.91	**0.34**	0.24	**8.69e-1**
IFFO1	50.32	**-0.32**	0.25	**9.30e-1**
IFI16	1099.7	**-0.13**	0.19	**9.90e-1**
IFI27L1	23.7	**-0.09**	0.24	**9.90e-1**
IFI30	2495.35	**0.68**	0.19	**5.78e-2**
IFI35	25.84	**-0.03**	0.25	**9.93e-1**
IFIH1	319.91	**0.81**	0.22	**3.46e-2**
IFIT2	15.89	**0.08**	0.23	**9.91e-1**
IFIT3	21.77	**0.1**	0.24	**9.90e-1**
IFNAR1	376.76	**0.11**	0.21	**9.90e-1**
IFNAR2	296.26	**0.19**	0.22	**9.74e-1**
IFNG-AS1	70.35	**-0.63**	0.25	**4.14e-1**
IFNGR1	227.57	**0.28**	0.23	**9.26e-1**
IFNGR2	379.1	**0.53**	0.21	**3.72e-1**
IFNLR1	113.41	**0.13**	0.24	**9.90e-1**
IFRD1	248.74	**0.63**	0.22	**2.32e-1**
IFRD2	613.82	**-0.13**	0.22	**9.90e-1**
IFT122	202.67	**-0.13**	0.22	**9.90e-1**
IFT140	54.1	**0.06**	0.25	**9.93e-1**
IFT172	65.38	**-0.04**	0.25	**9.93e-1**
IFT20	32.51	**0.17**	0.25	**9.90e-1**
IFT22	136.83	**0.12**	0.23	**9.90e-1**
IFT27	23.92	**0.03**	0.24	**9.93e-1**
IFT43	19.59	**0.12**	0.24	**9.90e-1**
IFT46	81.42	**-0.28**	0.25	**9.47e-1**
IFT52	111.16	**0.38**	0.24	**8.40e-1**
IFT57	456.83	**0.1**	0.2	**9.90e-1**
IFT74	128.96	**0.09**	0.24	**9.90e-1**
IFT80	184.54	**0.24**	0.23	**9.54e-1**
IFT81	127.1	**0.17**	0.24	**9.87e-1**

IFT88	85.8	**0.07**	0.25	**9.93e-1**
IGBP1	276.57	**0.44**	0.22	**6.54e-1**
IGF1R	142.14	**-0.16**	0.23	**9.87e-1**
IGF2BP3	778.45	**0.21**	0.21	**9.54e-1**
IGF2R	710.08	**0.19**	0.2	**9.58e-1**
IGFLR1	44.5	**-0.13**	0.25	**9.90e-1**
IGHMBP2	150.94	**-0.22**	0.24	**9.71e-1**
IGIP	18.01	**0.04**	0.24	**9.93e-1**
IGLL5	1266.79	**-0.43**	0.22	**6.90e-1**
IGSF8	158.36	**-0.08**	0.25	**9.91e-1**
IK	893.7	**-0.23**	0.19	**9.37e-1**
IKBIP	186.22	**0.09**	0.23	**9.90e-1**
IKBKAP	669.77	**-0.02**	0.2	**9.93e-1**
IKBKB	227.13	**0.28**	0.22	**9.23e-1**
IKBKE	448.51	**-0.04**	0.22	**9.93e-1**
IKBKG	85.92	**0.25**	0.25	**9.58e-1**
IKZF1	2202.08	**-0.18**	0.18	**9.58e-1**
IKZF2	202.11	**-0.78**	0.23	**7.31e-2**
IKZF3	1942.49	**-0.08**	0.18	**9.90e-1**
IKZF4	57.96	**0.02**	0.25	**9.94e-1**
IKZF5	493.03	**-0.09**	0.2	**9.90e-1**
IL10	84.19	**0.53**	0.25	**5.91e-1**
IL10RA	438.23	**0.29**	0.21	**9.06e-1**
IL10RB	20.64	**0.12**	0.24	**9.90e-1**
IL12RB1	105.02	**0.13**	0.24	**9.90e-1**
IL15RA	72.2	**0.18**	0.25	**9.87e-1**
IL16	234.08	**-0.22**	0.22	**9.56e-1**
IL17RA	280.74	**-0.31**	0.22	**8.78e-1**
IL18BP	69.41	**0.06**	0.25	**9.93e-1**
IL1RAP	28.24	**-0.29**	0.25	**9.47e-1**
IL20RB	14.47	**-0.15**	0.23	**9.88e-1**

IL21R	688.82	**0.58**	0.21	**3.10e-1**
IL2RG	1160.9	**0.09**	0.19	**9.90e-1**
IL4I1	79.92	**1.09**	0.25	**6.40e-3**
IL4R	1172.56	**-0.09**	0.21	**9.90e-1**
IL6ST	150.15	**0.04**	0.24	**9.93e-1**
IL7	11.23	**0.17**	0.21	**9.83e-1**
IL7R	194.3	**-1.33**	0.23	**7.00e-6**
ILDR2	116.52	**0.02**	0.24	**9.94e-1**
ILF2	2477.15	**-0.19**	0.18	**9.52e-1**
ILF3	4875.41	**-0.24**	0.19	**9.25e-1**
ILF3-AS1	102.06	**-0.05**	0.25	**9.93e-1**
ILK	318.35	**0.07**	0.21	**9.91e-1**
ILKAP	215.02	**0.21**	0.22	**9.64e-1**
ILVBL	156.92	**-0.19**	0.25	**9.86e-1**
IMMP1L	20.26	**0.04**	0.24	**9.93e-1**
IMMP2L	51.77	**-0.01**	0.25	**9.96e-1**
IMMT	1325.32	**0.31**	0.2	**8.41e-1**
IMP3	238.48	**0.28**	0.22	**9.30e-1**
IMP4	868.12	**-0.44**	0.2	**5.91e-1**
IMPA1	307.98	**0.18**	0.22	**9.80e-1**
IMPA2	125.68	**0.14**	0.24	**9.90e-1**
IMPAD1	706.5	**0.01**	0.21	**9.96e-1**
IMPDH1	1736.68	**-0.36**	0.2	**7.54e-1**
IMPDH2	1805.3	**0.11**	0.18	**9.90e-1**
INADL	13.97	**-0.19**	0.23	**9.81e-1**
INAFM1	17.38	**-0.11**	0.22	**9.90e-1**
INAFM2	38.75	**0.05**	0.25	**9.93e-1**
INCENP	1286.01	**-0.32**	0.21	**8.41e-1**
INF2	61.49	**-0.26**	0.25	**9.54e-1**
ING1	189.64	**0.05**	0.22	**9.93e-1**
ING2	105.95	**0.53**	0.24	**5.79e-1**
ING3	201.16	**0.17**	0.23	**9.87e-1**

ING4	56.61	**0.24**	0.25	**9.64e-1**
ING5	341.96	**0.1**	0.21	**9.90e-1**
INHBE	17.95	**0.82**	0.23	**6.75e-2**
INIP	123.55	**0.01**	0.24	**9.96e-1**
INO80	509.73	**-0.3**	0.2	**8.53e-1**
INO80C	76.59	**0.17**	0.25	**9.88e-1**
INO80D	274.98	**-0.01**	0.22	**9.96e-1**
INO80E	489.24	**-0.47**	0.23	**6.35e-1**
INPP4A	191.87	**0.01**	0.22	**9.96e-1**
INPP4B	16.47	**-0.04**	0.23	**9.93e-1**
INPP5A	106.2	**0.43**	0.24	**7.57e-1**
INPP5B	515.63	**0.03**	0.2	**9.93e-1**
INPP5D	1802.51	**-0.26**	0.19	**9.04e-1**
INPP5E	179.88	**-0.16**	0.25	**9.90e-1**
INPP5F	122.73	**-0.07**	0.24	**9.91e-1**
INPP5K	168.65	**0.55**	0.23	**4.62e-1**
INPPL1	1125.42	**-0.24**	0.2	**9.42e-1**
INSIG1	1375.96	**0.24**	0.19	**9.30e-1**
INSIG2	22.4	**0.15**	0.24	**9.90e-1**
INTS1	1279.31	**-0.23**	0.23	**9.52e-1**
INTS10	978.07	**0.04**	0.19	**9.93e-1**
INTS12	140.05	**-0.04**	0.24	**9.93e-1**
INTS2	418.87	**0.28**	0.22	**9.25e-1**
INTS3	716.87	**-0.13**	0.19	**9.88e-1**
INTS4	196.9	**-0.02**	0.23	**9.96e-1**
INTS4P2	14.44	**-0.21**	0.23	**9.63e-1**
INTS5	286.35	**-0.28**	0.23	**9.47e-1**
INTS6	321.03	**-0.16**	0.21	**9.87e-1**
INTS7	472.67	**0.05**	0.21	**9.93e-1**
INTS8	526.25	**0.11**	0.21	**9.90e-1**
INTS9	280.14	**-0.17**	0.21	**9.82e-1**
INVS	68.81	**0.17**	0.25	**9.90e-1**
IP6K1	347.3	**-0.36**	0.23	**8.38e-1**
IP6K2	292.21	**-0.02**	0.22	**9.96e-1**
IPMK	301.44	**0.01**	0.22	**9.98e-1**
IPO11	343.45	**-0.09**	0.21	**9.90e-1**
IPO13	453.32	**-0.18**	0.22	**9.80e-1**
IPO4	1484.34	**-0.26**	0.2	**9.13e-1**
IPO5	5041.5	**0.09**	0.19	**9.90e-1**
IPO5P1	129.02	**-0.18**	0.24	**9.87e-1**
IPO7	4786.71	**0.16**	0.19	**9.83e-1**
IPO8	584.49	**0.35**	0.2	**7.63e-1**
IPO9	1199.83	**-0.05**	0.19	**9.93e-1**
IPP	45.64	**0.14**	0.25	**9.90e-1**
IPPK	198.66	**0.01**	0.22	**9.96e-1**
IPW	149.99	**0.59**	0.25	**4.73e-1**
IQCB1	392.22	**0.22**	0.22	**9.56e-1**
IQCC	81.9	**-0.11**	0.25	**9.90e-1**
IQCD	88.42	**-0.06**	0.25	**9.93e-1**
IQCE	90.29	**0.08**	0.25	**9.91e-1**
IQCG	27.28	**0.12**	0.25	**9.90e-1**
IQCH	24.79	**-0.01**	0.25	**9.98e-1**
IQCH-AS1	28.76	**0.18**	0.25	**9.87e-1**
IQCK	25.17	**-0.02**	0.25	**9.95e-1**
IQGAP1	1880.32	**-0.06**	0.19	**9.91e-1**
IQSEC1	1213.47	**0.15**	0.19	**9.87e-1**
IRAK1	1481.49	**-0.4**	0.23	**7.57e-1**
IRAK1BP1	44.68	**0.08**	0.25	**9.91e-1**
IRAK4	139.14	**0.29**	0.24	**9.35e-1**
IREB2	903.52	**0.09**	0.21	**9.90e-1**
IRF1	403.92	**-0.03**	0.21	**9.93e-1**
IRF2	384.04	**0.25**	0.21	**9.43e-1**
IRF2BP1	164.62	**-0.18**	0.25	**9.87e-1**

IRF2BP2	145.94	**0.1**	0.23	**9.90e-1**
IRF2BPL	105.77	**-0.21**	0.25	**9.80e-1**
IRF3	496	**-0.46**	0.23	**6.69e-1**
IRF4	17.65	**0.4**	0.23	**7.75e-1**
IRF5	57.04	**-0.11**	0.25	**9.90e-1**
IRF7	29.6	**-0.02**	0.24	**9.95e-1**
IRF8	988.65	**0.25**	0.19	**9.10e-1**
IRF9	69.53	**0.52**	0.25	**6.14e-1**
IRGQ	110.37	**0**	0.24	**9.99e-1**
IRS1	169.86	**-0.59**	0.24	**4.11e-1**
ISCA1	387.99	**-0.01**	0.21	**9.96e-1**
ISCA2	99.17	**0.15**	0.24	**9.90e-1**
ISCU	298.65	**0.72**	0.22	**1.02e-1**
ISG15	31.83	**-0.06**	0.25	**9.93e-1**
ISG20	383.87	**0.11**	0.22	**9.90e-1**
ISG20L2	1122.79	**-0.48**	0.19	**3.80e-1**
ISL2	12.89	**0.17**	0.22	**9.87e-1**
ISOC1	225.51	**-0.01**	0.22	**9.96e-1**
ISOC2	465.27	**-0.42**	0.24	**7.57e-1**
IST1	751.09	**0.12**	0.2	**9.90e-1**
ISY1	48.49	**0.08**	0.25	**9.91e-1**
ISYNA1	14.63	**-0.04**	0.23	**9.93e-1**
ITCH	1010.86	**-0.07**	0.19	**9.90e-1**
ITFG1	223.89	**0.22**	0.22	**9.61e-1**
ITFG2	297.92	**0.02**	0.21	**9.93e-1**
ITFG3	260.4	**-0.14**	0.23	**9.90e-1**
ITGA10	11.9	**-0.07**	0.21	**9.91e-1**
ITGA4	818.72	**0.08**	0.2	**9.90e-1**
ITGA6	632	**0.06**	0.2	**9.91e-1**
ITGA7	11.21	**-0.11**	0.21	**9.90e-1**
ITGAE	55.12	**-0.03**	0.25	**9.93e-1**
ITGAL	361.53	**-0.3**	0.21	**8.80e-1**
ITGAM	21.9	**-0.2**	0.24	**9.81e-1**
ITGAV	95.91	**0.11**	0.25	**9.90e-1**
ITGB1	1735.85	**-0.15**	0.19	**9.82e-1**
ITGB1BP1	231.75	**0.09**	0.22	**9.90e-1**
ITGB1BP2	19.68	**-0.04**	0.24	**9.93e-1**
ITGB3BP	272.68	**0.13**	0.22	**9.90e-1**
ITGB7	613.51	**-0.17**	0.21	**9.81e-1**
ITM2B	154.77	**0.29**	0.24	**9.42e-1**
ITPA	305.52	**-0.34**	0.24	**8.68e-1**
ITPK1	501.96	**-0.28**	0.22	**9.25e-1**
ITPKB	453.71	**0.19**	0.21	**9.73e-1**
ITPKC	58.25	**0.05**	0.25	**9.93e-1**
ITPR1	270.29	**0.03**	0.22	**9.93e-1**
ITPR2	205.3	**-0.12**	0.22	**9.90e-1**
ITPR3	2062.65	**-0.23**	0.19	**9.47e-1**
ITPRIP	131.24	**0.09**	0.24	**9.90e-1**
ITPRIPL1	270.67	**-0.08**	0.21	**9.90e-1**
ITSN1	384.43	**-0.34**	0.2	**8.12e-1**
ITSN2	797.7	**-0.12**	0.19	**9.90e-1**
IVD	250.86	**-0.02**	0.22	**9.95e-1**
IVNS1ABP	773.13	**0.36**	0.2	**7.41e-1**
IWS1	361.07	**-0.01**	0.21	**9.96e-1**
IZUMO4	24.57	**-0.11**	0.24	**9.90e-1**
JADE1	418.71	**-0.07**	0.2	**9.90e-1**
JADE2	1867.2	**-0.33**	0.21	**8.39e-1**
JADE3	281.04	**-0.22**	0.21	**9.49e-1**
JAG1	28.66	**0.06**	0.25	**9.93e-1**
JAGN1	89.34	**0.15**	0.25	**9.90e-1**
JAK1	2457.64	**0.04**	0.19	**9.93e-1**
JAK2	46.62	**0.26**	0.25	**9.54e-1**
JAKMIP2	63.47	**-0.29**	0.25	**9.47e-1**
JARID2	170.3	**-0.2**	0.23	**9.73e-1**
JAZF1	202.92	**0.02**	0.22	**9.96e-1**

JCHAIN	4380.35	**-0.18**	0.19	**9.72e-1**
JKAMP	223.83	**0.16**	0.23	**9.87e-1**
JMJD1C	707.3	**0.08**	0.21	**9.90e-1**
JMJD4	194.68	**-0.35**	0.24	**8.69e-1**
JMJD6	195.92	**-0.05**	0.22	**9.93e-1**
JMJD8	255.42	**-0.26**	0.23	**9.47e-1**

JMY	268.98	**0.32**	0.22	**8.64e-1**
JOSD1	554.73	**-0.03**	0.2	**9.93e-1**
JOSD2	15.52	**-0.16**	0.22	**9.87e-1**
JPX	21.38	**-0.07**	0.24	**9.93e-1**
JRK	324.72	**-0.19**	0.22	**9.80e-1**
JRKL	105.22	**-0.03**	0.24	**9.93e-1**
JTB	354.96	**0.16**	0.22	**9.87e-1**
JUN	26.92	**0.09**	0.25	**9.90e-1**
JUNB	355.56	**-0.14**	0.24	**9.90e-1**
JUND	158.57	**0.45**	0.24	**7.04e-1**
JUP	37.87	**-0.01**	0.25	**9.97e-1**
KANK1	573.77	**1.1**	0.2	**3.80e-5**
KANK2	884.72	**-0.8**	0.2	**1.83e-2**
KANSL1	466.79	**-0.2**	0.2	**9.59e-1**
KANSL1L	52.03	**0.01**	0.25	**9.96e-1**
KANSL2	264.1	**0.03**	0.22	**9.93e-1**
KANSL3	690.66	**-0.24**	0.2	**9.42e-1**
KARS	1902.52	**0.01**	0.18	**9.96e-1**
KAT2A	1005.35	**-0.32**	0.2	**8.39e-1**
KAT2B	274.12	**0.3**	0.23	**9.11e-1**
KAT5	292.66	**0.24**	0.21	**9.48e-1**
KAT6A	908.79	**-0.2**	0.19	**9.49e-1**
KAT6B	688.28	**-0.25**	0.19	**9.20e-1**
KAT7	508.22	**0.09**	0.2	**9.90e-1**
KAT8	219.65	**0.18**	0.22	**9.86e-1**
KATNA1	168.59	**-0.05**	0.23	**9.93e-1**
KATNAL1	150.01	**-0.09**	0.23	**9.90e-1**
KATNAL2	51.78	**0.24**	0.25	**9.63e-1**
KATNB1	327.87	**-0.09**	0.23	**9.90e-1**
KATNBL1	102.56	**0.24**	0.25	**9.58e-1**
KBTBD2	224.69	**0.52**	0.22	**5.04e-1**
KBTBD4	140.36	**0.16**	0.23	**9.88e-1**
KBTBD6	143.34	**-0.17**	0.24	**9.87e-1**
KBTBD7	31.47	**-0.22**	0.25	**9.74e-1**
KBTBD8	401.93	**0.31**	0.22	**8.73e-1**
KCMF1	625.13	**0.3**	0.21	**8.64e-1**
KCNAB2	728.37	**-0.2**	0.22	**9.72e-1**
KCNAB3	42.5	**0.16**	0.25	**9.90e-1**
KCNC3	26.69	**-0.13**	0.25	**9.90e-1**
KCNC4	32.56	**0.04**	0.25	**9.93e-1**
KCND1	32.05	**-0.15**	0.25	**9.90e-1**
KCNH2	230.75	**-0.44**	0.23	**6.87e-1**
KCNIP2	22.02	**0.12**	0.24	**9.90e-1**
KCNJ11	119.06	**-0.09**	0.25	**9.90e-1**
KCNJ14	13.51	**0.11**	0.22	**9.90e-1**
KCNK12	58.85	**0.25**	0.25	**9.60e-1**
KCNMA1	42.1	**0.17**	0.25	**9.89e-1**
KCNMB4	103.25	**-0.13**	0.24	**9.90e-1**
KCNN3	1623.85	**-0.25**	0.18	**8.92e-1**
KCNQ1OT1	55.5	**-0.29**	0.25	**9.47e-1**
KCNQ5	1019.04	**0.05**	0.2	**9.93e-1**
KCTD1	49.64	**-0.24**	0.25	**9.66e-1**
KCTD10	333.13	**-0.16**	0.21	**9.87e-1**
KCTD11	29.82	**-0.15**	0.25	**9.90e-1**
KCTD13	86.34	**-0.14**	0.25	**9.90e-1**
KCTD15	358.11	**0.01**	0.21	**9.98e-1**
KCTD17	92.99	**-0.33**	0.25	**9.10e-1**

KCTD18	105.67	**0.11**	0.24	**9.90e-1**
KCTD2	328.37	**0.16**	0.21	**9.86e-1**
KCTD20	860.4	**0.13**	0.2	**9.90e-1**
KCTD21	28.08	**0.06**	0.25	**9.93e-1**
KCTD3	165.47	**0.08**	0.23	**9.90e-1**
KCTD5	329.91	**-0.12**	0.21	**9.90e-1**
KCTD6	54.74	**0.03**	0.25	**9.93e-1**
KCTD7	306.72	**-0.23**	0.21	**9.49e-1**
KCTD9	370.87	**0**	0.21	**9.98e-1**
KDELR1	623.03	**-0.32**	0.2	**8.34e-1**
KDELR2	799.23	**0.15**	0.2	**9.87e-1**
KDM1A	1127.8	**-0.07**	0.19	**9.90e-1**
KDM1B	920.35	**0.17**	0.2	**9.80e-1**
KDM2A	1432.14	**-0.1**	0.19	**9.90e-1**
KDM2B	1169.45	**-0.07**	0.19	**9.90e-1**
KDM3A	263.13	**0.33**	0.22	**8.51e-1**
KDM3B	1080.18	**-0.09**	0.19	**9.90e-1**
KDM4A	460.51	**0.3**	0.2	**8.64e-1**
KDM4A-AS1	21.86	**-0.4**	0.24	**8.29e-1**
KDM4B	212.8	**0**	0.24	**9.99e-1**
KDM4C	263.58	**0.36**	0.22	**8.11e-1**
KDM4D	12.66	**0.03**	0.22	**9.93e-1**
KDM5A	564.67	**-0.04**	0.2	**9.93e-1**
KDM5C	1009.83	**-0.19**	0.2	**9.66e-1**
KDM5D	363.52	**-0.13**	0.21	**9.90e-1**
KDM6A	202.26	**0.16**	0.22	**9.87e-1**

KDM6B	742.9	**-0.4**	0.22	**7.20e-1**
KDM7A	98.56	**0.09**	0.25	**9.90e-1**
KDM8	59.38	**-0.1**	0.25	**9.90e-1**
KDSR	195.21	**0.51**	0.23	**5.68e-1**
KEAP1	662.93	**-0.23**	0.22	**9.49e-1**
KHDC1	291.59	**-0.04**	0.21	**9.93e-1**
KHDRBS1	2336.96	**0.06**	0.18	**9.91e-1**
KHDRBS3	70.54	**-0.13**	0.25	**9.90e-1**
KHK	88.99	**-0.38**	0.25	**8.51e-1**
KHNYN	484.64	**0.15**	0.2	**9.87e-1**
KHSRP	3410.77	**-0.5**	0.22	**5.37e-1**
KIAA0020	1030.64	**-0.35**	0.19	**7.35e-1**
KIAA0040	741.57	**-0.25**	0.19	**9.20e-1**
KIAA0100	3005.68	**-0.07**	0.18	**9.90e-1**
KIAA0101	466.43	**0.16**	0.21	**9.87e-1**
KIAA0125	36.51	**-0.36**	0.25	**8.73e-1**
KIAA0141	447.69	**0.06**	0.21	**9.91e-1**
KIAA0195	465.55	**-0.06**	0.22	**9.93e-1**
KIAA0196	675.39	**-0.02**	0.21	**9.93e-1**
KIAA0226	646.17	**0.23**	0.19	**9.42e-1**
KIAA0226L	901.43	**-0.85**	0.19	**3.70e-3**
KIAA0232	146.8	**0.12**	0.23	**9.90e-1**
KIAA0319	43.74	**-0.14**	0.25	**9.90e-1**
KIAA0319L	378.27	**0.18**	0.21	**9.73e-1**
KIAA0355	164.98	**-0.04**	0.23	**9.93e-1**
KIAA0368	1572.4	**0.28**	0.19	**8.69e-1**
KIAA0391	508.28	**-0.23**	0.2	**9.47e-1**
KIAA0430	902.36	**0.03**	0.2	**9.93e-1**
KIAA0513	38.72	**-0.16**	0.25	**9.90e-1**
KIAA0556	99.58	**-0.31**	0.25	**9.29e-1**
KIAA0586	314.98	**-0.12**	0.22	**9.90e-1**
KIAA0753	236.9	**0.06**	0.22	**9.93e-1**
KIAA0895L	126.56	**0.04**	0.24	**9.93e-1**
KIAA0907	472.4	**-0.11**	0.2	**9.90e-1**
KIAA0922	2095.27	**-0.27**	0.19	**8.73e-1**
KIAA0930	534.29	**-0.07**	0.21	**9.90e-1**
KIAA1024	18.48	**0.09**	0.24	**9.90e-1**

KIAA1033	634.57	**-0.16**	0.21	**9.87e-1**
KIAA1109	373.51	**0.08**	0.21	**9.90e-1**
KIAA1143	666.8	**0.1**	0.2	**9.90e-1**
KIAA1147	378.06	**0.23**	0.21	**9.49e-1**
KIAA1161	118	**-0.3**	0.24	**9.25e-1**
KIAA1191	256.22	**-0.04**	0.22	**9.93e-1**
KIAA1211	278.64	**-0.46**	0.21	**5.87e-1**
KIAA1328	45.32	**0.16**	0.25	**9.90e-1**
KIAA1407	21.79	**0.03**	0.24	**9.93e-1**
KIAA1429	937.3	**0.03**	0.2	**9.93e-1**
KIAA1467	52.75	**0.06**	0.25	**9.93e-1**
KIAA1468	221.87	**0.11**	0.22	**9.90e-1**
KIAA1524	511.96	**0.02**	0.21	**9.93e-1**
KIAA1549L	297.22	**-0.03**	0.21	**9.93e-1**
KIAA1551	641.03	**-0.19**	0.21	**9.73e-1**
KIAA1586	44.24	**-0.01**	0.25	**9.98e-1**
KIAA1715	259.18	**0.17**	0.22	**9.86e-1**
KIAA1804	68.25	**0.01**	0.25	**9.96e-1**
KIAA1841	70.94	**0.03**	0.25	**9.93e-1**
KIAA1875	14.81	**-0.28**	0.23	**9.39e-1**
KIAA1919	106.33	**-0.06**	0.24	**9.93e-1**
KIAA1958	182.17	**0.07**	0.23	**9.91e-1**
KIAA2013	358.66	**-0.18**	0.23	**9.86e-1**
KIAA2018	278.74	**-0.12**	0.22	**9.90e-1**
KIAA2026	190.23	**0.1**	0.23	**9.90e-1**
KIDINS220	676.79	**-0.01**	0.2	**9.96e-1**
KIF11	1305.03	**-0.04**	0.19	**9.93e-1**
KIF13B	11.14	**-0.19**	0.21	**9.74e-1**
KIF14	318.24	**-0.04**	0.22	**9.93e-1**
KIF15	336.61	**0.12**	0.21	**9.90e-1**
KIF16B	130.62	**-0.08**	0.23	**9.90e-1**
KIF18A	246.16	**0.17**	0.23	**9.87e-1**
KIF18B	835.13	**-0.5**	0.22	**5.45e-1**
KIF1B	96.73	**-0.02**	0.24	**9.96e-1**
KIF1C	1242.39	**-0.3**	0.21	**8.80e-1**
KIF20A	530.03	**-0.24**	0.2	**9.42e-1**
KIF20B	1001.17	**-0.29**	0.2	**8.69e-1**
KIF21B	864.37	**0.15**	0.21	**9.87e-1**
KIF22	1160.3	**-0.46**	0.21	**5.62e-1**
KIF23	798.52	**-0.12**	0.2	**9.90e-1**
KIF24	199.21	**0**	0.22	**9.99e-1**
KIF2A	1185.23	**0.08**	0.2	**9.90e-1**
KIF2C	1121.68	**0.16**	0.19	**9.80e-1**
KIF3A	776.82	**-0.21**	0.2	**9.49e-1**
KIF3B	619.05	**0.25**	0.2	**9.22e-1**
KIF4A	390.4	**0.24**	0.21	**9.47e-1**
KIF5B	1915.91	**-0.09**	0.19	**9.90e-1**
KIF9	53.2	**0.12**	0.25	**9.90e-1**
KIFAP3	96.79	**0.38**	0.24	**8.44e-1**
KIFC1	788.28	**-0.23**	0.2	**9.47e-1**
KIFC2	323.82	**-0.25**	0.23	**9.49e-1**
KIN	93.33	**0.04**	0.24	**9.93e-1**
KIZ	99.66	**0.2**	0.24	**9.81e-1**
KLC1	577.63	**0.27**	0.2	**9.06e-1**
KLC2	376.08	**-0.23**	0.23	**9.54e-1**
KLC4	68.3	**0.21**	0.25	**9.80e-1**
KLF10	665.25	**-0.25**	0.2	**9.20e-1**
KLF12	190.34	**0.21**	0.23	**9.68e-1**
KLF13	1617.57	**-0.05**	0.2	**9.93e-1**
KLF15	20.3	**0.02**	0.24	**9.95e-1**
KLF16	278.71	**-0.2**	0.22	**9.68e-1**
KLF3	38.17	**-0.1**	0.25	**9.90e-1**
KLF6	133.41	**0.17**	0.23	**9.87e-1**

KLHDC10	477.96	**0.04**	0.2	**9.93e-1**
KLHDC2	164.06	**0.46**	0.23	**6.79e-1**
KLHDC3	565.97	**-0.13**	0.21	**9.90e-1**
KLHDC4	330.57	**-0.3**	0.23	**9.12e-1**
KLHL11	205.92	**-0.07**	0.23	**9.91e-1**
KLHL12	464.93	**0.23**	0.2	**9.47e-1**
KLHL14	59.92	**-0.69**	0.25	**3.07e-1**
KLHL15	165.47	**0.19**	0.24	**9.83e-1**
KLHL17	65.1	**-0.05**	0.25	**9.93e-1**
KLHL18	622.59	**-0.32**	0.2	**8.38e-1**
KLHL2	153.76	**0.45**	0.24	**6.92e-1**
KLHL20	140.28	**-0.09**	0.23	**9.90e-1**
KLHL21	349.17	**-0.15**	0.23	**9.90e-1**
KLHL22	39.43	**-0.03**	0.25	**9.93e-1**
KLHL24	231.24	**1.17**	0.23	**1.79e-4**
KLHL25	37.64	**-0.29**	0.25	**9.47e-1**
KLHL26	44.56	**-0.29**	0.25	**9.47e-1**
KLHL28	88.86	**0.03**	0.24	**9.93e-1**
KLHL32	18.61	**0.29**	0.24	**9.39e-1**
KLHL36	217.78	**-0.15**	0.22	**9.88e-1**
KLHL42	301.86	**-0.02**	0.21	**9.93e-1**
KLHL5	839.03	**0.11**	0.21	**9.90e-1**
KLHL6	841	**0.96**	0.19	**3.72e-4**
KLHL7	166.02	**0.25**	0.24	**9.52e-1**
KLHL8	408.01	**-0.11**	0.21	**9.90e-1**
KLHL9	82.13	**0.07**	0.25	**9.93e-1**
KLLN	36.8	**0.03**	0.25	**9.93e-1**
KLRAP1	21.53	**-0.09**	0.24	**9.90e-1**
KLRG1	16.16	**0.27**	0.23	**9.47e-1**
KMO	41.17	**0.6**	0.25	**5.22e-1**
KMT2A	1686.09	**-0.33**	0.19	**7.57e-1**
KMT2B	1013.95	**-0.57**	0.23	**4.32e-1**
KMT2C	1320.02	**-0.22**	0.19	**9.47e-1**
KMT2D	1745.73	**-0.59**	0.22	**3.26e-1**
KMT2E	1154.52	**-0.24**	0.19	**9.23e-1**
KMT2E-AS1	29.81	**-0.25**	0.25	**9.59e-1**
KNOP1	194.77	**-0.41**	0.23	**7.49e-1**
KNSTRN	500.05	**-0.24**	0.2	**9.46e-1**
KNTC1	680.94	**0.19**	0.21	**9.71e-1**
KPNA1	668.29	**0.05**	0.2	**9.93e-1**
KPNA2	1889.64	**-0.26**	0.18	**8.75e-1**
KPNA3	1179.31	**0.1**	0.2	**9.90e-1**
KPNA4	1012.83	**-0.07**	0.2	**9.90e-1**
KPNA5	70.71	**0.02**	0.25	**9.96e-1**
KPNA6	1322.54	**-0.24**	0.19	**9.25e-1**
KPNB1	4301.97	**-0.13**	0.18	**9.87e-1**
KPTN	74.82	**-0.01**	0.25	**9.96e-1**
KRAS	530.12	**0.11**	0.21	**9.90e-1**
KRBA1	130.94	**-0.33**	0.25	**9.10e-1**
KRBOX4	49.25	**0.13**	0.25	**9.90e-1**
KRCC1	170.85	**-0.09**	0.23	**9.90e-1**
KREMEN2	113.77	**-0.07**	0.19	**9.90e-1**
KRI1	600.46	**-0.18**	0.22	**9.81e-1**
KRIT1	535.43	**0.12**	0.21	**9.90e-1**
KRR1	387.06	**-0.08**	0.21	**9.90e-1**
KRT10	36.49	**0.49**	0.25	**6.84e-1**
KRTCAP2	200.52	**0.02**	0.22	**9.93e-1**
KSR1	128.03	**0.01**	0.24	**9.96e-1**
KTN1	2912.55	**0.08**	0.2	**9.90e-1**
KTN1-AS1	13.52	**-0.05**	0.22	**9.93e-1**
KXD1	697.15	**-0.47**	0.2	**5.31e-1**
L2HGDH	301.62	**-0.06**	0.21	**9.93e-1**
L3HYPDH	30.51	**0.04**	0.25	**9.93e-1**
L3MBTL1	50.63	**-0.07**	0.25	**9.93e-1**

L3MBTL2	647.07	**-0.03**	0.2	**9.93e-1**
L3MBTL3	20.22	**-0.1**	0.24	**9.90e-1**

LACC1	230.5	**0.02**	0.22	**9.95e-1**
LACE1	50.59	**0.03**	0.25	**9.93e-1**
LACTB	62.04	**0.1**	0.25	**9.90e-1**
LAGE3	58.37	**-0.16**	0.25	**9.90e-1**
LAIR1	107.56	**0.96**	0.24	**1.66e-2**
LAMC1	448.74	**-0.23**	0.2	**9.47e-1**
LAMC3	28.42	**0.12**	0.25	**9.90e-1**
LAMP1	406.56	**0.14**	0.2	**9.90e-1**
LAMP2	591.49	**0.16**	0.22	**9.87e-1**
LAMTOR1	358.03	**-0.31**	0.21	**8.73e-1**
LAMTOR2	112.99	**-0.51**	0.24	**6.01e-1**
LAMTOR3	220.66	**0.42**	0.23	**7.41e-1**
LAMTOR4	191.53	**-0.12**	0.22	**9.90e-1**
LAMTOR5	194.33	**0.02**	0.22	**9.93e-1**
LANCL1	513.7	**0.22**	0.21	**9.50e-1**
LANCL2	312.07	**-0.01**	0.21	**9.96e-1**
LAP3	841.83	**-0.23**	0.19	**9.39e-1**
LAPTM4A	262.43	**0.19**	0.22	**9.74e-1**
LAPTM5	1675.08	**0.32**	0.19	**7.97e-1**
LARGE	118.81	**-0.15**	0.24	**9.90e-1**
LARP1	5132.5	**-0.34**	0.18	**7.13e-1**
LARP1B	399.89	**-0.12**	0.21	**9.90e-1**
LARP4	1324.82	**-0.18**	0.2	**9.68e-1**
LARP4B	737.96	**0.04**	0.19	**9.93e-1**
LARP7	538.73	**-0.13**	0.2	**9.90e-1**
LARS	2192.53	**0.19**	0.19	**9.60e-1**
LARS2	854.4	**-0.24**	0.19	**9.29e-1**
LAS1L	942.41	**-0.07**	0.19	**9.90e-1**
LASP1	1635.54	**-0.34**	0.22	**8.38e-1**
LAT	36.45	**-0.12**	0.25	**9.90e-1**
LAT2	212.35	**0.99**	0.23	**5.69e-3**
LATS1	371.62	**-0.25**	0.21	**9.47e-1**
LBHD1	19.69	**0.07**	0.24	**9.93e-1**
LBR	3128.68	**0.03**	0.19	**9.93e-1**
LCAT	10.7	**0.1**	0.2	**9.90e-1**
LCK	511.5	**0.51**	0.2	**4.15e-1**
LCLAT1	178.27	**-0.02**	0.23	**9.95e-1**
LCMT1	126.69	**0.38**	0.24	**8.40e-1**
LCMT1-AS1	54.42	**-0.08**	0.25	**9.91e-1**
LCMT2	107	**0.09**	0.24	**9.90e-1**
LCOR	198.95	**0.06**	0.23	**9.93e-1**
LCORL	99.43	**0.02**	0.25	**9.95e-1**
LCP1	11530.84	**0.05**	0.18	**9.93e-1**
LDAH	255.23	**0.06**	0.22	**9.92e-1**
LDB1	540.36	**-0.4**	0.22	**7.49e-1**
LDHA	8066	**-0.15**	0.18	**9.81e-1**
LDHB	4339	**0.1**	0.18	**9.90e-1**
LDLR	901.29	**-0.56**	0.2	**2.89e-1**
LDLRAD4	70.16	**0.17**	0.25	**9.88e-1**
LDLRAP1	54.55	**-0.18**	0.25	**9.87e-1**
LEMD2	155.73	**0.09**	0.23	**9.90e-1**
LEMD3	368.43	**-0.01**	0.21	**9.96e-1**
LENG1	44.02	**-0.3**	0.25	**9.47e-1**
LENG8	2055.49	**-0.42**	0.21	**6.74e-1**
LENG8-AS1	20.27	**-0.17**	0.24	**9.87e-1**
LEO1	624.99	**-0.15**	0.2	**9.87e-1**
LEPR	95.38	**0.09**	0.25	**9.90e-1**
LEPROT	365.29	**-0.03**	0.21	**9.93e-1**
LEPROTL1	302.57	**0.14**	0.22	**9.90e-1**
LETM1	1041.66	**-0.21**	0.2	**9.49e-1**
LETM2	24.5	**0.05**	0.25	**9.93e-1**
LETMD1	306.25	**0.44**	0.21	**6.14e-1**

LGALS3BP	69.58	**-0.07**	0.25	**9.93e-1**
LGALSL	14.89	**-0.1**	0.22	**9.90e-1**
LGMN	554.29	**0.85**	0.2	**6.62e-3**
LHFP	255.19	**-0.15**	0.22	**9.88e-1**
LHFPL2	570.83	**0.12**	0.2	**9.90e-1**
LHPP	50.27	**-0.17**	0.25	**9.89e-1**
LHX4-AS1	61.85	**-0.25**	0.25	**9.58e-1**
LIAS	168.32	**0.05**	0.23	**9.93e-1**
LIG1	1022.32	**-0.13**	0.21	**9.90e-1**
LIG3	429.44	**-0.36**	0.2	**7.57e-1**
LIG4	228.41	**-0.1**	0.23	**9.90e-1**
LILRA4	10.05	**0.46**	0.2	**5.71e-1**
LILRB1	412.77	**0.29**	0.22	**9.12e-1**
LILRB4	20.17	**0.52**	0.24	**5.86e-1**
LIMD2	893.71	**-0.24**	0.24	**9.58e-1**
LIME1	151.17	**0.14**	0.25	**9.90e-1**
LIMK1	378.89	**-0.34**	0.23	**8.68e-1**
LIMK2	199.62	**-0.17**	0.22	**9.87e-1**
LIMS1	288.07	**-0.03**	0.23	**9.93e-1**
LIN37	22.76	**-0.04**	0.24	**9.93e-1**
LIN52	73.8	**-0.09**	0.25	**9.90e-1**
LIN54	340.38	**0.15**	0.22	**9.87e-1**
LIN7C	231.9	**0.16**	0.24	**9.89e-1**
LIN9	171.94	**0.25**	0.24	**9.49e-1**
LINC00094	204.07	**0.11**	0.22	**9.90e-1**
LINC00115	17.02	**-0.07**	0.23	**9.93e-1**
LINC00152	51.33	**0.06**	0.25	**9.93e-1**
LINC00173	24.96	**0.03**	0.25	**9.93e-1**
LINC00174	62.36	**0.18**	0.25	**9.87e-1**
LINC00176	89.23	**-0.06**	0.25	**9.93e-1**
LINC00265	171.05	**-0.27**	0.24	**9.47e-1**
LINC00294	66.45	**0.29**	0.25	**9.47e-1**
LINC00339	40.21	**0.3**	0.25	**9.43e-1**
LINC00342	24.7	**-0.18**	0.25	**9.87e-1**
LINC00426	42.42	**-0.05**	0.25	**9.93e-1**
LINC00476	34.24	**0.31**	0.25	**9.34e-1**
LINC00493	118.1	**0.16**	0.24	**9.89e-1**
LINC00494	27.18	**0.35**	0.25	**8.76e-1**
LINC00528	72.27	**-0.24**	0.25	**9.66e-1**
LINC00630	20.82	**0.07**	0.24	**9.93e-1**
LINC00641	223.95	**-0.2**	0.22	**9.66e-1**
LINC00657	2189.79	**0.2**	0.18	**9.49e-1**
LINC00664	45.82	**0.26**	0.25	**9.54e-1**
LINC00665	154.95	**-0.31**	0.23	**9.06e-1**
LINC00667	97.91	**0.28**	0.24	**9.47e-1**
LINC00847	127.17	**0.14**	0.24	**9.90e-1**
LINC00852	16.32	**-0.1**	0.23	**9.90e-1**
LINC00877	32.39	**-0.14**	0.25	**9.90e-1**
LINC00883	25.28	**-0.08**	0.25	**9.91e-1**
LINC00888	17.49	**-0.01**	0.23	**9.98e-1**
LINC00909	51.43	**0.13**	0.25	**9.90e-1**
LINC00926	189.61	**-0.07**	0.23	**9.91e-1**
LINC00938	62.05	**0.16**	0.25	**9.90e-1**
LINC00959	17.55	**0.22**	0.24	**9.66e-1**
LINC00998	102.09	**0.16**	0.24	**9.90e-1**
LINC00999	28.61	**-0.15**	0.24	**9.90e-1**
LINC01000	654.87	**-0.58**	0.23	**4.11e-1**
LINC01003	31.01	**0.3**	0.25	**9.42e-1**
LINC01004	32.74	**-0.09**	0.25	**9.90e-1**
LINC01021	15.78	**-0.02**	0.23	**9.96e-1**
LINC01061	130.23	**-0.44**	0.25	**7.59e-1**
LINC01089	45.18	**-0.23**	0.25	**9.72e-1**
LINC01128	176.41	**-0.01**	0.23	**9.96e-1**

LINC01138	10.3	**0.06**	0.21	**9.93e-1**
LINC01144	12.51	**-0.01**	0.22	**9.96e-1**
LINC01184	44.79	**0.16**	0.25	**9.90e-1**
LINC01215	301.66	**0.32**	0.21	**8.54e-1**
LINC01237	11.55	**-0.08**	0.22	**9.90e-1**
LINC01268	20.44	**0.1**	0.24	**9.90e-1**
LINC01311	16.84	**-0.1**	0.22	**9.90e-1**
LINC01347	28.84	**-0.11**	0.25	**9.90e-1**
LINC01355	21.74	**0.18**	0.24	**9.87e-1**
LINC01410	24.44	**0.14**	0.24	**9.90e-1**
LINC01420	88.65	**-0.25**	0.25	**9.54e-1**
LINC01481	19.99	**-0.25**	0.24	**9.53e-1**
LINC01521	35.96	**-0.07**	0.25	**9.93e-1**
LINC01534	10.61	**-0.16**	0.21	**9.86e-1**
LINC01547	10.26	**0.12**	0.21	**9.90e-1**
LINC01560	18.57	**0.07**	0.24	**9.91e-1**
LINC01572	29.13	**0.22**	0.25	**9.80e-1**
LINC01578	74.58	**0.3**	0.25	**9.42e-1**
LINC01604	24.93	**-0.05**	0.25	**9.93e-1**
LINC-PINT	81.71	**0.24**	0.25	**9.59e-1**
LINS	86.73	**-0.1**	0.25	**9.90e-1**
LIPA	277.01	**-0.02**	0.22	**9.93e-1**
LIPE	210.17	**-0.43**	0.24	**7.41e-1**
LIPT1	29.78	**-0.07**	0.25	**9.93e-1**
LIPT2	13.48	**0.29**	0.22	**9.12e-1**
LITAF	289.28	**-0.13**	0.21	**9.90e-1**
LIX1L	312.33	**0.01**	0.21	**9.96e-1**
LLGL1	291.12	**-0.24**	0.23	**9.53e-1**
LLGL2	48.47	**0.21**	0.25	**9.82e-1**
LLPH	281.12	**-0.33**	0.21	**8.41e-1**
LMAN1	1680.81	**-0.14**	0.19	**9.87e-1**
LMAN2	957.29	**-0.35**	0.21	**8.23e-1**
LMAN2L	104.47	**-0.07**	0.24	**9.92e-1**
LMBR1	815.34	**0.17**	0.2	**9.81e-1**
LMBR1L	55.17	**0.28**	0.25	**9.49e-1**
LMBRD1	79.62	**0.47**	0.25	**7.13e-1**
LMBRD2	68.09	**0.17**	0.25	**9.88e-1**
LMF1	27.3	**-0.19**	0.25	**9.86e-1**
LMF2	307.78	**-0.24**	0.25	**9.59e-1**
LMLN	143.32	**0.06**	0.24	**9.93e-1**
LMNB1	2367.1	**-0.12**	0.18	**9.90e-1**

LMNB2	1825.22	**-0.41**	0.22	**7.04e-1**
LMNTD2	24.14	**-0.03**	0.24	**9.93e-1**
LMO4	119.81	**0.2**	0.24	**9.81e-1**
LMO7	39.23	**0.26**	0.25	**9.54e-1**
LMTK2	425.02	**-0.18**	0.2	**9.72e-1**
LNP1	60.05	**-0.23**	0.25	**9.73e-1**
LNPEP	409.64	**0.33**	0.21	**8.41e-1**
LNX2	194.35	**-0.25**	0.23	**9.49e-1**
LOC100128361	27.04	**0.11**	0.25	**9.90e-1**
LOC100129034	852.56	**-0.02**	0.19	**9.93e-1**
LOC100129461	22.83	**-0.2**	0.24	**9.81e-1**
LOC100129917	22.67	**-0.32**	0.24	**9.07e-1**
LOC100130705	26.97	**-0.1**	0.25	**9.90e-1**
LOC100130744	119.35	**-0.08**	0.24	**9.90e-1**
LOC100130950	11.1	**0.12**	0.21	**9.90e-1**
LOC100131564	57.75	**0.19**	0.25	**9.87e-1**
LOC100132352	60.68	**0.31**	0.25	**9.37e-1**
LOC100133091	196.64	**0.05**	0.22	**9.93e-1**
LOC100133315	13.88	**-0.06**	0.23	**9.93e-1**
LOC100133331	92.56	**-0.53**	0.25	**6.07e-1**
LOC100287015	53.86	**-0.06**	0.25	**9.93e-1**
LOC100288069	38.05	**-0.35**	0.25	**8.98e-1**

LOC100288152	140.63	**-0.05**	0.25	**9.93e-1**
LOC100288637	96	**0.03**	0.24	**9.93e-1**
LOC100288778	143.8	**-0.28**	0.24	**9.47e-1**
LOC100288842	11.49	**0.11**	0.21	**9.90e-1**
LOC100294145	218.33	**0.01**	0.22	**9.96e-1**
LOC100419583	182.07	**0.34**	0.23	**8.56e-1**
LOC100420587	130.79	**-0.29**	0.24	**9.39e-1**
LOC100505549	40.33	**-0.18**	0.25	**9.87e-1**
LOC100505622	14.05	**-0.06**	0.22	**9.93e-1**
LOC100506100	10.86	**-0.09**	0.21	**9.90e-1**
LOC100506127	71.22	**-0.11**	0.25	**9.90e-1**
LOC100506258	475.87	**0.06**	0.2	**9.93e-1**
LOC100506302	52.81	**-0.12**	0.25	**9.90e-1**
LOC100506548	216.96	**0.3**	0.23	**9.10e-1**
LOC100506603	45.03	**-0.17**	0.25	**9.90e-1**
LOC100506639	23.49	**-0.25**	0.25	**9.56e-1**
LOC100506801	10.23	**-0.08**	0.21	**9.90e-1**
LOC100506804	11.12	**0.03**	0.21	**9.93e-1**
LOC100506844	38.01	**0.13**	0.25	**9.90e-1**
LOC100507006	17.32	**0.23**	0.23	**9.58e-1**
LOC100507437	17.7	**-0.23**	0.23	**9.54e-1**
LOC100507634	23.56	**-0.15**	0.24	**9.90e-1**
LOC100996437	12.56	**0.02**	0.22	**9.96e-1**
LOC100996579	87.59	**0.05**	0.25	**9.93e-1**
LOC101927021	26.1	**0.22**	0.25	**9.76e-1**
LOC101927045	22.86	**0.04**	0.24	**9.93e-1**
LOC101927181	15.94	**-0.16**	0.22	**9.87e-1**
LOC101927204	10.48	**0.22**	0.21	**9.49e-1**
LOC101927365	36.8	**0.14**	0.25	**9.90e-1**
LOC101927550	24.55	**0.13**	0.25	**9.90e-1**
LOC101927919	29.07	**-0.36**	0.25	**8.75e-1**
LOC101928068	23.1	**0.01**	0.24	**9.96e-1**
LOC101928069	11.14	**-0.05**	0.21	**9.93e-1**
LOC101928103	13.41	**-0.08**	0.22	**9.90e-1**
LOC101928525	12.19	**0.01**	0.21	**9.97e-1**
LOC101929057	10.31	**0.02**	0.21	**9.96e-1**
LOC101929147	53.28	**0.22**	0.25	**9.80e-1**
LOC101929294	34.05	**0.01**	0.25	**9.98e-1**
LOC101929709	22.54	**-0.09**	0.24	**9.90e-1**
LOC101929715	22.14	**-0.05**	0.24	**9.93e-1**
LOC101929767	17.9	**0.01**	0.24	**9.97e-1**
LOC102606465	34.7	**0.29**	0.25	**9.47e-1**
LOC102723927	17.89	**-0.08**	0.24	**9.90e-1**
LOC103344931	48.85	**-0.05**	0.25	**9.93e-1**
LOC105378732	23.89	**-0.08**	0.25	**9.91e-1**
LOC115110	58.5	**0.46**	0.25	**7.49e-1**
LOC146880	80.2	**-0.04**	0.25	**9.93e-1**
LOC148413	131.4	**-0.11**	0.24	**9.90e-1**
LOC150776	137.01	**-0.27**	0.24	**9.47e-1**
LOC155060	14.51	**0.1**	0.23	**9.90e-1**
LOC171391	11.54	**0.02**	0.22	**9.93e-1**
LOC220729	99.39	**0.36**	0.25	**8.68e-1**
LOC257396	17.61	**0.05**	0.23	**9.93e-1**
LOC283710	141.31	**0.02**	0.23	**9.94e-1**
LOC283922	43.54	**-0.05**	0.25	**9.93e-1**
LOC285074	112.83	**0.22**	0.24	**9.72e-1**
LOC286437	17.12	**-0.18**	0.23	**9.86e-1**
LOC339803	63.26	**-0.04**	0.25	**9.93e-1**
LOC374443	35.47	**0.13**	0.25	**9.90e-1**
LOC389641	113.49	**0.07**	0.24	**9.93e-1**
LOC389765	17.21	**0.26**	0.23	**9.48e-1**

LOC389906	44.84	**0.1**	0.25	**9.90e-1**
LOC400958	21.07	**0.37**	0.24	**8.47e-1**
LOC401320	10.27	**0.21**	0.2	**9.53e-1**

LOC439994	36.82	**-0.36**	0.25	**8.73e-1**
LOC440434	80.83	**0.23**	0.25	**9.66e-1**
LOC440461	15.27	**-0.01**	0.23	**9.96e-1**
LOC440600	13.56	**-0.23**	0.22	**9.50e-1**
LOC440704	22.7	**0.04**	0.24	**9.93e-1**
LOC441242	24.41	**-0.05**	0.25	**9.93e-1**
LOC613037	84.36	**-0.5**	0.25	**6.61e-1**
LOC63930	34.63	**0.02**	0.25	**9.93e-1**
LOC642361	32.64	**-0.27**	0.25	**9.49e-1**
LOC642846	240.61	**0**	0.22	**9.98e-1**
LOC642852	55.52	**0.07**	0.25	**9.93e-1**
LOC645513	27.11	**0.21**	0.25	**9.80e-1**
LOC646214	10.28	**0.25**	0.21	**9.42e-1**
LOC646762	146.76	**0.05**	0.23	**9.93e-1**
LOC648987	15.71	**0.13**	0.22	**9.90e-1**
LOC652276	39.02	**-0.28**	0.25	**9.48e-1**
LOC728323	34.68	**0.14**	0.25	**9.90e-1**
LOC728554	91.24	**0.43**	0.24	**7.57e-1**
LOC728613	11.53	**-0.14**	0.22	**9.90e-1**
LOC728673	19.29	**0.35**	0.24	**8.64e-1**
LOC728743	55.63	**-0.04**	0.25	**9.93e-1**
LOC729218	271.47	**-0.5**	0.23	**5.83e-1**
LOC729683	43.02	**0.05**	0.25	**9.93e-1**
LOC81691	63.42	**0.18**	0.25	**9.87e-1**
LOC90784	29.36	**0.07**	0.25	**9.93e-1**
LOC93622	168.94	**0.36**	0.23	**8.41e-1**
LOH12CR1	54.62	**0.03**	0.25	**9.93e-1**
LONP1	1763.23	**0.14**	0.2	**9.89e-1**
LONP2	176.77	**0.04**	0.23	**9.93e-1**
LONRF1	424.9	**0.32**	0.21	**8.52e-1**
LOXL2	229.41	**0.49**	0.22	**5.83e-1**
LPAR2	80.7	**-0.04**	0.25	**9.93e-1**
LPCAT1	1345.03	**0.96**	0.19	**1.89e-4**
LPCAT3	366.62	**-0.34**	0.21	**8.30e-1**
LPCAT4	151.4	**-0.11**	0.23	**9.90e-1**
LPGAT1	569.17	**0.22**	0.2	**9.49e-1**
LPIN1	249.06	**0.79**	0.22	**3.99e-2**
LPIN2	116.6	**-0.1**	0.24	**9.90e-1**
LPP	380.37	**-0.14**	0.21	**9.89e-1**
LPP-AS2	10.01	**-0.07**	0.2	**9.91e-1**
LPXN	1532.89	**0.12**	0.19	**9.90e-1**
LRBA	806.2	**0.03**	0.19	**9.93e-1**
LRCH1	529.95	**0.12**	0.2	**9.90e-1**
LRCH3	247.59	**-0.09**	0.22	**9.90e-1**
LRCH4	370	**-0.28**	0.24	**9.47e-1**
LRFN4	280.65	**-0.51**	0.25	**6.34e-1**
LRG1	25.9	**-0.27**	0.24	**9.47e-1**
LRIF1	235.36	**-0.09**	0.22	**9.90e-1**
LRIG1	1147.65	**-0.23**	0.19	**9.35e-1**
LRIG2	85.53	**0.12**	0.25	**9.90e-1**
LRMP	4256.13	**0.77**	0.19	**1.05e-2**
LRP10	345.51	**-0.05**	0.24	**9.93e-1**
LRP11	207.96	**0.45**	0.22	**6.54e-1**
LRP5L	13.4	**-0.16**	0.22	**9.87e-1**
LRP8	1720.4	**-0.03**	0.18	**9.93e-1**
LRPAP1	353.11	**0.09**	0.21	**9.90e-1**
LRPPRC	3778.95	**0.32**	0.2	**8.32e-1**
LRR1	173.61	**-0.05**	0.23	**9.93e-1**
LRRC1	56.51	**0.37**	0.25	**8.66e-1**
LRRC14	380.92	**-0.39**	0.23	**8.10e-1**
LRRC16A	124.39	**-0.19**	0.24	**9.86e-1**
LRRC16B	22.12	**-0.17**	0.24	**9.87e-1**
LRRC20	80.49	**-0.41**	0.25	**8.21e-1**
LRRC23	33.08	**0**	0.25	**9.98e-1**

LRRC27	27.27	**0.03**	0.25	**9.93e-1**
LRRC28	75.03	**0.23**	0.25	**9.73e-1**
LRRC34	49.74	**0.09**	0.25	**9.90e-1**
LRRC37A	15.23	**0.08**	0.23	**9.90e-1**
LRRC37A2	35.73	**-0.08**	0.25	**9.92e-1**
LRRC37A3	18.97	**0.12**	0.24	**9.90e-1**
LRRC37A4P	144.38	**-0.03**	0.23	**9.93e-1**
LRRC37B	67.63	**0.09**	0.25	**9.90e-1**
LRRC37BP1	291.67	**0.05**	0.22	**9.93e-1**
LRRC40	349.53	**-0.01**	0.22	**9.96e-1**
LRRC41	382.38	**-0.02**	0.21	**9.95e-1**
LRRC42	152.63	**-0.05**	0.23	**9.93e-1**
LRRC45	310.17	**-0.14**	0.23	**9.90e-1**
LRRC46	12.69	**-0.19**	0.22	**9.76e-1**
LRRC47	441.42	**-0.07**	0.21	**9.91e-1**
LRRC56	86.15	**-0.36**	0.25	**8.74e-1**

LRRC57	90.42	**0.06**	0.25	**9.93e-1**
LRRC58	1032.9	**0.16**	0.21	**9.86e-1**
LRRC59	1729.55	**-0.1**	0.19	**9.90e-1**
LRRC61	91.86	**-0.24**	0.25	**9.64e-1**
LRRC75A-AS1	2072.21	**0.38**	0.18	**6.07e-1**
LRRC8A	232.09	**-0.11**	0.22	**9.90e-1**
LRRC8B	220.38	**0.09**	0.23	**9.90e-1**
LRRC8C	250.76	**-0.03**	0.23	**9.93e-1**
LRRC8D	612.44	**0.13**	0.21	**9.90e-1**
LRRCC1	345.38	**-0.34**	0.21	**8.38e-1**
LRRFIP1	2763.87	**-0.24**	0.18	**9.08e-1**
LRRFIP2	306.73	**0.1**	0.22	**9.90e-1**
LRRK1	1315.93	**-0.22**	0.2	**9.49e-1**
LRSAM1	168.12	**-0.03**	0.23	**9.93e-1**
LRTOMT	46.87	**0.21**	0.25	**9.81e-1**
LRWD1	434.47	**-0.28**	0.23	**9.41e-1**
LSAMP	46.47	**0.53**	0.25	**6.14e-1**
LSG1	597.45	**-0.04**	0.2	**9.93e-1**
LSM1	145.56	**-0.03**	0.23	**9.93e-1**
LSM10	390.72	**-0.21**	0.22	**9.58e-1**
LSM11	89.18	**0.37**	0.25	**8.62e-1**
LSM12	375.31	**-0.1**	0.21	**9.90e-1**
LSM14A	1746.65	**0.02**	0.18	**9.94e-1**
LSM14B	361.49	**0.12**	0.21	**9.90e-1**
LSM2	128.41	**0.17**	0.24	**9.87e-1**
LSM3	277.55	**0.15**	0.22	**9.87e-1**
LSM4	466.75	**0.11**	0.21	**9.90e-1**
LSM5	307.23	**0.25**	0.22	**9.47e-1**
LSM6	164.21	**-0.15**	0.23	**9.90e-1**
LSM7	193.45	**-0.05**	0.24	**9.93e-1**
LSM8	545.84	**0.27**	0.2	**9.06e-1**
LSP1	2748.84	**-0.6**	0.22	**3.01e-1**
LSR	333.75	**-0.38**	0.24	**8.44e-1**
LSS	1054.81	**-0.56**	0.22	**4.11e-1**
LTA	361.04	**0.55**	0.24	**5.31e-1**
LTA4H	1085.07	**0.01**	0.19	**9.96e-1**
LTB	751.67	**0.15**	0.24	**9.90e-1**
LTB4R	248.18	**-0.13**	0.22	**9.90e-1**
LTB4R2	20.69	**0.07**	0.24	**9.93e-1**
LTBP1	989.15	**0.48**	0.19	**4.11e-1**
LTBP3	12.01	**0.03**	0.22	**9.93e-1**
LTBP4	287.72	**-0.33**	0.23	**8.75e-1**
LTN1	332.75	**0.17**	0.22	**9.87e-1**
LTV1	550.25	**0.16**	0.21	**9.87e-1**
LUC7L	274.33	**-0.11**	0.21	**9.90e-1**
LUC7L2	153.06	**-0.67**	0.25	**3.16e-1**
LUC7L3	1584.05	**-0.39**	0.18	**6.06e-1**

LUZP1	366.38	**-0.45**	0.21	**5.91e-1**
LY6G5B	100.77	**-0.08**	0.24	**9.91e-1**
LY75	34.59	**0.14**	0.25	**9.90e-1**
LY86	28.72	**0.15**	0.25	**9.90e-1**
LY86-AS1	52.3	**0.14**	0.25	**9.90e-1**
LYAR	864.21	**-0.19**	0.19	**9.58e-1**
LYL1	81.53	**-0.03**	0.25	**9.93e-1**
LYN	465.45	**0.13**	0.21	**9.90e-1**
LYPLA1	1489.58	**0.09**	0.2	**9.90e-1**
LYPLA2	359.09	**-0.5**	0.24	**6.28e-1**
LYPLAL1	76.34	**0.2**	0.25	**9.86e-1**
LYRM1	183.77	**0.49**	0.23	**5.86e-1**
LYRM2	439.08	**0.07**	0.22	**9.91e-1**
LYRM4	180.04	**0.17**	0.22	**9.87e-1**
LYRM5	37.33	**0.03**	0.25	**9.93e-1**
LYRM7	652.06	**0**	0.21	**9.99e-1**
LYSMD1	47.26	**-0.31**	0.25	**9.39e-1**
LYSMD2	91.43	**0.18**	0.25	**9.87e-1**
LYSMD3	233.61	**-0.1**	0.23	**9.90e-1**
LYSMD4	34.29	**0.27**	0.25	**9.49e-1**
LYST	70.74	**0.58**	0.25	**5.31e-1**
LZIC	103.4	**-0.17**	0.24	**9.88e-1**
LZTR1	445.11	**-0.44**	0.23	**7.07e-1**
LZTS2	142.31	**-0.43**	0.25	**7.97e-1**
LZTS3	101.37	**-0.17**	0.25	**9.89e-1**
M6PR	996.74	**0.05**	0.19	**9.93e-1**
MACC1	282.61	**-0.4**	0.22	**7.41e-1**
MACF1	769.48	**-0.17**	0.2	**9.80e-1**
MACROD1	60.39	**0.1**	0.25	**9.90e-1**
MAD1L1	214.63	**0**	0.22	**9.99e-1**
MAD2L1	563.07	**0.12**	0.2	**9.90e-1**
MAD2L1BP	113.6	**0**	0.24	**9.98e-1**
MAD2L2	161.51	**0.19**	0.23	**9.80e-1**
MADD	567.65	**0.03**	0.2	**9.93e-1**
MAEA	493.65	**-0.14**	0.2	**9.89e-1**
MAF1	845.44	**-0.05**	0.21	**9.93e-1**
MAFF	18.64	**0.5**	0.23	**5.91e-1**
MAFG	288.09	**0.16**	0.23	**9.88e-1**
MAFG-AS1	31.17	**-0.07**	0.24	**9.91e-1**
MAFK	337.18	**-0.47**	0.24	**6.69e-1**
MAGED1	1077.28	**-0.49**	0.21	**5.16e-1**
MAGED2	143.74	**-0.24**	0.25	**9.59e-1**
MAGEF1	133.4	**0.28**	0.23	**9.42e-1**
MAGI3	46.1	**0.13**	0.25	**9.90e-1**
MAGOH	264.72	**-0.17**	0.21	**9.81e-1**
MAGOHB	203.08	**0.15**	0.22	**9.88e-1**
MAGT1	403.91	**0.07**	0.21	**9.90e-1**
MAK16	747.91	**-0.11**	0.2	**9.90e-1**
MALAT1	673.36	**-0.42**	0.19	**5.86e-1**
MALSU1	165.05	**0.05**	0.23	**9.93e-1**
MALT1	409.29	**0.49**	0.22	**5.59e-1**
MAMDC4	173.07	**-0.25**	0.25	**9.57e-1**
MAML1	409.6	**-0.24**	0.21	**9.47e-1**
MAML2	220.16	**-0.07**	0.22	**9.90e-1**
MAML3	11.63	**-0.06**	0.22	**9.93e-1**
MAN1A1	259.12	**-0.05**	0.22	**9.93e-1**
MAN1A2	459.71	**0.16**	0.21	**9.87e-1**
MAN1B1	243.03	**-0.05**	0.22	**9.93e-1**
MAN1B1-AS1	21.23	**-0.02**	0.24	**9.95e-1**
MAN2A1	346.42	**0.24**	0.21	**9.47e-1**
MAN2A2	180.09	**-0.29**	0.23	**9.23e-1**
MAN2B1	883.28	**-0.1**	0.2	**9.90e-1**
MAN2B2	136.03	**0.18**	0.24	**9.86e-1**

MAN2C1	153.23	**0.24**	0.24	**9.60e-1**
MANBA	216.79	**0.29**	0.23	**9.20e-1**
MANBAL	113.71	**-0.01**	0.24	**9.96e-1**
MANEA	173.34	**0.16**	0.24	**9.90e-1**
MANEAL	472.19	**-0.14**	0.22	**9.90e-1**
MANF	511.49	**0.26**	0.2	**9.22e-1**
MAP1A	50.16	**-0.5**	0.25	**6.69e-1**
MAP1LC3B	168.61	**0.36**	0.23	**8.39e-1**
MAP1S	382.33	**-0.23**	0.23	**9.56e-1**
MAP2K1	406.26	**0.5**	0.2	**4.57e-1**
MAP2K2	610.19	**-0.26**	0.23	**9.48e-1**
MAP2K3	367.62	**-0.15**	0.21	**9.88e-1**
MAP2K4	316.15	**0.24**	0.22	**9.49e-1**
MAP2K5	120.06	**-0.26**	0.24	**9.49e-1**
MAP2K6	28.4	**0.02**	0.25	**9.95e-1**
MAP2K7	407.13	**-0.3**	0.24	**9.30e-1**
MAP3K1	340.91	**0.05**	0.21	**9.93e-1**
MAP3K10	55.7	**0.02**	0.25	**9.95e-1**
MAP3K11	256.07	**-0.08**	0.24	**9.90e-1**
MAP3K12	21.89	**-0.03**	0.24	**9.93e-1**
MAP3K14	309.18	**-0.2**	0.22	**9.73e-1**
MAP3K2	201.81	**0.17**	0.23	**9.87e-1**
MAP3K3	330.17	**-0.16**	0.22	**9.87e-1**
MAP3K4	248.45	**-0.17**	0.22	**9.86e-1**
MAP3K5	350.33	**0.12**	0.21	**9.90e-1**
MAP3K7	900.15	**0.1**	0.19	**9.90e-1**
MAP3K7CL	74.14	**0.23**	0.25	**9.68e-1**
MAP3K8	135.08	**0.37**	0.24	**8.41e-1**
MAP3K9	110.29	**-0.15**	0.24	**9.90e-1**
MAP4	3531.29	**-0.5**	0.18	**3.22e-1**
MAP4K1	1580.18	**-0.26**	0.2	**9.22e-1**
MAP4K2	353.57	**-0.34**	0.22	**8.52e-1**
MAP4K3	83.39	**0.2**	0.25	**9.81e-1**
MAP4K4	2827.79	**-0.06**	0.18	**9.91e-1**
MAP4K5	537.48	**-0.29**	0.21	**8.82e-1**
MAP6D1	18.22	**0.17**	0.24	**9.87e-1**
MAP7D1	1037.46	**-0.22**	0.22	**9.59e-1**
MAP7D2	24.86	**0.18**	0.25	**9.87e-1**
MAP7D3	411.58	**-0.28**	0.2	**8.99e-1**
MAP9	224.84	**0.1**	0.22	**9.90e-1**
MAPK1	844.76	**0.09**	0.2	**9.90e-1**
MAPK12	449.16	**-0.05**	0.22	**9.93e-1**
MAPK14	294.4	**0.26**	0.22	**9.42e-1**
MAPK1IP1L	1159.53	**-0.41**	0.19	**5.86e-1**
MAPK3	310.25	**-0.31**	0.22	**8.80e-1**
MAPK6	1417.39	**-0.09**	0.2	**9.90e-1**
MAPK7	189.85	**-0.35**	0.25	**8.68e-1**
MAPK8	205.74	**0.43**	0.23	**7.31e-1**
MAPK8IP2	13.77	**-0.06**	0.22	**9.93e-1**
MAPK8IP3	488.76	**-0.24**	0.23	**9.54e-1**
MAPK9	397.56	**0.3**	0.21	**8.78e-1**
MAPKAP1	1104.15	**0**	0.19	**9.98e-1**
MAPKAPK2	1147.63	**0.11**	0.19	**9.90e-1**
MAPKAPK3	327.82	**-0.15**	0.22	**9.88e-1**
MAPKAPK5	358.28	**0.21**	0.21	**9.59e-1**
MAPKAPK5-AS1	79.34	**0.15**	0.25	**9.90e-1**

MAPKBP1	173.08	**-0.54**	0.24	**5.45e-1**
MAPRE1	1967.18	**0.15**	0.19	**9.81e-1**
MAPRE2	657.49	**0.05**	0.2	**9.93e-1**
MARCH1	34.1	**-0.22**	0.25	**9.75e-1**
MARCH2	22.61	**-0.17**	0.24	**9.87e-1**
MARCH3	19.02	**0.14**	0.24	**9.90e-1**
MARCH5	218.45	**0.09**	0.22	**9.90e-1**

MARCH6	718.45	**0.25**	0.2	**9.25e-1**
MARCH7	563.62	**0.09**	0.21	**9.90e-1**
MARCH8	273.82	**0.08**	0.21	**9.90e-1**
MARCH9	148.3	**0.02**	0.23	**9.93e-1**
MARCKSL1	4469.39	**0.04**	0.2	**9.93e-1**
MARK2	565.23	**-0.45**	0.21	**5.94e-1**
MARK3	610.96	**0.11**	0.2	**9.90e-1**
MARK4	156.45	**-0.14**	0.24	**9.90e-1**
MARS	1783.12	**0.34**	0.18	**7.13e-1**
MARS2	378.69	**-0.35**	0.21	**8.10e-1**
MAST1	163.85	**-0.3**	0.24	**9.31e-1**
MAST2	1734	**-0.24**	0.19	**9.23e-1**
MAST3	499.4	**-0.43**	0.22	**6.69e-1**
MAST4	117.85	**-0.33**	0.24	**8.80e-1**
MASTL	313.26	**0.11**	0.21	**9.90e-1**
MAT1A	147.54	**-0.51**	0.24	**5.91e-1**
MAT2A	3686.78	**0**	0.19	**9.98e-1**
MAT2B	407.44	**0.27**	0.21	**9.12e-1**
MATR3	3546.54	**0.09**	0.19	**9.90e-1**
MAU2	366.18	**-0.19**	0.22	**9.78e-1**
MAVS	1070.13	**-0.42**	0.21	**6.49e-1**
MAX	568.66	**-0.15**	0.2	**9.87e-1**
MAZ	2372.85	**-0.28**	0.21	**9.12e-1**
MBD1	444.95	**-0.2**	0.21	**9.60e-1**
MBD2	943.12	**0.27**	0.2	**9.10e-1**
MBD3	665.25	**-0.06**	0.24	**9.93e-1**
MBD4	380	**0.17**	0.21	**9.86e-1**
MBD6	507.73	**-0.19**	0.23	**9.81e-1**
MBIP	166.81	**0.01**	0.23	**9.96e-1**
MBLAC2	220.43	**-0.15**	0.22	**9.88e-1**
MBNL1	2454.66	**-0.35**	0.19	**7.13e-1**
MBNL2	69.7	**0.1**	0.25	**9.90e-1**
MBNL3	334.86	**0.06**	0.22	**9.93e-1**
MBOAT2	99.73	**0.18**	0.24	**9.87e-1**
MBOAT7	268.35	**-0.08**	0.24	**9.91e-1**
MBP	221.6	**0.15**	0.22	**9.88e-1**
MBTD1	526.56	**0.07**	0.2	**9.91e-1**
MBTPS1	738.3	**0.23**	0.2	**9.47e-1**
MBTPS2	268.08	**0.01**	0.22	**9.97e-1**
MC1R	19.39	**-0.15**	0.23	**9.90e-1**
MCAT	155.02	**-0.14**	0.23	**9.90e-1**
MCCC1	370	**0.33**	0.21	**8.40e-1**
MCCC2	1534.45	**0.07**	0.19	**9.90e-1**
MCEE	32.38	**0.13**	0.25	**9.90e-1**
MCFD2	1117.55	**-0.11**	0.19	**9.90e-1**
MCIDAS	33.57	**-0.36**	0.25	**8.75e-1**
MCL1	2044.05	**0.31**	0.19	**8.17e-1**
MCM10	700.96	**-0.22**	0.2	**9.47e-1**
MCM2	2260.33	**-0.09**	0.19	**9.90e-1**
MCM3	3843.01	**0.04**	0.18	**9.93e-1**
MCM3AP	1030.21	**-0.01**	0.19	**9.96e-1**
MCM3AP-AS1	35.21	**0.01**	0.25	**9.98e-1**
MCM4	4301.79	**-0.04**	0.18	**9.93e-1**
MCM5	3516.68	**-0.49**	0.2	**4.16e-1**
MCM6	1254.46	**0.08**	0.19	**9.90e-1**
MCM7	5040.61	**-0.15**	0.19	**9.86e-1**
MCM8	817.29	**0.02**	0.2	**9.93e-1**
MCM9	237.91	**0.22**	0.22	**9.54e-1**
MCMBP	1329.46	**0.05**	0.19	**9.93e-1**
MCOLN1	94.52	**0.13**	0.24	**9.90e-1**
MCOLN2	264.96	**0.21**	0.22	**9.59e-1**
MCPH1	358.08	**-0.02**	0.21	**9.95e-1**
MCRS1	465.82	**-0.05**	0.21	**9.93e-1**
MCTP1	53.15	**-0.17**	0.25	**9.89e-1**
MCTP2	195.34	**0.46**	0.22	**6.36e-1**

MCTS1	250.81	**0.29**	0.22	**9.12e-1**
MCTS2P	110.98	**-0.2**	0.24	**9.81e-1**
MCU	238.15	**-0.31**	0.22	**8.92e-1**
MCUR1	499.78	**0.23**	0.21	**9.49e-1**
MDC1	2161.59	**-0.54**	0.2	**3.51e-1**
MDFIC	146.26	**0.13**	0.24	**9.90e-1**
MDH1	565.5	**0.36**	0.2	**7.57e-1**
MDH1B	12.85	**0.09**	0.22	**9.90e-1**
MDH2	3564.63	**-0.21**	0.2	**9.50e-1**
MDK	15.65	**0.07**	0.23	**9.91e-1**
MDM1	227.38	**0.03**	0.22	**9.93e-1**
MDM2	1460.74	**-0.15**	0.2	**9.86e-1**
MDM4	431.98	**0.01**	0.21	**9.96e-1**
MDN1	2443.62	**-0.4**	0.18	**5.91e-1**
ME2	2272.01	**0.02**	0.2	**9.93e-1**
MEA1	316.82	**-0.53**	0.23	**5.40e-1**
MEAF6	593.54	**0.02**	0.2	**9.93e-1**
MECP2	408.77	**-0.16**	0.21	**9.87e-1**
MECR	124.61	**0.05**	0.24	**9.93e-1**
MED1	1415.3	**-0.22**	0.19	**9.47e-1**
MED10	222.29	**-0.29**	0.22	**9.10e-1**
MED11	74.98	**-0.21**	0.25	**9.81e-1**
MED12	600.35	**-0.13**	0.2	**9.90e-1**
MED12L	167.98	**-0.09**	0.23	**9.90e-1**
MED13	823.68	**0.22**	0.2	**9.49e-1**
MED13L	1547.36	**-0.13**	0.19	**9.87e-1**
MED14	878.04	**-0.04**	0.2	**9.93e-1**
MED15	486.64	**-0.33**	0.2	**8.29e-1**
MED16	339.11	**-0.07**	0.22	**9.92e-1**
MED17	262.3	**0.1**	0.22	**9.90e-1**
MED18	94.05	**0.13**	0.24	**9.90e-1**
MED19	65.88	**-0.12**	0.25	**9.90e-1**
MED20	206	**0.13**	0.22	**9.90e-1**
MED21	117.96	**0.19**	0.24	**9.86e-1**
MED22	552.44	**-0.4**	0.23	**7.87e-1**
MED23	227.49	**0.31**	0.22	**8.88e-1**
MED24	761.73	**-0.25**	0.2	**9.25e-1**
MED25	641.67	**-0.69**	0.24	**2.38e-1**
MED26	297.99	**-0.25**	0.23	**9.49e-1**
MED27	121.48	**0.16**	0.24	**9.89e-1**
MED28	372.41	**0.09**	0.21	**9.90e-1**
MED29	249.21	**0.08**	0.22	**9.90e-1**
MED30	50.79	**0.35**	0.25	**8.95e-1**
MED31	36.41	**-0.16**	0.25	**9.90e-1**
MED4	346.11	**0.07**	0.21	**9.91e-1**
MED6	147.9	**0.26**	0.24	**9.47e-1**
MED7	66.21	**0.02**	0.25	**9.96e-1**
MED8	261.58	**0.25**	0.22	**9.47e-1**
MED9	87.38	**0.09**	0.25	**9.90e-1**
MEF2A	604.14	**0.23**	0.2	**9.47e-1**
MEF2BNB	33	**-0.27**	0.25	**9.49e-1**
MEF2C	791.99	**-0.41**	0.2	**6.03e-1**
MEF2D	1005.26	**-0.39**	0.22	**7.59e-1**
MEGF8	287.01	**-0.03**	0.25	**9.93e-1**
MEGF9	323.58	**-0.13**	0.21	**9.90e-1**
MEIS1	31.54	**-0.3**	0.25	**9.47e-1**
MEIS2	94.83	**-0.11**	0.24	**9.90e-1**
MELK	358.65	**0.14**	0.21	**9.90e-1**
MEMO1	298.01	**0.17**	0.21	**9.83e-1**
MEN1	920.47	**-0.42**	0.22	**6.87e-1**
MEPCE	1198.01	**-0.4**	0.23	**7.86e-1**
MESDC1	143.04	**0.21**	0.23	**9.74e-1**
MESDC2	403.03	**-0.26**	0.21	**9.25e-1**

MET	401.48	**-0.4**	0.21	**7.04e-1**
METAP1	897.96	**0.11**	0.2	**9.90e-1**
METAP1D	57.64	**0.14**	0.25	**9.90e-1**
METAP2	1881.35	**-0.17**	0.19	**9.72e-1**
METRNL	37.84	**0.16**	0.25	**9.90e-1**
METTL1	143.55	**-0.4**	0.23	**7.87e-1**
METTL10	125.39	**0.24**	0.24	**9.53e-1**
METTL12	37.34	**-0.24**	0.25	**9.61e-1**
METTL13	445.04	**-0.11**	0.2	**9.90e-1**
METTL14	178.38	**0.07**	0.23	**9.91e-1**
METTL15	118.17	**0.22**	0.24	**9.66e-1**
METTL16	560.54	**-0.21**	0.2	**9.49e-1**
METTL17	738.67	**0.09**	0.19	**9.90e-1**
METTL18	40.64	**0.03**	0.25	**9.93e-1**
METTL21A	134.91	**0.22**	0.23	**9.66e-1**
METTL21B	25.08	**-0.07**	0.25	**9.93e-1**
METTL22	102.35	**-0.08**	0.25	**9.90e-1**
METTL23	52.74	**0.23**	0.25	**9.74e-1**
METTL25	29.22	**0.2**	0.25	**9.86e-1**
METTL2A	186.74	**-0.2**	0.22	**9.74e-1**
METTL2B	315.03	**-0.18**	0.21	**9.80e-1**
METTL3	734.13	**0.2**	0.2	**9.57e-1**
METTL4	95.21	**0.26**	0.24	**9.49e-1**
METTL5	170.56	**0.07**	0.23	**9.91e-1**
METTL6	121.21	**-0.23**	0.24	**9.61e-1**
METTL7A	521.94	**-0.28**	0.2	**8.76e-1**
METTL8	345.49	**0**	0.22	**9.98e-1**
METTL9	655.75	**0.17**	0.21	**9.83e-1**
MEX3A	26.64	**-0.2**	0.25	**9.81e-1**
MEX3B	25.34	**0.02**	0.25	**9.94e-1**
MEX3C	803.56	**0.18**	0.2	**9.71e-1**

MEX3D	77.55	**-0.15**	0.25	**9.90e-1**
MFAP1	608.41	**-0.09**	0.2	**9.90e-1**
MFAP3	216.89	**0.14**	0.22	**9.90e-1**
MFF	353.38	**0.37**	0.22	**8.07e-1**
MFGE8	64.06	**0.37**	0.25	**8.64e-1**
MFHAS1	434.47	**-0.12**	0.2	**9.90e-1**
MFI2	17.89	**-0.1**	0.24	**9.90e-1**
MFI2-AS1	13.58	**-0.08**	0.22	**9.90e-1**
MFN1	576.24	**0.45**	0.2	**5.60e-1**
MFN2	1356.85	**-0.25**	0.2	**9.20e-1**
MFNG	1261.14	**-0.4**	0.22	**7.41e-1**
MFSD1	336.03	**0.49**	0.21	**5.36e-1**
MFSD10	111.32	**-0.25**	0.25	**9.58e-1**
MFSD11	105.43	**0.17**	0.24	**9.87e-1**
MFSD12	260.36	**-0.11**	0.24	**9.90e-1**
MFSD2A	295.57	**-0.24**	0.23	**9.49e-1**
MFSD3	124.86	**-0.43**	0.25	**7.99e-1**
MFSD5	158.55	**-0.2**	0.24	**9.80e-1**
MFSD6	345.63	**-0.04**	0.21	**9.93e-1**
MFSD8	78.9	**0.1**	0.25	**9.90e-1**
MFSD9	58.06	**0.08**	0.25	**9.91e-1**
MGA	1031.71	**-0.07**	0.19	**9.90e-1**
MGAT1	348.68	**-0.28**	0.24	**9.47e-1**
MGAT2	460.12	**0.06**	0.2	**9.92e-1**
MGAT3	461.95	**0.14**	0.23	**9.90e-1**
MGAT4A	144.59	**0.55**	0.24	**5.45e-1**
MGAT4B	453.56	**0.26**	0.21	**9.42e-1**
MGAT5	388.75	**-0.19**	0.21	**9.66e-1**
MGAT5B	17.73	**-0.07**	0.23	**9.92e-1**
MGC27345	248.67	**-0.21**	0.22	**9.66e-1**
MGC57346	73.1	**-0.17**	0.25	**9.89e-1**
MGC72080	128.95	**0.05**	0.24	**9.93e-1**

MGEA5	1081.32	**-0.07**	0.19	**9.90e-1**
MGLL	322.12	**0.17**	0.23	**9.87e-1**
MGME1	413.93	**0.15**	0.21	**9.87e-1**
MGMT	62.38	**0.27**	0.25	**9.49e-1**
MGRN1	623.86	**-0.34**	0.22	**8.56e-1**
MGST3	28.48	**0.07**	0.25	**9.93e-1**
MIA3	380.35	**-0.08**	0.21	**9.90e-1**
MIB1	527.19	**0.03**	0.2	**9.93e-1**
MIB2	87.43	**0.11**	0.25	**9.90e-1**
MICA	20.6	**0.11**	0.24	**9.90e-1**
MICAL1	728.68	**0.37**	0.22	**7.93e-1**
MICAL3	832.23	**-0.15**	0.2	**9.87e-1**
MICALL1	185.14	**-0.3**	0.24	**9.25e-1**
MICB	153.72	**-0.03**	0.24	**9.93e-1**
MICU1	327.36	**0**	0.21	**9.98e-1**
MICU2	229.2	**0.45**	0.22	**6.59e-1**
MICU3	23.43	**0.08**	0.24	**9.90e-1**
MID1IP1	311.25	**-0.34**	0.22	**8.44e-1**
MID1IP1-AS1	15.11	**-0.38**	0.23	**7.99e-1**
MIDN	1184.81	**-0.37**	0.23	**8.38e-1**
MIEF1	1008.95	**-0.04**	0.19	**9.93e-1**
MIEF2	19.25	**0.15**	0.24	**9.90e-1**
MIEN1	140.99	**-0.23**	0.24	**9.59e-1**
MIER1	254.73	**0.17**	0.22	**9.87e-1**
MIER2	181.71	**-0.06**	0.24	**9.93e-1**
MIER3	268.81	**0.24**	0.22	**9.49e-1**
MIF	789.75	**-0.1**	0.22	**9.90e-1**
MIF4GD	62.23	**0.11**	0.25	**9.90e-1**
MIIP	272.01	**-0.3**	0.24	**9.33e-1**
MILR1	19.76	**0.26**	0.24	**9.49e-1**
MINA	312.36	**-0.22**	0.21	**9.54e-1**
MINK1	684.45	**-0.48**	0.21	**5.79e-1**
MINOS1	197.84	**0.16**	0.22	**9.87e-1**
MINPP1	78.71	**0.29**	0.25	**9.47e-1**
MIOS	476.61	**0.35**	0.22	**8.36e-1**
MIPEP	221.27	**0.22**	0.22	**9.54e-1**
MIPEPP3	15.38	**-0.04**	0.23	**9.93e-1**
MIR142	29.28	**0.06**	0.25	**9.93e-1**
MIR155HG	42.73	**0.28**	0.25	**9.47e-1**
MIR17HG	96.98	**-0.06**	0.25	**9.93e-1**
MIR1914	10.37	**-0.01**	0.21	**9.98e-1**
MIR22HG	19.27	**0.36**	0.24	**8.62e-1**
MIR25	16.45	**-0.04**	0.23	**9.93e-1**
MIR3064	23.69	**0.33**	0.25	**9.10e-1**
MIR378I	17.44	**0.3**	0.24	**9.20e-1**
MIR4426	26.07	**0.4**	0.25	**8.33e-1**
MIR4435-2HG	77.2	**0.1**	0.25	**9.90e-1**
MIR5047	11.6	**0.16**	0.22	**9.87e-1**
MIR5195	30.54	**0.14**	0.25	**9.90e-1**
MIR600HG	170.74	**-0.28**	0.23	**9.42e-1**
MIR762HG	21.32	**0.17**	0.24	**9.88e-1**

MIS12	287.54	**-0.01**	0.21	**9.96e-1**
MIS18A	140.04	**-0.04**	0.23	**9.93e-1**
MIS18BP1	786.25	**0.11**	0.21	**9.90e-1**
MISP	10.34	**0.05**	0.2	**9.93e-1**
MITD1	125.48	**0.23**	0.24	**9.60e-1**
MKI67	6974	**-0.41**	0.18	**5.45e-1**
MKKS	221.81	**0.33**	0.22	**8.54e-1**
MKL1	480.54	**-0.36**	0.22	**8.28e-1**
MKL2	221.51	**-0.02**	0.22	**9.94e-1**
MKLN1	766.71	**0.1**	0.2	**9.90e-1**
MKLN1-AS	47.45	**0.01**	0.25	**9.98e-1**
MKNK1	173.68	**0.08**	0.23	**9.90e-1**
MKNK2	1619.04	**-0.25**	0.23	**9.49e-1**

MKRN1	739.02	**0.3**	0.19	**8.49e-1**
MKRN2	211.37	**0.21**	0.23	**9.72e-1**
MKRN3	41.25	**-0.26**	0.25	**9.54e-1**
MLEC	3551.18	**-0.05**	0.18	**9.93e-1**
MLF2	792.84	**-0.39**	0.24	**8.15e-1**
MLH1	670.12	**0.07**	0.2	**9.90e-1**
MLH3	140.41	**0.04**	0.24	**9.93e-1**
MLLT1	1107.73	**-0.53**	0.22	**4.81e-1**
MLLT10	498	**-0.1**	0.2	**9.90e-1**
MLLT11	57.14	**-0.29**	0.25	**9.47e-1**
MLLT3	263.37	**-0.14**	0.22	**9.90e-1**
MLLT4	652.94	**-0.13**	0.2	**9.89e-1**
MLLT6	1836.46	**-0.39**	0.22	**7.57e-1**
MLST8	560.56	**-0.1**	0.22	**9.90e-1**
MLX	379.97	**-0.34**	0.21	**8.29e-1**
MLXIP	781.74	**-0.53**	0.21	**4.11e-1**
MMAA	72.06	**0.06**	0.25	**9.93e-1**
MMAB	178.76	**-0.21**	0.23	**9.67e-1**
MMACHC	293.08	**-0.74**	0.23	**1.05e-1**
MMADHC	162.6	**0.3**	0.23	**9.12e-1**
MMD	199.13	**0.27**	0.23	**9.47e-1**
MME	1608.88	**-0.64**	0.2	**1.15e-1**
MMGT1	319.18	**0.04**	0.22	**9.93e-1**
MMP14	15.84	**-0.09**	0.23	**9.90e-1**
MMP24-AS1	67.25	**-0.02**	0.25	**9.96e-1**
MMP25-AS1	30.48	**-0.43**	0.25	**7.80e-1**
MMP9	23.78	**-0.03**	0.24	**9.93e-1**
MMS19	704.97	**0.09**	0.19	**9.90e-1**
MMS22L	523.6	**0.17**	0.2	**9.80e-1**
MNAT1	161.05	**0.01**	0.23	**9.96e-1**
MND1	227.61	**0.17**	0.22	**9.87e-1**
MNT	428.96	**-0.6**	0.23	**3.70e-1**
MNX1	20.93	**-0.04**	0.24	**9.93e-1**
MOAP1	83.98	**0.34**	0.25	**8.98e-1**
MOB1A	491.4	**0.03**	0.21	**9.93e-1**
MOB1B	571.36	**0.01**	0.22	**9.97e-1**
MOB2	121.87	**-0.15**	0.25	**9.90e-1**
MOB3A	1243.85	**0.03**	0.2	**9.93e-1**
MOCS2	278.53	**0.13**	0.22	**9.90e-1**
MOCS3	77.59	**-0.12**	0.25	**9.90e-1**
MOGS	590.53	**-0.54**	0.24	**5.68e-1**
MOK	28.41	**-0.09**	0.25	**9.90e-1**
MON1A	121.42	**-0.23**	0.24	**9.69e-1**
MON1B	415.28	**-0.32**	0.22	**8.64e-1**
MON2	287.12	**0.13**	0.22	**9.90e-1**
MORC2	485.08	**-0.11**	0.2	**9.90e-1**
MORC3	213.99	**-0.03**	0.23	**9.93e-1**
MORF4L1	1667.15	**0.11**	0.19	**9.90e-1**
MORF4L2	1142.49	**0.07**	0.2	**9.90e-1**
MORF4L2-AS1	14.27	**0.11**	0.22	**9.90e-1**
MORN1	29.15	**-0.13**	0.25	**9.90e-1**
MOSPD1	33.19	**0.25**	0.25	**9.58e-1**
MOSPD2	106.68	**0.12**	0.24	**9.90e-1**
MOSPD3	36.75	**-0.3**	0.25	**9.47e-1**
MOV10	67.45	**-0.37**	0.25	**8.64e-1**
MPC1	255.71	**0.4**	0.22	**7.13e-1**
MPC2	289.78	**-0.17**	0.21	**9.87e-1**
MPDU1	507.69	**-0.19**	0.21	**9.71e-1**
MPEG1	96.57	**0.58**	0.24	**4.83e-1**
MPG	152.89	**-0.23**	0.25	**9.73e-1**
MPHOSPH10	727.83	**-0.28**	0.2	**8.73e-1**
MPHOSPH6	205.26	**0.34**	0.23	**8.56e-1**
MPHOSPH8	402.12	**-0.48**	0.21	**5.31e-1**
MPHOSPH9	303.63	**0.08**	0.22	**9.90e-1**

MPI	276.72	**-0.1**	0.21	**9.90e-1**
MPLKIP	135.85	**0.02**	0.24	**9.95e-1**
MPND	29.7	**-0.04**	0.25	**9.93e-1**
MPP2	58.89	**-0.29**	0.25	**9.47e-1**
MPP5	273.95	**-0.1**	0.22	**9.90e-1**
MPP6	599.61	**0.13**	0.21	**9.90e-1**
MPP7	51.78	**-0.2**	0.25	**9.86e-1**
MPPE1	51.58	**0.27**	0.25	**9.50e-1**
MPRIP	910.29	**-0.11**	0.19	**9.90e-1**
MPST	120.34	**0.04**	0.25	**9.93e-1**
MPV17	166.43	**-0.06**	0.23	**9.93e-1**
MPV17L2	259.91	**-0.36**	0.23	**8.40e-1**
MPZ	170.63	**-0.42**	0.25	**8.04e-1**
MPZL1	642.76	**-0.4**	0.2	**6.56e-1**
MPZL3	23.58	**0.11**	0.25	**9.90e-1**
MR1	98.15	**0.26**	0.24	**9.49e-1**
MRE11A	507.4	**0.07**	0.21	**9.91e-1**
MREG	144.38	**0.54**	0.24	**5.42e-1**
MRFAP1	1333.9	**0.2**	0.19	**9.49e-1**
MRFAP1L1	260.04	**0.32**	0.22	**8.64e-1**
MRGBP	249.73	**0.19**	0.22	**9.74e-1**
MRI1	89.67	**-0.3**	0.25	**9.37e-1**
MRM1	143.52	**-0.3**	0.24	**9.33e-1**
MROH1	153.25	**-0.08**	0.24	**9.91e-1**
MROH6	95.78	**-0.36**	0.25	**8.78e-1**
MROH8	12.17	**-0.06**	0.21	**9.93e-1**
MRPL1	166.38	**0.16**	0.23	**9.88e-1**
MRPL10	483.1	**-0.18**	0.22	**9.86e-1**
MRPL11	430.72	**-0.09**	0.22	**9.90e-1**
MRPL12	487.65	**-0.18**	0.2	**9.79e-1**
MRPL13	219.18	**0.13**	0.22	**9.90e-1**
MRPL14	213.22	**-0.29**	0.22	**9.12e-1**
MRPL15	529.57	**-0.17**	0.2	**9.80e-1**
MRPL16	516.73	**0.1**	0.2	**9.90e-1**
MRPL17	239.29	**-0.1**	0.22	**9.90e-1**
MRPL18	506.76	**0.14**	0.2	**9.88e-1**
MRPL19	620.25	**-0.05**	0.21	**9.93e-1**
MRPL2	301.67	**-0.01**	0.22	**9.96e-1**
MRPL20	370.8	**-0.16**	0.21	**9.87e-1**
MRPL21	200.7	**0.08**	0.22	**9.90e-1**
MRPL22	205.59	**-0.11**	0.22	**9.90e-1**
MRPL23	159.03	**-0.02**	0.24	**9.93e-1**
MRPL24	237.35	**-0.12**	0.23	**9.90e-1**
MRPL27	182.47	**-0.16**	0.23	**9.87e-1**
MRPL28	370.76	**-0.41**	0.23	**7.57e-1**
MRPL3	1595.33	**0.08**	0.19	**9.90e-1**
MRPL30	561.65	**-0.01**	0.21	**9.96e-1**
MRPL32	346.89	**0.12**	0.21	**9.90e-1**
MRPL33	90.54	**-0.07**	0.25	**9.93e-1**
MRPL34	359.78	**-0.08**	0.23	**9.90e-1**
MRPL35	618.74	**-0.05**	0.21	**9.93e-1**
MRPL36	241.54	**-0.17**	0.22	**9.86e-1**
MRPL37	1910.31	**-0.1**	0.18	**9.90e-1**
MRPL38	515.98	**-0.06**	0.22	**9.93e-1**
MRPL39	271	**0.29**	0.22	**9.12e-1**
MRPL4	1428.13	**-0.31**	0.21	**8.66e-1**
MRPL40	85.8	**0.16**	0.25	**9.89e-1**
MRPL41	88.41	**0.19**	0.25	**9.87e-1**
MRPL42	339.32	**0.03**	0.22	**9.93e-1**
MRPL43	182.12	**-0.46**	0.24	**6.79e-1**
MRPL44	408.65	**0.17**	0.21	**9.85e-1**
MRPL45	492.62	**0.23**	0.2	**9.47e-1**
MRPL45P2	10.77	**0.08**	0.21	**9.90e-1**
MRPL46	213.72	**0.03**	0.22	**9.93e-1**

MRPL47	304.52	**0.11**	0.21	**9.90e-1**
MRPL48	230.47	**-0.08**	0.22	**9.90e-1**
MRPL49	613.21	**-0.32**	0.2	**8.45e-1**
MRPL50	340.94	**0.04**	0.22	**9.93e-1**
MRPL51	520.24	**-0.18**	0.21	**9.74e-1**
MRPL52	137.69	**-0.04**	0.24	**9.93e-1**
MRPL53	94.95	**0.06**	0.24	**9.93e-1**
MRPL54	67.58	**-0.19**	0.25	**9.87e-1**
MRPL55	76.9	**-0.14**	0.25	**9.90e-1**
MRPL57	200.38	**-0.09**	0.23	**9.90e-1**
MRPL9	271.55	**0.19**	0.21	**9.74e-1**
MRPS10	480.23	**0.17**	0.21	**9.86e-1**
MRPS11	316.83	**-0.13**	0.21	**9.90e-1**
MRPS12	342.27	**-0.52**	0.25	**5.94e-1**
MRPS14	185.27	**0.09**	0.23	**9.90e-1**
MRPS15	830.99	**-0.12**	0.19	**9.90e-1**
MRPS16	708.64	**-0.09**	0.19	**9.90e-1**
MRPS17	117.72	**-0.06**	0.24	**9.93e-1**
MRPS18A	321.92	**-0.22**	0.22	**9.54e-1**
MRPS18B	701.49	**0.21**	0.19	**9.49e-1**
MRPS18C	164.85	**-0.1**	0.23	**9.90e-1**
MRPS2	1220.22	**-0.36**	0.21	**7.84e-1**
MRPS21	356.23	**-0.12**	0.21	**9.90e-1**
MRPS22	327.36	**0.07**	0.21	**9.90e-1**
MRPS23	312.53	**0.24**	0.21	**9.47e-1**

MRPS25	693.66	**-0.09**	0.19	**9.90e-1**
MRPS26	297.51	**0.44**	0.21	**6.34e-1**
MRPS27	1517.32	**0.06**	0.18	**9.91e-1**
MRPS28	139.11	**0.21**	0.23	**9.74e-1**
MRPS30	477.4	**0.11**	0.2	**9.90e-1**
MRPS31	300.98	**-0.27**	0.21	**9.25e-1**
MRPS31P5	44.73	**0.03**	0.25	**9.93e-1**
MRPS33	293.61	**0.23**	0.21	**9.49e-1**
MRPS34	718.38	**-0.27**	0.22	**9.25e-1**
MRPS35	578.31	**0.36**	0.2	**7.69e-1**
MRPS36	78.58	**0.1**	0.25	**9.90e-1**
MRPS5	757	**-0.27**	0.2	**9.06e-1**
MRPS6	293.61	**-0.02**	0.22	**9.94e-1**
MRPS7	520.58	**-0.11**	0.21	**9.90e-1**
MRPS9	400.84	**0.21**	0.21	**9.54e-1**
MRRF	354.14	**0.13**	0.21	**9.90e-1**
MRS2	378.65	**-0.13**	0.21	**9.90e-1**
MRTO4	847.05	**-0.32**	0.19	**8.21e-1**
MS4A1	5824.33	**0.5**	0.19	**3.44e-1**
MS4A7	24.01	**0.67**	0.24	**3.01e-1**
MSANTD2	62.65	**0.1**	0.25	**9.90e-1**
MSANTD3	71.92	**0.02**	0.25	**9.95e-1**
MSANTD4	229.93	**0.15**	0.23	**9.90e-1**
MSH2	1243.52	**0.12**	0.2	**9.90e-1**
MSH3	301.46	**0.12**	0.21	**9.90e-1**
MSH6	2192.13	**-0.02**	0.18	**9.93e-1**
MSI2	372.48	**-0.05**	0.21	**9.93e-1**
MSL1	585.06	**0.09**	0.2	**9.90e-1**
MSL2	370.5	**0.07**	0.21	**9.91e-1**
MSL3	192.02	**0.11**	0.22	**9.90e-1**
MSMO1	275.64	**-0.24**	0.22	**9.47e-1**
MSN	5819.95	**-0.12**	0.18	**9.90e-1**
MSRB1	197.1	**-0.16**	0.23	**9.87e-1**
MSRB2	10.71	**0.11**	0.21	**9.90e-1**
MST1P2	18.09	**-0.01**	0.24	**9.96e-1**
MSTO2P	54.58	**0.12**	0.25	**9.90e-1**
MT1X	44.92	**-0.01**	0.25	**9.96e-1**
MT2A	157	**-0.77**	0.23	**1.03e-1**

MTA1	1210.46	**-0.04**	0.2	**9.93e-1**
MTA2	1669.9	**-0.39**	0.19	**6.07e-1**
MTA3	609.74	**-0.1**	0.2	**9.90e-1**
MTAP	625.45	**-0.19**	0.19	**9.58e-1**
MTBP	104.65	**0.01**	0.24	**9.96e-1**
MTCH1	541.09	**-0.05**	0.22	**9.93e-1**
MTCH2	880.07	**0.16**	0.19	**9.80e-1**
MTCL1	156.52	**-0.47**	0.24	**6.69e-1**
MTCP1	16.58	**-0.05**	0.23	**9.93e-1**
MTDH	2502.73	**0.03**	0.19	**9.93e-1**
MTERF1	179.37	**0.05**	0.23	**9.93e-1**
MTERF3	148.34	**0.37**	0.24	**8.41e-1**
MTERF4	311.85	**-0.06**	0.21	**9.91e-1**
MTF1	413.79	**-0.14**	0.21	**9.90e-1**
MTF2	330.04	**0.12**	0.21	**9.90e-1**
MTFMT	159.04	**-0.1**	0.23	**9.90e-1**
MTFP1	306.75	**-0.02**	0.23	**9.93e-1**
MTFR1	267.4	**0.15**	0.23	**9.90e-1**
MTFR1L	96.1	**-0.02**	0.24	**9.95e-1**
MTFR2	177.42	**0.05**	0.24	**9.93e-1**
MTG1	291.13	**-0.24**	0.21	**9.49e-1**
MTG2	293.77	**-0.23**	0.23	**9.58e-1**
MTHFD1	1765.69	**-0.01**	0.18	**9.96e-1**
MTHFD1L	843.45	**0.38**	0.2	**6.87e-1**
MTHFD2	1595.59	**0.58**	0.19	**2.02e-1**
MTHFD2L	62.36	**-0.01**	0.25	**9.96e-1**
MTHFR	179.76	**-0.14**	0.24	**9.90e-1**
MTHFSD	91.4	**0.1**	0.25	**9.90e-1**
MTIF2	855.52	**0.08**	0.2	**9.90e-1**
MTIF3	80.04	**0.23**	0.25	**9.72e-1**
MTM1	64.16	**0.14**	0.25	**9.90e-1**
MTMR1	309.33	**0.27**	0.22	**9.39e-1**
MTMR10	222.89	**0.28**	0.22	**9.32e-1**
MTMR12	583.54	**-0.08**	0.2	**9.90e-1**
MTMR14	306.73	**0.17**	0.21	**9.81e-1**
MTMR2	394.23	**0.11**	0.22	**9.90e-1**
MTMR3	231.82	**0.03**	0.22	**9.93e-1**
MTMR4	974.71	**0.17**	0.19	**9.74e-1**
MTMR6	309.25	**0.19**	0.22	**9.80e-1**
MTMR9	320.66	**0.11**	0.21	**9.90e-1**
MTO1	2443.88	**0.08**	0.18	**9.90e-1**
MTOR	1260.48	**-0.23**	0.19	**9.42e-1**
MTPAP	279.7	**0.19**	0.23	**9.80e-1**
MTR	862.31	**-0.05**	0.19	**9.93e-1**
MTRF1	83.9	**0.06**	0.25	**9.93e-1**

MTRF1L	153.44	**0.24**	0.24	**9.55e-1**
MTRR	702.96	**-0.15**	0.2	**9.87e-1**
MTSS1	57.53	**0.01**	0.25	**9.96e-1**
MTURN	377.21	**-0.06**	0.21	**9.93e-1**
MTUS1	27.62	**-0.12**	0.25	**9.90e-1**
MTUS2	79.03	**-0.77**	0.25	**1.45e-1**
MTX1	198	**-0.32**	0.23	**8.95e-1**
MTX2	259.96	**0.2**	0.22	**9.72e-1**
MTX3	119.5	**0.07**	0.24	**9.93e-1**
MUL1	155.71	**-0.13**	0.23	**9.90e-1**
MUM1	363.74	**-0.15**	0.21	**9.87e-1**
MURC	41.16	**0.15**	0.25	**9.90e-1**
MUS81	265.5	**-0.15**	0.23	**9.90e-1**
MUT	178.86	**0.29**	0.23	**9.39e-1**
MUTYH	316.54	**0**	0.22	**9.98e-1**
MVB12A	107.79	**-0.1**	0.24	**9.90e-1**
MVD	316.37	**-0.51**	0.24	**6.01e-1**
MVK	124.29	**-0.14**	0.24	**9.90e-1**

MVP	81.6	**-0.01**	0.25	**9.96e-1**
MXD1	30.86	**-0.08**	0.25	**9.91e-1**
MXD3	29.07	**-0.14**	0.25	**9.90e-1**
MXD4	91.5	**0.28**	0.25	**9.47e-1**
MXI1	205.7	**0.11**	0.23	**9.90e-1**
MYADM	141.27	**-0.47**	0.24	**6.80e-1**
MYB	541.54	**-0.03**	0.21	**9.93e-1**
MYBBP1A	2392.6	**-0.5**	0.21	**5.13e-1**
MYBL1	943.42	**-0.18**	0.2	**9.66e-1**
MYBL2	5707.98	**-0.3**	0.2	**8.52e-1**
MYC	2729.72	**-0.59**	0.19	**1.42e-1**
MYCBP2	1886.54	**-0.14**	0.19	**9.87e-1**
MYCL	19.36	**-0.03**	0.24	**9.93e-1**
MYD88	692.22	**-0.49**	0.2	**4.53e-1**
MYDGF	161.74	**0.35**	0.23	**8.53e-1**
MYEOV	70.09	**0.89**	0.25	**6.46e-2**
MYEOV2	40.87	**0**	0.25	**9.98e-1**
MYH10	488.92	**-0.18**	0.2	**9.73e-1**
MYH3	32.4	**0.1**	0.25	**9.90e-1**
MYH9	7113.63	**-0.3**	0.19	**8.30e-1**
MYL12A	336.06	**0.15**	0.21	**9.87e-1**
MYL12B	325.47	**0.31**	0.21	**8.64e-1**
MYL5	32.82	**0.02**	0.25	**9.95e-1**
MYL6	372.96	**0.04**	0.22	**9.93e-1**
MYL6B	166.81	**0.15**	0.24	**9.90e-1**
MYLIP	138.08	**0.18**	0.23	**9.86e-1**
MYLK4	16.18	**0.29**	0.23	**9.25e-1**
MYNN	209.34	**0.18**	0.23	**9.86e-1**
MYO18A	491.83	**-0.22**	0.21	**9.49e-1**
MYO19	443.13	**-0.09**	0.21	**9.90e-1**
MYO1C	603.73	**-0.05**	0.2	**9.93e-1**
MYO1D	294.47	**-0.02**	0.21	**9.93e-1**
MYO1E	241.17	**0.23**	0.22	**9.49e-1**
MYO1G	201.05	**0.35**	0.23	**8.53e-1**
MYO5A	382.43	**-0.05**	0.21	**9.93e-1**
MYO9A	344.42	**-0.27**	0.21	**9.23e-1**
MYO9B	1038.61	**-0.14**	0.2	**9.87e-1**
MYOM2	13.87	**-0.06**	0.22	**9.93e-1**
MYPOP	53.15	**-0.24**	0.25	**9.66e-1**
MYSM1	719.46	**-0.03**	0.2	**9.93e-1**
MZB1	945.79	**-0.48**	0.21	**5.22e-1**
MZF1	54.08	**-0.08**	0.25	**9.91e-1**
MZF1-AS1	58.67	**-0.03**	0.25	**9.93e-1**
MZT1	205.18	**0.25**	0.23	**9.49e-1**
MZT2A	45.42	**-0.03**	0.25	**9.93e-1**
MZT2B	79.26	**0.04**	0.25	**9.93e-1**
N4BP1	364.03	**-0.19**	0.21	**9.66e-1**
N4BP2	529.02	**-0.12**	0.22	**9.90e-1**
N4BP2L1	24.67	**-0.1**	0.25	**9.90e-1**
N4BP2L2	265.5	**0.06**	0.22	**9.93e-1**
N6AMT1	11.31	**-0.02**	0.22	**9.93e-1**
NAA10	463.34	**0**	0.2	**9.98e-1**
NAA15	1767.61	**-0.15**	0.2	**9.87e-1**
NAA16	261.84	**-0.24**	0.22	**9.49e-1**
NAA20	434.64	**0.14**	0.2	**9.87e-1**
NAA25	701.93	**0.03**	0.2	**9.93e-1**
NAA30	182.12	**0.14**	0.23	**9.90e-1**
NAA35	192.21	**0.13**	0.23	**9.90e-1**
NAA38	158.95	**-0.24**	0.23	**9.54e-1**
NAA40	327.29	**-0.13**	0.21	**9.90e-1**
NAA50	2503.13	**-0.25**	0.18	**8.95e-1**
NAA60	449.94	**-0.36**	0.22	**8.30e-1**
NAAA	129.22	**0.16**	0.24	**9.90e-1**
NAALADL2-AS2	128.85	**-0.17**	0.23	**9.87e-1**
NAB1	236.35	**0.1**	0.23	**9.90e-1**

NAB2	60.96	**-0.02**	0.25	**9.94e-1**
NABP1	117.21	**-0.27**	0.24	**9.47e-1**
NABP2	244.99	**-0.06**	0.22	**9.93e-1**
NACA	2066.23	**0.27**	0.18	**8.66e-1**
NACC1	1202.07	**-0.65**	0.24	**3.14e-1**
NADK	555.66	**-0.06**	0.21	**9.92e-1**
NADK2	209.65	**0.18**	0.22	**9.81e-1**
NADSYN1	242.67	**-0.17**	0.22	**9.87e-1**
NAE1	845.5	**0.21**	0.21	**9.54e-1**
NAF1	234.83	**0.08**	0.23	**9.90e-1**
NAGA	128.81	**-0.03**	0.23	**9.93e-1**
NAGK	129.66	**-0.03**	0.24	**9.93e-1**
NAGLU	148.77	**-0.04**	0.25	**9.93e-1**
NAGPA	65.42	**0.02**	0.25	**9.94e-1**
NAIF1	63.36	**-0.1**	0.25	**9.90e-1**
NAMPT	1857.16	**-0.3**	0.19	**8.49e-1**
NANP	122.53	**-0.01**	0.24	**9.97e-1**
NANS	459.88	**0.21**	0.2	**9.52e-1**
NAP1L1	7882.31	**0.4**	0.19	**6.01e-1**
NAP1L4	1442.73	**-0.06**	0.19	**9.90e-1**
NAPA	436.85	**-0.26**	0.21	**9.42e-1**
NAPA-AS1	10.04	**-0.11**	0.2	**9.90e-1**
NAPB	186.01	**0.09**	0.23	**9.90e-1**
NAPG	272.01	**-0.05**	0.22	**9.93e-1**
NAPRT	53.19	**-0.18**	0.25	**9.87e-1**
NAPSB	1159.29	**0.14**	0.21	**9.89e-1**
NARF	128.76	**0.34**	0.24	**8.68e-1**
NARFL	140.83	**-0.15**	0.24	**9.90e-1**
NARS	2005.43	**0.16**	0.18	**9.74e-1**
NARS2	249.18	**-0.03**	0.22	**9.93e-1**
NASP	4307.26	**0.03**	0.18	**9.93e-1**
NAT1	63.82	**-0.08**	0.25	**9.91e-1**
NAT10	1948.3	**-0.22**	0.18	**9.39e-1**
NAT14	49.19	**-0.1**	0.25	**9.90e-1**
NAT6	95.83	**-0.22**	0.25	**9.80e-1**
NAT9	183.19	**-0.23**	0.24	**9.60e-1**
NATD1	63.28	**-0.16**	0.25	**9.90e-1**
NAV1	18.39	**0.17**	0.24	**9.87e-1**
NAV2	14.3	**-0.57**	0.23	**4.11e-1**
NBAS	239.95	**0.09**	0.22	**9.90e-1**
NBEA	61.32	**0.08**	0.25	**9.91e-1**
NBEAL1	49.12	**0.04**	0.25	**9.93e-1**
NBEAL2	2052.53	**-0.41**	0.21	**6.87e-1**
NBN	961.7	**0.29**	0.2	**8.73e-1**
NBPF1	200.07	**0.1**	0.22	**9.90e-1**
NBPF10	20.02	**0.03**	0.24	**9.93e-1**
NBPF11	17.66	**-0.15**	0.24	**9.90e-1**
NBPF12	26.37	**-0.06**	0.25	**9.93e-1**
NBPF15	163.08	**0.08**	0.23	**9.90e-1**
NBPF3	66.57	**-0.02**	0.25	**9.94e-1**
NBPF8	53.27	**-0.06**	0.25	**9.93e-1**
NBR1	370.39	**0.56**	0.21	**3.41e-1**
NBR2	40.83	**0.18**	0.25	**9.87e-1**
NCALD	17.69	**-0.34**	0.24	**8.68e-1**
NCAPD2	2331.19	**0**	0.18	**9.98e-1**
NCAPD3	1078.55	**-0.12**	0.19	**9.90e-1**
NCAPG	906.03	**-0.02**	0.2	**9.93e-1**
NCAPG2	887.29	**0.07**	0.19	**9.90e-1**
NCAPH	376.94	**-0.16**	0.21	**9.87e-1**
NCAPH2	461.3	**-0.19**	0.23	**9.80e-1**
NCBP1	1035.93	**0.06**	0.2	**9.91e-1**
NCBP2	556.94	**0.11**	0.2	**9.90e-1**
NCBP2-AS2	106.66	**0.2**	0.24	**9.81e-1**

NCDN	511.48	**-0.38**	0.23	**8.27e-1**
NCEH1	79.16	**-0.15**	0.25	**9.90e-1**
NCF1	2825	**0.24**	0.19	**9.23e-1**
NCF1B	494.76	**0.33**	0.21	**8.30e-1**
NCF1C	621.98	**0.88**	0.2	**4.63e-3**
NCF2	12.76	**0.19**	0.22	**9.80e-1**
NCF4	46.82	**-0.2**	0.25	**9.87e-1**
NCK1	297.71	**0.26**	0.22	**9.42e-1**
NCK1-AS1	33.34	**-0.12**	0.25	**9.90e-1**
NCK2	133.61	**-0.09**	0.23	**9.90e-1**
NCKAP1L	863.4	**0.24**	0.19	**9.31e-1**
NCKIPSD	235.21	**-0.14**	0.23	**9.90e-1**
NCL	20600.98	**-0.4**	0.18	**5.62e-1**
NCLN	969.81	**-0.43**	0.23	**7.13e-1**
NCOA1	330.62	**0.11**	0.21	**9.90e-1**
NCOA2	355.17	**-0.21**	0.21	**9.58e-1**
NCOA3	3912.61	**0.19**	0.19	**9.56e-1**
NCOA4	1098.38	**0.11**	0.19	**9.90e-1**
NCOA5	897.26	**-0.15**	0.19	**9.81e-1**
NCOA6	1133.47	**-0.37**	0.19	**6.79e-1**
NCOA7	282.63	**0.08**	0.22	**9.90e-1**
NCOR1	1336.83	**-0.16**	0.19	**9.80e-1**
NCOR2	2408.67	**-0.33**	0.22	**8.64e-1**
NCR3LG1	689.08	**-0.22**	0.19	**9.47e-1**
NCSTN	543.8	**0.2**	0.2	**9.58e-1**
NDC1	2046.79	**-0.08**	0.2	**9.90e-1**
NDC80	420.02	**0.13**	0.22	**9.90e-1**
NDE1	361.99	**-0.23**	0.21	**9.49e-1**
NDEL1	191.63	**0.18**	0.22	**9.86e-1**
NDFIP1	174.31	**0.33**	0.23	**8.73e-1**
NDFIP2	82.36	**0.49**	0.25	**6.69e-1**
NDNL2	131.98	**0.28**	0.24	**9.45e-1**
NDOR1	713.18	**-0.66**	0.24	**3.07e-1**
NDRG3	562.98	**-0.08**	0.2	**9.90e-1**
NDST1	1115.09	**0.08**	0.2	**9.90e-1**
NDST2	208.98	**0.05**	0.23	**9.93e-1**
NDUFA1	170.88	**0**	0.24	**9.98e-1**
NDUFA10	962.67	**-0.08**	0.19	**9.90e-1**
NDUFA11	560.53	**-0.15**	0.21	**9.87e-1**
NDUFA12	254.3	**0.34**	0.22	**8.45e-1**
NDUFA13	341.19	**0.14**	0.21	**9.88e-1**
NDUFA2	110.79	**0.15**	0.24	**9.90e-1**
NDUFA3	177.98	**-0.34**	0.25	**9.06e-1**
NDUFA4	455.97	**0.14**	0.2	**9.87e-1**
NDUFA4L2	22.16	**0.05**	0.24	**9.93e-1**
NDUFA5	856.47	**0.16**	0.2	**9.81e-1**
NDUFA6	310.67	**-0.01**	0.21	**9.96e-1**
NDUFA7	280.08	**-0.24**	0.23	**9.49e-1**
NDUFA8	194.25	**-0.13**	0.23	**9.90e-1**
NDUFA9	468.15	**0.03**	0.2	**9.93e-1**
NDUFAB1	277.96	**0.18**	0.21	**9.80e-1**
NDUFAF1	125.4	**-0.04**	0.24	**9.93e-1**
NDUFAF2	255.18	**-0.24**	0.21	**9.47e-1**
NDUFAF3	128.46	**0.04**	0.24	**9.93e-1**
NDUFAF4	267.32	**0.5**	0.22	**5.45e-1**
NDUFAF5	115.21	**0.16**	0.24	**9.90e-1**
NDUFAF6	155.52	**0.31**	0.23	**9.06e-1**
NDUFAF7	191.51	**-0.09**	0.23	**9.90e-1**
NDUFB1	59.76	**0.35**	0.25	**8.87e-1**
NDUFB10	422	**-0.09**	0.21	**9.90e-1**
NDUFB11	214.44	**0.03**	0.22	**9.93e-1**
NDUFB2	163.61	**0.02**	0.23	**9.93e-1**
NDUFB2-AS1	26.53	**-0.17**	0.24	**9.88e-1**

NDUFB3	188.98	**0.05**	0.22	**9.93e-1**
NDUFB4	174.65	**-0.11**	0.23	**9.90e-1**
NDUFB5	345.91	**0.41**	0.21	**6.87e-1**
NDUFB6	75.2	**0.4**	0.25	**8.35e-1**
NDUFB7	211.22	**-0.22**	0.23	**9.64e-1**
NDUFB8	394.6	**-0.28**	0.22	**9.25e-1**
NDUFB9	489.7	**0.08**	0.2	**9.90e-1**
NDUFC1	106.97	**-0.21**	0.24	**9.80e-1**
NDUFC2	52.98	**0.14**	0.25	**9.90e-1**
NDUFS1	1090.8	**0.02**	0.19	**9.93e-1**
NDUFS2	655.31	**0.27**	0.19	**8.95e-1**
NDUFS3	276.65	**0.1**	0.22	**9.90e-1**
NDUFS4	79.68	**0.02**	0.25	**9.93e-1**
NDUFS5	811.56	**0.18**	0.19	**9.64e-1**
NDUFS6	447.51	**-0.04**	0.21	**9.93e-1**
NDUFS7	222.18	**-0.12**	0.25	**9.90e-1**
NDUFS8	291.93	**-0.12**	0.23	**9.90e-1**
NDUFV1	1761.34	**0.06**	0.2	**9.92e-1**
NDUFV2	567.71	**-0.02**	0.2	**9.93e-1**
NDUFV3	194.37	**-0.03**	0.22	**9.93e-1**
NEAT1	3492.37	**-0.36**	0.18	**6.87e-1**
NECAB3	104.2	**-0.08**	0.25	**9.91e-1**
NECAP1	209.16	**-0.08**	0.22	**9.90e-1**
NECAP2	531.02	**-0.17**	0.22	**9.86e-1**
NEDD1	426.33	**0.14**	0.21	**9.90e-1**
NEDD4	114.91	**0.04**	0.24	**9.93e-1**
NEDD4L	315.82	**-0.39**	0.21	**7.05e-1**
NEDD8	90.3	**0.21**	0.25	**9.77e-1**
NEDD9	228.11	**0.35**	0.22	**8.40e-1**
NEIL1	102.5	**0.26**	0.25	**9.50e-1**
NEIL2	29.65	**0.26**	0.25	**9.54e-1**
NEIL3	99.96	**-0.02**	0.24	**9.96e-1**
NEK1	139.42	**-0.01**	0.23	**9.98e-1**
NEK2	259.4	**0.1**	0.23	**9.90e-1**
NEK4	307.63	**-0.05**	0.21	**9.93e-1**
NEK6	605.45	**0.23**	0.2	**9.47e-1**
NEK7	142.96	**0.5**	0.24	**6.07e-1**
NEK8	131.44	**-0.18**	0.24	**9.87e-1**
NEK9	815.14	**0.1**	0.19	**9.90e-1**
NELFA	423.93	**-0.12**	0.23	**9.90e-1**

NELFB	419.03	**0.03**	0.22	**9.93e-1**
NELFCD	1030.33	**0.05**	0.19	**9.93e-1**
NELFE	441.85	**0.01**	0.2	**9.97e-1**
NEMF	698.01	**-0.33**	0.2	**8.08e-1**
NEMP1	695.15	**0.24**	0.2	**9.43e-1**
NEMP2	60.24	**0.24**	0.25	**9.66e-1**
NENF	55.48	**0.5**	0.25	**6.79e-1**
NEO1	335.7	**0.09**	0.21	**9.90e-1**
NET1	466.64	**0.1**	0.21	**9.90e-1**
NETO2	292.79	**0.04**	0.22	**9.93e-1**
NEU1	105.37	**0.46**	0.24	**7.04e-1**
NEU3	238.03	**-0.5**	0.22	**5.37e-1**
NEURL4	767.46	**-0.26**	0.21	**9.39e-1**
NF1	478.16	**-0.05**	0.21	**9.93e-1**
NF2	387.17	**0.02**	0.21	**9.94e-1**
NFAM1	41.56	**0.55**	0.25	**5.91e-1**
NFAT5	461.9	**-0.14**	0.21	**9.89e-1**
NFATC1	560.22	**0.04**	0.21	**9.93e-1**
NFATC2	679.09	**0**	0.19	**9.98e-1**
NFATC2IP	502.55	**0.02**	0.2	**9.93e-1**
NFATC3	784.29	**-0.1**	0.19	**9.90e-1**
NFATC4	181.68	**0.17**	0.24	**9.88e-1**
NFE2L1	2243.64	**0.31**	0.2	**8.49e-1**

NFE2L2	696.33	**0.45**	0.21	**5.91e-1**
NFE2L3	427.42	**0.1**	0.21	**9.90e-1**
NFIA	187.33	**-0.22**	0.22	**9.59e-1**
NFIB	22.59	**-0.11**	0.25	**9.90e-1**
NFIC	44.16	**-0.29**	0.25	**9.47e-1**
NFIL3	65.35	**0.45**	0.25	**7.49e-1**
NFKB1	742.9	**0.27**	0.19	**8.91e-1**
NFKB2	928.06	**0.34**	0.21	**8.34e-1**
NFKBIA	480.58	**0.3**	0.2	**8.68e-1**
NFKBIB	269.22	**-0.24**	0.24	**9.57e-1**
NFKBID	73.16	**0**	0.25	**9.98e-1**
NFKBIE	260.09	**0.16**	0.24	**9.90e-1**
NFKBIL1	53.23	**-0.38**	0.25	**8.62e-1**
NFKBIZ	236.29	**0.11**	0.22	**9.90e-1**
NFRKB	737.01	**-0.37**	0.2	**7.04e-1**
NFS1	455.74	**-0.18**	0.2	**9.73e-1**
NFU1	35.85	**0.01**	0.25	**9.96e-1**
NFX1	880.88	**0.15**	0.2	**9.87e-1**
NFXL1	209.4	**0.3**	0.23	**9.06e-1**
NFYA	496.53	**0.19**	0.2	**9.66e-1**
NFYB	219.78	**0.02**	0.22	**9.93e-1**
NFYC	875.99	**0.04**	0.19	**9.93e-1**
NFYC-AS1	36.13	**0.16**	0.25	**9.90e-1**
NGDN	284.92	**0.08**	0.21	**9.90e-1**
NGLY1	422.16	**0.25**	0.21	**9.43e-1**
NGRN	313.03	**-0.03**	0.21	**9.93e-1**
NHEJ1	165.19	**0.32**	0.23	**8.95e-1**
NHLRC2	151.59	**-0.13**	0.23	**9.90e-1**
NHLRC3	131.7	**0.34**	0.24	**8.69e-1**
NHP2	744.01	**-0.23**	0.22	**9.52e-1**
NHP2L1	947.61	**0.12**	0.19	**9.90e-1**
NICN1	96.53	**-0.01**	0.24	**9.97e-1**
NIF3L1	287.63	**-0.04**	0.21	**9.93e-1**
NIFK	362.46	**0.15**	0.22	**9.87e-1**
NIFK-AS1	14.35	**0.05**	0.22	**9.93e-1**
NIN	1874.9	**0.25**	0.19	**9.10e-1**
NINJ1	67.46	**-0.13**	0.25	**9.90e-1**
NINJ2	15.88	**0.14**	0.23	**9.90e-1**
NIP7	473.31	**-0.19**	0.2	**9.65e-1**
NIPA1	218.4	**0.05**	0.22	**9.93e-1**
NIPA2	836.57	**0.3**	0.2	**8.64e-1**
NIPAL2	55.36	**0.24**	0.25	**9.66e-1**
NIPAL3	55.37	**0.21**	0.25	**9.81e-1**
NIPBL	951.24	**-0.03**	0.2	**9.93e-1**
NIPBL-AS1	157.81	**0.29**	0.23	**9.25e-1**
NIPSNAP1	491.83	**-0.07**	0.21	**9.90e-1**
NIPSNAP3A	118.99	**-0.07**	0.24	**9.92e-1**
NIPSNAP3B	16.49	**-0.17**	0.23	**9.87e-1**
NISCH	488.8	**-0.13**	0.21	**9.90e-1**
NIT1	87.19	**-0.08**	0.25	**9.90e-1**
NIT2	196.84	**0.22**	0.22	**9.61e-1**
NKAP	56.58	**-0.19**	0.25	**9.87e-1**
NKIRAS1	56.49	**-0.07**	0.25	**9.93e-1**
NKIRAS2	322.59	**-0.4**	0.23	**7.57e-1**
NKRF	289.62	**0.17**	0.22	**9.86e-1**
NKTR	1034.79	**-0.2**	0.19	**9.54e-1**
NLE1	348.24	**-0.21**	0.23	**9.66e-1**
NLGN2	74.13	**-0.1**	0.25	**9.90e-1**
NLK	208.83	**0.02**	0.23	**9.93e-1**
NLN	1229.3	**-0.23**	0.19	**9.47e-1**

NLRC3	190.69	**-0.29**	0.22	**9.19e-1**
NLRC5	383.5	**-0.21**	0.23	**9.66e-1**
NLRP1	45.24	**-0.18**	0.25	**9.87e-1**

NLRP11	609.19	**0.66**	0.2	**1.12e-1**
NLRP4	502.19	**1.1**	0.2	**7.00e-5**
NLRP7	62.55	**0.13**	0.25	**9.90e-1**
NLRX1	119.76	**-0.02**	0.25	**9.96e-1**
NMD3	497.53	**0.31**	0.21	**8.64e-1**
NME1	265.34	**-0.03**	0.22	**9.93e-1**
NME4	433.84	**-0.36**	0.22	**8.31e-1**
NME6	150.05	**-0.22**	0.23	**9.66e-1**
NME7	53.05	**0.11**	0.25	**9.90e-1**
NMNAT1	89.95	**0.13**	0.24	**9.90e-1**
NMNAT3	69.49	**0.11**	0.25	**9.90e-1**
NMRAL1	337.74	**-0.24**	0.23	**9.49e-1**
NMT1	1305.06	**-0.15**	0.19	**9.86e-1**
NMT2	74.23	**0.01**	0.25	**9.96e-1**
NMU	46	**0.05**	0.25	**9.93e-1**
NNT	233.54	**0.23**	0.23	**9.54e-1**
NNT-AS1	94.67	**-0.21**	0.24	**9.80e-1**
NOA1	418.51	**0.22**	0.2	**9.49e-1**
NOB1	737.75	**0.04**	0.2	**9.93e-1**
NOC2L	2041.66	**-0.45**	0.21	**5.99e-1**
NOC3L	612.3	**0.15**	0.21	**9.87e-1**
NOC4L	442.32	**-0.32**	0.22	**8.75e-1**
NOCT	211.95	**0.09**	0.22	**9.90e-1**
NOD1	43.15	**-0.04**	0.25	**9.93e-1**
NOL10	535.42	**0.1**	0.21	**9.90e-1**
NOL11	1123.29	**0.04**	0.2	**9.93e-1**
NOL12	224.57	**-0.2**	0.23	**9.80e-1**
NOL3	19.71	**0.12**	0.23	**9.90e-1**
NOL6	1330.37	**-0.52**	0.22	**4.86e-1**
NOL7	457.9	**0.26**	0.2	**9.23e-1**
NOL8	869.62	**0.07**	0.2	**9.90e-1**
NOL9	441.06	**-0.02**	0.2	**9.95e-1**
NOLC1	4902.07	**-0.19**	0.18	**9.49e-1**
NOM1	844.98	**-0.11**	0.19	**9.90e-1**
NOMO1	665.71	**-0.27**	0.19	**8.90e-1**
NOMO2	351.69	**-0.24**	0.21	**9.47e-1**
NOMO3	20.85	**-0.04**	0.24	**9.93e-1**
NONO	4083	**-0.01**	0.18	**9.96e-1**
NOP10	350.71	**-0.5**	0.22	**5.37e-1**
NOP14	1415.05	**0.09**	0.18	**9.90e-1**
NOP14-AS1	30.28	**-0.08**	0.25	**9.92e-1**
NOP16	610.89	**-0.14**	0.2	**9.88e-1**
NOP2	1473.27	**-0.3**	0.19	**8.30e-1**
NOP56	2506.94	**-0.11**	0.18	**9.90e-1**
NOP58	1369.3	**-0.19**	0.19	**9.56e-1**
NOP9	997.97	**-0.4**	0.2	**6.59e-1**
NOS3	22.59	**-0.07**	0.24	**9.93e-1**
NOSIP	203.43	**-0.27**	0.24	**9.47e-1**
NOTCH1	394.35	**-0.33**	0.22	**8.64e-1**
NOTCH2	654.43	**-0.14**	0.19	**9.87e-1**
NOTCH2NL	49.94	**-0.04**	0.25	**9.93e-1**
NPAS1	29.82	**0.1**	0.25	**9.90e-1**
NPAT	358.35	**0.22**	0.21	**9.49e-1**
NPC1	173.09	**0.11**	0.23	**9.90e-1**
NPC2	112.64	**0.47**	0.24	**6.84e-1**
NPEPPS	1131.47	**0.12**	0.19	**9.90e-1**
NPHP4	151.32	**-0.08**	0.23	**9.90e-1**
NPIPA1	59.41	**-0.12**	0.25	**9.90e-1**
NPIPB11	50.52	**-0.3**	0.25	**9.45e-1**
NPIPB15	14.84	**-0.03**	0.23	**9.93e-1**
NPIPB3	95.96	**-0.23**	0.25	**9.66e-1**
NPIPB4	70.59	**-0.17**	0.25	**9.90e-1**
NPIPB5	193.05	**-0.57**	0.24	**5.09e-1**
NPL	46.18	**0.07**	0.25	**9.93e-1**
NPLOC4	782.28	**-0.16**	0.19	**9.81e-1**

NPM1	9958.44	**0.31**	0.19	**8.27e-1**
NPM3	560.04	**-0.07**	0.2	**9.91e-1**
NPR2	40.91	**0.04**	0.25	**9.93e-1**
NPRL2	153.7	**0.08**	0.23	**9.91e-1**
NPRL3	390.29	**-0.27**	0.22	**9.31e-1**
NPTN	317.46	**0.19**	0.21	**9.73e-1**
NPTN-IT1	16.96	**0.2**	0.23	**9.80e-1**
NQO1	157.79	**-0.28**	0.23	**9.42e-1**
NQO2	180.02	**0.24**	0.22	**9.49e-1**
NR1D1	199.6	**-0.38**	0.23	**8.07e-1**
NR1D2	279.32	**0.25**	0.23	**9.49e-1**
NR1H2	161.67	**-0.11**	0.25	**9.90e-1**
NR1H3	26.66	**0**	0.25	**9.99e-1**
NR2C1	204.71	**-0.01**	0.22	**9.96e-1**
NR2C2	268.46	**0.18**	0.22	**9.82e-1**

NR2C2AP	78.96	**-0.1**	0.25	**9.90e-1**
NR2F6	144.17	**-0.07**	0.25	**9.92e-1**
NR3C1	387.43	**0.08**	0.21	**9.90e-1**
NR3C2	15.11	**0.07**	0.23	**9.91e-1**
NR4A3	10.65	**0.11**	0.21	**9.90e-1**
NR6A1	243.41	**-0.34**	0.22	**8.48e-1**
NRADDP	22.87	**0.06**	0.24	**9.93e-1**
NRARP	17.99	**-0.07**	0.23	**9.91e-1**
NRAS	1086.97	**-0.05**	0.2	**9.93e-1**
NRAV	70.3	**-0.1**	0.25	**9.90e-1**
NRBF2	184.22	**-0.04**	0.22	**9.93e-1**
NRBP1	298.02	**-0.08**	0.21	**9.90e-1**
NRD1	1927.01	**0**	0.19	**9.98e-1**
NRDE2	120.39	**0.03**	0.24	**9.93e-1**
NREP	217.48	**-0.88**	0.22	**1.60e-2**
NRF1	191.12	**-0.38**	0.22	**8.08e-1**
NRG4	19.07	**-0.19**	0.24	**9.86e-1**
NRGN	16.47	**-0.19**	0.23	**9.86e-1**
NRM	188.29	**-0.24**	0.23	**9.53e-1**
NRROS	155.19	**-0.15**	0.24	**9.90e-1**
NRSN2-AS1	34.99	**-0.17**	0.25	**9.90e-1**
NSA2	1351.61	**-0.06**	0.19	**9.92e-1**
NSD1	1134.67	**0.03**	0.19	**9.93e-1**
NSDHL	209.86	**-0.41**	0.23	**7.56e-1**
NSF	520.46	**0.1**	0.21	**9.90e-1**
NSFL1C	800.9	**-0.28**	0.2	**8.91e-1**
NSG1	43.79	**1.41**	0.25	**3.80e-5**
NSL1	240.27	**-0.02**	0.23	**9.96e-1**
NSMAF	697.33	**0.05**	0.2	**9.93e-1**
NSMCE1	216.91	**0.26**	0.22	**9.47e-1**
NSMCE2	62.71	**0.12**	0.25	**9.90e-1**
NSMCE4A	370.47	**0.35**	0.21	**8.33e-1**
NSMF	928.73	**-0.27**	0.2	**9.11e-1**
NSRP1	460.2	**-0.79**	0.21	**3.07e-2**
NSUN2	1473.42	**0.12**	0.19	**9.90e-1**
NSUN3	61.06	**0**	0.25	**9.98e-1**
NSUN4	262.81	**0.2**	0.22	**9.72e-1**
NSUN5	398.93	**-0.09**	0.22	**9.90e-1**
NSUN5P1	226.87	**-0.09**	0.22	**9.90e-1**
NSUN5P2	188.06	**0.04**	0.24	**9.93e-1**
NSUN6	145.58	**0.11**	0.23	**9.90e-1**
NT5C	90.1	**0**	0.25	**9.98e-1**
NT5C2	695.5	**-0.17**	0.2	**9.81e-1**
NT5C3A	335.87	**0.2**	0.22	**9.72e-1**
NT5C3B	124.32	**0.15**	0.24	**9.90e-1**
NT5DC1	190.45	**0.32**	0.22	**8.76e-1**
NT5DC2	1083.78	**-0.24**	0.2	**9.42e-1**
NT5DC3	147.55	**0.06**	0.23	**9.93e-1**

NT5M	61.73	**-0.26**	0.25	**9.55e-1**
NTAN1	88.42	**0.29**	0.25	**9.47e-1**
NTHL1	168.55	**-0.2**	0.24	**9.80e-1**
NTMT1	173.98	**0**	0.23	**9.99e-1**
NTPCR	72.62	**0.04**	0.25	**9.93e-1**
NUAK2	94.05	**-0.01**	0.25	**9.96e-1**
NUB1	985.38	**-0.11**	0.19	**9.90e-1**
NUBP1	246.36	**0.21**	0.22	**9.58e-1**
NUBP2	251.61	**-0.19**	0.25	**9.87e-1**
NUBPL	83.76	**-0.16**	0.25	**9.90e-1**
NUCB1	391.87	**0.09**	0.22	**9.90e-1**
NUCB2	430.37	**0.21**	0.21	**9.53e-1**
NUCKS1	4284.92	**-0.15**	0.18	**9.81e-1**
NUDC	1801.82	**-0.37**	0.2	**7.04e-1**
NUDCD1	377.2	**0.03**	0.21	**9.93e-1**
NUDCD2	211.92	**-0.06**	0.22	**9.92e-1**
NUDCD3	607.77	**0.03**	0.2	**9.93e-1**
NUDT1	73.04	**-0.15**	0.25	**9.90e-1**
NUDT14	28.01	**0.13**	0.25	**9.90e-1**
NUDT15	316.22	**0.33**	0.21	**8.44e-1**
NUDT16	29.44	**-0.08**	0.25	**9.91e-1**
NUDT16L1	62.93	**-0.03**	0.25	**9.93e-1**
NUDT17	20.84	**-0.05**	0.23	**9.93e-1**
NUDT18	25.45	**-0.13**	0.25	**9.90e-1**
NUDT19	101.28	**0.08**	0.24	**9.90e-1**
NUDT2	35.89	**0.02**	0.25	**9.96e-1**
NUDT21	2286.99	**-0.1**	0.19	**9.90e-1**
NUDT22	134.39	**-0.22**	0.25	**9.74e-1**
NUDT3	21.78	**0.04**	0.23	**9.93e-1**
NUDT5	409.64	**-0.13**	0.21	**9.90e-1**
NUDT6	24.62	**0.22**	0.25	**9.73e-1**
NUDT7	12.92	**0.08**	0.22	**9.90e-1**
NUDT8	66.09	**0.33**	0.25	**9.12e-1**
NUDT9	155.25	**0.04**	0.23	**9.93e-1**
NUF2	326.3	**0.26**	0.21	**9.33e-1**

NUFIP1	326.24	**-0.24**	0.21	**9.47e-1**
NUFIP2	1507.27	**-0.24**	0.19	**9.25e-1**
NUGGC	474.26	**-0.17**	0.2	**9.80e-1**
NUMA1	1745.74	**-0.36**	0.2	**7.41e-1**
NUMB	415.3	**-0.24**	0.2	**9.47e-1**
NUMBL	189.87	**-0.64**	0.25	**3.52e-1**
NUP107	855.1	**0.21**	0.21	**9.57e-1**
NUP133	734.27	**0.04**	0.19	**9.93e-1**
NUP153	3022.98	**0.01**	0.19	**9.98e-1**
NUP155	809.08	**-0.11**	0.2	**9.90e-1**
NUP160	801.52	**0.11**	0.19	**9.90e-1**
NUP188	2000.72	**-0.19**	0.18	**9.49e-1**
NUP205	2004.41	**0.08**	0.19	**9.90e-1**
NUP210	4595.61	**-0.29**	0.21	**8.78e-1**
NUP214	1623.08	**-0.49**	0.19	**3.41e-1**
NUP35	227.59	**-0.14**	0.22	**9.90e-1**
NUP37	258.82	**0.18**	0.22	**9.80e-1**
NUP43	485.63	**0.04**	0.2	**9.93e-1**
NUP50	1542.08	**0.06**	0.19	**9.91e-1**
NUP50-AS1	22.31	**0.08**	0.24	**9.90e-1**
NUP54	353.47	**0.06**	0.21	**9.93e-1**
NUP62	1972.66	**-0.47**	0.21	**5.68e-1**
NUP62CL	41.55	**0.06**	0.25	**9.93e-1**
NUP85	464.52	**0.09**	0.2	**9.90e-1**
NUP88	752.43	**0.02**	0.19	**9.94e-1**
NUP93	971.06	**0.16**	0.19	**9.80e-1**
NUP98	2184.92	**-0.22**	0.19	**9.47e-1**
NUPL1	1233.54	**-0.04**	0.19	**9.93e-1**

NUPL2	275.7	**0.11**	0.22	**9.90e-1**
NUS1	1395.32	**0.18**	0.2	**9.73e-1**
NUSAP1	1249.51	**0.08**	0.19	**9.90e-1**
NUTF2	917.91	**-0.08**	0.19	**9.90e-1**
NUTM2A-AS1	112.46	**-0.04**	0.24	**9.93e-1**
NUTM2B-AS1	124.79	**-0.06**	0.24	**9.93e-1**
NUTM2D	13.46	**-0.08**	0.22	**9.90e-1**
NVL	340.67	**-0.06**	0.21	**9.93e-1**
NXF1	861.75	**-0.28**	0.19	**8.66e-1**
NXPE3	187.15	**0**	0.23	**9.98e-1**
NXPH4	119.87	**-0.27**	0.25	**9.49e-1**
NXT1	166.51	**0.04**	0.23	**9.93e-1**
NXT2	184.57	**0.14**	0.23	**9.90e-1**
OARD1	177.25	**0.26**	0.23	**9.47e-1**
OAS1	45.69	**-0.38**	0.25	**8.61e-1**
OAS2	268.54	**-0.2**	0.21	**9.66e-1**
OAT	653.42	**0.06**	0.2	**9.92e-1**
OAZ1	1557.91	**-0.14**	0.2	**9.87e-1**
OAZ2	198.13	**-0.13**	0.23	**9.90e-1**
OBFC1	96.94	**0.29**	0.24	**9.43e-1**
OBSCN	158.19	**-0.28**	0.24	**9.47e-1**
OCEL1	74.95	**-0.37**	0.25	**8.64e-1**
OCIAD1	392.2	**0.32**	0.21	**8.41e-1**
OCIAD2	50.23	**0.04**	0.25	**9.93e-1**
ODC1	4228.32	**0.22**	0.19	**9.43e-1**
ODF2	1278.65	**-0.14**	0.19	**9.87e-1**
ODF2L	78.27	**-0.02**	0.25	**9.94e-1**
OFD1	253.74	**0.08**	0.22	**9.90e-1**
OGDH	2817.3	**-0.45**	0.2	**5.37e-1**
OGFOD1	948.26	**-0.29**	0.19	**8.52e-1**
OGFOD2	153.66	**-0.24**	0.25	**9.60e-1**
OGFOD3	128.84	**0.13**	0.24	**9.90e-1**
OGFR	695.22	**-0.53**	0.23	**5.45e-1**
OGFRL1	551.55	**-0.1**	0.21	**9.90e-1**
OGFRP1	12.11	**0**	0.22	**9.98e-1**
OGG1	182.8	**-0.32**	0.23	**8.90e-1**
OGT	1605.39	**0.24**	0.2	**9.29e-1**
OIP5	88.59	**0.15**	0.25	**9.90e-1**
OIP5-AS1	207.52	**0.14**	0.23	**9.90e-1**
OLA1	1222.66	**0.1**	0.19	**9.90e-1**
OLFML2A	10.29	**0.1**	0.2	**9.90e-1**
OLMALINC	70.26	**-0.13**	0.25	**9.90e-1**
OMA1	284.04	**0.32**	0.22	**8.68e-1**
OPA1	1221.08	**0.16**	0.2	**9.86e-1**
OPA3	400.26	**-0.08**	0.21	**9.90e-1**
OPRL1	57.82	**0.04**	0.25	**9.93e-1**
OR13A1	59.4	**-0.34**	0.25	**9.03e-1**
ORAI1	131.88	**0.09**	0.25	**9.90e-1**
ORAI2	2829.98	**-0.29**	0.23	**9.21e-1**
ORAOV1	81.05	**0.02**	0.25	**9.93e-1**
ORC1	905.42	**0.03**	0.19	**9.93e-1**
ORC2	348.73	**-0.09**	0.21	**9.90e-1**
ORC3	475.34	**0.19**	0.21	**9.74e-1**
ORC4	82.23	**0.16**	0.25	**9.90e-1**
ORC5	364.32	**0.2**	0.21	**9.61e-1**

ORC6	249	**0.1**	0.22	**9.90e-1**
ORMDL1	224.97	**0.21**	0.23	**9.72e-1**
ORMDL2	72.05	**-0.11**	0.25	**9.90e-1**
ORMDL3	188.99	**-0.11**	0.23	**9.90e-1**
OS9	903.23	**0.1**	0.19	**9.90e-1**
OSBP	822.6	**0.14**	0.2	**9.87e-1**
OSBPL10	812.76	**-0.12**	0.19	**9.90e-1**
OSBPL11	342.24	**-0.01**	0.21	**9.96e-1**
OSBPL2	184.46	**0.11**	0.22	**9.90e-1**

OSBPL3	748.28	**0.44**	0.21	**5.94e-1**
OSBPL7	186.41	**-0.12**	0.23	**9.90e-1**
OSBPL8	1240.31	**-0.01**	0.21	**9.96e-1**
OSBPL9	1377.15	**0.04**	0.19	**9.93e-1**
OSCP1	15.03	**-0.12**	0.23	**9.90e-1**
OSER1	239.19	**0.39**	0.22	**7.57e-1**
OSGEP	287.72	**0.19**	0.21	**9.71e-1**
OSGEPL1	30.95	**0.19**	0.25	**9.87e-1**
OSGIN2	294.99	**0.14**	0.22	**9.90e-1**
OST4	295.84	**-0.07**	0.21	**9.90e-1**
OSTC	373.97	**0.42**	0.21	**6.69e-1**
OSTF1	200.9	**-0.12**	0.22	**9.90e-1**
OSTM1	196.92	**0.29**	0.23	**9.25e-1**
OTUB1	571.84	**-0.26**	0.22	**9.46e-1**
OTUD1	13.85	**0.06**	0.23	**9.93e-1**
OTUD3	268.67	**-0.4**	0.21	**7.13e-1**
OTUD4	1400.61	**-0.17**	0.19	**9.78e-1**
OTUD5	611.59	**0**	0.21	**9.99e-1**
OTUD6B	394.72	**-0.17**	0.21	**9.86e-1**
OTUD6B-AS1	228.73	**-0.28**	0.22	**9.20e-1**
OTUD7B	24.77	**-0.23**	0.25	**9.68e-1**
OTULIN	538.54	**0.3**	0.2	**8.64e-1**
OTX1	27.74	**-0.28**	0.25	**9.47e-1**
OXA1L	1102.55	**0.14**	0.19	**9.87e-1**
OXCT1	1208.38	**0.09**	0.19	**9.90e-1**
OXLD1	73.37	**-0.03**	0.25	**9.93e-1**
OXNAD1	146.59	**0.06**	0.23	**9.93e-1**
OXR1	272.38	**0.21**	0.23	**9.72e-1**
OXSM	47.92	**0.33**	0.25	**9.14e-1**
OXSR1	853.63	**0.21**	0.2	**9.50e-1**
OXTR	10.83	**-0.32**	0.21	**8.51e-1**
P2RX4	55.06	**0.26**	0.25	**9.54e-1**
P2RX5	336.22	**0.01**	0.21	**9.97e-1**
P2RX5-TAX1BP3	17.16	**0.03**	0.24	**9.93e-1**
P2RY10	79.98	**-0.39**	0.25	**8.41e-1**
P2RY11	30.13	**-0.18**	0.25	**9.87e-1**
P2RY8	1673.02	**0.05**	0.2	**9.93e-1**
P3H1	335.26	**-0.15**	0.21	**9.87e-1**
P4HA1	301.66	**0.08**	0.22	**9.90e-1**
P4HB	2404.79	**0.16**	0.18	**9.75e-1**
P4HTM	73.19	**0.08**	0.25	**9.91e-1**
PA2G4	4696.93	**-0.37**	0.18	**6.54e-1**
PA2G4P4	21.98	**0.17**	0.24	**9.88e-1**
PAAF1	181.03	**-0.16**	0.22	**9.88e-1**
PABPC1	20309.25	**0.01**	0.18	**9.96e-1**
PABPC1L	196.28	**0.17**	0.23	**9.87e-1**
PABPC3	94.74	**0.73**	0.25	**2.15e-1**
PABPC4	3497.11	**-0.15**	0.18	**9.81e-1**
PABPN1	88.15	**-0.25**	0.18	**8.91e-1**
PACRGL	101.5	**0.15**	0.24	**9.90e-1**
PACS1	1140.53	**-0.44**	0.21	**6.07e-1**
PACS2	365.08	**-0.05**	0.22	**9.93e-1**
PACSIN1	18.5	**-0.43**	0.24	**7.50e-1**
PACSIN2	415.29	**0.13**	0.21	**9.90e-1**
PAF1	743.29	**-0.24**	0.2	**9.47e-1**
PAFAH1B1	905.23	**0.4**	0.2	**6.54e-1**
PAFAH1B2	702.88	**-0.03**	0.21	**9.93e-1**
PAFAH1B3	92.29	**-0.08**	0.25	**9.91e-1**
PAFAH2	61.18	**-0.02**	0.25	**9.94e-1**
PAG1	699.71	**0.06**	0.2	**9.93e-1**
PAGR1	496.29	**-0.45**	0.23	**6.90e-1**
PAICS	5562.4	**-0.2**	0.18	**9.49e-1**
PAIP1	346.83	**0.39**	0.21	**7.41e-1**
PAIP2	610.22	**0.17**	0.2	**9.80e-1**

PAIP2B	25.07	**-0.07**	0.25	**9.92e-1**
PAK1	312.28	**-0.03**	0.21	**9.93e-1**
PAK1IP1	217.23	**0.02**	0.22	**9.93e-1**
PAK2	2027.76	**-0.11**	0.19	**9.90e-1**
PAK4	265.51	**-0.42**	0.25	**8.08e-1**
PALB2	412.81	**0.02**	0.21	**9.93e-1**
PALD1	791.4	**0.02**	0.22	**9.93e-1**
PALLD	299.95	**-0.13**	0.21	**9.90e-1**
PAM	42.33	**0.03**	0.25	**9.93e-1**
PAN2	367.63	**0.17**	0.21	**9.80e-1**
PAN3	405.59	**0.15**	0.21	**9.88e-1**
PAN3-AS1	17.12	**0.03**	0.23	**9.93e-1**
PANK1	154.5	**0.11**	0.23	**9.90e-1**
PANK2	240.6	**0.44**	0.22	**6.69e-1**
PANK3	513.86	**-0.03**	0.21	**9.93e-1**
PANK4	206.74	**-0.6**	0.23	**3.46e-1**
PAPD4	476.29	**-0.01**	0.21	**9.96e-1**
PAPD5	274.15	**-0.32**	0.21	**8.56e-1**
PAPD7	438.41	**-0.2**	0.2	**9.58e-1**
PAPOLA	3147.52	**0**	0.2	**9.98e-1**
PAPOLG	196.93	**0.15**	0.23	**9.90e-1**
PAPSS1	344.86	**0.1**	0.21	**9.90e-1**
PAQR3	261.62	**0.35**	0.23	**8.52e-1**
PAQR4	627.97	**-0.33**	0.23	**8.76e-1**
PAQR6	27.5	**-0.05**	0.25	**9.93e-1**
PAQR8	147.13	**0.49**	0.23	**6.03e-1**
PARD6A	76.34	**-0.06**	0.25	**9.93e-1**
PARD6B	37.88	**0.12**	0.25	**9.90e-1**
PARG	209.79	**0.1**	0.23	**9.90e-1**
PARGP1	13.13	**-0.26**	0.22	**9.47e-1**
PARK7	990.14	**0.13**	0.19	**9.88e-1**
PARL	250.42	**0.27**	0.22	**9.37e-1**
PARN	797.19	**0.13**	0.2	**9.88e-1**
PARP1	7429.26	**-0.04**	0.18	**9.93e-1**
PARP10	237.56	**-0.2**	0.24	**9.80e-1**
PARP11	102.48	**0.12**	0.24	**9.90e-1**
PARP12	32.18	**0.33**	0.25	**9.12e-1**
PARP15	10.96	**0.16**	0.21	**9.87e-1**
PARP16	109.84	**0.02**	0.24	**9.96e-1**
PARP2	499.1	**-0.08**	0.2	**9.90e-1**
PARP3	136.32	**-0.1**	0.24	**9.90e-1**
PARP4	867.69	**-0.02**	0.19	**9.94e-1**
PARP6	323.22	**-0.08**	0.21	**9.90e-1**
PARP8	303.64	**0.19**	0.22	**9.80e-1**
PARP9	400.98	**0.27**	0.21	**9.12e-1**
PARPBP	287.59	**-0.09**	0.22	**9.90e-1**
PARS2	115.25	**0.06**	0.24	**9.93e-1**
PARTICL	11.58	**0**	0.21	**9.98e-1**
PARVB	283.24	**0.34**	0.21	**8.39e-1**
PARVG	81.18	**-0.06**	0.25	**9.93e-1**
PASK	302.88	**-0.16**	0.23	**9.87e-1**
PATL1	1064.13	**0.03**	0.2	**9.93e-1**
PATZ1	564.12	**-0.33**	0.21	**8.39e-1**
PAWR	230.82	**0.17**	0.22	**9.86e-1**
PAX5	3179.5	**-0.32**	0.2	**8.29e-1**
PAXBP1	446.45	**0.13**	0.21	**9.90e-1**
PAXIP1	555.18	**-0.22**	0.2	**9.47e-1**
PAXIP1-AS1	62.44	**-0.01**	0.25	**9.96e-1**
PAXIP1-AS2	18.57	**0.01**	0.24	**9.96e-1**
PBDC1	212.36	**-0.26**	0.22	**9.47e-1**
PBK	208.65	**-0.21**	0.23	**9.66e-1**
PBLD	20.27	**0.18**	0.24	**9.87e-1**
PBRM1	905.54	**0.02**	0.19	**9.93e-1**
PBX2	535.54	**-0.27**	0.21	**9.21e-1**

PBX3	204.24	**0.1**	0.22	**9.90e-1**
PBX4	24.21	**-0.18**	0.24	**9.87e-1**
PBXIP1	356.38	**-0.24**	0.22	**9.49e-1**
PCBD2	55.17	**0.34**	0.25	**9.06e-1**
PCBP1	2172.43	**-0.36**	0.2	**7.41e-1**
PCBP1-AS1	37.91	**0.05**	0.25	**9.93e-1**
PCBP2	2900.89	**0.19**	0.18	**9.49e-1**
PCCA	31.22	**0.2**	0.25	**9.86e-1**
PCCB	357.95	**0.2**	0.21	**9.61e-1**
PCDH9	39.91	**-0.44**	0.25	**7.75e-1**
PCDHGA12	19.55	**-0.02**	0.24	**9.94e-1**
PCDHGB2	18.61	**0.13**	0.24	**9.90e-1**
PCDHGB3	11.53	**-0.04**	0.22	**9.93e-1**
PCDHGC3	197.35	**-0.3**	0.23	**9.10e-1**
PCED1A	105.39	**-0.1**	0.25	**9.90e-1**
PCF11	945.99	**-0.02**	0.19	**9.95e-1**
PCGF1	67.84	**0.2**	0.25	**9.83e-1**
PCGF2	37.82	**-0.18**	0.25	**9.87e-1**
PCGF3	368.56	**-0.16**	0.21	**9.86e-1**
PCGF5	821.69	**0**	0.22	**9.98e-1**
PCGF6	86.7	**0.36**	0.25	**8.68e-1**
PCID2	314.24	**0.3**	0.21	**8.84e-1**
PCIF1	262.92	**-0.05**	0.21	**9.93e-1**
PCK2	362.09	**0.52**	0.23	**5.37e-1**
PCM1	1996.2	**0.15**	0.2	**9.86e-1**
PCMT1	482.41	**0.39**	0.2	**6.84e-1**
PCMTD1	122.93	**0.27**	0.24	**9.47e-1**
PCMTD2	334.92	**0.46**	0.22	**6.07e-1**
PCNA	2559.88	**0.14**	0.18	**9.87e-1**

PCNP	1106.25	**0.06**	0.2	**9.91e-1**
PCNT	841.13	**-0.01**	0.19	**9.97e-1**
PCNX	588.05	**0.05**	0.2	**9.93e-1**
PCNXL2	19.23	**0.16**	0.24	**9.90e-1**
PCNXL3	791.65	**-0.3**	0.23	**9.08e-1**
PCNXL4	432.33	**0.42**	0.22	**6.90e-1**
PCOLCE	10.26	**0.15**	0.21	**9.87e-1**
PCSK7	210.47	**-0.14**	0.23	**9.90e-1**
PCYOX1	49.75	**-0.17**	0.25	**9.88e-1**
PCYOX1L	229.96	**-0.02**	0.22	**9.93e-1**
PCYT1A	161.34	**-0.07**	0.23	**9.92e-1**
PCYT2	269.75	**-0.33**	0.22	**8.64e-1**
PDAP1	1175.88	**-0.21**	0.2	**9.49e-1**
PDCD10	405.81	**0.18**	0.22	**9.81e-1**
PDCD11	2054.23	**-0.24**	0.18	**9.12e-1**
PDCD2	458.21	**0.22**	0.21	**9.49e-1**
PDCD2L	85.9	**0.24**	0.25	**9.58e-1**
PDCD4	1505.5	**0.43**	0.19	**5.47e-1**
PDCD4-AS1	70.45	**0.26**	0.25	**9.52e-1**
PDCD5	493.71	**-0.13**	0.2	**9.90e-1**
PDCD6	352.12	**0.09**	0.21	**9.90e-1**
PDCD6IP	1576.37	**-0.02**	0.19	**9.93e-1**
PDCD7	209.64	**-0.09**	0.22	**9.90e-1**
PDCL	162.16	**0.14**	0.23	**9.90e-1**
PDCL3	257.19	**-0.13**	0.22	**9.90e-1**
PDDC1	503.43	**-0.38**	0.24	**8.38e-1**
PDE12	431.29	**-0.19**	0.2	**9.66e-1**
PDE1B	13.23	**-0.06**	0.22	**9.93e-1**
PDE3B	123.44	**-0.08**	0.24	**9.90e-1**
PDE4A	459.45	**-0.27**	0.21	**9.33e-1**
PDE4B	501.22	**-0.46**	0.2	**5.31e-1**
PDE4D	30.54	**0.13**	0.25	**9.90e-1**
PDE4DIP	249.15	**-0.01**	0.22	**9.96e-1**
PDE6B	42.66	**0.15**	0.25	**9.90e-1**

PDE6D	188.54	**0.11**	0.23	**9.90e-1**
PDE7A	437.45	**0.08**	0.21	**9.90e-1**
PDE8A	206.83	**-0.29**	0.22	**9.12e-1**
PDGFD	61.96	**0.4**	0.25	**8.41e-1**
PDHA1	1588.27	**0.05**	0.18	**9.93e-1**
PDHB	550.92	**0.31**	0.2	**8.52e-1**
PDHX	345.5	**0.08**	0.21	**9.90e-1**
PDIA3	3987.24	**0.32**	0.18	**7.57e-1**
PDIA3P1	35.91	**0.44**	0.25	**7.61e-1**
PDIA4	2440.98	**0.17**	0.18	**9.64e-1**
PDIA5	73.23	**0.63**	0.25	**4.11e-1**
PDIA6	3120.34	**0.34**	0.19	**7.41e-1**
PDIK1L	114.46	**0.12**	0.24	**9.90e-1**
PDK1	440.72	**0.39**	0.21	**7.22e-1**
PDK2	105.9	**0.02**	0.24	**9.96e-1**
PDK3	286.08	**0.21**	0.22	**9.58e-1**
PDLIM2	117.9	**-0.43**	0.25	**8.04e-1**
PDLIM5	333.41	**0.03**	0.21	**9.93e-1**
PDLIM7	86.43	**-0.21**	0.25	**9.81e-1**
PDP1	140.15	**0.2**	0.23	**9.80e-1**
PDP2	466.75	**-0.27**	0.2	**9.10e-1**
PDPK1	524.13	**-0.07**	0.2	**9.90e-1**
PDPR	830.3	**-0.19**	0.19	**9.60e-1**
PDRG1	135.7	**-0.2**	0.24	**9.80e-1**
PDS5A	2415.3	**0.13**	0.2	**9.90e-1**
PDS5B	615.43	**-0.09**	0.2	**9.90e-1**
PDSS1	207.72	**0.31**	0.23	**9.01e-1**
PDSS2	247.47	**-0.09**	0.22	**9.90e-1**
PDXDC1	969.66	**0.15**	0.19	**9.86e-1**
PDXDC2P	80.53	**0.17**	0.25	**9.89e-1**
PDXK	410.32	**-0.08**	0.22	**9.90e-1**
PDXP	361.86	**0.12**	0.22	**9.90e-1**
PDZD11	141.83	**0.04**	0.23	**9.93e-1**
PDZD8	393.34	**0.01**	0.21	**9.96e-1**
PEA15	1910.86	**-0.39**	0.2	**6.83e-1**
PEAK1	286.22	**-0.14**	0.22	**9.90e-1**
PEBP1	1577.02	**-0.27**	0.19	**8.80e-1**
PEF1	499.47	**-0.07**	0.21	**9.90e-1**
PEG10	129.95	**-0.78**	0.24	**1.03e-1**
PELI1	304.32	**0.1**	0.22	**9.90e-1**
PELI3	37.01	**-0.28**	0.25	**9.49e-1**
PELO	65.36	**0.18**	0.25	**9.87e-1**
PELP1	1605.19	**-0.46**	0.22	**6.03e-1**
PEMT	138.24	**-0.09**	0.24	**9.90e-1**
PEPD	91.48	**0.17**	0.25	**9.88e-1**
PER1	339.2	**-0.31**	0.23	**9.12e-1**
PER2	436.75	**-0.03**	0.2	**9.93e-1**
PER3	22.1	**-0.27**	0.24	**9.49e-1**
PES1	2172.48	**-0.34**	0.2	**8.14e-1**

PET100	55.13	**0.36**	0.25	**8.73e-1**
PET117	30.55	**-0.53**	0.25	**5.94e-1**
PEX1	179.34	**0.2**	0.23	**9.72e-1**
PEX10	75.37	**0.2**	0.25	**9.86e-1**
PEX11B	113.6	**0.27**	0.24	**9.47e-1**
PEX12	57.15	**-0.09**	0.25	**9.90e-1**
PEX13	86.77	**0.1**	0.25	**9.90e-1**
PEX14	123.09	**-0.32**	0.24	**9.10e-1**
PEX16	83	**-0.04**	0.25	**9.93e-1**
PEX19	395.19	**0**	0.2	**1.00e+0**
PEX2	182.3	**0.21**	0.23	**9.66e-1**
PEX26	436.86	**-0.29**	0.2	**8.68e-1**
PEX3	259.87	**0.04**	0.22	**9.93e-1**
PEX5	624.77	**-0.1**	0.2	**9.90e-1**

PEX6	164.56	**-0.09**	0.25	**9.90e-1**
PEX7	20.44	**0.24**	0.24	**9.58e-1**
PFAS	1892.36	**-0.28**	0.21	**9.08e-1**
PFDN1	348.84	**-0.25**	0.21	**9.47e-1**
PFDN2	227.22	**0.06**	0.22	**9.93e-1**
PFDN4	192.42	**0.23**	0.22	**9.50e-1**
PFDN5	413.95	**-0.03**	0.2	**9.93e-1**
PFDN6	252.95	**-0.41**	0.23	**7.57e-1**
PFKFB2	43.85	**0.06**	0.25	**9.93e-1**
PFKFB3	296.88	**-0.27**	0.21	**9.23e-1**
PFKFB4	55.43	**-0.07**	0.25	**9.93e-1**
PFKL	1380.36	**0.01**	0.21	**9.97e-1**
PFKM	1193.14	**-0.06**	0.19	**9.91e-1**
PFKP	917.86	**-0.3**	0.2	**8.52e-1**
PFN1	4182.03	**-0.04**	0.18	**9.93e-1**
PGAM1	2014.19	**-0.19**	0.18	**9.54e-1**
PGAM5	776.99	**-0.45**	0.21	**5.91e-1**
PGAP1	78.43	**0.13**	0.25	**9.90e-1**
PGAP2	265.94	**-0.24**	0.22	**9.49e-1**
PGAP3	35.43	**0.06**	0.25	**9.93e-1**
PGBD2	75.27	**0.01**	0.25	**9.98e-1**
PGBD4	31.22	**-0.18**	0.25	**9.87e-1**
PGD	3037.72	**-0.15**	0.18	**9.84e-1**
PGGT1B	101.03	**0.2**	0.25	**9.81e-1**
PGK1	2659.01	**-0.1**	0.18	**9.90e-1**
PGLS	283.63	**0.25**	0.22	**9.47e-1**
PGM1	859.1	**-0.19**	0.2	**9.59e-1**
PGM2	521.01	**0.09**	0.21	**9.90e-1**
PGM2L1	11.89	**0.21**	0.22	**9.60e-1**
PGM3	183.55	**0.16**	0.23	**9.87e-1**
PGP	148.09	**0.1**	0.23	**9.90e-1**
PGPEP1	56.98	**0.29**	0.25	**9.47e-1**
PGRMC1	284.08	**0.22**	0.22	**9.58e-1**
PGRMC2	345.06	**0.2**	0.21	**9.60e-1**
PGS1	132.16	**0.28**	0.24	**9.42e-1**
PHACTR1	117.57	**0.46**	0.24	**6.87e-1**
PHACTR4	487.31	**-0.22**	0.2	**9.49e-1**
PHAX	354.29	**-0.12**	0.21	**9.90e-1**
PHB	1654.88	**-0.25**	0.2	**9.14e-1**
PHB2	2423.21	**0.09**	0.18	**9.90e-1**
PHC1	356.37	**-0.21**	0.21	**9.56e-1**
PHC2	517.64	**0.01**	0.21	**9.96e-1**
PHC3	495.87	**-0.18**	0.21	**9.80e-1**
PHF1	144.84	**-0.19**	0.25	**9.87e-1**
PHF10	195.3	**0.27**	0.23	**9.47e-1**
PHF11	121.27	**0.44**	0.25	**7.47e-1**
PHF12	719.86	**-0.26**	0.19	**9.10e-1**
PHF13	104.14	**0.09**	0.24	**9.90e-1**
PHF14	974.42	**-0.04**	0.2	**9.93e-1**
PHF19	782.34	**0.49**	0.21	**5.31e-1**
PHF2	298.17	**0.05**	0.22	**9.93e-1**
PHF20	536.88	**-0.09**	0.2	**9.90e-1**
PHF20L1	493.25	**0.12**	0.21	**9.90e-1**
PHF21A	401.48	**-0.34**	0.2	**8.07e-1**
PHF21B	14.08	**-0.24**	0.22	**9.49e-1**
PHF23	519.63	**-0.33**	0.22	**8.52e-1**
PHF3	1353.98	**-0.15**	0.19	**9.82e-1**
PHF5A	302.53	**-0.08**	0.21	**9.90e-1**
PHF6	443	**0.26**	0.22	**9.42e-1**
PHF7	51.1	**0.17**	0.25	**9.90e-1**
PHF8	593.1	**-0.27**	0.2	**8.97e-1**
PHGDH	1105.92	**0.26**	0.22	**9.39e-1**
PHIP	1178.09	**0.03**	0.2	**9.93e-1**
PHKA2	349.3	**-0.07**	0.21	**9.91e-1**
PHKB	458.34	**0.22**	0.21	**9.49e-1**

PHKG2	185.25	**-0.22**	0.23	**9.59e-1**
PHLDB3	30.18	**-0.02**	0.25	**9.94e-1**
PHLPP1	372.77	**-0.16**	0.21	**9.86e-1**
PHLPP2	278.54	**0.07**	0.21	**9.90e-1**

PHOSPHO2	13.21	**0.15**	0.22	**9.88e-1**
PHPT1	300.86	**-0.03**	0.24	**9.93e-1**
PHRF1	963.36	**-0.47**	0.22	**5.86e-1**
PHTF1	143.91	**0.33**	0.23	**8.77e-1**
PHTF2	430.69	**0.13**	0.22	**9.90e-1**
PHYKPL	73.34	**-0.02**	0.25	**9.95e-1**
PI16	27.6	**0.56**	0.25	**5.51e-1**
PI4K2A	202.32	**0.06**	0.23	**9.93e-1**
PI4K2B	466.44	**0.22**	0.21	**9.49e-1**
PI4KA	948.53	**0.03**	0.19	**9.93e-1**
PI4KAP1	64.73	**-0.29**	0.25	**9.47e-1**
PI4KAP2	113.43	**-0.06**	0.24	**9.93e-1**
PI4KB	693.84	**-0.19**	0.19	**9.61e-1**
PIAS1	416.88	**-0.2**	0.21	**9.61e-1**
PIAS2	400.12	**0.03**	0.21	**9.93e-1**
PIAS3	381.24	**-0.31**	0.21	**8.69e-1**
PIAS4	228.48	**-0.39**	0.23	**8.08e-1**
PIBF1	144.31	**0.14**	0.24	**9.90e-1**
PICALM	790.57	**-0.03**	0.2	**9.93e-1**
PICK1	110.41	**-0.17**	0.24	**9.88e-1**
PIDD1	266.76	**-0.53**	0.25	**5.91e-1**
PIEZO1	1751.07	**-0.21**	0.22	**9.66e-1**
PIF1	194.06	**-0.29**	0.24	**9.45e-1**
PIGA	153.62	**-0.06**	0.23	**9.93e-1**
PIGB	70.47	**0.53**	0.25	**6.03e-1**
PIGBOS1	17.97	**0.21**	0.24	**9.73e-1**
PIGC	64.3	**0.46**	0.25	**7.41e-1**
PIGF	30.67	**0.22**	0.25	**9.74e-1**
PIGG	159.65	**0.33**	0.23	**8.66e-1**
PIGH	48.02	**0.28**	0.25	**9.47e-1**
PIGK	156.87	**0.26**	0.23	**9.49e-1**
PIGL	11.73	**0.22**	0.21	**9.51e-1**
PIGM	57.93	**-0.02**	0.25	**9.95e-1**
PIGN	177.3	**0.46**	0.24	**6.76e-1**
PIGO	186.52	**-0.12**	0.23	**9.90e-1**
PIGP	23.07	**0.52**	0.24	**6.03e-1**
PIGQ	193.9	**-0.11**	0.25	**9.90e-1**
PIGS	426.87	**-0.16**	0.21	**9.86e-1**
PIGT	1490.35	**-0.26**	0.2	**9.06e-1**
PIGU	385.78	**0.15**	0.2	**9.87e-1**
PIGV	67.97	**0.43**	0.25	**8.04e-1**
PIGW	220.88	**0.33**	0.22	**8.64e-1**
PIGX	166.6	**0.38**	0.23	**8.30e-1**
PIH1D1	524.97	**-0.11**	0.2	**9.90e-1**
PIK3AP1	2420.87	**0.39**	0.19	**6.14e-1**
PIK3C2A	731.92	**-0.12**	0.22	**9.90e-1**
PIK3C2B	877.08	**-0.15**	0.2	**9.87e-1**
PIK3C3	233.25	**0.29**	0.22	**9.10e-1**
PIK3CA	253.96	**0.25**	0.23	**9.49e-1**
PIK3CB	329.61	**0**	0.22	**9.98e-1**
PIK3CD	1717.35	**-0.3**	0.2	**8.52e-1**
PIK3CD-AS1	12.96	**-0.15**	0.22	**9.89e-1**
PIK3CG	215.32	**0.22**	0.22	**9.58e-1**
PIK3IP1	52.32	**0.44**	0.25	**7.80e-1**
PIK3R1	480.44	**0.03**	0.21	**9.93e-1**
PIK3R2	555.21	**-0.19**	0.22	**9.80e-1**
PIK3R3	114.26	**-0.55**	0.24	**5.37e-1**
PIK3R4	513.37	**-0.14**	0.2	**9.88e-1**
PIKFYVE	653.43	**0.13**	0.2	**9.90e-1**

PILRA	15.1	**0.09**	0.23	**9.90e-1**
PIM1	1018.27	**0.04**	0.2	**9.93e-1**
PIM2	1152.66	**0.18**	0.19	**9.61e-1**
PIM3	305.36	**0.01**	0.23	**9.96e-1**
PIN1	270.74	**-0.38**	0.24	**8.29e-1**
PIN4	55.13	**0.1**	0.25	**9.90e-1**
PINK1-AS	179.58	**-0.06**	0.23	**9.93e-1**
PINX1	283.89	**-0.16**	0.21	**9.87e-1**
PIP4K2A	1154.42	**0.07**	0.19	**9.90e-1**
PIP4K2B	787.1	**-0.14**	0.2	**9.87e-1**
PIP4K2C	202.04	**-0.03**	0.22	**9.93e-1**
PIP5K1A	829.52	**-0.16**	0.19	**9.80e-1**
PIP5K1B	21.51	**-0.27**	0.24	**9.47e-1**
PIP5K1C	257.13	**-0.37**	0.24	**8.52e-1**
PISD	245.56	**0**	0.22	**1.00e+0**
PITHD1	335.18	**0.34**	0.21	**8.31e-1**
PITPNA	888.38	**0.29**	0.19	**8.56e-1**
PITPNA-AS1	34.86	**-0.02**	0.25	**9.95e-1**
PITPNB	931.01	**0.18**	0.2	**9.73e-1**
PITPNC1	206.92	**0.36**	0.22	**8.29e-1**
PITPNM1	320.97	**-0.3**	0.24	**9.25e-1**
PITRM1	763	**-0.04**	0.2	**9.93e-1**
PITRM1-AS1	10.49	**-0.1**	0.21	**9.90e-1**
PITX1	56.48	**-0.03**	0.25	**9.93e-1**

PJA1	182.13	**-0.26**	0.23	**9.47e-1**
PJA2	861.69	**0.47**	0.2	**5.36e-1**
PKD1	501.09	**-0.3**	0.24	**9.25e-1**
PKD1P1	351.33	**-0.23**	0.22	**9.50e-1**
PKD1P6	323.56	**-0.39**	0.23	**7.97e-1**
PKD2	100.1	**0.23**	0.24	**9.66e-1**
PKHD1L1	16.51	**0.11**	0.23	**9.90e-1**
PKI55	75.91	**0.16**	0.25	**9.90e-1**
PKIA	68.75	**0.03**	0.25	**9.93e-1**
PKIG	140.19	**-0.43**	0.24	**7.49e-1**
PKM	12256.2	**-0.24**	0.18	**9.10e-1**
PKMYT1	583.29	**-0.2**	0.21	**9.66e-1**
PKN1	1496.37	**-0.05**	0.23	**9.93e-1**
PKN2	332.24	**0.22**	0.22	**9.56e-1**
PKNOX1	227.49	**-0.12**	0.22	**9.90e-1**
PKP4	543.53	**-0.15**	0.2	**9.87e-1**
PLA2G12A	261.09	**0.21**	0.22	**9.64e-1**
PLA2G15	28.9	**-0.11**	0.25	**9.90e-1**
PLA2G4C	13.23	**0.22**	0.22	**9.59e-1**
PLA2G6	143.97	**-0.03**	0.25	**9.93e-1**
PLAA	623.86	**0.13**	0.2	**9.89e-1**
PLAC8	79.71	**0.19**	0.25	**9.86e-1**
PLAG1	51.88	**-0.1**	0.25	**9.90e-1**
PLAGL2	702.74	**-0.37**	0.21	**7.41e-1**
PLBD2	191.78	**-0.2**	0.24	**9.80e-1**
PLCB3	40.42	**-0.15**	0.25	**9.90e-1**
PLCD3	82.99	**-0.42**	0.25	**8.12e-1**
PLCG1	786.13	**-0.22**	0.2	**9.47e-1**
PLCG2	2626.42	**-0.1**	0.18	**9.90e-1**
PLCL2	168.13	**0.01**	0.23	**9.98e-1**
PLCXD1	683.36	**-0.24**	0.21	**9.47e-1**
PLD2	51.47	**-0.13**	0.25	**9.90e-1**
PLD3	201.24	**-0.14**	0.24	**9.90e-1**
PLD4	124.28	**-0.33**	0.25	**9.10e-1**
PLD6	61.26	**-0.24**	0.25	**9.61e-1**
PLEC	759.34	**-0.17**	0.22	**9.87e-1**
PLEK	3277.37	**0.65**	0.18	**4.72e-2**
PLEKHA1	89.54	**0.01**	0.25	**9.96e-1**
PLEKHA2	1418.63	**0.01**	0.19	**9.96e-1**

PLEKHA3	135.49	**0.25**	0.24	**9.49e-1**
PLEKHA5	280.87	**-0.2**	0.22	**9.74e-1**
PLEKHA8	323.85	**-0.03**	0.22	**9.93e-1**
PLEKHA8P1	22.32	**-0.02**	0.24	**9.94e-1**
PLEKHB1	31.49	**0.35**	0.25	**8.92e-1**
PLEKHB2	384.14	**0.17**	0.21	**9.81e-1**
PLEKHF2	409.16	**0.24**	0.21	**9.47e-1**
PLEKHG1	691.47	**0.3**	0.2	**8.53e-1**
PLEKHG2	232.22	**-0.14**	0.23	**9.90e-1**
PLEKHG4	73.68	**-0.06**	0.25	**9.93e-1**
PLEKHH3	20.72	**0.1**	0.23	**9.90e-1**
PLEKHJ1	265.6	**-0.08**	0.23	**9.91e-1**
PLEKHM1	172.47	**-0.32**	0.24	**9.04e-1**
PLEKHM1P	51.38	**-0.11**	0.25	**9.90e-1**
PLEKHM2	457.49	**-0.05**	0.21	**9.93e-1**
PLEKHM3	66.32	**0.1**	0.25	**9.90e-1**
PLEKHO2	130.57	**-0.14**	0.24	**9.90e-1**
PLGRKT	39.38	**0.57**	0.25	**5.62e-1**
PLIN2	225.66	**0.01**	0.22	**9.96e-1**
PLIN3	394.35	**0.12**	0.22	**9.90e-1**
PLK1	1683.12	**-0.63**	0.2	**1.12e-1**
PLK3	116.74	**-0.01**	0.24	**9.98e-1**
PLK4	506.42	**-0.01**	0.2	**9.96e-1**
PLOD1	476.77	**-0.49**	0.23	**5.96e-1**
PLOD3	38.18	**-0.02**	0.25	**9.96e-1**
PLP2	663.69	**0.26**	0.19	**9.11e-1**
PLRG1	363.21	**0.2**	0.21	**9.66e-1**
PLS1	218.56	**0.09**	0.23	**9.90e-1**
PLSCR1	38.69	**-0.25**	0.25	**9.59e-1**
PLTP	18.29	**0.16**	0.24	**9.88e-1**
PLXNA1	588.46	**-0.06**	0.22	**9.92e-1**
PLXNA3	99.83	**-0.26**	0.24	**9.49e-1**
PLXNB2	1142.68	**-0.32**	0.21	**8.62e-1**
PLXNC1	25.97	**0.27**	0.25	**9.49e-1**
PM20D2	1625.58	**-0.08**	0.2	**9.90e-1**
PMAIP1	525	**0.33**	0.21	**8.38e-1**
PMF1	45.65	**-0.05**	0.25	**9.93e-1**
PMFBP1	20.55	**0**	0.24	**9.99e-1**
PML	359.66	**-0.36**	0.22	**8.30e-1**
PMM1	44.96	**0.24**	0.25	**9.66e-1**
PMM2	277.34	**-0.2**	0.21	**9.61e-1**
PMPCA	1078.32	**-0.03**	0.19	**9.93e-1**
PMPCB	990.31	**0.12**	0.19	**9.90e-1**
PMS1	216.22	**0.16**	0.23	**9.87e-1**

PMS2	397.72	**0.08**	0.2	**9.90e-1**
PMS2CL	72.32	**-0.08**	0.25	**9.92e-1**
PMS2P1	310.61	**0.12**	0.21	**9.90e-1**
PMS2P3	75.97	**-0.14**	0.25	**9.90e-1**
PMS2P4	27.36	**-0.09**	0.25	**9.90e-1**
PMS2P5	78.12	**-0.27**	0.25	**9.49e-1**
PMS2P9	10.01	**-0.03**	0.21	**9.93e-1**
PMVK	156.89	**-0.27**	0.24	**9.47e-1**
PNISR	1747.8	**-0.28**	0.18	**8.49e-1**
PNKD	1652.93	**-0.39**	0.22	**7.57e-1**
PNKP	176.15	**-0.21**	0.25	**9.81e-1**
PNMA1	132.01	**-0.36**	0.24	**8.49e-1**
PNN	3527.53	**-0.29**	0.18	**8.30e-1**
PNO1	278.92	**-0.35**	0.21	**8.15e-1**
PNOC	73.61	**0.1**	0.25	**9.90e-1**
PNP	1527.08	**-0.1**	0.18	**9.90e-1**
PNPLA2	455.9	**-0.21**	0.23	**9.68e-1**
PNPLA4	65.83	**-0.05**	0.25	**9.93e-1**
PNPLA6	252.4	**-0.1**	0.23	**9.90e-1**

PNPLA7	18.12	**-0.36**	0.24	**8.53e-1**
PNPLA8	284.47	**0.12**	0.22	**9.90e-1**
PNPO	572.32	**-0.34**	0.2	**8.03e-1**
PNPT1	1162.17	**-0.2**	0.19	**9.50e-1**
PNRC1	227.62	**0.15**	0.22	**9.90e-1**
PNRC2	1634.52	**-0.15**	0.19	**9.83e-1**
POC1A	233.73	**-0.14**	0.22	**9.90e-1**
POC1B	148.36	**0.08**	0.23	**9.91e-1**
POC5	115.2	**0.22**	0.24	**9.71e-1**
PODXL	787.21	**-0.66**	0.2	**8.97e-2**
POF1B	30.69	**-0.09**	0.25	**9.90e-1**
POFUT1	671.46	**-0.26**	0.2	**9.21e-1**
POFUT2	91.31	**-0.1**	0.25	**9.90e-1**
POGK	678.12	**-0.07**	0.19	**9.90e-1**
POGLUT1	169.4	**0.38**	0.24	**8.39e-1**
POGZ	1176.71	**-0.13**	0.19	**9.87e-1**
POLA1	835.61	**0.14**	0.19	**9.87e-1**
POLA2	691.91	**-0.07**	0.19	**9.90e-1**
POLB	59.86	**0.01**	0.25	**9.96e-1**
POLD1	1080.23	**-0.39**	0.23	**7.75e-1**
POLD2	2469.4	**-0.36**	0.21	**7.57e-1**
POLD3	515.55	**0.08**	0.2	**9.90e-1**
POLD4	326.03	**-0.35**	0.24	**8.64e-1**
POLDIP2	1577.03	**-0.16**	0.19	**9.80e-1**
POLDIP3	867.32	**-0.15**	0.2	**9.87e-1**
POLE	1478.95	**-0.27**	0.19	**8.73e-1**
POLE2	209.28	**-0.03**	0.23	**9.93e-1**
POLE3	2271.33	**-0.5**	0.18	**3.01e-1**
POLE4	50.86	**-0.03**	0.25	**9.93e-1**
POLG	627.71	**-0.16**	0.21	**9.86e-1**
POLG2	101.13	**0.2**	0.24	**9.81e-1**
POLH	252.06	**-0.19**	0.22	**9.80e-1**
POLI	49.22	**0.19**	0.25	**9.87e-1**
POLK	183.98	**-0.02**	0.23	**9.94e-1**
POLL	121.51	**-0.36**	0.24	**8.64e-1**
POLM	279.42	**-0.41**	0.24	**7.77e-1**
POLQ	720.5	**-0.15**	0.2	**9.87e-1**
POLR1A	1671.28	**-0.38**	0.19	**6.79e-1**
POLR1B	585.4	**0.05**	0.2	**9.93e-1**
POLR1C	341.89	**-0.19**	0.21	**9.74e-1**
POLR1D	865.7	**0.04**	0.2	**9.93e-1**
POLR1E	407.07	**0.29**	0.21	**8.78e-1**
POLR2A	3491.46	**-0.35**	0.2	**7.99e-1**
POLR2B	1926.31	**0.06**	0.19	**9.91e-1**
POLR2C	363.62	**0.01**	0.21	**9.96e-1**
POLR2D	285.35	**-0.02**	0.21	**9.95e-1**
POLR2E	1056.89	**-0.38**	0.22	**7.97e-1**
POLR2F	284.05	**-0.29**	0.22	**9.17e-1**
POLR2G	189.36	**0.03**	0.23	**9.93e-1**
POLR2H	305.19	**0.46**	0.21	**5.86e-1**
POLR2I	138.6	**0.16**	0.23	**9.87e-1**
POLR2J	485.94	**-0.77**	0.22	**6.75e-2**
POLR2J2	30.58	**-0.34**	0.25	**9.03e-1**
POLR2J3	197.89	**-0.64**	0.24	**3.04e-1**
POLR2J4	109.25	**-0.44**	0.25	**7.57e-1**
POLR2K	272.02	**-0.14**	0.22	**9.90e-1**
POLR2L	225.82	**-0.18**	0.23	**9.86e-1**
POLR2M	18.12	**-0.2**	0.21	**9.64e-1**
POLR3A	560.9	**-0.21**	0.2	**9.53e-1**
POLR3B	349.32	**0.06**	0.21	**9.92e-1**
POLR3C	484.6	**0.11**	0.2	**9.90e-1**
POLR3D	304.87	**0.16**	0.21	**9.86e-1**
POLR3E	740.47	**-0.17**	0.2	**9.73e-1**
POLR3F	161.08	**0**	0.23	**9.98e-1**

POLR3G	999.21	**-0.37**	0.2	**7.22e-1**
POLR3GL	130.72	**-0.05**	0.24	**9.93e-1**
POLR3H	401.74	**-0.4**	0.22	**7.49e-1**
POLR3K	230.19	**-0.06**	0.22	**9.93e-1**
POLRMT	599.27	**-0.18**	0.23	**9.87e-1**
POM121	2730.79	**-0.55**	0.2	**2.98e-1**
POM121C	1950.99	**-0.52**	0.2	**3.61e-1**
POMGNT1	361.73	**-0.1**	0.22	**9.90e-1**
POMK	20.16	**0.25**	0.24	**9.49e-1**
POMP	372.36	**-0.08**	0.21	**9.90e-1**
POMT1	71.1	**-0.01**	0.25	**9.96e-1**
POMT2	154.68	**-0.12**	0.23	**9.90e-1**
POMZP3	13.41	**0.06**	0.22	**9.93e-1**
POP1	228.86	**-0.16**	0.22	**9.87e-1**
POP4	258.96	**0.1**	0.22	**9.90e-1**
POP5	98.06	**0.21**	0.24	**9.76e-1**
POP7	329.58	**-0.32**	0.23	**8.73e-1**
POR	697.15	**-0.39**	0.23	**7.87e-1**
PORCN	30.4	**0.12**	0.25	**9.90e-1**
POT1	421.05	**0.19**	0.21	**9.73e-1**
POTEE	16.36	**0.25**	0.23	**9.49e-1**
POU2AF1	4398.84	**-0.52**	0.19	**3.14e-1**
POU2F1	462.97	**-0.22**	0.2	**9.48e-1**
POU2F2	2371.1	**-0.63**	0.22	**2.49e-1**
POU6F1	30.69	**0.21**	0.25	**9.81e-1**
PP7080	107.26	**0.05**	0.24	**9.93e-1**
PPA1	1754.98	**0.31**	0.19	**8.39e-1**
PPA2	55.49	**0.31**	0.25	**9.42e-1**
PPAN	25.49	**-0.3**	0.24	**9.25e-1**
PPAP2A	66.45	**0.31**	0.25	**9.33e-1**
PPAPDC2	67.11	**0.27**	0.25	**9.49e-1**
PPARA	162.66	**0.05**	0.23	**9.93e-1**
PPARD	205.79	**-0.41**	0.24	**7.96e-1**
PPARGC1B	705.23	**-0.29**	0.2	**8.64e-1**
PPAT	858.71	**0.06**	0.21	**9.93e-1**
PPCDC	76.16	**0.03**	0.25	**9.93e-1**
PPCS	152.05	**0.25**	0.23	**9.49e-1**
PPDPF	230.95	**-0.09**	0.19	**9.90e-1**
PPFIA1	550.94	**0.22**	0.2	**9.49e-1**
PPFIA3	96.13	**-0.23**	0.25	**9.72e-1**
PPFIBP1	130.88	**0.22**	0.24	**9.66e-1**
PPFIBP2	174.7	**0.19**	0.23	**9.80e-1**
PPHLN1	604.64	**0.09**	0.2	**9.90e-1**
PPIA	4203.06	**-0.04**	0.18	**9.93e-1**
PPIB	1104.8	**0.36**	0.19	**6.87e-1**
PPID	302.59	**-0.04**	0.21	**9.93e-1**
PPIE	140.09	**0.03**	0.23	**9.93e-1**
PPIEL	19.72	**0.07**	0.24	**9.92e-1**
PPIF	2435.32	**-0.06**	0.19	**9.91e-1**
PPIG	916.67	**-0.78**	0.2	**1.77e-2**
PPIH	535	**-0.27**	0.2	**9.03e-1**
PPIL1	493.91	**0.15**	0.2	**9.87e-1**
PPIL2	919.47	**-0.36**	0.21	**7.59e-1**
PPIL3	99.51	**0.25**	0.24	**9.54e-1**
PPIL4	314.24	**0.02**	0.22	**9.96e-1**
PPIP5K1	330.3	**-0.05**	0.21	**9.93e-1**
PPIP5K2	539.51	**0.1**	0.21	**9.90e-1**
PPM1A	1104.65	**0.13**	0.2	**9.90e-1**
PPM1B	392.35	**0.19**	0.21	**9.73e-1**
PPM1D	165	**-0.19**	0.23	**9.82e-1**
PPM1E	292.52	**-0.07**	0.22	**9.90e-1**
PPM1F	267.84	**-0.12**	0.24	**9.90e-1**
PPM1G	3456.57	**-0.34**	0.18	**7.33e-1**
PPM1K	646.1	**0.08**	0.2	**9.90e-1**

PPM1L	82.52	**0.17**	0.25	**9.88e-1**
PPM1M	31.5	**0.38**	0.25	**8.52e-1**
PPME1	272.74	**-0.11**	0.21	**9.90e-1**
PPOX	60.5	**0.06**	0.25	**9.93e-1**
PPP1CA	1255.23	**-0.22**	0.19	**9.47e-1**
PPP1CB	1239.18	**0.09**	0.21	**9.90e-1**
PPP1CC	3008.19	**0.24**	0.19	**9.25e-1**
PPP1R10	794	**-0.33**	0.2	**8.10e-1**
PPP1R11	351.44	**-0.19**	0.21	**9.74e-1**
PPP1R12A	600.03	**-0.11**	0.2	**9.90e-1**
PPP1R12B	252.23	**-0.07**	0.22	**9.91e-1**
PPP1R12C	568.47	**-0.27**	0.24	**9.47e-1**
PPP1R13B	204.24	**-0.42**	0.22	**7.04e-1**
PPP1R13L	33.55	**-0.23**	0.25	**9.72e-1**
PPP1R14B	621.03	**0.3**	0.2	**8.64e-1**
PPP1R15A	161.15	**0.52**	0.24	**5.91e-1**
PPP1R15B	947.45	**0.15**	0.19	**9.86e-1**
PPP1R16A	132.96	**0.06**	0.25	**9.93e-1**
PPP1R16B	2214.8	**0.25**	0.19	**9.17e-1**

PPP1R18	1140.53	**-0.42**	0.23	**7.31e-1**
PPP1R2	352.97	**0.06**	0.21	**9.92e-1**
PPP1R21	131.84	**0.3**	0.24	**9.31e-1**
PPP1R35	97.99	**-0.28**	0.25	**9.47e-1**
PPP1R37	103.38	**-0.04**	0.25	**9.93e-1**
PPP1R3D	18.97	**0.09**	0.24	**9.90e-1**
PPP1R3E	159.2	**0.24**	0.23	**9.49e-1**
PPP1R3F	23.81	**0.2**	0.24	**9.85e-1**
PPP1R7	356.91	**0.05**	0.21	**9.93e-1**
PPP1R8	608.1	**-0.07**	0.2	**9.90e-1**
PPP1R9B	1739.29	**0**	0.21	**9.98e-1**
PPP2CA	913.23	**0.22**	0.2	**9.47e-1**
PPP2CB	196.71	**0.18**	0.23	**9.86e-1**
PPP2R1A	1317.97	**-0.02**	0.19	**9.94e-1**
PPP2R1B	483.14	**0.07**	0.21	**9.90e-1**
PPP2R2A	538.56	**0.23**	0.21	**9.49e-1**
PPP2R2D	213.61	**0.22**	0.22	**9.58e-1**
PPP2R3B	150.8	**0.1**	0.23	**9.90e-1**
PPP2R3C	151.39	**-0.14**	0.23	**9.90e-1**
PPP2R4	768.11	**-0.08**	0.21	**9.90e-1**
PPP2R5A	297.21	**0.33**	0.21	**8.40e-1**
PPP2R5B	21.45	**-0.19**	0.24	**9.86e-1**
PPP2R5C	1075.49	**0.54**	0.2	**3.30e-1**
PPP2R5D	617.5	**-0.11**	0.2	**9.90e-1**
PPP2R5E	617.94	**0.04**	0.2	**9.93e-1**
PPP3CA	292.96	**-0.05**	0.21	**9.93e-1**
PPP3CB	324.22	**0.21**	0.21	**9.58e-1**
PPP3CB-AS1	13.18	**0.06**	0.22	**9.93e-1**
PPP3CC	216.81	**0.41**	0.22	**7.31e-1**
PPP3R1	821.2	**0.04**	0.2	**9.93e-1**
PPP4C	441.61	**-0.12**	0.22	**9.90e-1**
PPP4R1	483.97	**0.01**	0.2	**9.96e-1**
PPP4R1L	53.92	**0.13**	0.25	**9.90e-1**
PPP4R2	296.52	**0.08**	0.22	**9.90e-1**
PPP4R3A	1033.04	**0.05**	0.19	**9.93e-1**
PPP4R3B	1029.29	**0.04**	0.2	**9.93e-1**
PPP4R4	14.16	**-0.1**	0.22	**9.90e-1**
PPP5C	940.37	**-0.24**	0.19	**9.25e-1**
PPP6C	746.85	**0.17**	0.2	**9.80e-1**
PPP6R1	3563.18	**-0.43**	0.22	**6.87e-1**
PPP6R2	445.25	**-0.15**	0.2	**9.87e-1**
PPP6R3	1118.84	**-0.02**	0.19	**9.95e-1**
PPRC1	2184.13	**-0.41**	0.2	**6.07e-1**
PPT1	1845.7	**0.17**	0.19	**9.66e-1**

PPTC7	566.82	**0.17**	0.21	**9.86e-1**
PPWD1	266.2	**-0.02**	0.22	**9.95e-1**
PQBP1	319.53	**0.13**	0.21	**9.90e-1**
PQLC1	185.31	**-0.11**	0.24	**9.90e-1**
PQLC2	37.81	**0.1**	0.25	**9.90e-1**
PRADC1	91.58	**-0.26**	0.25	**9.51e-1**
PRAF2	15.34	**0.26**	0.23	**9.47e-1**
PRC1	958.44	**-0.12**	0.19	**9.90e-1**
PRCC	729.23	**-0.68**	0.22	**1.44e-1**
PRCP	213.38	**0.01**	0.22	**9.96e-1**
PRDM1	46.78	**-0.72**	0.25	**2.56e-1**
PRDM10	681.77	**-0.15**	0.2	**9.87e-1**
PRDM11	61.39	**0.19**	0.25	**9.87e-1**
PRDM15	678.93	**-0.19**	0.2	**9.65e-1**
PRDM2	1915.42	**0.14**	0.18	**9.86e-1**
PRDM4	459.39	**-0.04**	0.2	**9.93e-1**
PRDX1	4430.4	**0.38**	0.18	**6.07e-1**
PRDX3	1224.39	**0.3**	0.2	**8.53e-1**
PRDX4	236.62	**0.23**	0.22	**9.50e-1**
PRDX5	662.72	**-0.07**	0.23	**9.91e-1**
PRDX6	961.1	**0.14**	0.19	**9.87e-1**
PREB	647.31	**-0.26**	0.22	**9.45e-1**
PRELID1	1414.79	**0.11**	0.19	**9.90e-1**
PRELP	30.93	**-0.08**	0.25	**9.91e-1**
PREP	519.09	**0.09**	0.2	**9.90e-1**
PREPL	965.52	**0.05**	0.2	**9.93e-1**
PREX1	837.46	**-0.27**	0.21	**9.12e-1**
PRICKLE1	15.67	**0.15**	0.23	**9.90e-1**
PRICKLE3	68.9	**-0.13**	0.25	**9.90e-1**
PRICKLE4	37.18	**-0.21**	0.25	**9.80e-1**
PRIM1	248.57	**0.4**	0.22	**7.57e-1**
PRIM2	164.34	**0.02**	0.23	**9.95e-1**
PRIMPOL	28.48	**0.07**	0.25	**9.93e-1**
PRKAA1	413.18	**0.02**	0.21	**9.93e-1**
PRKAB1	262.6	**-0.3**	0.22	**9.06e-1**
PRKAB2	246.2	**-0.08**	0.22	**9.90e-1**
PRKACA	286.2	**-0.44**	0.22	**6.54e-1**
PRKACB	355.43	**-0.65**	0.21	**1.57e-1**
PRKAG1	234.06	**0.15**	0.22	**9.88e-1**
PRKAG2	121.67	**0.25**	0.24	**9.49e-1**
PRKAR1A	1233.5	**0.06**	0.19	**9.90e-1**
PRKAR1B	572.49	**-0.31**	0.22	**8.92e-1**
PRKAR2A	268.58	**0.14**	0.22	**9.89e-1**
PRKAR2B	1204.88	**-0.08**	0.21	**9.90e-1**
PRKCA	207.76	**-0.07**	0.22	**9.90e-1**
PRKCB	1433.3	**-0.39**	0.19	**6.07e-1**
PRKCD	985.04	**-0.1**	0.19	**9.90e-1**
PRKCE	214.29	**0.14**	0.22	**9.90e-1**
PRKCI	931.19	**-0.07**	0.21	**9.90e-1**
PRKCQ-AS1	28.42	**0.03**	0.25	**9.93e-1**
PRKCSH	2089.02	**-0.28**	0.21	**9.04e-1**
PRKCZ	129.54	**0.13**	0.23	**9.90e-1**
PRKD2	316.33	**-0.36**	0.23	**8.41e-1**
PRKD3	594.2	**0.12**	0.2	**9.90e-1**
PRKDC	5387.01	**0.05**	0.19	**9.93e-1**
PRKRA	254.82	**0.26**	0.22	**9.47e-1**
PRKRIP1	34.84	**-0.15**	0.25	**9.90e-1**
PRKRIR	1007.78	**0.1**	0.2	**9.90e-1**
PRKX	258.65	**-0.22**	0.22	**9.58e-1**
PRKXP1	66.71	**0.12**	0.25	**9.90e-1**
PRKY	122.45	**-0.1**	0.24	**9.90e-1**
PRMT1	2616.13	**-0.15**	0.2	**9.86e-1**
PRMT2	211.87	**0.09**	0.22	**9.90e-1**

PRMT3	512.9	**0.19**	0.21	**9.68e-1**
PRMT5	1866.86	**-0.17**	0.18	**9.68e-1**
PRMT6	187.28	**0.01**	0.23	**9.96e-1**
PRMT7	239.3	**-0.06**	0.22	**9.93e-1**
PRMT9	152.35	**-0.03**	0.23	**9.93e-1**
PRNP	316.18	**0.19**	0.21	**9.74e-1**
PROB1	86.01	**-0.53**	0.25	**6.07e-1**
PROCA1	18.04	**-0.04**	0.24	**9.93e-1**
PRORSD1P	18.58	**0.04**	0.24	**9.93e-1**
PROSC	462.03	**0.02**	0.21	**9.93e-1**
PROSER1	1869.78	**-0.24**	0.19	**9.25e-1**
PROSER2	11.02	**-0.16**	0.21	**9.86e-1**
PROSER3	153.97	**-0.39**	0.24	**8.30e-1**
PRPF18	137.22	**0.01**	0.23	**9.98e-1**
PRPF19	2158.56	**-0.22**	0.19	**9.47e-1**
PRPF3	489.95	**-0.22**	0.2	**9.49e-1**
PRPF31	962.15	**-0.33**	0.2	**8.29e-1**
PRPF38A	1198.66	**0.13**	0.19	**9.87e-1**
PRPF38B	1180.76	**-0.68**	0.2	**7.79e-2**
PRPF39	355.74	**0.08**	0.21	**9.90e-1**
PRPF4	865.13	**-0.14**	0.19	**9.87e-1**
PRPF40A	1928.94	**-0.2**	0.19	**9.49e-1**
PRPF40B	21.26	**-0.01**	0.24	**9.96e-1**
PRPF4B	1669.12	**-0.04**	0.19	**9.93e-1**
PRPF6	1588.76	**-0.14**	0.19	**9.87e-1**
PRPF8	7305.75	**-0.32**	0.18	**7.61e-1**
PRPS1	649.65	**-0.01**	0.19	**9.96e-1**
PRPS2	770.91	**0.11**	0.2	**9.90e-1**
PRPSAP1	199.28	**0.36**	0.22	**8.29e-1**
PRPSAP2	340.35	**0.26**	0.21	**9.25e-1**
PRR11	869.84	**-0.32**	0.2	**8.19e-1**
PRR12	706.74	**-0.26**	0.23	**9.47e-1**
PRR13	902.3	**-0.36**	0.19	**7.13e-1**
PRR14	474.59	**-0.35**	0.23	**8.53e-1**
PRR14L	533.92	**-0.11**	0.2	**9.90e-1**
PRR22	63.6	**-0.38**	0.25	**8.53e-1**
PRR3	441.68	**-0.26**	0.2	**9.21e-1**
PRR5	36.19	**-0.19**	0.25	**9.87e-1**
PRR7	51.24	**0.06**	0.25	**9.93e-1**
PRRC1	645.27	**0.05**	0.2	**9.93e-1**
PRRC2A	5216.9	**-0.66**	0.22	**2.15e-1**
PRRC2B	2372.87	**-0.35**	0.2	**7.57e-1**
PRRC2C	5232.5	**-0.41**	0.18	**5.45e-1**
PRSS53	31.12	**-0.41**	0.25	**8.25e-1**
PRUNE	221.86	**-0.03**	0.22	**9.93e-1**
PSAP	4685.4	**0.81**	0.18	**3.36e-3**
PSAT1	835.89	**0.89**	0.2	**2.67e-3**
PSD3	11.48	**0.12**	0.21	**9.90e-1**
PSD4	442.06	**-0.28**	0.23	**9.42e-1**
PSEN1	247.94	**0.18**	0.22	**9.80e-1**
PSENEN	73	**-0.03**	0.25	**9.93e-1**
PSIP1	2090.71	**-0.51**	0.18	**2.57e-1**
PSKH1	222.33	**0.05**	0.23	**9.93e-1**
PSMA1	770.81	**0.29**	0.2	**8.68e-1**
PSMA2	597.73	**0.22**	0.2	**9.47e-1**
PSMA3	851.16	**0.3**	0.2	**8.64e-1**
PSMA3-AS1	132.8	**0.03**	0.24	**9.93e-1**
PSMA4	1086.72	**0.14**	0.19	**9.87e-1**
PSMA5	713.81	**0.22**	0.19	**9.47e-1**

PSMA6	689.21	**0.26**	0.2	**9.17e-1**
PSMA7	918.73	**0.03**	0.19	**9.93e-1**
PSMB1	699.86	**0.16**	0.19	**9.82e-1**
PSMB10	241.52	**-0.44**	0.24	**7.41e-1**
PSMB2	2534.31	**-0.08**	0.18	**9.90e-1**

PSMB3	584.12	**0.06**	0.2	**9.93e-1**
PSMB4	850.87	**0.13**	0.19	**9.90e-1**
PSMB5	612.39	**-0.07**	0.2	**9.90e-1**
PSMB6	495.98	**-0.19**	0.2	**9.64e-1**
PSMB7	589.36	**-0.05**	0.2	**9.93e-1**
PSMB8	473.99	**-0.04**	0.2	**9.93e-1**
PSMB8-AS1	82.24	**0.04**	0.25	**9.93e-1**
PSMB9	241.51	**-0.1**	0.22	**9.90e-1**
PSMC1	848.01	**-0.28**	0.19	**8.64e-1**
PSMC2	1013.53	**0.09**	0.19	**9.90e-1**
PSMC3	1044.96	**0.02**	0.19	**9.95e-1**
PSMC3IP	156.5	**0.07**	0.23	**9.93e-1**
PSMC4	728.27	**-0.09**	0.19	**9.90e-1**
PSMC5	932.46	**-0.17**	0.19	**9.80e-1**
PSMC6	673.12	**-0.05**	0.2	**9.93e-1**
PSMD1	1656.56	**-0.16**	0.18	**9.74e-1**
PSMD10	204.16	**0.25**	0.23	**9.47e-1**
PSMD11	1343.93	**-0.2**	0.19	**9.49e-1**
PSMD12	728.22	**-0.01**	0.2	**9.98e-1**
PSMD13	860.29	**0.19**	0.19	**9.59e-1**
PSMD14	648.94	**0.39**	0.2	**6.80e-1**
PSMD2	2334.42	**0.06**	0.18	**9.91e-1**
PSMD3	1902.7	**-0.17**	0.2	**9.74e-1**
PSMD4	440.06	**0.17**	0.2	**9.80e-1**
PSMD5	472.41	**-0.16**	0.2	**9.82e-1**
PSMD5-AS1	147.17	**0.25**	0.23	**9.49e-1**
PSMD6	464.44	**0.46**	0.21	**5.89e-1**
PSMD6-AS2	19.23	**0.01**	0.24	**9.96e-1**
PSMD7	1129.14	**0.09**	0.19	**9.90e-1**
PSMD8	1098.03	**-0.21**	0.19	**9.49e-1**
PSMD9	238.43	**0**	0.23	**9.98e-1**
PSME1	927.38	**0.09**	0.19	**9.90e-1**
PSME2	734.79	**-0.05**	0.19	**9.93e-1**
PSME3	2136.09	**-0.23**	0.18	**9.23e-1**
PSME4	1936.05	**0.09**	0.2	**9.90e-1**
PSMF1	926.94	**-0.24**	0.2	**9.42e-1**
PSMG1	561.14	**0.2**	0.2	**9.58e-1**
PSMG2	262.62	**0.48**	0.22	**5.91e-1**
PSMG3	142.4	**-0.09**	0.25	**9.90e-1**
PSMG3-AS1	25.82	**-0.25**	0.25	**9.54e-1**
PSMG4	86.23	**-0.25**	0.25	**9.58e-1**
PSPC1	462.01	**-0.04**	0.2	**9.93e-1**
PSPH	353.17	**0.22**	0.21	**9.51e-1**
PSRC1	25.48	**0.07**	0.25	**9.93e-1**
PSTK	21	**0.1**	0.24	**9.90e-1**
PTAFR	303.46	**-0.71**	0.23	**1.42e-1**
PTAR1	333.98	**0.03**	0.23	**9.93e-1**
PTBP1	3430.76	**-0.39**	0.2	**6.87e-1**
PTBP2	135.1	**-0.09**	0.24	**9.90e-1**
PTBP3	1423.72	**-0.07**	0.19	**9.90e-1**
PTCD2	99.27	**0.09**	0.24	**9.90e-1**
PTCD3	1234.07	**0.02**	0.19	**9.93e-1**
PTCH1	91.65	**-0.04**	0.24	**9.93e-1**
PTDSS1	1634.98	**0.21**	0.19	**9.47e-1**
PTDSS2	165.31	**0.2**	0.24	**9.81e-1**
PTEN	796.86	**0.28**	0.2	**8.92e-1**
PTENP1	12.73	**0.18**	0.22	**9.81e-1**
PTER	455.61	**0.14**	0.21	**9.90e-1**
PTGER4	168.17	**0.16**	0.23	**9.87e-1**
PTGES2	360.53	**-0.03**	0.22	**9.93e-1**
PTGES3	3605.09	**-0.12**	0.19	**9.90e-1**
PTGS1	44.49	**0.09**	0.25	**9.90e-1**
PTK2	435.4	**0.06**	0.21	**9.93e-1**
PTK2B	1602.93	**-0.31**	0.2	**8.52e-1**

PTMA	13550.84	**-0.4**	0.19	**6.06e-1**
PTMS	68.88	**-0.13**	0.25	**9.90e-1**
PTOV1	224.55	**-0.06**	0.24	**9.93e-1**
PTOV1-AS2	54.7	**0.07**	0.25	**9.93e-1**
PTP4A1	1005.03	**0.05**	0.21	**9.93e-1**
PTP4A2	3871.1	**0.03**	0.19	**9.93e-1**
PTPMT1	120.72	**0.04**	0.24	**9.93e-1**
PTPN1	794.92	**-0.21**	0.2	**9.49e-1**
PTPN11	2060.14	**-0.04**	0.19	**9.93e-1**
PTPN12	222.05	**-0.13**	0.23	**9.90e-1**
PTPN18	800.72	**-0.59**	0.2	**2.07e-1**
PTPN2	442.14	**0.18**	0.21	**9.74e-1**
PTPN22	517.05	**-0.23**	0.21	**9.49e-1**
PTPN23	593.69	**-0.49**	0.24	**6.14e-1**
PTPN3	19.23	**-0.01**	0.24	**9.96e-1**
PTPN4	69.67	**0.05**	0.25	**9.93e-1**
PTPN6	303.03	**1.63**	0.22	**0.00e+0**
PTPN7	493.41	**-0.4**	0.21	**6.87e-1**
PTPN9	358.82	**0.09**	0.21	**9.90e-1**
PTPRA	810.61	**0.17**	0.19	**9.75e-1**
PTPRB	15.06	**0.22**	0.23	**9.62e-1**
PTPRC	2551.33	**-0.42**	0.19	**5.60e-1**
PTPRCAP	523.74	**-0.04**	0.24	**9.93e-1**
PTPRE	70.12	**0.65**	0.25	**3.67e-1**
PTPRJ	383.72	**0.02**	0.21	**9.95e-1**
PTPRR	121.64	**0.32**	0.24	**9.11e-1**
PTPRU	17.42	**-0.09**	0.23	**9.90e-1**
PTRH1	16.41	**0.04**	0.23	**9.93e-1**
PTRH2	199.08	**-0.13**	0.23	**9.90e-1**
PTRHD1	129.65	**-0.01**	0.24	**9.97e-1**
PTS	56.07	**0.22**	0.25	**9.74e-1**
PTTG1	439.8	**-0.25**	0.2	**9.40e-1**
PTTG1IP	393.46	**0.22**	0.2	**9.49e-1**
PUF60	886.21	**-0.34**	0.22	**8.39e-1**
PUM1	1192.4	**-0.1**	0.19	**9.90e-1**
PUM2	1310.54	**0.2**	0.2	**9.60e-1**
PURA	234.2	**-0.39**	0.22	**7.46e-1**
PURB	647.57	**-0.07**	0.2	**9.90e-1**
PUS1	319.08	**-0.63**	0.23	**3.32e-1**
PUS10	122.41	**0.08**	0.24	**9.90e-1**
PUS3	161.39	**-0.03**	0.23	**9.93e-1**
PUS7	1164.83	**-0.07**	0.2	**9.90e-1**
PUS7L	226.51	**-0.04**	0.23	**9.93e-1**
PUSL1	60.55	**-0.09**	0.25	**9.90e-1**
PVRIG	269.68	**-0.19**	0.23	**9.81e-1**
PVRL1	1655.88	**0.55**	0.22	**4.11e-1**
PVT1	61.48	**0.28**	0.25	**9.47e-1**
PWAR5	10.41	**-0.18**	0.21	**9.80e-1**
PWARSN	17.08	**-0.06**	0.24	**9.93e-1**
PWP1	817.96	**0.09**	0.19	**9.90e-1**
PWP2	810.12	**-0.21**	0.2	**9.52e-1**
PWWP2A	239.21	**0.01**	0.22	**9.96e-1**
PXK	883.72	**-0.04**	0.2	**9.93e-1**
PXMP2	103.24	**-0.08**	0.24	**9.91e-1**
PXN	202.04	**-0.33**	0.24	**8.97e-1**
PXN-AS1	15.16	**-0.1**	0.22	**9.90e-1**
PYCR1	880.87	**-0.17**	0.22	**9.87e-1**
PYCR2	523.01	**-0.25**	0.22	**9.47e-1**
PYCRL	184.47	**-0.51**	0.25	**6.49e-1**
PYGB	546.16	**-0.09**	0.2	**9.90e-1**
PYGO2	460.14	**-0.33**	0.22	**8.66e-1**
PYROXD1	84.12	**0.33**	0.25	**9.12e-1**
QARS	2922.19	**-0.07**	0.19	**9.90e-1**
QKI	657.35	**0.18**	0.21	**9.80e-1**

QPCTL	234.61	**-0.17**	0.23	**9.87e-1**
QPRT	28.67	**-0.01**	0.25	**9.98e-1**
QRICH1	1199.99	**-0.23**	0.19	**9.42e-1**
QRSL1	595.43	**0.1**	0.2	**9.90e-1**
QSER1	1313.04	**-0.24**	0.2	**9.47e-1**
QSOX1	61.85	**-0.4**	0.25	**8.40e-1**
QSOX2	498.78	**0.06**	0.2	**9.92e-1**
QTRT1	287.56	**0.07**	0.23	**9.93e-1**
QTRTD1	572.29	**-0.07**	0.2	**9.90e-1**
R3HCC1	200.97	**-0.22**	0.23	**9.66e-1**
R3HCC1L	196.8	**0.1**	0.23	**9.90e-1**
R3HDM1	846.45	**-0.25**	0.19	**9.12e-1**
R3HDM2	317.61	**0.09**	0.21	**9.90e-1**
R3HDM4	172.73	**-0.24**	0.25	**9.59e-1**
RAB10	1335.78	**0.09**	0.19	**9.90e-1**
RAB11A	932.5	**0.54**	0.21	**3.52e-1**
RAB11B	382.21	**0**	0.22	**9.98e-1**
RAB11B-AS1	13.97	**0.12**	0.22	**9.90e-1**
RAB11FIP1	627.48	**0.19**	0.2	**9.66e-1**
RAB11FIP2	364.77	**0.11**	0.21	**9.90e-1**
RAB11FIP3	344.57	**-0.17**	0.22	**9.86e-1**
RAB11FIP4	486.42	**-0.44**	0.21	**6.07e-1**
RAB12	127.05	**0.08**	0.24	**9.91e-1**
RAB14	670.32	**0.24**	0.2	**9.43e-1**
RAB18	316.17	**0.12**	0.22	**9.90e-1**
RAB1A	629.54	**0.26**	0.2	**9.20e-1**
RAB1B	1055.29	**-0.37**	0.22	**8.16e-1**
RAB20	61.68	**-0.05**	0.25	**9.93e-1**
RAB21	325.26	**0.24**	0.21	**9.47e-1**
RAB22A	355.39	**0.22**	0.21	**9.49e-1**
RAB23	66.22	**0.22**	0.25	**9.74e-1**
RAB24	83.51	**0.18**	0.25	**9.87e-1**
RAB28	125.63	**0.03**	0.24	**9.93e-1**

RAB29	314.34	**-0.04**	0.21	**9.93e-1**
RAB2A	445.78	**0.24**	0.21	**9.47e-1**
RAB2B	172.54	**0**	0.23	**9.98e-1**
RAB30	716.55	**0.29**	0.2	**8.64e-1**
RAB30-AS1	14.32	**0.11**	0.22	**9.90e-1**
RAB33A	34.34	**-0.02**	0.25	**9.96e-1**
RAB33B	121.19	**0.27**	0.24	**9.49e-1**
RAB35	762.74	**-0.31**	0.21	**8.64e-1**
RAB39A	52.45	**-0.27**	0.25	**9.49e-1**
RAB39B	55.44	**0.64**	0.25	**4.11e-1**
RAB3A	77.83	**-0.18**	0.25	**9.87e-1**
RAB3GAP1	229.81	**0.32**	0.22	**8.66e-1**
RAB3GAP2	495.06	**0.22**	0.21	**9.49e-1**
RAB3IP	252.53	**-0.06**	0.22	**9.93e-1**
RAB40C	124.61	**-0.19**	0.25	**9.87e-1**
RAB5A	332.62	**0.15**	0.21	**9.87e-1**
RAB5B	485.53	**0.23**	0.2	**9.47e-1**
RAB5C	722.12	**-0.39**	0.21	**7.05e-1**
RAB6A	659.71	**0.13**	0.2	**9.90e-1**
RAB7A	1701.13	**0.03**	0.19	**9.93e-1**
RAB8A	1082.42	**-0.41**	0.19	**6.03e-1**
RAB8B	426.43	**0.61**	0.21	**2.45e-1**
RAB9A	91.38	**0.14**	0.25	**9.90e-1**
RABAC1	139.4	**-0.01**	0.25	**9.97e-1**
RABEP1	1270.34	**0.17**	0.19	**9.80e-1**
RABEP2	170.14	**0.01**	0.24	**9.96e-1**
RABEPK	230.59	**-0.04**	0.22	**9.93e-1**
RABGAP1	492.44	**0.11**	0.21	**9.90e-1**
RABGAP1L	1039.52	**-0.25**	0.2	**9.25e-1**
RABGEF1	383.6	**0.29**	0.21	**8.78e-1**

RABGGTA	152.7	**0.05**	0.24	**9.93e-1**
RABGGTB	497.96	**0.07**	0.2	**9.90e-1**
RABIF	133.92	**0.24**	0.24	**9.54e-1**
RABL2A	13.25	**0.06**	0.22	**9.93e-1**
RABL2B	148.17	**-0.15**	0.23	**9.90e-1**
RABL3	271.71	**-0.12**	0.22	**9.90e-1**
RABL6	1377.95	**-0.27**	0.21	**9.25e-1**
RAC1	1810.07	**0.14**	0.19	**9.87e-1**
RAC2	1995.72	**-0.28**	0.22	**9.17e-1**
RAC3	58.99	**-0.23**	0.25	**9.71e-1**
RACGAP1	735.67	**-0.19**	0.2	**9.59e-1**
RAD1	345.93	**0.05**	0.21	**9.93e-1**
RAD17	701.26	**-0.09**	0.2	**9.90e-1**
RAD18	536.87	**-0.12**	0.21	**9.90e-1**
RAD21	2429.54	**0.31**	0.2	**8.38e-1**
RAD23A	1072.29	**-0.33**	0.21	**8.41e-1**
RAD23B	2543.18	**0.04**	0.19	**9.93e-1**
RAD50	774.6	**-0.16**	0.2	**9.80e-1**
RAD51	272.86	**0.02**	0.21	**9.93e-1**
RAD51AP1	225.82	**0.12**	0.22	**9.90e-1**
RAD51-AS1	10.86	**-0.15**	0.21	**9.87e-1**
RAD51B	39.46	**0.3**	0.25	**9.47e-1**
RAD51C	163.4	**0.06**	0.23	**9.93e-1**
RAD51D	79.1	**-0.03**	0.25	**9.93e-1**
RAD52	112.47	**-0.06**	0.24	**9.93e-1**
RAD54B	140.48	**0.05**	0.23	**9.93e-1**
RAD54L	732.61	**-0.17**	0.2	**9.74e-1**
RAD54L2	206.1	**-0.26**	0.22	**9.47e-1**
RAD9A	175.46	**-0.33**	0.24	**8.92e-1**
RAE1	538.24	**-0.06**	0.2	**9.91e-1**
RAET1K	25.47	**0.1**	0.25	**9.90e-1**
RAF1	651	**0.08**	0.2	**9.90e-1**
RAI1	618.51	**-0.5**	0.24	**6.28e-1**
RALA	526.23	**0.27**	0.2	**9.08e-1**
RALB	28.68	**0.51**	0.25	**6.34e-1**
RALBP1	777.72	**-0.07**	0.2	**9.90e-1**
RALGAPA2	203.98	**0.1**	0.22	**9.90e-1**
RALGAPB	834.56	**0.02**	0.2	**9.95e-1**
RALGDS	307.7	**-0.03**	0.22	**9.93e-1**
RALGPS1	74.18	**-0.02**	0.25	**9.95e-1**
RALGPS2	485.61	**0**	0.21	**9.99e-1**
RALY	1150.31	**-0.28**	0.22	**9.25e-1**
RAMP1	26.45	**-0.08**	0.25	**9.91e-1**
RAN	3660.02	**0.19**	0.19	**9.58e-1**
RANBP1	1550.05	**0.23**	0.19	**9.32e-1**
RANBP10	471.88	**-0.22**	0.22	**9.54e-1**
RANBP2	1427.94	**-0.02**	0.2	**9.93e-1**
RANBP3	652.62	**-0.18**	0.2	**9.72e-1**
RANBP6	254.99	**0.23**	0.23	**9.58e-1**
RANBP9	490.1	**0.16**	0.21	**9.86e-1**
RANGAP1	1649.06	**-0.32**	0.21	**8.52e-1**
RANGRF	195.17	**-0.16**	0.23	**9.88e-1**
RAP1A	591.72	**0.31**	0.21	**8.73e-1**
RAP1B	1129.46	**0.06**	0.2	**9.92e-1**
RAP1GAP2	22.66	**-0.32**	0.24	**9.17e-1**
RAP1GDS1	308.27	**0.21**	0.21	**9.60e-1**
RAP2A	384.12	**0.04**	0.21	**9.93e-1**
RAP2B	161.49	**0.11**	0.23	**9.90e-1**
RAP2C	252.35	**0.34**	0.22	**8.52e-1**
RAPGEF1	2142.37	**-0.2**	0.19	**9.55e-1**
RAPGEF2	560.77	**-0.6**	0.2	**2.23e-1**
RAPGEF5	179.01	**0.15**	0.23	**9.90e-1**
RAPGEF6	430.98	**0.06**	0.22	**9.93e-1**

RAPGEFL1	26.75	**-0.04**	0.25	**9.93e-1**
RARA	334.32	**-0.33**	0.24	**8.98e-1**
RARG	44.56	**-0.15**	0.25	**9.90e-1**
RARRES3	15.9	**0.2**	0.23	**9.80e-1**
RARS	729.71	**0.12**	0.21	**9.90e-1**
RARS2	320.87	**0.16**	0.22	**9.87e-1**
RASA1	333.62	**-0.02**	0.22	**9.96e-1**
RASA2	217.39	**0.37**	0.23	**8.38e-1**
RASA4	18.29	**-0.13**	0.24	**9.90e-1**
RASA4B	21.77	**0.11**	0.24	**9.90e-1**
RASA4CP	26.17	**-0.24**	0.25	**9.59e-1**
RASAL1	139.01	**-0.29**	0.24	**9.42e-1**
RASGEF1B	76.27	**0.48**	0.25	**6.87e-1**
RASGRF1	13.7	**0.03**	0.22	**9.93e-1**
RASGRP1	478.94	**0.46**	0.21	**5.60e-1**
RASGRP2	507.82	**-0.19**	0.2	**9.72e-1**
RASGRP3	1061.57	**0.64**	0.2	**1.03e-1**
RASL11A	14.16	**0.04**	0.22	**9.93e-1**
RASSF1	83.43	**0.04**	0.25	**9.93e-1**
RASSF2	1942.25	**-0.22**	0.18	**9.39e-1**
RASSF3	584.49	**-0.01**	0.2	**9.96e-1**
RASSF4	93.58	**-0.16**	0.25	**9.90e-1**
RASSF5	572.84	**-0.03**	0.2	**9.93e-1**
RASSF6	1009.41	**-0.9**	0.19	**1.79e-3**
RASSF7	44.1	**-0.04**	0.25	**9.93e-1**
RAVER1	1664.74	**-0.28**	0.23	**9.45e-1**
RB1	761.37	**-0.03**	0.21	**9.93e-1**
RB1CC1	558.65	**0.05**	0.21	**9.93e-1**
RBAK	384.34	**-0.06**	0.21	**9.92e-1**
RBBP4	4070.38	**0.33**	0.18	**7.57e-1**
RBBP5	333.73	**0.1**	0.21	**9.90e-1**
RBBP6	1389.38	**-0.32**	0.19	**7.89e-1**
RBBP7	1957.71	**-0.17**	0.18	**9.66e-1**
RBBP8	1286.63	**0.21**	0.2	**9.50e-1**
RBBP9	38.75	**-0.02**	0.25	**9.94e-1**
RBCK1	470.55	**-0.15**	0.23	**9.89e-1**
RBFA	286.82	**0.03**	0.21	**9.93e-1**
RBFOX2	537.59	**-0.08**	0.2	**9.90e-1**
RBL1	471.96	**-0.03**	0.2	**9.93e-1**
RBL2	608.51	**0.44**	0.2	**5.79e-1**
RBM10	973.32	**-0.26**	0.21	**9.30e-1**
RBM12	1550.83	**-0.61**	0.18	**1.02e-1**
RBM12B	303.98	**-0.14**	0.21	**9.89e-1**
RBM14	939.6	**-0.43**	0.22	**6.84e-1**
RBM15	197.2	**-0.18**	0.22	**9.86e-1**
RBM15B	812.25	**-0.21**	0.2	**9.52e-1**
RBM17	1057.5	**0.06**	0.19	**9.92e-1**
RBM18	278.67	**-0.07**	0.22	**9.90e-1**
RBM19	706.4	**-0.23**	0.2	**9.47e-1**
RBM22	536.96	**0.23**	0.2	**9.47e-1**
RBM23	518.55	**-0.09**	0.2	**9.90e-1**
RBM25	2787.29	**-0.67**	0.18	**3.73e-2**
RBM26	1211.16	**-0.3**	0.19	**8.41e-1**
RBM26-AS1	14.66	**0.01**	0.23	**9.96e-1**
RBM27	1037.09	**-0.08**	0.2	**9.90e-1**
RBM28	779.68	**-0.3**	0.19	**8.51e-1**
RBM3	1623.73	**0.05**	0.18	**9.93e-1**
RBM33	843.75	**-0.22**	0.19	**9.47e-1**
RBM34	427.34	**-0.08**	0.21	**9.90e-1**
RBM38	1762	**-0.35**	0.21	**8.06e-1**
RBM39	1993.31	**0.04**	0.19	**9.93e-1**
RBM4	259.52	**-0.15**	0.22	**9.87e-1**
RBM41	154.15	**-0.09**	0.23	**9.90e-1**
RBM42	374.6	**-0.33**	0.24	**8.86e-1**
RBM45	86.81	**0.12**	0.25	**9.90e-1**

RBM48	50.52	**0.06**	0.25	**9.93e-1**
RBM4B	114.38	**0.12**	0.24	**9.90e-1**
RBM5	803.06	**0.04**	0.19	**9.93e-1**
RBM6	1896.97	**-0.12**	0.18	**9.90e-1**
RBM7	233.06	**0.03**	0.23	**9.93e-1**
RBM8A	861.01	**-0.05**	0.2	**9.93e-1**
RBMS2	38.14	**-0.15**	0.25	**9.90e-1**
RBMX	3035.45	**0.03**	0.18	**9.93e-1**

RBMX2	111.54	**-0.38**	0.24	**8.39e-1**
RBMXL1	192.73	**0.07**	0.23	**9.91e-1**
RBPJ	814.6	**-0.08**	0.2	**9.90e-1**
RBSN	150.25	**-0.11**	0.23	**9.90e-1**
RBX1	259.13	**0.15**	0.22	**9.88e-1**
RC3H1	354.16	**-0.09**	0.22	**9.90e-1**
RC3H2	362.02	**-0.03**	0.21	**9.93e-1**
RCAN3	72.44	**0.2**	0.25	**9.83e-1**
RCBTB1	265.29	**0.33**	0.21	**8.52e-1**
RCBTB2	41.92	**-0.02**	0.25	**9.94e-1**
RCC1	1929.9	**-0.19**	0.19	**9.58e-1**
RCC2	3314.59	**-0.1**	0.18	**9.90e-1**
RCCD1	166.69	**0.21**	0.24	**9.77e-1**
RCE1	88.39	**-0.09**	0.25	**9.90e-1**
RCHY1	210.16	**0.37**	0.24	**8.39e-1**
RCL1	308.21	**0.03**	0.21	**9.93e-1**
RCN2	273.75	**0.38**	0.22	**8.03e-1**
RCOR1	694.78	**0.25**	0.2	**9.25e-1**
RCOR3	263.39	**0.07**	0.22	**9.91e-1**
RCSD1	1227.04	**-0.43**	0.19	**5.37e-1**
RDH10	96.77	**0.15**	0.24	**9.90e-1**
RDH11	463.78	**-0.05**	0.2	**9.93e-1**
RDH13	245.36	**-0.69**	0.23	**2.07e-1**
REC8	431.79	**-0.44**	0.21	**6.14e-1**
RECQL	604.4	**0.24**	0.21	**9.47e-1**
RECQL4	468.73	**-0.36**	0.24	**8.56e-1**
RECQL5	397.31	**0.3**	0.23	**9.12e-1**
REEP3	90.55	**0.13**	0.25	**9.90e-1**
REEP4	284.7	**-0.26**	0.24	**9.49e-1**
REEP5	422.26	**0.11**	0.21	**9.90e-1**
REEP6	44.92	**-0.12**	0.25	**9.90e-1**
REL	890.13	**-0.59**	0.2	**2.31e-1**
RELA	737.92	**-0.44**	0.21	**6.07e-1**
RELB	426.96	**0.74**	0.22	**8.97e-2**
RELT	206.56	**-0.19**	0.24	**9.83e-1**
REPIN1	1443.06	**-0.36**	0.22	**8.30e-1**
REPS1	506.91	**-0.16**	0.21	**9.86e-1**
RER1	427.73	**0.26**	0.2	**9.25e-1**
RERE	2248.37	**-0.49**	0.21	**5.31e-1**
REST	409.47	**0.11**	0.22	**9.90e-1**
RETSAT	189.1	**-0.14**	0.22	**9.90e-1**
REV1	330.11	**0.1**	0.22	**9.90e-1**
REV3L	1002.42	**0.11**	0.2	**9.90e-1**
REXO1	401.29	**-0.45**	0.25	**7.40e-1**
REXO2	193.59	**-0.06**	0.23	**9.93e-1**
REXO4	478.02	**-0.25**	0.22	**9.47e-1**
RFC1	1499.83	**-0.29**	0.19	**8.51e-1**
RFC2	526.53	**0.19**	0.2	**9.64e-1**
RFC3	768.23	**0**	0.21	**9.98e-1**
RFC4	372.9	**0.32**	0.21	**8.52e-1**
RFC5	459.55	**-0.2**	0.2	**9.58e-1**
RFFL	199.53	**-0.37**	0.23	**8.39e-1**
RFK	293.12	**-0.06**	0.22	**9.93e-1**
RFNG	94.59	**-0.15**	0.25	**9.90e-1**
RFT1	354.01	**0.13**	0.21	**9.90e-1**

RFTN1	928.19	**-0.23**	0.2	**9.45e-1**
RFWD2	330.71	**0.26**	0.22	**9.47e-1**
RFWD3	1281.35	**-0.12**	0.19	**9.90e-1**
RFX1	111.92	**-0.13**	0.25	**9.90e-1**
RFX2	119.94	**-0.15**	0.24	**9.90e-1**
RFX3	95.72	**0.2**	0.25	**9.81e-1**
RFX5	1383.3	**0.1**	0.19	**9.90e-1**
RFX7	809.29	**-0.4**	0.2	**6.47e-1**
RFXANK	328.86	**-0.44**	0.23	**6.69e-1**
RFXAP	97.61	**0.06**	0.24	**9.93e-1**
RGCC	24.17	**-0.18**	0.24	**9.87e-1**
RGL1	22.63	**0.06**	0.24	**9.93e-1**
RGL2	193.38	**-0.22**	0.25	**9.72e-1**
RGMB	76.43	**0**	0.25	**9.98e-1**
RGP1	144.67	**-0.33**	0.24	**8.88e-1**
RGS1	132.44	**1.19**	0.24	**5.35e-4**
RGS10	204.02	**0.44**	0.22	**6.69e-1**
RGS13	1197.75	**0.23**	0.21	**9.47e-1**
RGS14	368.1	**-0.34**	0.22	**8.52e-1**
RGS16	227.19	**0.14**	0.22	**9.90e-1**
RGS19	309.57	**0.21**	0.23	**9.66e-1**
RGS2	10.82	**0.05**	0.2	**9.93e-1**
RGS3	182.52	**-0.46**	0.24	**7.09e-1**
RGS5	12.88	**0.01**	0.22	**9.96e-1**
RHBDD1	169.88	**0.26**	0.23	**9.47e-1**
RHBDD2	376.94	**-0.21**	0.22	**9.66e-1**
RHBDD3	148.42	**-0.3**	0.25	**9.40e-1**
RHBDF2	379.89	**-0.38**	0.24	**8.38e-1**

RHBDL1	23.51	**0.08**	0.24	**9.90e-1**
RHEB	657.31	**0.43**	0.2	**5.94e-1**
RHNO1	345.53	**-0.44**	0.21	**6.06e-1**
RHOA	2852.42	**0.22**	0.18	**9.47e-1**
RHOBTB2	1870.62	**0.28**	0.22	**9.23e-1**
RHOF	343.55	**0.07**	0.22	**9.90e-1**
RHOG	446.04	**-0.16**	0.23	**9.89e-1**
RHOH	587.7	**-0.13**	0.2	**9.90e-1**
RHOQ	767.84	**0.42**	0.2	**6.03e-1**
RHOT1	379.72	**0.29**	0.22	**9.13e-1**
RHOT2	634.72	**-0.27**	0.23	**9.42e-1**
RHOV	93.01	**-0.11**	0.25	**9.90e-1**
RHPN2	129.58	**-0.25**	0.23	**9.49e-1**
RIC1	681.74	**0.14**	0.2	**9.88e-1**
RIC8A	717.41	**-0.21**	0.21	**9.56e-1**
RICTOR	326.9	**0.08**	0.22	**9.90e-1**
RIF1	625.56	**0.02**	0.21	**9.94e-1**
RILP	11.24	**-0.12**	0.21	**9.90e-1**
RILPL2	170.81	**0.18**	0.24	**9.87e-1**
RIMKLA	147.33	**0.15**	0.23	**9.90e-1**
RIMKLB	128.33	**-0.18**	0.24	**9.87e-1**
RIMS2	36.6	**-0.18**	0.25	**9.87e-1**
RIMS3	1576.07	**0.57**	0.2	**2.48e-1**
RIN1	19.54	**-0.19**	0.24	**9.81e-1**
RING1	192.67	**0.01**	0.23	**9.96e-1**
RINL	148.82	**-0.26**	0.25	**9.52e-1**
RINT1	416.72	**0.13**	0.21	**9.90e-1**
RIOK1	544.79	**-0.11**	0.2	**9.90e-1**
RIOK2	259.45	**0.09**	0.22	**9.90e-1**
RIOK3	287.02	**0.31**	0.22	**8.84e-1**
RIPK1	225.99	**0.09**	0.22	**9.90e-1**
RIPK2	342.97	**0.2**	0.22	**9.64e-1**
RIT1	52.93	**0.34**	0.25	**9.06e-1**
RITA1	598.31	**-0.52**	0.23	**5.45e-1**
RLF	477.12	**0.03**	0.21	**9.93e-1**

RLIM	349.58	**0.16**	0.22	**9.87e-1**
RLTPR	1108.67	**-0.25**	0.22	**9.49e-1**
RMDN1	203.43	**0.28**	0.23	**9.30e-1**
RMDN3	180.17	**-0.11**	0.23	**9.90e-1**
RMI1	399.21	**0.06**	0.22	**9.93e-1**
RMI2	265.1	**0.99**	0.23	**5.15e-3**
RMND1	126.57	**0.22**	0.24	**9.72e-1**
RMND5A	969.25	**0.05**	0.2	**9.93e-1**
RMND5B	158.76	**0.01**	0.23	**9.96e-1**
RMRP	16.34	**-0.4**	0.22	**7.33e-1**
RNASEH1	406.17	**-0.07**	0.21	**9.90e-1**
RNASEH1-AS1	64.77	**-0.13**	0.25	**9.90e-1**
RNASEH2A	249.25	**-0.07**	0.22	**9.91e-1**
RNASEH2B	229.41	**0.31**	0.23	**9.04e-1**
RNASEH2C	250.46	**-0.11**	0.23	**9.90e-1**
RNASEK	21.64	**-0.2**	0.24	**9.80e-1**
RNASET2	11.56	**0.23**	0.22	**9.50e-1**
RND1	86.6	**0.07**	0.25	**9.91e-1**
RNF10	964.43	**0.01**	0.19	**9.98e-1**
RNF103	101.42	**0.35**	0.25	**8.73e-1**
RNF11	93.07	**0.31**	0.24	**9.25e-1**
RNF111	377.2	**0.09**	0.21	**9.90e-1**
RNF113A	86.97	**0.26**	0.25	**9.50e-1**
RNF114	483.36	**0.15**	0.2	**9.87e-1**
RNF115	299.24	**0.06**	0.21	**9.93e-1**
RNF121	131.66	**0.19**	0.23	**9.81e-1**
RNF123	312.54	**-0.09**	0.22	**9.90e-1**
RNF126	407.9	**-0.2**	0.24	**9.80e-1**
RNF13	222.87	**0.11**	0.23	**9.90e-1**
RNF135	23.95	**0.05**	0.25	**9.93e-1**
RNF138	637.51	**-0.12**	0.2	**9.90e-1**
RNF139	228.46	**0.48**	0.23	**6.07e-1**
RNF14	363.82	**0.53**	0.22	**4.37e-1**
RNF141	214.52	**0.1**	0.23	**9.90e-1**
RNF144B	872.67	**-0.58**	0.2	**2.15e-1**
RNF145	358.43	**1.18**	0.22	**5.60e-5**
RNF146	90.98	**0.64**	0.24	**3.61e-1**
RNF149	149.95	**0.39**	0.24	**8.23e-1**
RNF166	177.31	**-0.04**	0.24	**9.93e-1**
RNF167	334.03	**-0.31**	0.22	**8.73e-1**
RNF168	444.12	**-0.17**	0.2	**9.80e-1**
RNF169	270.13	**-0.1**	0.22	**9.90e-1**
RNF170	78.17	**0.29**	0.25	**9.47e-1**
RNF181	114.52	**0.3**	0.24	**9.32e-1**
RNF185	273.52	**-0.18**	0.22	**9.81e-1**
RNF187	1093.9	**0.44**	0.22	**6.74e-1**
RNF19A	181.1	**0.15**	0.23	**9.88e-1**
RNF19B	1318.15	**-0.01**	0.19	**9.96e-1**

RNF20	653.56	**0.03**	0.2	**9.93e-1**
RNF213	607.44	**0.01**	0.2	**9.96e-1**
RNF214	172.66	**-0.18**	0.23	**9.86e-1**
RNF215	27.86	**0.17**	0.25	**9.89e-1**
RNF216	597.47	**-0.07**	0.2	**9.90e-1**
RNF216P1	221.01	**-0.27**	0.22	**9.30e-1**
RNF219	393.25	**-0.07**	0.22	**9.90e-1**
RNF220	770.02	**0.06**	0.2	**9.91e-1**
RNF24	58.55	**0.03**	0.25	**9.93e-1**
RNF25	144.27	**-0.08**	0.23	**9.90e-1**
RNF26	564.89	**-0.28**	0.22	**9.25e-1**
RNF31	371.76	**-0.12**	0.21	**9.90e-1**
RNF32	22.48	**-0.09**	0.24	**9.90e-1**
RNF34	344.34	**0.08**	0.21	**9.90e-1**
RNF38	582.48	**0.13**	0.2	**9.90e-1**

RNF4	1153.47	**-0.25**	0.19	**9.01e-1**
RNF40	1119.3	**-0.26**	0.2	**9.23e-1**
RNF41	183.78	**0.13**	0.23	**9.90e-1**
RNF44	462.87	**-0.11**	0.24	**9.90e-1**
RNF6	657.51	**-0.26**	0.2	**9.10e-1**
RNF7	185.58	**-0.1**	0.23	**9.90e-1**
RNF8	600.98	**0**	0.2	**9.98e-1**
RNFT1	78.3	**-0.11**	0.25	**9.90e-1**
RNFT2	39.17	**-0.21**	0.25	**9.81e-1**
RNGTT	713.72	**0.17**	0.2	**9.80e-1**
RNH1	597.72	**-0.37**	0.23	**8.39e-1**
RNMT	427.92	**0.38**	0.21	**7.41e-1**
RNMTL1	253.95	**-0.11**	0.22	**9.90e-1**
RNPC3	151.35	**0.01**	0.24	**9.96e-1**
RNPEP	233.38	**0.14**	0.22	**9.90e-1**
RNPEPL1	298.17	**-0.27**	0.24	**9.49e-1**
RNPS1	2285.86	**-0.33**	0.19	**7.97e-1**
ROCK1	1103.9	**-0.02**	0.19	**9.93e-1**
ROCK1P1	12.12	**0.44**	0.21	**6.28e-1**
ROCK2	446.69	**0**	0.21	**9.98e-1**
ROGDI	54.29	**-0.37**	0.25	**8.66e-1**
ROMO1	125.45	**-0.21**	0.24	**9.74e-1**
ROR1	59.64	**-0.83**	0.25	**1.04e-1**
RP2	110.32	**-0.05**	0.24	**9.93e-1**
RP9	62.39	**0.1**	0.25	**9.90e-1**
RPA1	1426.5	**0.06**	0.19	**9.91e-1**
RPA2	550.15	**0.08**	0.2	**9.90e-1**
RPA3	124.33	**0.27**	0.24	**9.47e-1**
RPAIN	127.05	**0.18**	0.24	**9.87e-1**
RPAP1	306.2	**-0.33**	0.23	**8.73e-1**
RPAP2	120.32	**0.13**	0.24	**9.90e-1**
RPAP3	743.46	**-0.19**	0.2	**9.66e-1**
RPARP-AS1	189.28	**-0.14**	0.22	**9.90e-1**
RPE	674.43	**0.01**	0.2	**9.96e-1**
RPF1	191.65	**-0.11**	0.23	**9.90e-1**
RPF2	730.72	**0**	0.2	**9.98e-1**
RPGR	134.88	**0.24**	0.24	**9.54e-1**
RPGRIP1L	128.2	**-0.02**	0.24	**9.95e-1**
RPIA	374.36	**-0.15**	0.21	**9.87e-1**
RPL10	2504.4	**-0.2**	0.21	**9.66e-1**
RPL10A	2632.09	**0.36**	0.18	**6.59e-1**
RPL11	3271.88	**0.15**	0.18	**9.80e-1**
RPL12	2649.24	**0.06**	0.18	**9.91e-1**
RPL13	2280.57	**0.41**	0.18	**5.68e-1**
RPL13A	642.37	**0.75**	0.2	**2.42e-2**
RPL13AP20	22.32	**0.59**	0.24	**4.59e-1**
RPL14	3378.59	**0.28**	0.18	**8.58e-1**
RPL15	3689.55	**0.22**	0.18	**9.42e-1**
RPL17	175.07	**-0.26**	0.21	**9.33e-1**
RPL18	2105.62	**-0.11**	0.2	**9.90e-1**
RPL18A	2517.86	**-0.24**	0.21	**9.47e-1**
RPL19	4232.31	**0.26**	0.18	**8.64e-1**
RPL22	1540.27	**0.11**	0.19	**9.90e-1**
RPL22L1	570.7	**0.05**	0.2	**9.93e-1**
RPL23	1842.34	**0.39**	0.19	**6.49e-1**
RPL23A	2295.24	**0.22**	0.18	**9.42e-1**
RPL23AP53	154.27	**0.13**	0.23	**9.90e-1**
RPL23AP7	28.75	**0.02**	0.25	**9.95e-1**
RPL23AP82	62.15	**-0.22**	0.25	**9.80e-1**
RPL24	1456.28	**0**	0.19	**9.99e-1**
RPL26	2418.56	**0.26**	0.19	**8.87e-1**
RPL26L1	124.07	**-0.03**	0.24	**9.93e-1**
RPL27	1529.72	**0.02**	0.18	**9.93e-1**
RPL27A	3191.56	**0.11**	0.18	**9.90e-1**

RPL28	3271.35	**-0.15**	0.19	**9.86e-1**
RPL29	1764.04	**0.03**	0.19	**9.93e-1**
RPL3	8225.4	**0.29**	0.18	**8.34e-1**
RPL30	1874.23	**0.17**	0.18	**9.72e-1**

RPL31	818.18	**0.48**	0.19	**4.32e-1**
RPL32	2438.82	**0.24**	0.18	**9.06e-1**
RPL32P3	23.35	**-0.1**	0.25	**9.90e-1**
RPL34	532.58	**0.44**	0.2	**5.86e-1**
RPL35	1822.92	**0.14**	0.18	**9.86e-1**
RPL35A	1099.8	**-0.14**	0.19	**9.87e-1**
RPL36	880.28	**-0.14**	0.21	**9.88e-1**
RPL36A	43.06	**-0.14**	0.25	**9.90e-1**
RPL36AL	695.38	**-0.03**	0.19	**9.93e-1**
RPL37	1514.56	**0.05**	0.19	**9.93e-1**
RPL37A	1072	**0.14**	0.19	**9.87e-1**
RPL38	720.67	**0.2**	0.19	**9.54e-1**
RPL39	653.55	**0.16**	0.2	**9.83e-1**
RPL39L	61.32	**-0.25**	0.25	**9.59e-1**
RPL4	9640.13	**0.24**	0.18	**9.06e-1**
RPL41	773.25	**0.14**	0.21	**9.88e-1**
RPL5	4320.1	**0.4**	0.19	**5.91e-1**
RPL6	4849.48	**0.24**	0.18	**9.10e-1**
RPL7	3910.08	**0.41**	0.19	**5.84e-1**
RPL7A	4990.04	**0.16**	0.18	**9.77e-1**
RPL7L1	909.21	**-0.31**	0.19	**8.30e-1**
RPL8	5063.51	**-0.13**	0.22	**9.90e-1**
RPL9	1987.46	**0.2**	0.18	**9.49e-1**
RPLP0	5379.35	**0.07**	0.18	**9.90e-1**
RPLP1	1367.58	**-0.22**	0.23	**9.58e-1**
RPLP2	1315.67	**0.24**	0.19	**9.23e-1**
RPN1	2010.02	**0.1**	0.18	**9.90e-1**
RPN2	2243.57	**0.2**	0.18	**9.49e-1**
RPP14	288.52	**-0.11**	0.21	**9.90e-1**
RPP25L	67.55	**-0.06**	0.25	**9.93e-1**
RPP30	257.66	**-0.11**	0.22	**9.90e-1**
RPP38	125.82	**0.05**	0.24	**9.93e-1**
RPP40	140.51	**-0.22**	0.23	**9.61e-1**
RPRD1A	512.84	**0.06**	0.21	**9.91e-1**
RPRD1B	586.11	**-0.02**	0.2	**9.94e-1**
RPRD2	1171.53	**-0.42**	0.19	**5.83e-1**
RPS10	92.82	**-1.04**	0.25	**1.20e-2**
RPS10P7	10.71	**0.05**	0.21	**9.93e-1**
RPS11	3033.31	**-0.08**	0.19	**9.90e-1**
RPS12	1157.07	**0.47**	0.19	**4.07e-1**
RPS13	1236.7	**0.47**	0.2	**4.84e-1**
RPS14	1447.29	**-0.01**	0.19	**9.96e-1**
RPS15	1390.77	**-0.09**	0.2	**9.90e-1**
RPS15A	1673.57	**-0.01**	0.18	**9.96e-1**
RPS16	2243	**0.21**	0.18	**9.47e-1**
RPS17	255.77	**0.62**	0.22	**2.45e-1**
RPS18	2811.29	**0.25**	0.18	**8.80e-1**
RPS19	1468.07	**0.24**	0.19	**9.25e-1**
RPS19BP1	232.24	**-0.35**	0.24	**8.64e-1**
RPS2	6069.69	**-0.09**	0.21	**9.90e-1**
RPS20	1839.27	**0.26**	0.19	**8.98e-1**
RPS21	721.02	**0.09**	0.19	**9.90e-1**
RPS23	2397.04	**0.2**	0.18	**9.47e-1**
RPS24	2375.65	**0.2**	0.18	**9.49e-1**
RPS25	1543.34	**-0.11**	0.19	**9.90e-1**
RPS26	1148.94	**-0.11**	0.19	**9.90e-1**
RPS27	874.04	**0.18**	0.19	**9.63e-1**
RPS27A	1215.85	**0.13**	0.19	**9.88e-1**
RPS27L	119.96	**0.22**	0.24	**9.66e-1**
RPS28	692.66	**0.15**	0.19	**9.86e-1**

RPS29	335.65	**0.03**	0.21	**9.93e-1**
RPS3	4048.83	**0.03**	0.18	**9.93e-1**
RPS3A	3499.12	**0.57**	0.19	**2.11e-1**
RPS4X	3884.04	**0.19**	0.18	**9.54e-1**
RPS4Y1	1026.05	**0.41**	0.19	**5.88e-1**
RPS5	2307.91	**0.25**	0.18	**9.03e-1**
RPS6	5789.45	**0.36**	0.18	**6.40e-1**
RPS6KA1	953.3	**0.17**	0.19	**9.73e-1**
RPS6KA3	686.52	**0.01**	0.21	**9.98e-1**
RPS6KA4	237.43	**-0.36**	0.25	**8.69e-1**
RPS6KA5	71.23	**-0.07**	0.25	**9.92e-1**
RPS6KB1	776.18	**-0.31**	0.19	**8.39e-1**
RPS6KB2	298.5	**-0.45**	0.24	**7.04e-1**
RPS6KC1	45.67	**-0.1**	0.25	**9.90e-1**
RPS7	2704.52	**0.21**	0.18	**9.47e-1**
RPS8	3567.24	**0.49**	0.18	**3.20e-1**
RPS9	1788.18	**0.21**	0.19	**9.47e-1**
RPSA	4530.66	**0.28**	0.18	**8.45e-1**
RPSAP58	83.82	**0.29**	0.25	**9.47e-1**
RPTOR	516.46	**-0.23**	0.21	**9.49e-1**
RPUSD1	415.29	**-0.44**	0.24	**7.56e-1**
RPUSD2	174.45	**0**	0.23	**9.99e-1**
RPUSD3	116.86	**-0.18**	0.24	**9.87e-1**

RPUSD4	314.78	**0.22**	0.21	**9.49e-1**
RQCD1	1150.51	**-0.09**	0.19	**9.90e-1**
RRAGA	137.95	**0.21**	0.23	**9.74e-1**
RRAGB	33.72	**-0.08**	0.25	**9.91e-1**
RRAGC	282.49	**0.24**	0.22	**9.49e-1**
RRAS	11.38	**0.14**	0.21	**9.90e-1**
RRAS2	533.5	**0.47**	0.21	**5.62e-1**
RRBP1	1804.12	**0.04**	0.19	**9.93e-1**
RREB1	339.01	**-0.24**	0.21	**9.47e-1**
RRM1	1755.39	**0.23**	0.19	**9.47e-1**
RRM2	1539.25	**-0.07**	0.19	**9.90e-1**
RRM2B	1061.84	**-0.3**	0.2	**8.64e-1**
RRN3	477.09	**0.1**	0.2	**9.90e-1**
RRN3P1	99.47	**0.32**	0.25	**9.12e-1**
RRN3P2	27.22	**0.17**	0.25	**9.89e-1**
RRN3P3	62.57	**0.13**	0.25	**9.90e-1**
RRNAD1	77.72	**0.22**	0.25	**9.80e-1**
RRP1	627.66	**-0.24**	0.21	**9.47e-1**
RRP12	998.46	**-0.21**	0.2	**9.49e-1**
RRP15	406.31	**-0.09**	0.21	**9.90e-1**
RRP1B	2627.37	**-0.39**	0.18	**5.91e-1**
RRP36	337.32	**0**	0.22	**9.99e-1**
RRP7A	886.49	**-0.25**	0.21	**9.47e-1**
RRP7BP	247.66	**-0.41**	0.22	**7.31e-1**
RRP8	209.43	**-0.23**	0.22	**9.49e-1**
RRP9	479.03	**-0.41**	0.22	**7.04e-1**
RRS1	539.55	**-0.53**	0.22	**4.44e-1**
RSAD1	135.19	**0.05**	0.24	**9.93e-1**
RSBN1	197.12	**0.08**	0.23	**9.90e-1**
RSBN1L	449.24	**-0.09**	0.21	**9.90e-1**
RSC1A1	208.57	**-0.41**	0.22	**7.36e-1**
RSF1	480.51	**-0.16**	0.21	**9.87e-1**
RSG1	20.09	**-0.02**	0.24	**9.95e-1**
RSL1D1	2740.51	**-0.12**	0.18	**9.90e-1**
RSL24D1	778.31	**0.69**	0.21	**9.64e-2**
RSPH3	21.93	**-0.03**	0.24	**9.93e-1**
RSPRY1	245.72	**0.05**	0.22	**9.93e-1**
RSRC1	289.7	**-0.21**	0.21	**9.60e-1**
RSRC2	842.78	**-0.41**	0.19	**5.96e-1**
RSRP1	155.7	**0.2**	0.23	**9.80e-1**

RSU1	352.59	**-0.06**	0.21	**9.93e-1**
RTCA	353.33	**0.26**	0.21	**9.23e-1**
RTCB	748.21	**0**	0.19	**1.00e+0**
RTF1	935.62	**-0.35**	0.19	**7.31e-1**
RTFDC1	669.41	**0.1**	0.19	**9.90e-1**
RTN2	29.98	**0.05**	0.25	**9.93e-1**
RTN3	1029.68	**0.13**	0.19	**9.88e-1**
RTN4	618.8	**-0.05**	0.2	**9.93e-1**
RTN4IP1	93.76	**0.36**	0.25	**8.64e-1**
RTTN	162.24	**0.24**	0.23	**9.54e-1**
RUFY1	332.68	**0.28**	0.21	**9.07e-1**
RUFY2	59.78	**0.17**	0.25	**9.89e-1**
RUFY3	523.7	**-0.16**	0.21	**9.86e-1**
RUNDC1	122.53	**0.07**	0.24	**9.93e-1**
RUNX1	365.8	**0.04**	0.21	**9.93e-1**
RUNX1T1	59.1	**-0.31**	0.25	**9.39e-1**
RUNX3	1756.49	**0.02**	0.21	**9.95e-1**
RUSC1	63.31	**-0.15**	0.25	**9.90e-1**
RUVBL1	1294.85	**-0.07**	0.19	**9.90e-1**
RUVBL2	1260.46	**-0.23**	0.22	**9.50e-1**
RWDD1	465.2	**-0.24**	0.2	**9.42e-1**
RWDD2A	19.83	**0.12**	0.24	**9.90e-1**
RWDD2B	199.84	**0.04**	0.23	**9.93e-1**
RWDD3	26.08	**0.29**	0.25	**9.47e-1**
RWDD4	368.61	**0.19**	0.22	**9.80e-1**
RXRA	23.75	**-0.13**	0.25	**9.90e-1**
RXRB	271.54	**-0.06**	0.24	**9.93e-1**
RYBP	176.54	**0.27**	0.23	**9.45e-1**
RYK	252.43	**-0.26**	0.21	**9.42e-1**
S100A13	11.87	**0.21**	0.22	**9.63e-1**
S100PBP	383.24	**0.11**	0.21	**9.90e-1**
S1PR2	1279.43	**-0.26**	0.22	**9.47e-1**
S1PR4	201.47	**-0.14**	0.2	**9.87e-1**
SAAL1	342.04	**0.08**	0.21	**9.90e-1**
SAC3D1	65.36	**0.12**	0.25	**9.90e-1**
SACM1L	409.1	**0.09**	0.22	**9.90e-1**
SACS	374.87	**-0.11**	0.22	**9.90e-1**
SAE1	1417.85	**0.06**	0.19	**9.91e-1**
SAFB	1772.93	**-0.3**	0.19	**8.38e-1**
SAFB2	1125.15	**-0.57**	0.21	**3.01e-1**
SAMD1	527.47	**-0.28**	0.23	**9.39e-1**
SAMD10	408.2	**0.01**	0.23	**9.97e-1**
SAMD12	85.98	**-0.19**	0.25	**9.87e-1**

SAMD13	13.29	**-0.03**	0.22	**9.93e-1**
SAMD15	33.52	**-0.11**	0.25	**9.90e-1**
SAMD4A	38.6	**0.25**	0.25	**9.58e-1**
SAMD4B	564.67	**-0.42**	0.22	**6.90e-1**
SAMD8	145.13	**0.28**	0.24	**9.47e-1**
SAMD9	235.61	**-0.12**	0.23	**9.90e-1**
SAMD9L	23.46	**-0.07**	0.25	**9.93e-1**
SAMHD1	620.06	**-0.09**	0.2	**9.90e-1**
SAMM50	715.66	**0.03**	0.19	**9.93e-1**
SAMSN1	88.96	**0.11**	0.25	**9.90e-1**
SAP130	302.07	**-0.17**	0.21	**9.86e-1**
SAP18	645.15	**-0.13**	0.19	**9.90e-1**
SAP25	27.89	**-0.07**	0.24	**9.92e-1**
SAP30	127.61	**-0.17**	0.23	**9.87e-1**
SAP30BP	644.49	**0.15**	0.19	**9.86e-1**
SAP30L	134.25	**0.42**	0.23	**7.41e-1**
SAPCD2	925.74	**-0.18**	0.23	**9.87e-1**
SAR1A	590.9	**0.03**	0.2	**9.93e-1**
SAR1B	224.66	**0.18**	0.23	**9.86e-1**
SARAF	698.56	**0.32**	0.2	**8.29e-1**

SARNP	409.78	**0.12**	0.21	**9.90e-1**
SARS	1329.33	**0.45**	0.19	**4.40e-1**
SARS2	335.12	**-0.25**	0.22	**9.47e-1**
SART1	988.47	**-0.14**	0.2	**9.88e-1**
SART3	882.08	**-0.03**	0.19	**9.93e-1**
SASH3	1602.4	**-0.29**	0.21	**8.94e-1**
SASS6	433.98	**-0.11**	0.21	**9.90e-1**
SAT1	283.61	**0.08**	0.21	**9.90e-1**
SAT2	19.64	**0.12**	0.24	**9.90e-1**
SATB1	75.58	**0.24**	0.25	**9.61e-1**
SATB2	13.73	**-0.2**	0.22	**9.73e-1**
SAV1	155.25	**0.14**	0.23	**9.90e-1**
SAYSD1	104.32	**0.18**	0.24	**9.87e-1**
SBDS	769.69	**0.21**	0.2	**9.49e-1**
SBDSP1	567.85	**0.09**	0.2	**9.90e-1**
SBF1	1869.52	**0.04**	0.22	**9.93e-1**
SBF2	178.58	**0.12**	0.23	**9.90e-1**
SBK1	11.51	**-0.04**	0.21	**9.93e-1**
SBNO1	1368.85	**0.09**	0.2	**9.90e-1**
SBNO2	292.42	**-0.16**	0.23	**9.87e-1**
SC5D	311.76	**0.28**	0.21	**9.17e-1**
SCAF1	558.32	**-0.17**	0.23	**9.87e-1**
SCAF11	1629.24	**-0.02**	0.19	**9.93e-1**
SCAF4	1246.86	**-0.3**	0.19	**8.30e-1**
SCAF8	791.14	**-0.12**	0.19	**9.90e-1**
SCAI	155.31	**-0.12**	0.24	**9.90e-1**
SCAMP1	412.05	**-0.05**	0.22	**9.93e-1**
SCAMP1-AS1	25.76	**0.25**	0.25	**9.57e-1**
SCAMP2	520.39	**-0.46**	0.23	**6.47e-1**
SCAMP3	414.74	**-0.21**	0.21	**9.58e-1**
SCAMP4	294.43	**-0.28**	0.24	**9.47e-1**
SCAMP5	121.02	**0.01**	0.25	**9.96e-1**
SCAND1	88.09	**-0.13**	0.25	**9.90e-1**
SCAND2P	30.37	**0.04**	0.25	**9.93e-1**
SCAP	683.6	**-0.32**	0.22	**8.64e-1**
SCAPER	61.81	**0.17**	0.25	**9.89e-1**
SCARB1	1189.38	**-0.56**	0.21	**3.26e-1**
SCARB2	128.09	**0.1**	0.24	**9.90e-1**
SCARF1	29.16	**-0.11**	0.25	**9.90e-1**
SCARNA12	22.85	**-0.02**	0.24	**9.95e-1**
SCART1	175.84	**-0.51**	0.23	**5.83e-1**
SCCPDH	53.51	**0.07**	0.25	**9.93e-1**
SCD	5837.15	**-0.66**	0.18	**3.91e-2**
SCD5	14.44	**0.09**	0.23	**9.90e-1**
SCFD1	341.39	**0.37**	0.23	**8.20e-1**
SCFD2	172.36	**-0.16**	0.23	**9.89e-1**
SCLT1	176.87	**0.21**	0.23	**9.72e-1**
SCMH1	1052.04	**-0.36**	0.19	**7.24e-1**
SCN4A	128.34	**-0.13**	0.24	**9.90e-1**
SCNN1D	31.28	**-0.31**	0.25	**9.25e-1**
SCO1	516.19	**0.06**	0.2	**9.91e-1**
SCO2	83.71	**-0.14**	0.25	**9.90e-1**
SCOC	87.03	**0.32**	0.25	**9.23e-1**
SCP2	404.15	**0.05**	0.2	**9.93e-1**
SCPEP1	177.28	**0.2**	0.23	**9.72e-1**
SCRIB	543.19	**-0.32**	0.24	**9.18e-1**
SCRN2	25.76	**-0.29**	0.24	**9.47e-1**
SCRN3	12.38	**0.04**	0.21	**9.93e-1**
SCYL1	742.25	**-0.45**	0.22	**6.54e-1**
SCYL2	388.61	**0.18**	0.21	**9.81e-1**
SCYL3	51.13	**0.2**	0.25	**9.86e-1**
SDAD1	689.36	**0.12**	0.2	**9.90e-1**
SDCBP	81.38	**0.29**	0.25	**9.47e-1**
SDCBP2-AS1	11.92	**-0.05**	0.22	**9.93e-1**

SDCCAG3	677.86	**-0.08**	0.2	**9.90e-1**
SDCCAG8	56.21	**0.25**	0.25	**9.59e-1**
SDE2	170.21	**0.18**	0.23	**9.86e-1**
SDF2	90.55	**0.18**	0.24	**9.87e-1**
SDF2L1	140.38	**0.27**	0.24	**9.47e-1**
SDF4	772.82	**-0.2**	0.22	**9.72e-1**
SDHA	1061.48	**0.11**	0.19	**9.90e-1**
SDHAF1	90.37	**0.15**	0.25	**9.90e-1**
SDHAF2	212.53	**-0.08**	0.22	**9.90e-1**
SDHAF3	160.46	**0.16**	0.24	**9.88e-1**
SDHAF4	22.75	**0**	0.25	**9.98e-1**
SDHAP1	147.99	**0.13**	0.24	**9.90e-1**
SDHAP2	62.26	**-0.04**	0.25	**9.93e-1**
SDHAP3	96.29	**-0.25**	0.24	**9.54e-1**
SDHB	774.87	**0.13**	0.19	**9.89e-1**
SDHC	131.71	**0.11**	0.24	**9.90e-1**
SDHD	599.89	**-0.04**	0.2	**9.93e-1**
SDK1	55.26	**-0.05**	0.25	**9.93e-1**
SDR39U1	163.75	**-0.21**	0.23	**9.73e-1**
SEC11A	267.7	**0.36**	0.22	**8.28e-1**
SEC11C	307.83	**0.48**	0.21	**5.45e-1**
SEC13	553.88	**0.05**	0.21	**9.93e-1**
SEC14L1	1077.14	**-0.32**	0.19	**7.99e-1**
SEC16A	1555.02	**-0.34**	0.2	**7.75e-1**
SEC22A	71.75	**0.24**	0.25	**9.59e-1**
SEC22B	364.97	**0.05**	0.21	**9.93e-1**
SEC22C	190.9	**0.15**	0.23	**9.89e-1**
SEC23A	293.3	**0.03**	0.22	**9.93e-1**
SEC23B	790.02	**0.25**	0.19	**9.11e-1**
SEC23IP	697.04	**-0.14**	0.2	**9.88e-1**
SEC24A	631.43	**0.1**	0.21	**9.90e-1**
SEC24B	468.3	**0.04**	0.21	**9.93e-1**
SEC24C	1593.6	**-0.41**	0.2	**6.54e-1**
SEC24D	308.14	**-0.04**	0.21	**9.93e-1**
SEC31A	1140.67	**-0.11**	0.19	**9.90e-1**
SEC31B	152.7	**-0.06**	0.23	**9.93e-1**
SEC61A1	2206.95	**-0.04**	0.18	**9.93e-1**
SEC61A2	48.97	**0.21**	0.25	**9.81e-1**
SEC61B	270.8	**-0.01**	0.22	**9.96e-1**
SEC61G	218.11	**0.11**	0.22	**9.90e-1**
SEC62	1139.55	**0.09**	0.19	**9.90e-1**
SEC63	1685.79	**0.11**	0.19	**9.90e-1**
SECISBP2	569.3	**0.29**	0.2	**8.68e-1**
SECISBP2L	233.36	**0.21**	0.23	**9.66e-1**
SEH1L	1252.85	**0.15**	0.2	**9.87e-1**
SEL1L	710.76	**0.28**	0.2	**8.90e-1**
SEL1L3	979.36	**0.16**	0.19	**9.80e-1**
SELK	94.32	**0.26**	0.25	**9.49e-1**
SELL	156.25	**-0.34**	0.23	**8.64e-1**
SELO	158.84	**-0.18**	0.23	**9.86e-1**
SELPLG	77.63	**-0.14**	0.25	**9.90e-1**
SELT	713.42	**0.22**	0.22	**9.52e-1**
SEMA3G	41.45	**-0.5**	0.25	**6.69e-1**
SEMA4A	61.5	**0**	0.25	**9.98e-1**
SEMA4B	143.52	**-0.46**	0.23	**6.79e-1**
SEMA4D	262.79	**0.09**	0.22	**9.90e-1**
SEMA4F	14.44	**0.04**	0.23	**9.93e-1**
SEMA7A	179.67	**0.57**	0.23	**4.15e-1**
SENP1	527.74	**-0.2**	0.2	**9.59e-1**
SENP2	573.97	**-0.25**	0.2	**9.25e-1**
SENP3	22.1	**-0.14**	0.24	**9.90e-1**
SENP5	289.9	**-0.03**	0.21	**9.93e-1**
SENP6	4067.86	**0.15**	0.2	**9.87e-1**
SENP7	38.1	**-0.01**	0.25	**9.97e-1**

SENP8	10.11	**0.04**	0.2	**9.93e-1**
SEP15	637.67	**0.22**	0.21	**9.54e-1**
SEPHS1	721.26	**0.2**	0.2	**9.58e-1**
SEPHS2	452.17	**0.37**	0.2	**7.33e-1**
SEPSECS	75.91	**0.03**	0.25	**9.93e-1**
SEPT1	258.99	**0.05**	0.22	**9.93e-1**
SEPT11	1016.31	**0.03**	0.2	**9.93e-1**
SEPT2	2797.76	**-0.04**	0.19	**9.93e-1**
SEPT6	3219.26	**-0.53**	0.18	**2.24e-1**
SEPT7	1583.46	**0.27**	0.19	**8.97e-1**
SEPT7P2	86.05	**0.25**	0.25	**9.54e-1**
SEPT8	273.74	**0.26**	0.22	**9.47e-1**
SEPT9	5790.77	**-0.26**	0.21	**9.30e-1**
SEPW1	61.67	**-1.08**	0.25	**6.96e-3**
SERAC1	47.56	**0.06**	0.25	**9.93e-1**
SERBP1	6599.28	**-0.23**	0.18	**9.12e-1**
SERF2	384.34	**-0.02**	0.21	**9.93e-1**
SERGEF	56.18	**0.07**	0.25	**9.93e-1**

SERHL2	12.99	**-0.15**	0.22	**9.89e-1**
SERINC1	258.38	**0.41**	0.22	**7.13e-1**
SERINC3	680.7	**0.21**	0.2	**9.49e-1**
SERINC5	78.56	**-0.18**	0.25	**9.87e-1**
SERP1	1113.65	**0.47**	0.2	**4.63e-1**
SERPINA9	1601.59	**0.27**	0.19	**8.73e-1**
SERPINB1	11.42	**0.35**	0.21	**8.21e-1**
SERPINB8	107.09	**0.07**	0.24	**9.92e-1**
SERPINB9	733.69	**0.46**	0.2	**5.32e-1**
SERPINB9P1	159.58	**0.37**	0.23	**8.34e-1**
SERTAD1	14.23	**-0.09**	0.22	**9.90e-1**
SERTAD2	653.83	**-0.45**	0.2	**5.37e-1**
SERTAD3	45.68	**0.06**	0.25	**9.93e-1**
SESN1	177.28	**-0.05**	0.23	**9.93e-1**
SESN2	252.1	**0.84**	0.23	**3.89e-2**
SESN3	170.19	**-0.25**	0.23	**9.49e-1**
SESTD1	148.86	**0.04**	0.23	**9.93e-1**
SET	6319.63	**0.05**	0.18	**9.93e-1**
SETBP1	110.06	**-0.21**	0.24	**9.74e-1**
SETD1A	1175.97	**-0.45**	0.22	**6.52e-1**
SETD1B	382.45	**-0.42**	0.22	**7.05e-1**
SETD2	1537.32	**-0.09**	0.19	**9.90e-1**
SETD3	681.99	**0.06**	0.2	**9.91e-1**
SETD4	62.59	**0.06**	0.25	**9.93e-1**
SETD5	1452.96	**-0.24**	0.19	**9.23e-1**
SETD6	214.93	**-0.07**	0.22	**9.90e-1**
SETD7	1733.25	**-0.21**	0.18	**9.47e-1**
SETD8	917.44	**-0.08**	0.19	**9.90e-1**
SETD9	22.3	**0.11**	0.24	**9.90e-1**
SETDB1	491.49	**0.09**	0.2	**9.90e-1**
SETDB2	447.79	**0.38**	0.21	**7.57e-1**
SETMAR	93.6	**-0.25**	0.24	**9.53e-1**
SETSIP	25.01	**0.22**	0.25	**9.72e-1**
SETX	1083	**0.48**	0.2	**4.40e-1**
SEZ6L2	20.86	**-0.26**	0.23	**9.47e-1**
SF1	3443.87	**-0.56**	0.2	**2.89e-1**
SF3A1	2815.84	**-0.42**	0.19	**5.68e-1**
SF3A2	1236.65	**-0.65**	0.23	**2.80e-1**
SF3A3	2502.25	**-0.07**	0.18	**9.90e-1**
SF3B1	3401.83	**0.07**	0.19	**9.90e-1**
SF3B2	2645.93	**-0.24**	0.18	**9.10e-1**
SF3B3	3562.18	**0**	0.18	**9.98e-1**
SF3B4	981.75	**-0.42**	0.21	**6.42e-1**
SF3B5	348.12	**-0.13**	0.21	**9.90e-1**
SF3B6	370.18	**0.08**	0.21	**9.90e-1**

SFI1	302.06	**0.06**	0.21	**9.93e-1**
SFMBT1	202.54	**-0.17**	0.22	**9.87e-1**
SFMBT2	347.71	**-0.04**	0.21	**9.93e-1**
SFPQ	5593.35	**-0.34**	0.18	**7.13e-1**
SFR1	24.9	**0.12**	0.25	**9.90e-1**
SFSWAP	795.78	**-0.38**	0.2	**6.81e-1**
SFT2D1	217.12	**0.9**	0.22	**1.28e-2**
SFT2D2	25.98	**0.04**	0.25	**9.93e-1**
SFT2D3	13.66	**0.07**	0.22	**9.91e-1**
SFXN1	882.03	**0.12**	0.2	**9.90e-1**
SFXN2	244.74	**-0.22**	0.22	**9.56e-1**
SFXN4	334.72	**0.26**	0.22	**9.45e-1**
SFXN5	22.12	**-0.08**	0.24	**9.91e-1**
SGCB	60.96	**0.26**	0.25	**9.54e-1**
SGCE	77.82	**-0.09**	0.25	**9.90e-1**
SGK1	381.49	**1.37**	0.21	**0.00e+0**
SGK223	201.66	**-0.23**	0.23	**9.59e-1**
SGK494	145.27	**-0.45**	0.23	**6.87e-1**
SGMS1	180.21	**-0.39**	0.23	**7.98e-1**
SGOL1	194.98	**0.07**	0.22	**9.90e-1**
SGOL2	367.67	**-0.07**	0.22	**9.91e-1**
SGPL1	282.34	**0.19**	0.21	**9.73e-1**
SGPP1	425.85	**0.73**	0.2	**5.15e-2**
SGPP2	67.64	**0.32**	0.25	**9.23e-1**
SGSM2	461.18	**-0.19**	0.22	**9.80e-1**
SGSM3	270.45	**-0.1**	0.24	**9.90e-1**
SGTA	1518.77	**-0.34**	0.19	**7.41e-1**
SGTB	170.86	**0.22**	0.23	**9.66e-1**
SH2B1	463.13	**-0.37**	0.24	**8.40e-1**
SH2B2	729.96	**-0.05**	0.22	**9.93e-1**
SH2B3	590.46	**-0.03**	0.2	**9.93e-1**
SH2D3A	15.65	**-0.02**	0.21	**9.95e-1**
SH2D3C	217.58	**0.61**	0.23	**3.64e-1**
SH3BGR	17.87	**-0.11**	0.24	**9.90e-1**
SH3BGRL	419.26	**0.16**	0.22	**9.87e-1**
SH3BGRL3	314.27	**-0.42**	0.21	**6.69e-1**
SH3BP1	348.74	**-0.34**	0.22	**8.53e-1**
SH3BP2	289.2	**-0.09**	0.22	**9.90e-1**
SH3BP5	127.58	**-0.35**	0.24	**8.62e-1**
SH3BP5-AS1	72.14	**0.17**	0.25	**9.88e-1**
SH3BP5L	185.7	**0.02**	0.24	**9.93e-1**
SH3D21	45.84	**-0.11**	0.25	**9.90e-1**
SH3GL1	481.12	**-0.3**	0.24	**9.32e-1**
SH3GLB1	567.22	**0.09**	0.21	**9.90e-1**
SH3GLB2	500.45	**-0.34**	0.22	**8.41e-1**
SH3KBP1	1585.67	**0.19**	0.18	**9.49e-1**
SH3PXD2A	222.3	**-0.02**	0.22	**9.95e-1**
SH3RF1	37.99	**-0.01**	0.25	**9.96e-1**
SH3TC1	257.65	**-0.14**	0.24	**9.90e-1**
SHANK2	99.68	**-0.54**	0.24	**5.70e-1**
SHARPIN	130.35	**-0.28**	0.25	**9.47e-1**
SHC1	423.94	**-0.42**	0.23	**7.31e-1**
SHCBP1	318.18	**0.16**	0.21	**9.87e-1**
SHFM1	325.06	**0.25**	0.21	**9.45e-1**
SHISA5	1365.15	**-0.4**	0.22	**7.41e-1**
SHKBP1	522.2	**-0.18**	0.23	**9.86e-1**
SHMT1	489.52	**-0.14**	0.2	**9.88e-1**
SHMT2	2826.92	**-0.04**	0.21	**9.93e-1**
SHOC2	623.91	**0.15**	0.21	**9.87e-1**
SHPK	231.97	**-0.09**	0.22	**9.90e-1**
SHPRH	308.74	**-0.04**	0.22	**9.93e-1**
SHQ1	221.21	**0.1**	0.22	**9.90e-1**
SHROOM3	103.66	**-0.71**	0.24	**2.15e-1**

SIAE	82.57	**0.13**	0.25	**9.90e-1**
SIAH1	103.62	**0.27**	0.25	**9.49e-1**
SIAH2	190.37	**0.18**	0.22	**9.83e-1**
SIDT2	225.94	**-0.11**	0.23	**9.90e-1**
SIGLEC10	360.63	**-0.43**	0.22	**6.90e-1**
SIGMAR1	1179.82	**-0.37**	0.21	**7.57e-1**
SIK1	171.72	**-0.28**	0.24	**9.47e-1**
SIK2	239.84	**-0.13**	0.22	**9.90e-1**
SIK3	645.44	**-0.31**	0.2	**8.40e-1**
SIKE1	401.41	**0.1**	0.22	**9.90e-1**
SIL1	47.93	**0.15**	0.25	**9.90e-1**
SIMC1	230.53	**-0.43**	0.22	**6.84e-1**
SIN3A	786.33	**-0.01**	0.19	**9.96e-1**
SIN3B	435.25	**-0.08**	0.21	**9.90e-1**
SIPA1	265.79	**0.01**	0.24	**9.98e-1**
SIPA1L1	262.81	**0.04**	0.22	**9.93e-1**
SIPA1L3	806.55	**-0.09**	0.22	**9.90e-1**
SIRT1	480.42	**0.28**	0.21	**9.04e-1**
SIRT2	111.78	**-0.15**	0.25	**9.90e-1**
SIRT3	104.37	**-0.14**	0.24	**9.90e-1**
SIRT5	103.72	**0.04**	0.25	**9.93e-1**
SIRT6	165.48	**-0.25**	0.25	**9.58e-1**
SIRT7	99.15	**-0.11**	0.25	**9.90e-1**
SIT1	358.37	**0.26**	0.23	**9.47e-1**
SIVA1	135.13	**-0.25**	0.25	**9.60e-1**
SKA1	245.91	**0.01**	0.22	**9.96e-1**
SKA2	398.64	**-0.04**	0.21	**9.93e-1**
SKA3	534.77	**-0.15**	0.21	**9.88e-1**
SKAP2	245.79	**0.28**	0.22	**9.25e-1**
SKI	339.51	**-0.15**	0.21	**9.87e-1**
SKIDA1	12.52	**-0.02**	0.21	**9.93e-1**
SKIL	266.11	**0.52**	0.22	**4.96e-1**
SKIV2L	584.94	**-0.33**	0.21	**8.52e-1**
SKIV2L2	1393.65	**-0.11**	0.2	**9.90e-1**
SKP1	849.43	**0.15**	0.2	**9.87e-1**
SKP2	361.15	**-0.16**	0.21	**9.87e-1**
SLAIN1	347.6	**-0.03**	0.21	**9.93e-1**
SLAIN2	443.7	**-0.06**	0.21	**9.91e-1**
SLAMF1	56.03	**0.74**	0.25	**2.24e-1**
SLAMF6	442.7	**-0.55**	0.2	**3.13e-1**
SLBP	683.04	**0.41**	0.21	**6.69e-1**
SLC10A3	117.91	**-0.16**	0.25	**9.90e-1**
SLC10A7	59.19	**0.01**	0.25	**9.96e-1**
SLC11A2	205.67	**0.19**	0.23	**9.81e-1**
SLC12A2	276.74	**0.14**	0.22	**9.90e-1**
SLC12A4	91.68	**-0.19**	0.25	**9.87e-1**
SLC12A5	12.9	**-0.02**	0.22	**9.95e-1**
SLC12A6	113.6	**-0.5**	0.24	**6.10e-1**
SLC12A8	59.6	**0.07**	0.25	**9.93e-1**
SLC12A9	313.76	**-0.45**	0.24	**7.04e-1**
SLC15A2	34.12	**0.18**	0.25	**9.87e-1**
SLC15A3	29.05	**0.34**	0.25	**8.97e-1**
SLC15A4	183.9	**0.68**	0.23	**2.15e-1**
SLC16A1	1875.83	**0.04**	0.19	**9.93e-1**
SLC16A13	38.79	**-0.25**	0.25	**9.58e-1**
SLC16A1-AS1	30.09	**-0.32**	0.25	**9.17e-1**
SLC16A6	339.24	**-0.22**	0.21	**9.52e-1**
SLC16A7	192.44	**-0.03**	0.24	**9.93e-1**
SLC17A5	671.38	**0.43**	0.2	**6.03e-1**
SLC17A9	764.81	**-0.27**	0.24	**9.47e-1**
SLC19A1	453.32	**-0.6**	0.24	**4.14e-1**
SLC19A2	102.49	**0.05**	0.24	**9.93e-1**
SLC1A1	164.87	**-0.15**	0.23	**9.90e-1**

SLC1A4	319.14	**0.44**	0.21	**6.14e-1**
SLC1A5	2141.04	**-0.23**	0.22	**9.52e-1**
SLC20A1	363.6	**0.3**	0.21	**8.73e-1**
SLC20A2	227.59	**0.09**	0.22	**9.90e-1**
SLC22A5	48.79	**-0.27**	0.25	**9.49e-1**
SLC23A1	12.86	**0.13**	0.22	**9.90e-1**
SLC23A2	751.68	**0.17**	0.19	**9.74e-1**
SLC23A3	11.86	**-0.08**	0.22	**9.90e-1**
SLC24A1	17.49	**-0.22**	0.24	**9.70e-1**
SLC25A1	350.9	**-0.28**	0.23	**9.40e-1**
SLC25A10	283.02	**-0.54**	0.23	**5.31e-1**
SLC25A11	330.62	**-0.31**	0.23	**9.06e-1**
SLC25A12	310.52	**-0.04**	0.21	**9.93e-1**
SLC25A13	191.39	**0.08**	0.23	**9.90e-1**
SLC25A14	45.43	**0.11**	0.25	**9.90e-1**
SLC25A15	248.28	**-0.01**	0.22	**9.98e-1**
SLC25A16	42.8	**0.11**	0.25	**9.90e-1**
SLC25A17	216.79	**-0.16**	0.22	**9.87e-1**
SLC25A19	419.95	**-0.1**	0.21	**9.90e-1**
SLC25A20	186.83	**0.24**	0.22	**9.49e-1**
SLC25A22	265.74	**-0.26**	0.25	**9.50e-1**
SLC25A23	732.17	**-0.45**	0.2	**5.71e-1**
SLC25A25	150.32	**0.53**	0.24	**5.86e-1**
SLC25A25-AS1	232.23	**-0.25**	0.24	**9.51e-1**
SLC25A26	67.08	**0.34**	0.25	**9.03e-1**
SLC25A27	137.9	**-0.03**	0.23	**9.93e-1**
SLC25A28	121.18	**0.03**	0.24	**9.93e-1**
SLC25A3	2027.28	**0.18**	0.18	**9.58e-1**
SLC25A32	581.33	**0.08**	0.21	**9.90e-1**
SLC25A33	146.46	**0.41**	0.24	**7.59e-1**
SLC25A35	11.04	**-0.09**	0.21	**9.90e-1**
SLC25A36	867.32	**0.07**	0.21	**9.91e-1**
SLC25A37	397	**-0.12**	0.21	**9.90e-1**
SLC25A38	272.16	**0.26**	0.21	**9.46e-1**
SLC25A39	1641.12	**-0.28**	0.22	**9.25e-1**
SLC25A4	168.66	**-0.05**	0.23	**9.93e-1**
SLC25A40	225.09	**0.3**	0.22	**8.99e-1**
SLC25A42	54.39	**-0.12**	0.25	**9.90e-1**
SLC25A43	208.11	**0.19**	0.23	**9.83e-1**
SLC25A44	357.78	**-0.33**	0.21	**8.38e-1**
SLC25A45	53.25	**-0.2**	0.25	**9.86e-1**
SLC25A46	908.62	**-0.07**	0.2	**9.90e-1**
SLC25A5	1954.15	**0.4**	0.18	**5.86e-1**
SLC25A51	131.96	**0.11**	0.24	**9.90e-1**
SLC25A6	3553.87	**0**	0.21	**9.99e-1**
SLC26A2	79.02	**0.2**	0.25	**9.85e-1**
SLC26A6	223.93	**-0.26**	0.23	**9.47e-1**
SLC27A1	19.17	**0.1**	0.24	**9.90e-1**
SLC27A3	32.28	**-0.15**	0.25	**9.90e-1**
SLC27A4	345.21	**-0.22**	0.22	**9.59e-1**
SLC27A5	57	**-0.33**	0.25	**9.12e-1**
SLC29A1	2446.24	**-0.4**	0.19	**5.96e-1**
SLC29A2	308.63	**-0.55**	0.24	**5.37e-1**
SLC29A3	65.16	**-0.21**	0.25	**9.80e-1**
SLC2A1	960.82	**-0.27**	0.22	**9.25e-1**
SLC2A11	80.52	**-0.02**	0.25	**9.96e-1**
SLC2A13	15.88	**0.16**	0.23	**9.87e-1**
SLC2A3	15.29	**0.51**	0.23	**5.71e-1**
SLC2A4RG	149.51	**0.19**	0.24	**9.86e-1**
SLC2A5	2002.19	**-0.51**	0.19	**3.49e-1**
SLC2A6	76.59	**-0.31**	0.25	**9.41e-1**
SLC2A8	60.27	**-0.01**	0.25	**9.96e-1**
SLC30A1	81.87	**-0.09**	0.25	**9.90e-1**
SLC30A5	378.38	**0.32**	0.21	**8.49e-1**
SLC30A6	256.04	**0.1**	0.22	**9.90e-1**

SLC30A7	139.13	**0.2**	0.24	**9.81e-1**
SLC30A9	572.12	**0.28**	0.2	**8.83e-1**
SLC31A1	414.6	**-0.05**	0.21	**9.93e-1**
SLC33A1	265.59	**0.35**	0.22	**8.30e-1**
SLC35A1	127.61	**0.41**	0.24	**8.10e-1**
SLC35A2	103.24	**-0.25**	0.25	**9.54e-1**
SLC35A3	231.4	**-0.08**	0.23	**9.90e-1**
SLC35A4	416.14	**-0.22**	0.21	**9.49e-1**
SLC35A5	187.8	**0.31**	0.23	**9.10e-1**
SLC35B1	158.14	**0.51**	0.24	**5.91e-1**
SLC35B2	146.64	**-0.19**	0.24	**9.86e-1**
SLC35B3	76.09	**0.14**	0.25	**9.90e-1**
SLC35B4	584.11	**0.22**	0.2	**9.49e-1**

SLC35C1	134.15	**-0.13**	0.25	**9.90e-1**
SLC35C2	346.24	**-0.02**	0.22	**9.94e-1**
SLC35D1	231.58	**-0.03**	0.22	**9.93e-1**
SLC35E1	703.72	**-0.04**	0.2	**9.93e-1**
SLC35E2	71.03	**0.26**	0.25	**9.53e-1**
SLC35E2B	318.78	**-0.01**	0.21	**9.97e-1**
SLC35E3	151.23	**-0.27**	0.23	**9.47e-1**
SLC35F2	579.75	**0.11**	0.2	**9.90e-1**
SLC35F5	163.62	**0.23**	0.23	**9.59e-1**
SLC35F6	184.42	**-0.29**	0.22	**9.19e-1**
SLC36A1	216.81	**-0.2**	0.22	**9.72e-1**
SLC36A4	120.15	**0.19**	0.24	**9.86e-1**
SLC37A1	272.33	**0.06**	0.22	**9.93e-1**
SLC37A3	43.91	**0.16**	0.25	**9.90e-1**
SLC37A4	280.42	**-0.26**	0.22	**9.47e-1**
SLC38A1	3509.45	**0.14**	0.19	**9.87e-1**
SLC38A10	419.8	**-0.16**	0.24	**9.89e-1**
SLC38A2	637.29	**0.83**	0.21	**1.33e-2**
SLC38A5	747.82	**-0.34**	0.19	**7.69e-1**
SLC38A6	31.9	**0.05**	0.25	**9.93e-1**
SLC38A7	105.83	**-0.19**	0.24	**9.86e-1**
SLC38A9	138.71	**-0.07**	0.23	**9.91e-1**
SLC39A1	409.51	**-0.28**	0.23	**9.42e-1**
SLC39A10	243.32	**-0.04**	0.24	**9.93e-1**
SLC39A11	218.02	**0.22**	0.22	**9.58e-1**
SLC39A13	89.07	**-0.14**	0.25	**9.90e-1**
SLC39A14	1083.83	**-0.06**	0.19	**9.92e-1**
SLC39A3	193.04	**-0.03**	0.23	**9.93e-1**
SLC39A4	89.42	**-0.07**	0.25	**9.93e-1**
SLC39A6	585.41	**-0.09**	0.21	**9.90e-1**
SLC39A7	531.85	**-0.09**	0.21	**9.90e-1**
SLC39A8	367.17	**0.39**	0.22	**7.57e-1**
SLC39A9	764.8	**0.23**	0.19	**9.47e-1**
SLC3A2	783.77	**0.2**	0.21	**9.58e-1**
SLC41A1	1345.72	**-0.73**	0.19	**2.34e-2**
SLC41A2	88.51	**0.17**	0.25	**9.89e-1**
SLC41A3	100.36	**0.17**	0.24	**9.88e-1**
SLC43A1	466.44	**0.69**	0.2	**8.18e-2**
SLC43A2	137.54	**-0.52**	0.25	**6.07e-1**
SLC43A3	2012.25	**-0.44**	0.18	**4.72e-1**
SLC44A1	489.62	**0.12**	0.21	**9.90e-1**
SLC44A2	1032.68	**-0.03**	0.2	**9.93e-1**
SLC45A3	306.52	**-0.03**	0.24	**9.93e-1**
SLC45A4	68.96	**-0.12**	0.25	**9.90e-1**
SLC46A3	88.72	**0.11**	0.25	**9.90e-1**
SLC48A1	194.23	**-0.42**	0.24	**7.76e-1**
SLC4A1AP	316.59	**-0.07**	0.21	**9.90e-1**
SLC4A2	496.22	**-0.34**	0.23	**8.69e-1**
SLC4A7	720.87	**0.1**	0.2	**9.90e-1**
SLC4A8	31.51	**0.1**	0.25	**9.90e-1**

SLC50A1	263.74	**0.02**	0.22	**9.95e-1**
SLC52A2	180.32	**-0.12**	0.25	**9.90e-1**
SLC5A3	1127.93	**-0.53**	0.2	**3.10e-1**
SLC5A5	10.05	**0.24**	0.21	**9.47e-1**
SLC5A6	773.39	**-0.34**	0.2	**8.03e-1**
SLC6A16	25.45	**-0.03**	0.25	**9.93e-1**
SLC6A6	805.95	**-0.35**	0.19	**7.41e-1**
SLC6A9	80.34	**0.4**	0.25	**8.38e-1**
SLC7A1	2603.19	**-0.23**	0.19	**9.39e-1**
SLC7A11	623.13	**0.78**	0.21	**3.89e-2**
SLC7A5	4071.56	**-0.26**	0.22	**9.42e-1**
SLC7A5P1	20.95	**0.01**	0.24	**9.97e-1**
SLC7A5P2	21.16	**-0.02**	0.24	**9.93e-1**
SLC7A6	849.87	**0.03**	0.19	**9.93e-1**
SLC7A6OS	111.87	**0.05**	0.24	**9.93e-1**
SLC7A7	55.77	**0.24**	0.25	**9.61e-1**
SLC8B1	28.59	**-0.36**	0.25	**8.69e-1**
SLC9A1	471.62	**-0.42**	0.23	**7.23e-1**
SLC9A3R1	620.41	**-0.38**	0.22	**7.64e-1**
SLC9A6	197.72	**0.13**	0.23	**9.90e-1**
SLC9A7	595.21	**0.14**	0.2	**9.87e-1**
SLC9A8	243.89	**-0.13**	0.22	**9.90e-1**
SLC9A9	16.94	**0.07**	0.23	**9.91e-1**
SLC9B2	125.93	**-0.02**	0.24	**9.95e-1**
SLCO3A1	350.44	**0.01**	0.21	**9.96e-1**
SLCO4A1	432.97	**-0.31**	0.23	**9.06e-1**
SLFN11	86.14	**-0.3**	0.25	**9.42e-1**
SLFNL1-AS1	42.01	**-0.4**	0.25	**8.41e-1**
SLIRP	274.98	**0.01**	0.22	**9.96e-1**
SLK	787.03	**-0.21**	0.21	**9.57e-1**
SLMAP	448.18	**0.03**	0.21	**9.93e-1**
SLMO1	67.24	**-0.08**	0.25	**9.91e-1**
SLMO2	1042.77	**0.04**	0.21	**9.93e-1**

SLTM	2188.88	**-0.17**	0.18	**9.71e-1**
SLU7	291.52	**0.02**	0.21	**9.94e-1**
SLX4	298.55	**-0.36**	0.22	**8.30e-1**
SLX4IP	30.58	**-0.11**	0.25	**9.90e-1**
SMA4	15.89	**-0.1**	0.23	**9.90e-1**
SMAD2	537.27	**0.37**	0.21	**7.55e-1**
SMAD3	252.39	**0.02**	0.22	**9.94e-1**
SMAD4	467.96	**0.05**	0.21	**9.93e-1**
SMAD5	442.46	**-0.3**	0.21	**8.69e-1**
SMAD7	19.68	**-0.07**	0.24	**9.91e-1**
SMAP1	411.99	**0.27**	0.21	**9.14e-1**
SMAP2	1704.95	**0.01**	0.18	**9.96e-1**
SMARCA2	655.3	**0.14**	0.19	**9.87e-1**
SMARCA4	5601.11	**-0.15**	0.19	**9.87e-1**
SMARCA5	2246.5	**-0.09**	0.19	**9.90e-1**
SMARCAD1	470.36	**0.17**	0.22	**9.83e-1**
SMARCAL1	148.89	**0.05**	0.23	**9.93e-1**
SMARCB1	942.36	**0.25**	0.19	**9.12e-1**
SMARCC1	3423.26	**-0.36**	0.18	**6.69e-1**
SMARCC2	1664.15	**-0.35**	0.2	**7.56e-1**
SMARCD1	1101.73	**-0.17**	0.19	**9.79e-1**
SMARCD2	1053	**-0.14**	0.2	**9.88e-1**
SMARCE1	1165.09	**0.1**	0.19	**9.90e-1**
SMC1A	3095.42	**-0.16**	0.18	**9.72e-1**
SMC2	1388.94	**0.14**	0.2	**9.88e-1**
SMC3	2171.16	**-0.03**	0.18	**9.93e-1**
SMC4	3151.24	**-0.19**	0.19	**9.58e-1**
SMC5	729.46	**-0.1**	0.2	**9.90e-1**
SMC6	725.43	**0.14**	0.2	**9.87e-1**
SMCHD1	1499.61	**-0.08**	0.2	**9.90e-1**

SMCO4	29.94	**0.26**	0.25	**9.50e-1**
SMCR8	483.18	**-0.3**	0.2	**8.64e-1**
SMDT1	66.31	**0.28**	0.25	**9.48e-1**
SMG1	2160.7	**-0.03**	0.2	**9.93e-1**
SMG1P1	35.12	**0**	0.25	**9.98e-1**
SMG1P2	27.45	**0.01**	0.25	**9.96e-1**
SMG1P3	56.56	**0.02**	0.25	**9.95e-1**
SMG1P7	83.12	**-0.2**	0.25	**9.86e-1**
SMG5	1177.41	**-0.23**	0.2	**9.47e-1**
SMG6	383.12	**-0.42**	0.22	**6.87e-1**
SMG7	1806.8	**-0.53**	0.18	**2.33e-1**
SMG8	216.89	**0.01**	0.22	**9.96e-1**
SMG9	345.48	**-0.25**	0.22	**9.47e-1**
SMIM10L1	156.54	**0.39**	0.23	**8.11e-1**
SMIM11	59.53	**-0.27**	0.25	**9.49e-1**
SMIM12	393.33	**-0.24**	0.21	**9.47e-1**
SMIM13	286.51	**0.25**	0.22	**9.47e-1**
SMIM14	1198.23	**0.21**	0.19	**9.49e-1**
SMIM15	34.7	**-0.05**	0.25	**9.93e-1**
SMIM19	67.24	**0.33**	0.25	**9.10e-1**
SMIM20	99.08	**0**	0.24	**9.99e-1**
SMIM4	32.39	**-0.2**	0.25	**9.86e-1**
SMIM7	180.17	**0**	0.23	**9.98e-1**
SMIM8	66.18	**0.07**	0.25	**9.93e-1**
SMNDC1	422.39	**0.21**	0.21	**9.57e-1**
SMPD1	38.36	**0.12**	0.25	**9.90e-1**
SMPD4	879.51	**-0.62**	0.22	**2.33e-1**
SMS	1313.62	**0.08**	0.19	**9.90e-1**
SMTN	49.91	**-0.14**	0.25	**9.90e-1**
SMU1	554.03	**0**	0.2	**9.98e-1**
SMUG1	63.81	**0.03**	0.25	**9.93e-1**
SMURF1	287.11	**-0.08**	0.21	**9.90e-1**
SMURF2	153.77	**0.16**	0.23	**9.88e-1**
SMYD2	155.08	**0.34**	0.23	**8.64e-1**
SMYD3	74.62	**-0.03**	0.25	**9.93e-1**
SMYD4	282.26	**-0.07**	0.21	**9.91e-1**
SMYD5	410.52	**-0.24**	0.21	**9.47e-1**
SNAI3	18.99	**-0.25**	0.24	**9.49e-1**
SNAI3-AS1	19	**-0.17**	0.24	**9.87e-1**
SNAP23	496.34	**-0.01**	0.21	**9.96e-1**
SNAP29	318.05	**-0.19**	0.21	**9.74e-1**
SNAP47	110.81	**0.17**	0.24	**9.87e-1**
SNAPC1	81.94	**0.01**	0.25	**9.98e-1**
SNAPC2	93.65	**-0.06**	0.25	**9.93e-1**
SNAPC3	158.09	**-0.07**	0.23	**9.91e-1**
SNAPC4	727.08	**-0.56**	0.23	**4.62e-1**
SNAPC5	48.32	**-0.08**	0.25	**9.91e-1**
SNAPIN	87.42	**0.08**	0.25	**9.91e-1**
SND1	2944.65	**0.08**	0.18	**9.90e-1**
SNF8	255.38	**0.19**	0.22	**9.80e-1**
SNHG1	816.5	**0.13**	0.19	**9.89e-1**
SNHG10	52.16	**0.1**	0.25	**9.90e-1**
SNHG11	37.41	**0.11**	0.25	**9.90e-1**
SNHG12	73.89	**0.14**	0.25	**9.90e-1**
SNHG15	195.07	**0.06**	0.23	**9.93e-1**
SNHG16	772.81	**0.1**	0.19	**9.90e-1**
SNHG17	262.34	**0.12**	0.22	**9.90e-1**
SNHG19	29.13	**-0.22**	0.25	**9.73e-1**
SNHG20	55.41	**-0.19**	0.25	**9.87e-1**
SNHG21	31.55	**0.04**	0.25	**9.93e-1**
SNHG3	547.4	**0.45**	0.2	**5.83e-1**
SNHG4	123.13	**-0.08**	0.24	**9.90e-1**
SNHG5	773.06	**0.58**	0.2	**2.15e-1**
SNHG6	208.83	**0.44**	0.22	**6.69e-1**

SNHG7	249.08	**0.01**	0.23	**9.96e-1**
SNHG8	75.28	**0.35**	0.25	**8.87e-1**
SNIP1	220.24	**-0.05**	0.22	**9.93e-1**
SNN	435.25	**0.7**	0.21	**1.04e-1**
SNORA18	25.63	**0.27**	0.24	**9.49e-1**
SNORA40	34.27	**0.15**	0.25	**9.90e-1**
SNORA6	17.21	**0.4**	0.23	**7.98e-1**
SNORA61	31.68	**0.49**	0.25	**6.87e-1**
SNORA64	15.3	**0.23**	0.23	**9.58e-1**
SNORA67	18.52	**0.07**	0.24	**9.93e-1**
SNORA70	12.77	**0.19**	0.21	**9.74e-1**
SNORA8	29.32	**0.17**	0.25	**9.89e-1**
SNORA9	28.91	**0.33**	0.25	**9.12e-1**
SNORD10	14.52	**-0.14**	0.23	**9.90e-1**
SNORD101	10.8	**0.01**	0.21	**9.96e-1**
SNORD102	14.58	**0.31**	0.23	**8.94e-1**
SNORD104	29.34	**-0.25**	0.25	**9.59e-1**
SNORD16	12.41	**-0.02**	0.22	**9.95e-1**
SNORD17	91.82	**-0.55**	0.25	**5.68e-1**
SNORD22	13.22	**0.18**	0.22	**9.81e-1**
SNORD25	11.03	**0.07**	0.21	**9.91e-1**
SNORD26	30.94	**-0.09**	0.25	**9.90e-1**
SNORD30	13.13	**-0.01**	0.22	**9.96e-1**
SNORD31	20.14	**0.17**	0.24	**9.87e-1**
SNORD35A	12.84	**-0.12**	0.22	**9.90e-1**
SNORD35B	15.71	**0.04**	0.23	**9.93e-1**
SNORD44	18.11	**0.12**	0.23	**9.90e-1**
SNORD47	13.21	**0.21**	0.22	**9.61e-1**
SNORD58A	11.04	**0.05**	0.2	**9.93e-1**
SNORD76	15.77	**-0.17**	0.23	**9.87e-1**
SNORD88B	38.61	**-0.44**	0.24	**7.41e-1**
SNRK	152.6	**0.11**	0.23	**9.90e-1**
SNRNP200	4033.48	**-0.16**	0.18	**9.73e-1**
SNRNP25	329.12	**-0.08**	0.21	**9.90e-1**
SNRNP27	228.68	**-0.2**	0.22	**9.66e-1**
SNRNP35	130.93	**-0.54**	0.24	**5.68e-1**
SNRNP40	692.94	**0.04**	0.19	**9.93e-1**
SNRNP48	228.66	**0.16**	0.23	**9.87e-1**
SNRNP70	2108.56	**-0.55**	0.23	**4.46e-1**
SNRPA	1032.92	**-0.3**	0.21	**8.64e-1**
SNRPA1	810.46	**-0.04**	0.19	**9.93e-1**
SNRPB	1095.81	**-0.32**	0.22	**8.64e-1**
SNRPB2	410.98	**-0.2**	0.2	**9.58e-1**
SNRPC	756.87	**-0.15**	0.2	**9.86e-1**
SNRPD1	909.74	**-0.02**	0.2	**9.93e-1**
SNRPD2	742.2	**-0.05**	0.2	**9.93e-1**
SNRPD3	1251.21	**-0.27**	0.19	**8.73e-1**
SNRPE	328.74	**0.25**	0.21	**9.47e-1**
SNRPF	520.75	**-0.19**	0.2	**9.64e-1**
SNRPG	348.51	**-0.21**	0.21	**9.54e-1**
SNTA1	31.17	**-0.27**	0.25	**9.49e-1**
SNTB2	270.09	**-0.05**	0.22	**9.93e-1**
SNUPN	259.51	**0.21**	0.22	**9.61e-1**
SNW1	691.27	**0.04**	0.2	**9.93e-1**
SNX1	724.51	**0.01**	0.19	**9.98e-1**
SNX10	263.27	**0.27**	0.23	**9.47e-1**
SNX11	162.01	**0.25**	0.23	**9.49e-1**
SNX12	245.13	**-0.24**	0.22	**9.47e-1**
SNX13	302.01	**0.15**	0.22	**9.89e-1**
SNX14	452.27	**0.23**	0.21	**9.47e-1**
SNX16	35.89	**0.42**	0.25	**8.14e-1**
SNX17	198.09	**0.14**	0.23	**9.90e-1**
SNX18	76.31	**-0.26**	0.25	**9.53e-1**
SNX19	208.18	**-0.06**	0.22	**9.93e-1**

SNX2	989.64	**0.02**	0.2	**9.95e-1**
SNX22	399.97	**-0.13**	0.21	**9.90e-1**
SNX25	307.51	**0.14**	0.22	**9.90e-1**
SNX27	376.64	**-0.04**	0.21	**9.93e-1**
SNX29	367.82	**0.06**	0.21	**9.93e-1**
SNX29P1	17.19	**0.16**	0.23	**9.88e-1**
SNX29P2	214.94	**0.49**	0.23	**5.91e-1**
SNX3	917.18	**0.3**	0.2	**8.52e-1**

SNX30	279.51	**-0.01**	0.21	**9.96e-1**
SNX4	313.08	**0.46**	0.22	**6.21e-1**
SNX5	1335.25	**0.29**	0.19	**8.52e-1**
SNX6	480.48	**0.18**	0.22	**9.83e-1**
SNX8	638.08	**-0.1**	0.22	**9.90e-1**
SOAT1	443.18	**0.15**	0.21	**9.87e-1**
SOBP	307.35	**-0.31**	0.21	**8.64e-1**
SOCS1	67.69	**0.45**	0.25	**7.57e-1**
SOCS4	401.16	**0.14**	0.22	**9.90e-1**
SOCS5	136.76	**0.04**	0.24	**9.93e-1**
SOCS7	306.78	**0.03**	0.21	**9.93e-1**
SOD1	1395.05	**0.19**	0.19	**9.51e-1**
SOD2	496.15	**-0.11**	0.2	**9.90e-1**
SOGA1	357.96	**-0.01**	0.22	**9.96e-1**
SON	3636.84	**-0.11**	0.18	**9.90e-1**
SORD	40.17	**-0.09**	0.25	**9.90e-1**
SORL1	1344.99	**0.77**	0.19	**1.19e-2**
SOS1	792.42	**-0.12**	0.2	**9.90e-1**
SOS2	258.24	**0.57**	0.22	**3.77e-1**
SOX12	342.61	**-0.46**	0.23	**6.79e-1**
SOX4	90.65	**-0.36**	0.25	**8.64e-1**
SOX5	62.62	**-0.41**	0.25	**8.30e-1**
SP1	1051.22	**-0.06**	0.19	**9.91e-1**
SP100	497.57	**0.11**	0.21	**9.90e-1**
SP110	576.64	**-0.57**	0.2	**2.52e-1**
SP140	485.92	**-0.27**	0.2	**9.07e-1**
SP140L	76.77	**-0.3**	0.25	**9.42e-1**
SP2	423.67	**-0.41**	0.23	**7.57e-1**
SP3	897.57	**0.12**	0.2	**9.90e-1**
SP4	190.02	**-0.13**	0.23	**9.90e-1**
SPAG1	17.32	**-0.07**	0.23	**9.91e-1**
SPAG5	1007.24	**-0.07**	0.19	**9.90e-1**
SPAG7	227.57	**0.17**	0.22	**9.86e-1**
SPAG9	815.77	**0.17**	0.21	**9.81e-1**
SPARCL1	605.61	**-0.37**	0.2	**7.14e-1**
SPAST	417.66	**0.07**	0.21	**9.90e-1**
SPATA13	612.88	**-0.39**	0.2	**6.69e-1**
SPATA2	218.91	**0.04**	0.22	**9.93e-1**
SPATA24	11.82	**-0.09**	0.22	**9.90e-1**
SPATA2L	13.63	**-0.06**	0.22	**9.93e-1**
SPATA33	78.79	**-0.16**	0.25	**9.90e-1**
SPATA5	112.53	**-0.08**	0.24	**9.90e-1**
SPATA5L1	132.14	**0.3**	0.23	**9.17e-1**
SPATA7	14.75	**0.19**	0.22	**9.74e-1**
SPATS2	418.22	**-0.22**	0.21	**9.49e-1**
SPC24	77.56	**-0.26**	0.25	**9.49e-1**
SPC25	145.32	**-0.11**	0.23	**9.90e-1**
SPCS1	355.11	**0.33**	0.21	**8.38e-1**
SPCS2	423.04	**0.19**	0.2	**9.66e-1**
SPCS3	1240.53	**0.35**	0.2	**7.79e-1**
SPDL1	347	**0.23**	0.22	**9.49e-1**
SPECC1	87.35	**0.03**	0.25	**9.93e-1**
SPECC1L	211.41	**0.05**	0.23	**9.93e-1**
SPEN	1874.2	**-0.39**	0.19	**5.99e-1**
SPG11	391.94	**0.29**	0.21	**9.06e-1**
SPG21	735.6	**0.43**	0.2	**6.03e-1**

SPG7	398.15	**0.06**	0.2	**9.93e-1**
SPHK2	256.44	**-0.38**	0.25	**8.52e-1**
SPI1	451.87	**-0.42**	0.22	**7.04e-1**
SPIB	1599.24	**-0.06**	0.22	**9.93e-1**
SPICE1	134	**0.18**	0.24	**9.87e-1**
SPIDR	361.11	**-0.09**	0.21	**9.90e-1**
SPIN1	594.85	**-0.01**	0.21	**9.96e-1**
SPINK2	18.86	**0.11**	0.24	**9.90e-1**
SPINT2	192.57	**0.19**	0.23	**9.80e-1**
SPIRE1	218.36	**-0.07**	0.22	**9.91e-1**
SPIRE2	13.4	**0.27**	0.21	**9.25e-1**
SPN	75.26	**-0.11**	0.25	**9.90e-1**
SPNS1	264.21	**-0.08**	0.24	**9.91e-1**
SPOCK2	30.73	**-0.08**	0.25	**9.91e-1**
SPOP	394.96	**0.09**	0.21	**9.90e-1**
SPOPL	105.12	**0.03**	0.25	**9.93e-1**
SPPL2A	120.02	**0.44**	0.24	**7.41e-1**
SPPL2B	279.47	**-0.27**	0.24	**9.47e-1**
SPPL3	277.72	**0.35**	0.21	**8.15e-1**
SPRED1	149.88	**0.77**	0.24	**1.12e-1**
SPRED2	158.71	**0.35**	0.23	**8.53e-1**
SPRED3	11.67	**-0.09**	0.21	**9.90e-1**
SPRTN	118.52	**-0.01**	0.24	**9.96e-1**
SPRYD3	241.65	**-0.26**	0.24	**9.49e-1**
SPRYD4	106.48	**-0.28**	0.24	**9.47e-1**
SPRYD7	115.93	**0.08**	0.24	**9.91e-1**
SPSB1	84.09	**0.39**	0.25	**8.40e-1**

SPSB2	15.6	**-0.09**	0.21	**9.90e-1**
SPSB3	36.01	**-0.07**	0.25	**9.93e-1**
SPTAN1	1741.69	**-0.04**	0.18	**9.93e-1**
SPTLC1	489.84	**0.09**	0.21	**9.90e-1**
SPTLC2	586.86	**0.49**	0.2	**4.66e-1**
SPTSSA	328.35	**-0.05**	0.22	**9.93e-1**
SPTY2D1	325.13	**-0.05**	0.21	**9.93e-1**
SQLE	1480.16	**-0.09**	0.19	**9.90e-1**
SQSTM1	1581.52	**0.39**	0.2	**6.87e-1**
SRA1	68.75	**0.18**	0.25	**9.87e-1**
SRBD1	154.35	**0.05**	0.23	**9.93e-1**
SRC	31.51	**0.59**	0.25	**5.09e-1**
SRCAP	2663.3	**-0.52**	0.2	**3.80e-1**
SRD5A1	129.55	**0.37**	0.24	**8.49e-1**
SRD5A3	239.4	**0.17**	0.23	**9.87e-1**
SREBF1	753.25	**-0.38**	0.23	**8.12e-1**
SREBF2	2141.34	**-0.06**	0.2	**9.91e-1**
SREK1	856.55	**-0.49**	0.19	**3.80e-1**
SREK1IP1	113.89	**-0.09**	0.25	**9.90e-1**
SRF	869.91	**-0.56**	0.22	**4.11e-1**
SRFBP1	106.38	**0.06**	0.25	**9.93e-1**
SRGAP2	265.98	**-0.24**	0.21	**9.47e-1**
SRGAP2B	118.66	**0.07**	0.24	**9.92e-1**
SRGN	67.23	**0.02**	0.25	**9.96e-1**
SRI	393.32	**0.24**	0.21	**9.47e-1**
SRM	1870.14	**-0.2**	0.19	**9.49e-1**
SRP14	1260.39	**-0.2**	0.19	**9.49e-1**
SRP14-AS1	19.4	**0.13**	0.24	**9.90e-1**
SRP19	259.37	**-0.17**	0.21	**9.81e-1**
SRP54	798.33	**0.11**	0.2	**9.90e-1**
SRP68	715.37	**0.27**	0.2	**8.91e-1**
SRP72	1777	**-0.08**	0.19	**9.90e-1**
SRP9	688.87	**0.19**	0.2	**9.63e-1**
SRPK1	2250.2	**-0.09**	0.19	**9.90e-1**
SRPK2	408.81	**-0.37**	0.2	**7.41e-1**
SRPR	1050.98	**0.06**	0.19	**9.92e-1**

SRPRB	522.72	**0.19**	0.2	**9.60e-1**
SRR	36.64	**0.15**	0.25	**9.90e-1**
SRRD	228.97	**0.14**	0.22	**9.90e-1**
SRRM1	2644.17	**-0.56**	0.19	**2.00e-1**
SRRM2	12829.03	**-0.49**	0.19	**3.52e-1**
SRRT	2286.25	**-0.38**	0.2	**7.04e-1**
SRSF1	4253.35	**-0.05**	0.18	**9.93e-1**
SRSF10	1984.21	**-0.03**	0.19	**9.93e-1**
SRSF11	1587.93	**-0.42**	0.18	**5.45e-1**
SRSF2	2764.71	**0.15**	0.18	**9.81e-1**
SRSF3	2415.06	**0.21**	0.19	**9.49e-1**
SRSF4	1011.42	**0.05**	0.19	**9.93e-1**
SRSF5	1603.73	**-0.08**	0.18	**9.90e-1**
SRSF6	2255.39	**0.11**	0.18	**9.90e-1**
SRSF7	1315.47	**0.04**	0.19	**9.93e-1**
SRSF8	371.23	**0.04**	0.21	**9.93e-1**
SRSF9	645.21	**0.33**	0.2	**7.97e-1**
SRXN1	419.86	**-0.07**	0.2	**9.90e-1**
SS18	1323.35	**-0.25**	0.19	**9.06e-1**
SS18L1	140.35	**0.11**	0.23	**9.90e-1**
SS18L2	96.17	**0.31**	0.25	**9.29e-1**
SSB	2153.09	**-0.27**	0.18	**8.59e-1**
SSBP1	986.99	**-0.09**	0.19	**9.90e-1**
SSBP2	294.08	**-0.04**	0.21	**9.93e-1**
SSBP3	584.53	**-0.5**	0.22	**5.36e-1**
SSBP4	160.15	**-0.4**	0.25	**8.40e-1**
SSC5D	16.25	**-0.01**	0.22	**9.96e-1**
SSFA2	145.44	**0.06**	0.23	**9.93e-1**
SSH1	222.49	**0.01**	0.22	**9.96e-1**
SSH2	855.23	**-0.3**	0.19	**8.38e-1**
SSH3	10.9	**-0.07**	0.21	**9.91e-1**
SSNA1	258.91	**0**	0.23	**1.00e+0**
SSR1	1562.26	**0.32**	0.2	**8.40e-1**
SSR2	698.52	**0.07**	0.2	**9.90e-1**
SSR3	665.1	**0.34**	0.2	**8.12e-1**
SSR4	357.82	**0.02**	0.22	**9.93e-1**
SSRP1	4060.1	**0.02**	0.18	**9.93e-1**
SSSCA1	124.5	**-0.26**	0.24	**9.49e-1**
SSU72	765.05	**0.42**	0.2	**6.10e-1**
SSX2IP	229.83	**0.08**	0.23	**9.90e-1**
ST13	2178.82	**0.06**	0.18	**9.91e-1**
ST14	904.65	**-0.25**	0.21	**9.40e-1**
ST20	20.96	**0.16**	0.24	**9.90e-1**
ST20-AS1	13.34	**-0.12**	0.22	**9.90e-1**
ST3GAL1	59.53	**0.45**	0.25	**7.56e-1**
ST3GAL2	367.62	**-0.16**	0.23	**9.87e-1**
ST3GAL3	119.66	**0.43**	0.24	**7.36e-1**
ST3GAL4	60.06	**-0.07**	0.25	**9.93e-1**
ST3GAL5	14.34	**-0.04**	0.22	**9.93e-1**
ST6GAL1	3898.56	**0.27**	0.18	**8.52e-1**
ST6GALNAC4	414.42	**-0.39**	0.24	**8.38e-1**
ST6GALNAC6	166.3	**-0.29**	0.24	**9.39e-1**
ST7	241.77	**-0.13**	0.22	**9.90e-1**
ST7L	40.98	**0**	0.25	**9.99e-1**
ST8SIA4	66.31	**0.11**	0.25	**9.90e-1**
STAC3	48.8	**-0.05**	0.25	**9.93e-1**
STAG1	404.98	**0.01**	0.21	**9.96e-1**
STAG2	1473.48	**0.14**	0.2	**9.87e-1**
STAG3	11.19	**-0.23**	0.21	**9.49e-1**
STAG3L1	62.54	**-0.3**	0.25	**9.42e-1**
STAG3L2	163.79	**-0.51**	0.24	**5.92e-1**
STAG3L4	63.28	**0.04**	0.25	**9.93e-1**
STAG3L5P-PVRIG2P-PILRB	327.87	**-0.34**	0.22	**8.44e-1**

STAM	195.79	**-0.13**	0.23	**9.90e-1**
STAM2	235.65	**0.3**	0.23	**9.12e-1**
STAMBP	358.56	**0.09**	0.21	**9.90e-1**
STAMBPL1	110.82	**0.27**	0.24	**9.49e-1**
STAP1	437.19	**-0.2**	0.2	**9.58e-1**
STARD10	15.51	**0**	0.23	**9.99e-1**
STARD3	199.01	**-0.09**	0.24	**9.90e-1**
STARD3NL	144.95	**0.26**	0.23	**9.47e-1**
STARD4	190.85	**0.26**	0.23	**9.47e-1**
STARD5	17.13	**0.11**	0.23	**9.90e-1**
STARD7	2149.8	**0**	0.19	**9.99e-1**
STARD7-AS1	29.35	**0.27**	0.25	**9.49e-1**
STARD9	32.16	**-0.28**	0.25	**9.47e-1**
STAT1	217.72	**0.45**	0.23	**6.59e-1**
STAT2	304.64	**0.29**	0.21	**8.98e-1**
STAT3	340.89	**-0.09**	0.21	**9.90e-1**
STAT5B	644.64	**-0.06**	0.2	**9.91e-1**
STAT6	2865.76	**-0.3**	0.21	**8.75e-1**
STAU1	2067.16	**-0.21**	0.18	**9.47e-1**
STAU2	432.11	**-0.1**	0.21	**9.90e-1**
STIL	939.36	**-0.03**	0.19	**9.93e-1**
STIM1	461.15	**0.07**	0.2	**9.90e-1**
STIM2	550.03	**-0.26**	0.2	**9.25e-1**
STIP1	3138.04	**-0.4**	0.18	**5.71e-1**
STK10	663.74	**0.01**	0.2	**9.96e-1**
STK11	323.33	**-0.04**	0.22	**9.93e-1**
STK11IP	282.1	**-0.34**	0.24	**8.66e-1**
STK16	98.19	**0.07**	0.24	**9.92e-1**
STK17A	634.28	**0.42**	0.21	**6.69e-1**
STK17B	1136.68	**0.18**	0.2	**9.76e-1**
STK19	45.24	**0.19**	0.25	**9.87e-1**
STK24	1105.24	**0.1**	0.2	**9.90e-1**
STK25	323.14	**-0.09**	0.23	**9.90e-1**
STK26	602.73	**-0.03**	0.2	**9.93e-1**
STK3	23.87	**-0.05**	0.25	**9.93e-1**
STK32C	13.78	**0.09**	0.23	**9.90e-1**
STK33	89.99	**0.17**	0.25	**9.88e-1**
STK35	730.54	**-0.37**	0.2	**7.41e-1**
STK36	308.94	**0.08**	0.22	**9.90e-1**
STK38	567.88	**-0.15**	0.2	**9.86e-1**
STK38L	226.28	**0.11**	0.22	**9.90e-1**
STK39	560.4	**-0.02**	0.2	**9.93e-1**
STK4	1874.71	**0.08**	0.19	**9.90e-1**
STK40	1171.48	**-0.02**	0.22	**9.96e-1**
STMN1	1813.73	**0.44**	0.19	**5.37e-1**
STOML1	14.57	**-0.13**	0.22	**9.90e-1**
STOML2	649.46	**-0.05**	0.19	**9.93e-1**
STOX1	31.11	**0.07**	0.25	**9.93e-1**
STRA13	172.04	**-0.14**	0.24	**9.90e-1**
STRADA	210.45	**-0.1**	0.22	**9.90e-1**
STRADB	119.97	**0.25**	0.24	**9.52e-1**
STRAP	1209.51	**-0.03**	0.19	**9.93e-1**
STRBP	1890.16	**0.06**	0.19	**9.90e-1**
STRIP1	196.31	**0.02**	0.22	**9.95e-1**
STRIP2	117.39	**0.21**	0.24	**9.74e-1**
STRN	666.61	**-0.04**	0.21	**9.93e-1**
STRN3	224.46	**0.03**	0.22	**9.93e-1**
STRN4	731.21	**-0.25**	0.23	**9.49e-1**
STS	593.41	**0.56**	0.2	**3.01e-1**
STT3A	1588.21	**0.09**	0.19	**9.90e-1**
STT3B	1211.28	**0.37**	0.2	**7.22e-1**
STUB1	365.19	**-0.16**	0.21	**9.87e-1**
STX10	149.19	**-0.1**	0.23	**9.90e-1**
STX11	14.36	**0**	0.23	**9.98e-1**
STX12	231.67	**0.36**	0.22	**8.33e-1**

STX16	655.83	**0.03**	0.2	**9.93e-1**
STX17	268.18	**0.02**	0.22	**9.95e-1**

STX18	226.85	**0.07**	0.22	**9.91e-1**
STX18-AS1	46.19	**-0.02**	0.25	**9.95e-1**
STX1A	41.03	**-0.43**	0.25	**7.94e-1**
STX2	141.07	**0.27**	0.24	**9.47e-1**
STX3	235.07	**0.44**	0.22	**6.54e-1**
STX4	133.57	**-0.07**	0.24	**9.91e-1**
STX5	121.8	**0.43**	0.24	**7.33e-1**
STX6	198.33	**-0.1**	0.22	**9.90e-1**
STX7	529.53	**0.05**	0.21	**9.93e-1**
STX8	135.94	**-0.03**	0.23	**9.93e-1**
STXBP1	434.66	**-0.15**	0.2	**9.87e-1**
STXBP2	260.37	**-0.24**	0.22	**9.49e-1**
STXBP3	221.87	**0.44**	0.23	**7.04e-1**
STXBP4	50.15	**-0.04**	0.25	**9.93e-1**
STXBP5	155.1	**0.04**	0.23	**9.93e-1**
STYX	341.4	**-0.22**	0.22	**9.56e-1**
STYXL1	129.49	**0.15**	0.23	**9.90e-1**
SUB1	515.31	**0.17**	0.21	**9.81e-1**
SUCLA2	381.22	**0.12**	0.21	**9.90e-1**
SUCLG1	361.21	**0.31**	0.21	**8.52e-1**
SUCLG2	321.6	**0.16**	0.21	**9.87e-1**
SUCO	348.69	**0.17**	0.22	**9.86e-1**
SUDS3	560.36	**-0.05**	0.2	**9.93e-1**
SUFU	189.42	**-0.38**	0.23	**8.30e-1**
SUGP1	318.68	**-0.24**	0.21	**9.47e-1**
SUGP2	1661.1	**-0.15**	0.19	**9.83e-1**
SUGT1	311.29	**0.08**	0.21	**9.90e-1**
SULT1A1	221.35	**-0.32**	0.23	**8.90e-1**
SUMF1	20.2	**-0.14**	0.24	**9.90e-1**
SUMF2	610.49	**0.02**	0.22	**9.93e-1**
SUMO1	721.91	**0.04**	0.2	**9.93e-1**
SUMO1P3	11.49	**0.08**	0.21	**9.90e-1**
SUMO2	1230.97	**0.09**	0.19	**9.90e-1**
SUMO3	666.52	**-0.07**	0.19	**9.90e-1**
SUN1	673.09	**0.02**	0.19	**9.94e-1**
SUN2	107.76	**-0.21**	0.25	**9.81e-1**
SUPT16H	7734.63	**-0.21**	0.18	**9.47e-1**
SUPT20H	447.9	**-0.2**	0.2	**9.58e-1**
SUPT3H	35.38	**0.08**	0.25	**9.91e-1**
SUPT4H1	309.39	**0.18**	0.21	**9.81e-1**
SUPT5H	2209.12	**-0.43**	0.21	**6.60e-1**
SUPT6H	1399.34	**-0.27**	0.19	**8.77e-1**
SUPT7L	349.92	**-0.08**	0.21	**9.90e-1**
SUPV3L1	737.22	**0.28**	0.2	**8.73e-1**
SURF1	63.65	**0.41**	0.25	**8.30e-1**
SURF2	128.96	**-0.4**	0.24	**8.10e-1**
SURF4	932.12	**0.24**	0.19	**9.30e-1**
SURF6	610.94	**-0.25**	0.21	**9.47e-1**
SUSD3	353.47	**0.34**	0.21	**8.30e-1**
SUSD6	370.77	**-0.12**	0.21	**9.90e-1**
SUV39H1	251.24	**-0.29**	0.23	**9.13e-1**
SUV39H2	324.2	**-0.1**	0.22	**9.90e-1**
SUV420H1	233.73	**0.13**	0.22	**9.90e-1**
SUV420H2	61.31	**0.04**	0.25	**9.93e-1**
SUZ12	1533.44	**0**	0.2	**9.98e-1**
SUZ12P1	71.71	**0.34**	0.25	**9.06e-1**
SVBP	68.23	**0.01**	0.25	**9.96e-1**
SWAP70	3674.13	**0.48**	0.19	**3.77e-1**
SWI5	71.02	**-0.11**	0.25	**9.90e-1**
SWSAP1	42.71	**-0.55**	0.25	**5.86e-1**
SWT1	18.37	**0.28**	0.24	**9.42e-1**

SYAP1	324.15	**0.05**	0.21	**9.93e-1**
SYBU	21.17	**-0.38**	0.24	**8.40e-1**
SYCE2	12.84	**0**	0.22	**9.98e-1**
SYF2	225.56	**0.28**	0.22	**9.25e-1**
SYK	1509.64	**-0.41**	0.18	**5.79e-1**
SYMPK	1499.54	**-0.25**	0.2	**9.25e-1**
SYNCRIP	7510.84	**-0.4**	0.18	**5.76e-1**
SYNE1	283.37	**0.41**	0.21	**7.03e-1**
SYNE2	2643.83	**-0.17**	0.19	**9.71e-1**
SYNGAP1	706.38	**-0.43**	0.22	**6.88e-1**
SYNGR2	1305.65	**0.4**	0.21	**6.93e-1**
SYNGR3	73.56	**0.29**	0.25	**9.47e-1**
SYNJ1	68.98	**-0.04**	0.25	**9.93e-1**
SYNJ2	425.66	**0.03**	0.2	**9.93e-1**
SYNPO	49.26	**-0.15**	0.25	**9.90e-1**
SYNRG	329.64	**0.06**	0.21	**9.93e-1**
SYP	30.15	**-0.12**	0.25	**9.90e-1**
SYPL1	1435.04	**0.32**	0.2	**8.38e-1**
SYS1	357.36	**0.69**	0.21	**1.03e-1**
SYTL1	22.16	**0.12**	0.24	**9.90e-1**
SYVN1	3482.81	**-0.24**	0.2	**9.42e-1**
SZRD1	1504.46	**-0.48**	0.21	**5.68e-1**

SZT2	650.89	**-0.32**	0.21	**8.54e-1**
TAB1	411.04	**-0.18**	0.22	**9.81e-1**
TAB2	481.35	**-0.14**	0.2	**9.87e-1**
TAB3	586.49	**-0.27**	0.21	**9.17e-1**
TACC1	1417.32	**0.25**	0.19	**9.12e-1**
TACC3	1352.43	**-0.21**	0.19	**9.49e-1**
TACO1	185.93	**0.23**	0.23	**9.54e-1**
TADA1	173.97	**0.15**	0.23	**9.89e-1**
TADA2A	180.31	**0.12**	0.22	**9.90e-1**
TADA2B	151.25	**-0.1**	0.23	**9.90e-1**
TADA3	201.49	**-0.05**	0.23	**9.93e-1**
TAF1	477.6	**0.15**	0.2	**9.87e-1**
TAF10	126.24	**0.06**	0.24	**9.93e-1**
TAF11	174.69	**-0.22**	0.23	**9.59e-1**
TAF12	177.74	**-0.16**	0.23	**9.88e-1**
TAF13	104.07	**-0.01**	0.24	**9.98e-1**
TAF15	3293.84	**-0.66**	0.2	**8.97e-2**
TAF1A	54.98	**-0.02**	0.25	**9.95e-1**
TAF1B	87.12	**-0.02**	0.25	**9.93e-1**
TAF1C	535.46	**-0.36**	0.24	**8.61e-1**
TAF1D	451.13	**-0.18**	0.22	**9.84e-1**
TAF2	703.01	**-0.08**	0.2	**9.90e-1**
TAF3	239.02	**-0.32**	0.22	**8.64e-1**
TAF4	450.33	**0.12**	0.2	**9.90e-1**
TAF4B	802.4	**0.06**	0.2	**9.91e-1**
TAF5	258.71	**0.05**	0.22	**9.93e-1**
TAF5L	425.22	**-0.09**	0.21	**9.90e-1**
TAF6	738.53	**-0.31**	0.21	**8.64e-1**
TAF6L	130.27	**-0.04**	0.25	**9.93e-1**
TAF7	1083.39	**0.09**	0.19	**9.90e-1**
TAF8	273.92	**0.36**	0.21	**8.04e-1**
TAF9	504.17	**-0.12**	0.2	**9.90e-1**
TAF9B	170.29	**-0.11**	0.23	**9.90e-1**
TAGAP	435.52	**0.41**	0.2	**6.54e-1**
TAGLN2	2825.32	**-0.24**	0.19	**9.33e-1**
TALDO1	1387.49	**0.05**	0.19	**9.93e-1**
TAMM41	95.31	**0.05**	0.24	**9.93e-1**
TANC1	419.25	**-0.06**	0.2	**9.92e-1**
TANGO2	137.78	**-0.06**	0.23	**9.93e-1**
TANGO6	205.57	**-0.04**	0.22	**9.93e-1**
TANK	371.97	**0.34**	0.21	**8.36e-1**

TAOK1	686.47	**0.11**	0.2	**9.90e-1**
TAOK2	465.03	**-0.27**	0.22	**9.43e-1**
TAOK3	759.49	**0.08**	0.19	**9.90e-1**
TAP1	595.51	**0.04**	0.21	**9.93e-1**
TAP2	2147.07	**-0.25**	0.19	**9.04e-1**
TAPBP	1757.58	**-0.11**	0.21	**9.90e-1**
TAPBPL	44.57	**-0.09**	0.25	**9.90e-1**
TAPT1	199.36	**0.04**	0.23	**9.93e-1**
TAPT1-AS1	10.81	**-0.02**	0.21	**9.95e-1**
TARBP1	338.63	**0.3**	0.21	**8.78e-1**
TARBP2	184.37	**-0.03**	0.24	**9.93e-1**
TARDBP	2457.2	**-0.06**	0.19	**9.91e-1**
TARS	1006.58	**0.4**	0.19	**6.14e-1**
TARS2	632.46	**-0.13**	0.2	**9.89e-1**
TARSL2	191.26	**-0.13**	0.23	**9.90e-1**
TASP1	74.99	**0.04**	0.25	**9.93e-1**
TATDN1	158.17	**0.34**	0.24	**8.66e-1**
TATDN2	809.07	**-0.16**	0.19	**9.81e-1**
TATDN3	117	**0.33**	0.24	**9.07e-1**
TAX1BP1	990.97	**0.11**	0.2	**9.90e-1**
TAZ	82.41	**0.14**	0.25	**9.90e-1**
TBC1D1	812.73	**0.24**	0.2	**9.39e-1**
TBC1D10A	84.17	**-0.33**	0.25	**9.11e-1**
TBC1D10B	432.57	**-0.13**	0.24	**9.90e-1**
TBC1D10C	153.78	**-0.36**	0.25	**8.73e-1**
TBC1D12	117.22	**0.08**	0.24	**9.91e-1**
TBC1D13	274.96	**-0.21**	0.22	**9.58e-1**
TBC1D14	937.41	**-0.03**	0.19	**9.93e-1**
TBC1D15	163.71	**0.07**	0.23	**9.91e-1**
TBC1D17	117.22	**-0.05**	0.25	**9.93e-1**
TBC1D19	22.81	**0.15**	0.24	**9.90e-1**
TBC1D2	19.95	**-0.05**	0.24	**9.93e-1**
TBC1D20	244.9	**0.09**	0.22	**9.90e-1**
TBC1D22A	310.76	**-0.05**	0.22	**9.93e-1**
TBC1D22B	226.32	**-0.11**	0.22	**9.90e-1**
TBC1D23	212.63	**0.17**	0.23	**9.87e-1**
TBC1D24	286.54	**-0.44**	0.24	**7.36e-1**
TBC1D25	116.92	**-0.01**	0.24	**9.96e-1**
TBC1D2B	394.43	**-0.1**	0.2	**9.90e-1**
TBC1D31	81.2	**0.03**	0.25	**9.93e-1**
TBC1D32	37.62	**0.01**	0.25	**9.97e-1**
TBC1D4	232.96	**0.1**	0.22	**9.90e-1**

TBC1D5	441.18	**0.02**	0.2	**9.93e-1**
TBC1D7	31.69	**0.19**	0.25	**9.87e-1**
TBC1D8B	34.51	**-0.04**	0.25	**9.93e-1**
TBC1D9	91.48	**-0.57**	0.24	**5.31e-1**
TBC1D9B	860.72	**0.01**	0.21	**9.96e-1**
TBCA	618.5	**0.09**	0.2	**9.90e-1**
TBCB	274.57	**0.23**	0.21	**9.49e-1**
TBCC	96.39	**0.06**	0.24	**9.93e-1**
TBCCD1	124.18	**0.33**	0.24	**8.89e-1**
TBCD	498.33	**-0.08**	0.2	**9.90e-1**
TBCE	197.11	**0.14**	0.23	**9.90e-1**
TBCEL	65.98	**0.18**	0.25	**9.87e-1**
TBCK	108	**0.32**	0.24	**9.10e-1**
TBK1	489.81	**0.04**	0.21	**9.93e-1**
TBL1X	501.07	**0**	0.2	**9.98e-1**
TBL1XR1	1138.94	**0.32**	0.2	**8.40e-1**
TBL2	286.82	**-0.24**	0.21	**9.47e-1**
TBL3	617.7	**-0.32**	0.23	**8.73e-1**
TBP	273.04	**-0.31**	0.21	**8.64e-1**
TBPL1	187.91	**-0.22**	0.23	**9.60e-1**
TBRG1	245.38	**-0.13**	0.22	**9.90e-1**

TBRG4	1107.79	**-0.31**	0.2	**8.53e-1**
TCAIM	142.47	**0.13**	0.23	**9.90e-1**
TCEA1	1652.97	**0.19**	0.19	**9.58e-1**
TCEA2	44.36	**0.22**	0.25	**9.78e-1**
TCEANC	11.88	**0.06**	0.21	**9.93e-1**
TCEANC2	139.01	**0.11**	0.23	**9.90e-1**
TCEB1	289.34	**-0.11**	0.21	**9.90e-1**
TCEB2	376.42	**0.09**	0.21	**9.90e-1**
TCEB3	1143.18	**-0.38**	0.19	**6.34e-1**
TCERG1	2215.81	**-0.31**	0.18	**8.18e-1**
TCF12	553.38	**-0.1**	0.21	**9.90e-1**
TCF19	355.38	**-0.05**	0.21	**9.93e-1**
TCF20	1390.77	**0**	0.19	**9.99e-1**
TCF25	791.57	**-0.27**	0.21	**9.12e-1**
TCF3	5377.28	**-0.54**	0.23	**4.73e-1**
TCF4	880.69	**0.39**	0.19	**6.56e-1**
TCF7L2	43.09	**-0.42**	0.25	**8.11e-1**
TCFL5	200.05	**0.31**	0.22	**8.87e-1**
TCHP	231.61	**-0.22**	0.22	**9.58e-1**
TCIRG1	82.76	**-0.17**	0.25	**9.89e-1**
TCL1A	391.4	**-0.26**	0.22	**9.47e-1**
TCL6	13.14	**-0.19**	0.22	**9.80e-1**
TCOF1	1818.41	**-0.53**	0.21	**4.11e-1**
TCONS_00029157	35.61	**-0.39**	0.25	**8.50e-1**
TCP1	4358.82	**0.01**	0.19	**9.96e-1**
TCP11L1	122.07	**0**	0.24	**9.98e-1**
TCTA	103.25	**0.15**	0.24	**9.90e-1**
TCTEX1D2	17.68	**-0.05**	0.23	**9.93e-1**
TCTN1	509.94	**1.01**	0.2	**3.61e-4**
TCTN2	26.56	**0.34**	0.25	**9.03e-1**
TCTN3	271.1	**0.19**	0.22	**9.74e-1**
TDG	725.93	**-0.31**	0.2	**8.40e-1**
TDP1	253.38	**0.11**	0.21	**9.90e-1**
TDP2	304.76	**-0.12**	0.21	**9.90e-1**
TDRD3	169.85	**-0.04**	0.23	**9.93e-1**
TDRD7	84.07	**0.13**	0.25	**9.90e-1**
TDRKH	74.45	**0.12**	0.25	**9.90e-1**
TEC	101.89	**0.79**	0.24	**1.05e-1**
TECPR1	83.03	**-0.08**	0.25	**9.90e-1**
TECPR2	120.03	**-0.24**	0.24	**9.58e-1**
TECR	763.88	**-0.4**	0.21	**7.22e-1**
TEF	164.57	**-0.35**	0.23	**8.53e-1**
TEFM	56.84	**-0.12**	0.25	**9.90e-1**
TEKT4P2	56.68	**-0.24**	0.25	**9.66e-1**
TELO2	415.05	**-0.4**	0.25	**8.31e-1**
TEP1	231.43	**0.03**	0.22	**9.93e-1**
TERF1	312.29	**-0.05**	0.21	**9.93e-1**
TERF2	469.78	**-0.08**	0.2	**9.90e-1**
TERF2IP	649.03	**0.31**	0.2	**8.41e-1**
TERT	82.75	**-0.29**	0.25	**9.47e-1**
TES	507.1	**0.54**	0.2	**3.41e-1**
TESC	114.5	**0.27**	0.24	**9.47e-1**
TESK1	587.68	**-0.2**	0.24	**9.83e-1**
TESK2	79.94	**0.19**	0.25	**9.87e-1**
TESPA1	12.2	**-0.13**	0.22	**9.90e-1**
TET2	81.08	**-0.15**	0.25	**9.90e-1**
TET3	486.8	**-0.17**	0.21	**9.81e-1**
TEX10	871.94	**-0.25**	0.2	**9.39e-1**
TEX19	32.78	**0.22**	0.25	**9.75e-1**
TEX2	225.46	**-0.05**	0.22	**9.93e-1**
TEX22	11.9	**-0.07**	0.21	**9.91e-1**
TEX261	986.22	**-0.13**	0.19	**9.89e-1**
TEX264	199.04	**-0.21**	0.23	**9.70e-1**

TEX30	14.36	**0.15**	0.23	**9.90e-1**
TEX9	62.8	**-0.12**	0.25	**9.90e-1**
TFAM	1133.28	**0.07**	0.2	**9.90e-1**
TFAP4	359.29	**-0.39**	0.23	**8.03e-1**
TFB1M	152.55	**0.08**	0.23	**9.90e-1**
TFB2M	221.25	**0.06**	0.22	**9.93e-1**
TFCP2	260.93	**0.14**	0.22	**9.90e-1**
TFDP1	2521.67	**-0.03**	0.18	**9.93e-1**
TFDP2	773.68	**-0.51**	0.19	**3.41e-1**
TFE3	334.49	**-0.05**	0.23	**9.93e-1**
TFEB	431.28	**0.01**	0.23	**9.96e-1**
TFEC	391.25	**0.91**	0.22	**1.19e-2**
TFG	272.35	**0.05**	0.21	**9.93e-1**
TFIP11	535.29	**0.06**	0.2	**9.91e-1**
TFPT	106.28	**-0.14**	0.25	**9.90e-1**
TFRC	2782.87	**0.28**	0.19	**8.68e-1**
TGDS	146.16	**-0.09**	0.23	**9.90e-1**
TGFB1	1437.32	**-0.54**	0.22	**4.17e-1**
TGFBR1	362.74	**0.26**	0.22	**9.42e-1**
TGFBR2	156.96	**0.05**	0.23	**9.93e-1**
TGFBRAP1	605.96	**-0.16**	0.2	**9.81e-1**
TGIF2	917.83	**-0.34**	0.2	**7.73e-1**
TGOLN2	927.19	**-0.1**	0.19	**9.90e-1**
TGS1	424.57	**-0.2**	0.21	**9.58e-1**
THADA	397.27	**0.1**	0.21	**9.90e-1**
THAP1	130.59	**-0.12**	0.24	**9.90e-1**
THAP11	265.53	**0.16**	0.22	**9.87e-1**
THAP2	38.9	**-0.02**	0.25	**9.96e-1**
THAP3	66.77	**0.03**	0.25	**9.93e-1**
THAP4	855.02	**-0.41**	0.21	**6.69e-1**
THAP5	346.38	**-0.09**	0.22	**9.90e-1**
THAP6	85.16	**0.15**	0.25	**9.90e-1**
THAP7	136.16	**-0.21**	0.25	**9.80e-1**
THAP7-AS1	12.12	**-0.13**	0.22	**9.90e-1**
THAP8	18.27	**-0.05**	0.23	**9.93e-1**
THAP9	72.9	**0.04**	0.25	**9.93e-1**
THAP9-AS1	186.58	**0.09**	0.23	**9.90e-1**
THBS3	40.82	**0.18**	0.25	**9.87e-1**
THEM4	44.84	**0.1**	0.25	**9.90e-1**
THEM6	74.07	**-0.2**	0.25	**9.86e-1**
THEMIS2	61.54	**-0.63**	0.25	**4.16e-1**
THG1L	166.82	**0.25**	0.23	**9.49e-1**
THNSL1	186.83	**0.24**	0.23	**9.51e-1**
THOC1	348.96	**0.1**	0.21	**9.90e-1**
THOC2	723.38	**-0.03**	0.2	**9.93e-1**
THOC3	360.61	**-0.28**	0.21	**9.12e-1**
THOC5	421.63	**-0.05**	0.21	**9.93e-1**
THOC6	329.8	**-0.05**	0.22	**9.93e-1**
THOC7	379.31	**0.26**	0.22	**9.47e-1**
THOP1	1031.02	**-0.31**	0.22	**8.70e-1**
THRA	63.12	**-0.47**	0.25	**7.14e-1**
THRAP3	3604.71	**-0.33**	0.18	**7.56e-1**
THTPA	58.75	**-0.16**	0.25	**9.90e-1**
THUMPD1	644.57	**-0.06**	0.21	**9.91e-1**
THUMPD2	62.85	**-0.02**	0.25	**9.96e-1**
THUMPD3	337.58	**0.08**	0.21	**9.90e-1**
THUMPD3-AS1	76.8	**0.49**	0.25	**6.69e-1**
THYN1	205.1	**0.01**	0.22	**9.96e-1**
TIA1	420.65	**0.09**	0.21	**9.90e-1**
TIAL1	799.23	**0.08**	0.19	**9.90e-1**
TIAM1	135.2	**0.01**	0.23	**9.96e-1**
TIAM2	261.29	**0.35**	0.22	**8.30e-1**
TICAM1	311.3	**-0.28**	0.22	**9.16e-1**
TICRR	553.6	**-0.39**	0.2	**6.69e-1**
TIFA	358.92	**0.54**	0.22	**4.22e-1**

TIGAR	222.14	**0.04**	0.22	**9.93e-1**
TIGD1	95.38	**0.11**	0.24	**9.90e-1**
TIGD2	29.92	**0.11**	0.25	**9.90e-1**
TIGD4	10.5	**-0.14**	0.21	**9.90e-1**
TIGD5	33.59	**-0.12**	0.25	**9.90e-1**
TIGD6	23.51	**-0.02**	0.25	**9.95e-1**
TIMELESS	1539.59	**0.09**	0.18	**9.90e-1**
TIMM10	265.68	**-0.17**	0.22	**9.86e-1**
TIMM10B	372.08	**-0.1**	0.21	**9.90e-1**
TIMM13	348.92	**-0.14**	0.23	**9.90e-1**
TIMM17A	542.6	**-0.07**	0.2	**9.90e-1**
TIMM17B	181.55	**-0.18**	0.2	**9.74e-1**
TIMM21	324.44	**0.36**	0.22	**8.09e-1**
TIMM22	173.87	**-0.22**	0.23	**9.58e-1**
TIMM23	275.02	**0.18**	0.22	**9.81e-1**
TIMM23B	95.48	**0.09**	0.24	**9.90e-1**
TIMM44	775.55	**-0.11**	0.2	**9.90e-1**

TIMM50	398.28	**-0.02**	0.21	**9.93e-1**
TIMM8A	91.26	**0.07**	0.24	**9.91e-1**
TIMM8B	185.25	**-0.22**	0.23	**9.61e-1**
TIMM9	169.2	**0.13**	0.23	**9.90e-1**
TIMMDC1	311.31	**0.18**	0.22	**9.80e-1**
TINF2	247.78	**0.05**	0.22	**9.93e-1**
TIPARP	86.21	**0.13**	0.25	**9.90e-1**
TIPIN	207.96	**0.05**	0.22	**9.93e-1**
TIPRL	516.97	**0.21**	0.21	**9.58e-1**
TJAP1	232.09	**-0.12**	0.23	**9.90e-1**
TJP2	268.89	**-0.54**	0.21	**3.95e-1**
TJP3	76.66	**-0.22**	0.25	**9.80e-1**
TK1	394.75	**-0.15**	0.22	**9.88e-1**
TKFC	163.43	**-0.15**	0.24	**9.90e-1**
TKT	4306.32	**-0.35**	0.2	**7.59e-1**
TLCD1	35.28	**0.16**	0.25	**9.90e-1**
TLDC1	64.85	**0.1**	0.25	**9.90e-1**
TLE3	835.53	**-0.5**	0.22	**5.37e-1**
TLE4	346.46	**-0.14**	0.21	**9.90e-1**
TLE6	25.07	**0.08**	0.25	**9.91e-1**
TLK1	830.99	**0.05**	0.19	**9.93e-1**
TLK2	385.02	**0.12**	0.21	**9.90e-1**
TLN1	2247.43	**-0.09**	0.19	**9.90e-1**
TLN2	199.75	**-0.12**	0.22	**9.90e-1**
TLR1	158.32	**0.18**	0.23	**9.87e-1**
TLR10	880.54	**0.07**	0.2	**9.90e-1**
TLR3	20.38	**-0.25**	0.24	**9.49e-1**
TLR4	69.03	**0.03**	0.25	**9.93e-1**
TLR6	171.53	**0.15**	0.23	**9.89e-1**
TLR9	942.11	**-0.77**	0.23	**7.89e-2**
TM2D1	87.95	**0.06**	0.24	**9.93e-1**
TM2D2	115.69	**-0.02**	0.24	**9.96e-1**
TM2D3	68.93	**0.29**	0.25	**9.47e-1**
TM7SF2	47.18	**-0.44**	0.25	**7.94e-1**
TM7SF3	361.38	**0.32**	0.21	**8.52e-1**
TM9SF1	180.08	**0.47**	0.23	**6.03e-1**
TM9SF2	551.57	**0.31**	0.21	**8.56e-1**
TM9SF3	1187.97	**0.35**	0.2	**7.66e-1**
TM9SF4	1107.03	**-0.26**	0.19	**8.91e-1**
TMA16	284.23	**-0.06**	0.21	**9.92e-1**
TMA7	436.05	**-0.1**	0.21	**9.90e-1**
TMBIM1	602.77	**-0.31**	0.2	**8.40e-1**
TMBIM4	35.53	**0.25**	0.25	**9.60e-1**
TMBIM6	2275.23	**0.23**	0.19	**9.40e-1**
TMC3-AS1	13.08	**-0.04**	0.22	**9.93e-1**
TMC6	252.38	**0**	0.24	**1.00e+0**

TMC8	1156.48	**0.22**	0.23	**9.64e-1**
TMCC1	121.97	**0.16**	0.24	**9.89e-1**
TMCC2	48.06	**-0.32**	0.25	**9.29e-1**
TMCO1	315.46	**0.13**	0.21	**9.90e-1**
TMCO3	89.3	**0.29**	0.24	**9.47e-1**
TMCO6	122.33	**-0.11**	0.24	**9.90e-1**
TMED1	54.33	**0**	0.25	**1.00e+0**
TMED10	1641.86	**0.35**	0.19	**7.33e-1**
TMED2	1322.27	**0.35**	0.19	**7.41e-1**
TMED3	197.57	**0**	0.24	**9.99e-1**
TMED4	403.17	**0.07**	0.2	**9.90e-1**
TMED5	772.09	**-0.02**	0.21	**9.95e-1**
TMED7	299.37	**0.45**	0.23	**6.69e-1**
TMED8	104.9	**-0.44**	0.24	**7.36e-1**
TMED9	510.08	**-0.01**	0.2	**9.96e-1**
TMEM101	123.48	**-0.04**	0.24	**9.93e-1**
TMEM102	103.45	**-0.26**	0.25	**9.49e-1**
TMEM104	172.14	**-0.49**	0.24	**6.54e-1**
TMEM106A	45.76	**0.04**	0.25	**9.93e-1**
TMEM106C	496.43	**0.24**	0.2	**9.42e-1**
TMEM107	62.29	**-0.14**	0.25	**9.90e-1**
TMEM109	1259.74	**-0.36**	0.22	**8.30e-1**
TMEM11	209.49	**-0.17**	0.23	**9.87e-1**
TMEM110	103.95	**0.04**	0.24	**9.93e-1**
TMEM115	142.12	**-0.31**	0.25	**9.25e-1**
TMEM116	97.11	**0.16**	0.24	**9.90e-1**
TMEM117	25.24	**-0.09**	0.25	**9.90e-1**
TMEM120A	115.03	**0.13**	0.24	**9.90e-1**
TMEM120B	280.43	**-0.44**	0.22	**6.79e-1**
TMEM123	3037.71	**0.3**	0.19	**8.40e-1**
TMEM126A	33.13	**0.14**	0.25	**9.90e-1**
TMEM126B	192.51	**0.1**	0.23	**9.90e-1**
TMEM127	323.53	**-0.09**	0.21	**9.90e-1**
TMEM128	47.19	**0.36**	0.25	**8.76e-1**
TMEM129	241.08	**-0.09**	0.21	**9.90e-1**
TMEM131	602.45	**0.03**	0.2	**9.93e-1**
TMEM134	62.74	**-0.1**	0.25	**9.90e-1**

TMEM135	188.29	**0.18**	0.23	**9.83e-1**
TMEM138	132.5	**0.05**	0.24	**9.93e-1**
TMEM140	10.36	**-0.11**	0.21	**9.90e-1**
TMEM141	115.48	**-0.26**	0.25	**9.49e-1**
TMEM143	106.58	**-0.08**	0.24	**9.91e-1**
TMEM147	346.33	**0.26**	0.22	**9.45e-1**
TMEM147-AS1	88.94	**0.05**	0.25	**9.93e-1**
TMEM14A	76.98	**0.44**	0.25	**7.57e-1**
TMEM14B	205.36	**0.19**	0.22	**9.74e-1**
TMEM14C	133.46	**0.17**	0.23	**9.87e-1**
TMEM156	214.23	**0.19**	0.23	**9.81e-1**
TMEM159	58.06	**0.48**	0.25	**6.90e-1**
TMEM160	25.35	**-0.1**	0.24	**9.90e-1**
TMEM161A	310.06	**-0.27**	0.24	**9.47e-1**
TMEM161B	162.19	**0.18**	0.23	**9.86e-1**
TMEM161B-AS1	10.11	**0.14**	0.21	**9.88e-1**
TMEM164	106.7	**-0.13**	0.24	**9.90e-1**
TMEM165	341.46	**0.26**	0.21	**9.25e-1**
TMEM167A	448.6	**0.14**	0.21	**9.88e-1**
TMEM167B	140.57	**0.19**	0.23	**9.82e-1**
TMEM168	29.17	**0.14**	0.25	**9.90e-1**
TMEM170A	176.17	**0.05**	0.23	**9.93e-1**
TMEM170B	205.87	**0.29**	0.24	**9.37e-1**
TMEM175	85.23	**0.06**	0.25	**9.93e-1**
TMEM177	38.31	**-0.2**	0.25	**9.84e-1**
TMEM178B	12.78	**0.19**	0.22	**9.80e-1**

TMEM179B	89.29	**0.06**	0.24	**9.93e-1**
TMEM18	89.42	**0.19**	0.25	**9.87e-1**
TMEM180	62.16	**-0.04**	0.25	**9.93e-1**
TMEM181	236.77	**0.35**	0.22	**8.40e-1**
TMEM182	22.24	**0.27**	0.24	**9.49e-1**
TMEM183A	27.9	**0.12**	0.25	**9.90e-1**
TMEM184B	329.36	**-0.43**	0.22	**6.84e-1**
TMEM184C	201.05	**0.02**	0.22	**9.95e-1**
TMEM185A	34.16	**-0.01**	0.25	**9.98e-1**
TMEM186	69.62	**0.09**	0.25	**9.90e-1**
TMEM189	165.9	**-0.26**	0.24	**9.49e-1**
TMEM19	205.05	**-0.06**	0.23	**9.93e-1**
TMEM192	335.41	**-0.15**	0.21	**9.87e-1**
TMEM198	30.66	**-0.02**	0.24	**9.93e-1**
TMEM198B	201.9	**-0.34**	0.23	**8.52e-1**
TMEM199	220.69	**0.33**	0.22	**8.64e-1**
TMEM201	639.52	**-0.51**	0.23	**5.79e-1**
TMEM203	134.53	**0.51**	0.24	**5.91e-1**
TMEM205	170.4	**0.16**	0.24	**9.88e-1**
TMEM206	76.4	**0.19**	0.25	**9.87e-1**
TMEM208	79.17	**-0.01**	0.25	**9.98e-1**
TMEM209	741.84	**-0.16**	0.2	**9.81e-1**
TMEM214	570.35	**-0.14**	0.21	**9.88e-1**
TMEM218	63.66	**0.35**	0.25	**8.91e-1**
TMEM219	77.2	**0.19**	0.25	**9.87e-1**
TMEM222	204.04	**0.09**	0.23	**9.90e-1**
TMEM223	91.91	**-0.34**	0.25	**9.01e-1**
TMEM229B	58.64	**-0.35**	0.25	**8.96e-1**
TMEM230	664.58	**0.13**	0.19	**9.88e-1**
TMEM231	123.36	**0.37**	0.24	**8.40e-1**
TMEM234	23.37	**0.08**	0.24	**9.90e-1**
TMEM237	37.76	**0.1**	0.25	**9.90e-1**
TMEM241	115.11	**0.06**	0.24	**9.93e-1**
TMEM242	42.44	**0.39**	0.25	**8.52e-1**
TMEM243	197.71	**0.61**	0.23	**3.09e-1**
TMEM245	600.79	**-0.08**	0.2	**9.90e-1**
TMEM248	918.24	**0.07**	0.19	**9.90e-1**
TMEM249	18.24	**-0.08**	0.23	**9.91e-1**
TMEM251	50.59	**0.48**	0.25	**7.02e-1**
TMEM254	41.58	**0.15**	0.25	**9.90e-1**
TMEM256	12.75	**-0.06**	0.22	**9.93e-1**
TMEM258	95.34	**0.25**	0.24	**9.52e-1**
TMEM259	1084.4	**-0.16**	0.22	**9.87e-1**
TMEM260	88.01	**0.08**	0.25	**9.91e-1**
TMEM261	147.83	**0.03**	0.23	**9.93e-1**
TMEM263	65.91	**0.25**	0.25	**9.58e-1**
TMEM265	62.18	**0.18**	0.25	**9.87e-1**
TMEM30A	1941.25	**0.36**	0.2	**7.56e-1**
TMEM33	651.02	**-0.12**	0.2	**9.90e-1**
TMEM38A	143.49	**-0.08**	0.23	**9.91e-1**
TMEM38B	256.35	**0.3**	0.22	**9.10e-1**
TMEM39A	162.72	**0.29**	0.23	**9.25e-1**
TMEM39B	207.71	**0.05**	0.22	**9.93e-1**
TMEM41A	52.48	**-0.07**	0.25	**9.93e-1**
TMEM41B	129.15	**0.16**	0.24	**9.90e-1**
TMEM43	330.3	**0.03**	0.21	**9.93e-1**
TMEM5	140.16	**0.21**	0.23	**9.71e-1**

TMEM50A	431.82	**0.34**	0.21	**8.38e-1**
TMEM50B	204.02	**0.63**	0.23	**2.89e-1**
TMEM53	40.7	**-0.26**	0.25	**9.54e-1**
TMEM55A	39.59	**0.03**	0.25	**9.93e-1**
TMEM55B	163.9	**-0.08**	0.24	**9.90e-1**
TMEM57	296.68	**0.08**	0.21	**9.90e-1**
TMEM59	362.86	**0.56**	0.21	**3.52e-1**

TMEM60	47.97	**0.5**	0.25	**6.79e-1**
TMEM62	184.13	**0.08**	0.23	**9.90e-1**
TMEM63A	159.85	**-0.28**	0.23	**9.47e-1**
TMEM63B	151.97	**0.05**	0.23	**9.93e-1**
TMEM63C	146.52	**-0.36**	0.24	**8.53e-1**
TMEM64	205.9	**0.27**	0.23	**9.47e-1**
TMEM65	129.95	**0.31**	0.24	**9.22e-1**
TMEM67	95.77	**-0.04**	0.25	**9.93e-1**
TMEM68	64.01	**0.14**	0.25	**9.90e-1**
TMEM69	478.79	**-0.14**	0.2	**9.88e-1**
TMEM70	158.08	**0.27**	0.24	**9.47e-1**
TMEM79	67.45	**0.04**	0.25	**9.93e-1**
TMEM80	75.08	**0.15**	0.25	**9.90e-1**
TMEM86B	95.22	**-0.18**	0.25	**9.88e-1**
TMEM87A	233.16	**0.07**	0.22	**9.91e-1**
TMEM87B	138.73	**0.11**	0.24	**9.90e-1**
TMEM8A	241.17	**-0.17**	0.24	**9.88e-1**
TMEM8B	39.05	**-0.13**	0.25	**9.90e-1**
TMEM9	85.96	**0.13**	0.25	**9.90e-1**
TMEM97	724.41	**-0.19**	0.19	**9.61e-1**
TMEM99	25.26	**0.26**	0.25	**9.49e-1**
TMEM9B	116.74	**0.32**	0.24	**9.10e-1**
TMF1	308.23	**0.07**	0.22	**9.90e-1**
TMLHE	75.14	**-0.01**	0.25	**9.98e-1**
TMOD2	370.71	**-0.02**	0.21	**9.93e-1**
TMOD3	359.94	**-0.03**	0.22	**9.93e-1**
TMPO	2604.66	**-0.03**	0.19	**9.93e-1**
TMPO-AS1	91.28	**0.06**	0.24	**9.93e-1**
TMPPE	26.08	**0.17**	0.25	**9.89e-1**
TMPRSS13	11	**0.16**	0.21	**9.87e-1**
TMSB10	868.17	**-0.1**	0.2	**9.90e-1**
TMSB4X	1629.65	**0.96**	0.19	**4.96e-4**
TMTC2	66.7	**0.02**	0.25	**9.96e-1**
TMTC3	106.07	**0**	0.24	**9.99e-1**
TMTC4	147.5	**0.2**	0.23	**9.80e-1**
TMUB1	373.36	**-0.33**	0.24	**8.97e-1**
TMUB2	150.52	**-0.11**	0.24	**9.90e-1**
TMX1	605.49	**0.2**	0.21	**9.60e-1**
TMX2	631.95	**-0.08**	0.2	**9.90e-1**
TMX3	371.86	**0.33**	0.22	**8.53e-1**
TMX4	665.68	**0.33**	0.2	**8.30e-1**
TNF	171.44	**0.26**	0.24	**9.49e-1**
TNFAIP1	122.85	**-0.1**	0.24	**9.90e-1**
TNFAIP3	383.95	**0.53**	0.21	**3.77e-1**
TNFAIP8	231.09	**0.17**	0.22	**9.87e-1**
TNFAIP8L1	85.5	**-0.23**	0.25	**9.72e-1**
TNFRSF10A	196.19	**0.23**	0.22	**9.52e-1**
TNFRSF10B	474.48	**0.29**	0.2	**8.73e-1**
TNFRSF13B	93.31	**-0.64**	0.25	**3.64e-1**
TNFRSF13C	82.51	**-0.17**	0.25	**9.89e-1**
TNFRSF14	172.79	**0.22**	0.24	**9.74e-1**
TNFRSF17	23.2	**0.25**	0.25	**9.54e-1**
TNFRSF1A	11.18	**-0.17**	0.2	**9.80e-1**
TNFRSF21	32.72	**-0.34**	0.25	**9.04e-1**
TNFRSF9	10.87	**-0.18**	0.21	**9.75e-1**
TNFSF9	111.89	**0.13**	0.25	**9.90e-1**
TNIP1	2131.11	**-0.05**	0.19	**9.93e-1**
TNIP2	180.48	**0.24**	0.23	**9.50e-1**
TNK2	206.14	**-0.65**	0.25	**3.50e-1**
TNKS	403.4	**0.14**	0.21	**9.89e-1**
TNKS1BP1	315.53	**-0.36**	0.24	**8.53e-1**
TNKS2	480	**0.45**	0.22	**6.07e-1**
TNPO1	2636.49	**-0.04**	0.2	**9.93e-1**
TNPO2	1285.13	**-0.48**	0.2	**4.22e-1**

TNPO3	1418.07	**-0.07**	0.19	**9.90e-1**
TNRC18	1009.43	**-0.12**	0.23	**9.90e-1**
TNRC6A	1088.68	**-0.44**	0.19	**5.27e-1**
TNRC6B	343.36	**-0.33**	0.22	**8.52e-1**
TNRC6C	42.71	**-0.12**	0.25	**9.90e-1**
TNRC6C-AS1	21.35	**0.14**	0.24	**9.90e-1**
TNS3	1635.45	**-0.19**	0.19	**9.58e-1**
TOB1	427.77	**0.02**	0.2	**9.95e-1**
TOB1-AS1	11.11	**0.07**	0.21	**9.91e-1**
TOB2	442.65	**-0.43**	0.22	**6.90e-1**
TOE1	381.56	**-0.18**	0.21	**9.80e-1**
TOLLIP	181.08	**0.19**	0.23	**9.83e-1**

TOM1	105.9	**-0.04**	0.25	**9.93e-1**
TOM1L2	90.73	**0.05**	0.25	**9.93e-1**
TOMM20	1868.47	**0.24**	0.19	**9.25e-1**
TOMM22	873.27	**-0.09**	0.19	**9.90e-1**
TOMM34	986.45	**-0.25**	0.19	**9.12e-1**
TOMM40	1608.44	**-0.58**	0.23	**4.22e-1**
TOMM40L	134.11	**-0.23**	0.24	**9.60e-1**
TOMM5	572.34	**-0.17**	0.2	**9.80e-1**
TOMM6	943.45	**-0.3**	0.19	**8.40e-1**
TOMM7	179.87	**-0.28**	0.24	**9.47e-1**
TOMM70A	1443.05	**0.1**	0.2	**9.90e-1**
TONSL	702.56	**-0.43**	0.24	**7.41e-1**
TOP1	4760.25	**-0.45**	0.18	**4.15e-1**
TOP1MT	522.66	**-0.08**	0.2	**9.90e-1**
TOP2A	3441.97	**-0.13**	0.19	**9.88e-1**
TOP2B	2492.5	**0.17**	0.19	**9.80e-1**
TOP3A	647.19	**-0.29**	0.19	**8.64e-1**
TOP3B	334.53	**-0.4**	0.23	**7.57e-1**
TOPBP1	1793.44	**0.16**	0.19	**9.82e-1**
TOPORS	366.99	**-0.13**	0.21	**9.90e-1**
TOR1A	204.39	**0.25**	0.22	**9.47e-1**
TOR1AIP1	211.62	**0.24**	0.22	**9.49e-1**
TOR1AIP2	354.94	**0.04**	0.21	**9.93e-1**
TOR1B	92.55	**0.03**	0.24	**9.93e-1**
TOR2A	90.86	**0.16**	0.25	**9.90e-1**
TOR3A	616.92	**0.41**	0.2	**6.32e-1**
TOX	50.09	**-0.07**	0.25	**9.93e-1**
TOX4	882.64	**-0.5**	0.2	**4.11e-1**
TP53	1688.38	**0.1**	0.2	**9.90e-1**
TP53BP1	809.19	**-0.06**	0.19	**9.91e-1**
TP53BP2	11.73	**-0.03**	0.21	**9.93e-1**
TP53I11	26.29	**-0.37**	0.25	**8.62e-1**
TP53I13	49.2	**-0.05**	0.25	**9.93e-1**
TP53INP1	38.93	**-0.16**	0.25	**9.90e-1**
TP53INP2	180.4	**-0.13**	0.23	**9.90e-1**
TP53RK	230.58	**0.3**	0.23	**9.06e-1**
TP63	441.34	**0.01**	0.2	**9.97e-1**
TPCN1	1288.32	**-0.1**	0.2	**9.90e-1**
TPCN2	88.2	**0.2**	0.25	**9.81e-1**
TPD52	847.2	**0.24**	0.21	**9.47e-1**
TPD52L2	888.15	**-0.06**	0.19	**9.91e-1**
TPGS1	22.98	**0.01**	0.23	**9.96e-1**
TPGS2	929.54	**0.1**	0.19	**9.90e-1**
TPI1	3998.88	**-0.11**	0.2	**9.90e-1**
TPI1P2	29.95	**0.05**	0.25	**9.93e-1**
TPK1	16.23	**-0.07**	0.23	**9.91e-1**
TPM3	3002.12	**0.06**	0.18	**9.90e-1**
TPM3P9	72.39	**0.03**	0.25	**9.93e-1**
TPM4	902.38	**-0.17**	0.19	**9.74e-1**
TPMT	212.22	**-0.05**	0.22	**9.93e-1**
TPP1	1574.53	**0.07**	0.18	**9.90e-1**
TPP2	1408.32	**0.01**	0.2	**9.96e-1**

TPR	2980.91	**-0.01**	0.19	**9.96e-1**
TPRA1	82.41	**0.21**	0.25	**9.80e-1**
TPRG1L	81.52	**0.03**	0.25	**9.93e-1**
TPRKB	108.82	**-0.08**	0.24	**9.90e-1**
TPRN	300.38	**-0.37**	0.24	**8.42e-1**
TPST2	61.58	**0.18**	0.25	**9.87e-1**
TPT1	5110.15	**0.37**	0.19	**6.59e-1**
TPT1-AS1	27.71	**-0.02**	0.25	**9.95e-1**
TPX2	2999.49	**-0.22**	0.18	**9.42e-1**
TRA2A	923.28	**-0.2**	0.19	**9.50e-1**
TRA2B	2286.03	**-0.08**	0.18	**9.90e-1**
TRABD	537.4	**-0.27**	0.23	**9.47e-1**
TRADD	33.33	**-0.27**	0.25	**9.49e-1**
TRAF1	259.74	**0.53**	0.22	**4.62e-1**
TRAF2	293.46	**-0.01**	0.22	**9.96e-1**
TRAF3	846.1	**-0.19**	0.19	**9.59e-1**
TRAF3IP1	160.9	**-0.17**	0.23	**9.87e-1**
TRAF3IP2-AS1	81.83	**0.22**	0.25	**9.74e-1**
TRAF4	1062.42	**0.32**	0.19	**8.08e-1**
TRAF5	272.16	**0.07**	0.22	**9.91e-1**
TRAF6	113.12	**0.32**	0.24	**9.08e-1**
TRAF7	1329.08	**-0.55**	0.22	**4.22e-1**
TRAFD1	271.85	**-0.2**	0.22	**9.72e-1**
TRAIP	154.45	**0.07**	0.23	**9.92e-1**
TRAK1	838.49	**0**	0.19	**9.99e-1**
TRAK2	322.15	**-0.16**	0.21	**9.87e-1**
TRAM1	1481.05	**0.15**	0.2	**9.87e-1**
TRAM2	85.43	**-0.23**	0.25	**9.66e-1**
TRAM2-AS1	20.8	**0.2**	0.24	**9.81e-1**
TRANK1	1024.13	**-0.12**	0.19	**9.90e-1**
TRAP1	1885.98	**-0.13**	0.19	**9.87e-1**

TRAPPC1	284.03	**-0.02**	0.21	**9.95e-1**
TRAPPC10	819.48	**0.02**	0.19	**9.94e-1**
TRAPPC11	427.14	**0.19**	0.21	**9.72e-1**
TRAPPC12	133.65	**0.09**	0.23	**9.90e-1**
TRAPPC13	116.94	**-0.01**	0.24	**9.98e-1**
TRAPPC2	60.86	**0.14**	0.25	**9.90e-1**
TRAPPC2L	188.91	**0.19**	0.22	**9.80e-1**
TRAPPC3	330.14	**0.07**	0.21	**9.91e-1**
TRAPPC4	167.36	**0.16**	0.23	**9.87e-1**
TRAPPC5	65.12	**0.35**	0.25	**8.92e-1**
TRAPPC6A	90.16	**-0.08**	0.25	**9.91e-1**
TRAPPC6B	195.71	**0.27**	0.23	**9.46e-1**
TRAPPC8	651.52	**0.09**	0.21	**9.90e-1**
TRAPPC9	113.58	**-0.06**	0.24	**9.93e-1**
TRDMT1	107.94	**0**	0.24	**9.99e-1**
TREML2	14.7	**0.42**	0.22	**7.01e-1**
TRERF1	254.4	**-0.42**	0.22	**6.94e-1**
TREX1	93.31	**-0.06**	0.25	**9.93e-1**
TRIAP1	189.11	**-0.02**	0.23	**9.93e-1**
TRIB1	290.06	**-0.16**	0.22	**9.87e-1**
TRIB2	127.96	**0.17**	0.24	**9.87e-1**
TRIM11	214.92	**-0.17**	0.24	**9.87e-1**
TRIM13	142.87	**0.23**	0.24	**9.60e-1**
TRIM14	1410.99	**-0.2**	0.19	**9.54e-1**
TRIM16	22.56	**0.28**	0.25	**9.47e-1**
TRIM21	132.24	**0.16**	0.24	**9.88e-1**
TRIM22	59.69	**-0.18**	0.25	**9.87e-1**
TRIM23	82.17	**0.27**	0.25	**9.49e-1**
TRIM24	834.36	**-0.17**	0.19	**9.73e-1**
TRIM25	994.35	**-0.07**	0.19	**9.90e-1**
TRIM26	874.14	**-0.34**	0.21	**8.38e-1**
TRIM27	599.3	**0.02**	0.2	**9.93e-1**

TRIM28	3377.63	**-0.11**	0.19	**9.90e-1**
TRIM32	109.94	**0.11**	0.24	**9.90e-1**
TRIM33	874.91	**-0.07**	0.2	**9.90e-1**
TRIM35	276.42	**-0.22**	0.22	**9.59e-1**
TRIM37	640.67	**0.04**	0.2	**9.93e-1**
TRIM38	198.69	**0.06**	0.22	**9.93e-1**
TRIM39	101.11	**-0.07**	0.24	**9.93e-1**
TRIM4	121.35	**0.51**	0.24	**5.91e-1**
TRIM41	378.93	**-0.23**	0.23	**9.58e-1**
TRIM44	1531.85	**0.13**	0.18	**9.87e-1**
TRIM52	72.4	**-0.31**	0.25	**9.25e-1**
TRIM52-AS1	40.01	**-0.02**	0.25	**9.94e-1**
TRIM56	532.25	**-0.6**	0.23	**3.50e-1**
TRIM59	178.26	**0.12**	0.23	**9.90e-1**
TRIM62	138.55	**-0.33**	0.24	**8.92e-1**
TRIM65	431.44	**-0.37**	0.22	**7.89e-1**
TRIM66	178.71	**-0.17**	0.23	**9.87e-1**
TRIM8	407.15	**-0.09**	0.22	**9.90e-1**
TRIM9	222.2	**-0.19**	0.22	**9.74e-1**
TRIO	737.55	**-0.21**	0.19	**9.49e-1**
TRIOBP	153.53	**-0.08**	0.24	**9.91e-1**
TRIP11	375.33	**-0.02**	0.21	**9.93e-1**
TRIP12	1582.37	**0.03**	0.19	**9.93e-1**
TRIP13	564.41	**0.01**	0.2	**9.96e-1**
TRIP4	145.95	**-0.03**	0.23	**9.93e-1**
TRIT1	465.97	**-0.01**	0.2	**9.96e-1**
TRMT1	768.89	**-0.13**	0.22	**9.90e-1**
TRMT10A	148.56	**-0.12**	0.23	**9.90e-1**
TRMT10B	22.89	**-0.07**	0.25	**9.93e-1**
TRMT10C	271.34	**0.07**	0.22	**9.91e-1**
TRMT11	152.15	**0**	0.23	**9.98e-1**
TRMT112	218.01	**0.11**	0.22	**9.90e-1**
TRMT12	85.13	**0.02**	0.25	**9.96e-1**
TRMT13	191.67	**0.05**	0.23	**9.93e-1**
TRMT1L	236.19	**0.32**	0.22	**8.73e-1**
TRMT2A	413.14	**-0.34**	0.23	**8.73e-1**
TRMT2B	131.53	**0.16**	0.24	**9.90e-1**
TRMT44	73.96	**-0.16**	0.25	**9.90e-1**
TRMT5	250.26	**0.16**	0.23	**9.87e-1**
TRMT6	745.18	**-0.17**	0.19	**9.74e-1**
TRMT61A	306.51	**-0.37**	0.24	**8.51e-1**
TRMT61B	120.81	**0.21**	0.24	**9.74e-1**
TRMU	186.28	**0.02**	0.22	**9.93e-1**
TRNAU1AP	94.78	**0.29**	0.24	**9.42e-1**
TRNT1	246	**-0.03**	0.22	**9.93e-1**
TROAP	625.19	**-0.59**	0.22	**3.48e-1**
TROVE2	159.17	**0.02**	0.23	**9.95e-1**
TRPC4AP	519.72	**-0.02**	0.2	**9.94e-1**
TRPM7	978.43	**0.23**	0.2	**9.47e-1**
TRPS1	75.78	**-0.18**	0.25	**9.87e-1**
TRPT1	42.51	**0.03**	0.25	**9.93e-1**

TRPV1	11.52	**0.06**	0.21	**9.93e-1**
TRPV2	294.03	**0.01**	0.21	**9.96e-1**
TRRAP	1745.85	**-0.18**	0.19	**9.61e-1**
TRUB1	495.01	**0.16**	0.22	**9.87e-1**
TRUB2	470.68	**-0.11**	0.2	**9.90e-1**
TSC1	661.36	**0.38**	0.2	**6.90e-1**
TSC2	717.39	**-0.24**	0.21	**9.47e-1**
TSC22D1	346.27	**0**	0.21	**9.98e-1**
TSC22D2	164.96	**-0.15**	0.23	**9.90e-1**
TSC22D3	76.24	**-0.15**	0.25	**9.90e-1**
TSC22D4	385.84	**-0.47**	0.25	**6.93e-1**
TSEN15	175.95	**0.65**	0.24	**2.89e-1**

TSEN2	251.81	**0.01**	0.22	**9.97e-1**
TSEN34	117.95	**-0.12**	0.25	**9.90e-1**
TSEN54	227.47	**0.09**	0.23	**9.90e-1**
TSFM	345.28	**-0.22**	0.21	**9.49e-1**
TSG101	392.31	**0.21**	0.21	**9.58e-1**
TSGA10	16.34	**0.06**	0.23	**9.93e-1**
TSHZ1	298.28	**-0.08**	0.21	**9.90e-1**
TSN	455.67	**-0.05**	0.2	**9.93e-1**
TSNARE1	22.72	**0.2**	0.23	**9.80e-1**
TSNAX	99.66	**0.23**	0.24	**9.66e-1**
TSPAN14	1232.6	**-0.05**	0.2	**9.93e-1**
TSPAN17	140.6	**-0.25**	0.24	**9.54e-1**
TSPAN3	459.04	**0.25**	0.2	**9.39e-1**
TSPAN33	162.85	**0.22**	0.23	**9.61e-1**
TSPAN4	20.72	**0.09**	0.24	**9.90e-1**
TSPO	12.2	**-0.03**	0.2	**9.93e-1**
TSPYL1	834.71	**-0.09**	0.19	**9.90e-1**
TSPYL2	250.72	**-0.1**	0.22	**9.90e-1**
TSPYL4	79.85	**0.04**	0.25	**9.93e-1**
TSR1	1867.78	**-0.15**	0.19	**9.86e-1**
TSR2	329.56	**-0.37**	0.22	**7.97e-1**
TSR3	183.98	**-0.01**	0.24	**9.98e-1**
TSSC1	200.25	**0.07**	0.22	**9.91e-1**
TSSC4	137.73	**-0.36**	0.25	**8.73e-1**
TST	29.98	**-0.19**	0.24	**9.86e-1**
TSTA3	250.11	**-0.23**	0.22	**9.52e-1**
TSTD1	27.59	**-0.12**	0.25	**9.90e-1**
TSTD2	232.83	**0.04**	0.22	**9.93e-1**
TTBK2	108.99	**0.06**	0.24	**9.93e-1**
TTC1	477.74	**-0.07**	0.21	**9.91e-1**
TTC13	177.04	**-0.02**	0.23	**9.96e-1**
TTC14	382.29	**0.18**	0.22	**9.81e-1**
TTC17	440.99	**0.09**	0.2	**9.90e-1**
TTC19	334.74	**0.44**	0.22	**6.60e-1**
TTC21A	31.18	**-0.32**	0.25	**9.21e-1**
TTC21B	205.45	**0.08**	0.23	**9.90e-1**
TTC23	18.67	**0.32**	0.24	**8.98e-1**
TTC26	28	**0.18**	0.25	**9.88e-1**
TTC27	350.79	**0.15**	0.21	**9.88e-1**
TTC3	1388.32	**-0.05**	0.19	**9.93e-1**
TTC30A	10.77	**-0.05**	0.21	**9.93e-1**
TTC31	199.79	**0.03**	0.23	**9.93e-1**
TTC32	14.79	**0.2**	0.23	**9.75e-1**
TTC33	175.45	**0.06**	0.23	**9.93e-1**
TTC37	944.2	**0.18**	0.21	**9.73e-1**
TTC39C	20.03	**-0.29**	0.24	**9.40e-1**
TTC4	41.9	**-0.75**	0.25	**2.15e-1**
TTC5	176.92	**0.34**	0.23	**8.64e-1**
TTC7A	545.39	**-0.3**	0.22	**8.92e-1**
TTC8	88.97	**0.03**	0.25	**9.93e-1**
TTC9	392.53	**0.4**	0.21	**6.87e-1**
TTC9C	140.97	**-0.07**	0.24	**9.92e-1**
TTF1	180.33	**0.03**	0.23	**9.93e-1**
TTF2	1342.19	**-0.06**	0.19	**9.91e-1**
TTI1	602.12	**-0.14**	0.2	**9.87e-1**
TTI2	107.04	**-0.08**	0.24	**9.90e-1**
TTK	867.5	**0.14**	0.21	**9.90e-1**
TTL	259.06	**-0.03**	0.21	**9.93e-1**
TTLL11	45.75	**0.08**	0.25	**9.91e-1**
TTLL12	2243.84	**-0.57**	0.22	**3.69e-1**
TTLL3	17.69	**0.02**	0.24	**9.95e-1**
TTLL4	725.82	**-0.37**	0.19	**7.04e-1**
TTLL5	391.07	**-0.17**	0.21	**9.81e-1**
TTPAL	249.97	**0**	0.22	**9.98e-1**
TTTY15	163.05	**0.1**	0.23	**9.90e-1**

TTYH3	88.83	**-0.05**	0.25	**9.93e-1**
TUBA1A	1243.04	**-0.37**	0.19	**6.83e-1**
TUBA1B	10195.85	**-0.25**	0.18	**8.80e-1**
TUBA1C	2611.97	**-0.34**	0.18	**7.13e-1**
TUBA4A	2414.42	**-0.65**	0.18	**5.90e-2**
TUBA4B	16.74	**0.06**	0.23	**9.93e-1**

TUBB	14989.06	**-0.27**	0.19	**8.64e-1**
TUBB2A	28.67	**-0.36**	0.25	**8.73e-1**
TUBB3	332.87	**-0.18**	0.22	**9.81e-1**
TUBB4B	2973.8	**-0.47**	0.22	**5.96e-1**
TUBB6	194.94	**-0.25**	0.23	**9.49e-1**
TUBD1	34.8	**0.04**	0.25	**9.93e-1**
TUBE1	153.6	**0.38**	0.23	**8.21e-1**
TUBG1	988.28	**-0.47**	0.2	**5.32e-1**
TUBG2	73.64	**-0.29**	0.25	**9.47e-1**
TUBGCP2	661.21	**-0.12**	0.2	**9.90e-1**
TUBGCP3	312.05	**0.2**	0.21	**9.63e-1**
TUBGCP4	468.32	**-0.31**	0.2	**8.44e-1**
TUBGCP5	274.54	**0.05**	0.21	**9.93e-1**
TUBGCP6	426.7	**-0.17**	0.22	**9.86e-1**
TUFM	2971.2	**-0.02**	0.19	**9.95e-1**
TUG1	2042.43	**-0.07**	0.19	**9.90e-1**
TULP3	306.24	**-0.32**	0.21	**8.53e-1**
TULP4	252.48	**-0.14**	0.22	**9.90e-1**
TUSC2	207.01	**-0.01**	0.23	**9.98e-1**
TUT1	343.01	**-0.37**	0.24	**8.56e-1**
TVP23B	75.17	**0.35**	0.25	**8.74e-1**
TWF1	400.78	**-0.02**	0.22	**9.93e-1**
TWF2	405.08	**0.11**	0.21	**9.90e-1**
TWISTNB	378.6	**0.08**	0.21	**9.90e-1**
TWSG1	110.47	**0.45**	0.25	**7.23e-1**
TXLNA	1319.43	**-0.07**	0.19	**9.90e-1**
TXLNB	105.81	**0.06**	0.24	**9.93e-1**
TXLNG	1094.52	**-0.2**	0.19	**9.49e-1**
TXLNGY	289.87	**0.18**	0.23	**9.86e-1**
TXN	688.59	**0**	0.19	**9.98e-1**
TXN2	742.2	**-0.19**	0.21	**9.73e-1**
TXNDC11	434.6	**0.33**	0.2	**8.37e-1**
TXNDC12	493.57	**0.27**	0.21	**9.12e-1**
TXNDC15	263.64	**0.18**	0.22	**9.80e-1**
TXNDC16	162.91	**0.18**	0.23	**9.87e-1**
TXNDC17	142.59	**-0.12**	0.23	**9.90e-1**
TXNDC5	12.34	**0.25**	0.22	**9.47e-1**
TXNDC9	174.87	**0.06**	0.23	**9.93e-1**
TXNIP	721.43	**0.22**	0.19	**9.47e-1**
TXNL1	547.22	**-0.1**	0.2	**9.90e-1**
TXNL4A	284.44	**0.39**	0.22	**7.41e-1**
TXNL4B	155.6	**0.06**	0.23	**9.93e-1**
TXNRD1	2304.17	**-0.29**	0.19	**8.51e-1**
TXNRD2	66.29	**0.09**	0.25	**9.90e-1**
TYK2	1093.25	**-0.16**	0.22	**9.87e-1**
TYMP	17.1	**-0.13**	0.23	**9.90e-1**
TYMS	1368.1	**0.29**	0.19	**8.52e-1**
TYSND1	325.14	**-0.31**	0.24	**9.23e-1**
TYW1	409.05	**0.17**	0.21	**9.81e-1**
TYW1B	93.28	**-0.12**	0.24	**9.90e-1**
TYW3	650.15	**0.15**	0.2	**9.87e-1**
TYW5	52.32	**0.28**	0.25	**9.47e-1**
U2AF1	855.59	**0.02**	0.19	**9.95e-1**
U2AF1L4	58.69	**0.02**	0.25	**9.96e-1**
U2AF2	2234.28	**-0.3**	0.22	**8.97e-1**
U2SURP	3293.66	**-0.16**	0.19	**9.80e-1**
UACA	277.69	**-0.07**	0.22	**9.91e-1**

UAP1	654.67	**-0.03**	0.2	**9.93e-1**
UAP1L1	190.56	**0.32**	0.24	**9.10e-1**
UBA1	3232.46	**-0.22**	0.19	**9.47e-1**
UBA2	2437.28	**0.23**	0.19	**9.39e-1**
UBA3	343.95	**-0.03**	0.21	**9.93e-1**
UBA5	345.24	**0.34**	0.22	**8.43e-1**
UBA52	1955.68	**0.09**	0.18	**9.90e-1**
UBA6	484.13	**-0.03**	0.21	**9.93e-1**
UBA6-AS1	54.2	**0.05**	0.25	**9.93e-1**
UBA7	74.12	**-0.1**	0.25	**9.90e-1**
UBAC1	343.72	**0.03**	0.21	**9.93e-1**
UBAC2	237.74	**0.57**	0.22	**3.64e-1**
UBAC2-AS1	14.4	**-0.01**	0.22	**9.96e-1**
UBALD1	183.42	**-0.26**	0.25	**9.51e-1**
UBALD2	110.8	**0.59**	0.25	**4.73e-1**
UBAP1	492.2	**-0.23**	0.2	**9.47e-1**
UBAP2	1675.94	**-0.38**	0.19	**6.49e-1**
UBAP2L	3729.42	**-0.48**	0.19	**3.69e-1**
UBASH3A	14.87	**-0.38**	0.23	**8.12e-1**
UBASH3B	140.52	**0.77**	0.24	**1.12e-1**
UBB	2159.18	**0.15**	0.18	**9.80e-1**
UBC	2637.57	**0.19**	0.19	**9.54e-1**
UBE2A	435.44	**0.17**	0.21	**9.81e-1**
UBE2B	225.41	**0.34**	0.23	**8.64e-1**
UBE2C	673.08	**-0.19**	0.19	**9.60e-1**
UBE2D1	111.61	**0.18**	0.24	**9.87e-1**
UBE2D2	550.04	**0.17**	0.2	**9.75e-1**
UBE2D3	2329.37	**-0.09**	0.19	**9.90e-1**
UBE2D4	170.12	**-0.19**	0.23	**9.80e-1**
UBE2E1	577.06	**-0.16**	0.2	**9.86e-1**
UBE2E2	192.74	**-0.22**	0.22	**9.58e-1**
UBE2E3	93.58	**-0.01**	0.24	**9.98e-1**
UBE2F	48.92	**0.09**	0.25	**9.90e-1**
UBE2G1	1073.04	**0.02**	0.2	**9.93e-1**
UBE2G2	1215.6	**-0.26**	0.19	**8.88e-1**
UBE2H	456.27	**0.43**	0.2	**6.07e-1**
UBE2I	1182.04	**-0.13**	0.19	**9.89e-1**
UBE2J1	5858.45	**0.09**	0.19	**9.90e-1**
UBE2J2	257.57	**-0.02**	0.22	**9.94e-1**
UBE2K	1265.89	**0.05**	0.2	**9.93e-1**
UBE2L3	1315.53	**-0.34**	0.19	**7.19e-1**
UBE2L6	588.78	**-0.15**	0.2	**9.87e-1**
UBE2M	446.11	**0.04**	0.21	**9.93e-1**
UBE2N	793.23	**-0.19**	0.19	**9.56e-1**
UBE2O	1157.76	**-0.03**	0.2	**9.93e-1**
UBE2Q1	816.39	**0.02**	0.19	**9.95e-1**
UBE2Q2	226.8	**0.03**	0.22	**9.93e-1**
UBE2R2	606.43	**-0.06**	0.2	**9.91e-1**
UBE2S	721.5	**-0.26**	0.23	**9.48e-1**
UBE2T	367.09	**0.18**	0.21	**9.80e-1**
UBE2V1	25.94	**-0.13**	0.25	**9.90e-1**
UBE2V2	541.89	**-0.01**	0.2	**9.96e-1**
UBE2W	101.47	**0.15**	0.25	**9.90e-1**
UBE2Z	865.57	**-0.14**	0.2	**9.88e-1**
UBE3A	1160.98	**-0.05**	0.2	**9.93e-1**
UBE3B	286.45	**0**	0.21	**9.98e-1**
UBE3C	1015.52	**0.08**	0.19	**9.90e-1**
UBE3D	62.3	**-0.05**	0.25	**9.93e-1**
UBE4A	958.59	**-0.02**	0.2	**9.93e-1**
UBE4B	750.57	**-0.14**	0.19	**9.87e-1**
UBFD1	800.74	**0.27**	0.2	**8.98e-1**
UBIAD1	434.11	**-0.3**	0.21	**8.89e-1**
UBL3	150.19	**0.24**	0.23	**9.54e-1**

UBL4A	201.13	**-0.21**	0.24	**9.75e-1**
UBL5	145.49	**-0.19**	0.23	**9.86e-1**
UBL7	267.88	**-0.08**	0.22	**9.90e-1**
UBL7-AS1	22.79	**0.21**	0.25	**9.80e-1**
UBLCP1	141.46	**0.04**	0.24	**9.93e-1**
UBN1	865.21	**-0.33**	0.2	**8.07e-1**
UBN2	355	**-0.06**	0.21	**9.93e-1**
UBOX5	104.43	**-0.36**	0.25	**8.64e-1**
UBP1	1685.97	**0.03**	0.2	**9.93e-1**
UBQLN1	1474.56	**0.05**	0.19	**9.93e-1**
UBQLN2	334.68	**-0.01**	0.21	**9.98e-1**
UBQLN4	1001.95	**-0.4**	0.2	**6.69e-1**
UBR1	273.37	**0.02**	0.23	**9.93e-1**
UBR2	561.54	**0.18**	0.21	**9.80e-1**
UBR3	298.7	**0.24**	0.22	**9.49e-1**
UBR4	2019.48	**-0.09**	0.18	**9.90e-1**
UBR5	2343.65	**0.17**	0.19	**9.73e-1**
UBR5-AS1	25.07	**-0.17**	0.25	**9.87e-1**
UBR7	598.04	**0.26**	0.2	**9.11e-1**
UBTD1	16.41	**-0.15**	0.22	**9.88e-1**
UBTD2	212.73	**0.11**	0.22	**9.90e-1**
UBTF	3158.16	**-0.21**	0.19	**9.47e-1**
UBXN1	679.82	**0.01**	0.21	**9.96e-1**
UBXN11	299.52	**0.24**	0.21	**9.47e-1**
UBXN2A	113.16	**-0.06**	0.24	**9.93e-1**
UBXN2B	355.84	**0.05**	0.21	**9.93e-1**
UBXN4	374.73	**0.1**	0.21	**9.90e-1**
UBXN6	271.04	**0.19**	0.23	**9.81e-1**
UBXN7	396.87	**-0.06**	0.21	**9.93e-1**
UBXN8	145.76	**0.22**	0.23	**9.66e-1**
UCHL1	1380.01	**0.26**	0.19	**9.03e-1**
UCHL3	251.61	**0.27**	0.22	**9.39e-1**
UCHL5	717.24	**0.01**	0.2	**9.96e-1**
UCK1	150.33	**-0.1**	0.23	**9.90e-1**
UCK2	555.83	**-0.07**	0.2	**9.90e-1**
UCKL1	454.17	**-0.42**	0.21	**6.53e-1**
UCP2	1478.06	**-0.21**	0.19	**9.47e-1**
UFC1	377.34	**0.06**	0.21	**9.93e-1**
UFD1L	427.82	**-0.09**	0.2	**9.90e-1**
UFL1	783.02	**0.33**	0.21	**8.41e-1**
UFM1	559.87	**0.17**	0.21	**9.81e-1**
UFSP2	190.79	**0.16**	0.23	**9.87e-1**
UGCG	339.79	**1.32**	0.22	**3.00e-6**
UGDH	356.02	**0.17**	0.21	**9.86e-1**
UGGT1	442.38	**0.16**	0.21	**9.86e-1**
UGP2	612.84	**0**	0.2	**9.99e-1**

UGT8	86.23	**0.28**	0.25	**9.47e-1**
UHMK1	1219.64	**0.16**	0.2	**9.86e-1**
UHRF1	930.57	**-0.13**	0.2	**9.90e-1**
UHRF1BP1	618.78	**-0.17**	0.2	**9.80e-1**
UHRF1BP1L	356.24	**0.21**	0.22	**9.59e-1**
UHRF2	491.8	**-0.07**	0.2	**9.90e-1**
UIMC1	428.97	**0.21**	0.2	**9.52e-1**
ULBP2	14.86	**0.11**	0.23	**9.90e-1**
ULK1	168.65	**-0.37**	0.24	**8.53e-1**
ULK3	266.39	**-0.11**	0.23	**9.90e-1**
ULK4	126.07	**-0.11**	0.24	**9.90e-1**
UMAD1	178.69	**0.27**	0.23	**9.47e-1**
UMPS	374.84	**0.15**	0.21	**9.87e-1**
UNC119	329.28	**-0.03**	0.22	**9.93e-1**
UNC119B	447.49	**-0.07**	0.2	**9.90e-1**
UNC13A	13.27	**-0.22**	0.22	**9.58e-1**
UNC45A	503.47	**0.02**	0.21	**9.93e-1**

UNC50	79.93	**0.42**	0.25	**8.08e-1**
UNC93B1	232.36	**-0.13**	0.23	**9.90e-1**
UNG	731.89	**-0.1**	0.2	**9.90e-1**
UNK	374.68	**-0.25**	0.22	**9.47e-1**
UNKL	232.5	**-0.2**	0.24	**9.80e-1**
UPF1	1113.69	**-0.14**	0.2	**9.87e-1**
UPF2	1002.96	**-0.11**	0.19	**9.90e-1**
UPF3A	681.66	**-0.63**	0.2	**1.25e-1**
UPF3B	332.31	**-0.41**	0.21	**6.87e-1**
UPP1	49.69	**0.27**	0.25	**9.49e-1**
UPRT	41.35	**0.09**	0.25	**9.90e-1**
UQCC1	466.09	**0**	0.2	**9.98e-1**
UQCC2	62.67	**0.13**	0.25	**9.90e-1**
UQCC3	61.19	**0.1**	0.25	**9.90e-1**
UQCR10	315.18	**-0.4**	0.22	**7.41e-1**
UQCR11	286.02	**-0.15**	0.22	**9.89e-1**
UQCRB	671.9	**-0.02**	0.19	**9.95e-1**
UQCRC1	1153.38	**-0.02**	0.2	**9.94e-1**
UQCRC2	1518.1	**0.11**	0.19	**9.90e-1**
UQCRFS1	455.99	**0.25**	0.2	**9.37e-1**
UQCRH	911.86	**0.3**	0.19	**8.40e-1**
UQCRHL	37.27	**0.45**	0.25	**7.55e-1**
UQCRQ	234.3	**0.03**	0.22	**9.93e-1**
URB1	752	**-0.34**	0.19	**7.59e-1**
URB2	447.61	**-0.06**	0.2	**9.93e-1**
URGCP	291.32	**0.03**	0.21	**9.93e-1**
URI1	768.06	**0.27**	0.21	**9.12e-1**
URM1	636.86	**-0.38**	0.22	**7.75e-1**
UROD	342.18	**-0.15**	0.22	**9.88e-1**
UROS	263.22	**0.3**	0.22	**8.91e-1**
USB1	569.48	**-0.22**	0.2	**9.49e-1**
USE1	50.07	**0.51**	0.25	**6.59e-1**
USF1	362.19	**-0.31**	0.22	**8.73e-1**
USF2	783.36	**0.33**	0.2	**8.30e-1**
USMG5	305.15	**-0.08**	0.21	**9.90e-1**
USO1	1170.13	**0.31**	0.2	**8.52e-1**
USP1	2136.25	**0.03**	0.2	**9.93e-1**
USP10	1935.64	**-0.19**	0.18	**9.54e-1**
USP11	670.5	**0.13**	0.19	**9.89e-1**
USP12	1002.97	**0.24**	0.2	**9.46e-1**
USP13	549.45	**0.02**	0.2	**9.93e-1**
USP14	1150.25	**0.13**	0.2	**9.89e-1**
USP15	404.56	**0.21**	0.22	**9.63e-1**
USP16	612.29	**0.08**	0.21	**9.90e-1**
USP19	719.09	**-0.16**	0.2	**9.86e-1**
USP2	11.96	**-0.17**	0.22	**9.86e-1**
USP20	120.41	**-0.04**	0.24	**9.93e-1**
USP21	202.8	**-0.28**	0.22	**9.29e-1**
USP22	2748.64	**0.01**	0.18	**9.96e-1**
USP24	1916.83	**-0.06**	0.19	**9.91e-1**
USP25	463.04	**0.09**	0.21	**9.90e-1**
USP28	430.36	**0**	0.2	**9.98e-1**
USP2-AS1	23.67	**-0.31**	0.24	**9.31e-1**
USP3	289.62	**0**	0.21	**9.98e-1**
USP30	78.94	**0.06**	0.25	**9.93e-1**
USP31	225.45	**0.31**	0.23	**8.95e-1**
USP32	293.88	**-0.07**	0.22	**9.90e-1**
USP33	477.76	**0.12**	0.21	**9.90e-1**
USP34	2174.54	**0.08**	0.19	**9.90e-1**
USP35	29.87	**0.11**	0.25	**9.90e-1**
USP36	1247.13	**-0.61**	0.21	**2.52e-1**
USP37	271.25	**-0.05**	0.22	**9.93e-1**
USP38	344.2	**0.06**	0.21	**9.93e-1**
USP39	853.91	**0.04**	0.19	**9.93e-1**

USP4	481.38	**-0.15**	0.2	**9.87e-1**
USP42	420.71	**-0.23**	0.2	**9.47e-1**

USP45	262.33	**0.17**	0.23	**9.87e-1**
USP46	112.99	**-0.02**	0.24	**9.93e-1**
USP47	613.68	**-0.05**	0.2	**9.93e-1**
USP48	1010.1	**0.04**	0.2	**9.93e-1**
USP49	245.68	**0.37**	0.22	**7.89e-1**
USP5	1582.38	**-0.34**	0.2	**7.97e-1**
USP53	123.55	**-0.09**	0.25	**9.90e-1**
USP54	174.61	**-0.18**	0.23	**9.82e-1**
USP6NL	575.43	**-0.02**	0.2	**9.94e-1**
USP7	3348.44	**0.14**	0.19	**9.87e-1**
USP8	544.05	**-0.36**	0.2	**7.57e-1**
USP9X	1261.72	**0.11**	0.2	**9.90e-1**
USP9Y	275.12	**0.14**	0.22	**9.90e-1**
USPL1	279.58	**-0.15**	0.22	**9.88e-1**
UST	182.62	**0.22**	0.23	**9.58e-1**
UTP11L	587.66	**-0.07**	0.2	**9.90e-1**
UTP14A	712.31	**-0.01**	0.2	**9.96e-1**
UTP14C	182.7	**0.05**	0.23	**9.93e-1**
UTP15	469.11	**-0.04**	0.22	**9.93e-1**
UTP18	372.35	**0.31**	0.21	**8.64e-1**
UTP20	1320.22	**-0.15**	0.2	**9.87e-1**
UTP23	233.97	**-0.32**	0.22	**8.64e-1**
UTP3	948.31	**-0.41**	0.19	**5.87e-1**
UTP6	696.94	**0.22**	0.2	**9.48e-1**
UTRN	261.25	**0**	0.22	**9.98e-1**
UTS2	25.29	**0.16**	0.25	**9.90e-1**
UTY	246.55	**0.19**	0.22	**9.81e-1**
UVRAG	446.6	**0.22**	0.21	**9.49e-1**
UVSSA	107.94	**0.1**	0.24	**9.90e-1**
UXS1	60.45	**0.09**	0.25	**9.90e-1**
UXT	170.67	**0.11**	0.23	**9.90e-1**
VAC14	776.08	**-0.12**	0.2	**9.90e-1**
VAMP1	758.77	**-0.38**	0.2	**6.90e-1**
VAMP2	184.52	**-0.02**	0.23	**9.94e-1**
VAMP3	199.47	**0.2**	0.23	**9.74e-1**
VAMP4	60.02	**0.27**	0.25	**9.49e-1**
VAMP7	337.8	**0.26**	0.22	**9.42e-1**
VAMP8	368.95	**0.22**	0.21	**9.49e-1**
VAPA	722.69	**0.25**	0.21	**9.39e-1**
VAPB	551.97	**0.05**	0.2	**9.93e-1**
VARS	2387.44	**-0.52**	0.22	**5.37e-1**
VARS2	669.65	**-0.46**	0.23	**6.69e-1**
VASP	637.39	**-0.23**	0.23	**9.59e-1**
VAV1	567.07	**0.07**	0.21	**9.91e-1**
VAV2	414.84	**0.02**	0.2	**9.93e-1**
VBP1	381.04	**0.16**	0.21	**9.87e-1**
VCAM1	24.29	**0.27**	0.25	**9.49e-1**
VCL	292.96	**-0.05**	0.21	**9.93e-1**
VCP	2587.94	**0.22**	0.18	**9.39e-1**
VCPIP1	315.01	**0.09**	0.21	**9.90e-1**
VCPKMT	78.23	**0.19**	0.25	**9.87e-1**
VDAC1	3276.58	**-0.07**	0.18	**9.90e-1**
VDAC2	929.53	**0.1**	0.19	**9.90e-1**
VDAC3	746.12	**-0.21**	0.2	**9.49e-1**
VEGFA	207.13	**0.12**	0.23	**9.90e-1**
VEGFB	236.5	**0.04**	0.24	**9.93e-1**
VEZF1	471.44	**-0.03**	0.21	**9.93e-1**
VEZT	609.5	**-0.08**	0.21	**9.90e-1**
VGF	20.79	**0.14**	0.24	**9.90e-1**
VGLL4	356.69	**-0.17**	0.21	**9.81e-1**
VHL	667.49	**0.07**	0.19	**9.90e-1**
VIM	834.92	**0.7**	0.2	**5.90e-2**

VIMP	83.11	**0.12**	0.25	**9.90e-1**
VIPAS39	189.49	**-0.12**	0.22	**9.90e-1**
VKORC1	128.13	**0**	0.24	**9.99e-1**
VKORC1L1	927.14	**0.03**	0.2	**9.93e-1**
VMA21	473.07	**0.09**	0.21	**9.90e-1**
VMP1	318.59	**0.15**	0.22	**9.87e-1**
VNN2	364.8	**-0.29**	0.21	**8.96e-1**
VOPP1	1062.48	**-0.14**	0.19	**9.87e-1**
VPRBP	958.91	**-0.18**	0.19	**9.61e-1**
VPREB3	436.37	**-0.31**	0.22	**8.92e-1**
VPS11	339.53	**0**	0.21	**9.99e-1**
VPS13A	819.53	**0.01**	0.2	**9.96e-1**
VPS13B	291.18	**0.11**	0.22	**9.90e-1**
VPS13C	920.8	**0.09**	0.2	**9.90e-1**
VPS13D	419.23	**0.03**	0.2	**9.93e-1**
VPS16	146.58	**0.14**	0.23	**9.90e-1**
VPS18	369.21	**-0.2**	0.22	**9.72e-1**
VPS25	257.95	**-0.14**	0.22	**9.90e-1**
VPS26A	450.31	**0.27**	0.22	**9.25e-1**
VPS26B	151.65	**0.04**	0.23	**9.93e-1**
VPS28	99.08	**-0.02**	0.25	**9.96e-1**

VPS29	258.66	**-0.15**	0.22	**9.89e-1**
VPS33A	333.67	**0.05**	0.21	**9.93e-1**
VPS33B	57.22	**0.1**	0.25	**9.90e-1**
VPS35	1250.69	**0.1**	0.2	**9.90e-1**
VPS36	472.97	**0.24**	0.21	**9.47e-1**
VPS37A	304.8	**-0.06**	0.22	**9.93e-1**
VPS37B	22.4	**-0.2**	0.24	**9.81e-1**
VPS37C	97.06	**-0.33**	0.25	**9.21e-1**
VPS39	472.11	**0**	0.2	**9.98e-1**
VPS41	285.27	**0.05**	0.22	**9.93e-1**
VPS45	181.76	**0.17**	0.23	**9.87e-1**
VPS4A	524.82	**-0.16**	0.21	**9.87e-1**
VPS4B	471.77	**0.11**	0.21	**9.90e-1**
VPS50	184.15	**0.49**	0.23	**5.96e-1**
VPS51	527.83	**-0.12**	0.23	**9.90e-1**
VPS52	487.55	**0.04**	0.2	**9.93e-1**
VPS53	265.62	**-0.16**	0.21	**9.87e-1**
VPS54	122.63	**0.26**	0.24	**9.49e-1**
VPS72	250.05	**-0.35**	0.22	**8.38e-1**
VPS8	200.47	**0.34**	0.22	**8.52e-1**
VPS9D1-AS1	395.99	**-0.81**	0.23	**7.46e-2**
VRK1	455.77	**0.16**	0.22	**9.87e-1**
VRK2	169.85	**0.25**	0.23	**9.49e-1**
VRK3	237.85	**-0.06**	0.22	**9.93e-1**
VSIG10L	28.21	**-0.17**	0.25	**9.88e-1**
VTA1	520.68	**-0.19**	0.21	**9.68e-1**
VTI1A	234.25	**0.19**	0.22	**9.81e-1**
VTI1B	539.05	**-0.07**	0.2	**9.90e-1**
VWA7	23.05	**-0.24**	0.24	**9.60e-1**
VWA8	405.05	**0.01**	0.21	**9.98e-1**
VWA9	458.09	**0.06**	0.2	**9.91e-1**
WAC	1857.2	**-0.05**	0.19	**9.93e-1**
WAC-AS1	146.02	**0.18**	0.23	**9.87e-1**
WAPAL	972.92	**0.01**	0.2	**9.96e-1**
WARS	1968.73	**0.89**	0.18	**7.42e-4**
WARS2	146.9	**0.4**	0.24	**7.97e-1**
WAS	657.69	**-0.28**	0.22	**9.21e-1**
WASF1	1044.29	**-0.39**	0.19	**6.28e-1**
WASF2	1735.51	**-0.32**	0.2	**8.22e-1**
WASF3	99.61	**-0.85**	0.24	**7.22e-2**
WASH1	27.46	**0.08**	0.25	**9.91e-1**
WASH2P	56.58	**-0.03**	0.25	**9.93e-1**

WASH3P	41.9	**-0.23**	0.25	**9.73e-1**
WASH7P	107.71	**-0.2**	0.25	**9.81e-1**
WASL	189.6	**-0.11**	0.22	**9.90e-1**
WBP11	2059.27	**-0.31**	0.18	**7.99e-1**
WBP1L	268.06	**0.02**	0.21	**9.93e-1**
WBP2	507.08	**-0.21**	0.23	**9.73e-1**
WBP4	155.38	**-0.18**	0.23	**9.86e-1**
WBSCR16	594.04	**0.02**	0.2	**9.95e-1**
WBSCR22	525.01	**-0.13**	0.21	**9.90e-1**
WDFY1	395.76	**0.06**	0.21	**9.93e-1**
WDFY2	66.36	**0.28**	0.25	**9.47e-1**
WDFY4	2082.34	**-0.2**	0.18	**9.49e-1**
WDHD1	514.54	**0.07**	0.21	**9.90e-1**
WDPCP	39	**-0.05**	0.25	**9.93e-1**
WDR1	1799.76	**-0.16**	0.18	**9.80e-1**
WDR11	608.8	**0.41**	0.2	**6.52e-1**
WDR12	620.74	**-0.18**	0.2	**9.72e-1**
WDR13	156.42	**-0.05**	0.23	**9.93e-1**
WDR17	68.45	**0.01**	0.25	**9.97e-1**
WDR18	518.72	**-0.18**	0.23	**9.87e-1**
WDR19	387.11	**0.4**	0.22	**7.31e-1**
WDR20	178.27	**-0.12**	0.23	**9.90e-1**
WDR24	261.2	**-0.18**	0.22	**9.81e-1**
WDR25	42.34	**0.08**	0.25	**9.91e-1**
WDR26	908.66	**0.21**	0.19	**9.49e-1**
WDR27	100.46	**0.24**	0.24	**9.58e-1**
WDR3	1150.96	**-0.16**	0.19	**9.80e-1**
WDR33	512.27	**-0.28**	0.2	**9.04e-1**
WDR34	372.11	**-0.17**	0.23	**9.87e-1**
WDR35	127.98	**-0.24**	0.24	**9.59e-1**
WDR36	1146.53	**-0.03**	0.2	**9.93e-1**
WDR37	144.51	**0.01**	0.23	**9.98e-1**
WDR4	333.28	**-0.28**	0.22	**9.23e-1**
WDR41	291.37	**0.31**	0.22	**8.68e-1**
WDR43	1714.42	**-0.01**	0.19	**9.96e-1**
WDR44	114.2	**0.38**	0.24	**8.39e-1**
WDR45	159.95	**0.32**	0.23	**8.97e-1**
WDR45B	311.23	**0.02**	0.21	**9.95e-1**
WDR46	551.03	**-0.17**	0.21	**9.81e-1**
WDR47	123.72	**0.18**	0.24	**9.87e-1**
WDR48	413.59	**0.14**	0.21	**9.90e-1**

WDR5	727.51	**0.07**	0.19	**9.90e-1**
WDR53	68.69	**-0.05**	0.25	**9.93e-1**
WDR54	140.11	**0.13**	0.23	**9.90e-1**
WDR55	130.43	**-0.31**	0.24	**9.23e-1**
WDR59	291.29	**-0.01**	0.21	**9.96e-1**
WDR5B	38.53	**0.38**	0.25	**8.64e-1**
WDR6	639.37	**-0.26**	0.23	**9.47e-1**
WDR60	224.06	**-0.19**	0.22	**9.80e-1**
WDR61	211.69	**0.24**	0.22	**9.49e-1**
WDR62	753.3	**-0.42**	0.22	**6.79e-1**
WDR66	29.83	**-0.16**	0.25	**9.90e-1**
WDR7	230.15	**-0.08**	0.22	**9.90e-1**
WDR70	145.28	**0.09**	0.23	**9.90e-1**
WDR73	139.63	**-0.07**	0.23	**9.91e-1**
WDR74	519.49	**-0.17**	0.22	**9.86e-1**
WDR75	845.97	**0**	0.2	**9.98e-1**
WDR76	986.74	**-0.09**	0.19	**9.90e-1**
WDR77	701.15	**0.09**	0.19	**9.90e-1**
WDR81	274.8	**-0.18**	0.24	**9.87e-1**
WDR82	1137.37	**0.05**	0.19	**9.93e-1**
WDR83	49.9	**-0.34**	0.25	**9.06e-1**
WDR83OS	134.04	**0.15**	0.24	**9.90e-1**

WDR89	170.47	**0.14**	0.23	**9.90e-1**
WDR90	335.32	**-0.24**	0.24	**9.57e-1**
WDR91	201.45	**0.14**	0.23	**9.90e-1**
WDR92	140.29	**-0.08**	0.24	**9.91e-1**
WDSUB1	38.29	**0.16**	0.25	**9.90e-1**
WDTC1	738.63	**-0.19**	0.22	**9.80e-1**
WDYHV1	65.83	**0.08**	0.25	**9.91e-1**
WEE1	837.61	**0.6**	0.21	**2.47e-1**
WFS1	51.96	**-0.08**	0.25	**9.92e-1**
WHAMM	138.69	**-0.01**	0.23	**9.98e-1**
WHAMMP1	40.11	**0.17**	0.25	**9.90e-1**
WHSC1	2029.81	**-0.01**	0.18	**9.96e-1**
WHSC1L1	860.11	**-0.19**	0.19	**9.58e-1**
WIBG	142.82	**0.18**	0.24	**9.87e-1**
WIPF1	3049.36	**-0.34**	0.19	**7.43e-1**
WIPF2	283.14	**-0.3**	0.22	**8.96e-1**
WIPI1	17.32	**0.04**	0.24	**9.93e-1**
WIPI2	857.12	**0.35**	0.19	**7.22e-1**
WIZ	451.14	**-0.42**	0.24	**7.57e-1**
WNK1	3312.57	**-0.26**	0.18	**8.75e-1**
WNK2	394.4	**-0.56**	0.24	**5.09e-1**
WNT10A	218.35	**0.31**	0.23	**9.08e-1**
WNT3	45.97	**-0.2**	0.25	**9.86e-1**
WNT5A	150.11	**-0.29**	0.23	**9.27e-1**
WRAP53	241.34	**-0.23**	0.22	**9.49e-1**
WRAP73	176.97	**0.04**	0.23	**9.93e-1**
WRB	99.32	**0.44**	0.25	**7.41e-1**
WRN	338.99	**0.18**	0.22	**9.80e-1**
WRNIP1	514.46	**0.07**	0.2	**9.90e-1**
WSB1	483.71	**0.49**	0.21	**4.95e-1**
WTAP	768.03	**0.04**	0.2	**9.93e-1**
WWC1	393.12	**0.13**	0.2	**9.90e-1**
WWC3	363.76	**-0.1**	0.21	**9.90e-1**
WWOX	114.06	**-0.12**	0.24	**9.90e-1**
WWP1	335.85	**0.08**	0.21	**9.90e-1**
WWP2	455.68	**-0.26**	0.21	**9.31e-1**
XAB2	527.05	**-0.19**	0.21	**9.73e-1**
XBP1	677.16	**0.26**	0.2	**9.12e-1**
XIAP	307.06	**0.02**	0.22	**9.96e-1**
XKR3	18.12	**-0.04**	0.23	**9.93e-1**
XKR6	22.75	**0**	0.24	**9.99e-1**
XPA	63.14	**0.37**	0.25	**8.64e-1**
XPC	417.85	**-0.04**	0.21	**9.93e-1**
XPNPEP1	706.43	**0.19**	0.19	**9.58e-1**
XPNPEP3	359.57	**-0.26**	0.21	**9.25e-1**
XPO1	3411.69	**-0.15**	0.19	**9.87e-1**
XPO4	891.06	**-0.14**	0.2	**9.88e-1**
XPO5	1118.23	**-0.14**	0.19	**9.87e-1**
XPO6	1916.51	**-0.15**	0.18	**9.86e-1**
XPO7	1431.02	**0**	0.19	**9.98e-1**
XPOT	3039.31	**0.29**	0.19	**8.64e-1**
XPR1	398.14	**-0.07**	0.21	**9.90e-1**
XRCC1	321.26	**-0.31**	0.23	**9.06e-1**
XRCC2	450.35	**-0.19**	0.21	**9.70e-1**
XRCC3	275.12	**-0.36**	0.23	**8.52e-1**
XRCC4	116.31	**0.34**	0.24	**8.89e-1**
XRCC5	3198.11	**0.01**	0.19	**9.98e-1**
XRCC6	4441.51	**-0.13**	0.18	**9.87e-1**
XRCC6BP1	73.88	**0.35**	0.25	**8.87e-1**
XRN1	259.12	**0.34**	0.22	**8.52e-1**
XRN2	1600.22	**-0.17**	0.19	**9.73e-1**

XRRA1	102.51	**-0.03**	0.24	**9.93e-1**
XXYLT1	197.02	**0.02**	0.22	**9.95e-1**
XYLT1	188.86	**0.19**	0.23	**9.81e-1**

XYLT2	159.88	**-0.34**	0.24	**8.73e-1**
YAE1D1	54.22	**0.23**	0.25	**9.74e-1**
YAF2	108.21	**0.1**	0.24	**9.90e-1**
YARS	2591.53	**0.2**	0.18	**9.49e-1**
YARS2	165.29	**0.08**	0.23	**9.90e-1**
YBEY	87.62	**0.14**	0.25	**9.90e-1**
YBX1	14010.64	**-0.12**	0.18	**9.90e-1**
YBX3	2321.78	**0.15**	0.19	**9.81e-1**
YBX3P1	12.9	**0.29**	0.22	**9.12e-1**
YDJC	181.35	**-0.05**	0.24	**9.93e-1**
YEATS2	1317.02	**-0.13**	0.19	**9.89e-1**
YEATS4	286.4	**0.32**	0.22	**8.70e-1**
YIF1A	352.98	**-0.14**	0.21	**9.90e-1**
YIF1B	204.85	**-0.23**	0.24	**9.60e-1**
YIPF1	151.42	**0.05**	0.24	**9.93e-1**
YIPF2	46.29	**-0.11**	0.25	**9.90e-1**
YIPF3	224.07	**0.04**	0.23	**9.93e-1**
YIPF4	91.37	**0.37**	0.25	**8.52e-1**
YIPF5	123.98	**0.23**	0.24	**9.61e-1**
YIPF6	59.55	**0.33**	0.25	**9.17e-1**
YJEFN3	27.57	**-0.11**	0.24	**9.90e-1**
YKT6	674.07	**-0.19**	0.2	**9.68e-1**
YLPM1	1716.73	**-0.48**	0.19	**3.69e-1**
YME1L1	1544.99	**0.01**	0.19	**9.96e-1**
YOD1	190.18	**-0.01**	0.23	**9.97e-1**
YPEL1	20.79	**0.07**	0.24	**9.93e-1**
YPEL2	31.56	**0.11**	0.25	**9.90e-1**
YPEL5	70.3	**0.55**	0.25	**5.87e-1**
YRDC	264.17	**0.12**	0.21	**9.90e-1**
YTHDC1	989.7	**0.02**	0.19	**9.93e-1**
YTHDC2	619.25	**0.12**	0.2	**9.90e-1**
YTHDF1	936.43	**-0.1**	0.19	**9.90e-1**
YTHDF2	816.87	**0.11**	0.2	**9.90e-1**
YTHDF3	772.47	**-0.23**	0.2	**9.47e-1**
YWHAB	2808.77	**0.14**	0.19	**9.87e-1**
YWHAE	3103.58	**0.01**	0.18	**9.96e-1**
YWHAG	3648.5	**-0.22**	0.18	**9.39e-1**
YWHAH	999.1	**-0.04**	0.19	**9.93e-1**
YWHAQ	2281.95	**0.23**	0.19	**9.42e-1**
YWHAZ	5820.73	**0.09**	0.19	**9.90e-1**
YY1	945.62	**0.05**	0.19	**9.93e-1**
YY1AP1	769.99	**-0.34**	0.19	**7.57e-1**
YY2	45.21	**-0.18**	0.25	**9.87e-1**
ZADH2	162.37	**0.32**	0.23	**8.92e-1**
ZAK	301.94	**-0.16**	0.22	**9.87e-1**
ZBED1	534.18	**0.07**	0.2	**9.90e-1**
ZBED4	734.3	**-0.03**	0.19	**9.93e-1**
ZBED5	282.76	**-0.18**	0.22	**9.81e-1**
ZBED5-AS1	14.15	**0.04**	0.23	**9.93e-1**
ZBED6	82.32	**0.35**	0.25	**8.88e-1**
ZBED6CL	73.23	**-0.1**	0.25	**9.90e-1**
ZBTB1	461.69	**0.59**	0.21	**2.59e-1**
ZBTB10	282.35	**0.14**	0.21	**9.90e-1**
ZBTB11	529.7	**0.1**	0.21	**9.90e-1**
ZBTB11-AS1	20.52	**0.03**	0.24	**9.93e-1**
ZBTB12	103.18	**-0.25**	0.25	**9.56e-1**
ZBTB14	191.56	**0.24**	0.22	**9.49e-1**
ZBTB17	259.09	**-0.21**	0.24	**9.74e-1**
ZBTB18	230.71	**-0.12**	0.22	**9.90e-1**
ZBTB2	554.86	**-0.3**	0.2	**8.53e-1**
ZBTB20	42.7	**-0.28**	0.25	**9.49e-1**
ZBTB21	169.4	**-0.06**	0.23	**9.93e-1**
ZBTB22	33.47	**-0.11**	0.25	**9.90e-1**
ZBTB24	657.62	**-0.21**	0.2	**9.49e-1**

ZBTB25	96.94	**-0.11**	0.24	**9.90e-1**
ZBTB26	61.69	**-0.05**	0.25	**9.93e-1**
ZBTB3	40.04	**-0.09**	0.25	**9.90e-1**
ZBTB32	26.89	**-0.35**	0.25	**8.81e-1**
ZBTB33	398.29	**0.04**	0.21	**9.93e-1**
ZBTB34	68.13	**-0.15**	0.25	**9.90e-1**
ZBTB37	20.72	**-0.02**	0.24	**9.93e-1**
ZBTB38	183.57	**0.1**	0.23	**9.90e-1**
ZBTB39	170.67	**-0.12**	0.23	**9.90e-1**
ZBTB4	57.65	**-0.13**	0.25	**9.90e-1**
ZBTB40	315.28	**-0.04**	0.22	**9.93e-1**
ZBTB41	112.22	**-0.12**	0.24	**9.90e-1**
ZBTB43	124.93	**-0.12**	0.24	**9.90e-1**
ZBTB44	1002.12	**-0.04**	0.2	**9.93e-1**
ZBTB45	74.51	**-0.37**	0.25	**8.68e-1**
ZBTB46	26.39	**0.17**	0.25	**9.88e-1**

ZBTB48	178.96	**-0.2**	0.24	**9.81e-1**
ZBTB49	40.87	**0.15**	0.25	**9.90e-1**
ZBTB5	224.04	**0.12**	0.22	**9.90e-1**
ZBTB6	112.22	**-0.01**	0.24	**9.96e-1**
ZBTB7A	471.27	**-0.65**	0.23	**2.57e-1**
ZBTB7B	114.78	**-0.28**	0.25	**9.47e-1**
ZBTB8A	103.95	**0.58**	0.25	**5.31e-1**
ZBTB8OS	272.81	**0.72**	0.22	**1.02e-1**
ZBTB9	153.57	**-0.16**	0.23	**9.88e-1**
ZC2HC1A	28.71	**0.18**	0.25	**9.87e-1**
ZC3H10	44.08	**-0.08**	0.25	**9.91e-1**
ZC3H11A	941.48	**0.16**	0.2	**9.81e-1**
ZC3H12A	172.24	**-0.21**	0.24	**9.80e-1**
ZC3H12D	173.87	**-0.2**	0.23	**9.80e-1**
ZC3H13	1219.34	**-0.49**	0.19	**3.49e-1**
ZC3H14	747.51	**0.02**	0.2	**9.95e-1**
ZC3H15	981.8	**-0.07**	0.19	**9.90e-1**
ZC3H18	1538.28	**-0.57**	0.2	**2.52e-1**
ZC3H3	229.51	**-0.51**	0.24	**6.07e-1**
ZC3H4	870.39	**-0.36**	0.22	**8.31e-1**
ZC3H6	18.49	**0.06**	0.24	**9.93e-1**
ZC3H7A	460.92	**0.28**	0.21	**9.20e-1**
ZC3H7B	1463.98	**-0.46**	0.21	**5.96e-1**
ZC3H8	114.21	**0.1**	0.24	**9.90e-1**
ZC3HAV1	1162.82	**-0.06**	0.19	**9.91e-1**
ZC3HC1	284.82	**-0.02**	0.21	**9.95e-1**
ZC4H2	43	**-0.14**	0.25	**9.90e-1**
ZCCHC10	324.21	**-0.03**	0.22	**9.93e-1**
ZCCHC11	1081.06	**-0.06**	0.19	**9.90e-1**
ZCCHC14	104.73	**-0.02**	0.24	**9.93e-1**
ZCCHC17	339	**-0.22**	0.21	**9.49e-1**
ZCCHC2	568.75	**-0.37**	0.2	**7.09e-1**
ZCCHC3	178.53	**0.04**	0.23	**9.93e-1**
ZCCHC4	91.74	**0**	0.24	**9.98e-1**
ZCCHC6	454.11	**-0.14**	0.21	**9.90e-1**
ZCCHC7	824.83	**0.05**	0.19	**9.93e-1**
ZCCHC8	476.4	**0.2**	0.2	**9.59e-1**
ZCCHC9	129.01	**-0.18**	0.24	**9.87e-1**
ZCRB1	211.3	**-0.45**	0.22	**6.28e-1**
ZCWPW1	53.86	**0.31**	0.25	**9.41e-1**
ZDHHC12	135.52	**-0.29**	0.25	**9.47e-1**
ZDHHC13	149.62	**0.37**	0.24	**8.45e-1**
ZDHHC14	254.2	**-0.21**	0.21	**9.58e-1**
ZDHHC16	353.36	**0.02**	0.21	**9.93e-1**
ZDHHC17	157.26	**0.25**	0.23	**9.49e-1**
ZDHHC18	263.04	**-0.24**	0.24	**9.52e-1**
ZDHHC2	235.81	**0.18**	0.22	**9.81e-1**

ZDHHC20	511.64	**0.13**	0.21	**9.90e-1**
ZDHHC21	199.93	**0.04**	0.23	**9.93e-1**
ZDHHC23	195.08	**-0.05**	0.23	**9.93e-1**
ZDHHC24	24.42	**-0.14**	0.23	**9.90e-1**
ZDHHC3	512.04	**-0.03**	0.2	**9.93e-1**
ZDHHC4	144.65	**0.52**	0.23	**5.70e-1**
ZDHHC5	1070.91	**-0.18**	0.2	**9.73e-1**
ZDHHC6	256.75	**0.16**	0.22	**9.87e-1**
ZDHHC7	320.08	**0.08**	0.21	**9.90e-1**
ZDHHC9	31.25	**0.14**	0.25	**9.90e-1**
ZEB1	338.57	**0.02**	0.21	**9.93e-1**
ZEB1-AS1	101.39	**-0.01**	0.24	**9.96e-1**
ZEB2	172.87	**-0.37**	0.23	**8.33e-1**
ZER1	123.49	**-0.03**	0.24	**9.93e-1**
ZFAND1	173.73	**0.32**	0.23	**8.91e-1**
ZFAND2A	49.52	**0.26**	0.25	**9.54e-1**
ZFAND2B	99.67	**0.08**	0.24	**9.90e-1**
ZFAND3	198.83	**0.09**	0.22	**9.90e-1**
ZFAND4	263.36	**0.04**	0.22	**9.93e-1**
ZFAND5	409.65	**0.18**	0.21	**9.78e-1**
ZFAND6	250.38	**0.4**	0.22	**7.41e-1**
ZFAS1	316.26	**0.34**	0.22	**8.38e-1**
ZFAT	121.65	**0.19**	0.24	**9.81e-1**
ZFC3H1	732.74	**-0.21**	0.2	**9.54e-1**
ZFHX3	255.8	**-0.35**	0.22	**8.28e-1**
ZFP1	189.95	**0.14**	0.23	**9.90e-1**
ZFP14	16.61	**-0.06**	0.23	**9.93e-1**
ZFP30	17.52	**-0.04**	0.23	**9.93e-1**
ZFP36	139.42	**-0.42**	0.25	**8.16e-1**
ZFP36L1	1467.67	**-0.17**	0.21	**9.81e-1**
ZFP36L2	403.48	**0.03**	0.21	**9.93e-1**
ZFP41	95.35	**-0.18**	0.25	**9.87e-1**
ZFP62	225.32	**0.14**	0.22	**9.90e-1**
ZFP64	373.93	**-0.23**	0.21	**9.49e-1**
ZFP69	132.75	**0.14**	0.23	**9.90e-1**
ZFP69B	52.98	**-0.01**	0.25	**9.98e-1**

ZFP82	25.75	**0.02**	0.24	**9.95e-1**
ZFP90	43.13	**0.37**	0.25	**8.64e-1**
ZFP91	1134.66	**-0.06**	0.19	**9.93e-1**
ZFPL1	200.37	**-0.37**	0.23	**8.39e-1**
ZFPM1	63.62	**-0.07**	0.25	**9.93e-1**
ZFR	1625.81	**-0.07**	0.19	**9.90e-1**
ZFX	264.65	**0.12**	0.22	**9.90e-1**
ZFY	125.7	**0.22**	0.24	**9.66e-1**
ZFYVE1	102.93	**0.07**	0.24	**9.93e-1**
ZFYVE16	130.66	**0.12**	0.24	**9.90e-1**
ZFYVE19	171.93	**-0.19**	0.23	**9.84e-1**
ZFYVE21	46	**0.32**	0.25	**9.23e-1**
ZFYVE26	326.19	**-0.01**	0.21	**9.98e-1**
ZFYVE27	219.05	**-0.26**	0.23	**9.47e-1**
ZGPAT	327.15	**-0.16**	0.24	**9.89e-1**
ZGRF1	211.03	**0.2**	0.23	**9.80e-1**
ZHX1	396.79	**-0.05**	0.22	**9.93e-1**
ZHX2	1132.08	**-0.23**	0.19	**9.47e-1**
ZHX3	326.7	**-0.19**	0.21	**9.73e-1**
ZKSCAN1	573.96	**0.03**	0.2	**9.93e-1**
ZKSCAN2	192.97	**-0.05**	0.22	**9.93e-1**
ZKSCAN3	35.81	**0.1**	0.25	**9.90e-1**
ZKSCAN4	17.16	**0.17**	0.24	**9.87e-1**
ZKSCAN5	264.26	**0.15**	0.21	**9.88e-1**
ZKSCAN8	473.69	**-0.08**	0.21	**9.90e-1**
ZMAT1	12.28	**0.12**	0.22	**9.90e-1**
ZMAT2	540.88	**-0.09**	0.2	**9.90e-1**

ZMAT3	195.11	**0.35**	0.23	**8.52e-1**
ZMAT5	43.48	**-0.05**	0.25	**9.93e-1**
ZMIZ1	906.17	**-0.7**	0.22	**1.25e-1**
ZMIZ2	3035.92	**-0.28**	0.23	**9.30e-1**
ZMPSTE24	944.75	**0.06**	0.2	**9.91e-1**
ZMYM1	131.95	**0.04**	0.24	**9.93e-1**
ZMYM2	622.95	**-0.02**	0.21	**9.93e-1**
ZMYM3	775.57	**-0.17**	0.2	**9.74e-1**
ZMYM4	1156.62	**0.06**	0.19	**9.91e-1**
ZMYM5	68.08	**0.03**	0.25	**9.93e-1**
ZMYM6	240.4	**0.12**	0.22	**9.90e-1**
ZMYM6NB	14.79	**0.02**	0.23	**9.94e-1**
ZMYND10	10.59	**0**	0.21	**9.98e-1**
ZMYND19	399.47	**0.34**	0.2	**8.21e-1**
ZMYND8	740.42	**-0.24**	0.19	**9.25e-1**
ZNF100	96.35	**-0.13**	0.25	**9.90e-1**
ZNF101	301.48	**-0.29**	0.21	**8.92e-1**
ZNF106	1392.95	**0.03**	0.2	**9.93e-1**
ZNF107	1024.97	**-0.32**	0.2	**8.34e-1**
ZNF117	108.92	**0.13**	0.25	**9.90e-1**
ZNF12	285.26	**0.15**	0.22	**9.89e-1**
ZNF121	124.34	**-0.25**	0.24	**9.49e-1**
ZNF124	58.13	**0.1**	0.25	**9.90e-1**
ZNF131	444.5	**0.05**	0.21	**9.93e-1**
ZNF132	11.83	**-0.02**	0.22	**9.93e-1**
ZNF133	30.69	**-0.01**	0.25	**9.96e-1**
ZNF136	49.99	**0.18**	0.25	**9.87e-1**
ZNF137P	32.33	**0.03**	0.25	**9.93e-1**
ZNF138	322.92	**-0.05**	0.21	**9.93e-1**
ZNF14	44.26	**0.12**	0.25	**9.90e-1**
ZNF140	30.82	**0.07**	0.25	**9.92e-1**
ZNF141	130.18	**-0.16**	0.24	**9.89e-1**
ZNF142	732.48	**-0.55**	0.21	**3.49e-1**
ZNF143	142.85	**0.03**	0.23	**9.93e-1**
ZNF146	1217.53	**-0.02**	0.2	**9.95e-1**
ZNF148	459.5	**-0.1**	0.21	**9.90e-1**
ZNF16	51.55	**0.19**	0.25	**9.87e-1**
ZNF160	219.81	**0.26**	0.22	**9.47e-1**
ZNF165	64.8	**0.24**	0.25	**9.66e-1**
ZNF169	26.51	**-0.15**	0.25	**9.90e-1**
ZNF17	50.57	**0.14**	0.25	**9.90e-1**
ZNF174	201.63	**-0.25**	0.22	**9.47e-1**
ZNF175	63.54	**0.02**	0.25	**9.96e-1**
ZNF18	47.87	**0.18**	0.25	**9.87e-1**
ZNF180	45.48	**0.01**	0.25	**9.96e-1**
ZNF181	28.15	**0.43**	0.25	**7.94e-1**
ZNF182	97.63	**0.16**	0.24	**9.90e-1**
ZNF184	120.46	**0.1**	0.24	**9.90e-1**
ZNF185	17.65	**0.02**	0.24	**9.93e-1**
ZNF189	96.06	**0.27**	0.25	**9.49e-1**
ZNF195	346.41	**0.2**	0.22	**9.66e-1**
ZNF197	49.26	**0.1**	0.25	**9.90e-1**
ZNF2	40.75	**-0.15**	0.25	**9.90e-1**
ZNF200	163.98	**0.05**	0.23	**9.93e-1**
ZNF202	190.57	**0**	0.23	**9.98e-1**
ZNF207	2031.31	**-0.07**	0.19	**9.90e-1**
ZNF211	24.07	**0.14**	0.25	**9.90e-1**
ZNF212	110.13	**0.1**	0.24	**9.90e-1**
ZNF213	97.02	**-0.31**	0.25	**9.39e-1**
ZNF213-AS1	23.45	**0.11**	0.25	**9.90e-1**
ZNF215	83.26	**-0.09**	0.25	**9.90e-1**
ZNF217	723.96	**0.34**	0.2	**8.04e-1**
ZNF219	29.78	**0.05**	0.24	**9.93e-1**

ZNF22	559.74	**0.14**	0.2	**9.88e-1**
ZNF226	29.53	**0.1**	0.25	**9.90e-1**
ZNF23	104.17	**0.21**	0.24	**9.74e-1**
ZNF232	188.7	**0.01**	0.23	**9.97e-1**
ZNF236	144.43	**-0.07**	0.23	**9.93e-1**
ZNF24	747.89	**0.1**	0.21	**9.90e-1**
ZNF248	124.95	**0.21**	0.24	**9.74e-1**
ZNF25	53.2	**0.11**	0.25	**9.90e-1**
ZNF250	75.86	**0.04**	0.25	**9.93e-1**
ZNF251	114.27	**0.13**	0.24	**9.90e-1**
ZNF252P	288.77	**0.17**	0.22	**9.86e-1**
ZNF253	93.61	**0.26**	0.24	**9.49e-1**
ZNF254	170.87	**0.1**	0.23	**9.90e-1**
ZNF260	114.02	**0.07**	0.24	**9.93e-1**
ZNF263	576.66	**-0.19**	0.21	**9.72e-1**
ZNF266	268.16	**0.23**	0.22	**9.52e-1**
ZNF267	454.09	**0.27**	0.21	**9.14e-1**
ZNF268	130.9	**0.04**	0.24	**9.93e-1**
ZNF271P	161.3	**-0.07**	0.23	**9.91e-1**
ZNF273	195.69	**-0.11**	0.23	**9.90e-1**
ZNF274	100.06	**0.24**	0.24	**9.58e-1**
ZNF275	233.28	**0.28**	0.22	**9.30e-1**
ZNF276	255.17	**-0.09**	0.22	**9.90e-1**
ZNF277	202.97	**0.37**	0.22	**8.12e-1**
ZNF28	192.06	**0.11**	0.23	**9.90e-1**
ZNF280B	16.75	**-0.09**	0.23	**9.90e-1**
ZNF280C	147.57	**-0.01**	0.23	**9.98e-1**
ZNF280D	62.04	**-0.29**	0.25	**9.47e-1**
ZNF281	430.22	**-0.11**	0.21	**9.90e-1**
ZNF282	358.89	**-0.1**	0.22	**9.90e-1**
ZNF286A	166.59	**-0.08**	0.23	**9.90e-1**
ZNF286B	26.22	**0.11**	0.25	**9.90e-1**
ZNF292	510.29	**0.19**	0.22	**9.80e-1**
ZNF296	219.44	**-0.18**	0.24	**9.87e-1**
ZNF3	418.44	**0.22**	0.2	**9.49e-1**
ZNF304	102.56	**0.01**	0.24	**9.97e-1**
ZNF316	353.96	**-0.05**	0.23	**9.93e-1**
ZNF317	544.11	**0.01**	0.2	**9.96e-1**
ZNF318	948.08	**0.59**	0.19	**1.79e-1**
ZNF319	138.04	**-0.16**	0.25	**9.90e-1**
ZNF320	232.42	**-0.08**	0.22	**9.90e-1**
ZNF322	20.26	**-0.01**	0.24	**9.97e-1**
ZNF324	96.56	**-0.14**	0.25	**9.90e-1**
ZNF324B	63.56	**-0.11**	0.25	**9.90e-1**
ZNF326	485.13	**-0.3**	0.2	**8.64e-1**
ZNF330	508.33	**0.19**	0.2	**9.64e-1**
ZNF331	111.17	**-0.08**	0.24	**9.91e-1**
ZNF333	20.97	**0.21**	0.24	**9.80e-1**
ZNF335	582.04	**-0.2**	0.21	**9.60e-1**
ZNF337	113.78	**0.13**	0.24	**9.90e-1**
ZNF337-AS1	47.42	**-0.32**	0.25	**9.25e-1**
ZNF33A	630.93	**0.02**	0.2	**9.93e-1**
ZNF33B	401.58	**0.42**	0.22	**6.90e-1**
ZNF34	17.48	**0.13**	0.24	**9.90e-1**
ZNF341	88.83	**-0.26**	0.25	**9.49e-1**
ZNF343	328.14	**-0.29**	0.21	**9.03e-1**
ZNF346	154.64	**-0.11**	0.23	**9.90e-1**
ZNF347	36.62	**0.03**	0.25	**9.93e-1**
ZNF35	49.95	**-0.12**	0.25	**9.90e-1**
ZNF354A	108.97	**0.01**	0.24	**9.98e-1**
ZNF354B	16.59	**0.06**	0.23	**9.93e-1**
ZNF367	252.72	**0.21**	0.22	**9.61e-1**
ZNF37A	462.2	**-0.06**	0.21	**9.93e-1**
ZNF37BP	408.34	**-0.11**	0.21	**9.90e-1**
ZNF383	31.02	**0.1**	0.25	**9.90e-1**

ZNF384	799.67	**-0.19**	0.2	**9.64e-1**
ZNF394	174.49	**0.49**	0.23	**5.91e-1**
ZNF395	664.94	**0.04**	0.21	**9.93e-1**
ZNF397	73.16	**0.21**	0.25	**9.81e-1**
ZNF398	366.51	**-0.08**	0.21	**9.90e-1**
ZNF407	147.72	**0.14**	0.23	**9.90e-1**
ZNF408	68.82	**-0.1**	0.25	**9.90e-1**
ZNF41	137.19	**0.28**	0.24	**9.42e-1**
ZNF410	201.42	**0.31**	0.22	**8.91e-1**
ZNF414	94.16	**-0.21**	0.25	**9.81e-1**
ZNF417	74.72	**0.03**	0.25	**9.93e-1**

ZNF419	17.03	**-0.15**	0.24	**9.90e-1**
ZNF420	29.06	**0.18**	0.25	**9.87e-1**
ZNF425	17.2	**0.05**	0.23	**9.93e-1**
ZNF428	99.97	**-0.2**	0.25	**9.81e-1**
ZNF429	93.54	**-0.12**	0.25	**9.90e-1**
ZNF43	352.51	**0.03**	0.22	**9.93e-1**
ZNF430	182.88	**-0.03**	0.23	**9.93e-1**
ZNF431	150.52	**-0.04**	0.23	**9.93e-1**
ZNF432	19.82	**-0.07**	0.24	**9.93e-1**
ZNF436	108.64	**-0.02**	0.24	**9.95e-1**
ZNF436-AS1	12.85	**0.04**	0.22	**9.93e-1**
ZNF438	45.63	**-0.23**	0.25	**9.74e-1**
ZNF44	44.31	**0.13**	0.25	**9.90e-1**
ZNF440	37.88	**-0.08**	0.25	**9.92e-1**
ZNF441	52.23	**0.08**	0.25	**9.91e-1**
ZNF443	15.52	**0.08**	0.22	**9.90e-1**
ZNF444	119.77	**-0.1**	0.25	**9.90e-1**
ZNF445	189.89	**-0.19**	0.23	**9.81e-1**
ZNF446	10.67	**0.12**	0.2	**9.90e-1**
ZNF449	29.5	**0.14**	0.25	**9.90e-1**
ZNF45	112.07	**0.2**	0.24	**9.80e-1**
ZNF451	327.32	**0.06**	0.21	**9.93e-1**
ZNF460	16.29	**-0.19**	0.23	**9.81e-1**
ZNF468	186.29	**-0.06**	0.23	**9.93e-1**
ZNF473	191.59	**0.17**	0.22	**9.87e-1**
ZNF48	216.25	**-0.25**	0.24	**9.51e-1**
ZNF480	264.2	**0.06**	0.23	**9.93e-1**
ZNF484	31.97	**0.16**	0.25	**9.90e-1**
ZNF485	62.4	**-0.09**	0.25	**9.90e-1**
ZNF486	38.78	**0.14**	0.25	**9.90e-1**
ZNF487	21.01	**0.03**	0.24	**9.93e-1**
ZNF490	56.88	**0.45**	0.25	**7.49e-1**
ZNF493	41.26	**0.18**	0.25	**9.87e-1**
ZNF497	24.63	**0.01**	0.25	**9.98e-1**
ZNF500	76.37	**-0.37**	0.25	**8.64e-1**
ZNF506	131.36	**0.21**	0.24	**9.73e-1**
ZNF507	407.59	**-0.1**	0.21	**9.90e-1**
ZNF510	86.57	**0.16**	0.25	**9.90e-1**
ZNF511	164.5	**0.23**	0.23	**9.58e-1**
ZNF512	409.02	**0.14**	0.21	**9.88e-1**
ZNF513	41.15	**-0.28**	0.25	**9.49e-1**
ZNF518A	390.78	**0.2**	0.22	**9.73e-1**
ZNF519	65.63	**0.12**	0.25	**9.90e-1**
ZNF521	35.95	**0.18**	0.25	**9.87e-1**
ZNF524	15.37	**0.05**	0.22	**9.93e-1**
ZNF525	181.7	**0.09**	0.23	**9.90e-1**
ZNF526	119.84	**-0.37**	0.25	**8.56e-1**
ZNF527	12.05	**0.12**	0.21	**9.90e-1**
ZNF532	325.64	**-0.2**	0.21	**9.66e-1**
ZNF543	52.71	**0.08**	0.25	**9.91e-1**
ZNF544	108.65	**0.15**	0.24	**9.90e-1**
ZNF546	17.31	**0.03**	0.24	**9.93e-1**

ZNF547	16.18	**0.2**	0.23	**9.75e-1**
ZNF548	52.76	**0.08**	0.25	**9.91e-1**
ZNF550	57.44	**0.12**	0.25	**9.90e-1**
ZNF551	104.18	**0.06**	0.24	**9.93e-1**
ZNF552	68.3	**0**	0.25	**9.98e-1**
ZNF554	19.08	**0.04**	0.24	**9.93e-1**
ZNF555	40.81	**0.09**	0.25	**9.90e-1**
ZNF556	15.68	**0.12**	0.23	**9.90e-1**
ZNF557	88.2	**0.01**	0.25	**9.96e-1**
ZNF559	42.56	**0.11**	0.25	**9.90e-1**
ZNF561	166.07	**0.07**	0.23	**9.91e-1**
ZNF561-AS1	14.06	**0.01**	0.23	**9.97e-1**
ZNF562	146.01	**0.25**	0.23	**9.49e-1**
ZNF563	10.46	**0.15**	0.21	**9.87e-1**
ZNF564	45.31	**0.31**	0.25	**9.42e-1**
ZNF565	14.06	**-0.08**	0.23	**9.90e-1**
ZNF566	25.85	**0.28**	0.25	**9.47e-1**
ZNF567	43.14	**-0.19**	0.25	**9.87e-1**
ZNF569	45.98	**0.03**	0.25	**9.93e-1**
ZNF57	60.29	**0**	0.25	**9.99e-1**
ZNF572	38.19	**0.23**	0.25	**9.68e-1**
ZNF574	296.65	**-0.36**	0.22	**8.38e-1**
ZNF576	82.93	**-0.45**	0.25	**7.49e-1**
ZNF579	41.49	**0**	0.25	**1.00e+0**
ZNF580	78.88	**-0.06**	0.25	**9.93e-1**
ZNF581	192.29	**0.02**	0.24	**9.96e-1**
ZNF583	34.15	**0.25**	0.25	**9.59e-1**
ZNF584	117.47	**-0.18**	0.24	**9.87e-1**
ZNF585A	20.94	**0.05**	0.24	**9.93e-1**
ZNF585B	38.75	**0.14**	0.25	**9.90e-1**
ZNF586	112.4	**0.22**	0.24	**9.72e-1**

ZNF587	293.61	**-0.08**	0.22	**9.90e-1**
ZNF587B	96.57	**-0.18**	0.24	**9.87e-1**
ZNF589	757.27	**-0.39**	0.2	**6.69e-1**
ZNF592	952.04	**-0.43**	0.2	**5.99e-1**
ZNF593	142.9	**-0.25**	0.25	**9.54e-1**
ZNF594	167.7	**0.32**	0.23	**8.91e-1**
ZNF596	28.27	**0.05**	0.25	**9.93e-1**
ZNF597	46.54	**0**	0.25	**9.98e-1**
ZNF598	845.77	**-0.36**	0.23	**8.41e-1**
ZNF600	99.79	**0.11**	0.24	**9.90e-1**
ZNF605	87.74	**0.28**	0.25	**9.47e-1**
ZNF607	98.17	**0.02**	0.24	**9.96e-1**
ZNF608	439.25	**0.7**	0.21	**8.70e-2**
ZNF609	778.51	**-0.29**	0.19	**8.64e-1**
ZNF611	92.92	**-0.03**	0.25	**9.93e-1**
ZNF613	32.23	**0.02**	0.25	**9.95e-1**
ZNF614	108.6	**0.14**	0.25	**9.90e-1**
ZNF615	12.81	**0**	0.22	**9.99e-1**
ZNF616	64.15	**0.27**	0.25	**9.49e-1**
ZNF619	25.6	**0.25**	0.25	**9.57e-1**
ZNF621	205.87	**-0.14**	0.22	**9.90e-1**
ZNF622	184	**0.16**	0.22	**9.88e-1**
ZNF623	99.81	**0.11**	0.24	**9.90e-1**
ZNF624	24.5	**0.23**	0.24	**9.63e-1**
ZNF626	76.77	**0**	0.25	**9.99e-1**
ZNF627	32.47	**0.31**	0.25	**9.31e-1**
ZNF628	91.37	**-0.01**	0.25	**9.96e-1**
ZNF638	824.24	**0.18**	0.21	**9.73e-1**
ZNF639	314.97	**0.28**	0.23	**9.42e-1**
ZNF641	28.75	**0.18**	0.25	**9.87e-1**
ZNF644	559.97	**0.05**	0.21	**9.93e-1**
ZNF646	364.32	**-0.39**	0.23	**8.10e-1**

ZNF649	22.1	**-0.14**	0.24	**9.90e-1**
ZNF652	321.6	**-0.22**	0.21	**9.53e-1**
ZNF653	44.69	**0.27**	0.25	**9.51e-1**
ZNF654	97.34	**0.13**	0.24	**9.90e-1**
ZNF655	587.15	**0.12**	0.2	**9.90e-1**
ZNF658	28	**-0.11**	0.25	**9.90e-1**
ZNF664	1505.64	**-0.11**	0.19	**9.90e-1**
ZNF665	18.23	**0**	0.24	**9.98e-1**
ZNF668	98.45	**-0.33**	0.25	**9.08e-1**
ZNF669	11.97	**0.12**	0.22	**9.90e-1**
ZNF670	64.5	**0**	0.25	**9.99e-1**
ZNF671	20.61	**0.14**	0.24	**9.90e-1**
ZNF672	440.79	**0.08**	0.21	**9.90e-1**
ZNF674	19.27	**0.1**	0.24	**9.90e-1**
ZNF674-AS1	32.66	**-0.2**	0.25	**9.83e-1**
ZNF675	196.54	**0.06**	0.22	**9.93e-1**
ZNF678	154.4	**0.22**	0.23	**9.66e-1**
ZNF680	179.49	**0.03**	0.23	**9.93e-1**
ZNF681	145.16	**0.29**	0.24	**9.41e-1**
ZNF684	33.38	**0.02**	0.25	**9.96e-1**
ZNF687	237.17	**-0.25**	0.24	**9.53e-1**
ZNF688	23.27	**-0.08**	0.23	**9.90e-1**
ZNF689	205.3	**-0.03**	0.22	**9.93e-1**
ZNF691	122.35	**-0.23**	0.24	**9.60e-1**
ZNF692	231.79	**-0.02**	0.22	**9.95e-1**
ZNF695	17.63	**0.26**	0.23	**9.47e-1**
ZNF696	84.91	**0.02**	0.25	**9.96e-1**
ZNF699	10.38	**0.19**	0.21	**9.73e-1**
ZNF7	171.86	**0.2**	0.23	**9.73e-1**
ZNF70	50.57	**-0.14**	0.25	**9.90e-1**
ZNF700	91.1	**0.35**	0.25	**8.80e-1**
ZNF701	99.5	**-0.01**	0.24	**9.98e-1**
ZNF706	300.26	**0.02**	0.21	**9.93e-1**
ZNF707	33	**0.06**	0.25	**9.93e-1**
ZNF708	68.74	**-0.25**	0.25	**9.56e-1**
ZNF709	16.91	**0.2**	0.23	**9.80e-1**
ZNF71	60.5	**-0.1**	0.25	**9.90e-1**
ZNF710	201.47	**-0.59**	0.24	**4.14e-1**
ZNF711	243.99	**0.03**	0.22	**9.93e-1**
ZNF713	18.9	**0**	0.24	**9.98e-1**
ZNF714	241.69	**-0.11**	0.22	**9.90e-1**
ZNF718	76.61	**0.16**	0.25	**9.90e-1**
ZNF720	55.54	**0.09**	0.25	**9.90e-1**
ZNF721	415.46	**0.03**	0.21	**9.93e-1**
ZNF726	18.59	**-0.04**	0.24	**9.93e-1**
ZNF730	46.49	**0.03**	0.25	**9.93e-1**
ZNF736	275.55	**0.23**	0.21	**9.49e-1**
ZNF737	129.57	**0.07**	0.24	**9.93e-1**
ZNF738	136.01	**0.22**	0.24	**9.72e-1**
ZNF740	309.07	**0.16**	0.21	**9.87e-1**
ZNF746	241.47	**-0.22**	0.23	**9.66e-1**

ZNF747	147.72	**-0.12**	0.23	**9.90e-1**
ZNF749	68.52	**0.02**	0.25	**9.94e-1**
ZNF75A	31.21	**0.05**	0.25	**9.93e-1**
ZNF75D	55.67	**0.41**	0.25	**8.30e-1**
ZNF76	295.12	**0.14**	0.21	**9.90e-1**
ZNF761	219.94	**0.03**	0.22	**9.93e-1**
ZNF764	53.76	**-0.1**	0.25	**9.90e-1**
ZNF765	128.45	**-0.17**	0.24	**9.87e-1**
ZNF766	158.52	**0**	0.23	**9.98e-1**
ZNF767P	157.38	**0.31**	0.23	**9.03e-1**
ZNF768	307.87	**-0.12**	0.23	**9.90e-1**
ZNF77	24.29	**0.09**	0.25	**9.90e-1**
ZNF770	767.96	**0.2**	0.21	**9.61e-1**

ZNF771	15.27	**0.26**	0.23	**9.47e-1**
ZNF772	12.26	**0.16**	0.22	**9.87e-1**
ZNF773	15.91	**0.13**	0.23	**9.90e-1**
ZNF775	40.12	**-0.06**	0.25	**9.93e-1**
ZNF776	158.1	**0.11**	0.23	**9.90e-1**
ZNF777	297.11	**0.04**	0.22	**9.93e-1**
ZNF778	46.94	**-0.11**	0.25	**9.90e-1**
ZNF780A	26.36	**-0.02**	0.25	**9.96e-1**
ZNF780B	65.2	**0.32**	0.25	**9.25e-1**
ZNF782	43.85	**0.07**	0.25	**9.93e-1**
ZNF783	22.14	**-0.12**	0.24	**9.90e-1**
ZNF784	16.52	**0.06**	0.23	**9.93e-1**
ZNF786	77.06	**-0.22**	0.25	**9.80e-1**
ZNF787	167.01	**-0.29**	0.25	**9.47e-1**
ZNF789	58.96	**0.1**	0.25	**9.90e-1**
ZNF79	50.93	**-0.09**	0.25	**9.90e-1**
ZNF791	143.32	**0.68**	0.24	**2.42e-1**
ZNF792	18.51	**-0.11**	0.23	**9.90e-1**
ZNF799	17.14	**0.21**	0.23	**9.69e-1**
ZNF8	68.63	**-0.23**	0.25	**9.71e-1**
ZNF800	379.78	**0.01**	0.22	**9.98e-1**
ZNF804A	231.13	**-0.03**	0.22	**9.93e-1**
ZNF805	57.55	**0.18**	0.25	**9.87e-1**
ZNF808	77.28	**-0.01**	0.25	**9.96e-1**
ZNF81	51.4	**0.23**	0.25	**9.72e-1**
ZNF813	107.97	**-0.02**	0.24	**9.95e-1**
ZNF814	10.58	**-0.06**	0.21	**9.92e-1**
ZNF815P	15.21	**-0.07**	0.23	**9.91e-1**
ZNF816	58.8	**0.21**	0.25	**9.81e-1**
ZNF821	20.22	**0.15**	0.24	**9.90e-1**
ZNF823	47.74	**0.22**	0.25	**9.79e-1**
ZNF827	445.88	**-0.01**	0.2	**9.97e-1**
ZNF83	149.62	**0.16**	0.23	**9.87e-1**
ZNF830	117.03	**0.11**	0.24	**9.90e-1**
ZNF831	148.45	**-0.92**	0.24	**1.96e-2**
ZNF837	15.08	**0.26**	0.22	**9.47e-1**
ZNF839	99.92	**0.16**	0.24	**9.90e-1**
ZNF844	31.21	**0.15**	0.25	**9.90e-1**
ZNF845	134.72	**-0.02**	0.24	**9.95e-1**
ZNF85	117.86	**-0.07**	0.24	**9.93e-1**
ZNF852	31.11	**-0.2**	0.25	**9.86e-1**
ZNF860	185.19	**-0.41**	0.23	**7.49e-1**
ZNF862	18.82	**-0.03**	0.24	**9.93e-1**
ZNF865	113.19	**-0.05**	0.25	**9.93e-1**
ZNF888	64.18	**-0.13**	0.25	**9.90e-1**
ZNF91	113.63	**0.01**	0.25	**9.96e-1**
ZNF92	509.63	**-0.3**	0.22	**8.92e-1**
ZNF93	48.21	**0.06**	0.25	**9.93e-1**
ZNFX1	654.34	**-0.12**	0.19	**9.90e-1**
ZNHIT1	169.51	**0.07**	0.23	**9.93e-1**
ZNHIT2	17.39	**-0.18**	0.23	**9.86e-1**
ZNHIT3	122.33	**0.47**	0.24	**6.69e-1**
ZNHIT6	530.25	**-0.19**	0.2	**9.66e-1**
ZNRD1	59.8	**-0.21**	0.25	**9.81e-1**
ZNRD1-AS1	24.48	**0.05**	0.25	**9.93e-1**
ZNRF1	185.16	**-0.13**	0.23	**9.90e-1**
ZNRF2	101.08	**0.21**	0.24	**9.80e-1**
ZP3	10.05	**-0.03**	0.21	**9.93e-1**
ZPBP2	17.15	**0**	0.23	**9.98e-1**
ZPR1	769.95	**-0.08**	0.19	**9.90e-1**
ZRANB1	312.62	**0.05**	0.21	**9.93e-1**
ZRANB2	1324.14	**0.01**	0.2	**9.96e-1**
ZRANB3	61.72	**0.14**	0.25	**9.90e-1**
ZRSR2	113.79	**-0.37**	0.24	**8.41e-1**

ZSCAN12P1	73.25	**0.26**	0.25	**9.54e-1**
ZSCAN16-AS1	33.16	**-0.2**	0.25	**9.84e-1**
ZSCAN2	60.04	**0.02**	0.25	**9.94e-1**
ZSCAN20	45.3	**0.07**	0.25	**9.93e-1**
ZSCAN21	49.07	**0.09**	0.25	**9.90e-1**
ZSCAN22	35.94	**0.07**	0.25	**9.93e-1**
ZSCAN25	166.55	**-0.18**	0.23	**9.81e-1**
ZSCAN26	41.82	**0.03**	0.25	**9.93e-1**
ZSCAN29	293.23	**0.18**	0.21	**9.80e-1**
ZSCAN30	34	**0.16**	0.25	**9.90e-1**
ZSCAN32	200.04	**0.15**	0.22	**9.88e-1**
ZSCAN5A	48.77	**0.17**	0.25	**9.89e-1**
ZSWIM1	180.83	**-0.37**	0.23	**8.30e-1**
ZSWIM3	42.31	**0.2**	0.25	**9.86e-1**
ZSWIM4	33.36	**0.37**	0.25	**8.66e-1**
ZSWIM6	33.15	**0.04**	0.25	**9.93e-1**
ZSWIM7	69.45	**0.42**	0.25	**8.12e-1**
ZSWIM8	406.84	**-0.22**	0.22	**9.58e-1**
ZUFSP	223.64	**0.15**	0.22	**9.88e-1**
ZW10	288.21	**0.21**	0.22	**9.64e-1**
ZWILCH	750.63	**0.02**	0.21	**9.95e-1**
ZWINT	782.3	**-0.16**	0.19	**9.83e-1**
ZXDB	95.86	**0.06**	0.24	**9.93e-1**
ZXDC	174.83	**0.24**	0.23	**9.49e-1**
ZYG11B	286.85	**0.15**	0.21	**9.88e-1**
ZZEF1	565.26	**-0.07**	0.2	**9.91e-1**
ZZZ3	469.55	**0.05**	0.2	**9.93e-1**

International Journal of *Molecular Sciences*

IMPACT FACTOR 4.9 | Indexed in: PubMed | CITESCORE 8.1

Review

The Interplay between Autophagy and Mitochondria in Cancer

Aleksandra Zdanowicz and Emilia Grosicka-Maciąg

Special Issue
Autophagy and Cellular Oxidative Stress: Molecular Mechanisms and Diagnostic Biomarkers
Edited by
Dr. Ramona D'Amico and Dr. Daniela Impellizzeri

MDPI

https://doi.org/10.3390/ijms25179143

International Journal of
Molecular Sciences

MDPI

Review

The Interplay between Autophagy and Mitochondria in Cancer

Aleksandra Zdanowicz [1,2] and Emilia Grosicka-Maciąg [3,*]

[1] Department of Biochemistry, Medical University of Warsaw, Banacha 1 Str., 02-097 Warsaw, Poland; aleksandra.zdanowicz@wum.edu.pl
[2] Doctoral School, Medical University of Warsaw, Zwirki i Wigury 81 Str., 02-091 Warsaw, Poland
[3] Department of Biochemistry and Laboratory Diagnostic, Collegium Medicum Cardinal Stefan Wyszyński University, Kazimierza Wóycickiego 1 Str., 01-938 Warsaw, Poland
* Correspondence: e.grosicka-maciag@uksw.edu.pl

Abstract: Besides producing cellular energy, mitochondria are crucial in controlling oxidative stress and modulating cellular metabolism, particularly under stressful conditions. A key aspect of this regulatory role involves the recycling process of autophagy, which helps to sustain energy homeostasis. Autophagy, a lysosome-dependent degradation pathway, plays a fundamental role in maintaining cellular homeostasis by degrading damaged organelles and misfolded proteins. In the context of tumor formation, autophagy significantly influences cancer metabolism and chemotherapy resistance, contributing to both tumor suppression and surveillance. This review focuses on the relationship between mitochondria and autophagy, specifically in the context of cancer progression. Investigating the interaction between autophagy and mitochondria reveals new possibilities for cancer treatments and may result in the development of more effective therapies targeting mitochondria, which could have significant implications for cancer treatment. Additionally, this review highlights the increasing understanding of autophagy's role in tumor development, with a focus on modulating mitochondrial function and autophagy in both pre-clinical and clinical cancer research. It also explores the potential for developing more-targeted and personalized therapies by investigating autophagy-related biomarkers.

Keywords: mitochondria; mitophagy; autophagy; oxidative stress; cancer; autophagy-related biomarkers

Citation: Zdanowicz, A.; Grosicka-Maciąg, E. The Interplay between Autophagy and Mitochondria in Cancer. *Int. J. Mol. Sci.* **2024**, *25*, 9143. https://doi.org/10.3390/ijms25179143

Academic Editors: Daniela Impellizzeri and Ramona D'Amico

Received: 15 July 2024
Revised: 16 August 2024
Accepted: 21 August 2024
Published: 23 August 2024

1. Introduction: The Function of Mitochondria

Mitochondria are often termed the "powerhouse" of the cell because of their ability to transform the energy contained in glucose or other organic molecules into adenosine triphosphate (ATP).

During cellular respiration, apart from ATP production (Figure 1), mitochondria primarily generate reactive oxygen species (ROS), mainly superoxide (O^{2-}), due to electron leakage at complexes I and III [1]. Under typical physiological conditions, mitochondria produce a modest level of mtROS (mitochondrial ROS), but in the presence of a mitochondrial dysfunction, the production of mtROS escalates uncontrollably. This excessive, unmanageable level of mtROS leads to modified mitochondrial redox signaling. Oxidative stress conditions within mitochondria are heralded by the impairment of the Krebs cycle, the degradation of mitochondrial proteins through their unfolding, also impacting cell death, mitochondrial DNA (mtDNA) mutations, and lipid damage [2]. Moreover, mitochondrial oxidative stress induces the expression of genes that activate stress response pathways, including the activation of Nrf2 (nuclear factor erythroid 2-related factor 2). The Nrf2 transcription factor controls the expression of antioxidant response genes related to glutathione, thioredoxin, iron metabolism, and NADPH production. Disruption of mtDNA by mtROS can impair ETC function because mtDNA encodes 13 mRNAs for mitochondrial respiratory complexes, 22 tRNAs, and 2 rRNAs [3]. The control of the accumulation and elimination of mtROS can be executed by either superoxide dismutase (SOD), NADPH

oxidase (NOX), catalase (CAT), glutathione peroxidase (GSH-Px), or thioredoxin peroxidase (TRX-Px) [4]. The effectiveness of GSH-Px and TRX-Px is contingent upon the presence of reduced glutathione (GSH) and reduced thioredoxin (TRX). The replenishment of GSH and TRX relies on the functionality of reductases and the quantity of their cofactor, NADPH. Additionally, mtROS can be eliminated through the controlled removal of mitochondria, known as mitophagy [2].

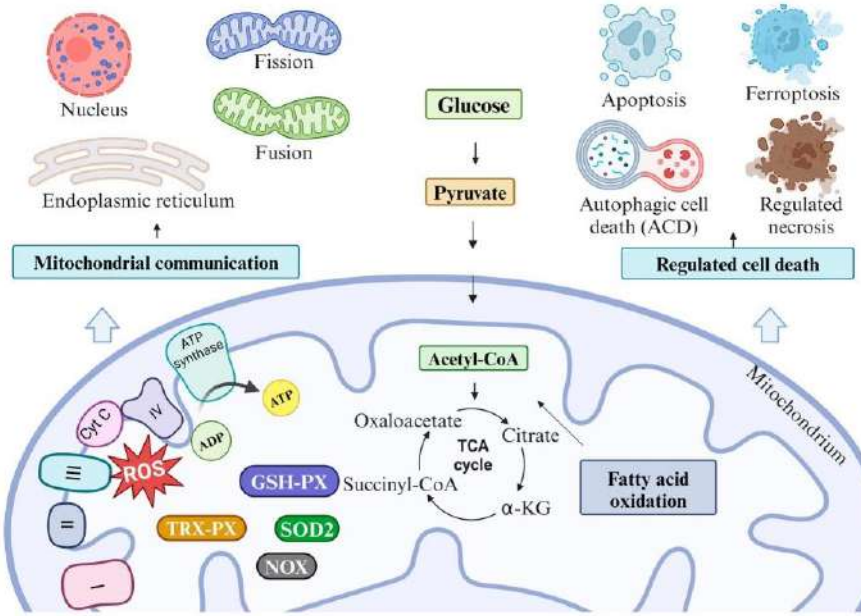

Figure 1. Overview of mitochondrial functions. Mitochondria perform several essential functions within the cell, including ATP production; reactive oxygen species (ROS) generation and elimination through superoxide dismutase (SOD), NADPH oxidase (NOX), catalase (CAT), glutathione peroxidase (GSH-Px), or thioredoxin peroxidase (TRX-Px); mitochondrial communication; and regulation of cell death. This image was created on BioRender.com.

Mitochondria play crucial roles in maintaining calcium homeostasis, the reprogramming of metabolism to suit physiological needs, and the regulation of the cell and organelles' death. To maintain cellular homeostasis, mitochondria engage in communication with each other and with other organelles through various mechanisms, such as retrograde signaling, vesicular transport, signaling molecules, or direct interaction with the mitochondria-associated membrane (MAM) of the endoplasmic reticulum (ER). Collaboration with ER supports mitochondria in regulating Ca^{2+} transport, apoptosis, and phospholipids delivery. Additionally, cooperation with peroxisomes assists in fatty acid oxidation and the elimination of mtROS [5]. The formation of a mitochondrial network occurs through the processes of the fission and fusion of both the outer (OMM) and the inner (IMM) mitochondrial membranes. A proper balance between mitochondrial fusion and fission is vital for ensuring effective cell metabolism and adaptation to stress. The fusion of mitochondria facilitates the mixing of mtDNA and enhances MMP, mitochondrial respiration, and ATP production. Conversely, mitochondrial fission regulates apoptosis and mitophagy [6]. Furthermore, intact mitochondria possessing mtDNA are capable of transferring between cells via a mechanism termed horizontal mitochondrial transfer (HMT). The primary purpose of HMT is to share functional mitochondria with cells exhibiting aberrant mitochondrial functions. Consequently, cells receiving mitochondria restore mitochondrial respiration [3].

The ability of mitochondria to dynamically modulate and adapt cellular functions in response to stressful conditions is considered a pivotal factor in cancer development.

The key difference in cancer cells' mitochondria compared to those in healthy cells lies in the switching between the Warburg effect and OXPHOS, along with altered ROS production, disrupted calcium regulation, and aberrant interactions within the mitochondrial network [7]. This switch allows cancer cells to generate energy and biosynthetic precursors, enabling their rapid proliferation even in oxygen-deprived conditions. Alongside the Warburg effect, cancer cell mitochondria may undergo modifications in fatty acid oxidation and glutamine metabolism [8]. In cancer, mitochondria exhibit notable heterogeneity and dysregulation across various cellular processes, such as apoptosis, regulated necrosis, ferroptosis, and autophagic cell death (ACD). These characteristics significantly contribute to increasing the therapeutic resistance of patients [9].

The inhibition of mitochondrial function in malignant cells represents a promising strategy for selectively targeting malignant cells and reducing their adaptation to the tumor microenvironment, thereby impeding tumor progression. Mitochondria-targeted cancer therapy relies on distinctions between mitochondrial function in cancerous and healthy cells. One widely employed therapeutic approach involves inhibiting ATP production by suppressing either complex I or II in ETC. This generates significant energy stress in cancer cells, resulting in the initiation of autophagic cell death. Additionally, mitochondrial respiration can be inhibited by targeting specific enzymes in the TCA cycle, such as α-ketoglutarate dehydrogenase (KGDH) or pyruvate dehydrogenase (PDH) [10]. Another approach to targeting mitochondria in cancer involves promoting oxidative stress or inducing autophagy.

2. Autophagy

Originally, autophagy was defined as a cell survival mechanism that occurs under starvation or oxidative stress (hypoxia, ROS) conditions, wherein the cell degrades damaged or unnecessary organelles to generate nutrients. Recently, it was discovered that autophagy is involved in the quality control of organelles/proteins by degrading dysfunctional proteins/organelles. Autophagy is divided into selective and nonselective types. Nonselective autophagy is a process that transforms cellular energy by randomly removing organelles. In contrast, selective autophagy specifically targets damaged organelles, such as the ER, mitochondria, and peroxisomes, as well as cellular proteins. Nonselective autophagy is triggered under starvation or nutrient deprivation conditions, while selective autophagy is more prevalent in nutrient-rich environments [11].

It was recently reported that autophagic cell death (ACD) is likely an outcome of either extensive autophagy, prolonged stress, or inhibited apoptosis [12]. During ACD, nuclear condensation increases, caspase activity decreases, and cellular vacuoles are generated [13].

Selective autophagy is a multistage process that includes the following steps: initiation, elongation, maturation, fusion, and degradation. Initiation (Figure 2A) commences with the activation of the ULK (Unc-51-like kinase) complex. This complex controls the commencement of selective autophagy by forming a stable protein assembly that includes ULK1/2 (serine/threonine Unc-51 like kinase 1/2), FIP200 (also known as RB1CC1), ATG13, and ATG101. Once this complex is formed, it initializes and regulates the formation of the pre-autophagosomal structure (PAS) and recruits ATG9 vesicles [14], which facilitate PAS expansion and are often referred to as the "seeds" of autophagosome formation [15]. The activity of the ULK complex is regulated by leading regulators of nutrient stress sensors, namely, mechanistic target of rapamycin complex 1 (mTORC1) and AMP-activated protein kinase (AMPK) [16]. Specifically, mTORC1 suppresses the function of the ULK complex through the phosphorylation of ATG13 and ULK1 proteins [17]. Furthermore, mTORC1 modulates the location of transcription factor EB (TFEB) by directing it to lysosomes. The key regulator of the autophagy pathway, TFEB, orchestrates the transcriptional regulation of autophagy genes via binding to the CLEAR (coordinated lysosomal expression and regulation) element in the nucleus. The interaction between TFEB and CLEAR promotes autophagy and facilitates lysosomal biogenesis [17]. The initiation of autophagy requires either the inactivation of mTORC1 or the activation of AMPK. The activity of AMPK de-

pends on the availability of cellular energy. When ATP is depleted, AMPK phosphorylates ULK1 and inhibits the activity of mTORC1 [18].

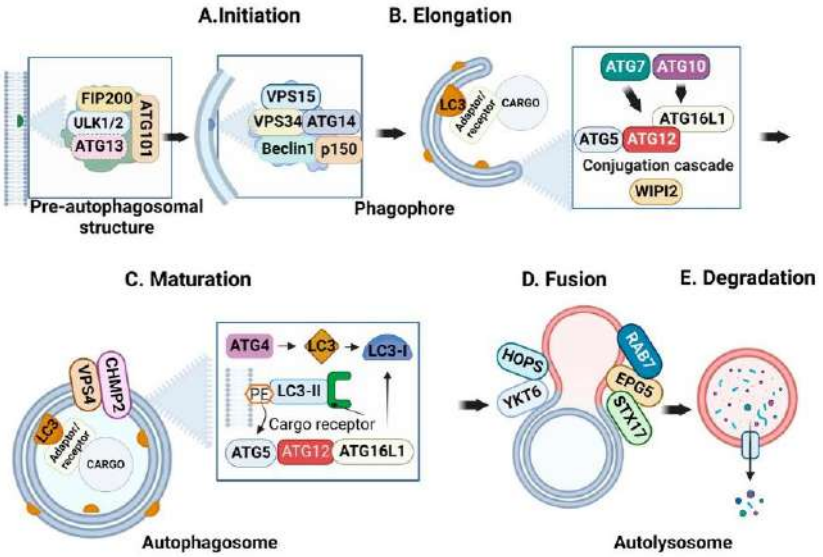

Figure 2. The autophagy pathway, which is subdivided into the following steps: (**A**) Initiation—the ULK complex, consisting of FIP200, ULK1/2, ATG13, and ATG101, mediates pre-autophagosomal structure formation. (**B**) Elongation—the PI3K complex, consisting of VPS15, VPS34, ATG14, Beclin1, and p150, generates the phagophore. Phagophore elongation is mediated by WIPI2, conjugation cascade ATG5-ATG12-ATG16L, ATG7, and ATG10. (**C**) Maturation—ATG4 convertss LC3 (an ATG8 family protein)-to-LC3-I and the conjugation cascade attaches LC3-I to PE (phosphatidylethanolamine) in the lipid membrane and generates lipidated LC3-II. The autophagosome's closure is mediated by VPS4 and CHMP2 proteins. (**D**) Fusion—autophagososme–lysosome fusion is initiated by SNARE proteins (YKT6, STX17), tethering factors (HOPS, EPG5), and GTPase (RAB7). (**E**) Degradation. This image was created on BioRender.com.

The complex ULK initializes the formation of the second autophagic complex, also known as the PI3K (phosphatidylinositol 3-kinase) complex. It is composed of VPS34 (Vacuolar protein sorting 34, a class III Pi3K), VPS15, Beclin1 (Bcl-2-interacting myosin-like coiled-coil), ATG14, p150, and NRBF2 (nuclear-receptor-binding factor 2). This complex is engaged in the extension of the phagophore (an isolated lipid double-membrane structure) and the production of phosphoinositide 3-phosphate (PI3P) on the autophagic membrane (Figure 2). The elongation of the phagophore (Figure 2B) is initiated by the production of PI3P and the recruitment of the scaffold protein WIPI2 (WD-repeat domain phosphoinositide-interacting 2). Subsequently, WIPI2 facilitates the tethering of the endoplasmic reticulum membrane and phagophore via ATG2 and supports the assembly of the ATG5-ATG12-ATG16L1 complex, along with ATG3 and ATG7. These proteins are essential for the expansion and formation of the phagophore membrane, as they provide a physical platform and facilitate the lipidation of ATG8 family proteins (LC3 (microtubule-associated protein 1 light chain 3) or GABARAP (GABA type A receptor-associated protein)) [19]. The ubiquitin-like proteins LC3 and GABARAP facilitate the attachment of the cargo adaptor/receptor to the lipid membrane (specifically to phosphatidylethanolamine (PE)), acting as a binding platform [17]. The protein ATG4, along with its partners ATG7 (ubiquitin-activating enzyme (E1)) and ATG3 (ubiquitin conjugation enzyme (E2)), facilitate the transformation of LC3 into its soluble form, LC3-I [20]. The ATG5-ATG12-ATG16L conjugation cascade is essential for attaching soluble LC3-I to PE in the lipid membrane. This attachment leads to the generation of lipidated LC3-II, which acts as a docking site for

autophagy cargo adaptors/receptors. But on the outer membrane, LC3-II promotes autophagosome maturation (Figure 2C) and lysosome merging. Autophagic cargo adaptors in the autophagosomal membrane, including p62/SQSTM1 and NRB1, selectively identify and associate with ubiquitinated cargo material [13].

The autophagosome membrane is closed by the activity of ESCRT components (endosomal sorting complex required for transport)—CHMP2 (charged multivesicular body protein 2) and VPS4 [21]. The Fusion (Figure 2D) of mature autophagosome with lysosomes is initiated by SNARE (soluble N-ethylmaleimide-sensitive attachment protein receptors) superfamily proteins, including STX17, SNAP29, VAMP3, VAMP7, VAMP8, and YKT6 [14]. They are both found on the autophagosome and lysosome membranes [22]. The process of fusion between the autophagosome and lysosome is promoted by tethering factors, including the HOPS (homotypic fusion and protein sorting) complex (VPS11, VPS18, VPS33A, VPS39, and VPS41), PLEKHM1 (pleckstrin-homology-domain-containing family M member 1), and EPG5 [23]. The tethering factors interact with GTPases, including ARL8B and RAB7, located in the lysosome membrane. Additionally, they bind to ATG8 family proteins present on the outer membrane of autophagosomes [22]. After the autophagosome fuses with the lysosome, the autophagic cargo undergoes degradation (Figure 2E) mediated by lysosomal enzymes. This process causes the degradation of organelles and the release of metabolic components.

2.1. Selective Autophagy—Mitophagy

Selective autophagy is a process that selectively, i.e., according to specific receptors, targets and degrades old and dysfunctional organelles, including mitochondria (mitophagy), ribosomes (ribophagy), peroxisomes (pexophagy), and the endoplasmic reticulum (ER) (reticulophagy).

The primary purpose of mitophagy is to regulate the quality and quantity of mitochondria via the selective elimination of dysfunctional or damaged organelles [24], and it is important for embryonic development, apoptosis, and cell differentiation. The main role of mitophagy is to maintain mitochondrial quality control and homeostasis. When mitophagy is ineffective at removing damaged mitochondria, the accumulation of dysfunctional or deficient mitochondria increases, resulting in decreased OXPHOS performance and increased levels of ROS. This imbalance can disrupt metabolism, cause cellular damage, and eventually result in cell death. Improper mitophagy contributes to the development of various pathological states, such as cancer and metabolic, neurodegenerative, cardiovascular, and skeletal muscle diseases [25]. Mitophagy can be activated by nutrient limitation or mitochondrial dysfunction, among which the latter is caused by different types of stress factors, such as mtDNA damage, elevated levels of mtROS, misfolded mitochondrial proteins, hypoxia, and declined mitochondrial membrane potential (MMP) [26]. Mitophagy is divided into ubiquitin-dependent (PARKIN-dependent and -independent) and ubiquitin-independent (receptor-based) types.

2.1.1. Ubiquitin-Mediated Mitophagy

Ubiquitin-dependent mitophagy is a selective mechanism wherein mitochondria that are specifically marked with ubiquitin molecules are removed from the cell [26]. The initiation of PINK1 (PTEN-induced putative kinase 1)/Parkin-mediated mitophagy occurs in response to mitochondrial stress, including mitochondrial membrane depolarization or the extreme misfolding of mitochondrial proteins (Figure 3). Mitochondrial dysfunction leads to the accumulation of the serine/threonine PINK1 kinase at the OMM, whereas under physiological conditions, the levels of PINK1 in mitochondria are typically low. The durability of PINK1 protein at the OMM depends on the activity of TOMM7 (translocase of outer mitochondrial membrane 7), Hsp70 (heat shock protein), PHB2 (prohibitin 2), and PGAM5 (mitochondrial serine/threonine protein phosphatase) [27]. At a damaged OMM, PINK1 auto-activates, dimerizes, and induces cytosolic Parkin ligase (U3 ubiquitin ligase) activity via phosphorylation. The active Parkin ligase produces ubiquitin chains

and tags OMM proteins, such as MFN2 (Mitofusin-2), VDAC-1 (voltage-dependent anion channel-1), and Miro (mitochondrial Rho GTPase), for mitophagy. Ubiquitinated OMM proteins provide a scaffold for the binding of autophagy adaptor proteins (also named autophagy receptor proteins). Besides Parkin ligase, other E3 ubiquitin ligases like GP78 (glycoprotein 78), MUL1 (mitochondrial E3 ubiquitin ligase 1), and SIAH1 (seven in absentia homolog 1) are also responsible for ubiquitinating mitochondrial proteins [24]. The tagged mitochondria are isolated from the healthy mitochondrial network through the activity of RHOT1 (Ras homolog family member T1) [28]. However, some studies have indicated that mitochondria are fragmented and separated from the ER before they can be tagged for mitophagy [29]. Additionally, mitochondrial proteins that are improperly tagged with ubiquitin chains are modified by deubiquitinase (DUB) enzymes [26].

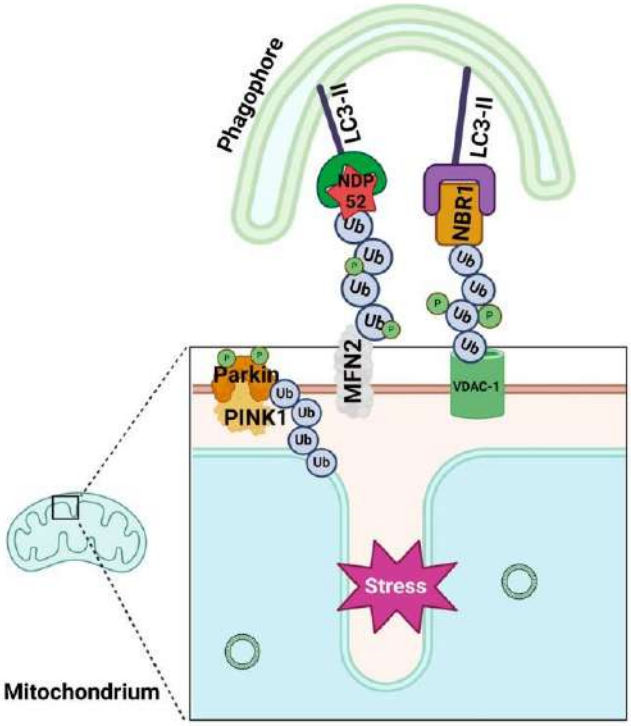

Figure 3. PINK1/Parkin-dependent mitophagy. Under conditions of mitochondrial stress, PINK1 accumulates on the outer mitochondrial membrane (OMM), where it undergoes phosphorylation and activation. This activation subsequently triggers Parkin ligase, which ubiquitinates mitochondrial proteins, such as MFN2 and VDAC-1. Mitochondria with polyubiquitinated OMM proteins recruit mitophagy cargo receptors/adaptors, such as NDP52 and NBR1, to their surfaces. The mitophagy cargo receptor/adaptors connect both with LC3-II, present on the phagophore membrane, and with ubiquitinated chains. This image was created on BioRender.com.

In the next step, PINK1 phosphorylates ubiquitin chains that are attached to OMM proteins to enhance the mitophagy process. Finally, OMM proteins marked with ubiquitin are recognized by autophagy receptors/adaptors of ubiquitin-dependent mitophagy SQSTM1/p62 (sequestosome 1), OPTN (optineurin), CALCOCO2/NDP52 (calcium binding and coiled-coil domain 2), NBR1 (neighbor of BRCA1 gene 1 protein), AMBRA1, and TAX1BP1 (Tax1 binding protein 1) [25] (Table 1). At the N-terminal arm, these receptors possess an LC3-interacting region (LIR) that enables them to interact with the MAP1LC3/LC3 (microtubule-associated protein 1 light chain 3) and LC3 protein families, which are anchored in the phagophore membrane. The mitophagy receptors/adaptors can bind to

the ubiquitinated OMM proteins through their ubiquitin-binding domain, thus forming mitophagy cargo. Once the mitophagic cargo binds to the mitophagy receptor, it triggers the formation of the mitophagosome. The mitophagosome, which encapsulates the marked mitochondrium, subsequently merges with lysosomes [30].

2.1.2. Ubiquitin-Independent Mitophagy

Ubiquitin-independent mitophagy is a process where damaged mitochondria are directed to the mitophagosome without relying on ubiquitin tagging. Instead, this process depends on the presence of mitophagy receptors/adaptors, as summarized in Table 1. These receptors/adaptors directly interact with MAP1LC3/LC3 and LC3/GABARAP, which are localized on the phagophore membrane [31]. Ubiquitin-independent mitophagy receptors/adaptors, such as BNIP3 (BCL2/adenovirus E1B 19 kDa protein-interacting protein 3), BNIP3L/NIX, FUNDC1 (FUN14 Domain-Containing 1), BCL2L13 (BCL2-Like 13), FKBP8 (FKBP Prolyl Isomerase 8), and AMBRA1 (the activating molecule in BECLIN1-regulated autophagy 1), are directly located on the mitochondria membrane. The expression levels of these receptors are regulated by transcriptional and post-transcriptional modifications [26]. Besides protein mitophagic receptors, mitochondria also exploit lipid-based receptors like cardiolipin (CL) and ceramide [30] (Table 1). CL is typically found in the IMM, where it supports the activity of ETC complexes I, III, and IV and ATP synthase. However, under mitochondrial stress, CL can translocate to the OMM [32].

Table 1. Mitophagy receptors.

Type of Mitophagy Receptors	Key Properties	Regulators (Positive [+]/Negative [-])	Ubiquitin Dependent (+/-)	Location
Protein receptors				
SQSTM/p62	Oxidative-stress-inducible protein; regulator of Nrf2 factor, NF-kB [33]	ULK1 [+]; CK2 [+]; TBK1 [+]; mTORC1 [+];	+	Cytoplasm
CALCOCO2/NDP52	Promotor of phagophore biogenesis [34]	TANK binding kinase 1 (TBK1), [+];	+	Cytoplasm
OPTN (Optineurin)	Promotor of phagophore biogenesis [35]	TNF-α [+]; Interferons [+];	+	Cytoplasm
NBR1	Oxidative-stress-inducible protein; cooperates with p62 [35];	-	+	Cytoplasm
TAX1BP1	Eliminator of excessive ROS [36,37]	-	+	Cytoplasm
BNIP3	BCL2 apoptosis regulator protein (pro-apoptotic); promotes hypoxia-induced autophagy; regulator of mTOR [32];	FOXO3 (starvation, [+]); HIF-1 [+]; MA-5 [+];	-/+	OMM
BNIP3L/NIX	Stress sensor; inducer of cell death and mitophagy (ischemia, erythrocyte development [38])	HIF1A (hypoxia, [+]); GTPase RHEB (phosphorylation, [+]); PKA (phosphorylation, [-]);	-/+	OMM
FUNDC1	Involved in hypoxia-induced mitophagy; dephosphorylated form activates fission and mitophagy; connects with fission (DNM1L, DRP1)/fusion (OPA1) proteins; regulator of proteostasis [39]	SRC (kinase, [-]); CK2 (kinase, [-]); ULK1(kinase, [+]); PGAM5 (phosphatase, [+]); MARCH5 (ubiquitin ligase E3, [-]); MIR137 [-];	-	OMM

Table 1. *Cont.*

Type of Mitophagy Receptors	Key Properties	Regulators (Positive [+]/Negative [-])	Ubiquitin Dependent (+/-)	Location
BCL2L13	Promotor of mitochondrial fragmentation; regulator of fission; maintainer of mitochondrial quality; inducer of apoptosis [32,40]	Unknown;	-	OMM
FKBP8	Anti-apoptotic protein; regulator of mTORC1; exerts peptidylprolyl isomerase activity [32,41]	RHEB [-];	-	OMM
AMBRA1	Phagophore activator; along with BECN1, it is an activator of PtdIns3k (phosphatidylinositol 3-kinase); interacts with HUWE1 (E3 ubiquitin ligase) and thus induces ubiquitin-independent mitophagy [32,42]	NFKBI [+]; BCL2 family proteins [-]; MCL1 [-]; CHUK [+]; GSK3B [+];	-/+	OMM
PHB2 (prohibitin 2)	Regulator of mitochondrial proteases; maintainer of mitochondrial genome; promotor of PINK1-PARKIN-dependent mitophagy; along with AURKA, it is a kinase promotor of PARKIN-independent mitophagy [32]	AURKA [+]	-/+	OMM/IMM
Lipid receptors				
CL (cardiolipin)	Maintainer of electron transport chain function; involved in apoptosis; cooperates with BECN1 (mitophagy) and DNM1L (mitochondrial division) [43]	CRLS1 (cardiolipin synthase 1, [+]); PLSCR3 ((phospholipid scramblase 3), transport CL to OMM [+]); NDPK-D (kinase, [+]) PRRT2/PKC [+]; SNCA[+];	-	OMM/IMM
Ceramide	Ceramide-induced mitophagy [32]	CERS1(ceramide synthase 1, [+]); DNM1L [+];	-	OMM

2.1.3. Chaperone-Mediated Autophagy

Chaperone-mediated autophagy (CMA) is a distinctive type of selective autophagy responsible for the lysosomal degradation of misfolded or damaged proteins. In contrast to ubiquitin-dependent/independent autophagy, during the CMA process, proteins are not enclosed in the autophagosome; instead, they are directly targeted by the chaperone Hsc70 (heat shock cognate protein 70) in the cytosol. The mechanism of CMA is categorized into distinct stages (Figure 4): 1. substrate recognition; 2. the binding of the substrate to the lysosomal membrane; 3. the multimerization of translocation complex; 4. substrate unfolding; 5. substrate translocation and degradation in the lysosomal lumen; and 6. dissociation of the translocation complex. Hsc70 recognizes CMA's substrates by binding to the KFERQ motif in target proteins [44]. The function of Hsc70 is supported by various co-chaperons, including Hsp40 (heat shock protein 40), CHIP (carboxyl terminus of hsc70-interacting protein), BAG1 (Bcl2-associated athano-gene 1 protein), and HOP (hsp70-hsp90 organizing protein) [45]. In addition to recognizing substrates, the complex HOP is actively engaged in protein stabilization and unfolding [46]. After the substrate recognition step, Hsc70, along with the target protein, binds to the lysosomal receptor LAMP-2A (lysosome-associated membrane protein type 2A) [47]. LAMP-2A forms a dynamic translocation channel via

multimerization and interaction with GFAP (glial fibrillary acidic protein), which is responsible for maintaining the structure of the multimeric LAMP-2A complex in the lysosomal membrane. Consequently, the CMA substrate is unfolded and transported into the lysosomal lumen, where it undergoes immediate degradation by lysosomal proteases [48]. After CMA substrate translocation, the interaction between GFAP and EF1α (elongation factor 1-α) is disrupted by GTP (guanosine triphosphate). This disturbance results in the release of EF1α to phosphorylated GFAP, which, in turn, facilitates the disassembly of LAMP-2A into its individual monomers [49]. The phosphorylation of GFAP on the lysosomal membrane supports the dissociation of GFAP from the LAMP-2A multimeric complex through the dimerization of phosphorylated GFAP with unmodified GFAP. The level of GFAP phosphorylation is controlled by the activity of AKT1 (AKT serine/threonine kinase 1), which becomes active when phosphorylated by mTORC2 (mammalian target of rapamycin complex 2) and inactive when dephosphorylated by PHLPP1 (PH domain and leucine-rich repeat protein phosphatase 1) [45].

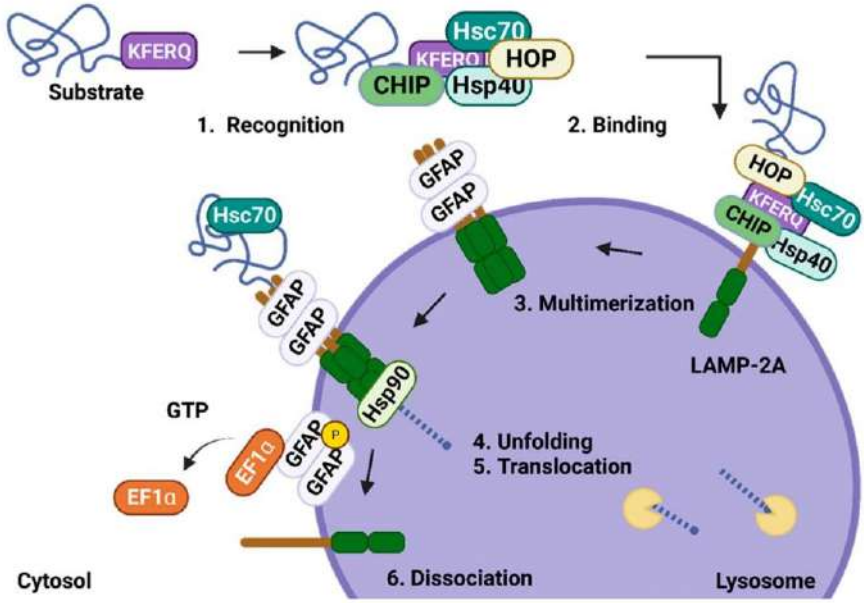

Figure 4. Mechanism of CMA (chaperone-mediated autophagy): 1. Recognition: Hsc70 and co-chaperons, such as Hsp40 (heat shock protein 40), CHIP (carboxyl terminus of hsc70-interacting protein), and HOP (hsp70-hsp90 organizing protein), recognize CMA substrates by specifically targeting the KFERQ motif present within the substrate. 2. Binding: CMA substrate binds to the lysomal surface receptor LAMP-2A (lysosome-associated membrane protein type 2A). 3. Multimerization: LAMP-2A forms a translocation channel through LAMP-2A multimerization and stabilization via GFAP (glial fibrillary acidic protein). 4. Unfolding: CMA substrate is unfolded by Hsc70 and stabilized by Hsc90. 5. Translocation: CMA substrate is transported into lysosomal lumen. 6. Dissociation: upon phosphorylation by EF1α, GFAP undergoes dissociation from the LAMP-2A channel, resulting in the disassembly of the LAMP-2A multimeric complex into monomeric form. This image was created on BioRender.com.

The transport of LAMP-2A to the lysosomal surface represents a crucial stage in CMA. Moreover, the level of LAMP-2A directly affects CMA activity. The translocation of LAMP-2A to lysosomal membrane is determined by the involvement of Rab-7A (Ras-related protein Rab-7A), Rab-11A, DYNC1LI2 (Dynein Cytoplasmic 1 Light Intermediate Chain 2), and RILP (Rab-interacting lysosomal protein) [45]. CMA activity is regulated by the amounts of the key CMA proteins (Hsc70, GFAP, and LAMP-2A), as well as by

the kinase AKT1 and circadian cycle regulators, such as BMAL1 (basic helix–loop–helix ARNT-like 1), PER1/2 (period circadian protein homolog 1/2), or RARα (retinoic acid receptor alpha) [50]. Increased CMA activity is usually related to lipotoxicity (cytosolic lipid overload), starvation, hypoxia, and mitochondrial or ER stress. The elevated CMA activity is affected by the transcriptional upregulation of LAMP-2A (mostly by NFE2L2 (NFE2-Like BZIP transcription factor 2), Nrf2, and NFAT1 (nuclear factor of activated T cells) [51].

The CMA pathway supports a range of cellular processes, including the maintenance of protein quality, the regulation of the cell cycle, and the modulation of immune responses. Especially, CMA contributes to the quality control of mitochondrial proteins, such as COX IV (cytochrome c oxidase subunit 4), Tom20 (mitochondrial import receptor subunit TOM20 homolog), DJ-1 (nucleic acid deglycase), Parkin, MFN2, ATP5F1A (ATP synthase F1 subunit alpha), and VDAC1, which modulate mitochondrial function and protect the integrity of mitochondria [45].

3. Role of Autophagy in Tumorigenesis

In cancer, the autophagy process serves a dual and complex function, acting either as a suppressor or initiator of tumorigenesis, depending on the type of tumor and the stage of disease advancement. On the one hand, autophagy might promote cancer suppression by abolishing oxidative stress, inhibiting cellular transformation, preventing the accumulation of damaged cellular components, and maintaining cell homeostasis [11]. Transcription factors like p53, death-associated protein kinase (DAPK), tuberous sclerosis proteins 1 and 2 (TSC1/2), and phosphatase and tensin homolog (PTEN) are essential contributors to the tumor-suppressive function of autophagy [11].

On the other hand, autophagy can support tumor development and metastasis by providing nutrients to cancer cells [52], allowing cancer cells to survive under metabolic stress. Tumor oncogenes, like RAS and BRAF, promote tumor growth by upregulating the process of autophagy [11]. In developing novel cancer therapies or enhancing the efficacy of chemotherapy, comprehending the involvement of autophagy at all phases of tumor formation is crucial. This knowledge contributes to the advancement of precision therapies that can effectively modulate autophagy [53].

The involvement of the autophagy activator Beclin-1 in tumorigenesis is linked to its phosphorylation level and interactions with various partner proteins [54]. DAPK is a key regulator protein that contributes to the phosphorylation status of Beclin-1 and the formation of the autophagosome [55]. Autophagy inhibition is achieved through the interaction of Beclin-1 with its inhibitor, BCL2. In contrast, the interaction of Beclin-1 with AMBRA1, UVRAG (UV-radiation-resistance-associated gene protein), and BIF1 (Bax interacting factor 1) disrupts the binding of Beclin-1 with BCL2, which subsequently leads to autophagy initiation [11]. In solid tumors, a decrease in Beclin-1 expression is often observed and correlated with metastasis development. On other hand, in colorectal cancers and gastric carcinomas, Beclin-1 expression is elevated, resulting in enhanced autophagy. This observation has led to the suggestion that Beclin-1 promotes cell proliferation and tumorigenesis under stress conditions like hypoxia and starvation [56]. Furthermore, Beclin-1 cooperates with another autophagy regulator, PTEN, which negatively controls the activity of the PI3K/AKT pathway. A reduced expression of PTEN and Beclin-1 has been observed in chemoresistant ovarian cancers [57]. This discovery indicates that PTEN and Beclin-1 play roles in regulating autophagy in ovarian cancer, and their decreased expression levels contribute to reducing autophagy activity and increasing chemoresistance [58].

The modulation of autophagy by the major transcription factor p53 is determined by its subcellular localization, which determines whether cancer cells will survive or die. Nuclear p53 facilitates autophagy activation by promoting the transcription of autophagy-related genes, while cytoplasmic p53 suppresses autophagy by inhibiting autophagy regulators [11]. Upon encountering cellular stress, nuclear p53 initiates autophagy through inducing the expression of DRAM (damage-regulated autophagy modulator), DAPK, and ULK1/2 [59].

Moreover, p53, through the promotion of autophagy, can increase the proliferation and resistance to chemotherapy of malignant liposarcoma cells [60].

The accumulation of autophagy cargo receptor p62 (also known as SQSTM1) is a notable feature observed in many cancers, and it is correlated with poor clinical outcomes among hepatocellular carcinoma patients [61] and increased metastasis occurrence in nasopharyngeal carcinoma. The accumulation of p62 supports tumor development and cancer cell growth via the activation of Nrf2, mTORC1, TRAF6 (tumor-necrosis-factor-receptor-associated factor 6), TNFa (tumor necrosis factor α), and NF-kB (nuclear factor kappa-light-chain-enhancer of activated B cells) [54]. Consequently, an increased presence of p62 in tumors implies its involvement in promoting the development and progression of cancer. Therefore, inhibiting p62 during autophagy holds promise as a strategy for treating cancer [62].

Among mitophagy regulators, it has been observed that the tumor suppression Parkin protein encoded by the *PARK2* gene is frequently deleted in colorectal, lung, breast, glioblastoma, and melanoma cancers. The absence of Parkin E3 ubiquitin ligase leads to the accumulation of dysfunctional mitochondria, resulting in elevated levels of glycolysis and ROS, reduced OXPHOS, and increased resistance to apoptosis in cells [22].

The mitochondrial kinase PINK1 is implicated in tumor suppression due to its role in detecting and removing damaged mitochondria. In certain cancers, there is a noted decrease in PINK1 expression (such as sarcomas, neuroblastomas, and leukemias), while in others, there is an increase (such as lung and breast cancers and carcinoma) [63].

Autophagy has been demonstrated to play a pivotal role in promoting drug resistance in chemotherapy-treated cancer cells. It also regulates cell migration and metastasis by affecting the interactions between cancer and healthy cells [11]. Despite the complex role of autophagy in cancer, inhibiting this process can make cancer cells more sensitive to chemotherapy and enhance cell death [24].

4. Modulation of Mitochondria and Autophagy Exhibits Promise in Cancer Treatment

Cancer cells frequently demonstrate the capacity to reprogram their metabolism, allowing them to survive and thrive in challenging conditions, including those generated by chemotherapy [6]. Targeting metabolic plasticity in cancer has been shown to significantly enhance the effectiveness of cancer therapies [64]. A recent study has shown that decreased expression of mitochondrial fission regulator protein DRP1 affects metabolic plasticity and reduces the survival of breast-cancer--induced brain metastases [65].

Mitochondria primarily drive the bioenergetic adaptation that facilitates tumor growth. It is well established that mitochondrial reprogramming promotes tumor growth and cancer cell proliferation via retrograde signaling involving ROS, Ca^{2+}, ATP, or TCA intermediates, which can modify gene expression [6]. It has recently been identified that the knockout of *MTCH1* (*mitochondrial carrier 1*) in cervical cancer (in HeLa cells) activates retrograde signaling through the FOXO1-GPX4 axis, leading to increased accumulation of mtROS and ferroptosis. The study in question proposes the use of MTCH1 as a candidate target for retrograde signaling pathways in cervical cancer [66].

Modifying mitochondrial metabolism (Tables 2 and 3) offers a strategy for reshaping cancer cell metabolism and combatting drug resistance. Current strategies for targeting mitochondrial function include inhibiting ETC, modulating redox balance, affecting Ca^{2+} homeostasis or the apoptotic pathway, and disrupting the TCA cycle. Disruption of ETC can be achieved through the inhibition of ETC complexes I–V. The effectiveness of several complex I inhibitors is limited by issues like poor potency, toxicity, or unintended off-target actions, such as targeting rotenone and BAY 87-2243 [67]. While some complex I inhibitors have failed to translate successfully to preclinical studies, others are currently being tested in clinical trials (Table 3). Phenformin, an antidiabetic drug, inhibits complex I and disrupts the redox balance (NADH/NAD+) and energetic state (AMP/ATP), resulting in AMPK activation [68]. Atovaquone, used as an antimalarial drug, interferes with complex III,

reducing oxygen consumption and subsequently decreasing tumor hypoxia in individuals with non-small-cell lung cancer [69].

Through the excessive activation of mitochondrial respiration, the loss of MMP can cause a breakdown in mitochondrial metabolism and ATP production, resulting in cell death. A newly identified complex IV activator, the fungal natural product ophiobolin A (OPA), significantly decreases NCI-H1703 cells' proliferation [70]. Bedaquiline interferes with ATP production by targeting complex V, which lowers DA-MB-231 breast cancer cell proliferation, enhances ovarian cancer cells' sensitivity to cisplatin, and helped prevent metastasis in a xenograft model [71,72].

The disruption of mitochondrial metabolism through TCA cycle inhibition using devimistat (CPI-613), PDH, and KGDH inhibitors is being tested in patients with advanced biliary tract cancer in vitro and in a Phase Ib clinical trial, in combination with gemcitabine and cisplatin [73]. Current clinical trials are investigating devimistat (CPI-613) as a monotherapy for refractory Burkitt's lymphoma/leukemia (NCT03793140) and in combination with chemotherapies for advanced pancreatic cancer (NCT03699319) and with chemoradiation for pancreatic adenocarcinoma (NCT05325281) (Table 3).

Inhibiting the apoptosis regulator BCL-2 (B-cell lymphoma-2) is one of the most extensively investigated approaches for triggering the mitochondrial apoptotic pathway in cancer therapy. Venetoclax (ABT199) was the first FDA-approved BH3-mimetic drug, originally indicated for the treatment of chronic lymphocytic leukemia [74]. Subsequent studies revealed its effectiveness in treating acute myeloid leukemia. It is commonly administered either as monotherapy or in combination with monoclonal antibodies, such as rituximab, or alongside chemotherapy. The molecular action of ventoclax is driven by the activation of BAK and BAX proteins, leading to the permeabilization of the mitochondrial outer membrane and inducing apoptosis [75]. Ongoing preclinical and clinical (Table 3) studies are investigating the efficacy and safety of venetoclax, both as a monotherapy and in combination with other anti-cancer drugs, in treating breast cancer (NCT03900884), myeloma (NCT05455294), lung cancer (NCT04274907), prostate cancer (NCT03751436), and solid tumors [76].

Alongside its mitochondrial function, autophagy helps facilitate cancer plasticity under nutrient deprivation conditions. Inducing autophagy can potentially prevent tumor development and growth in the early stages [77]. However, in advanced stages of cancer, autophagy supports tumor growth and metastasis by supplying the necessary substrates for cell proliferation [78]. The impact of autophagy activation on tumorigenesis is influenced by the degree of autophagy. A basic level of autophagy facilitates tumor growth and the development of drug resistance, while a high level of autophagy results in excessive removal of cellular components, leading to the cell death [79]. Relying only on autophagy targeting is insufficient for cancer treatment. Some studies have demonstrated that combining autophagy inhibitors or activators with chemotherapy, radiotherapy, or immunotherapy is a more effective treatment strategy [77]. By inhibiting autophagy, the susceptibility of cancer cells to chemotherapeutic drugs and treatments that induce apoptosis is heightened [78]. Tables 2 and 3 present a range of autophagy inhibitors and activators that are being investigated in preclinical studies and ongoing clinical trials. As FDA-approved antimalarial drugs, chloroquine (CQ) and hydroxychloroquine (HCQ) are some of the most prominent autophagy inhibitors being explored in cancer therapies based on autophagy mechanisms. Through their accumulation in lysosomes and inhibition of lysosomal acidification, they interrupt the autophagosome's fusion with lysosome and change signaling and transcriptional activity [80]. The antitumor effect of HCQ was increased when used in combination with monoclonal antibodies, namely, anti-PD1 (nivolumab), in advanced melanoma (Table 3, NCT04464759); inhibitor of MEK1/2 (trametinib) in pancreatic cancer (NCT03825289); a Ras/Raf/MEK/ERK signaling pathway inhibitor (sorafenib) in hepatocellular cancer (NCT03037437); and an Akt inhibitor (MK2206) in solid tumors (NCT01480154). CQ and HCQ, in addition to changing lysosomal pH, also impact the pH values of Golgi vesicles and endosomes [81]. CQ derivatives are also known to target and

suppress the function of PPT1 (palmitoyl-protein thioesterase 1) in melanoma cells [82]. The precise mechanisms of action of CQ and HCQ remain poorly understood and extend beyond their effects on autophagy. It has been observed that CQ activates the p53 pathway, resulting in apoptosis in glioma cells [83]. In clinical trials, adverse events associated with CQ and HCQ, including nausea, diarrhea, vomiting, myopathy, and cardiotoxic effects, are frequently reported [84].

Conversely, stimulating autophagy in cancer treatment can effectively impede cell proliferation and inhibit tumor growth. Among the leading autophagy inducers examined in clinical trials are the FDA-approved mTOR inhibitors rapamycin (sirolimus) and its analogue temsirolimus (CCI-779) and everolimus, which are FDA-approved for the treatment of malignancies and the prevention of transplant rejection [85]. Everolimus and temsirolimus are FDA-approved drugs used to treat advanced renal cell carcinoma. Ongoing research, including preclinical and clinical trials, is exploring their efficacy as a monotherapy and in combination with other therapies (CQ, radiation, and THZ1 (cyclin-dependent kinase 7 inhibitor)) across different cancer types (bladder, colorectal, and prostate cancers and carcinoma) in vitro and in vivo. Research is focusing on everolimus, both as a standalone treatment and in combination with CQ, HCQ, AKT inhibitors 1 and 2, arsenic trioxide, or propachlor, in breast, renal, and ovarian cancer cells; various carcinoma cell lines; and mouse models. Investigations have been conducted on rapamycin in cell lines of pancreatic, cervical, and lung carcinomas; melanomas; osteosarcomas; and liposarcomas, as well as in xenograft mice models [86]. Clinical trials have explored the use of rapamycin in combination with chloroquine (CQ) and hydroxychloroquine (HCQ). Current ongoing research includes a Phase I trial assessing rapamycin's combination with vorinostat for treating advanced cancers (NCT01087554), as well as a Phase I/II study evaluating its use with HCQ, metformin, dasatinib, or nelfinavir in treating relapsed prostate cancer and other solid tumors (NCT05036226).

Recently, the natural polyphenol epigallocatechin gallate (EGCG) deriving from green tea leaves has garnered interest for its ability to induce cell death through autophagy and apoptosis. EGCG is known to alter multiple cellular pathways in different types of cancer. Among the most notable pathways it effects is the RAS-Raf-MEK-ERK axis, where its action leads to the inhibition of cell proliferation and the induction of apoptosis in pancreatic cancer [87,88]. Moreover, EGCG attenuated the PTEN/AKT/mTOR pathway in ovarian cancer cell lines and mouse models [89]. In bladder cancer cell lines (5634 and T24), EGCG induces apoptosis through the regulation of autophagy in a dose-dependent manner. EGCG upregulates the expression of caspase 3, caspase 9, and Bax, and it also decreases BCL2 expression. Concurrently, EGCG stimulates the formation of autophagosomes and elevates the expression of the autophagy-related protein LC3II [90].

Table 2. Synthetic inducers and inhibitors of mitochondrial function and autophagy.

Compound	Mechanism	Ref.
	Mitochondria inhibitors	
Rotenone	Inhibits complex I in gastric cancer cells (MKN-1, MKN-B, and MKN-74)	[91]
BAY 87-2243	Inhibited complex I in melanoma tumor xenograft (SK-MEL-28 and G-361 cells) and in vitro (A-375, G-361, SK-MEL-5, SK-MEL-28 cells)	[92]
MitoVES (mitochondrially targeted vitamin E succinate)	Inhibits complex II in colon cancer (HCT116 cells in vitro and in BALB/c nu/nu mice)	[93]
Atovaquone (ATO)	Inhibits complex III in breast cancer cells (MCF7)	[94]
Antimycin A	Inhibits complex III in acute myeloid leukemia U937 and HL-60 cells	[95]

Table 2. *Cont.*

Compound	Mechanism	Ref.
VLX600	Acts as an OXPHOS inhibitor (inhibiting complexes I, II, IV) in colon cancer 3-D microtissues; Acts as an iron chelator; Induces autophagy-dependent cell death and mitophagy through BNIP3/BNIP3L activation in glioblastoma cells (U251, MZ54, NCH644) and organotypic brain slice cultures	[96]
BTB06584	Inhibits ATP synthase in non-small-cell lung cancer cells (A549)	[97]
Oligomycin	Inhibits ATP synthase in breast metastasis cells (MDA-MB-231)	[98]
	Mitochondrial activators	
Ophinobolin A (OPA)	Activates complex IV in lung squamous cell carcinoma (NCI-H1703)	[70]
	Autophagy inhibitors	
Vitexin	Inhibits LC3-associated autophagosome formation Decreases p-ERK1/2 levels in hepatocellular carcinoma (SK-Hep1 and Hepa1-6 cells)	[99]
RA-XII	Inhibits AMPK pathway; Induces apoptosis through the suppression of autophagy in liver cancer (HepG2 cells);	[100]
3-methyladenine (3-MA)	Inhibits LC3-I/II and class III PI3K complex; Increases p62 levels in colon cancer cells (LOVO and SW480)	[101]
Astragaloside II	Decreases the levels of LC3-II and Beclin-1 in hepatic cancer cell lines (Bel-7402 and Bel-7402/FU)	[102]
Bafilomycin A1	Increases LC3 levels; Promotes the association of Beclin-1 and Bcl-2; Blocks V-ATPase in B-cell acute lymphoblastic leukemia (697 cells)	[103]
SAR405	Suppresses VPS34 and PIK3C3 kinase in carcinoma cell line H1299	[104]
Clarithromycin	Upregulates LC3-II in primary colorectal cancer surgical samples; Induces autophagosome formation and decreases p62/SQSTM1 levels in colorectal cancer (HCT116 cells)	[105]
4-acetylantroquinonol B	Inhibits ATG5 in ovarian cell line ES-2	[106]
	Autophagy activators	
Salinomycin	Increases LC3B-II levels and vacuolization in melanoma SK-Mel-19 cells	[107]
Esomeprazole	Inhibits V-ATPase in lung cancer (A549/Taxol cells)	[108]
Niraparib	Inhibits AKT/mTOR pathway and increases ROS levels; Activates ERK1/2 and increases LC3-II in hepatocellular carcinoma (Huh7 and HepG2)	[109]

Table 2. *Cont.*

Compound	Mechanism	Ref.
Matrine	Leads to the accumulation of LC3-II; Reduces the levels of total AKT and mTOR in gastric cancer (SGC-7901)	[110]
Bisindolylmaleimide (BMA-155Cl)	Increases Beclin-1, NF-kB, and p65 levels in hepatocarcinoma HepG-2 cells	[111]
Resveratrol Spermidine	Activates SIRT1 in colon cancer HCT 116 cells	[112]
Bicyclol	Inhibits p-AKT and pERK; Decreases the levels of p-mTOR (Ser2448); Increases LC3-II levels in hepatocellular carcinoma cell HepG2	[113]
Glycochenodeoxycholate	Increases LC3-II and pAMPK levels; Decreases p63 and pmTOR levels in hepatocellular carcinoma (SMMC7721 and Huh7 cells)	[114]
Lapatinib	Increases LC3-II, ATG7, Beclin-1, and ATG5 levels in acute myeloblastic leukemia (U937 cells)	[115]
Lycorine	Decreases TCRP1 (tongue-cancer-resistance-associated protein 1) and p-AKT levels, increases LC3 II levels, and decreases Beclin-1 levels in hepatocellular carcinoma (HepG2 and SMMC-7721)	[116]
Baicalein/baicalin	Activates ATG5, ATG7, ATG12, Beclin-1, and LC3-IIB proteins in bladder cancer T24 cells	[117]
Epigallocatechin gallate (EGCG)	Elevates levels of LC3-II; Increases number of autophagosomes in cepatocellular carcinoma cell line HepG2	[118]

Table 3. Investigated drugs targeting autophagy and mitochondrial pathways in ongoing cancer clinical trials.

Title	Drug	Target	Cancer Type	ClinicalTrials.gov ID	Ref.
Targeted apoptotic pathway					
A Phase I clinical trial evaluating the tolerance and pharmacokinetics of TQB3909 tablets in patients with relapsed or refractory advanced malignant tumors (China)	TQB3909	BCL-2 inhibitor	Phase I: advanced malignant tumors	NCT04975204	[119]
A Phase Ib/ii study to investigate the safety, tolerance and pharmacokinetics of TQB3909 with HR-positive, HER2-negative advanced breast cancer (China)			Phase Ib/II: advanced breast cancer	NCT05775575	
A Phase Ib/II clinical trial on the safety and efficacy of TQB3909 tablets in patients with recurrent or refractory CLL/SLL (China)			Phase Ib/II: chronic lymphocytic leukemia/small lymphocytic lymphoma	NCT05959694	

Table 3. *Cont.*

Title	Drug	Target	Cancer Type	ClinicalTrials.gov ID	Ref.
A Phase 1a/1b open-label dose escalation and expansion study of Bcl-2 inhibitor BGB-11417 in patients with mature B-cell malignancies (United States)	Sonrotoclax (BGB-11417) or Sontroclax in combination with zanubrutinib and obinutuzumab	BCL-2 inhibitor	Phase Ia/Ib: mature B-cell malignancies	NCT04277637	
A Phase I study of venetoclax in combination with cytotoxic chemotherapy, including calaspargase pegol, for children, adolescents and young adults with high-risk hematologic malignancies (United States)	Venetoclax in combination with azacitidine cytarabine, methotrexate, hydrocortisone, leucovorin, dexamethasone, vincristine, doxorubicin, dexrazoxane, calaspargase, pegol, erwinia asparaginase		Acute myeloid leukemia/chronic lymphocytic leukemia Phase I: hematologic malignancies	FDA-approved NCT05292664	
A Phase 1 study of triplet therapy with navitoclax, venetoclax, and decitabine for high-risk myeloid malignancies (United States)	Venetoclax in combination with navitoclax and decitabine		Phase I: myeloid malignancy	NCT05455294	
Phase 1 study of venetoclax, a BCL2 antagonist, for patients with blastic plasmacytoid dendritic cell neoplasm (BPDCN) (United States)	Venetoclax		Phase I: dendritic cell neoplasm	NCT03485547	[120]
A Phase 1b study of palbociclib, letrozole and venetoclax in ER and BCL-2 positive locally advanced or metastatic breast cancer (Australia)	Venetoclax in combination with palbociclib and letrozole		Phase Ib: breast cancer	NCT03900884	
Phase Ib/II study of enzalutamide with venetoclax (ABT-199) in patients with metastatic castrate resistant prostate cancer (mCRPC) (United States)	Venetoclax in combination with enzalutamide		Phase Ib/II: prostate cancer	NCT03751436	
A Phase 1b study of venetoclax in combination with pembrolizumab in subjects with previously untreated NSCLC whose tumors have high PD-L1 expression (United States)	Venetoclax in combination with pembrolizumab		Phase Ib: non-small-cell lung cancer		
A Phase 1 study of oral LOXO-338, a selective BCL-2 inhibitor, in patients with advanced hematologic malignancies (United States)	LOXO-338		Phase I: advanced hematologic malignancies	NCT05024045	[121]
A Phase 1 study investigating the safety, tolerability, pharmacokinetics, pharmacodynamics, and preliminary antitumor activity of second mitochondrial-derived activator of caspases mimetic BGB-24714 as monotherapy and with combination therapies in patients with solid tumors	BGB-24714 or BGB-24714 in combination with paclitaxel, carboplatin, docetaxel	SMAC (mitochondrial-derived activator of caspases) mimetic and inhibitor of apoptosis protein	Phase I: solid tumors	NCT05381909	[122]

Table 3. *Cont.*

Title	Drug	Target	Cancer Type	ClinicalTrials.gov ID	Ref.
A randomized, double-blind placebo-controlled, Phase 3 study of Debio 1143 in combination with platinum-based chemotherapy and standard fractionation intensity-modulated radiotherapy in patients with locally advanced squamous cell carcinoma of the head and neck, suitable for definitive chemoradiotherapy (TrilynX) (United States)	Xevinapant (Debio 1143) in combination with chemotherapy	Second mitochondrial-derived activator of caspases	Phase III: advanced squamous cell carcinoma of the head and neck	NCT04459715	[123]
A Phase 1b study of the OxPhos inhibitor ME-344 combined with bevacizumab in previously treated metastatic colorectal cancer (United States)	Me-344 combined with bevacizumab	OxPhos pathway inhibitor; purine biosynthesis inhibitor	Phase Ib: previously treated metastatic colorectal cancer	NCT05824559	[124]
A Phase 1 open-label, dose-escalation, safety, pharmacokinetic, and pharmacodynamic study of Minnelide™ capsules given alone or in combination with paclitaxel in patients with advanced gastric cancer (Republic of Korea)	Minnelide (triptolide)	SIRT3 regulator; c-myc down-regulator	Phase I: gastric cancer	NCT05566834	
A Phase II trial of the superenhancer inhibitor minnelide in advanced refractory adenosquamous carcinoma of the pancreas (ASCP) (United States)			Phase II: advanced refractory adenosquamous carcinoma of the pancreas	NCT04896073	
A Phase 1b open-label, dose-escalation, safety, and pharmacodynamic study of Minnelide™ capsules given in combination with osimertinib in patients with EGFR mutated NSCLC (United States)	Minnelide in combination with osimertinib		Phase Ib: lung cancer	NCT05166616	[125]
A Phase 1b, open-label, safety, pharmacokinetic, and pharmacodynamic study of an anti-super-enhancer Minnelide given along with abraxane plus gemcitabine in patients with metastatic adenocarcinoma of the pancreas (Republic of Korea)	Minnelide in combination with Abraxane and gemcitabine		Phase Ib: metastatic adenocarcinoma of the pancreas	NCT05557851	
A Phase 1, multi-center, open-label, dose-escalation, safety, pharmacokinetic, and pharmacodynamic study of minnelide™ capsules given alone or in combination with protein-bound paclitaxel in patients with advanced solid tumors (United States)	Minnelide in combination with paclitaxel		Phase I: advanced solid tumors	NCT03129139	
Targeting mitochondrial metabolism					
A Phase I trial targeting mitochondrial metabolism with papaverine in combination with chemoradiation for stage II-III non-small cell lung cancer (United States)	Papaverine in combination with chemoradiation and immunotherapy	Mitochondrial Complex I inhibitor	Phase I: Stage II–III non-small-cell lung cancer	NCT05136846	[126]

Table 3. *Cont.*

Title	Drug	Target	Cancer Type	ClinicalTrials.gov ID	Ref.
Phase I trial of phenformin with patients with combination BRAF inhibitor/MEK inhibitor in patients with BRAFV600E/K-mutated melanoma (United States)	Phenformin in combination with dabrafenib and phenformin	Mitochondrial complex I inhibitor	Phase I: melanoma	NCT03026517	[68]
Phase II clinical trial repurposing atovaquone for the treatment of platinum-resistant ovarian cancer (United States)	Atovaquone (Mepron)	Mitochondrial complex III inhibitor	Phase II: ovarian cancer	NCT05998135	[127]
A Trial of atovaquone (Mepron®) combined with conventional chemotherapy for de novo acute myeloid leukemia (AML) adolescents, and young adults (ATACC AML) (United States)	Atovaquone in combination with conventional chemotherapy (cytarabine, daunorubicin, etoposide, gemtuzumab ozogamicin)	Mitochondrial complex III inhibitor	Phase I: acute myeloid leukemia	NCT03568994	
A Phase I study of oral carboxyamidotriazole orotate (CTO) titrated as a single agent in patients with advanced or metastatic solid tumors and titrated in combination therapy with temodar® for patients with glioblastoma and other recurrent malignant gliomas or in combination with temodar® and radiation therapy for patients with newly diagnosed glioblastoma and malignant gliomas (United States)	Carboxyamidotriazole orotate or in combination with temodar/radiation therapy	Non-voltage-dependent calcium channel inhibitor	Phase I: advanced or metastatic solid tumors Phase I: glioblastoma, malignant gliomas	NCT01107522	[128]
A Phase II clinical trial of CPI-613 in patients with relapsed or refractory Burkitt lymphoma/leukemia or high-grade B-cell lymphoma with rearrangements of MYC and BCL2 and/or BCL6 (United States)	Devimistat (CPI-613)	Pyruvate dehydrogenase and α-ketoglutarate dehydrogenase/2-oxoglutarate dehydrogenase	Phase II: relapsed/refractory Burkitt's Lymphoma/leukemia or high-grade B-cell lymphoma with rearrangements of MYC and BCL2 and/or BCL6	NCT03793140	[129]
A Phase II/I open-label clinical trial of CPI-613 in combination with modified FOLFIRINOX in patients with locally advanced pancreatic cancer and good performance status (United States)	Devimistat in combination with modified FOLFIRINOX (oxaliplatin, irinotecan, 5-flurouracil, and folinic acid)		Phase II/I: advanced pancreatic cancer	NCT03699319	
A Phase I dose-escalation study of CPI-613 (Devimistat) in combination with chemoradiation in patients with pancreatic adenocarcinoma (United States)	Devimistat in combination with chemoradiation		Phase I: pancreatic adenocarcinoma	NCT05325281	
Phase II open-label multi-cohort study evaluating CPI-613 (Devimistat) in combination with hydroxychloroquine and 5-fluorouracil or gemcitabine in patients with advanced chemorefractory colorectal, pancreatic, or other solid cancers (United States)	Devimistat in combination with hydroxychloroquine 5-fluorouracil or gemcitabine		Phase II: advanced chemorefractory colorectal, pancreatic or solid tumors	NCT05733000	

Table 3. *Cont.*

Title	Drug	Target	Cancer Type	ClinicalTrials.gov ID	Ref.
Phase II study of AG-120 in people with IDH1 mutant chondrosarcoma (United States)	Ivosidenib (AG-120)	IDH1 inhibitor	Acute myeloid leukemia Phase II: Chondrosarcoma	FDA-approved NCT04278781	[130]
A Phase I, multicenter, open-label, dose-escalation and expansion, safety, pharmacokinetic, pharmacodynamic, and clinical activity study of orally administered AG-120 in subjects with advanced hematologic malignancies with an IDH1 mutation (United States)			Phase I: advanced hematologic malignancies	NCT02074839	
Phase Ib/II investigator initiated study of the IDH1-mutant inhibitor ivosidenib (AG120) with the BCL2 inhibitor venetoclax +/- azacitidine in IDH1-mutated hematologic malignancies (United States)	Ivosidenib in combination with venetoclax +/- azacitidine		Phase Ib/II: IDH1-mutated hematologic malignancies	NCT03471260	
Phase II study of enasidenib in IDH2-mutated malignant sinonasal and skull base tumors (United States)	Enasidenib	IDH2 inhibitor	FDA-approved for acute myeloid leukemia Phase II: malignant sinonasal and skull base tumors	NCT06176989	[131]
Trial of dichloroacetate (DCA) in glioblastoma multiforme (GBM) (United States)	Dichloracetate	Pyruvate dehydrogenase complex inhibitor	Phase IIA: glioblastoma	NCT05120284	[132]
Targeting autophagy					
LIMIT melanoma: (lysosomal inhibition + melanoma immunotherapy) a Phase 1/2 open label trial of nivolumab and hydroxychloroquine or nivolumab/ipilimumab and hydroxychloroquine in patients with advanced melanoma (United States)	Hydroxychloroquine in combination with nivolumab/ipilimumab	Lysosomal acidification inhibitor; Disrupt the fusion of autophagosome with lysosome	Phase I/II: melanoma	NCT04464759	[81,133]
THREAD: A Phase I trial of trametinib and hydroxychloroquine in patients with advanced pancreatic cancer (United States)	Hydroxychloroquine in combination with trametinib		Phase I: advanced pancreatic cancer	NCT03825289	
Binimetinib plus hydroxychloroquine in KRAS mutant metastatic pancreatic cancer (United States)	Hydroxychloroquine in combination with binimetinib		Phase I: KRAS mutant metastatic pancreatic cancer	NCT04132505	
Modulation of sorafenib induced autophagy using hydroxychloroquine in hepatocellular cancer (United States)	Hydroxychloroquine in combination with sorafenib		Phase II: advanced hepatocellular cancer	NCT03037437	
A Phase I trial of MK-2206 and hydroxychloroquine in solid tumors, melanoma, renal and prostate cancer to examine the role of autophagy in tumorigenesis (United States)	Hydroxychloroquine in combination with Akt inhibitor MK2206		Phase I: advanced solid tumors, melanoma, prostate, kidney cancer	NCT01480154	

Table 3. *Cont.*

Title	Drug	Target	Cancer Type	ClinicalTrials.gov ID	Ref.
Treatment of adults with newly diagnosed glioblastoma with partial brain radiation therapy plus temozolomide and chloroquine followed by tumor treating fields plus temozolomide and chloroquine—a pilot study (United States)	Chloroquine in combination with radiotherapy or tumor-treating fields therapy	Lysosomal acidification inhibitor; Disrupt the fusion of autophagosome with lysosome	Phase I: glioblastoma	NCT04397679	[81,133]
Phase II study of oral metformin for intravesical treatment of non-muscle-invasive bladder cancer (Netherlands)	Metformin	AMPK activator; mTOR inhibitor; STAT3-mediated pathway inhibitor; autophagy inducer (decreases p62, increases LC3-II); Complex I inhibitor	Phase II: non-muscle-invasive bladder cancer	NCT03379909	[134–136]
STOP-LEUKEMIA: Repurposing metformin as a leukemia-preventive drug in CCUS and LR-MDS (Denmark)	Metformin		Phase II: clonal cytopenia, myelodysplastic neoplasms	NCT04741945	
Clinical effects of metformin on fertility-sparing treatment for early endometrial cancer (Republic of Korea)			Phase III: endometrial cancer	NCT04792749	
Profiling and reversing metabolic insufficiency in the tumor microenvironment in advanced melanoma: a trial of pembrolizumab and metformin versus pembrolizumab alone in advanced melanoma (United States)	Metformin in combination with pembrolizumab		Phase I: advanced melanoma	NCT03311308	
Phase 2A pilot trial of metformin, digoxin, simvastatin (C3) in combination with gemcitabine in subjects with recurrent/refractory metastatic advanced pancreatic cancer) (United States)	Metformin in combination with simvastatin, and digoxin +/- gemcitabine		Phase I/II: metastatic advanced pancreatic cancer	NCT06030622	
Effect of metformin plus tyrosine kinase inhibitors compared with tyrosine kinase inhibitors alone for patients with advanced non-small cell lung cancer and EGFR mutations: Phase 3 randomized clinical trial (Mexico)	Metformin in combination with tyrosine kinase inhibitors		Phase II: advanced non-small-cell lung cancer	NCT05445791	
A Phase 0, single-center, open-label, dose-escalating trial using super-selective intra-arterial infusion of a single dose of temsirolimus for the treatment of recurrent high-grade glioma (United states)	Temsirolimus (CCI-779)	Autophagy in-ducer; mTOR inhibitor	Advanced renal cell carcinoma Early phase 0: glioma, glioblastoma	FDA-approved NCT05773326	[137]
Phase II trial of encapsulated rapamycin (eRapa) for bladder cancer prevention (United States)	Rapamycin (Sirolimus)	Autophagy inducer; mTOR inhibitor	Phase II: bladder cancer	NCT04375813	[138]
A Phase I trial of sirolimus or everolimus or temsirolimus (mTOR inhibitor) and vorinostat (histone deacetylase inhibitor) in advanced cancer (United States)	Rapamycin in combination with vorinostat		Phase I: advanced cancer	NCT01087554	
Combination of autophagy selective therapeutics (COAST) in advanced solid tumors or relapsed prostate cancer, a Phase I/II Trial (United States)	Rapamycin in combination with hydroxychloroquine, metformin or dasatanib or nelfinavir		Phase I/II: advanced solid tumors, relapsed prostate cancer	NCT05036226	

Table 3. *Cont.*

Title	Drug	Target	Cancer Type	ClinicalTrials.gov ID	Ref.
	Everolimus (afinitor)	Autophagy in-ducer; mTOR inhibitor	HER2-negative advanced breast cancer, pancreatic neuroendocrine tumors, renal cell carcinoma, angiomyolipoma	FDA-approved	[139,140]
Efficacy and safety of epigallocatechin-3-gallate, an important polyphenolic that originates from tea, in patients with esophageal squamous cancer: a Phase II trial (China)	Epigallocatechin gallate (EGCG)	Autophagy activator through ROS elevation, Beclin-1- and LC3B-increasing	Phase II: esophageal squamous cancer	NCT06398405	[87]

5. Challenges Faced in Relation to Therapies Targeting Mitochondrial and Autophagic Processes

Utilizing autophagy and mitochondrial function modulators (Tables 2 and 3) in cancer therapy shows potential in overcoming tumor plasticity and drug resistance. However, some compounds exhibit dual effects, including non-specificity and undefined molecular mechanisms of action. For instance, EGCG activates autophagy and has been shown to suppress COX-2 in prostate, colon, and skin cancers in vitro and in mouse models as well as inhibit NF-kB in a melanoma mouse model [141]. In colorectal cancer (the HT-29 cell line), it triggers endoplasmic reticulum stress through the upregulation of BiP and PERK, leading to apoptosis via increased caspase-3/7 levels. In glioblastoma (the T98G and U87MG cell lines), EGCG elevates ROS levels, increases caspase 8 levels, and activates the JNK pathway [142]. Metformin is an exemplary mitochondria-targeted drug, as it decreases TCA cycle activity and inhibits complex I, leading to reduced ATP production. The resulting lower ATP levels activate AMPK and inhibit mTOR, which triggered autophagy in a myeloma cancer model (the RPMI8226 and U266 cell lines and NOD/SCID mice). In contrast, in leukemic cells (HL60 and MOLM14), metformin triggers apoptosis. Additionally, metformin has the ability to inhibit the NF-kB signaling pathway [143]. These examples underscore the pressing need to develop drugs that specifically target autophagy or mitochondria.

The development of autophagy inhibition methods centers on either inducing excessive autophagy or targeting the early stages of autophagy initiation [59]. A potential candidate for targeting autophagy initiation, the ULK1 inhibitor 13-oxyingenol-dodecanoate (13OD), is currently undergoing preclinical research. The associated study demonstrated that 13OD effectively inhibited the proliferation of non-small-cell lung cancer cells (A549 and H460) in vitro and in BALB/c athymic nude mice by promoting autophagic cell death [144].

Autophagy inducers, notably mTOR inhibitors, face challenges due to their incomplete targeting of mTORC1. This limitation arises as mTORC1 can bypass rapalog effects through the compensatory activation of other pathways, such as PI3K/Akt. Additionally, mutations in the FKBP12–rapamycin binding domain, including an alanine-to-valine substitution at position 2034 (A2034V) and a phenylalanine-to-leucine substitution at position 2108 (F2108L), as well as the activation of mTORC2-dependent pathways, contribute to the issue [145].

Following clinical trials, it was revealed that HCQ's therapeutic effects are not mainly induced by autophagy inhibition. Rather, HCQ accumulates in endosomes, inhibits the toll-like receptor (TLR) pathway, reduces self-antigen presentation, and curbs cytokine production. The acidic nature of the tumor microenvironment negatively impacts HCQ's efficacy by restricting its cellular transport. To address this challenge and minimize toxicity, targeted drug delivery systems like nanoparticles can be utilized [146].

Researchers conducting clinical trials struggle with the challenge of identifying which cancer types and grades are autophagy-dependent, requiring them to discern the function of autophagy each specific cancer patient [59]. To tackle the issue of identifying cancer's dependence on autophagy, some clinical studies employ biomarkers. A case in point is a clinical trial that evaluated glioblastoma patients' responses to combined CQ, chemotherapy, or radiotherapy by analyzing the EGFRvIII marker [147]. The level of the autophagy marker p62 is influenced not only by autophagy activity but also by its role in activating antioxidant gene expression, particularly NRF2, even when autophagy is not occurring [59].

For the mitochondria-targeted BCL-2 inhibitor venetoclax, clinical trials have revealed that secondary resistance can arise in multiple myeloma patients who have undergone long-term venetoclax therapy or possess missense mutations in BCL-2 and BAX. Venetoclax treatment, whether administered as a monotherapy or in combination with chemotherapy, can cause adverse events, including nausea, diarrhea, tumor lysis syndrome, and, most commonly, neutropenia and thrombocytopenia [148]. Studies investigating IDH1/IDH2 inhibitors indicate that resistance can occur in solid malignancies. It is hypothesized that this resistance arises from isotype switching, wherein patients with cytosolic IDH1 mutations develop mitochondrial IDH2 mutations after receiving IDH1 inhibitor therapy [149].

Despite their potential, the application of autophagy and mitochondria modulators in cancer treatment remains limited due to several challenges, including their lack of specificity, the development of resistance, cancer heterogeneity, and unclear molecular mechanisms underlying their actions. To address these issues, further studies are essential, especially those focused on discovering innovative drug targets and assessing synergistic combinations of drugs. Furthermore, creating autophagy-related biomarkers could help manage the variability among cancer patients and allow for more individualized treatment strategies.

6. Autophagy-Related Genes Hold Potential as Prognostic and Diagnostic Biomarkers for Cancer

Diagnosing and predicting the outcome of cancer in its early stages are essential for successful and effective treatment. Various types of cancer have unique autophagy-related biomarkers that serve as prognostic indicators. Identifying these biomarkers is essential for cancer diagnosis and can help predict the effectiveness of therapies that modulate autophagy.

In regard to melanoma, the extensively studied potential autophagy-related biomarkers are LC3, p62, and Beclin-1. Immunohistochemical analysis of malignant melanomas has revealed an increased expression of LC3 and decreased expression of Beclin-1, which are correlated with poorer patient outcomes and the progression of metastasis. However, there are instances of Beclin-1 overexpression and LC3 downregulation in advanced melanoma. The prognostic biomarker p62 is upregulated in the early stages of melanoma according to the AJCC (American Joint Committee on Cancer), but its expression is downregulated in advanced metastatic tumors [150]. In observational studies, these markers were validated in endometrial polyp tissue samples via immunohistochemistry (NCT04706000). Previous research on endometriosis has identified reduced levels of Beclin-1 mRNA and protein [151] (Table 4).

Analysis of mRNA expression in 52 normal and 495 tumor tissues from the Prostate Adenocarcinoma database identified mutations in *ATG9B*, *DNAJB1* (DnaJ heat shock protein family (Hsp40) member B1), *HSPB8*, *NKX2-3*, and *TP63* genes significantly associated with an increased risk of developing prostate cancer. Additionally, *BNIP3*, *NPC1*, and *TP53* genes serve as prognostic autophagy biomarkers for advanced stages of prostate cancer [152].

In oral squamous cell carcinoma (OSCC), RNA sequencing and clinical screening data analysis have identified *ATG12* and *BID* as potential prognostic autophagy-related biomarkers. Subsequent validation studies based on qRT-PCR, immunohistochemistry, and Western blot analysis have confirmed that these biomarkers are overexpressed in OSCC cell lines (SCC9, SCC15, SCC25) and tissues [153].

Table 4. Observational research on cancer patients derived from clinical trial database.

Title	Type of Study	Autophagy Markers/Evaluation	Type of Cancer	ClinicalTrials.gov ID
Investigation of autophagy markers in endometrial polyps (Turkey)	Observational	Beclin 1 LC3A/B P62/ Immunohistochemistry ELISA	Endometrial polyp	NCT04706000
Association of autophagy-related genes, LncRNA and SNPs with colorectal cancer in egyptian population (Egypt)	Observational	In PBMC and tissue, the levels of expression of EIF4EBP1, HOTTIP and serum SNP HOTTIP rs1859168	Colorectal cancer	NCT04729855
Identification of novel autophagy markers in bladder cancer patients (Egypt)	Observational	Atg7 (RTPCR) LC3A (immunohisto-chemistry)	Bladder cancer	NCT03254888
Immunohistochemical assessment of programmed death ligand 1 PDL-1 and autophagy marker LC3B in glioblastoma (Egypt)	Observational	LC3B (immunohisto-chemistry)	Glioblastoma	NCT04284306

Research employing tissue microarrays, immunohistochemistry, and Western blot analysis conducted on formalin-fixed, paraffin-embedded tissues from 352 gastric cancer patients has indicated that diminished expression of ULK1, Beclin 1, ATG3, and ATG10 is associated with improved prognosis [154].

The transcriptome profiles from the TCGA (The Cancer Genome Atlas) and GTEx (The Genotype-Tissue Expression) databases, supported by clinical data and qPCR analysis of fresh cervical cancer samples, revealed *ATG4D*, *CD46*, *TP73*, and *HSPB8* as autophagy-related risk biomarkers. These markers are downregulated in cervical cancer and are associated with favorable prognosis [155]. An additional autophagy-related long non-coding RNA (lncRNA) involved in cervical cancer identified using a public database has established 10 lncRNAs with prognostic potential, with *DBH-AS1* being the most notable. Moreover, the associated study confirmed the role of lncRNA in regulating autophagy, modulating tumor development, and altering sensitivity to treatment [156].

In regard to glioma, one well-known biomarker is *VMP1*. Data analyses based on various cancer genome atlases have shown that *VMP1* is upregulated in high-grade gliomas, and this is associated with a worse prognosis. Suppressing *VMP1* expression through CRISPR-Cas9 gene editing significantly inhibited the proliferation of LN299 cells, leading to partial autophagy as a result of disrupted autophagosome formation and the initiation of apoptosis. *VMP1* has the potential to be utilized as a predictor of survival for glioma patients [157].

In regard to bladder cancer, 11 autophagy-related biomarkers have been identified as key indicators of patient survival and clinical outcomes based on information from the Human Autophagy Database and Bladder Carcinoma databases. These biomarkers are *APOL1*, *ATG4B*, *BAG1*, *CASP3*, *DRAM1*, *ITGA3*, *KLHL24*, *P4HB*, *PRKCD*, *ULK2*, and *WDR45*. Notably, the overexpression of *ULK2* and *P4HB* is linked to high-risk bladder cancer. In contrast, the overexpression of *APOL1*, *ATG4B*, *BAG1*, *DRAM1*, *ITGA3*, *KLHL24*, *PRKCD*, and *WDR45* is correlated with low-risk bladder cancer [158]. A study (NCT03254888) on bladder cancer patients with confirmed histopathology employed quantitative real-time

PCR to estimate ATG7 levels and used immunohistochemistry to determine LC3A levels as markers of autophagy (Table 4).

In regard to esophageal cancer, RNA-sequencing data analysis and clinical information derived from TCGA database identified *DNAJB*, *BNIP1*, *VAMP7*, and *TBK1* (TANK binding kinase 1) as prognostic autophagy-related signatures. These biomarkers are significantly associated with overall patient survival [159].

Significant increases in autophagy and mitophagy markers, such as Beclin-1, LC-3, BNIP-3, and Parkin, were detected in breast cancer tissues compared to controls. The associated study also indicated that LC3 immunostaining was linked to younger breast cancer patients, while Parkin was associated with a history of breastfeeding [160].

An analysis of ovarian cancer gene expression profiles from the TCGA database, in conjunction with clinical data, uncovered 52 potential autophagy-related genes. LASSO-Cox analysis further revealed that FOXO1 and CASP8 are particularly promising for prognosis. Immunohistochemical analysis of tissue microarrays from 125 patients identified that elevated FOXO1 expression is linked to metastasis and a poorer prognosis in ovarian cancer [161].

Cancer prognosis and diagnosis are highly demanding disciplines owing to the diversity and intricacy of gene expression in individual patients. Each cancer patient possesses distinct genetic profiles and undergoes unique modifications in gene expression in response to cancer development. This uniqueness presents challenges in predicting cancer progression and treatment response. The heterogeneity in gene expression among cancer patients results in variation in tumor behavior and sensitivity to chemotherapy. Identifying specific prognostic biomarkers can contribute to early cancer patient diagnosis and enhance the effectiveness of personalized treatment strategies.

7. Conclusions

This review provides a comprehensive overview of the various functions of mitochondria within cancer cells, with a specific focus on their role in autophagy. Understanding the distinct characteristics of mitochondria in both healthy and cancerous cells, particularly in relation to autophagy, is crucial for developing more precise treatments, especially for cancer [9]. Strategies for inhibiting mitochondrial function or autophagy in cancer treatment include: 1. inducing oxidative stress; 2. disrupting mitochondrial respiration by targeting Complexes I through V; 3. inhibiting non-voltage calcium channels; 4. suppressing TCA cycle enzymes; and 5. modulating autophagy through activation or inhibition [162].

Autophagy is initiated under conditions of starvation and stress, such as organelle damage and the presence of misfolded proteins [163]. In cancer, autophagy plays a dual role: it can either promote tumorigenesis in certain cancers or suppress tumor development in others. Additionally, autophagy plays a role in the development of drug resistance and metastasis [12]. Modulating autophagy in cancer cells holds promise for cancer treatment. Autophagy inhibitors like chloroquine and hydroxychloroquine, as well as autophagy activators such as temsirolimus and rapamycin, have demonstrated efficacy in disrupting tumor growth, especially when combined with chemotherapy, according to both preclinical and clinical studies [164]. Despite the potential of mitochondrial function or autophagy modulators, their application is limited by several factors, including a lack of specificity, incomplete targeting due to mutations at binding sites, adverse events, and the development of secondary resistance.

Moreover, the precise diagnosis of specific cancer types is as crucial as the development of effective treatments. Early-stage cancer diagnosis significantly enhances the likelihood of successful treatment. Autophagy-related biomarkers are valuable for both cancer diagnosis and prognosis. This review also provides an overview of unique autophagy biomarkers across different types of cancer in pre-clinical and clinical studies.

Author Contributions: Conceptualization: A.Z.; literature search and writing: A.Z.; review and editing: E.G.-M. All authors have read and agreed to the published version of the manuscript.

Funding: This research received no external funding.

Conflicts of Interest: The authors declare no conflicts of interest. The funders had no role in the design of the study; in the collection, analyses, or interpretation of data; in the writing of the manuscript; or in the decision to publish the results.

Abbreviations

13OD	13-oxyingenol-dodecanoate
ACD	autophagic cell death
AJCC	American Joint Committee on Cancer
AKT1	AKT serine/threonine kinase 1
AMBRA1	the activating molecule in BECLIN1-regulated autophagy 1
AMPK	AMP-activated protein kinase
ATP	adenosine triphosphate
ATP5F1A	ATP synthase F1 subunit alpha
BAG1	Bcl2-associated athanogene 1 protein
BCL-2	B-cell lymphoma-2
BCL2L13	BCL2-Like 13
Beclin1	Bcl-2-interacting myosin-like coiled-coil
BIF1	Bax-interacting factor 1
BMAL1	basic helix–loop–helix ARNT-like 1
BNIP3	BCL2/adenovirus E1B 19 kDa protein-interacting protein 3
CALCOCO2/NDP52	calcium-binding and coiled-coil domain 2
CAT	catalase
CHIP	carboxyl terminus of hsc70-interacting protein
CHMP2	charged multivesicular body protein 2
CL	cardiolipin
CLEAR	coordinated lysosomal expression and regulation
CMA	chaperone-mediated autophagy
COX IV	cytochrome c oxidase subunit 4
DAPK	death-associated protein kinase
DAPK	death-associated protein kinase
DJ-1	nucleic acid deglycase
DNAJB1	DnaJ heat shock protein family (Hsp40) member B1
DRAM	damage-regulated autophagy modulator
DUB	deubiquitinase
DYNC1LI2	Dynein Cytoplasmic 1 Light Intermediate Chain 2
EF1α	elongation factor 1-α
EGCG	epigallocatechin gallate
ER	endoplasmic reticulum
ESCRT	endosomal sorting complex required for transport
ETC	electron transport chain
FKBP8	FKBP Prolyl Isomerase 8
FUNDC1	FUN14 Domain-Containing 1
GABARAP	GABA type A receptor-associated protein
GFAP	glial fibrillary acidic protein
GP78	glycoprotein 78
GSH	glutathione
GSH-Px	glutathione peroxidase
GTEx	genotype-tissue expression
GTP	guanosine triphosphate
HMT	horizontal mitochondrial transfer
HOP	hsp70-hsp90 organizing protein
HOPS	homotypic fusion and protein sorting
Hsp40	heat shock protein 40

Hsp70	heat shock protein 70
IMM	inner mitochondrial membrane
KGDH	α-ketoglutarate dehydrogenase
LAMP-2A	lysosome-associated membrane protein type 2A
LC3	microtubule-associated protein 1 light chain 3
LIR	LC3-interacting region
MAM	mitochondria-associated membrane
MAP1LC3/LC3	microtubule associated protein 1 light chain 3
MFN2	Mitofusin-2
Miro	mitochondrial Rho GTPase
MMP	mitochondrial membrane potential
MTCH1	mitochondrial carrier 1
mTORC1	mechanistic target of rapamycin complex 1
mTORC2	mammalian target of rapamycin complex 2
mtROS	mitochondrial reactive oxygen species
MUL1	mitochondrial E3 ubiquitin ligase 1
NBR1	neighbor of BRCA1 gene 1 protein
NFAT1	nuclear factor of activated T cells
NFE2L2	NFE2 Like BZIP transcription factor 2
NF-kB	nuclear factor kappa-light-chain-enhancer of activated B cells
NOX	NADPH oxidase
Nrf2	nuclear factor erythroid 2-related factor 2
OMM	outer mitochondrial membrane
OPTN	optineurin
OSCC	oral squamous cell carcinoma
OXPHOS	oxidative phosphorylation
PAS	pre-autophagosomal structure
PDH	pyruvate dehydrogenase
PE	phosphatidylethanolamine
PER1/2	period circadian protein homolog 1/2
PGAM5	mitochondrial serine/threonine protein phosphatase
PHB2	prohibitin 2
PHLPP1	PH Domain And Leucine Rich Repeat Protein Phosphatase 1
PI3K	phosphatidylinositol 3-kinase
PI3P	phosphoinositide 3-phosphate
PINK1	PTEN-induced putative kinase 1
PLEKHM1	pleckstrin homology domain-containing family M member 1
PPT1	palmitoyl-protein thioesterase 1
PTEN	phosphatase and tensin homolog
Rab-7A	Ras-related protein Rab-7A
RARα	retinoic acid receptor alpha
RHOT1	Ras homolog family member T1
RILP	Rab-interacting lysosomal protein
ROS	reactive oxygen species
SIAH1	seven in absentia homolog 1
SMAC	mitochondrial-derived activator of caspases
SNARE	soluble N-ethylmaleimide-sensitive attachment protein receptors
SOD	superoxide dismutase
SQSTM1/p62	sequestosome 1
TAX1BP1	Tax1 binding protein 1
TBK1	TANK binding kinase 1
TCA	tricarboxylic acid
TCGA	The Cancer Genome Atlas
TFEB	transcription factor EB
TLR	toll-like receptor
TNFa	tumor necrosis factor α
Tom20	mitochondrial import receptor subunit TOM20 homolog
TOMM7	translocase of outer mitochondrial membrane 7

TRAF6	tumor-necrosis-factor-receptor-associated factor 6
TRX	reduced thioredoxin
TRX-Px	thioredoxin peroxidase
TSC1/2	tuberous sclerosis protein 1 and 2
ULK	Unc-51-like kinase
ULK1/2	serine/threonine Unc-51 like kinase ½
UVRAG	UV radiation resistance-associated
VDAC-1	voltage-dependent anion channel-1
VPS34	vacuolar protein sorting 34
WIPI2	WD-repeat domain phosphoinositide-interacting 2

References

1. Murphy, M.P. How mitochondria produce reactive oxygen species. *Biochem. J.* **2009**, *417*, 1–13. [CrossRef]
2. Cheung, E.C.; Vousden, K.H. The role of ROS in tumour development and progression. *Nat. Rev. Cancer* **2022**, *22*, 280–297. [CrossRef]
3. Dong, L.F.; Rohlena, J.; Zobalova, R.; Nahacka, Z.; Rodriguez, A.M.; Berridge, M.V.; Neuzil, J. Mitochondria on the move: Horizontal mitochondrial transfer in disease and health. *J. Cell Biol.* **2023**, *222*, e202211044. [CrossRef] [PubMed]
4. Mailloux, R.J. Mitochondrial Antioxidants and the Maintenance of Cellular Hydrogen Peroxide Levels. *Oxid. Med. Cell. Longev.* **2018**, *2018*, 7857251. [CrossRef] [PubMed]
5. Xia, M.; Zhang, Y.; Jin, K.; Lu, Z.; Zeng, Z.; Xiong, W. Communication between mitochondria and other organelles: A brand-new perspective on mitochondria in cancer. *Cell Biosci.* **2019**, *9*, 27. [CrossRef] [PubMed]
6. Jin, P.; Jiang, J.; Zhou, L.; Huang, Z.; Nice, E.C.; Huang, C.; Fu, L. Mitochondrial adaptation in cancer drug resistance: Prevalence, mechanisms, and management. *J. Hematol. Oncol.* **2022**, *15*, 97. [CrossRef] [PubMed]
7. Kopinski, P.K.; Singh, L.N.; Zhang, S.; Lott, M.T.; Wallace, D.C. Mitochondrial DNA variation and cancer. *Nat. Rev. Cancer* **2021**, *21*, 431–445. [CrossRef]
8. Sainero-Alcolado, L.; Liano-Pons, J.; Ruiz-Perez, M.V.; Arsenian-Henriksson, M. Targeting mitochondrial metabolism for precision medicine in cancer. *Cell Death Differ.* **2022**, *29*, 1304–1317. [CrossRef]
9. Mukherjee, S.; Bhatti, G.K.; Chhabra, R.; Reddy, P.H.; Bhatti, J.S. Targeting mitochondria as a potential therapeutic strategy against chemoresistance in cancer. *Biomed. Pharmacother.* **2023**, *160*, 114398. [CrossRef]
10. Missiroli, S.; Perrone, M.; Genovese, I.; Pinton, P.; Giorgi, C. Cancer metabolism and mitochondria: Finding novel mechanisms to fight tumours. *eBioMedicine* **2020**, *59*, 102943. [CrossRef]
11. Rakesh, R.; PriyaDharshini, L.C.; Sakthivel, K.M.; Rasmi, R.R. Role and regulation of autophagy in cancer. *Biochim. Biophys. Acta Mol. Basis Dis.* **2022**, *1868*, 166400. [CrossRef] [PubMed]
12. Ahmadi-Dehlaghi, F.; Mohammadi, P.; Valipour, E.; Pournaghi, P.; Kiani, S.; Mansouri, K. Autophagy: A challengeable paradox in cancer treatment. *Cancer Med.* **2023**, *12*, 11542–11569. [CrossRef]
13. Noguchi, M.; Hirata, N.; Tanaka, T.; Suizu, F.; Nakajima, H.; Chiorini, J.A. Autophagy as a modulator of cell death machinery. *Cell Death Dis.* **2020**, *11*, 517. [CrossRef]
14. Rangel, M.; Kong, J.; Bhatt, V.; Khayati, K.; Guo, J.Y. Autophagy and tumorigenesis. *FEBS J.* **2022**, *289*, 7177–7198. [CrossRef]
15. Yamamoto, H.; Zhang, S.; Mizushima, N. Autophagy genes in biology and disease. *Nat. Rev. Genet.* **2023**, *24*, 382–400. [CrossRef] [PubMed]
16. Amaravadi, R.K.; Kimmelman, A.C.; Debnath, J. Targeting Autophagy in Cancer: Recent Advances and Future Directions. *Cancer Discov.* **2019**, *9*, 1167–1181. [CrossRef]
17. Ichimiya, T.; Yamakawa, T.; Hirano, T.; Yokoyama, Y.; Hayashi, Y.; Hirayama, D.; Wagatsuma, K.; Itoi, T.; Nakase, H. Autophagy and Autophagy-Related Diseases: A Review. *Int. J. Mol. Sci.* **2020**, *21*, 8974. [CrossRef] [PubMed]
18. Alers, S.; Loffler, A.S.; Wesselborg, S.; Stork, B. Role of AMPK-mTOR-Ulk1/2 in the regulation of autophagy: Cross talk, shortcuts, and feedbacks. *Mol. Cell. Biol.* **2012**, *32*, 2–11. [CrossRef]
19. Martens, S.; Fracchiolla, D. Activation and targeting of ATG8 protein lipidation. *Cell Discov.* **2020**, *6*, 23. [CrossRef]
20. Agrotis, A.; von Chamier, L.; Oliver, H.; Kiso, K.; Singh, T.; Ketteler, R. Human ATG4 autophagy proteases counteract attachment of ubiquitin-like LC3/GABARAP proteins to other cellular proteins. *J. Biol. Chem.* **2019**, *294*, 12610–12621. [CrossRef]
21. Chavez-Dominguez, R.; Perez-Medina, M.; Lopez-Gonzalez, J.S.; Galicia-Velasco, M.; Aguilar-Cazares, D. The Double-Edge Sword of Autophagy in Cancer: From Tumor Suppression to Pro-tumor Activity. *Front. Oncol.* **2020**, *10*, 578418. [CrossRef]
22. Hernandez, G.A.; Perera, R.M. Autophagy in cancer cell remodeling and quality control. *Mol. Cell* **2022**, *82*, 1514–1527. [CrossRef] [PubMed]
23. Yim, W.W.; Mizushima, N. Lysosome biology in autophagy. *Cell Discov.* **2020**, *6*, 6. [CrossRef]
24. Ferro, F.; Servais, S.; Besson, P.; Roger, S.; Dumas, J.F.; Brisson, L. Autophagy and mitophagy in cancer metabolic remodelling. *Semin. Cell Dev. Biol.* **2020**, *98*, 129–138. [CrossRef] [PubMed]
25. Doblado, L.; Lueck, C.; Rey, C.; Samhan-Arias, A.K.; Prieto, I.; Stacchiotti, A.; Monsalve, M. Mitophagy in Human Diseases. *Int. J. Mol. Sci.* **2021**, *22*, 3903. [CrossRef] [PubMed]
26. Choubey, V.; Zeb, A.; Kaasik, A. Molecular Mechanisms and Regulation of Mammalian Mitophagy. *Cells* **2021**, *11*, 38. [CrossRef]

27. Yan, C.; Gong, L.; Chen, L.; Xu, M.; Abou-Hamdan, H.; Tang, M.; Desaubry, L.; Song, Z. PHB2 (prohibitin 2) promotes PINK1-PRKN/Parkin-dependent mitophagy by the PARL-PGAM5-PINK1 axis. *Autophagy* **2020**, *16*, 419–434. [CrossRef]
28. Ajoolabady, A.; Chiong, M.; Lavandero, S.; Klionsky, D.J.; Ren, J. Mitophagy in cardiovascular diseases: Molecular mechanisms, pathogenesis, and treatment. *Trends Mol. Med.* **2022**, *28*, 836–849. [CrossRef]
29. Zuo, Z.; Jing, K.; Wu, H.; Wang, S.; Ye, L.; Li, Z.; Yang, C.; Pan, Q.; Liu, W.J.; Liu, H.F. Mechanisms and Functions of Mitophagy and Potential Roles in Renal Disease. *Front. Physiol.* **2020**, *11*, 935. [CrossRef]
30. Vara-Perez, M.; Felipe-Abrio, B.; Agostinis, P. Mitophagy in Cancer: A Tale of Adaptation. *Cells* **2019**, *8*, 493. [CrossRef]
31. Montava-Garriga, L.; Ganley, I.G. Outstanding Questions in Mitophagy: What We Do and Do Not Know. *J. Mol. Biol.* **2020**, *432*, 206–230. [CrossRef] [PubMed]
32. Teresak, P.; Lapao, A.; Subic, N.; Boya, P.; Elazar, Z.; Simonsen, A. Regulation of PRKN-independent mitophagy. *Autophagy* **2022**, *18*, 24–39. [CrossRef]
33. Sanchez-Martin, P.; Saito, T.; Komatsu, M. p62/SQSTM1: 'Jack of all trades' in health and cancer. *FEBS J.* **2019**, *286*, 8–23. [CrossRef]
34. Boyle, K.B.; Ravenhill, B.J.; Randow, F. CALCOCO2/NDP52 initiates selective autophagy through recruitment of ULK and TBK1 kinase complexes. *Autophagy* **2019**, *15*, 1655–1656. [CrossRef] [PubMed]
35. Padman, B.S.; Nguyen, T.N.; Uoselis, L.; Skulsuppaisarn, M.; Nguyen, L.K.; Lazarou, M. LC3/GABARAPs drive ubiquitin-independent recruitment of Optineurin and NDP52 to amplify mitophagy. *Nat. Commun.* **2019**, *10*, 408. [CrossRef]
36. Cerda-Troncoso, C.; Varas-Godoy, M.; Burgos, P.V. Pro-Tumoral Functions of Autophagy Receptors in the Modulation of Cancer Progression. *Front. Oncol.* **2020**, *10*, 619727. [CrossRef]
37. Fan, Y.; Cheng, Z.; Mao, L.; Xu, G.; Li, N.; Zhang, M.; Weng, P.; Zheng, L.; Dong, X.; Hu, S.; et al. PINK1/TAX1BP1-directed mitophagy attenuates vascular endothelial injury induced by copper oxide nanoparticles. *J. Nanobiotechnol.* **2022**, *20*, 149. [CrossRef] [PubMed]
38. Sandoval, H.; Thiagarajan, P.; Dasgupta, S.K.; Schumacher, A.; Prchal, J.T.; Chen, M.; Wang, J. Essential role for Nix in autophagic maturation of erythroid cells. *Nature* **2008**, *454*, 232–235. [CrossRef] [PubMed]
39. Wu, W.; Lin, C.; Wu, K.; Jiang, L.; Wang, X.; Li, W.; Zhuang, H.; Zhang, X.; Chen, H.; Li, S.; et al. FUNDC1 regulates mitochondrial dynamics at the ER-mitochondrial contact site under hypoxic conditions. *EMBO J.* **2016**, *35*, 1368–1384. [CrossRef]
40. Nakazawa, M.; Matsubara, H.; Matsushita, Y.; Watanabe, M.; Vo, N.; Yoshida, H.; Yamaguchi, M.; Kataoka, T. The Human Bcl-2 Family Member Bcl-rambo Localizes to Mitochondria and Induces Apoptosis and Morphological Aberrations in Drosophila. *PLoS ONE* **2016**, *11*, e0157823. [CrossRef]
41. Bai, X.; Ma, D.; Liu, A.; Shen, X.; Wang, Q.J.; Liu, Y.; Jiang, Y. Rheb activates mTOR by antagonizing its endogenous inhibitor, FKBP38. *Science* **2007**, *318*, 977–980. [CrossRef] [PubMed]
42. Cecconi, F.; Di Bartolomeo, S.; Nardacci, R.; Fuoco, C.; Corazzari, M.; Giunta, L.; Romagnoli, A.; Stoykova, A.; Chowdhury, K.; Fimia, G.M.; et al. A novel role for autophagy in neurodevelopment. *Autophagy* **2007**, *3*, 506–508. [CrossRef]
43. Li, X.X.; Tsoi, B.; Li, Y.F.; Kurihara, H.; He, R.R. Cardiolipin and its different properties in mitophagy and apoptosis. *J. Histochem. Cytochem.* **2015**, *63*, 301–311. [CrossRef] [PubMed]
44. Andrade-Tomaz, M.; de Souza, L.; Rocha, C.R.R.; Gomes, L.R. The Role of Chaperone-Mediated Autophagy in Cell Cycle Control and Its Implications in Cancer. *Cells* **2020**, *9*, 2140. [CrossRef]
45. Jafari, M.; McCabe, M.; Cuervo, A.M. Chaperone-mediated autophagy: Mechanisms and physiological relevance. *Curr. Opin. Physiol.* **2022**, *30*, 100597. [CrossRef]
46. Agarraberes, F.A.; Dice, J.F. A molecular chaperone complex at the lysosomal membrane is required for protein translocation. *J. Cell Sci.* **2001**, *114*, 2491–2499. [CrossRef]
47. Kaushik, S.; Cuervo, A.M. The coming of age of chaperone-mediated autophagy. *Nat. Rev. Mol. Cell Biol.* **2018**, *19*, 365–381. [CrossRef]
48. Kanno, H.; Handa, K.; Murakami, T.; Aizawa, T.; Ozawa, H. Chaperone-Mediated Autophagy in Neurodegenerative Diseases and Acute Neurological Insults in the Central Nervous System. *Cells* **2022**, *11*, 1205. [CrossRef]
49. Hubert, V.; Weiss, S.; Rees, A.J.; Kain, R. Modulating Chaperone-Mediated Autophagy and Its Clinical Applications in Cancer. *Cells* **2022**, *11*, 2562. [CrossRef]
50. Zhang, J.; Johnson, J.L.; He, J.; Napolitano, G.; Ramadass, M.; Rocca, C.; Kiosses, W.B.; Bucci, C.; Xin, Q.; Gavathiotis, E.; et al. Cystinosin, the small GTPase Rab11, and the Rab7 effector RILP regulate intracellular trafficking of the chaperone-mediated autophagy receptor LAMP2A. *J. Biol. Chem.* **2017**, *292*, 10328–10346. [CrossRef] [PubMed]
51. Pajares, M.; Rojo, A.I.; Arias, E.; Diaz-Carretero, A.; Cuervo, A.M.; Cuadrado, A. Transcription factor NFE2L2/NRF2 modulates chaperone-mediated autophagy through the regulation of LAMP2A. *Autophagy* **2018**, *14*, 1310–1322. [CrossRef] [PubMed]
52. Cui, J.; Shen, H.M.; Lim, L.H.K. The Role of Autophagy in Liver Cancer: Crosstalk in Signaling Pathways and Potential Therapeutic Targets. *Pharmaceuticals* **2020**, *13*, 432. [CrossRef]
53. Jain, V.; Singh, M.P.; Amaravadi, R.K. Recent advances in targeting autophagy in cancer. *Trends Pharmacol. Sci.* **2023**, *44*, 290–302. [CrossRef] [PubMed]
54. Yun, C.W.; Jeon, J.; Go, G.; Lee, J.H.; Lee, S.H. The Dual Role of Autophagy in Cancer Development and a Therapeutic Strategy for Cancer by Targeting Autophagy. *Int. J. Mol. Sci.* **2020**, *22*, 179. [CrossRef]

55. Movahhed, P.; Saberiyan, M.; Safi, A.; Arshadi, Z.; Kazerouni, F.; Teimori, H. The impact of DAPK1 and mTORC1 signaling association on autophagy in cancer. *Mol. Biol. Rep.* **2022**, *49*, 4959–4964. [CrossRef]
56. Hu, Y.J.; Zhong, J.T.; Gong, L.; Zhang, S.C.; Zhou, S.H. Autophagy-Related Beclin 1 and Head and Neck Cancers. *OncoTargets Ther.* **2020**, *13*, 6213–6227. [CrossRef]
57. Usman, R.M.; Razzaq, F.; Akbar, A.; Farooqui, A.A.; Iftikhar, A.; Latif, A.; Hassan, H.; Zhao, J.; Carew, J.S.; Nawrocki, S.T.; et al. Role and mechanism of autophagy-regulating factors in tumorigenesis and drug resistance. *Asia Pac. J. Clin. Oncol.* **2021**, *17*, 193–208. [CrossRef]
58. Ying, H.; Qu, D.; Liu, C.; Ying, T.; Lv, J.; Jin, S.; Xu, H. Chemoresistance is associated with Beclin-1 and PTEN expression in epithelial ovarian cancers. *Oncol. Lett.* **2015**, *9*, 1759–1763. [CrossRef]
59. Debnath, J.; Gammoh, N.; Ryan, K.M. Autophagy and autophagy-related pathways in cancer. *Nat. Rev. Mol. Cell Biol.* **2023**, *24*, 560–575. [CrossRef] [PubMed]
60. Hu, Y.; Li, X.; Xue, W.; Pang, J.; Meng, Y.; Shen, Y.; Xu, Q. TP53INP2-related basal autophagy is involved in the growth and malignant progression in human liposarcoma cells. *Biomed. Pharmacother.* **2017**, *88*, 562–568. [CrossRef]
61. Pan, J.; Lu, C.; Jun, W.; Wu, Y.; Shi, X.; Ding, Y. The up-regulation of P62 levels is associated with resistance of sorafenib in hepatocarcinoma cells. *Int. J. Clin. Exp. Pathol.* **2019**, *12*, 2622–2630. [PubMed]
62. Shin, D.W. Dual Roles of Autophagy and Their Potential Drugs for Improving Cancer Therapeutics. *Biomol. Ther.* **2020**, *28*, 503–511. [CrossRef]
63. Panigrahi, D.P.; Praharaj, P.P.; Bhol, C.S.; Mahapatra, K.K.; Patra, S.; Behera, B.P.; Mishra, S.R.; Bhutia, S.K. The emerging, multifaceted role of mitophagy in cancer and cancer therapeutics. *Semin. Cancer Biol.* **2020**, *66*, 45–58. [CrossRef]
64. Fendt, S.M.; Frezza, C.; Erez, A. Targeting Metabolic Plasticity and Flexibility Dynamics for Cancer Therapy. *Cancer Discov.* **2020**, *10*, 1797–1807. [CrossRef] [PubMed]
65. Parida, P.K.; Marquez-Palencia, M.; Ghosh, S.; Khandelwal, N.; Kim, K.; Nair, V.; Liu, X.Z.; Vu, H.S.; Zacharias, L.G.; Gonzalez-Ericsson, P.I.; et al. Limiting mitochondrial plasticity by targeting DRP1 induces metabolic reprogramming and reduces breast cancer brain metastases. *Nat. Cancer* **2023**, *4*, 893–907. [CrossRef]
66. Wang, X.; Ji, Y.; Qi, J.; Zhou, S.; Wan, S.; Fan, C.; Gu, Z.; An, P.; Luo, Y.; Luo, J. Mitochondrial carrier 1 (MTCH1) governs ferroptosis by triggering the FoxO1-GPX4 axis-mediated retrograde signaling in cervical cancer cells. *Cell Death Dis.* **2023**, *14*, 508. [CrossRef]
67. Yap, T.A.; Daver, N.; Mahendra, M.; Zhang, J.; Kamiya-Matsuoka, C.; Meric-Bernstam, F.; Kantarjian, H.M.; Ravandi, F.; Collins, M.E.; Francesco, M.E.D.; et al. Complex I inhibitor of oxidative phosphorylation in advanced solid tumors and acute myeloid leukemia: Phase I trials. *Nat. Med.* **2023**, *29*, 115–126. [CrossRef] [PubMed]
68. Di Magno, L.; Manni, S.; Di Pastena, F.; Coni, S.; Macone, A.; Cairoli, S.; Sambucci, M.; Infante, P.; Moretti, M.; Petroni, M.; et al. Phenformin Inhibits Hedgehog-Dependent Tumor Growth through a Complex I-Independent Redox/Corepressor Module. *Cell Rep.* **2020**, *30*, 1735–1752.e7. [CrossRef]
69. Skwarski, M.; McGowan, D.R.; Belcher, E.; Di Chiara, F.; Stavroulias, D.; McCole, M.; Derham, J.L.; Chu, K.Y.; Teoh, E.; Chauhan, J.; et al. Mitochondrial Inhibitor Atovaquone Increases Tumor Oxygenation and Inhibits Hypoxic Gene Expression in Patients with Non-Small Cell Lung Cancer. *Clin. Cancer Res.* **2021**, *27*, 2459–2469. [CrossRef]
70. Gowans, F.A.; Thach, D.Q.; Wang, Y.; Altamirano Poblano, B.E.; Dovala, D.; Tallarico, J.A.; McKenna, J.M.; Schirle, M.; Maimone, T.J.; Nomura, D.K. Ophiobolin A Covalently Targets Complex IV Leading to Mitochondrial Metabolic Collapse in Cancer Cells. *bioRxiv* **2023**. [CrossRef]
71. Fiorillo, M.; Scatena, C.; Naccarato, A.G.; Sotgia, F.; Lisanti, M.P. Bedaquiline, an FDA-approved drug, inhibits mitochondrial ATP production and metastasis in vivo, by targeting the gamma subunit (ATP5F1C) of the ATP synthase. *Cell Death Differ.* **2021**, *28*, 2797–2817. [CrossRef] [PubMed]
72. Zhu, H.; Chen, Q.; Zhao, L.; Hu, P. Targeting ATP Synthase by Bedaquiline as a Therapeutic Strategy to Sensitize Ovarian Cancer to Cisplatin. *Nutr. Cancer* **2023**, *75*, 1271–1280. [CrossRef] [PubMed]
73. Mohan, A.; Griffith, K.A.; Wuchu, F.; Zhen, D.B.; Kumar-Sinha, C.; Crysler, O.; Hsiehchen, D.; Enzler, T.; Dippman, D.; Gunchick, V.; et al. Devimistat in Combination with Gemcitabine and Cisplatin in Biliary Tract Cancer: Preclinical Evaluation and Phase Ib Multicenter Clinical Trial (BilT-04). *Clin. Cancer Res.* **2023**, *29*, 2394–2400. [CrossRef] [PubMed]
74. Deeks, E.D. Venetoclax: First Global Approval. *Drugs* **2016**, *76*, 979–987. [CrossRef]
75. Xu, J.; Dong, X.; Huang, D.C.S.; Xu, P.; Zhao, Q.; Chen, B. Current Advances and Future Strategies for BCL-2 Inhibitors: Potent Weapons against Cancers. *Cancers* **2023**, *15*, 4957. [CrossRef]
76. Ploumaki, I.; Triantafyllou, E.; Koumprentziotis, I.A.; Karampinos, K.; Drougkas, K.; Karavolias, I.; Trontzas, I.; Kotteas, E.A. Bcl-2 pathway inhibition in solid tumors: A review of clinical trials. *Clin. Transl. Oncol.* **2023**, *25*, 1554–1578. [CrossRef]
77. Liu, J.; Wu, Y.; Meng, S.; Xu, P.; Li, S.; Li, Y.; Hu, X.; Ouyang, L.; Wang, G. Selective autophagy in cancer: Mechanisms, therapeutic implications, and future perspectives. *Mol. Cancer* **2024**, *23*, 22. [CrossRef]
78. Chen, J.L.; Wu, X.; Yin, D.; Jia, X.H.; Chen, X.; Gu, Z.Y.; Zhu, X.M. Autophagy inhibitors for cancer therapy: Small molecules and nanomedicines. *Pharmacol. Ther.* **2023**, *249*, 108485. [CrossRef]
79. Chang, H.; Zou, Z. Targeting autophagy to overcome drug resistance: Further developments. *J. Hematol. Oncol.* **2020**, *13*, 159. [CrossRef] [PubMed]

80. Zeh, H.J.; Bahary, N.; Boone, B.A.; Singhi, A.D.; Miller-Ocuin, J.L.; Normolle, D.P.; Zureikat, A.H.; Hogg, M.E.; Bartlett, D.L.; Lee, K.K.; et al. A Randomized Phase II Preoperative Study of Autophagy Inhibition with High-Dose Hydroxychloroquine and Gemcitabine/Nab-Paclitaxel in Pancreatic Cancer Patients. *Clin. Cancer Res.* **2020**, *26*, 3126–3134. [CrossRef]
81. Ferreira, P.M.P.; Sousa, R.W.R.; Ferreira, J.R.O.; Militao, G.C.G.; Bezerra, D.P. Chloroquine and hydroxychloroquine in antitumor therapies based on autophagy-related mechanisms. *Pharmacol. Res.* **2021**, *168*, 105582. [CrossRef] [PubMed]
82. Rebecca, V.W.; Nicastri, M.C.; Fennelly, C.; Chude, C.I.; Barber-Rotenberg, J.S.; Ronghe, A.; McAfee, Q.; McLaughlin, N.P.; Zhang, G.; Goldman, A.R.; et al. PPT1 Promotes Tumor Growth and Is the Molecular Target of Chloroquine Derivatives in Cancer. *Cancer Discov.* **2019**, *9*, 220–229. [CrossRef] [PubMed]
83. Kim, E.L.; Wustenberg, R.; Rubsam, A.; Schmitz-Salue, C.; Warnecke, G.; Bucker, E.M.; Pettkus, N.; Speidel, D.; Rohde, V.; Schulz-Schaeffer, W.; et al. Chloroquine activates the p53 pathway and induces apoptosis in human glioma cells. *Neuro Oncol.* **2010**, *12*, 389–400. [CrossRef]
84. Schrezenmeier, E.; Dorner, T. Mechanisms of action of hydroxychloroquine and chloroquine: Implications for rheumatology. *Nat. Rev. Rheumatol.* **2020**, *16*, 155–166. [CrossRef]
85. Buzun, K.; Gornowicz, A.; Lesyk, R.; Bielawski, K.; Bielawska, A. Autophagy Modulators in Cancer Therapy. *Int. J. Mol. Sci.* **2021**, *22*, 5804. [CrossRef]
86. Elshazly, A.M.; Elzahed, A.A.; Gewirtz, D.A. The Cytoprotective and Cytotoxic Functions of Autophagy in Response to mTOR Inhibitors. *Front. Biosci.* **2024**, *29*, 231. [CrossRef]
87. Ferrari, E.; Bettuzzi, S.; Naponelli, V. The Potential of Epigallocatechin Gallate (EGCG) in Targeting Autophagy for Cancer Treatment: A Narrative Review. *Int. J. Mol. Sci.* **2022**, *23*, 6075. [CrossRef]
88. Shankar, S.; Suthakar, G.; Srivastava, R.K. Epigallocatechin-3-gallate inhibits cell cycle and induces apoptosis in pancreatic cancer. *Front. Biosci.* **2007**, *12*, 5039–5051. [CrossRef] [PubMed]
89. Qin, J.; Fu, M.; Wang, J.; Huang, F.; Liu, H.; Huangfu, M.; Yu, D.; Liu, H.; Li, X.; Guan, X.; et al. PTEN/AKT/mTOR signaling mediates anticancer effects of epigallocatechin-3-gallate in ovarian cancer. *Oncol. Rep.* **2020**, *43*, 1885–1896. [CrossRef]
90. Yin, Z.; Li, J.; Kang, L.; Liu, X.; Luo, J.; Zhang, L.; Li, Y.; Cai, J. Epigallocatechin-3-gallate induces autophagy-related apoptosis associated with LC3B II and Beclin expression of bladder cancer cells. *J. Food Biochem.* **2021**, *45*, e13758. [CrossRef]
91. Yoshida, J.; Ohishi, T.; Abe, H.; Ohba, S.I.; Inoue, H.; Usami, I.; Amemiya, M.; Oriez, R.; Sakashita, C.; Dan, S.; et al. Mitochondrial complex I inhibitors suppress tumor growth through concomitant acidification of the intra- and extracellular environment. *iScience* **2021**, *24*, 103497. [CrossRef] [PubMed]
92. Schockel, L.; Glasauer, A.; Basit, F.; Bitschar, K.; Truong, H.; Erdmann, G.; Algire, C.; Hagebarth, A.; Willems, P.H.; Kopitz, C.; et al. Targeting mitochondrial complex I using BAY 87-2243 reduces melanoma tumor growth. *Cancer Metab.* **2015**, *3*, 11. [CrossRef] [PubMed]
93. Dong, L.F.; Jameson, V.J.; Tilly, D.; Cerny, J.; Mahdavian, E.; Marin-Hernandez, A.; Hernandez-Esquivel, L.; Rodriguez-Enriquez, S.; Stursa, J.; Witting, P.K.; et al. Mitochondrial targeting of vitamin E succinate enhances its pro-apoptotic and anti-cancer activity via mitochondrial complex II. *J. Biol. Chem.* **2011**, *286*, 3717–3728. [CrossRef]
94. Cheng, G.; Hardy, M.; Topchyan, P.; Zander, R.; Volberding, P.; Cui, W.; Kalyanaraman, B. Potent inhibition of tumour cell proliferation and immunoregulatory function by mitochondria-targeted atovaquone. *Sci. Rep.* **2020**, *10*, 17872. [CrossRef]
95. Zhang, Y.; Luo, T.; Ding, X.; Chang, Y.; Liu, C.; Zhang, Y.; Hao, S.; Yin, Q.; Jiang, B. Inhibition of mitochondrial complex III induces differentiation in acute myeloid leukemia. *Biochem. Biophys. Res. Commun.* **2021**, *547*, 162–168. [CrossRef]
96. Reisbeck, L.; Linder, B.; Tascher, G.; Bozkurt, S.; Weber, K.J.; Herold-Mende, C.; van Wijk, S.J.L.; Marschalek, R.; Schaefer, L.; Munch, C.; et al. The iron chelator and OXPHOS inhibitor VLX600 induces mitophagy and an autophagy-dependent type of cell death in glioblastoma cells. *Am. J. Physiol. Cell Physiol.* **2023**, *325*, C1451–C1469. [CrossRef]
97. Wang, Y.; Hou, Q.; Xiao, G.; Yang, S.; Di, C.; Si, J.; Zhou, R.; Ye, Y.; Zhang, Y.; Zhang, H. Selective ATP hydrolysis inhibition in F1Fo ATP synthase enhances radiosensitivity in non-small-cell lung cancer cells (A549). *Oncotarget* **2017**, *8*, 53602–53612. [CrossRef] [PubMed]
98. Davis, R.T.; Blake, K.; Ma, D.; Gabra, M.B.I.; Hernandez, G.A.; Phung, A.T.; Yang, Y.; Maurer, D.; Lefebvre, A.; Alshetaiwi, H.; et al. Transcriptional diversity and bioenergetic shift in human breast cancer metastasis revealed by single-cell RNA sequencing. *Nat. Cell Biol.* **2020**, *22*, 310–320. [CrossRef]
99. He, J.D.; Wang, Z.; Li, S.P.; Xu, Y.J.; Yu, Y.; Ding, Y.J.; Yu, W.L.; Zhang, R.X.; Zhang, H.M.; Du, H.Y. Vitexin suppresses autophagy to induce apoptosis in hepatocellular carcinoma via activation of the JNK signaling pathway. *Oncotarget* **2016**, *7*, 84520–84532. [CrossRef]
100. Song, L.; Wang, Z.; Wang, Y.; Guo, D.; Yang, J.; Chen, L.; Tan, N. Natural Cyclopeptide RA-XII, a New Autophagy Inhibitor, Suppresses Protective Autophagy for Enhancing Apoptosis through AMPK/mTOR/P70S6K Pathways in HepG2 Cells. *Molecules* **2017**, *22*, 1934. [CrossRef]
101. Zhang, X.; Wang, H.; Yu, M.; Ma, K.; Ning, L. Inhibition of autophagy by 3-methyladenine promotes migration and invasion of colon cancer cells through epithelial mesenchymal transformation. *Transl. Cancer Res.* **2022**, *11*, 2834–2842. [CrossRef] [PubMed]
102. Wang, M.; Huang, C.; Su, Y.; Yang, C.; Xia, Q.; Xu, D.J. Astragaloside II sensitizes human hepatocellular carcinoma cells to 5-fluorouracil via suppression of autophagy. *J. Pharm. Pharmacol.* **2017**, *69*, 743–752. [CrossRef] [PubMed]

103. Yuan, N.; Song, L.; Zhang, S.; Lin, W.; Cao, Y.; Xu, F.; Fang, Y.; Wang, Z.; Zhang, H.; Li, X.; et al. Bafilomycin A1 targets both autophagy and apoptosis pathways in pediatric B-cell acute lymphoblastic leukemia. *Haematologica* **2015**, *100*, 345–356. [CrossRef] [PubMed]
104. Pasquier, B. SAR405, a PIK3C3/Vps34 inhibitor that prevents autophagy and synergizes with MTOR inhibition in tumor cells. *Autophagy* **2015**, *11*, 725–726. [CrossRef]
105. Petroni, G.; Bagni, G.; Iorio, J.; Duranti, C.; Lottini, T.; Stefanini, M.; Kragol, G.; Becchetti, A.; Arcangeli, A. Clarithromycin inhibits autophagy in colorectal cancer by regulating the hERG1 potassium channel interaction with PI3K. *Cell Death Dis.* **2020**, *11*, 161. [CrossRef]
106. Liu, M.; Bamodu, O.A.; Huang, W.C.; Zucha, M.A.; Lin, Y.K.; Wu, A.T.H.; Huang, C.C.; Lee, W.H.; Yuan, C.C.; Hsiao, M.; et al. 4-Acetylantroquinonol B suppresses autophagic flux and improves cisplatin sensitivity in highly aggressive epithelial cancer through the PI3K/Akt/mTOR/p70S6K signaling pathway. *Toxicol. Appl. Pharmacol.* **2017**, *325*, 48–60. [CrossRef]
107. Liu, Y.; Hao, Y.; Li, Y.; Zheng, Y.; Dai, J.; Zhong, F.; Wei, W.; Fang, Z. Salinomycin induces autophagic cell death in salinomycin-sensitive melanoma cells through inhibition of autophagic flux. *Sci. Rep.* **2020**, *10*, 18515. [CrossRef] [PubMed]
108. Bai, Z.; Ding, N.; Ge, J.; Wang, Y.; Wang, L.; Wu, N.; Wei, Q.; Xu, S.; Liu, X.; Zhou, G. Esomeprazole overcomes paclitaxel-resistance and enhances anticancer effects of paclitaxel by inducing autophagy in A549/Taxol cells. *Cell Biol. Int.* **2021**, *45*, 177–187. [CrossRef]
109. Zai, W.; Chen, W.; Han, Y.; Wu, Z.; Fan, J.; Zhang, X.; Luan, J.; Tang, S.; Jin, X.; Fu, X.; et al. Targeting PARP and autophagy evoked synergistic lethality in hepatocellular carcinoma. *Carcinogenesis* **2020**, *41*, 345–357. [CrossRef]
110. Li, Y.; Zhang, J.; Ma, H.; Chen, X.; Liu, T.; Jiao, Z.; He, W.; Wang, F.; Liu, X.; Zeng, X. Protective role of autophagy in matrine-induced gastric cancer cell death. *Int. J. Oncol.* **2013**, *42*, 1417–1426. [CrossRef]
111. Sun, X.; Li, L.; Ma, H.G.; Sun, P.; Wang, Q.L.; Zhang, T.T.; Shen, Y.M.; Zhu, W.M.; Li, X. Bisindolylmaleimide alkaloid BMA-155Cl induces autophagy and apoptosis in human hepatocarcinoma HepG-2 cells through the NF-kappaB p65 pathway. *Acta Pharmacol. Sin.* **2017**, *38*, 524–538. [CrossRef]
112. Morselli, E.; Marino, G.; Bennetzen, M.V.; Eisenberg, T.; Megalou, E.; Schroeder, S.; Cabrera, S.; Benit, P.; Rustin, P.; Criollo, A.; et al. Spermidine and resveratrol induce autophagy by distinct pathways converging on the acetylproteome. *J. Cell Biol.* **2011**, *192*, 615–629. [CrossRef] [PubMed]
113. Wang, Y.; Nie, H.; Zhao, X.; Qin, Y.; Gong, X. Bicyclol induces cell cycle arrest and autophagy in HepG2 human hepatocellular carcinoma cells through the PI3K/AKT and Ras/Raf/MEK/ERK pathways. *BMC Cancer* **2016**, *16*, 742. [CrossRef] [PubMed]
114. Gao, L.; Lv, G.; Li, R.; Liu, W.T.; Zong, C.; Ye, F.; Li, X.Y.; Yang, X.; Jiang, J.H.; Hou, X.J.; et al. Glycochenodeoxycholate promotes hepatocellular carcinoma invasion and migration by AMPK/mTOR dependent autophagy activation. *Cancer Lett.* **2019**, *454*, 215–223. [CrossRef]
115. Chen, Y.J.; Fang, L.W.; Su, W.C.; Hsu, W.Y.; Yang, K.C.; Huang, H.L. Lapatinib induces autophagic cell death and differentiation in acute myeloblastic leukemia. *OncoTargets Ther.* **2016**, *9*, 4453–4464. [CrossRef]
116. Yu, H.; Qiu, Y.; Pang, X.; Li, J.; Wu, S.; Yin, S.; Han, L.; Zhang, Y.; Jin, C.; Gao, X.; et al. Lycorine Promotes Autophagy and Apoptosis via TCRP1/Akt/mTOR Axis Inactivation in Human Hepatocellular Carcinoma. *Mol. Cancer Ther.* **2017**, *16*, 2711–2723. [CrossRef]
117. Lin, C.; Tsai, S.C.; Tseng, M.T.; Peng, S.F.; Kuo, S.C.; Lin, M.W.; Hsu, Y.M.; Lee, M.R.; Amagaya, S.; Huang, W.W.; et al. AKT serine/threonine protein kinase modulates baicalin-triggered autophagy in human bladder cancer T24 cells. *Int. J. Oncol.* **2013**, *42*, 993–1000. [CrossRef]
118. Zhou, J.; Farah, B.L.; Sinha, R.A.; Wu, Y.; Singh, B.K.; Bay, B.H.; Yang, C.S.; Yen, P.M. Epigallocatechin-3-gallate (EGCG), a green tea polyphenol, stimulates hepatic autophagy and lipid clearance. *PLoS ONE* **2014**, *9*, e87161. [CrossRef] [PubMed]
119. D'Aguanno, S.; Brignone, M.; Scalera, S.; Chiacchiarini, M.; Di Martile, M.; Valentini, E.; De Nicola, F.; Ricci, A.; Pelle, F.; Botti, C.; et al. Bcl-2 dependent modulation of Hippo pathway in cancer cells. *Cell Commun. Signal* **2024**, *22*, 277. [CrossRef]
120. Bruzzese, A.; Martino, E.A.; Labanca, C.; Mendicino, F.; Lucia, E.; Olivito, V.; Neri, A.; Morabito, F.; Vigna, E.; Gentile, M. Potential of BGB-11417, a BCL2 inhibitor, in hematological malignancies. *Expert. Opin. Investig. Drugs* **2024**, *33*, 73–77. [CrossRef]
121. Alencar, A.J.; Roeker, L.E.; Hoffmann, M.; Murthy, G.S.G.; Patel, V.; Ku, N.C.; Pauff, J.M.; Eyre, T.A.; Jurczak, W.; Le Gouill, S. A First-in-Human Phase 1 Study of Oral LOXO-338, a Selective BCL2 Inhibitor, in Patients with Advanced Hematologic Malignancies (Trial in Progress). *Blood* **2021**, *138*, 2424. [CrossRef]
122. Li, J.; Hu, N.; Zhang, Y.; Yang, X.; Deng, M.; Gong, W.; Yin, L.; Liu, Y.; Gao, Y.; Wei, W.; et al. Abstract 6158: BGB-24714, a novel oral IAP antagonist, displayed significant anti-tumor activities in preclinical models as a monotherapy and in combination with paclitaxel. *Cancer Res.* **2023**, *83*, 6158. [CrossRef]
123. Bourhis, J.; Burtness, B.; Licitra, L.F.; Nutting, C.; Schoenfeld, J.D.; Omar, M.; Bouisset, F.; Nauwelaerts, H.; Urfer, Y.; Zanna, C.; et al. Xevinapant or placebo plus chemoradiotherapy in locally advanced squamous cell carcinoma of the head and neck: TrilynX phase III study design. *Future Oncol.* **2022**, *18*, 1669–1678. [CrossRef]
124. Hurrish, K.H.; Su, Y.; Patel, S.; Ramage, C.L.; Zhao, J.; Temby, B.R.; Carter, J.L.; Edwards, H.; Buck, S.A.; Wiley, S.E.; et al. Enhancing anti-AML activity of venetoclax by isoflavone ME-344 through suppression of OXPHOS and/or purine biosynthesis in vitro. *Biochem. Pharmacol.* **2024**, *220*, 115981. [CrossRef]
125. Kumar, A.; Corey, C.; Scott, I.; Shiva, S.; D'Cunha, J. Minnelide/Triptolide Impairs Mitochondrial Function by Regulating SIRT3 in P53-Dependent Manner in Non-Small Cell Lung Cancer. *PLoS ONE* **2016**, *11*, e0160783. [CrossRef]

126. Benej, M.; Hong, X.; Vibhute, S.; Scott, S.; Wu, J.; Graves, E.; Le, Q.T.; Koong, A.C.; Giaccia, A.J.; Yu, B.; et al. Papaverine and its derivatives radiosensitize solid tumors by inhibiting mitochondrial metabolism. *Proc. Natl. Acad. Sci. USA* **2018**, *115*, 10756–10761. [CrossRef]
127. Rodriguez-Berriguete, G.; Puliyadi, R.; Machado, N.; Barberis, A.; Prevo, R.; McLaughlin, M.; Buffa, F.M.; Harrington, K.J.; Higgins, G.S. Antitumour effect of the mitochondrial complex III inhibitor Atovaquone in combination with anti-PD-L1 therapy in mouse cancer models. *Cell Death Dis.* **2024**, *15*, 32. [CrossRef] [PubMed]
128. Omuro, A.; Beal, K.; McNeill, K.; Young, R.J.; Thomas, A.; Lin, X.; Terziev, R.; Kaley, T.J.; DeAngelis, L.M.; Daras, M.; et al. Multicenter Phase IB Trial of Carboxyamidotriazole Orotate and Temozolomide for Recurrent and Newly Diagnosed Glioblastoma and Other Anaplastic Gliomas. *J. Clin. Oncol.* **2018**, *36*, 1702–1709. [CrossRef]
129. Zachar, Z.; Marecek, J.; Maturo, C.; Gupta, S.; Stuart, S.D.; Howell, K.; Schauble, A.; Lem, J.; Piramzadian, A.; Karnik, S.; et al. Non-redox-active lipoate derivates disrupt cancer cell mitochondrial metabolism and are potent anticancer agents in vivo. *J. Mol. Med.* **2011**, *89*, 1137–1148. [CrossRef]
130. Abou-Alfa, G.K.; Macarulla, T.; Javle, M.M.; Kelley, R.K.; Lubner, S.J.; Adeva, J.; Cleary, J.M.; Catenacci, D.V.; Borad, M.J.; Bridgewater, J.; et al. Ivosidenib in IDH1-mutant, chemotherapy-refractory cholangiocarcinoma (ClarIDHy): A multicentre, randomised, double-blind, placebo-controlled, phase 3 study. *Lancet Oncol.* **2020**, *21*, 796–807. [CrossRef]
131. Thol, F.; Ganser, A. Treatment of Relapsed Acute Myeloid Leukemia. *Curr. Treat. Options Oncol.* **2020**, *21*, 66. [CrossRef]
132. Schoenmann, N.; Tannenbaum, N.; Hodgeman, R.M.; Raju, R.P. Regulating mitochondrial metabolism by targeting pyruvate dehydrogenase with dichloroacetate, a metabolic messenger. *Biochim. Biophys. Acta Mol. Basis Dis.* **2023**, *1869*, 166769. [CrossRef] [PubMed]
133. Manic, G.; Obrist, F.; Kroemer, G.; Vitale, I.; Galluzzi, L. Chloroquine and hydroxychloroquine for cancer therapy. *Mol. Cell. Oncol.* **2014**, *1*, e29911. [CrossRef]
134. Zhang, T.; Wang, X.; He, D.; Jin, X.; Guo, P. Metformin sensitizes human bladder cancer cells to TRAIL-induced apoptosis through mTOR/S6K1-mediated downregulation of c-FLIP. *Anticancer Drugs* **2014**, *25*, 887–897. [CrossRef] [PubMed]
135. Pan, Q.; Yang, G.L.; Yang, J.H.; Lin, S.L.; Liu, N.; Liu, S.S.; Liu, M.Y.; Zhang, L.H.; Huang, Y.R.; Shen, R.L.; et al. Metformin can block precancerous progression to invasive tumors of bladder through inhibiting STAT3-mediated signaling pathways. *J. Exp. Clin. Cancer Res.* **2015**, *34*, 77. [CrossRef] [PubMed]
136. Agius, L.; Ford, B.E.; Chachra, S.S. The Metformin Mechanism on Gluconeogenesis and AMPK Activation: The Metabolite Perspective. *Int. J. Mol. Sci.* **2020**, *21*, 3240. [CrossRef]
137. Schulze, M.; Stock, C.; Zaccagnini, M.; Teber, D.; Rassweiler, J.J. Temsirolimus. *Recent. Results Cancer Res.* **2014**, *201*, 393–403. [CrossRef]
138. Benjamin, D.; Colombi, M.; Moroni, C.; Hall, M.N. Rapamycin passes the torch: A new generation of mTOR inhibitors. *Nat. Rev. Drug Discov.* **2011**, *10*, 868–880. [CrossRef]
139. Hasskarl, J. Everolimus. *Recent. Results Cancer Res.* **2018**, *211*, 101–123. [CrossRef]
140. Saran, U.; Foti, M.; Dufour, J.F. Cellular and molecular effects of the mTOR inhibitor everolimus. *Clin. Sci.* **2015**, *129*, 895–914. [CrossRef]
141. Sharifi-Rad, M.; Pezzani, R.; Redaelli, M.; Zorzan, M.; Imran, M.; Ahmed Khalil, A.; Salehi, B.; Sharopov, F.; Cho, W.C.; Sharifi-Rad, J. Preclinical Pharmacological Activities of Epigallocatechin-3-gallate in Signaling Pathways: An Update on Cancer. *Molecules* **2020**, *25*, 467. [CrossRef]
142. Zhang, S.; Cao, M.; Fang, F. The Role of Epigallocatechin-3-Gallate in Autophagy and Endoplasmic Reticulum Stress (ERS)-Induced Apoptosis of Human Diseases. *Med. Sci. Monit.* **2020**, *26*, e924558. [CrossRef]
143. Zhao, B.; Luo, J.; Yu, T.; Zhou, L.; Lv, H.; Shang, P. Anticancer mechanisms of metformin: A review of the current evidence. *Life Sci.* **2020**, *254*, 117717. [CrossRef] [PubMed]
144. Wang, X.Y.; Wang, Y.J.; Guo, B.W.; Hou, Z.L.; Zhang, G.X.; Han, Z.; Liu, Q.; Yao, G.D.; Song, S.J. 13-Oxyingenol-dodecanoate inhibits the growth of non-small cell lung cancer cells by targeting ULK1. *Bioorg. Chem.* **2024**, *147*, 107367. [CrossRef]
145. Formisano, L.; Napolitano, F.; Rosa, R.; D'Amato, V.; Servetto, A.; Marciano, R.; De Placido, P.; Bianco, C.; Bianco, R. Mechanisms of resistance to mTOR inhibitors. *Crit. Rev. Oncol. Hematol.* **2020**, *147*, 102886. [CrossRef] [PubMed]
146. Low, L.E.; Kong, C.K.; Yap, W.H.; Siva, S.P.; Gan, S.H.; Siew, W.S.; Ming, L.C.; Lai-Foenander, A.S.; Chang, S.K.; Lee, W.L.; et al. Hydroxychloroquine: Key therapeutic advances and emerging nanotechnological landscape for cancer mitigation. *Chem. Biol. Interact.* **2023**, *386*, 110750. [CrossRef] [PubMed]
147. Du, W.; Xu, A.; Huang, Y.; Cao, J.; Zhu, H.; Yang, B.; Shao, X.; He, Q.; Ying, M. The role of autophagy in targeted therapy for acute myeloid leukemia. *Autophagy* **2021**, *17*, 2665–2679. [CrossRef]
148. Cao, Q.; Wu, X.; Zhang, Q.; Gong, J.; Chen, Y.; You, Y.; Shen, J.; Qiang, Y.; Cao, G. Mechanisms of action of the BCL-2 inhibitor venetoclax in multiple myeloma: A literature review. *Front. Pharmacol.* **2023**, *14*, 1291920. [CrossRef]
149. Zarei, M.; Hue, J.J.; Hajihassani, O.; Graor, H.J.; Katayama, E.S.; Loftus, A.W.; Bajor, D.; Rothermel, L.D.; Vaziri-Gohar, A.; Winter, J.M. Clinical development of IDH1 inhibitors for cancer therapy. *Cancer Treat. Rev.* **2022**, *103*, 102334. [CrossRef]
150. Tang, D.Y.; Ellis, R.A.; Lovat, P.E. Prognostic Impact of Autophagy Biomarkers for Cutaneous Melanoma. *Front. Oncol.* **2016**, *6*, 236. [CrossRef]
151. Zhang, L.; Liu, Y.; Xu, Y.; Wu, H.; Wei, Z.; Cao, Y. The expression of the autophagy gene beclin-1 mRNA and protein in ectopic and eutopic endometrium of patients with endometriosis. *Int. J. Fertil. Steril.* **2015**, *8*, 429–436. [CrossRef]

152. Cheng, Y.; Qi, F.; Li, L.; Qin, Z.; Li, X.; Wang, X. Autophagy-related genes are potential diagnostic and prognostic biomarkers in prostate cancer. *Transl. Androl. Urol.* **2020**, *9*, 2616–2628. [CrossRef]
153. Huang, G.Z.; Lu, Z.Y.; Rao, Y.; Gao, H.; Lv, X.Z. Screening and identification of autophagy-related biomarkers for oral squamous cell carcinoma (OSCC) via integrated bioinformatics analysis. *J. Cell Mol. Med.* **2021**, *25*, 4444–4454. [CrossRef]
154. Cao, Q.H.; Liu, F.; Yang, Z.L.; Fu, X.H.; Yang, Z.H.; Liu, Q.; Wang, L.; Wan, X.B.; Fan, X.J. Prognostic value of autophagy related proteins ULK1, Beclin 1, ATG3, ATG5, ATG7, ATG9, ATG10, ATG12, LC3B and p62/SQSTM1 in gastric cancer. *Am. J. Transl. Res.* **2016**, *8*, 3831–3847.
155. Meng, D.; Jin, H.; Zhang, X.; Yan, W.; Xia, Q.; Shen, S.; Xie, S.; Cui, M.; Ding, B.; Gu, Y.; et al. Identification of autophagy-related risk signatures for the prognosis, diagnosis, and targeted therapy in cervical cancer. *Cancer Cell Int.* **2021**, *21*, 362. [CrossRef]
156. Feng, Q.; Wang, J.; Cui, N.; Liu, X.; Wang, H. Autophagy-related long non-coding RNA signature for potential prognostic biomarkers of patients with cervical cancer: A study based on public databases. *Ann. Transl. Med.* **2021**, *9*, 1668. [CrossRef]
157. Lin, W.; Sun, Y.; Qiu, X.; Huang, Q.; Kong, L.; Lu, J.J. VMP1, a novel prognostic biomarker, contributes to glioma development by regulating autophagy. *J. Neuroinflamm.* **2021**, *18*, 165. [CrossRef]
158. Zhou, C.; Li, A.H.; Liu, S.; Sun, H. Identification of an 11-Autophagy-Related-Gene Signature as Promising Prognostic Biomarker for Bladder Cancer Patients. *Biology* **2021**, *10*, 375. [CrossRef]
159. Du, H.; Xie, S.; Guo, W.; Che, J.; Zhu, L.; Hang, J.; Li, H. Development and validation of an autophagy-related prognostic signature in esophageal cancer. *Ann. Transl. Med.* **2021**, *9*, 317. [CrossRef]
160. Mustafa, M.F.; Saliluddin, S.M.; Fakurazi, S.; Laim, N.M.S.T.; Pauzi, S.H.M.; Yahya, N.H.N.; Gopal, N.S.R.; Abdullah, M.A.; Maniam, S. Expression of Autophagy and Mitophagy Markers in Breast Cancer Tissues. *Front. Oncol.* **2021**, *11*, 612009. [CrossRef]
161. Yang, J.; Wang, C.; Zhang, Y.; Cheng, S.; Wu, M.; Gu, S.; Xu, S.; Wu, Y.; Wang, Y. A novel autophagy-related gene signature associated with prognosis and immune microenvironment in ovarian cancer. *J. Ovarian Res.* **2023**, *16*, 86. [CrossRef] [PubMed]
162. Qiu, Y.H.; Zhang, T.S.; Wang, X.W.; Wang, M.Y.; Zhao, W.X.; Zhou, H.M.; Zhang, C.H.; Cai, M.L.; Chen, X.F.; Zhao, W.L.; et al. Mitochondria autophagy: A potential target for cancer therapy. *J. Drug Target.* **2021**, *29*, 576–591. [CrossRef] [PubMed]
163. Yun, C.W.; Lee, S.H. The Roles of Autophagy in Cancer. *Int. J. Mol. Sci.* **2018**, *19*, 3466. [CrossRef]
164. Mohsen, S.; Sobash, P.T.; Algwaiz, G.F.; Nasef, N.; Al-Zeidaneen, S.A.; Karim, N.A. Autophagy Agents in Clinical Trials for Cancer Therapy: A Brief Review. *Curr. Oncol.* **2022**, *29*, 1695–1708. [CrossRef]

International Journal of *Molecular Sciences*

IMPACT FACTOR 4.9 | Indexed in: PubMed | CITESCORE 8.1

Article

Low-Dose Salinomycin Alters Mitochondrial Function and Reprograms Global Metabolism in Burkitt Lymphoma

Aleksandra Zdanowicz, Oleksandr Ilchenko, Andrzej Ciechanowicz, Haoyu Chi, Marta Struga and Beata Pyrzynska

Special Issue
Oxidative Stress and Mitochondria in Human Diseases
Edited by
Dr. Alejandra Espinosa

MDPI

https://doi.org/10.3390/ijms26115125

International Journal of
Molecular Sciences

MDPI

Article

Low-Dose Salinomycin Alters Mitochondrial Function and Reprograms Global Metabolism in Burkitt Lymphoma

Aleksandra Zdanowicz [1,2], Oleksandr Ilchenko [3,4], Andrzej Ciechanowicz [5], Haoyu Chi [6,7], Marta Struga [1] and Beata Pyrzynska [1,*]

1 Department of Biochemistry, Medical University of Warsaw, Banacha 1 Str., 02-097 Warsaw, Poland
2 Doctoral School, Medical University of Warsaw, Zwirki i Wigury 81 Str., 02-091 Warsaw, Poland
3 Department of Forest Genetics and Plant Physiology, Umeå Plant Science Centre, Swedish University of Agricultural Sciences, Skogsmarksgränd 17, 90183 Umea, Sweden; oleksandr.ilchenko@slu.se
4 Department of Chemistry, Umeå University, Linnaeus väg 10B, 90187 Umea, Sweden
5 Department of Regenerative Medicine, Center for Preclinical Research and Technology, Medical University of Warsaw, Banacha 1B Str., 02-097 Warsaw, Poland
6 Department of Cell and Developmental Biology, University College London, Gower Street, London WC1E 6BT, UK
7 Consortium for Mitochondrial Research, University College London, Gower Street, London WC1E 6BT, UK
* Correspondence: beata.pyrzynska@wum.edu.pl

Abstract: Salinomycin (SAL), originally identified for its potent antibacterial properties, has recently garnered attention for its remarkable activity against a variety of cancer types. Beyond its direct cytotoxic effects on cancer cells, SAL can also enhance the efficacy of anti-CD20 immunotherapy in B-cell malignancies, both *in vitro* and *in vivo*. Despite these promising findings, the precise molecular mechanisms underlying SAL's anticancer action remain poorly understood. Here, we demonstrate that even at low concentrations (0.25–0.5 mM), SAL disrupts mitochondrial membrane potential and induces oxidative stress in Burkitt lymphoma. Further investigations uncovered that SAL shifts cellular metabolism from mitochondrial respiration to aerobic glycolysis. Additionally, metabolomic profiling identified SAL-induced arginine depletion as a key metabolic alteration. These findings provide new insights into SAL's multifaceted mechanisms of action and support its potential as an adjunctive therapy in cancer treatment.

Keywords: salinomycin; mitochondria; mitochondrial respiration; oxidative stress; metabolomics

Academic Editor: Consolato M. Sergi

Received: 25 April 2025
Revised: 20 May 2025
Accepted: 23 May 2025
Published: 27 May 2025

Citation: Zdanowicz, A.; Ilchenko, O.; Ciechanowicz, A.; Chi, H.; Struga, M.; Pyrzynska, B. Low-Dose Salinomycin Alters Mitochondrial Function and Reprograms Global Metabolism in Burkitt Lymphoma. *Int. J. Mol. Sci.* **2025**, *26*, 5125. https://doi.org/10.3390/ijms26115125

1. Introduction

Polyether ionophores (cation carriers) constitute a significant class of natural compounds, capable of the selective binding and transporting of cations across cellular lipid membranes [1]. Among polyether ionophores, salinomycin (SAL) is the most extensively studied. Originally isolated from *Streptomyces albus*, it has been widely used as an anticoccidial and antibacterial agent against Gram-positive bacteria in veterinary medicine [2,3].

In a 2009 study, Gupta et al. were the first to demonstrate that SAL exhibited anticancer properties and a significantly greater potency and selectivity against breast cancer stem cells (CSCs) than conventional chemotherapeutic agents [4]. Since then, it has been demonstrated that SAL exhibits multi-targeted anticancer activity across diverse malignancies. In hepatocellular carcinoma, it induces cell cycle arrest in a cell line-dependent manner, causing G0/G1-phase arrest in HepG2 cells, while inducing G2/M-phase arrest in SMMC-7721 and BEL-7402 cells [5]. In colorectal cancer, SAL effectively suppresses

tumor proliferation via inhibition of the Wnt/β-catenin signaling pathway [6]. In both prostate (PC3 cell line) and breast cancer cells (SKBR3 and MDAMB468), SAL modulates the mitochondrial dynamic and promotes mitophagy [7].

Further studies have revealed that SAL overcomes multidrug resistance in cisplatin-resistant ovarian cancer cells (A2780cis) by enhancing apoptosis through the upregulation of DR5 (death receptor-5), caspase-8, and FADD (Fas-associated protein with death domain) [8]. Additionally, SAL sensitizes radiation-treated breast cancer cells (Hs578T) by increasing DNA damage and inducing G2 arrest [9].

Our recent studies have shown that SAL not only possesses direct anticancer effects but also enhances the effectiveness of anti-CD20 immunotherapy by upregulating the surface CD20 antigen on malignant B-cells, as demonstrated in both *in vitro* and *in vivo* models [10]. B-cell malignancies—including diffuse large B-cell lymphoma (DLBCL), Burkitt lymphoma, follicular lymphoma, and high-grade B-cell lymphoma—are commonly treated with anti-CD20 monoclonal antibody therapy (e.g., rituximab, ofatumumab, obinutuzumab) in combination with chemotherapy [11]. However, treatment efficacy is often hindered by variable CD20 expression across different B-cell malignancy subtypes and among individual patients [12]. Notably, SAL shows promise for the upregulation of low CD20 levels in B-cell malignancies, offering a potential strategy to enhance target antigen expression and improve therapeutic outcomes [10]. While SAL demonstrates therapeutic potential in B-cell malignancies, its precise molecular mechanisms remain incompletely characterized.

Despite its diverse anticancer properties, concerns have been raised regarding its potential toxicity. In 2004, a 35-year-old patient reported experiencing nausea, tachycardia, and muscle pain following the accidental inhalation of SAL [13]. However, a pilot clinical trial involving patients with ovarian, head and neck, and metastatic breast cancers revealed that SAL administered intravenously at doses of 200–250 μg/kg every other day over three weeks led to the regression of metastatic lesions. Acute side effects were infrequent, and no serious long-term adverse effects were reported [14]. In contrast, subsequent studies have reported dose-dependent toxicity in mammals. For example, weight loss and sensory polyneuropathy were observed in mice at doses exceeding 5 mg/kg [15], while muscular atrophy and ataxia were reported in horses at doses above 0.6 μg/kg [16]. To overcome the potential adverse effects associated with SAL, numerous derivatives of SAL with improved anticancer properties have been synthesized [17,18], and are currently being tested in numerous preclinical models [19]. Boehmerle and Endres (2011) demonstrated that SAL-induced neuro- and myotoxicity is associated with increased cytosolic Na^+ concentrations, which in turn trigger a rise in cytosolic Ca^{2+} levels [20]. Additionally, previous studies have demonstrated SAL's ability to bind both monovalent (K^+, Na^+, Cs^+) and divalent (Fe^{2+}, Ca^{2+}, Mg^{2+}) metal cations [18], with a marked preference for monovalent species, particularly K^+ and Na^+ [17]. SAL forms complexes with these ions, facilitating their transport across lipid bilayer membranes [21]. SAL's transport can occur through electroneutral, electrogenic or bio-mimetic mechanisms, depending on the surrounding environment—whether neutral, slightly alkaline, or acidic [17,22]. The ionophoric activity of SAL dysregulates the physiological Na^+/K^+ balance, alters the intracellular pH, and induces changes in osmotic pressure [17]. In breast CSCs, SAL has been shown to promote iron transport and storage within lysosomes, causing lysosomal membrane destabilization and ultimately triggering ferroptosis, a form of programmed cell death [18,23].

Recent studies have shown that SAL disrupts mitochondrial function in CSC [24], aligning with its well-established cationophoric activity across mitochondrial membranes [25]. In the MDA-MB-453 breast cancer cell line, treatment with 10 μM SAL for 48 h results in a reduction in MMP and a pronounced activation of caspases 3 and 7 [26]. In PC-3 prostate cancer cells, 48 h treatment with SAL (0.45–4 μM) promotes apoptosis through multiple

mitochondrial-associated mechanisms, including enhanced ROS generation, MMP disruption, BAX mitochondrial translocation, the cytosolic accumulation of cytochrome c, PARP-1 cleavage, and caspase-3 activation [27]. In U2OS osteosarcoma cells, treatment with SAL for 12 and 24 h increases ROS production, which in turn activates AMPK signaling and induces autophagy [28]. Proteomic functional enrichment analysis of the breast CSC model (human mammary HMLER CD24low/CD44high), following a 48 h treatment with 0.5 μM SAL, revealed that SAL suppresses the expression of mitochondrial proteins associated with the TCA (tricarboxylic acid) cycle, ETC (electron transport chain), glycolysis, B-oxidation and glutaminolysis [24].

While Managò et al. [29] reported the rapid mitochondrial effects of SAL (10 μM) (within 0–90 min) in B-CLL cells, our study is the first to investigate the impact of prolonged (12–24 h), low-concentration SAL exposure on mitochondrial function and the global remodeling of Burkitt lymphoma cells' metabolism.

2. Results

2.1. SAL Causes Mitochondrial Dysfunction and Induces Oxidative Stress in Burkitt Lymphoma Cells

To assess the effects of SAL on mitochondrial function in Burkitt lymphoma, we treated Raji cells with 0.25 μM, 0.5 μM, or 5 μM SAL for 12 and 36 h. Staining with membrane potential-sensitive fluorescent probes (JC-1 and TMRM), followed by flow cytometry analysis, revealed a significant reduction in mitochondrial membrane potential (MMP) following SAL treatment compared to matched controls (Figure 1A,B and Supplementary Figures S1 and S2). The MMP generated by mitochondrial complexes I, III, and IV reflects the mitochondrion's capacity for ATP production [30]. Based on this, we hypothesize that SAL induces mitochondrial dysfunction.

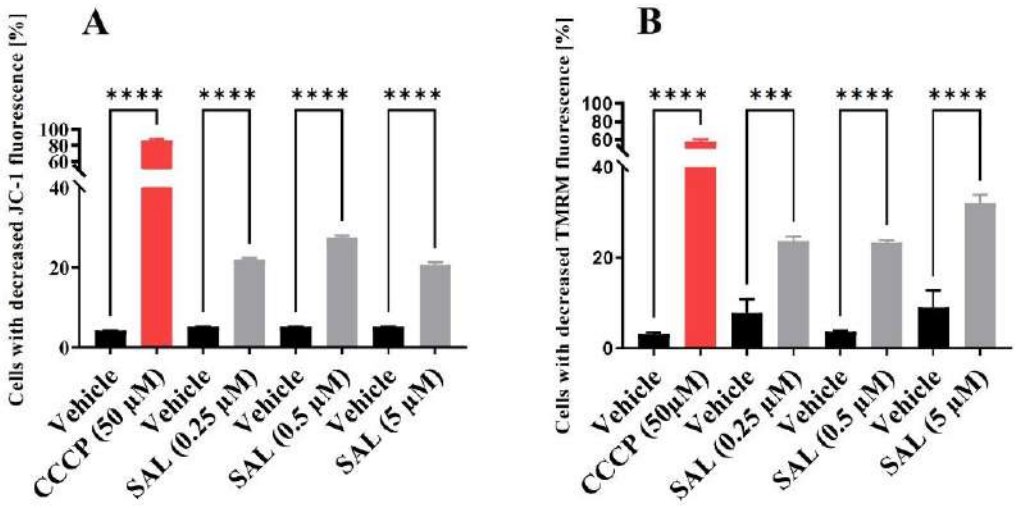

Figure 1. Salinomycin (SAL) reduces mitochondrial membrane potential (MMP) in live Raji cells. (**A**) MMP was assessed using the cationic carbocyanine dye JC-1 after 12 h of SAL treatment at concentrations of 0.25 μM, 0.5 μM, and 5 μM. (**B**) MMP was evaluated using tetramethylrhodamine methyl ester (TMRM) following 36 h of SAL treatment at the same concentrations. A positive control was included by treating cells with 50 μM carbonyl cyanide 3-chlorophenylhydrazone (CCCP) for 1 h. Data are expressed as mean ± SD from three experiments ($n = 3$), and statistical significance was assessed using one-way ANOVA (*** $p < 0.001$, **** $p < 0.0001$).

Given that mitochondrial dysfunction can influence respiratory chain activity and the production of mitochondrial reactive oxygen species (mtROS), we evaluated mtROS levels using MitoSOX Red, a fluorogenic dye that selectively detects superoxide in live mitochondria. Quantitative analysis using flow cytometry revealed a significant increase in the generation of mitochondrial superoxide following treatment with 0.25 µM, 0.5 µM, and 5 µM of SAL (Figure 2A and Supplementary Figure S3). The continuous elevation in mtROS disrupts redox homeostasis, leading to an imbalance between ROS production and the cellular antioxidant defense system [31,32]. To quantify this oxidative stress, we utilized CellROX Green reagent, a fluorogenic probe for live-cell ROS detection. Treatment with 0.25 and 0.5 µM SAL resulted in a significant increase in oxidative stress compared to vehicle-treated controls (Figure 2B and Supplementary Figure S4).

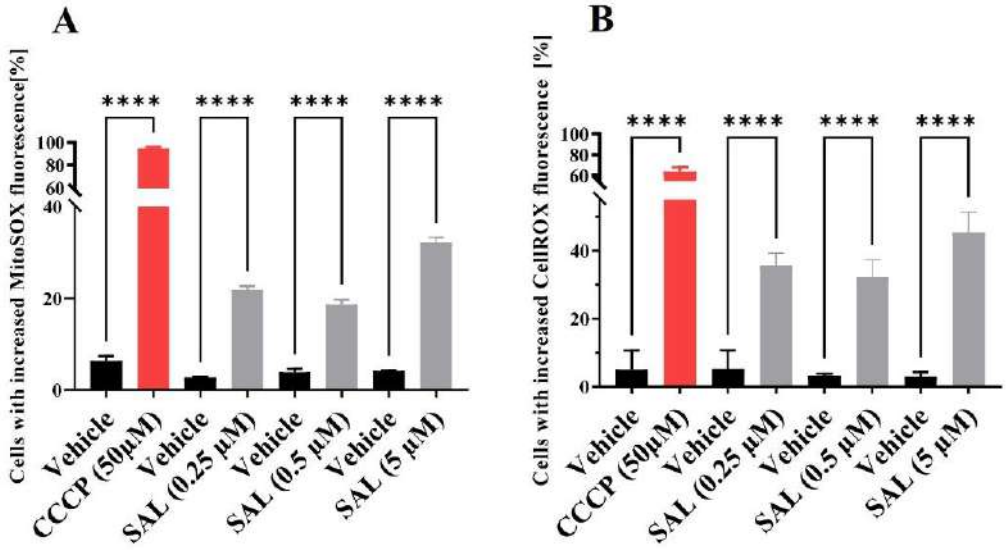

Figure 2. SAL induces the generation of reactive oxygen species (ROS) in Raji cells. (**A**) Mitochondrial superoxide production was detected using MitoSOX dye following 36 h of SAL treatment at concentrations of 0.25 µM, 0.5 µM, and 5 µM. (**B**) Total ROS levels were assessed using CellROX Green reagent after 48 h of SAL treatment at concentrations of 0.25 µM and 0.5 µM. As a positive control, cells were treated with 50 µM CCCP for 1 h. Results are expressed as mean ± SD from three experiments ($n = 3$), and statistical significance was evaluated using one-way ANOVA (**** $p < 0.0001$).

2.2. SAL Suppresses Mitochondrial Respiration and Glycolytic Activity

To directly evaluate mitochondrial dysfunction, we measured oxygen consumption rates (OCRs) using the Seahorse XFe96 extracellular flux analyzer. After 24 h of SAL treatment, both basal and maximal respiratory capacities were significantly reduced (Figure 3A–C), accompanied by a substantial decrease in ATP production (Figure 3D). These findings indicate a profound impairment of mitochondrial oxidative phosphorylation even at the lowest concentration of SAL (0.25 µM).

To examine the impact of SAL on glycolytic flux, we measured the extracellular acidification rate (ECAR). Notably, 24 h treatment with SAL led to significant metabolic reprogramming, as evidenced by a marked increase in basal ECAR at a concentration of 0.25 µM. While the glycolytic reserve remained unchanged at lower concentrations (0.25 µM and 0.5 µM), it was decreased at 5 µM (Figure 4A–C). These findings suggest that SAL suppresses oxidative phosphorylation, while enhancing glycolytic activity, in Burkitt lymphoma cells.

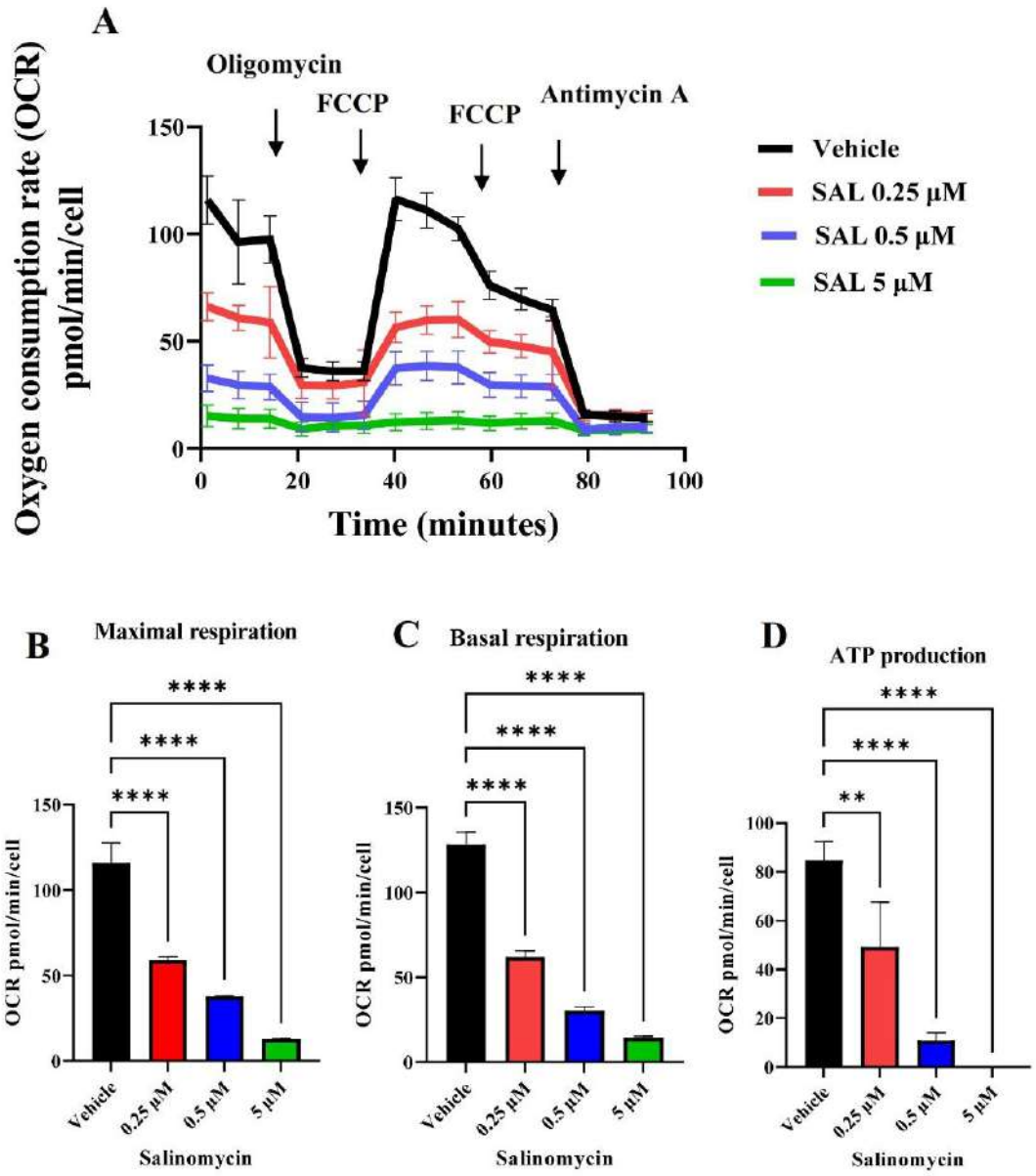

Figure 3. SAL suppresses mitochondrial respiration in Raji cells. (**A**) Oxygen consumption rate (OCR) was measured using a Seahorse XFe96 analyzer, following 24 h-long treatment with 0.25 µM, 0.5 µM, or 5 µM SAL. OCR was assessed under basal conditions and after the sequential addition of oligomycin (2.5 µM), carbonyl cyanide-p-trifluoromethoxyphenylhydrazone (FCCP, 1 µM and 1.5 µM), and antimycin A (2.5 µM). The data concerning maximal respiration (**B**), basal respiration (**C**), and ATP production (**D**) have been extracted from the analysis presented in (**A**). Data were normalized to cell number and represent the mean ± SD from experiments ($n = 3$). Statistical analysis was performed using one-way ANOVA (** $p < 0.01$, **** $p < 0.0001$).

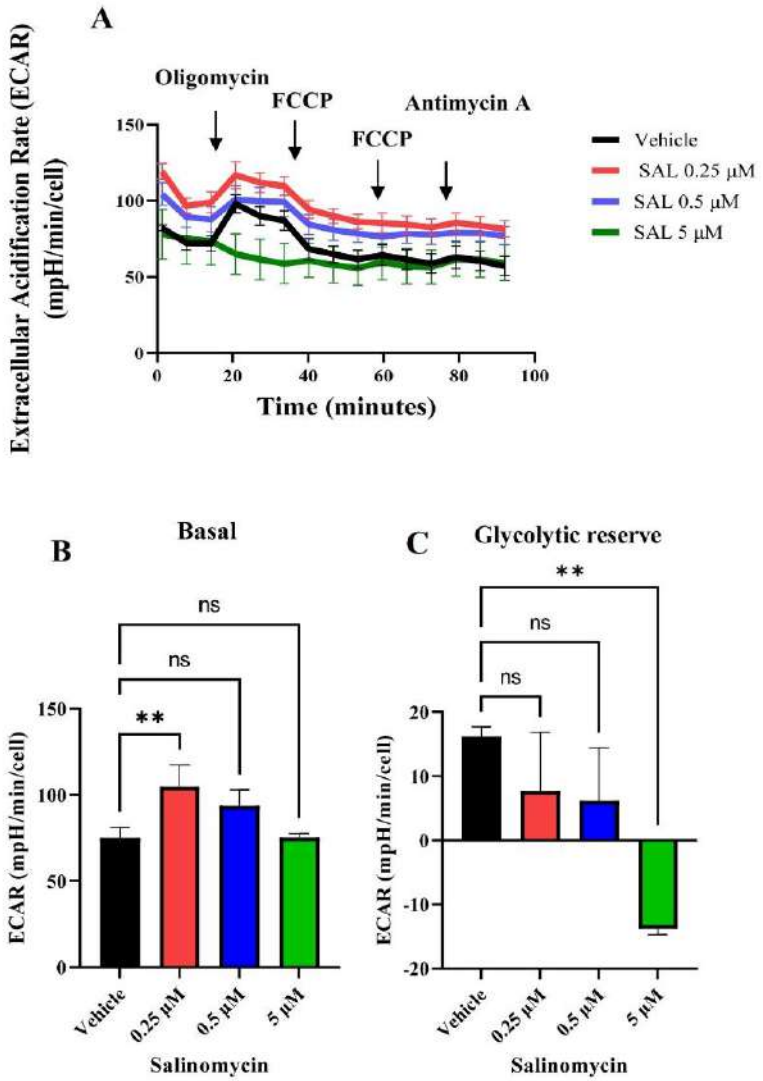

Figure 4. SAL reduces glycolytic activity in Raji cells. (**A**) Extracellular acidification rate (ECAR) was measured using the Seahorse XFe96 analyzer following treatment with 0.25 µM, 0.5 µM, and 5 µM SAL under basal conditions and after sequential injections of oligomycin (2.5 µM), FCCP (1 µM and 1.5 µM), and antimycin A (2.5 µM). (**B**,**C**) Quantification of basal ECAR (**B**) and glycolytic reserve in response to oligomycin (**C**) was extracted from the ECAR profiles shown in (**A**). Data were normalized to cell number and represent the mean ± SD from three experiments ($n = 3$). Statistical analysis was performed using one-way ANOVA (** $p < 0.01$, ns indicates non-significant differences ($p > 0.05$)).

2.3. SAL Reprograms Burkitt Lymphoma Metabolism

Mitochondria play a vital role in cancer cell adaptation and metabolic regulation, especially under stressful conditions [31,33]. To investigate the metabolic alterations associated with SAL-induced mitochondrial dysfunction, we conducted untargeted metabolomic profiling using a SolariX 2xR 7T FT-ICR MS on cells treated with 0.25 µM SAL for 24 h.

This analysis detected 9290 metabolic features—5492 in positive ion mode and 3798 in negative ion mode. Among these, 698 metabolites were annotated (425 in positive mode and 273 in negative mode). After filtering out duplicates and excluding metabolites present in fewer than 30% of samples, 93 metabolites (76 from positive mode and 17 from negative

mode) were retained for further analysis. Although different normalization methods were applied to the dataset, the subsequent analysis focused solely on the Pareto-normalized data. The Pareto-normalized dataset exhibits a kurtosis of 2.65 and a skewness of −0.49, with a coefficient of determination (R^2) fitted to a Gaussian distribution of 0.884 and 2.15% of significant *p*-values from the one-sample Kolmogorov–Smirnov test.

An OPLS-DA (Orthogonal Partial Least Squares Discriminant Analysis) model, along with PCA (Principal Component Analysis), was applied to compare the metabolomic profiles of SAL-treated and vehicle-treated cells (Figure 5A and Supplementary Figures S5 and S6). To pinpoint the most significant metabolic alterations, we examined the Variable Importance in Projection (VIP) scores derived from the OPLS model. This analysis highlighted marked changes in the levels of L-arginine and L-norleucine following SAL treatment (Figure 5B).

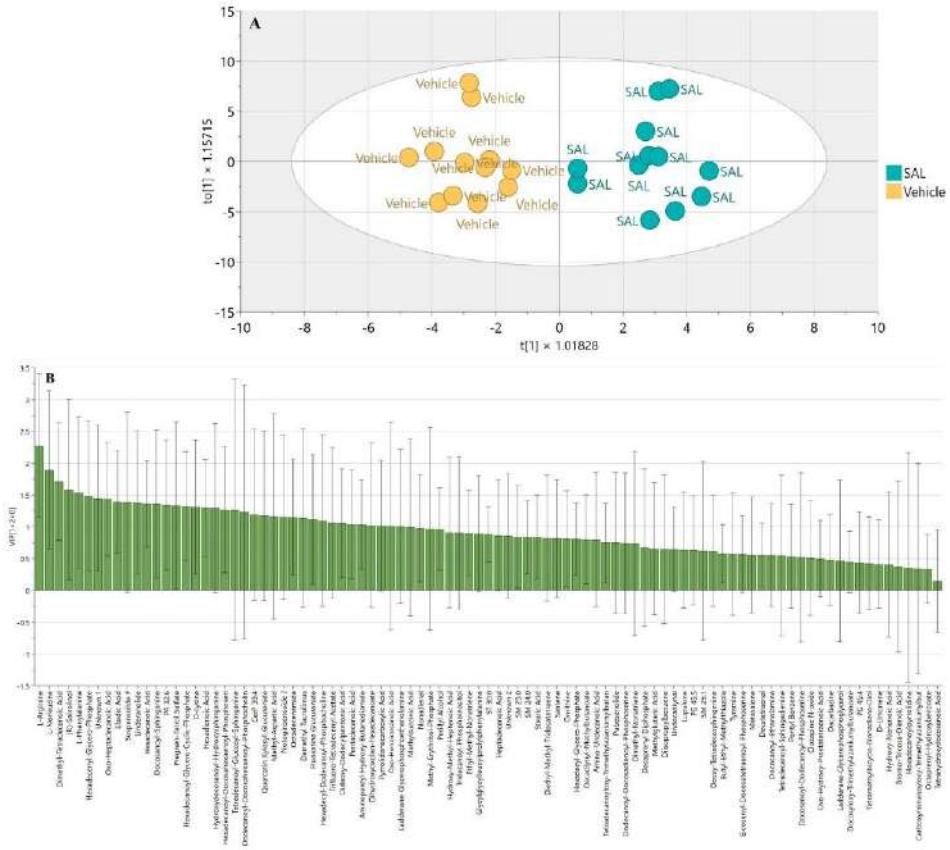

Figure 5. Untargeted metabolomic profiling of Raji cells treated with 0.25 µM SAL, analyzed using SolariX 2xT 7T. (**A**) OPLS-DA (Orthogonal Projections to Latent Structures–Discriminant Analysis) score plot R2X = 0.104, R2Y = 0.878, Q2 = 0.476; CV-ANOVA $p = 0.0399$. (**B**) OPLS-derived VIP (Variable Importance in Projection) score plot.

A pairwise comparison of normalized metabolomic data between SAL-treated and vehicle-treated samples was performed using Student's *t*-test ($p < 0.05$). The results were visualized using volcano plots (Figure 6A,B), highlighting statistically significant metabolites. This analysis revealed notable alterations in the levels of several metabolites following SAL treatment, including a marked decrease in L-arginine (*t*-test, $p = 0.000001$), L-norleucine ($p = 0.0002$), and L-phenylalanine ($p = 0.01$) (Figure 7 and Supplementary Figure S7). In

contrast, SAL treatment resulted in a significant increase in dimethyl-tetradecenoic acid ($p = 0.0003$), hexadecenoic acid ($p = 0.03$), and elaidic acid ($p = 0.015$).

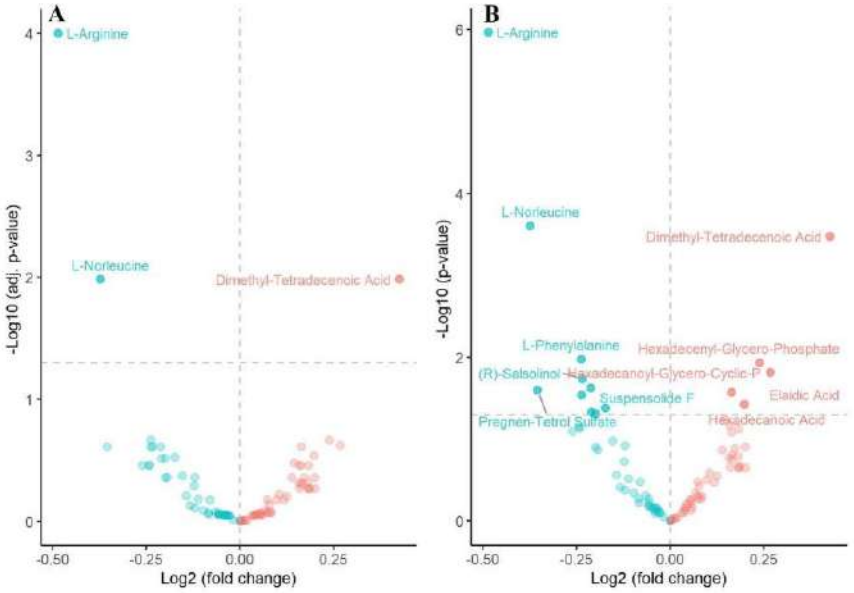

Figure 6. Metabolome of SAL-treated Raji cells. Volcano plots display differentially regulated metabolites, with the most significant ones marked with annotations, based on (**A**) FDR-adjusted p-values (t-test $p = 0.05$) and (**B**) unadjusted p-values (t-test $p = 0.05$). Blue represents metabolites that are lower in the SAL-treated group, while red denotes metabolites that are higher relative to the vehicle group. Horizontal dashed line indicates $p = 0.05$.

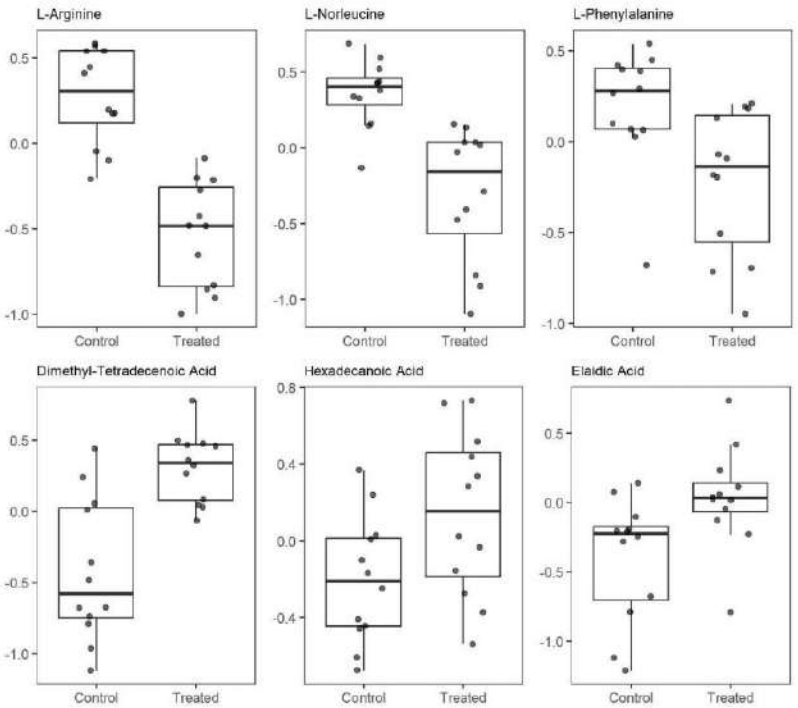

Figure 7. Levels of metabolites increased or decreased following treatment with 0.25 µM SAL (t-test $p = 0.05$).

To identify metabolic pathways altered in response to SAL's administration, we performed a metabolite set enrichment analysis (MSEA) using MetaboAnalyst 6.0 (Figure 8). The analysis revealed significant changes in pathways related to solute carrier (SLC)-mediated transmembrane transport and glucose homeostasis. Of note was that the revealed changes in glucose homeostasis aligned with the changes in glycolysis status, previously detected by the Seahorse extracellular flux analyzer.

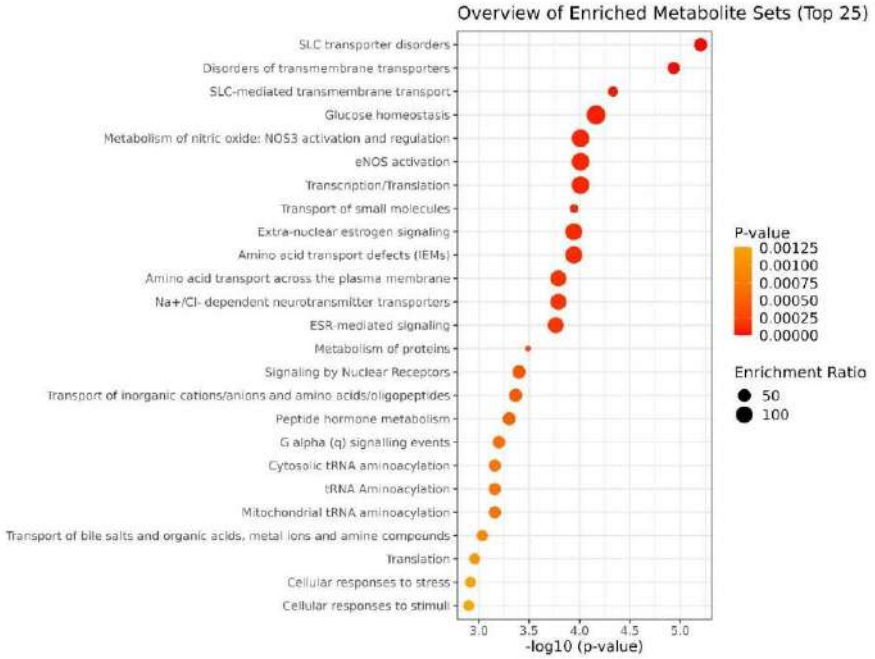

Figure 8. Enrichment analysis of metabolic pathways after SAL's administration using Metaboanalyst 6.0. The top 25 enriched pathways are displayed based on *p*-value and enrichment ratio.

3. Discussion

SAL not only demonstrates direct anticancer properties, but it has also recently been shown to enhance anti-CD20 immunotherapy in both *in vitro* and *in vivo* models of B-cell malignancies [10]. These findings underscore its potential for advancing into clinical trials and eventual therapeutic applications. Building on this, our study seeks to further elucidate the molecular mechanisms driving SAL's anticancer effects in Burkitt lymphoma. A more comprehensive and precise understanding of these mechanisms could substantially improve SAL's prospects for clinical success.

In the present study, we investigated the effects of a non-toxic concentration of SAL on mitochondrial function and metabolomic profiles in Burkitt lymphoma. Specifically, we focused on SAL's impact on MMP and mitochondrial respiration and its role in reprogramming cellular metabolism. The observed decrease in MMP in Burkitt lymphoma cells following 0.25 µM SAL treatment (Figure 1A,B and Supplementary Figure S1) is consistent with findings in other cancer models. For instance, SAL at 5 µM was reported to reduce MMP in retinoblastoma RB383 cells [34], and at 1.33 µM in human prostate cancer cells (PC-3) [27]. Similarly, a 10 µM concentration of SAL decreased MMP in PC-3, SKBR3, and MDA-MB-468 cancer cell lines [7]. In the melanoma SK-Mel-19 cell line, treatment with 1 µM SAL for 12 and 24 h resulted in a reduction in MMP levels [35].

Our data indicate that SAL induces a sustained reduction in MMP, a phenomenon whose pathological significance extends beyond simple ATP deficiency. Furthermore, MMP

plays a crucial role in maintaining mitochondrial homeostasis and provides the electrochemical gradient necessary for ion transport across the mitochondrial membrane [30]. As highlighted by Zorova et al., prolonged MMP suppression primarily affects ROS levels, potentially leading to oxidative stress [30]. Consistent with this, our findings show that SAL induces oxidative stress (Figure 2B and Supplementary Figure S4) in line with previous reports in various cancer models. For instance, Xipell et al. reported that SAL promotes global ROS generation in glioma cells (GSC11 and SF188) at a concentration of 0.1 μM [36]. Similarly, Yu et al. reported increased ROS levels in U87MG cells treated with 4 μM SAL [37]. A 6 h treatment with SAL at concentrations of 1.89 μM in A549 lung cancer cells and 1.22 μM in MDA-MB-231 breast cancer cells resulted in only a marginal, statistically insignificant increase in oxidative stress [38].

In our study, SAL treatment led to a marked increase in mtROS levels (Figure 2A and Supplementary Figure S3). Previous research using 10 μM SAL in B-CLL cells showed unchanged mtROS levels during over 60 min of exposure [29]. The observed increase in mtROS levels may be attributed to changes in mitochondrial respiration, as ROS production is closely linked to electron transport chain activity and oxygen consumption. While it is well established that an elevated MMP is associated with an increased production of mtROS, a reduction in MMP can lead to decreased ROS levels, primarily due to diminished activity of mitochondrial Complexes I and III, which are the main sites of mtROS generation [39,40]. Conversely, in pathological conditions such as hypoxia, a reduced MMP has been linked to elevated mtROS production, contributing to excessive overall oxidative stress [41]. This is further supported by the alterations in OCR detected following SAL treatment (Figure 3A), consistent with previous reports in retinoblastoma RB383 cells [34] and HMLE-Twist cells [29].

Our data demonstrate that SAL-induced mitochondrial dysfunction, characterized by a reduction in MMP (Figure 1A,B) and OCR (Figure 3), appears to elicit a compensatory upregulation of glycolytic metabolism. This is supported by a significant increase in the basal ECAR following treatment with 0.25 μM SAL (Figure 4A,B). Notably, this metabolic adaptation differs from observations in retinoblastoma RB383 cells, where SAL treatment did not result in a significant change in basal ECAR [34]. In HMLER $CD24^{-}$ cells, SAL treatment resulted in a greater reliance on glycolytic activity compared to mitochondrial respiration [24]. Together, these findings suggest that SAL treatment promotes metabolic reprogramming toward enhanced aerobic glycolysis as a primary source of ATP production.

Our metabolomic analysis revealed that a low concentration of SAL led to a decrease in L-arginine (Figure 7), a metabolite synthesized from citrulline and aspartate via arginosuccinate synthase 1 (ASS1) as part of the urea cycle [42]. Reduced arginine levels have been linked to mitochondrial dysfunction, primarily due to impaired oxidative phosphorylation (OXPHOS) and decreased ATP production in ASS1-deficient breast cancer [43]. In MDA-MB-231 breast adenocarcinoma cells, arginine deprivation disrupts both mitochondrial respiration and glycolytic flux, leading to extensive metabolic reprogramming [44]. This response is characterized by dysregulated ROS levels and altered acetyl-CoA production. Notably, cells with impaired mitochondrial function exhibit resistance to the effects of arginine starvation, highlighting the critical role of mitochondrial function in mediating this metabolic vulnerability [44]. In ASS1-deficient leiomyosarcoma (SKLMS1, SKUT1) and melanoma (SKMEL2) cells, arginine deprivation suppresses the Warburg effect while promoting OXPHOS [45]. In a 2020 study, Brashears et al. demonstrated that the cellular response to arginine starvation in sarcomas is mediated by ERK's upregulation and activation of the MYC signaling pathway [46].

Arginine deprivation has been associated with several forms of cell death, including caspase-dependent and -independent apoptosis, autophagic cell death, and necroptosis [42].

These mechanisms have been reported across a range of malignancies, including ovarian cancer [47], sarcoma [48], melanoma [49], and lymphoma [50]. As a result, arginine deprivation has emerged as a promising and advanced therapeutic strategy in cancer treatment. Several approaches have been investigated to achieve arginine depletion, including dietary restriction, inhibition of arginine transport, and enzymatic therapies such as recombinant human arginase and arginine deiminase [51]. Among these, human recombinant arginase I (PEG-BCT-100) and pegylated arginine deiminase (ADI-PEG20) are currently in clinical trials and have shown success in effectively depleting arginine levels in cancer cells. To date, more than 20 clinical trials have evaluated ADI-PEG20 as a monotherapy or in combination with other treatments across over 12 cancer types, including glioblastoma, melanoma, non-small cell lung cancer, mesothelioma, acute myeloid leukemia, pancreatic cancer, hepatocellular carcinoma, breast cancer, and uveal melanoma [42].

In summary, our findings demonstrate that SAL, even at low concentrations, diminishes MMP, elevates mtROS, and induces oxidative stress in Burkitt lymphoma cells. Furthermore, SAL disrupts mitochondrial respiration, boosts glycolytic activity, and decreases intracellular arginine levels. Furthermore, metabolic pathway enrichment analysis (Figure 8) revealed significant alterations in SLC-mediated transmembrane transport, which is an expected outcome given SAL's ability to influence ion transport via biological membranes.

However, this study has certain limitations, including the use of a single cell line and the absence of validation in additional lymphoma cell lines or primary patient samples. These factors may limit the generalizability of the results and underscore the need for further investigations in more physiologically relevant models to confirm and extend these findings.

4. Materials and Methods

4.1. Cell Line and Chemicals

The Burkitt lymphoma Raji cell line (RRID:CVCL_0511) was maintained in RPMI 1640 medium (Corning, NY, USA; cat. #10-040-CVR) supplemented with 10% fetal bovine serum (FBS; Fisher Scientific, Waltham, MA, USA; cat. #SH3007203), 100 U/mL penicillin, and 100 µg/mL streptomycin at 37 °C in a humidified 5% CO_2 atmosphere. The cell line was routinely tested and confirmed to be mycoplasma-free. Salinomycin (sodium salt) was obtained from Sigma-Aldrich, St. Louis, MO, USA (cat. #S4526) and dissolved in methanol.

4.2. Mitochondrial Membrane Potential (MMP) Assessment

Cells (1.5×10^5 per well) were seeded in 12-well plates and treated with either methanol (control vehicle) or salinomycin (SAL; 0.25 µM, 0.5 µM, or 5 µM). After 12 or 36 h of treatment, cells were harvested by centrifugation (1300 rpm, 5 min, 4 °C) and washed with phosphate-buffered saline (PBS).

MMP was evaluated using either the MitoPT JC-1 Assay Kit (ImmunoChemistry Technologies, Davis, CA, USA, cat. #6261) or the MitoProbe TMRM Assay Kit (Invitrogen, Waltham, MA, USA, cat. #M20036), following the manufacturer's instructions. As a positive control, cells were treated with 50 µM carbonyl cyanide 3-chlorophenylhydrazone (CCCP) for 60 min. Cells were co-stained with either JC-1 or TMRM and Zombie-NIR Dye (BioLegend, San Diego, CA, USA, cat. #423106) for 30 min at 37 °C in the dark, washed with PBS, and live cells were subsequently analyzed by flow cytometry using a FACS Verse instrument (Becton Dickinson, Franklin Lake, NJ, USA). In both the MitoPT JC-1 and MitoProbe TMRM assays, the percentage of live cells (Zombie-NIR-negative) displaying reduced fluorescence in the PE (phycoerythrin) channel was assessed.

4.3. Assessment of Mitochondrial Superoxide and Global Oxidative Stress

Cells (1.5×10^5 per well) were plated in 12-well plates and treated with either salinomycin (Sal; 0.25 µM, 0.5 µM, or 5 µM) or the control vehicle. Following treatment periods of 36 or 48 h, cells were harvested by centrifugation (1300 rpm, 5 min, 4 °C) and washed with ice-cold PBS. Mitochondrial superoxide production was measured using MitoSOX Red mitochondrial superoxide indicator (Invitrogen, Waltham, MA, USA, cat. #M36008), while general oxidative stress was assessed with CellROX Green Reagent (Invitrogen, Waltham, MA, USA, cat. #C10492), according to the manufacturer's protocols. As a positive control, cells were treated with 50 µM CCCP for 60 min. Following a 30 min co-staining with Zombie-NIR Dye (BioLegend, San Diego, USA, cat. #423106) under light-protected conditions, samples were immediately analyzed by flow cytometry using a FACS Verse instrument (Becton Dickinson, New Jersey, USA). In the MitoSOX Red assay, the percentage of live cells (Zombie-NIR-negative) exhibiting increased fluorescence in the PE channel was measured. For the CellROX Green Reagent assay, the percentage of live cells (Zombie-NIR-negative) showing elevated fluorescence in the FITC (fluorescein) channel was determined.

4.4. Measurement of Cellular Bioenergetics Using Seahorse XFe96 Extracellular Flux Analyzer

Cellular respiration and glycolysis were measured using the Seahorse XFe96 extracellular flux analyzer (Agilent, Santa Clara, CA, USA) with the XF Cell Mito Stress Test Kit (Agilent, Santa Clara, CA, USA, cat. #103015-100). Assays were conducted in Seahorse XF DMEM Medium (pH 7.4; Agilent), supplemented with glucose (1 mM; Gibco, Waltham, MA, USA, cat. #A24940-01), L-glutamine (1 mM; Gibco, Waltham, MA, cat. #25030), and sodium pyruvate (1 mM; Sigma, cat. #S8636). Non-adherent Raji cells (5×10^4 cells/well) were seeded onto Cell-Tak (Corning, Corning, NY, USA, cat. #354240)-coated XF96 microplates (Agilent, Santa Clara, CA, USA, cat. #102416-100) to ensure adhesion and incubated for 30 min at 37 °C in a CO_2-free incubator before the assay's initiation. Following baseline measurements, the following compounds were sequentially injected: oligomycin (2.5 µM; ATP synthase inhibitor), carbonyl cyanide-p-trifluoromethoxyphenylhydrazone (FCCP, 1 µM followed by 1.5 µM; mitochondrial uncoupler to assess maximal respiration), and antimycin A (2.5 µM; Complex III inhibitor). The initial low concentration of FCCP helps determine the minimal dose required to achieve a maximal OCR, while the subsequent higher concentration confirms whether maximal respiration has been fully reached. Data were analyzed using the XF Cell Mito Stress Test Report Generator (Agilent, Santa Clara, USA). Post-assay normalization was performed by staining cells with Hoechst 33342 (5 µM; Thermo Scientific, Waltham, MA, USA, cat. #62249) for 30 min. Nuclei were quantified using the ImageXpress imaging system (Molecular Devices, San Jose, CA, USA) to determine cell counts per well, and all Seahorse measurements were normalized accordingly.

4.5. Metabolomics Sample Preparation

Cells were normalized by count and lysed via a freeze–thaw cycle, followed by the addition of 100 µL of ice-cold (−20 °C) methanol (LC-MS hypergrade, Merck, Darmstadt, Germany). After centrifugation (18,000× g, −10 °C, 30 min), 80 µL of the supernatant was lyophilized at room temperature using an Eppendorf concentrator. The dried residue was reconstituted immediately prior to injection in a 50:50 (v/v) mixture of ddH_2O and acetonitrile (ACN) containing 0.1% formic acid.

Untargeted metabolomic profiling was conducted using a SolariX 2xR 7T FT-ICR MS (ultra-high-resolution Fourier-transform ion cyclotron resonance mass spectrometer) equipped with an electrospray ionization (ESI) source in direct injection mode. Samples were infused at a flow rate of 300 µL/h in both positive and negative ionization modes.

Key instrument parameters:
Ion accumulation time: 0.03 s;
Dry gas flow: 4.0 L/min;
Drying temperature: 200 °C;
Capillary voltage: 4500 V (positive mode)/3500 V (negative mode).

Mass spectra were acquired and processed using the T-Rex 2D algorithm (MRMS single spectra) within MetaboScape 5.0 software (Bruker, Billerica, MA, USA).

4.5.1. Sample Overview

The dataset, which comprised metabolomic profiles, was acquired in both positive and negative ionization modes using MetaboScape 5.0 software. Samples included the control group (vehicle-treated cells) and the treatment group (cells treated with 0.25 μM salinomycin for 24 h).

The experimental design consisted of 24 total samples:
12 control samples (6 independent replicates × 2 technical replicates);
12 treated samples (6 independent replicates × 2 technical replicates).

4.5.2. Data Treatment

To ensure a high data quality and analytical robustness, the following treatment steps were applied (Table 1):

1. Missing Value Imputation

Sparse data (zero values) were imputed to maintain dataset completeness and enhance statistical reliability.

2. Data Transformation

Variables were mathematically transformed to approximate normal distributions and reduce skewness, ensuring compliance with parametric test assumptions.

3. Data Centering

Values were adjusted to a common scale using min–max normalization ([0, 1] range) to facilitate direct comparison across variables and samples.

4. Data Normalization

Systematic technical variations were corrected using normalization methods to isolate biologically relevant patterns.

Table 1. Summary of data treatment steps.

Step	Type	Method	Equation
1	Missing Value Imputation	Half-minimum	$x_{ij} = \frac{\bar{x}_i}{2}$
2	Data Transformation	Log_{10}	$\tilde{x}_{ij} = log_{10}(x_{ij})$
3	Data Centering	Min–max centering	$\hat{x}_{ij} = \frac{\tilde{x}_{ij} - \tilde{x}_{j\ min}}{\tilde{x}_{j\ max} - \tilde{x}_{j\ min}}$
4	Data Normalization	Pareto	$\widetilde{x}_{ij} = \frac{(\hat{x}_{ij} - \bar{x}_i)}{\sqrt{s_i}}$

4.6. Statistical Analysis

4.6.1. Descriptive Statistical Analysis

Comprehensive quality control was performed using descriptive statistical analysis to assess data integrity and the effectiveness of treatments. The following metrics were calculated:

- Distribution characteristics: kurtosis and skewness—evaluated deviations from normality;

- Gaussian function fit R^2—assessed the goodness-of-fit to a normal distribution;
- One-sample Kolmogorov–Smirnov test—statistically tested normality assumptions.

4.6.2. Univariate Statistical Analysis

- One-sample test Kolmogorov–Smirnov—evaluated distribution normality;
- Student's *t*-test—applied to normally distributed data;
- Mann–Whitney U test—used for non-normally distributed data or in the presence of outliers;
- Multiple comparison correction: Benjamini–Hochberg procedure—controlled the false discovery rate (FDR).

4.6.3. Multivariate Statistical Analysis

To explore patterns and group separations in the metabolomic data, complementary multivariate approaches were applied:

1. Unsupervised Analysis:

- Principal Component Analysis (PCA): provided an initial unsupervised overview of data structure and helped identify outliers.

2. Supervised Modeling:

- Orthogonal Partial Least Squares Discriminant Analysis (OPLS-DA): used to enhance group separation and identify discriminant metabolites;
- Model optimization: performed through iterative component selection;
- Validation: conducted using leave-one-out cross-validation (LOOCV);
- Significance testing: assessed via cross-validated ANOVA (CV-ANOVA), with a $p < 0.05$ considered significant.

3. Model Quality Assessment:

- Permutation testing: evaluated potential overfitting.

4. Calculated model parameters:

- R^2X/R^2Y: goodness of fit of the model;
- Q^2: goodness of prediction of the model.

Supplementary Materials: The following supporting information can be downloaded at: https://www.mdpi.com/article/10.3390/ijms26115125/s1.

Author Contributions: Conceptualization, A.Z. and B.P.; methodology, A.Z., H.C. (Seahorse analysis), O.I. and A.C. (metabolomics); experiments performance: A.Z. and A.C.; data curation, O.I. and A.Z.; writing—original draft preparation, A.Z.; writing—review and editing, A.Z., B.P., O.I. and M.S.; visualization, A.Z. and O.I.; supervision, B.P.; funding acquisition, B.P. All authors have read and agreed to the published version of the manuscript.

Funding: This research was funded by the National Science Centre (NCN, Poland), grant no 2019/35/B/NZ5/01445 (to B.P.).

Institutional Review Board Statement: Not applicable.

Informed Consent Statement: Not applicable.

Data Availability Statement: Data are contained within the article and Supplementary Materials.

Acknowledgments: This work was conducted with support from the Seahorse facility of the UCL Consortium for Mitochondrial Research. Graphs and statistical analyses were generated using GraphPad Prism 9.5. Univariate data analysis was conducted in R version 4.4.2. Multivariate statistics were conducted using the SIMCA 18 software, Sartorius (https://www.sartorius.com/en/

products/process-analytical-technology/data-analytics-software/mvda-software/simca (accessed on 12 January 2023)). The authors have reviewed and edited the output and take full responsibility for the content of this publication.

Conflicts of Interest: The authors declare no conflicts of interest.

Abbreviations

The following abbreviations are used in this manuscript:

ASS1	Arginosuccinate synthase 1
CCCP	Carbonyl cyanide 3-chlorophenylhydrazone
CSC	Cancer stem cell
CV-ANOVA	Cross-validated ANOVA
DLBCL	Diffuse large B-cell lymphoma
DR5	Death receptor-5
ECAR	Extracellular acidification rate
ETC	Electron transport chain
FADD	Fas-associated protein with death domain
FCCP	Carbonyl cyanide-p-trifluoromethoxyphenylhydrazone
LOOCV	Leave-one-out cross-validation
MMP	Mitochondrial membrane potential
MSEA	Metabolite set enrichment analysis
mtROS	Mitochondrial reactive oxygen species
OCR	Oxygen consumption rates
OPLS-DA	Orthogonal Partial Least Squares Discriminant Analysis
OXPHOS	Oxidative phosphorylation
PCA	Principal Component Analysis
SAL	Salinomycin
SLC	Solute carrier
TCA	Tricarboxylic acid
TMRM	Tetramethylrhodamine methyl ester
VIP	Variable Importance in Projection

References

1. Dutton, C.J.; Banks, B.J.; Cooper, C.B. Polyether ionophores. *Nat. Prod. Rep.* **1995**, *12*, 165–181. [CrossRef] [PubMed]
2. Miyazaki, Y.; Shibuya, M.; Sugawara, H.; Kawaguchi, O.; Hirsoe, C. Salinomycin, a new polyether antibiotic. *J. Antibiot.* **1974**, *27*, 814–821. [CrossRef] [PubMed]
3. Ekinci, I.B.; Chlodowska, A.; Olejnik, M. Ionophore Toxicity in Animals: A Review of Clinical and Molecular Aspects. *Int. J. Mol. Sci.* **2023**, *24*, 1696. [CrossRef]
4. Gupta, P.B.; Onder, T.T.; Jiang, G.; Tao, K.; Kuperwasser, C.; Weinberg, R.A.; Lander, E.S. Identification of selective inhibitors of cancer stem cells by high-throughput screening. *Cell* **2009**, *138*, 645–659. [CrossRef] [PubMed]
5. Wang, F.; He, L.; Dai, W.Q.; Xu, Y.P.; Wu, D.; Lin, C.L.; Wu, S.M.; Cheng, P.; Zhang, Y.; Shen, M.; et al. Salinomycin inhibits proliferation and induces apoptosis of human hepatocellular carcinoma cells in vitro and in vivo. *PLoS ONE* **2012**, *7*, e50638. [CrossRef]
6. Lu, D.; Choi, M.Y.; Yu, J.; Castro, J.E.; Kipps, T.J.; Carson, D.A. Salinomycin inhibits Wnt signaling and selectively induces apoptosis in chronic lymphocytic leukemia cells. *Proc. Natl. Acad. Sci. USA* **2011**, *108*, 13253–13257. [CrossRef]
7. Jangamreddy, J.R.; Ghavami, S.; Grabarek, J.; Kratz, G.; Wiechec, E.; Fredriksson, B.A.; Rao Pariti, R.K.; Cieslar-Pobuda, A.; Panigrahi, S.; Los, M.J. Salinomycin induces activation of autophagy, mitophagy and affects mitochondrial polarity: Differences between primary and cancer cells. *Biochim. Biophys. Acta* **2013**, *1833*, 2057–2069. [CrossRef]
8. Parajuli, B.; Lee, H.G.; Kwon, S.H.; Cha, S.D.; Shin, S.J.; Lee, G.H.; Bae, I.; Cho, C.H. Salinomycin inhibits Akt/NF-kappaB and induces apoptosis in cisplatin resistant ovarian cancer cells. *Cancer Epidemiol.* **2013**, *37*, 512–517. [CrossRef]
9. Kim, W.K.; Kim, J.H.; Yoon, K.; Kim, S.; Ro, J.; Kang, H.S.; Yoon, S. Salinomycin, a p-glycoprotein inhibitor, sensitizes radiation-treated cancer cells by increasing DNA damage and inducing G2 arrest. *Investig. New Drugs* **2012**, *30*, 1311–1318. [CrossRef]

10. Torun, A.; Zdanowicz, A.; Miazek-Zapala, N.; Zapala, P.; Pradhan, B.; Jedrzejczyk, M.; Ciechanowicz, A.; Pilch, Z.; Skorzynski, M.; Slabicki, M.; et al. Potassium/sodium cation carriers robustly up-regulate CD20 antigen by targeting MYC, and synergize with anti-CD20 immunotherapies to eliminate malignant B cells. *Haematologica* **2024**. [CrossRef]
11. Casan, J.M.L.; Wong, J.; Northcott, M.J.; Opat, S. Anti-CD20 monoclonal antibodies: Reviewing a revolution. *Hum. Vaccines Immunother.* **2018**, *14*, 2820–2841. [CrossRef] [PubMed]
12. Tomita, A. Genetic and Epigenetic Modulation of CD20 Expression in B-Cell Malignancies: Molecular Mechanisms and Significance to Rituximab Resistance. *J. Clin. Exp. Hematop.* **2016**, *56*, 89–99. [CrossRef] [PubMed]
13. Story, P.; Doube, A. A case of human poisoning by salinomycin, an agricultural antibiotic. *N. Z. Med. J.* **2004**, *117*, U799.
14. Naujokat, C.; Steinhart, R. Salinomycin as a drug for targeting human cancer stem cells. *J. Biomed. Biotechnol.* **2012**, *2012*, 950658. [CrossRef]
15. Boehmerle, W.; Muenzfeld, H.; Springer, A.; Huehnchen, P.; Endres, M. Specific targeting of neurotoxic side effects and pharmacological profile of the novel cancer stem cell drug salinomycin in mice. *J. Mol. Med.* **2014**, *92*, 889–900. [CrossRef] [PubMed]
16. Soni, V.; Nagar, A.; Bardiya, R.; Mara, J.; Von Suskil, L.; Rose, S.; Sonawane, C. A Concise Review of Prodigious Salinomycin and Its Derivatives Effective in Treatment of Breast Cancer: (2012–2022). *Int. J. Transl. Med.* **2023**, *3*, 217–245. [CrossRef]
17. Antoszczak, M.; Huczynski, A. Salinomycin and its derivatives—A new class of multiple-targeted "magic bullets". *Eur. J. Med. Chem.* **2019**, *176*, 208–227. [CrossRef]
18. Versini, A.; Colombeau, L.; Hienzsch, A.; Gaillet, C.; Retailleau, P.; Debieu, S.; Muller, S.; Caneque, T.; Rodriguez, R. Salinomycin Derivatives Kill Breast Cancer Stem Cells by Lysosomal Iron Targeting. *Chemistry* **2020**, *26*, 7416–7424. [CrossRef]
19. Antoszczak, M. A comprehensive review of salinomycin derivatives as potent anticancer and anti-CSCs agents. *Eur. J. Med. Chem.* **2019**, *166*, 48–64. [CrossRef]
20. Boehmerle, W.; Endres, M. Salinomycin induces calpain and cytochrome c-mediated neuronal cell death. *Cell Death Dis.* **2011**, *2*, e168. [CrossRef]
21. Rutkowski, J.; Brzezinski, B. Structures and properties of naturally occurring polyether antibiotics. *BioMed Res. Int.* **2013**, *2013*, 162513. [CrossRef]
22. Versini, A.; Saier, L.; Sindikubwabo, F.; Muller, S.; Caneque, T.; Rodriguez, R. Chemical biology of salinomycin. *Tetrahedron* **2018**, *74*, 5585–5614. [CrossRef]
23. Mai, T.T.; Hamai, A.; Hienzsch, A.; Caneque, T.; Muller, S.; Wicinski, J.; Cabaud, O.; Leroy, C.; David, A.; Acevedo, V.; et al. Salinomycin kills cancer stem cells by sequestering iron in lysosomes. *Nat. Chem.* **2017**, *9*, 1025–1033. [CrossRef] [PubMed]
24. Cosialls, E.; Pacreau, E.; Duruel, C.; Ceccacci, S.; Elhage, R.; Desterke, C.; Roger, K.; Guerrera, C.; Ducloux, R.; Souquere, S.; et al. mTOR inhibition suppresses salinomycin-induced ferroptosis in breast cancer stem cells by ironing out mitochondrial dysfunctions. *Cell Death Dis.* **2023**, *14*, 744. [CrossRef]
25. Rokitskaya, T.I.; Firsov, A.M.; Khailova, L.S.; Kotova, E.A.; Antonenko, Y.N. Selectivity of cation transport across lipid membranes by the antibiotic salinomycin. *Biochim. Biophys. Acta Biomembr.* **2023**, *1865*, 184182. [CrossRef]
26. Verdoodt, B.; Vogt, M.; Schmitz, I.; Liffers, S.T.; Tannapfel, A.; Mirmohammadsadegh, A. Salinomycin induces autophagy in colon and breast cancer cells with concomitant generation of reactive oxygen species. *PLoS ONE* **2012**, *7*, e44132. [CrossRef] [PubMed]
27. Kim, K.Y.; Yu, S.N.; Lee, S.Y.; Chun, S.S.; Choi, Y.L.; Park, Y.M.; Song, C.S.; Chatterjee, B.; Ahn, S.C. Salinomycin-induced apoptosis of human prostate cancer cells due to accumulated reactive oxygen species and mitochondrial membrane depolarization. *Biochem. Biophys. Res. Commun.* **2011**, *413*, 80–86. [CrossRef]
28. Zhu, L.Q.; Zhen, Y.F.; Zhang, Y.; Guo, Z.X.; Dai, J.; Wang, X.D. Salinomycin activates AMP-activated protein kinase-dependent autophagy in cultured osteoblastoma cells: A negative regulator against cell apoptosis. *PLoS ONE* **2013**, *8*, e84175. [CrossRef]
29. Manago, A.; Leanza, L.; Carraretto, L.; Sassi, N.; Grancara, S.; Quintana-Cabrera, R.; Trimarco, V.; Toninello, A.; Scorrano, L.; Trentin, L.; et al. Early effects of the antineoplastic agent salinomycin on mitochondrial function. *Cell Death Dis.* **2015**, *6*, e1930. [CrossRef]
30. Zorova, L.D.; Popkov, V.A.; Plotnikov, E.Y.; Silachev, D.N.; Pevzner, I.B.; Jankauskas, S.S.; Babenko, V.A.; Zorov, S.D.; Balakireva, A.V.; Juhaszova, M.; et al. Mitochondrial membrane potential. *Anal. Biochem.* **2018**, *552*, 50–59. [CrossRef]
31. Zdanowicz, A.; Grosicka-Maciag, E. The Interplay between Autophagy and Mitochondria in Cancer. *Int. J. Mol. Sci.* **2024**, *25*, 9143. [CrossRef] [PubMed]
32. Zhang, B.; Pan, C.; Feng, C.; Yan, C.; Yu, Y.; Chen, Z.; Guo, C.; Wang, X. Role of mitochondrial reactive oxygen species in homeostasis regulation. *Redox Rep.* **2022**, *27*, 45–52. [CrossRef] [PubMed]
33. Casanova, A.; Wevers, A.; Navarro-Ledesma, S.; Pruimboom, L. Mitochondria: It is all about energy. *Front. Physiol.* **2023**, *14*, 1114231. [CrossRef]
34. Li, J.; Min, Y. Pre-clinical evidence that salinomycin is active against retinoblastoma via inducing mitochondrial dysfunction, oxidative damage and AMPK activation. *J. Bioenerg. Biomembr.* **2021**, *53*, 513–523. [CrossRef] [PubMed]

35. Liu, Y.; Hao, Y.; Li, Y.; Zheng, Y.; Dai, J.; Zhong, F.; Wei, W.; Fang, Z. Salinomycin induces autophagic cell death in salinomycin-sensitive melanoma cells through inhibition of autophagic flux. *Sci. Rep.* **2020**, *10*, 18515. [CrossRef]
36. Xipell, E.; Gonzalez-Huarriz, M.; Martinez de Irujo, J.J.; Garcia-Garzon, A.; Lang, F.F.; Jiang, H.; Fueyo, J.; Gomez-Manzano, C.; Alonso, M.M. Salinomycin induced ROS results in abortive autophagy and leads to regulated necrosis in glioblastoma. *Oncotarget* **2016**, *7*, 30626–30641. [CrossRef]
37. Yu, S.N.; Kim, S.H.; Kim, K.Y.; Ji, J.H.; Seo, Y.K.; Yu, H.S.; Ahn, S.C. Salinomycin induces endoplasmic reticulum stress-mediated autophagy and apoptosis through generation of reactive oxygen species in human glioma U87MG cells. *Oncol. Rep.* **2017**, *37*, 3321–3328. [CrossRef]
38. Jedrzejczyk, M.; Sulik, M.; Mielczarek-Puta, M.; Lim, G.Y.; Podsiad, M.; Hoser, J.; Bednarczyk, P.; Struga, M.; Huczynski, A. Anticancer activity of salinomycin quaternary phosphonium salts. *Eur. J. Med. Chem.* **2025**, *282*, 117055. [CrossRef]
39. Korshunov, S.S.; Skulachev, V.P.; Starkov, A.A. High protonic potential actuates a mechanism of production of reactive oxygen species in mitochondria. *FEBS Lett.* **1997**, *416*, 15–18. [CrossRef]
40. Suski, J.M.; Lebiedzinska, M.; Bonora, M.; Pinton, P.; Duszynski, J.; Wieckowski, M.R. Relation between mitochondrial membrane potential and ROS formation. *Methods Mol. Biol.* **2012**, *810*, 183–205. [CrossRef]
41. Salaroglio, I.C.; Belisario, D.C.; Akman, M.; La Vecchia, S.; Godel, M.; Anobile, D.P.; Ortone, G.; Digiovanni, S.; Fontana, S.; Costamagna, C.; et al. Mitochondrial ROS drive resistance to chemotherapy and immune-killing in hypoxic non-small cell lung cancer. *J. Exp. Clin. Cancer Res.* **2022**, *41*, 243. [CrossRef] [PubMed]
42. Chen, C.L.; Hsu, S.C.; Ann, D.K.; Yen, Y.; Kung, H.J. Arginine Signaling and Cancer Metabolism. *Cancers* **2021**, *13*, 3541. [CrossRef]
43. Qiu, F.; Chen, Y.R.; Liu, X.; Chu, C.Y.; Shen, L.J.; Xu, J.; Gaur, S.; Forman, H.J.; Zhang, H.; Zheng, S.; et al. Arginine starvation impairs mitochondrial respiratory function in ASS1-deficient breast cancer cells. *Sci. Signal.* **2014**, *7*, ra31. [CrossRef]
44. Cheng, C.T.; Qi, Y.; Wang, Y.C.; Chi, K.K.; Chung, Y.; Ouyang, C.; Chen, Y.R.; Oh, M.E.; Sheng, X.; Tang, Y.; et al. Arginine starvation kills tumor cells through aspartate exhaustion and mitochondrial dysfunction. *Commun. Biol.* **2018**, *1*, 178. [CrossRef]
45. Kremer, J.C.; Prudner, B.C.; Lange, S.E.S.; Bean, G.R.; Schultze, M.B.; Brashears, C.B.; Radyk, M.D.; Redlich, N.; Tzeng, S.C.; Kami, K.; et al. Arginine Deprivation Inhibits the Warburg Effect and Upregulates Glutamine Anaplerosis and Serine Biosynthesis in ASS1-Deficient Cancers. *Cell Rep.* **2017**, *18*, 991–1004. [CrossRef] [PubMed]
46. Brashears, C.B.; Barlin, M.; Ehrhardt, W.R.; Rathore, R.; Schultze, M.; Tzeng, S.C.; Van Tine, B.A.; Held, J.M. Systems level profiling of arginine starvation reveals MYC and ERK adaptive metabolic reprogramming. *Cell Death Dis.* **2020**, *11*, 662. [CrossRef]
47. Ji, J.X.; Cochrane, D.R.; Tessier-Cloutier, B.; Chen, S.Y.; Ho, G.; Pathak, K.V.; Alcazar, I.N.; Farnell, D.; Leung, S.; Cheng, A.; et al. Arginine Depletion Therapy with ADI-PEG20 Limits Tumor Growth in Argininosuccinate Synthase-Deficient Ovarian Cancer, Including Small-Cell Carcinoma of the Ovary, Hypercalcemic Type. *Clin. Cancer Res.* **2020**, *26*, 4402–4413. [CrossRef] [PubMed]
48. Bean, G.R.; Kremer, J.C.; Prudner, B.C.; Schenone, A.D.; Yao, J.C.; Schultze, M.B.; Chen, D.Y.; Tanas, M.R.; Adkins, D.R.; Bomalaski, J.; et al. A metabolic synthetic lethal strategy with arginine deprivation and chloroquine leads to cell death in ASS1-deficient sarcomas. *Cell Death Dis.* **2016**, *7*, e2406. [CrossRef]
49. Savaraj, N.; Wu, C.; Kuo, M.T.; You, M.; Wangpaichitr, M.; Robles, C.; Spector, S.; Feun, L. The relationship of arginine deprivation, argininosuccinate synthetase and cell death in melanoma. *Drug Target Insights* **2007**, *2*, 119–128. [CrossRef]
50. Delage, B.; Luong, P.; Maharaj, L.; O'Riain, C.; Syed, N.; Crook, T.; Hatzimichael, E.; Papoudou-Bai, A.; Mitchell, T.J.; Whittaker, S.J.; et al. Promoter methylation of argininosuccinate synthetase-1 sensitises lymphomas to arginine deiminase treatment, autophagy and caspase-dependent apoptosis. *Cell Death Dis.* **2012**, *3*, e342. [CrossRef]
51. Fultang, L.; Vardon, A.; De Santo, C.; Mussai, F. Molecular basis and current strategies of therapeutic arginine depletion for cancer. *Int. J. Cancer* **2016**, *139*, 501–509. [CrossRef] [PubMed]

Supplementary materials to:

Publication No. 3

Low-Dose Salinomycin Alters Mitochondrial Function and Reprograms Global Metabolism in Burkitt Lymphoma

Aleksandra Zdanowicz [1,2] Oleksandr Ilchenko [3,4] Andrzej Ciechanowicz [5] Haoyu Chi [6,7] Marta Struga [1] and Beata Pyrzynska [1,*]

1 Department of Biochemistry, Medical University of Warsaw, Banacha 1 Str., 02-097 Warsaw, Poland
2 Doctoral School, Medical University of Warsaw, Zwirki i Wigury 81 Str., 02-091 Warsaw, Poland
3 Department of Forest Genetics and Plant Physiology, Umeå Plant Science Centre, Swedish University of Agricultural Sciences, Skogsmarksgränd 17, 90183 Umea, Sweden
4 Department of Chemistry, Umeå University, Linnaeus väg 10B, 90187 Umea, Sweden
5 Department of Regenerative Medicine, Center for Preclinical Research and Technology, Medical University of Warsaw, Banacha 1B Str., 02-097 Warsaw, Poland
6 Department of Cell and Developmental Biology, University College London, Gower Street, London WC1E 6BT, UK
7 Consortium for Mitochondrial Research, University College London, Gower Street, London WC1E 6BT, UK
*Author to whom correspondence should be addressed.

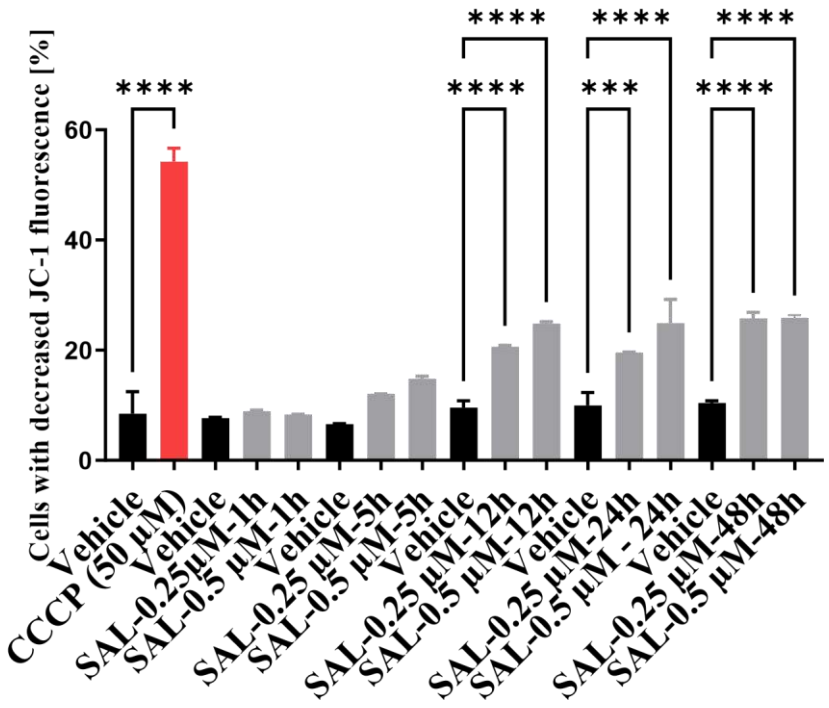

Supplementary Figure S1: Time-dependent changes in MMP following SAL treatment, visualized using JC-1 staining.

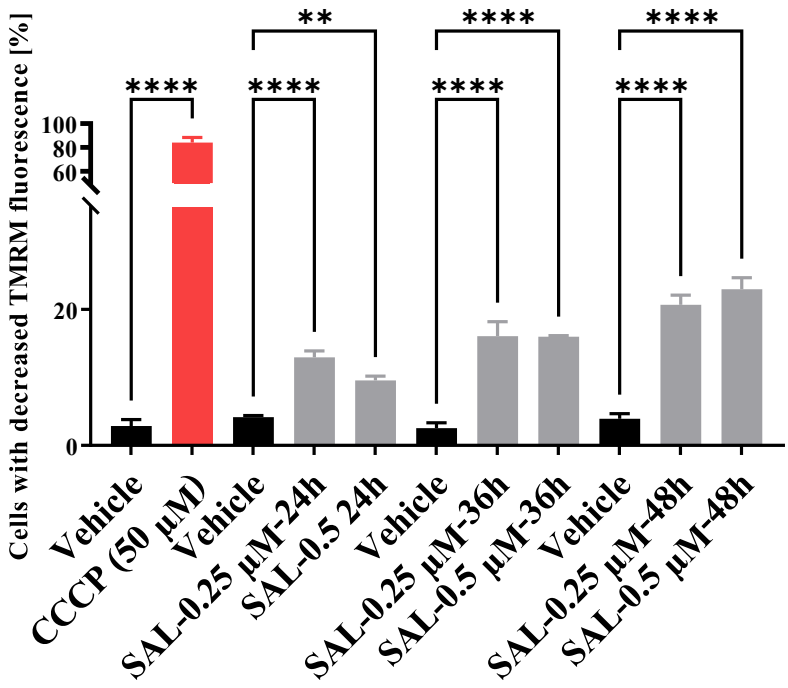

Supplementary Figure S2: Time-course analysis of SAL-induced changes in MMP using TMRM staining.

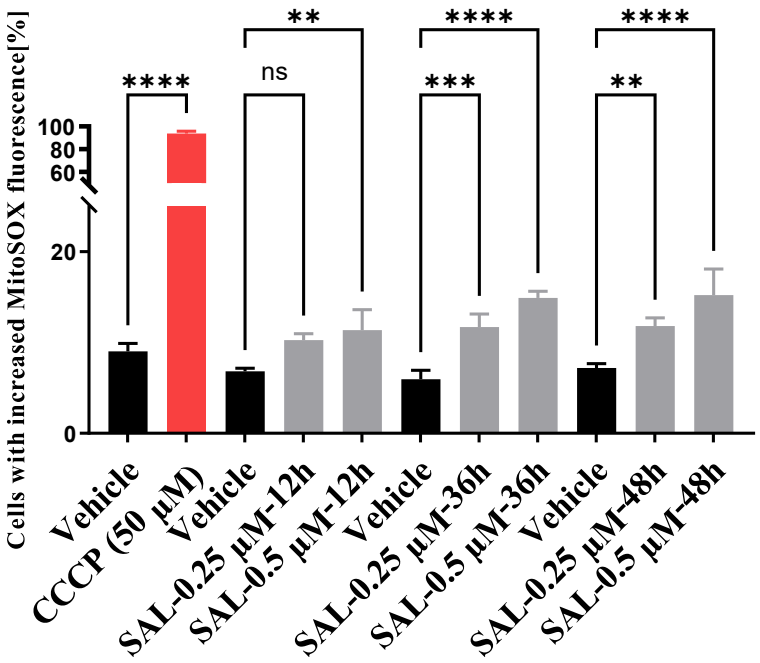

Supplementary Figure S3: Monitoring mitochondrial superoxide levels over time following SAL treatment using MitoSOX.

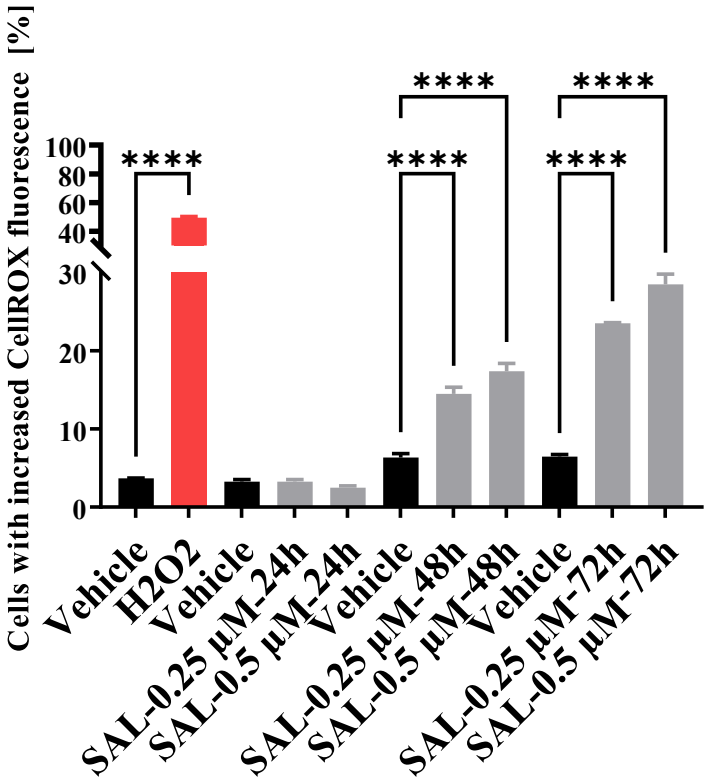

Supplementary Figure S4: Time-dependent changes in cellular oxidative stress in response to SAL treatment, detected via CellROX.

Supplementary Figure S5: Untargeted metabolomic profiling – Principal Component Analysis (PCA) plot.

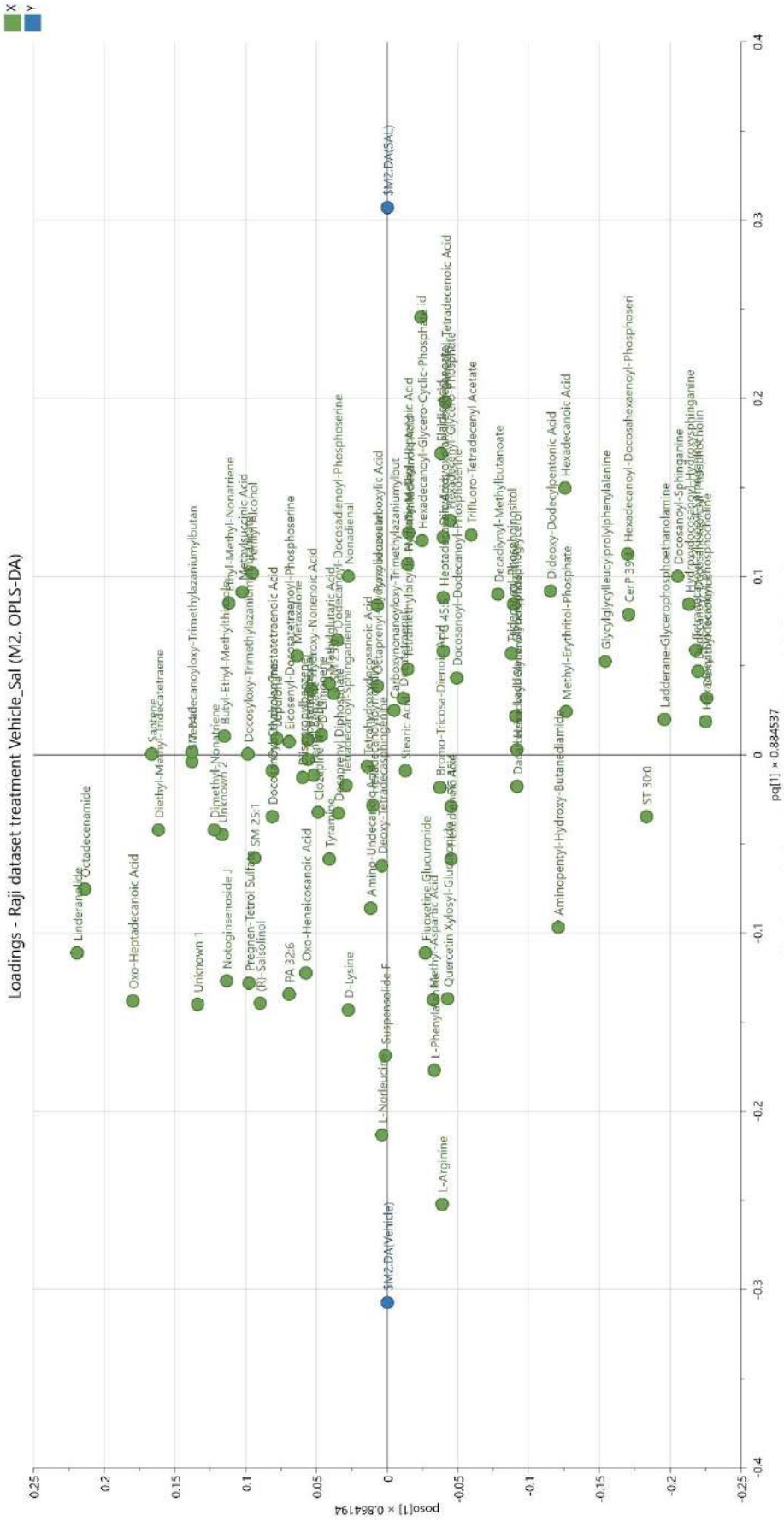

Supplementary Figure S6: Untargeted metabolomic profiling – Orthogonal Partial Least Squares Discriminant Analysis (OPLS-DA) loadings plot.

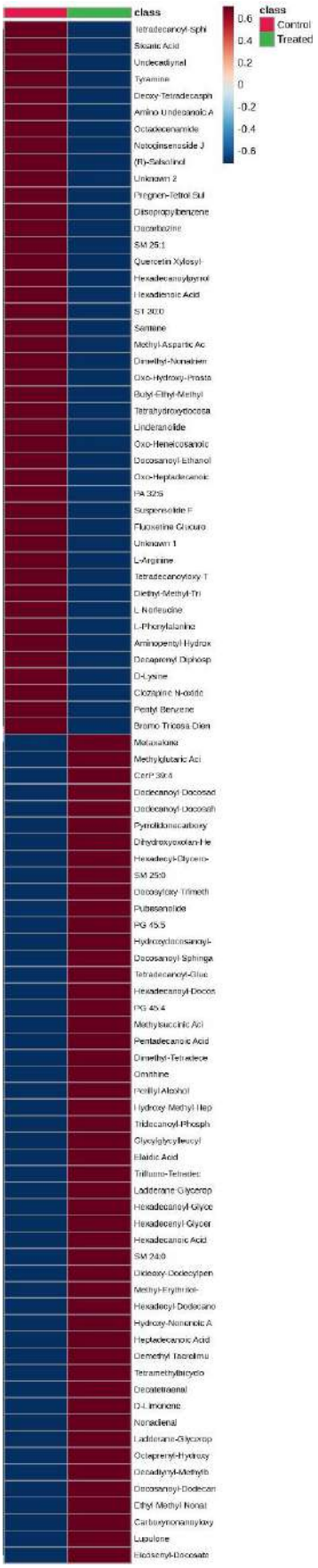

Supplementary Figure S7: Heatmap of metabolite expression patterns from untargeted metabolomic profiling, generated using MetaboAnalyst 6.0.

9. Summary and Conclusions

This PhD dissertation demonstrated that certain cation carriers can upregulate CD20 expression on malignant B cells, thereby enhancing the efficacy of anti-CD20 therapeutic antibodies through both *in vitro* mechanisms, such as complement-dependent cytotoxicity and antibody-dependent cellular cytotoxicity, and *in vivo* models. Furthermore, a comprehensive review of the literature, combined with original experimental research, revealed that salinomycin -induced CD20 upregulation is associated with MYC downregulation. Additionally, salinomycin directly affects mitochondrial function by disrupting mitochondrial respiration and altering cellular metabolism.

9.1 Publication No. 1: Enhancing anti-CD20 immunotherapy in B-cell malignancies cells.

Torun A.*, **Zdanowicz A**.*, Miazek-Zapala N., Zapala P., Pradhan B., Jedrzejczyk M., Ciechanowicz A., Pilch Z., Skorzynski M., Słabicki M., Rymkiewicz G., Barankiewicz J., Martines C., Laurenti L., Struga M., Winiarska M., Golab J., Kucia M., Ratajczak M.Z., Huczynski A., Calado D.P., Efremov D.G., Zerrouqi A., Pyrzynska B. Potassium /sodium cation carriers robustly up-regulate CD20 antigen by targeting MYC, and synergize with anti-CD20 immunotherapies to eliminate malignant B cells. Haematologica (Early view Dec 19, 2024).

*- AT and AZ contributed equally as co-first authors.

To address this, our team screened a range of cation carriers for their potential to enhance surface CD20 expression. Among the compounds tested, SAL, monensin (MON), narasin, and nigericin showed a notable ability to upregulate CD20 levels. Specifically, treatment with 0.25 µM SAL for 48 hours resulted in increased surface levels of CD20 antigen across several DLBCL and Burkitt lymphoma cell lines, as well as in primary CLL cells derived from patients' peripheral blood and DLBCL cells isolated from lymph nodes.

Our extended analyses demonstrate that SAL-induced upregulation of CD20 enhances the efficacy of therapeutic antibodies—particularly RTX, in both CDC and ADCC assays. To validate our *in vitro* findings, we proceeded with *in vivo* experiments using a SCID mouse model. This model was chosen due to its preserved complement system and natural killer (NK) cell activity, both of which are critical for RTX-mediated CDC and ADCC, respectively.

To investigate the molecular mechanism underlying CD20 upregulation, we initially observed that 12 hours of SAL and MON treatment affected levels of *MS4A1* mRNA. Based on this, we performed transcriptomic analysis on Raji cells treated with SAL and MON. The analysis

identified 65 significantly altered genes following SAL treatment and 896 following MON treatment. Furthermore, gene set enrichment analysis revealed modulation of 6 transcription factors/miRNAs by SAL and 101 by MON. Notably, four regulatory elements—FOXO, MYC, NF-Y, and miR-181—were commonly affected by both treatments.

To validate the transcriptomic data, we conducted qRT-PCR and Western blotting analyses, focusing on the FOXO and MYC regulatory pathways. In the FOXO signaling pathway, qRT-PCR showed that the expression of *IL7R* and *SGK1* was modulated by SAL treatment. These transcriptional changes were confirmed by Western blotting analysis, which revealed corresponding alterations in SGK1 protein levels and in phosphorylation of AKT (pAKT). In the MYC signaling pathway, qRT-PCR analysis revealed the downregulation of *MYC* mRNA and differential expression of several MYC-related target genes, including *PLK1*, *TNFAIP3*, and *PTPN6*, in response to SAL treatment.

To investigate the regulatory role of MYC in CD20 expression, we employed the MYC Tet-OFF system in the P493-6 cell line, where tetracycline/doxycycline treatment suppresses MYC expression. Repression of MYC led to increased levels of CD20, confirming MYC as a negative regulator of CD20. To further test this, we tested SAL derivatives that do not induce upregulation of CD20 expression and found that in contrast to these SAL derivatives, only the original SAL compound was capable of downregulating MYC. This suggests strong signalling connection between SAL-driven CD20 upregulation and suppression of MYC.

To further validate these findings, we used CRISPR/Cas9-mediated knockout of MYC and SGK1 in Raji cells. Following nucleofection, we assessed CD20 expression levels and observed that reduced MYC expression correlated with the increased levels of CD20, reinforcing its repressive role. This observation was further confirmed by pharmacological inhibition of MYC using 10058-F4, which similarly resulted in upregulation of CD20.

Additionally, CUT&RUN immunoprecipitation experiments demonstrated that MYC directly binds to the promoter region of MS4A1, the gene encoding CD20, providing direct evidence of MYC-mediated transcriptional regulation.

Overall, this study demonstrates that SAL and MON effectively upregulate CD20 expression in B-cell malignancies, thereby enhancing the efficacy of both anti-CD20 immunotherapy with monoclonal antibodies. Transcriptomic analysis, followed by validation through qRT-PCR, Western blotting, and CRISPR-Cas9 gene editing, elucidated the molecular mechanism of CD20 upregulation, highlighting the pivotal role of MYC.

9.2 Publication No. 2: A literature review focused on mitochondrial functionality in cancer.

Zdanowicz A., Grosicka-Maciąg E. The Interplay between Autophagy and Mitochondria in Cancer. Int. J. Mol. Sci. 2024, 25(17):9143.

This review manuscript examines existing literature from PubMed and Google Scholar on mitochondrial function in cancer. Beyond their established role in ATP (adenosine triphosphate) generation, mitochondria are crucial for cellular adaptation, regulation of oxidative stress, and metabolic processes—functions that become especially important under the stressful conditions typical of the tumor microenvironment.

Previous studies have demonstrated that cation carriers, such as SAL, affect mitochondrial function by promoting the accumulation of dysfunctional mitochondria, increasing the production of mtROS [37], and inducing both apoptosis [38] and autophagic cell death [26]. Analyzing and reviewing the available literature on the diverse functions of mitochondria and various forms of autophagy—including ubiquitin-mediated mitophagy, ubiquitin-independent mitophagy, and chaperone-mediated autophagy—and their roles in cancer development or regression increases the likelihood of understanding the impact of SAL on mitochondrial function.

Moreover, this publication lists the synthetic inhibitors and inducers of mitochondrial function and autophagy that have been investigated *in vitro*, as well as drugs currently undergoing evaluation in ongoing cancer clinical trials. Modulating mitochondrial homeostasis in cancer holds promise for drug development, as alterations in mitochondrial function have been shown to influence gene expression through retrograde signaling. Currently available strategies to reprogram cellular metabolism include targeting the mitochondrial electron transport chain (ETC) complexes, the tricarboxylic acid (TCA) cycle, and apoptosis regulators, such as BCL-2. Moreover, modulation of autophagy—either through activation or inhibition—plays a complex role in cancer progression. In the early stages of tumor development, inducing autophagy can suppress tumor growth by removing damaged organelles and limiting cellular stress. However, in later stages, autophagy may promote tumor progression and metastasis by providing essential nutrients to support cancer cell survival.

Despite their therapeutic potential, mitochondrial modulators face several limitations, including challenges in specific targeting, cancer heterogeneity, and incomplete understanding of their exact mechanisms of action. A major obstacle in the effective use of mitochondrial or autophagy modulators is the accurate diagnosis of cancer patients—particularly in identifying the cancer type, stage, and the extent to which the tumor depends on autophagy for survival. To aid in

this diagnostic process, the final section of this publication highlights autophagy-related genes with potential utility as prognostic and diagnostic biomarkers in cancer.

This overview summarizes current insights into mitochondrial and autophagy-related mechanisms in cancer cells, enhancing our understanding of mitochondrial homeostasis. Furthermore, it establishes a conceptual foundation for the formulation of hypotheses and the strategic direction of research into cation carriers as modulators of mitochondrial function in cancer.

9.3 Publication No. 3: The impact of SAL on mitochondrial function and the metabolomic profile of Burkitt lymphoma.

Zdanowicz A., Ilchenko O., Ciechanowicz A., Chi H., Struga M., Pyrzynska B., Low-Dose Salinomycin Alters Mitochondrial Function and Reprograms Metabolism in Burkitt Lymphoma. Int. J. Mol. Sci. 2025, 26(11), 5125.

As noted in Publication No. 2, cation carriers significantly affect mitochondrial function. Managò et al., 2015 reported that treatment with cation carriers (0–90 minutes) led to MMP reduction, acidification of the mitochondrial matrix (decreased pH) in HMLE-Twist cells, increased production of ROS in B-CLL cells, and reduced ATP levels in HMLE-Twist cells [38]. Additionally, research by Cosialls et al., 2023 has shown that a 48-hour treatment with 0.5 µM SAL inhibits the expression of mitochondrial proteins involved in key metabolic pathways, including the TCA cycle, ETC, glycolysis, glutaminolysis, and β-oxidation. It also affects proteins associated with mitochondrial biogenesis, such as those involved in mitochondrial RNA translation and mitochondrial ribosomal components [30].

Publication No. 1 demonstrated that SAL exerts anticancer effects and enhances anti-CD20 immunotherapy. Additionally, the literature review in Publication No. 2 and experimental studies by Managò et al. and Cosialls et al. highlighted SAL's impact on mitochondrial function. Building on this, Publication No. 3 aimed to investigate the effects of low concentrations of SAL on mitochondrial functionality and metabolism in lymphoma. A deeper understanding of the molecular mechanisms underlying SAL's action could facilitate its translation into clinical trials.

We investigated the effects of low concentrations of SAL (0.25 and 0.5 µM) on MMP, ROS production, OXPHOS, glycolytic activity, and metabolomic profiles in lymphoma cells. SAL treatment for 12-36 hours resulted in a reduction of MMP, which correlated with findings from oxygen consumption assays, showing a concentration-dependent decrease in basal respiration, maximal respiration, and ATP production.

The activity of the ETC is closely linked to mtROS production, as Complexes I and III are the primary sites of ROS generation. We examined mtROS levels and general oxidative stress in Raji cells and found that SAL treatment increased both. Under normal conditions, a higher MMP correlates with enhanced ETC activity, leading to increased ATP synthesis and mtROS production [39]. However, under pathological conditions—such as low oxygen availability—a decline in MMP can paradoxically result in excessive mtROS production, contributing to elevated overall oxidative stress [40].

Our results revealed that SAL, by inhibiting OXPHOS, shifts cellular metabolism toward increased glycolytic activity, as evidenced by elevated extracellular acidification rate (ECAR). Furthermore, metabolomic and subsequent data analysis demonstrated that 24-hour treatment with SAL leads to L-arginine depletion in Raji cells. In the study by Cheng et al., 2018 arginine depletion in MDA-MB-231 breast adenocarcinoma cells led to a reduction in mitochondrial respiration and extensive metabolic reprogramming [41]. Furthermore, depriving cancer cells of L-arginine can be therapeutically beneficial as arginine removal induces cell death in many cancer types [42].

9.4 Conclusions

My PhD thesis presents a strategy to increase CD20 expression and improve CD20-targeted immunotherapy, tackling the frequent issue of diminished CD20 levels seen across patients and with different B-cell malignancies. The approach involves pretreating malignant B cells with cation carriers that elevate CD20 expression on the cell surface, leading to significantly improved responses to anti-CD20 immunotherapy in both *in vitro* and *in vivo* studies, included in this dissertation. The evaluation of this strategy was based on screening various cation carriers for their ability to upregulate CD20 using flow cytometry. Selected cation carriers were then tested in CDC and ADCC assays. The initial findings obtained *in vitro* were subsequently confirmed in a mouse model.

Furthermore, the experimental results not only elucidated the molecular mechanism underlying CD20 upregulation, but also revealed the impact of cation carriers on mitochondrial function and cellular metabolic profiles. Notably, CD20 upregulation was found to be associated with MYC downregulation. To investigate the molecular basis of CD20 upregulation, changes in gene expression were analyzed using transcriptomics and qRT-PCR. Protein-level alterations following cation carrier treatment were assessed through Western blotting. Key findings were further validated using CRISPR-Cas9-mediated gene knockout.

The impact of cation carriers on mitochondria and cellular metabolism was analyzed through assessments of MMP, ROS production, mitochondrial respiration, and comprehensive metabolomic profiling. Importantly, it was found that cation carriers, particularly SAL, inhibit mitochondrial respiration, induce a metabolic shift toward glycolysis, and reduce intracellular L-arginine levels.

These findings underscore the therapeutic potential of cation carriers—as promising drug candidates for future clinical trials. At a low concentration (0.25 μM), SAL significantly upregulates CD20 expression on the surface of B-cell-derived malignancies, thereby enhancing the effectiveness of anti-CD20 immunotherapy. Moreover, at this dosage, SAL demonstrates a favorable safety profile while modulating mitochondrial function and certain cellular signaling pathways.

10. Approval of the Bioethics and Ethics Committee

Komisja Bioetyczna
przy Warszawskim Uniwersytecie Medycznym

Tel.: 022/ 57 - 20 -303
Fax: 022/ 57 - 20 -165

ul. Żwirki i Wigury nr 61
02-091 Warszawa

e-mail: komisja.bioetyczna@wum.edu.pl
www.komisja-bioetyczna.wum.edu.pl

KB/...65.../2023

Komisja Bioetyczna przy Warszawskim Uniwersytecie Medycznym
w dniu 08 maja 2023 r. po zapoznaniu się z wnioskiem

Dr hab.n.med. Grzegorz Rymkiewicz
Pracownia Cytometrii Przepływowej
Zakładu Patomorfologii Nowotworów
Narodowego Instytutu Nowotworów
ul. Rendgena 5, 02-781 Warszawa

dotyczącym: wyrażenia opinii w sprawie badania pt. "Testowanie pochodnych nośników kationowych jako potencjalnych terapeutyków w leczeniu nowotworów wywodzących się z limfocytów B"

- Badanie może być prowadzone wyłącznie w okresie obowiązywania polisy ubezpieczeniowej.

wyraża następującą
opinię

- stwierdza, że jest ono dopuszczalne i zgodne z zasadami naukowo-etycznymi*.
- ~~stwierdza, że jest ono niedopuszczalne i niezgodne z zasadami naukowo-etycznymi.*~~

Uwagi Komisji – ***verte***

Komisja działa na podstawie regulaminu działania Komisji Bioetycznej przy Warszawskim Uniwersytecie Medycznym, przyjętego zarządzeniem Rektora WUM nr 200/2022 z dnia 18 października 2022 r. oraz przepisów prawa powszechnie obowiązującego, w tym przede wszystkim ustawy z dnia 5 grudnia 1996 r. o zawodach lekarza i lekarza dentysty, ustawy z dnia 6 września 2001 r. Prawo farmaceutyczne, ustawy z 22 kwietnia 2022 r. o wyrobach medycznych oraz prawa międzynarodowego lub unijnego, a także odpowiednich norm naukowych lub zawodowych.

Przewodnicząca Komisji Bioetycznej

Prof. dr hab. n. med. Magdalena Kuźma-Kozakiewicz

*niepotrzebne skreślić

UCHWAŁA NR WAW2/095/2023

z dnia 5 lipca 2023 r.

II Lokalnej Komisji Etycznej do Spraw Doświadczeń na Zwierzętach w Warszawie

§ 1

Na podstawie art. 48 ust. 1 pkt. 1[1] ustawy z dnia 15 stycznia 2015r. o ochronie zwierząt wykorzystywanych do celów naukowych lub edukacyjnych (Dz. U. z 2021 r. poz. 1331), zwanej dalej „ustawą" po rozpatrzeniu wniosku pt.: **„Testowanie pochodnych salinomycyny jako potencjalnych terapeutyków przeciwnowotworowych, stosowanych razem z przeciwciałami anty-CD20."** z dnia 29.06.2023 roku, złożonego przez Centrum Badań Przedklinicznych (CBP) WUM, adres: ul. Banacha 1B, Warszawa 02-097, zaplanowanego przez dr Beatę Pyrzyńską[2],

przy udziale:[3] (nie dotyczy),

Lokalna Komisja Etyczna:

WYRAŻA ZGODĘ

na przeprowadzenie doświadczeń na zwierzętach w zakresie wniosku.

§ 2

W wyniku rozpatrzenia wniosku, o którym mowa w § 1, Lokalna Komisja Etyczna ustaliła, że:

1. Wniosek należy przypisać do kategorii: [PB1] (badania podstawowe) onkologia, niezależnie od badanego układu.
2. Najwyższy stopień dotkliwości proponowanych procedur to: umiarkowana.
3. Doświadczenia będą przeprowadzane na gatunkach lub grupach gatunków[4]:

Gatunek	Wiek/stadium rozwoju	Liczba
Mysz domowa SCID (CB17/icr-Prkdc scid/icrlcoCrl)	6 – 7 tygodni	144
Mysz domowa C57BL/6 lub C57BL/6/Clzd	6 – 7 tygodni	244
Mysz domowa NSG (NOD.Cg-Prkdcscid Il2rgtm1Wjl/SzJ)	6 – 7 tygodni	10

4. Doświadczenia będą przeprowadzane przez: Beata Pyrzyńska, Aleksandra Zdanowicz, Abdessamad Zerrouqi, Robert Wrzesień, Karolina Tyszkowska.
5. Doświadczenie będzie przeprowadzane w terminie[5] od 17.07.2023 r. do 13.02.2028 r.
6. Doświadczenie będzie przeprowadzone w ośrodku[6]: nie dotyczy.
7. Doświadczenie będzie przeprowadzone poza ośrodkiem, w: nie dotyczy.
8. Użyte do procedur zwierzęta dzikie zostaną odłowione przez: nie dotyczy.
9. Doświadczenie ~~zostanie~~/nie zostanie poddane ocenie retrospektywnej ~~na podstawie art. 53 ust. 1 ustawy w terminie do 6 miesięcy od dnia przekazania przez użytkownika dokumentacji,~~

[1] Niewłaściwy zapis usunąć
[2] imię i nazwisko osoby, która zaplanowała i jest odpowiedzialna za przeprowadzenie doświadczenia
[3] Wypełnić w przypadku dopuszczenia do postępowania organizacji społecznej.
[4] Podać liczbę, szczep/stado, wiek/stadium rozwoju
[5] Nie dłużej niż 5 lat
[6] Podać jeśli jest to inny ośrodek niż użytkownik

~~mającej stanowić podstawę dokonania oceny retrospektywnej. Użytkownik jest zobowiązany do przekazania ww. dokumentacji niezwłocznie, tj. w terminie, o którym mowa w art. 52 ust. 2 ustawy.~~

§ 3

Uzasadnienie:

Komisja oceniła wniosek zgodnie z art. 47 ust. 1 i 2 ustawy z dnia 15 stycznia 2015 r. o ochronie zwierząt wykorzystywanych do celów naukowych lub edukacyjnych (Dz. U. z 2021 r. poz. 1331). Po zapoznaniu się z problematyką badawczą przedstawioną we wniosku komisja stwierdza, że przedstawiony projekt spełnia zasady dopuszczenia doświadczeń na zwierzętach pod kątem oceny etycznej. Na podstawie art. 107 § 4 ustawy z dnia 14 czerwca 1960 r. – Kodeks postępowania administracyjnego z późniejszymi zmianami (Dz. U. 2020 r. poz. 256) odstąpiono od sporządzania uzasadnienia decyzji, ponieważ uwzględnia ona w całości żądanie strony.

§ 4

Integralną część niniejszej uchwały stanowi kopia wniosku, o którym mowa w § 1.

Szkoła Główna Gospodarstwa Wiejskiego
w Warszawie
II Lokalna Komisja Etyczna
ds. Doświadczeń na Zwierzętach
02-786 Warszawa, ul. Ciszewskiego 8
tel. 22 60 [illegible]

(Pieczęć lokalnej komisji etycznej)

PRZEWODNICZĄCA
II Lokalnej Komisji Etycznej
ds. Doświadczeń na Zwierzętach przy SGGW
/ Prof. dr hab. Joanna Gromadzka-Ostrowska /

(Podpis Przewodniczącej Komisji)

Pouczenie:

Zgodnie z art. 33 ust. 3 i art. 40 ustawy w zw. z art. 127 § 1 i 2 oraz 129 § 2 ustawy z dnia z dnia 14 czerwca 1960 r. Kodeks postępowania administracyjnego (Dz. U. 2017, poz. 1257 – tj.; dalej KPA) od uchwały Lokalnej Komisji Etycznej strona może wnieść, za jej pośrednictwem, odwołanie do Krajowej Komisji Etycznej do Spraw Doświadczeń na Zwierzętach w terminie 14 od dnia doręczenia uchwały.

Na podstawie art. 127a KPA w trakcie biegu terminu do wniesienia odwołania strona może zrzec się prawa do jego wniesienia, co należy uczynić wobec Lokalnej Komisji Etycznej, która wydała uchwałę. Z dniem doręczenia Lokalnej Komisji Etycznej oświadczenia o zrzeczeniu się prawa do wniesienia odwołania przez ostatnią ze stron postępowania, decyzja staje się ostateczna i prawomocna.

Otrzymuje:
1) Użytkownik.
2) Organizacja społeczna dopuszczona do udziału w postępowaniu (jeśli dotyczy)
3) a/a

Użytkownik kopię przekazuje:
- Osoba planująca doświadczenie
- Zespół ds. dobrostanu

11. Co-authors' statements

11. 1 Publication No. 1

Name and Surname: **Beata Pyrzyńska** Date: April 2nd, 2025

Statement

As a co-author of the research paper entitled:

"Potassium/sodium cation carriers robustly up-regulate CD20 antigen by targeting MYC and synergize with anti-CD20 immunotherapies to eliminate malignant B cells"

I formally consent to the inclusion of the aforementioned work as an integral component of the doctoral dissertation portfolio of Aleksandra Zdanowicz, MSc.

Additionally, I declare my contribution to the research as follows:

Author's Name and Surname	Contribution range
Anna Torun	Conducting experiments and statistical analysis; Critical evaluation and interpretation of results;
Aleksandra Zdanowicz	Conducting experiments and statistical analysis; Critical evaluation and interpretation of results; Manuscript revision;
Nina Miązek-Zapała	Conducting experiments and statistical analysis;
Piotr Zapała	Conducting experiments and statistical analysis;
Bhaskar Pradhan	Conducting experiments; Manuscript revision;
Marta Jędrzejczyk	Conducting experiments;
Andrzej Ciechanowicz	Conducting experiments;
Zofia Pilch	Conducting experiments;
Marcin Skórzynski	Conducting experiments;
Mikołaj Słabicki	Concept and study design;
Grzegorz Rymkiewicz	Delivery of patient samples; Diagnosis of patient samples;
Joanna Barankiewicz	Delivery of patient samples; Diagnosis of patient samples;

Claudio Martines	Conducting experiments;
Luca Laurenti	Delivery of patient samples; Diagnosis of patient samples;
Marta Struga	Concept and study design;
Magdalena Winiarska	Concept and study design;
Jakub Gołąb	Concept and study design;
Magdalena Kucia	Concept and study design;
Mariusz Z Ratajczak	Concept and study design;
Adam Huczyński	Study conception and design; Data summary;
Dinis P Calado	Study concept and design;
Dimitar G Efremov	Concept and study design; Delivery of patient samples;
Abdessamad Zerrouqi	Study concept and design, conducting experiments; Manuscript revision;
Beata Pyrzyńska	Study concept and design; Conducting experiments and statistical analysis; Critical evaluation and interpretation of results; Preparation of both the initial draft and the final version of the manuscript.

The following experimental results, prepared by Aleksandra Zdanowicz, MSc, are included in the article:

- Fig. 3C – Complement-dependent cytotoxicity (CDC) assay following treatment with ofatumumab.
- Fig. 6B – Western blot analysis of both phosphorylated and total protein levels of AKT, FOXO1, and SGK1 kinase in Raji cells, along with statistical quantification.
- Fig. 7A – qRT-PCR analysis measuring *MYC* mRNA levels.
- Fig. 8B – Western blot analysis of MYC and SGK1, along with statistical quantification.
- Fig. 8C – Western blot analysis of MYC and SGK1 in Raji cells nucleofected with RNP complexes containing sgRNA targeting either MYC (sgMYC) or SGK1 (sgSGK1) and Cas9 nuclease.
- Fig. 8D – Flow cytometry analysis estimating the surface expression level of CD20 in Raji cells pretreated with either SAL or a MYC inhibitor.
- Fig. 8E – Chromatin immunoprecipitation assay (CUT&RUN) examining MYC-DNA interaction, followed by RT-PCR amplification of the MS4A1 promoter fragment.
- Suppl. Fig. 7 – Flow cytometry assessment of surface CD20 expression in Raji cells following treatment with an NLRP3 inhibitor or cation carriers.
- Suppl. Fig 9A – Quantification and statistical analysis of MYC protein levels by Western blotting in Raji and P493-6 cell lines pretreated with SAL, MON, or vehicle.
- Suppl. Fig. 9B - Quantification of the binding of *MYC* to its target E-box DNA motif in nuclear extracts from from Raji cells using the TransAM MYC ELISA.
- Suppl. Fig. 11C – Western blot analysis of both phosphorylated and total protein levels of AKT and FOXO1 in Raji cells, along with statistical quantification.
- Suppl. Fig. 12A – Western blot analysis of MYC in extracts from Raji cells, either mock-nucleofected or genome-edited with sgMYC.
- Suppl. Fig. 12B – Flow cytometry analysis of surface CD20 on Raji cells, either mock-nucleofected or genome-edited with sgMYC, followed by treatment with SAL, MON, or corresponding controls for 48 hours.
- Suppl. Fig. 12C – Western blot analysis of MYC in extracts from Raji cells, either mock-nucleofected or genome-edited with sgSGK1.
- Suppl. Fig. 12D – Flow cytometry analysis of surface CD20 on Raji cells, either mock-nucleofected or genome-edited with sgSGK1, followed by treatment with SAL, MON, or corresponding controls.
- Suppl. Fig. 12E – Flow cytometry analysis of surface CD20 on Raji cells pretreated with EMD638683.

I confirm that the results obtained by Aleksandra Zdanowicz, Msc, are included in the paper as figures mentioned above.

Andrzej Ciechanowicz Warsaw, 30.05.2025

Statement

As a co-author of the research paper entitled:

"Potassium/sodium cation carriers robustly up-regulate CD20 antigen by targeting MYC and synergize with anti-CD20 immunotherapies to eliminate malignant B cells"

I formally consent to the inclusion of the aforementioned work as an integral component of the doctoral dissertation portfolio of Aleksandra Zdanowicz, MSc.

Additionally, I declare my contribution to the research as follows:

Author's Name and Surname	Contribution range
Anna Torun	Conducting experiments and statistical analysis; Critical evaluation and interpretation of results;
Aleksandra Zdanowicz	Conducting experiments and statistical analysis; Critical evaluation and interpretation of results; Manuscript revision;
Nina Miązek-Zapała	Conducting experiments and statistical analysis;
Piotr Zapała	Conducting experiments and statistical analysis;
Bhaskar Pradhan	Conducting experiments; Manuscript revision;
Marta Jędrzejczyk	Conducting experiments;
Andrzej Ciechanowicz	Conducting experiments;
Zofia Pilch	Conducting experiments;
Marcin Skórzynski	Conducting experiments;
Mikołaj Słabicki	Concept and study design;
Grzegorz Rymkiewicz	Delivery of patient samples; Diagnosis of patient samples;
Joanna Barankiewicz	Delivery of patient samples; Diagnosis of patient samples;

Claudio Martines	Conducting experiments;
Luca Laurenti	Delivery of patient samples; Diagnosis of patient samples;
Marta Struga	Concept and study design;
Magdalena Winiarska	Concept and study design;
Jakub Gołąb	Concept and study design;
Magdalena Kucia	Concept and study design;
Mariusz Z Ratajczak	Concept and study design;
Adam Huczyński	Study conception and design; Data summary;
Dinis P Calado	Study concept and design;
Dimitar G Efremov	Concept and study design; Delivery of patient samples;
Abdessamad Zerrouqi	Study concept and design, conducting experiments; Manuscript revision;
Beata Pyrzyńska	Study concept and design; Conducting experiments and statistical analysis; Critical evaluation and interpretation of results; Preparation of both the initial draft and the final version of the manuscript.

Sign Ciechanowicz Ciechanowicz (30-May-2025 14:24 GMT+2)

The following experimental results, prepared by Aleksandra Zdanowicz, MSc, are included in the article:

- Fig. 3C – Complement-dependent cytotoxicity (CDC) assay following treatment with ofatumumab.
- Fig. 6B – Western blot analysis of both phosphorylated and total protein levels of AKT, FOXO1, and SGK1 kinase in Raji cells, along with statistical quantification.
- Fig. 7A – qRT-PCR analysis measuring *MYC* mRNA levels.
- Fig. 8B – Western blot analysis of MYC and SGK1, along with statistical quantification.
- Fig. 8C – Western blot analysis of MYC and SGK1 in Raji cells nucleofected with RNP complexes containing sgRNA targeting either MYC (sgMYC) or SGK1 (sgSGK1) and Cas9 nuclease.
- Fig. 8D – Flow cytometry analysis estimating the surface expression level of CD20 in Raji cells pretreated with either SAL or a MYC inhibitor.
- Fig. 8E – Chromatin immunoprecipitation assay (CUT&RUN) examining MYC-DNA interaction, followed by RT-PCR amplification of the MS4A1 promoter fragment.
- Suppl. Fig. 7 – Flow cytometry assessment of surface CD20 expression in Raji cells following treatment with an NLRP3 inhibitor or cation carriers.
- Suppl. Fig 9A – Quantification and statistical analysis of MYC protein levels by Western blotting in Raji and P493-6 cell lines pretreated with SAL, MON, or vehicle.
- Suppl. Fig. 9B - Quantification of the binding of *MYC* to its target E-box DNA motif in nuclear extracts from from Raji cells using the TransAM MYC ELISA.
- Suppl. Fig. 11C – Western blot analysis of both phosphorylated and total protein levels of AKT and FOXO1 in Raji cells, along with statistical quantification.
- Suppl. Fig. 12A – Western blot analysis of MYC in extracts from Raji cells, either mock-nucleofected or genome-edited with sgMYC.
- Suppl. Fig. 12B – Flow cytometry analysis of surface CD20 on Raji cells, either mock-nucleofected or genome-edited with sgMYC, followed by treatment with SAL, MON, or corresponding controls for 48 hours.
- Suppl. Fig. 12C – Western blot analysis of MYC in extracts from Raji cells, either mock-nucleofected or genome-edited with sgSGK1.
- Suppl. Fig. 12D – Flow cytometry analysis of surface CD20 on Raji cells, either mock-nucleofected or genome-edited with sgSGK1, followed by treatment with SAL, MON, or corresponding controls.
- Suppl. Fig. 12E – Flow cytometry analysis of surface CD20 on Raji cells pretreated with EMD638683.

Marta Jędrzejczyk Warszawa, 29.05.2025

Statement

As a co-author of the research paper entitled:

"Potassium/sodium cation carriers robustly up-regulate CD20 antigen by targeting MYC and synergize with anti-CD20 immunotherapies to eliminate malignant B cells"

I formally consent to the inclusion of the aforementioned work as an integral component of the doctoral dissertation portfolio of Aleksandra Zdanowicz, MSc.

Additionally, I declare my contribution to the research as follows:

Author's Name and Surname	Contribution range
Anna Torun	Conducting experiments and statistical analysis; Critical evaluation and interpretation of results;
Aleksandra Zdanowicz	Conducting experiments and statistical analysis; Critical evaluation and interpretation of results; Manuscript revision;
Nina Miązek-Zapała	Conducting experiments and statistical analysis;
Piotr Zapała	Conducting experiments and statistical analysis;
Bhaskar Pradhan	Conducting experiments; Manuscript revision;
Marta Jędrzejczyk	Conducting experiments;
Andrzej Ciechanowicz	Conducting experiments;
Zofia Pilch	Conducting experiments;
Marcin Skórzynski	Conducting experiments;
Mikołaj Słabicki	Concept and study design;
Grzegorz Rymkiewicz	Delivery of patient samples; Diagnosis of patient samples;
Joanna Barankiewicz	Delivery of patient samples; Diagnosis of patient samples;

Claudio Martines	Conducting experiments;
Luca Laurenti	Delivery of patient samples; Diagnosis of patient samples;
Marta Struga	Concept and study design;
Magdalena Winiarska	Concept and study design;
Jakub Gołąb	Concept and study design;
Magdalena Kucia	Concept and study design;
Mariusz Z Ratajczak	Concept and study design;
Adam Huczyński	Study conception and design; Data summary;
Dinis P Calado	Study concept and design;
Dimitar G Efremov	Concept and study design; Delivery of patient samples;
Abdessamad Zerrouqi	Study concept and design, conducting experiments; Manuscript revision;
Beata Pyrzyńska	Study concept and design; Conducting experiments and statistical analysis; Critical evaluation and interpretation of results; Preparation of both the initial draft and the final version of the manuscript.

The following experimental results, prepared by Aleksandra Zdanowicz, MSc, are included in the article:

- Fig. 3C – Complement-dependent cytotoxicity (CDC) assay following treatment with ofatumumab.
- Fig. 6B – Western blot analysis of both phosphorylated and total protein levels of AKT, FOXO1, and SGK1 kinase in Raji cells, along with statistical quantification.
- Fig. 7A – qRT-PCR analysis measuring *MYC* mRNA levels.
- Fig. 8B – Western blot analysis of MYC and SGK1, along with statistical quantification.
- Fig. 8C – Western blot analysis of MYC and SGK1 in Raji cells nucleofected with RNP complexes containing sgRNA targeting either MYC (sgMYC) or SGK1 (sgSGK1) and Cas9 nuclease.
- Fig. 8D – Flow cytometry analysis estimating the surface expression level of CD20 in Raji cells pretreated with either SAL or a MYC inhibitor.
- Fig. 8E – Chromatin immunoprecipitation assay (CUT&RUN) examining MYC-DNA interaction, followed by RT-PCR amplification of the MS4A1 promoter fragment.
- Suppl. Fig. 7 – Flow cytometry assessment of surface CD20 expression in Raji cells following treatment with an NLRP3 inhibitor or cation carriers.
- Suppl. Fig 9A – Quantification and statistical analysis of MYC protein levels by Western blotting in Raji and P493-6 cell lines pretreated with SAL, MON, or vehicle.
- Suppl. Fig. 9B - Quantification of the binding of *MYC* to its target E-box DNA motif in nuclear extracts from from Raji cells using the TransAM MYC ELISA.
- Suppl. Fig. 11C – Western blot analysis of both phosphorylated and total protein levels of AKT and FOXO1 in Raji cells, along with statistical quantification.
- Suppl. Fig. 12A – Western blot analysis of MYC in extracts from Raji cells, either mock-nucleofected or genome-edited with sgMYC.
- Suppl. Fig. 12B – Flow cytometry analysis of surface CD20 on Raji cells, either mock-nucleofected or genome-edited with sgMYC, followed by treatment with SAL, MON, or corresponding controls for 48 hours.
- Suppl. Fig. 12C – Western blot analysis of MYC in extracts from Raji cells, either mock-nucleofected or genome-edited with sgSGK1.
- Suppl. Fig. 12D – Flow cytometry analysis of surface CD20 on Raji cells, either mock-nucleofected or genome-edited with sgSGK1, followed by treatment with SAL, MON, or corresponding controls.
- Suppl. Fig. 12E – Flow cytometry analysis of surface CD20 on Raji cells pretreated with EMD638683.

Bhaskar Pradhan Warszawa, 28-03-2025

Statement

As a co-author of the research paper entitled:

"Potassium/sodium cation carriers robustly up-regulate CD20 antigen by targeting MYC and synergize with anti-CD20 immunotherapies to eliminate malignant B cells"

I formally consent to the inclusion of the aforementioned work as an integral component of the doctoral dissertation portfolio of Aleksandra Zdanowicz, MSc.

Additionally, I declare my contribution to the research as follows:

Author's Name and Surname	Contribution range
Anna Torun	Conducting experiments and statistical analysis; Critical evaluation and interpretation of results;
Aleksandra Zdanowicz	Conducting experiments and statistical analysis; Critical evaluation and interpretation of results; Manuscript revision;
Nina Miązek-Zapała	Conducting experiments and statistical analysis;
Piotr Zapała	Conducting experiments and statistical analysis;
Bhaskar Pradhan	Conducting experiments; Manuscript revision;
Marta Jędrzejczyk	Conducting experiments;
Andrzej Ciechanowicz	Conducting experiments;
Zofia Pilch	Conducting experiments;
Marcin Skórzynski	Conducting experiments;
Mikołaj Słabicki	Concept and study design;
Grzegorz Rymkiewicz	Delivery of patient samples; Diagnosis of patient samples;
Joanna Barankiewicz	Delivery of patient samples; Diagnosis of patient samples;

Claudio Martines	Conducting experiments;
Luca Laurenti	Delivery of patient samples; Diagnosis of patient samples;
Marta Struga	Concept and study design;
Magdalena Winiarska	Concept and study design;
Jakub Gołąb	Concept and study design;
Magdalena Kucia	Concept and study design;
Mariusz Z Ratajczak	Concept and study design;
Adam Huczyński	Study conception and design; Data summary;
Dinis P Calado	Study concept and design;
Dimitar G Efremov	Concept and study design; Delivery of patient samples;
Abdessamad Zerrouqi	Study concept and design, conducting experiments; Manuscript revision;
Beata Pyrzyńska	Study concept and design; Conducting experiments and statistical analysis; Critical evaluation and interpretation of results; Preparation of both the initial draft and the final version of the manuscript.

Sign 

The following experimental results, prepared by Aleksandra Zdanowicz, MSc, are included in the article:

- Fig. 3C – Complement-dependent cytotoxicity (CDC) assay following treatment with ofatumumab.
- Fig. 6B – Western blot analysis of both phosphorylated and total protein levels of AKT, FOXO1, and SGK1 kinase in Raji cells, along with statistical quantification.
- Fig. 7A – qRT-PCR analysis measuring *MYC* mRNA levels.
- Fig. 8B – Western blot analysis of MYC and SGK1, along with statistical quantification.
- Fig. 8C – Western blot analysis of MYC and SGK1 in Raji cells nucleofected with RNP complexes containing sgRNA targeting either MYC (sgMYC) or SGK1 (sgSGK1) and Cas9 nuclease.
- Fig. 8D – Flow cytometry analysis estimating the surface expression level of CD20 in Raji cells pretreated with either SAL or a MYC inhibitor.
- Fig. 8E – Chromatin immunoprecipitation assay (CUT&RUN) examining MYC-DNA interaction, followed by RT-PCR amplification of the MS4A1 promoter fragment.
- Suppl. Fig. 7 – Flow cytometry assessment of surface CD20 expression in Raji cells following treatment with an NLRP3 inhibitor or cation carriers.
- Suppl. Fig 9A – Quantification and statistical analysis of MYC protein levels by Western blotting in Raji and P493-6 cell lines pretreated with SAL, MON, or vehicle.
- Suppl. Fig. 9B - Quantification of the binding of *MYC* to its target E-box DNA motif in nuclear extracts from from Raji cells using the TransAM MYC ELISA.
- Suppl. Fig. 11C – Western blot analysis of both phosphorylated and total protein levels of AKT and FOXO1 in Raji cells, along with statistical quantification.
- Suppl. Fig. 12A – Western blot analysis of MYC in extracts from Raji cells, either mock-nucleofected or genome-edited with sgMYC.
- Suppl. Fig. 12B – Flow cytometry analysis of surface CD20 on Raji cells, either mock-nucleofected or genome-edited with sgMYC, followed by treatment with SAL, MON, or corresponding controls for 48 hours.
- Suppl. Fig. 12C – Western blot analysis of MYC in extracts from Raji cells, either mock-nucleofected or genome-edited with sgSGK1.
- Suppl. Fig. 12D – Flow cytometry analysis of surface CD20 on Raji cells, either mock-nucleofected or genome-edited with sgSGK1, followed by treatment with SAL, MON, or corresponding controls.
- Suppl. Fig. 12E – Flow cytometry analysis of surface CD20 on Raji cells pretreated with EMD638683.

Piotr Zapała

Warszawa, 28.03.2025

Statement

As a co-author of the research paper entitled:

"Potassium/sodium cation carriers robustly up-regulate CD20 antigen by targeting MYC and synergize with anti-CD20 immunotherapies to eliminate malignant B cells"

I formally consent to the inclusion of the aforementioned work as an integral component of the doctoral dissertation portfolio of Aleksandra Zdanowicz, MSc.

Additionally, I declare my contribution to the research as follows:

Author's Name and Surname	Contribution range
Anna Torun	Conducting experiments and statistical analysis; Critical evaluation and interpretation of results;
Aleksandra Zdanowicz	Conducting experiments and statistical analysis; Critical evaluation and interpretation of results; Manuscript revision;
Nina Miązek-Zapała	Conducting experiments and statistical analysis;
Piotr Zapała	Conducting experiments and statistical analysis;
Bhaskar Pradhan	Conducting experiments; Manuscript revision;
Marta Jędrzejczyk	Conducting experiments;
Andrzej Ciechanowicz	Conducting experiments;
Zofia Pilch	Conducting experiments;
Marcin Skórzynski	Conducting experiments;
Mikołaj Słabicki	Concept and study design;
Grzegorz Rymkiewicz	Delivery of patient samples; Diagnosis of patient samples;
Joanna Barankiewicz	Delivery of patient samples; Diagnosis of patient samples;

Claudio Martines	Conducting experiments;
Luca Laurenti	Delivery of patient samples; Diagnosis of patient samples;
Marta Struga	Concept and study design;
Magdalena Winiarska	Concept and study design;
Jakub Gołąb	Concept and study design;
Magdalena Kucia	Concept and study design;
Mariusz Z Ratajczak	Concept and study design;
Adam Huczyński	Study conception and design; Data summary;
Dinis P Calado	Study concept and design;
Dimitar G Efremov	Concept and study design; Delivery of patient samples;
Abdessamad Zerrouqi	Study concept and design, conducting experiments; Manuscript revision;
Beata Pyrzyńska	Study concept and design; Conducting experiments and statistical analysis; Critical evaluation and interpretation of results; Preparation of both the initial draft and the final version of the manuscript.

The following experimental results, prepared by Aleksandra Zdanowicz, MSc, are included in the article:

- Fig. 3C – Complement-dependent cytotoxicity (CDC) assay following treatment with ofatumumab.
- Fig. 6B – Western blot analysis of both phosphorylated and total protein levels of AKT, FOXO1, and SGK1 kinase in Raji cells, along with statistical quantification.
- Fig. 7A – qRT-PCR analysis measuring *MYC* mRNA levels.
- Fig. 8B – Western blot analysis of MYC and SGK1, along with statistical quantification.
- Fig. 8C – Western blot analysis of MYC and SGK1 in Raji cells nucleofected with RNP complexes containing sgRNA targeting either MYC (sgMYC) or SGK1 (sgSGK1) and Cas9 nuclease.
- Fig. 8D – Flow cytometry analysis estimating the surface expression level of CD20 in Raji cells pretreated with either SAL or a MYC inhibitor.
- Fig. 8E – Chromatin immunoprecipitation assay (CUT&RUN) examining MYC-DNA interaction, followed by RT-PCR amplification of the MS4A1 promoter fragment.
- Suppl. Fig. 7 – Flow cytometry assessment of surface CD20 expression in Raji cells following treatment with an NLRP3 inhibitor or cation carriers.
- Suppl. Fig 9A – Quantification and statistical analysis of MYC protein levels by Western blotting in Raji and P493-6 cell lines pretreated with SAL, MON, or vehicle.
- Suppl. Fig. 9B - Quantification of the binding of *MYC* to its target E-box DNA motif in nuclear extracts from from Raji cells using the TransAM MYC ELISA.
- Suppl. Fig. 11C – Western blot analysis of both phosphorylated and total protein levels of AKT and FOXO1 in Raji cells, along with statistical quantification.
- Suppl. Fig. 12A – Western blot analysis of MYC in extracts from Raji cells, either mock-nucleofected or genome-edited with sgMYC.
- Suppl. Fig. 12B – Flow cytometry analysis of surface CD20 on Raji cells, either mock-nucleofected or genome-edited with sgMYC, followed by treatment with SAL, MON, or corresponding controls for 48 hours.
- Suppl. Fig. 12C – Western blot analysis of MYC in extracts from Raji cells, either mock-nucleofected or genome-edited with sgSGK1.
- Suppl. Fig. 12D – Flow cytometry analysis of surface CD20 on Raji cells, either mock-nucleofected or genome-edited with sgSGK1, followed by treatment with SAL, MON, or corresponding controls.
- Suppl. Fig. 12E – Flow cytometry analysis of surface CD20 on Raji cells pretreated with EMD638683.

Nina Miązek-Zapała

Statement

As a co-author of the research paper entitled:

"Potassium/sodium cation carriers robustly up-regulate CD20 antigen by targeting MYC and synergize with anti-CD20 immunotherapies to eliminate malignant B cells"

I formally consent to the inclusion of the aforementioned work as an integral component of the doctoral dissertation portfolio of Aleksandra Zdanowicz, MSc.

Additionally, I declare my contribution to the research as follows (highlighted above):

Author's Name and Surname	Contribution range
Anna Torun	Conducting experiments and statistical analysis; Critical evaluation and interpretation of results;
Aleksandra Zdanowicz	Conducting experiments and statistical analysis; Critical evaluation and interpretation of results; Manuscript revision;
Nina Miązek-Zapała	**Conducting experiments and statistical analysis; providing funding, design, and conceptualization of the RNA-seq experiment;**
Piotr Zapała	Conducting experiments and statistical analysis;
Bhaskar Pradhan	Conducting experiments; Manuscript revision;
Marta Jędrzejczyk	Conducting experiments;
Andrzej Ciechanowicz	Conducting experiments;
Zofia Pilch	Conducting experiments;
Marcin Skórzynski	Conducting experiments;
Mikołaj Słabicki	Concept and study design;
Grzegorz Rymkiewicz	Delivery of patient samples; Diagnosis of patient samples;
Joanna Barankiewicz	Delivery of patient samples; Diagnosis of patient samples;

Claudio Martines	Conducting experiments;
Luca Laurenti	Delivery of patient samples; Diagnosis of patient samples;
Marta Struga	Concept and study design;
Magdalena Winiarska	Concept and study design;
Jakub Gołąb	Concept and study design;
Magdalena Kucia	Concept and study design;
Mariusz Z Ratajczak	Concept and study design;
Adam Huczyński	Study conception and design; Data summary;
Dinis P Calado	Study concept and design;
Dimitar G Efremov	Concept and study design; Delivery of patient samples;
Abdessamad Zerrouqi	Study concept and design, conducting experiments; Manuscript revision;
Beata Pyrzyńska	Study concept and design; Conducting experiments and statistical analysis; Critical evaluation and interpretation of results; Preparation of both the initial draft and the final version of the manuscript.

The following experimental results, prepared by Aleksandra Zdanowicz, MSc, are included in the article:

- Fig. 3C – Complement-dependent cytotoxicity (CDC) assay following treatment with ofatumumab.
- Fig. 6B – Western blot analysis of both phosphorylated and total protein levels of AKT, FOXO1, and SGK1 kinase in Raji cells, along with statistical quantification.
- Fig. 7A – qRT-PCR analysis measuring *MYC* mRNA levels.
- Fig. 8B – Western blot analysis of MYC and SGK1, along with statistical quantification.
- Fig. 8C – Western blot analysis of MYC and SGK1 in Raji cells nucleofected with RNP complexes containing sgRNA targeting either MYC (sgMYC) or SGK1 (sgSGK1) and Cas9 nuclease.
- Fig. 8D – Flow cytometry analysis estimating the surface expression level of CD20 in Raji cells pretreated with either SAL or a MYC inhibitor.
- Fig. 8E – Chromatin immunoprecipitation assay (CUT&RUN) examining MYC-DNA interaction, followed by RT-PCR amplification of the MS4A1 promoter fragment.
- Suppl. Fig. 7 – Flow cytometry assessment of surface CD20 expression in Raji cells following treatment with an NLRP3 inhibitor or cation carriers.
- Suppl. Fig 9A – Quantification and statistical analysis of MYC protein levels by Western blotting in Raji and P493-6 cell lines pretreated with SAL, MON, or vehicle.
- Suppl. Fig. 9B - Quantification of the binding of *MYC* to its target E-box DNA motif in nuclear extracts from from Raji cells using the TransAM MYC ELISA.
- Suppl. Fig. 11C – Western blot analysis of both phosphorylated and total protein levels of AKT and FOXO1 in Raji cells, along with statistical quantification.
- Suppl. Fig. 12A – Western blot analysis of MYC in extracts from Raji cells, either mock-nucleofected or genome-edited with sgMYC.
- Suppl. Fig. 12B – Flow cytometry analysis of surface CD20 on Raji cells, either mock-nucleofected or genome-edited with sgMYC, followed by treatment with SAL, MON, or corresponding controls for 48 hours.
- Suppl. Fig. 12C – Western blot analysis of MYC in extracts from Raji cells, either mock-nucleofected or genome-edited with sgSGK1.
- Suppl. Fig. 12D – Flow cytometry analysis of surface CD20 on Raji cells, either mock-nucleofected or genome-edited with sgSGK1, followed by treatment with SAL, MON, or corresponding controls.
- Suppl. Fig. 12E – Flow cytometry analysis of surface CD20 on Raji cells pretreated with EMD638683.

haematologica

Journal of the Ferrata Storti Foundation

Change of Authorship Form for Authors and Contributors to *Haematologica*

This form must be completed and signed by ALL Authors.

Manuscript Title: Potassium/sodium cation carriers robustly upregulate CD20 antigen by targeting MYC and synergize with anti-CD20 immunotherapies to eliminate malignant B cells.

MS Number: HAEMATOL/2024/285826 Date: October 2nd, 2024

Please check ALL that apply:

- ☐ New author(s) have been added
- ☐ Author wishes to remove his/her name
- ☒ Order of authorship has changed

Manuscripts will not be processed until the *Haematologica* Editorial Office has received this signed form. Fax the completed form to the *Haematologica* Editorial Office at: +39 0382 394705, or scan and e-mail the form to office@haematologica.org

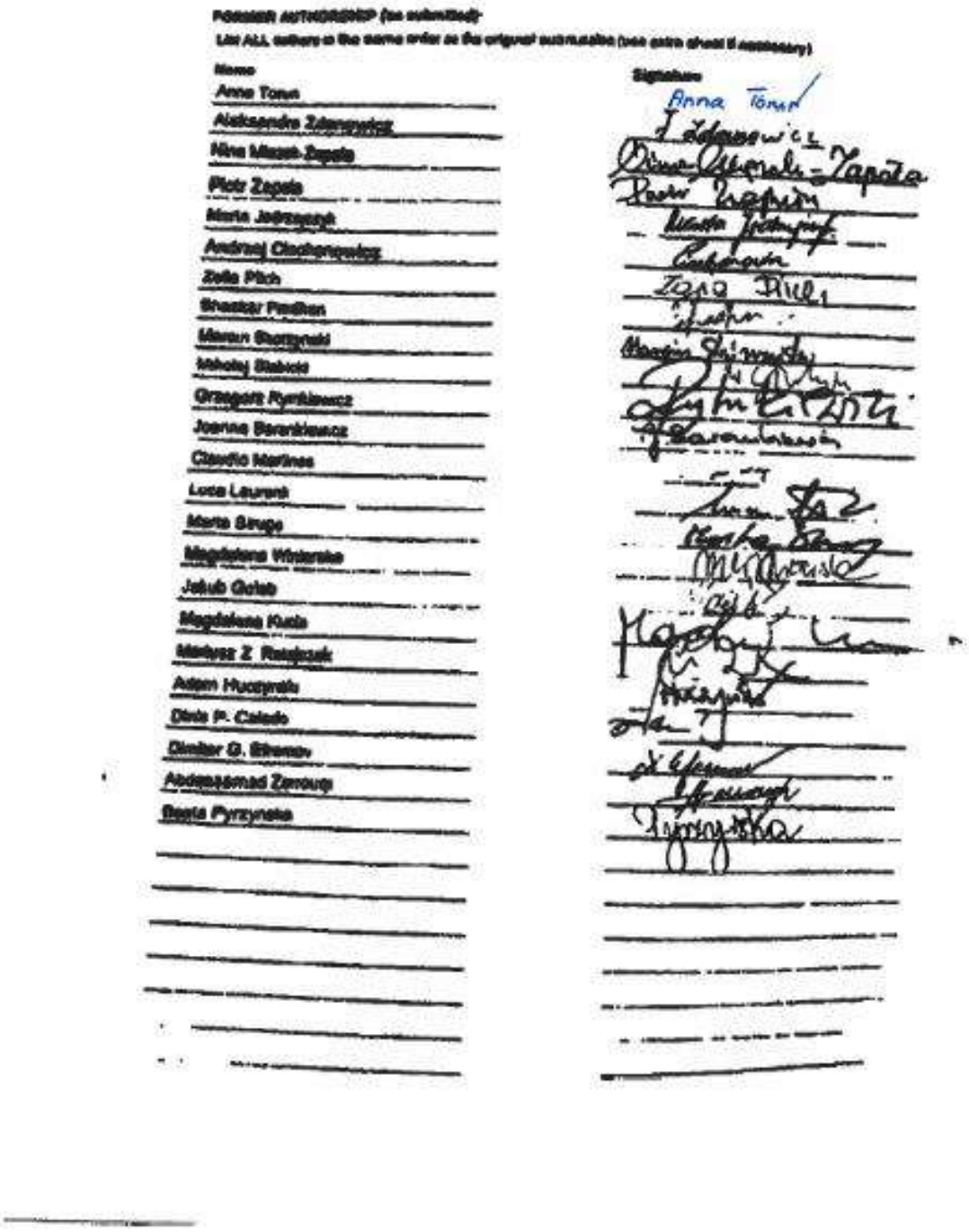
FORMER AUTHORSHIP (as submitted)
List ALL authors in the same order as the original submission (use extra sheet if necessary)
Name
Signature
Anna Town
Aleksandra Zdanowicz
Nina Mazur-Zapała
Piotr Zapała
Maria Jedrzejczyk
Andrzej Ciechanowicz
Zofia Pilch
Sławomir Pawlas
Marcin Słomiński
Mikołaj Słabicki
Grzegorz Rymkiewicz
Joanna Borankiewicz
Claudio Martinez
Luca Laurenti
Marta Sługa
Magdalena Wiśniewska
Jakub Golab
Magdalena Kuta
Mariusz Z. Ratajczak
Adam Huczyński
Dinis P. Calado
Dimitar G. Stanev
Abdessamad Zerouq
Beata Pyrzyńska

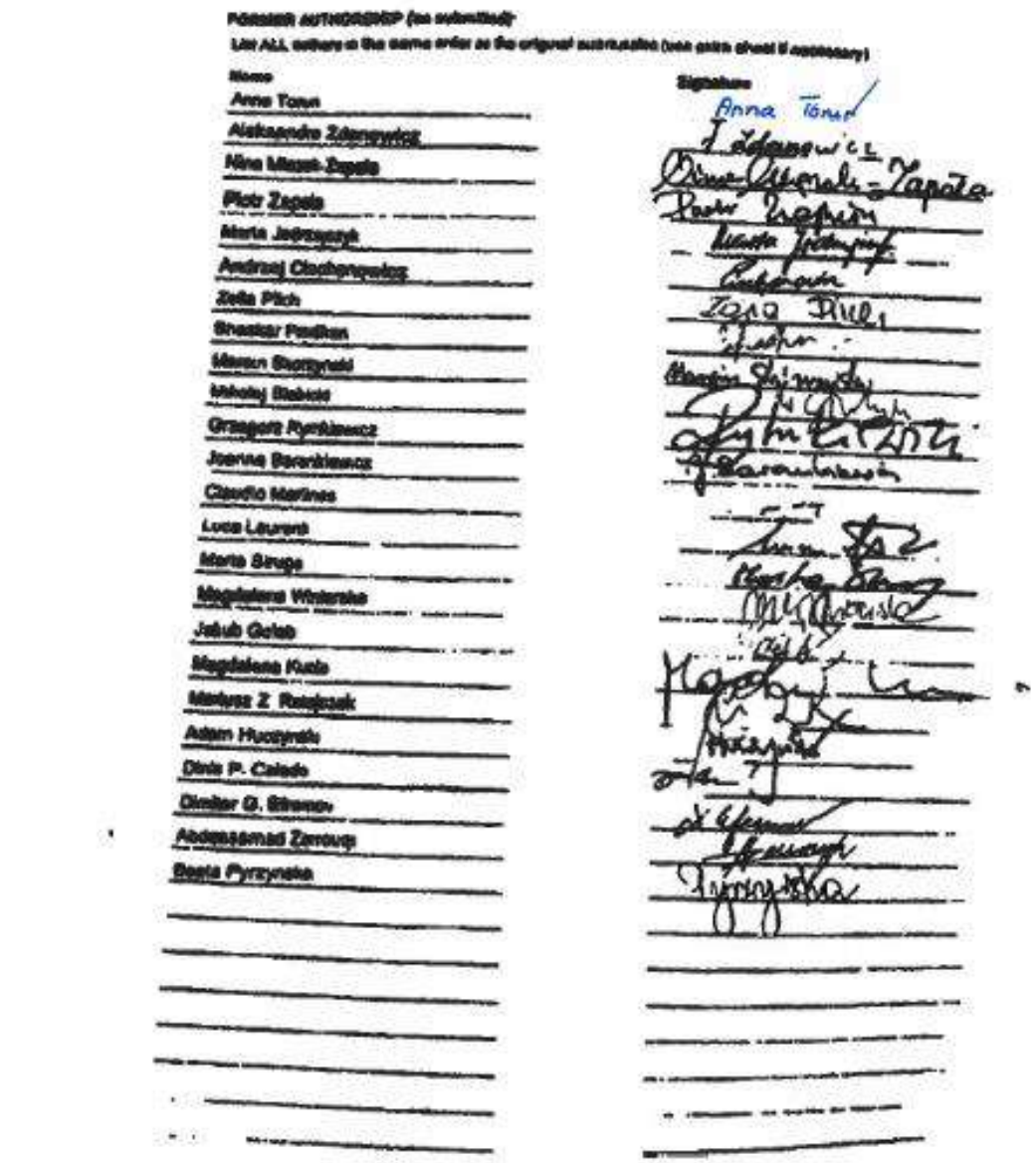
FORMER AUTHORSHIP (as submitted)
List ALL authors in the same order as the original submission (use extra sheet if necessary)
Name
Signature
Anna Tonn
Aleksandra Zdanowicz
Nina Mazur-Zapała
Piotr Zapała
Marta Jędrzejczyk
Andrzej Ciechanowicz
Zofia Pilch
Sławomir Pietras
Marcin Słomiński
Mikołaj Słabicki
Grzegorz Rymkiewicz
Joanna Barankiewicz
Claudio Martines
Lucia Laurent
Marta Sauga
Magdalena Wiśniska
Jakub Golab
Magdalena Kusia
Mariusz Z. Ratajczak
Adam Huczyński
Dinis P. Calado
Dimiter G. Stavrev
Abdessamad Zerouqi
Beata Pyrzyńska

Aleksandra Zdanowicz Warszawa, 27-05-2025

Statement

As a co-author of the research paper entitled:

"Potassium/sodium cation carriers robustly up-regulate CD20 antigen by targeting MYC and synergize with anti-CD20 immunotherapies to eliminate malignant B cells"

I formally consent to the inclusion of the aforementioned work as an integral component of the doctoral dissertation portfolio of Aleksandra Zdanowicz, MSc.

Additionally, I declare my contribution to the research as follows:

Author's Name and Surname	Contribution range
Anna Torun	Conducting experiments and statistical analysis; Critical evaluation and interpretation of results;
Aleksandra Zdanowicz	Conducting experiments and statistical analysis; Critical evaluation and interpretation of results; Manuscript revision;
Nina Miązek-Zapała	Conducting experiments and statistical analysis;
Piotr Zapała	Conducting experiments and statistical analysis;
Bhaskar Pradhan	Conducting experiments; Manuscript revision;
Marta Jędrzejczyk	Conducting experiments;
Andrzej Ciechanowicz	Conducting experiments;
Zofia Pilch	Conducting experiments;
Marcin Skórzynski	Conducting experiments;
Mikołaj Słabicki	Concept and study design;
Grzegorz Rymkiewicz	Delivery of patient samples; Diagnosis of patient samples;
Joanna Barankiewicz	Delivery of patient samples; Diagnosis of patient samples;

Claudio Martines	Conducting experiments;
Luca Laurenti	Delivery of patient samples; Diagnosis of patient samples;
Marta Struga	Concept and study design;
Magdalena Winiarska	Concept and study design;
Jakub Gołąb	Concept and study design;
Magdalena Kucia	Concept and study design;
Mariusz Z Ratajczak	Concept and study design;
Adam Huczyński	Study conception and design; Data summary;
Dinis P Calado	Study concept and design;
Dimitar G Efremov	Concept and study design; Delivery of patient samples;
Abdessamad Zerrouqi	Study concept and design, conducting experiments; Manuscript revision;
Beata Pyrzyńska	Study concept and design; Conducting experiments and statistical analysis; Critical evaluation and interpretation of results; Preparation of both the initial draft and the final version of the manuscript.

Sign A Adamowicz

The following experimental results, prepared by Aleksandra Zdanowicz, MSc, are included in the article:

- Fig. 3C – Complement-dependent cytotoxicity (CDC) assay following treatment with ofatumumab.
- Fig. 6B – Western blot analysis of both phosphorylated and total protein levels of AKT, FOXO1, and SGK1 kinase in Raji cells, along with statistical quantification.
- Fig. 7A – qRT-PCR analysis measuring *MYC* mRNA levels.
- Fig. 8B – Western blot analysis of MYC and SGK1, along with statistical quantification.
- Fig. 8C – Western blot analysis of MYC and SGK1 in Raji cells nucleofected with RNP complexes containing sgRNA targeting either MYC (sgMYC) or SGK1 (sgSGK1) and Cas9 nuclease.
- Fig. 8D – Flow cytometry analysis estimating the surface expression level of CD20 in Raji cells pretreated with either SAL or a MYC inhibitor.
- Fig. 8E – Chromatin immunoprecipitation assay (CUT&RUN) examining MYC-DNA interaction, followed by RT-PCR amplification of the MS4A1 promoter fragment.
- Suppl. Fig. 7 – Flow cytometry assessment of surface CD20 expression in Raji cells following treatment with an NLRP3 inhibitor or cation carriers.
- Suppl. Fig 9A – Quantification and statistical analysis of MYC protein levels by Western blotting in Raji and P493-6 cell lines pretreated with SAL, MON, or vehicle.
- Suppl. Fig. 9B - Quantification of the binding of *MYC* to its target E-box DNA motif in nuclear extracts from from Raji cells using the TransAM MYC ELISA.
- Suppl. Fig. 11C – Western blot analysis of both phosphorylated and total protein levels of AKT and FOXO1 in Raji cells, along with statistical quantification.
- Suppl. Fig. 12A – Western blot analysis of MYC in extracts from Raji cells, either mock-nucleofected or genome-edited with sgMYC.
- Suppl. Fig. 12B – Flow cytometry analysis of surface CD20 on Raji cells, either mock-nucleofected or genome-edited with sgMYC, followed by treatment with SAL, MON, or corresponding controls for 48 hours.
- Suppl. Fig. 12C – Western blot analysis of MYC in extracts from Raji cells, either mock-nucleofected or genome-edited with sgSGK1.
- Suppl. Fig. 12D – Flow cytometry analysis of surface CD20 on Raji cells, either mock-nucleofected or genome-edited with sgSGK1, followed by treatment with SAL, MON, or corresponding controls.
- Suppl. Fig. 12E – Flow cytometry analysis of surface CD20 on Raji cells pretreated with EMD638683.

11.2 Publication No. 2

WMCM UKSW Wydział Medyczny. Collegium Medicum UNIWERSYTET KARDYNAŁA STEFANA WYSZYŃSKIEGO W WARSZAWIE

Warszawa, 27 maja 2025

Emilia Grosicka-Maciąg, Ph.D. Assoc. Prof.

Statement

As a co-author of the research paper entitled:
" The Interplay between Autophagy and Mitochondria in Cancer "

I formally consent to the inclusion of the aforementioned work as an integral component of the doctoral dissertation portfolio of Aleksandra Zdanowicz, MSc.

Additionally, I declare my contribution to the research as follows:

Author's Name and Surname	Contribution range
Aleksandra Zdanowicz	Study concept and planning; comprehensive literature search; structuring the review; drafting and refining the manuscript; creating figures and tables; proofreading and revision; formatting according to journal guidelines; responding to reviewers' comments;
Emilia Grosicka-Maciąg	Manuscript editing and addressing editors' comments.

UKSW

Podpisany elektronicznie przez
Emilia Klementyna Grosicka-Maciąg
27.05.2025
11:09:51 +02'00'

Wydział Medyczny. Collegium Medicum Uniwersytetu Kardynała Stefana Wyszyńskiego
ul. Woyciickiego 1/3, 01-938 Warszawa | +48 22 380 96 95, 22 380 96 90
wmcm@uksw.edu.pl | www.wmcm.uksw.edu.pl

Aleksandra Zdanowicz Warszawa, 27-05-2025

Statement

As a co-author of the research paper entitled:

" The Interplay between Autophagy and Mitochondria in Cancer "

I formally consent to the inclusion of the aforementioned work as an integral component of the doctoral dissertation portfolio of Aleksandra Zdanowicz, MSc.

Additionally, I declare my contribution to the research as follows:

Author's Name and Surname	Contribution range
Aleksandra Zdanowicz	Study concept and planning; comprehensive literature search; structuring the review; drafting and refining the manuscript; creating figures and tables; proofreading and revision; formatting according to journal guidelines; responding to reviewers' comments;
Emilia Grosicka-Maciąg	Manuscript editing and addressing editors' comments.

Sign A. Zdanowicz

11.3 Publication No. 3

Beata Pyrzyńska Warsaw, May 26th, 2025

Statement

As a co-author of the research paper entitled:

" Low-Dose Salinomycin Alters Mitochondrial Function and Reprograms Global Metabolism in Burkitt Lymphoma"

I formally consent to the inclusion of the aforementioned work as an integral component of the doctoral dissertation portfolio of Aleksandra Zdanowicz, MSc.

Additionally, I declare my contribution to the research as follows:

Author's Name and Surname	Contribution range
Aleksandra Zdanowicz	Conceptualization and planning of the study; comprehensive literature search; drafting and refining the manuscript; performing the experiments; proofreading and revising; formatting the manuscript according to journal guidelines; addressing reviewers' feedback;
Oleksandr Ilchenko	Metabolomics data analysis and preparation of figures (Figures 5–8 and Supplementary Figures S5–S7); editing of the manuscript and addressing editors' comments.
Andrzej Ciechanowicz	Metabolomics experiments conduction;
Haoyu Chi	Seahorse experiment conduction and manuscript editing;
Marta Struga	Manuscript editing;
Beata Pyrzynska	Study conceptualization and planning; manuscript editing and revision; addressing editors' comments; supervision; and funding acquisition

Signature

The following experimental results, prepared by Aleksandra Zdanowicz, MSc, are included in the article:

Fig.1A and Suppl. Fig. S1– Measurement of mitochondrial membrane potential using the MitoPT JC-1 Assay kit.

Fig. 1B and Suppl. Fig. S2 – Measurement of mitochondrial membrane potential using the TMRM Assay Kit.

Fig. 2A and Suppl. Fig. S3 – Evaluation of mitochondrial superoxide production using the MitoSOX Red mitochondrial superoxide indicator.

Fig. 2B and Suppl. Fig. S4 – Assessment of general oxidative stress using the CellROX Green Reagent.

Fig. 3A-D – Measurement of oxygen consumption rate (OCR) using the Seahorse XFe96 extracellular flux analyzer.

Fig. 4A-C – Measurement of extracellular acidification rate (ECAR) using the Seahorse XFe96 extracellular flux analyzer.

Marta Struga, prof. Warszawa, 27-05-2025

Statement

As a co-author of the research paper entitled:

" Low-Dose Salinomycin Alters Mitochondrial Function and Reprograms Global Metabolism in Burkitt Lymphoma"

I formally consent to the inclusion of the aforementioned work as an integral component of the doctoral dissertation portfolio of Aleksandra Zdanowicz, MSc.

Additionally, I declare my contribution to the research as follows:

Author's Name and Surname	Contribution range
Aleksandra Zdanowicz	Conceptualization and planning of the study; comprehensive literature search; drafting and refining the manuscript; performing the experiments; proofreading and revising; formatting the manuscript according to journal guidelines; addressing reviewers' feedback;
Oleksandr Ilchenko	Metabolomics data analysis and preparation of figures (Figures 5–8 and Supplementary Figures S5–S7); editing of the manuscript and addressing editors' comments.
Andrzej Ciechanowicz	Metabolomics experiments conduction;
Haoyu Chi	Seahorse experiment conduction and manuscript editing;
Marta Struga	Manuscript editing;
Beata Pyrzynska	Study conceptualization and planning; manuscript editing and revision; addressing editors' comments; supervision; and funding acquisition

KIEROWNIK
Katedry i Zakładu Biochemii
prof. dr. hab. n. med. Marta Struga

Sign _____

The following experimental results, prepared by Aleksandra Zdanowicz, MSc, are included in the article:

Fig.1A and Suppl. Fig. S1– Measurement of mitochondrial membrane potential using the MitoPT JC-1 Assay kit.

Fig. 1B and Suppl. Fig. S2 – Measurement of mitochondrial membrane potential using the TMRM Assay Kit.

Fig. 2A and Suppl. Fig. S3 – Evaluation of mitochondrial superoxide production using the MitoSOX Red mitochondrial superoxide indicator.

Fig. 2B and Suppl. Fig. S4 – Assessment of general oxidative stress using the CellROX Green Reagent.

Fig. 3A-D – Measurement of oxygen consumption rate (OCR) using the Seahorse XFe96 extracellular flux analyzer.

Fig. 4A-C – Measurement of extracellular acidification rate (ECAR) using the Seahorse XFe96 extracellular flux analyzer.

Haoyu Chi London, 23-05-2025

Statement

As a co-author of the research paper entitled:

" Low-Dose Salinomycin Alters Mitochondrial Function and Reprograms Global Metabolism in Burkitt Lymphoma"

I formally consent to the inclusion of the aforementioned work as an integral component of the doctoral dissertation portfolio of Aleksandra Zdanowicz, MSc.

Additionally, I declare my contribution to the research as follows:

Author's Name and Surname	Contribution range
Aleksandra Zdanowicz	Conceptualization and planning of the study; comprehensive literature search; drafting and refining the manuscript; performing the experiments; proofreading and revising; formatting the manuscript according to journal guidelines; addressing reviewers' feedback;
Oleksandr Ilchenko	Metabolomics data analysis and preparation of figures (Figures 5–8 and Supplementary Figures S5–S7); editing of the manuscript and addressing editors' comments.
Andrzej Ciechanowicz	Metabolomics experiments conduction;
Haoyu Chi	Seahorse experiment conduction and manuscript editing;
Marta Struga	Manuscript editing;
Beata Pyrzynska	Study conceptualization and planning; manuscript editing and revision; addressing editors' comments; supervision; and funding acquisition

Sign Haoyu Chi

The following experimental results, prepared by Aleksandra Zdanowicz, MSc, are included in the article:

Fig.1A and Suppl. Fig. S1– Measurement of mitochondrial membrane potential using the MitoPT JC-1 Assay kit.

Fig. 1B and Suppl. Fig. S2 – Measurement of mitochondrial membrane potential using the TMRM Assay Kit.

Fig. 2A and Suppl. Fig. S3 – Evaluation of mitochondrial superoxide production using the MitoSOX Red mitochondrial superoxide indicator.

Fig. 2B and Suppl. Fig. S4 – Assessment of general oxidative stress using the CellROX Green Reagent.

Fig. 3A-D – Measurement of oxygen consumption rate (OCR) using the Seahorse XFe96 extracellular flux analyzer.

Fig. 4A-C – Measurement of extracellular acidification rate (ECAR) using the Seahorse XFe96 extracellular flux analyzer.

Andrzej Ciechanowicz Warsaw, 30.05.2025

Statement

As a co-author of the research paper entitled:

" Low-Dose Salinomycin Alters Mitochondrial Function and Reprograms Global Metabolism in Burkitt Lymphoma"

I formally consent to the inclusion of the aforementioned work as an integral component of the doctoral dissertation portfolio of Aleksandra Zdanowicz, MSc.

Additionally, I declare my contribution to the research as follows:

Author's Name and Surname	Contribution range
Aleksandra Zdanowicz	Conceptualization and planning of the study; comprehensive literature search; drafting and refining the manuscript; performing the experiments; proofreading and revising; formatting the manuscript according to journal guidelines; addressing reviewers' feedback;
Oleksandr Ilchenko	Metabolomics data analysis and preparation of figures (Figures 5–8 and Supplementary Figures S5–S7); editing of the manuscript and addressing editors' comments.
Andrzej Ciechanowicz	Metabolomics experiments conduction;
Haoyu Chi	Seahorse experiment conduction and manuscript editing;
Marta Struga	Manuscript editing;
Beata Pyrzynska	Study conceptualization and planning; manuscript editing and revision; addressing editors' comments; supervision; and funding acquisition

Sign Ciechanowicz Ciechanowicz (30-May-2025 14:20 GMT+2)

The following experimental results, prepared by Aleksandra Zdanowicz, MSc, are included in the article:

Fig.1A and Suppl. Fig. S1– Measurement of mitochondrial membrane potential using the MitoPT JC-1 Assay kit.

Fig. 1B and Suppl. Fig. S2 – Measurement of mitochondrial membrane potential using the TMRM Assay Kit.

Fig. 2A and Suppl. Fig. S3 – Evaluation of mitochondrial superoxide production using the MitoSOX Red mitochondrial superoxide indicator.

Fig. 2B and Suppl. Fig. S4 – Assessment of general oxidative stress using the CellROX Green Reagent.

Fig. 3A-D – Measurement of oxygen consumption rate (OCR) using the Seahorse XFe96 extracellular flux analyzer.

Fig. 4A-C – Measurement of extracellular acidification rate (ECAR) using the Seahorse XFe96 extracellular flux analyzer.

Oleksandr Ilchenko Umeå, Sweden, 29.05.2025

Statement

As a co-author of the research paper entitled:

" Low-Dose Salinomycin Alters Mitochondrial Function and Reprograms Global Metabolism in Burkitt Lymphoma"

I formally consent to the inclusion of the aforementioned work as an integral component of the doctoral dissertation portfolio of Aleksandra Zdanowicz, MSc.

Additionally, I declare my contribution to the research as follows:

Author's Name and Surname	Contribution range
Aleksandra Zdanowicz	Conceptualization and planning of the study; comprehensive literature search; drafting and refining the manuscript; performing the experiments; proofreading and revising; formatting the manuscript according to journal guidelines; addressing reviewers' feedback;
Oleksandr Ilchenko	Metabolomics data analysis and preparation of figures (Figures 5–8 and Supplementary Figures S5–S7); editing of the manuscript and addressing editors' comments.
Andrzej Ciechanowicz	Metabolomics experiments conduction;
Haoyu Chi	Seahorse experiment conduction and manuscript editing;
Marta Struga	Manuscript editing;
Beata Pyrzynska	Study conceptualization and planning; manuscript editing and revision; addressing editors' comments; supervision; and funding acquisition

Sign_____

The following experimental results, prepared by Aleksandra Zdanowicz, MSc, are included in the article:

Fig.1A and Suppl. Fig. S1 – Measurement of mitochondrial membrane potential using the MitoPT JC-1 Assay kit.

Fig. 1B and Suppl. Fig. S2 – Measurement of mitochondrial membrane potential using the TMRM Assay Kit.

Fig. 2A and Suppl. Fig. S3 – Evaluation of mitochondrial superoxide production using the MitoSOX Red mitochondrial superoxide indicator.

Fig. 2B and Suppl. Fig. S4 – Assessment of general oxidative stress using the CellROX Green Reagent.

Fig. 3A-D – Measurement of oxygen consumption rate (OCR) using the Seahorse XFe96 extracellular flux analyzer.

Fig. 4A-C – Measurement of extracellular acidification rate (ECAR) using the Seahorse XFe96 extracellular flux analyzer.

Aleksandra Zdanowicz Warszawa, 27-05-2025

Statement

As a co-author of the research paper entitled:

" Low-Dose Salinomycin Alters Mitochondrial Function and Reprograms Global Metabolism in Burkitt Lymphoma"

I formally consent to the inclusion of the aforementioned work as an integral component of the doctoral dissertation portfolio of Aleksandra Zdanowicz, MSc.

Additionally, I declare my contribution to the research as follows:

Author's Name and Surname	Contribution range
Aleksandra Zdanowicz	Conceptualization and planning of the study; comprehensive literature search; drafting and refining the manuscript; performing the experiments; proofreading and revising; formatting the manuscript according to journal guidelines; addressing reviewers' feedback;
Oleksandr Ilchenko	Metabolomics data analysis and preparation of figures (Figures 5–8 and Supplementary Figures S5–S7); editing of the manuscript and addressing editors' comments.
Andrzej Ciechanowicz	Metabolomics experiments conduction;
Haoyu Chi	Seahorse experiment conduction and manuscript editing;
Marta Struga	Manuscript editing;
Beata Pyrzynska	Study conceptualization and planning; manuscript editing and revision; addressing editors' comments; supervision; and funding acquisition

Sign A. Zdanowicz

The following experimental results, prepared by Aleksandra Zdanowicz, MSc, are included in the article:

Fig.1A and Suppl. Fig. S1– Measurement of mitochondrial membrane potential using the MitoPT JC-1 Assay kit.

Fig. 1B and Suppl. Fig. S2 – Measurement of mitochondrial membrane potential using the TMRM Assay Kit.

Fig. 2A and Suppl. Fig. S3 – Evaluation of mitochondrial superoxide production using the MitoSOX Red mitochondrial superoxide indicator.

Fig. 2B and Suppl. Fig. S4 – Assessment of general oxidative stress using the CellROX Green Reagent.

Fig. 3A-D – Measurement of oxygen consumption rate (OCR) using the Seahorse XFe96 extracellular flux analyzer.

Fig. 4A-C – Measurement of extracellular acidification rate (ECAR) using the Seahorse XFe96 extracellular flux analyzer.

12. References

1. Dabkowska, A., K. Domka, and M. Firczuk, *Advancements in cancer immunotherapies targeting CD20: from pioneering monoclonal antibodies to chimeric antigen receptor-modified T cells.* Front Immunol, 2024. **15**: p. 1363102.
2. Salles, G., et al., *Rituximab in B-Cell Hematologic Malignancies: A Review of 20 Years of Clinical Experience.* Adv Ther, 2017. **34**(10): p. 2232-2273.
3. Grillo-Lopez, A.J., et al., *Rituximab: the first monoclonal antibody approved for the treatment of lymphoma.* Curr Pharm Biotechnol, 2000. **1**(1): p. 1-9.
4. Boross, P. and J.H. Leusen, *Mechanisms of action of CD20 antibodies.* Am J Cancer Res, 2012. **2**(6): p. 676-90.
5. Brinkmann, U. and R.E. Kontermann, *The making of bispecific antibodies.* MAbs, 2017. **9**(2): p. 182-212.
6. Engelberts, P.J., et al., *DuoBody-CD3xCD20 induces potent T-cell-mediated killing of malignant B cells in preclinical models and provides opportunities for subcutaneous dosing.* EBioMedicine, 2020. **52**: p. 102625.
7. Pavlasova, G. and M. Mraz, *The regulation and function of CD20: an "enigma" of B-cell biology and targeted therapy.* Haematologica, 2020. **105**(6): p. 1494-1506.
8. Prevodnik, V.K., et al., *The predictive significance of CD20 expression in B-cell lymphomas.* Diagn Pathol, 2011. **6**: p. 33.
9. Drott, K., et al., *Valproate in combination with rituximab and CHOP as first-line therapy in diffuse large B-cell lymphoma (VALFRID).* Blood Adv, 2018. **2**(12): p. 1386-1392.
10. Shen, Q.D., et al., *Gemcitabine-oxaliplatin plus rituximab (R-GemOx) as first-line treatment in elderly patients with diffuse large B-cell lymphoma: a single-arm, open-label, phase 2 trial.* Lancet Haematol, 2018. **5**(6): p. e261-e269.
11. Torun, A., et al., *Potassium/sodium cation carriers robustly up-regulate CD20 antigen by targeting MYC, and synergize with anti-CD20 immunotherapies to eliminate malignant B cells.* Haematologica, 2024.
12. Dutton, C.J., B.J. Banks, and C.B. Cooper, *Polyether ionophores.* Nat Prod Rep, 1995. **12**(2): p. 165-81.
13. Kaushik, V., et al., *Ionophores: Potential Use as Anticancer Drugs and Chemosensitizers.* Cancers (Basel), 2018. **10**(10).
14. Antoszczak, M. and A. Huczynski, *Salinomycin and its derivatives - A new class of multiple-targeted "magic bullets".* Eur J Med Chem, 2019. **176**: p. 208-227.

15. Miyazaki, Y., et al., *Salinomycin, a new polyether antibiotic.* J Antibiot (Tokyo), 1974. **27**(11): p. 814-21.
16. Dewangan, J., S. Srivastava, and S.K. Rath, *Salinomycin: A new paradigm in cancer therapy.* Tumour Biol, 2017. **39**(3): p. 1010428317695035.
17. Antoszczak M., R.J., Huczynski A., *Structure and Biological Activity of Polyether Ionophores and Their Semisynthetic Derivatives.* In book: Bioactive Natural Products : Chemistry and Biology, 2015.
18. Gupta, P.B., et al., *Identification of selective inhibitors of cancer stem cells by high-throughput screening.* Cell, 2009. **138**(4): p. 645-659.
19. Kim, K.Y., et al., *Salinomycin-induced apoptosis of human prostate cancer cells due to accumulated reactive oxygen species and mitochondrial membrane depolarization.* Biochem Biophys Res Commun, 2011. **413**(1): p. 80-6.
20. Parajuli, B., et al., *Salinomycin inhibits Akt/NF-kappaB and induces apoptosis in cisplatin resistant ovarian cancer cells.* Cancer Epidemiol, 2013. **37**(4): p. 512-7.
21. Kim, S.H., et al., *Salinomycin simultaneously induces apoptosis and autophagy through generation of reactive oxygen species in osteosarcoma U2OS cells.* Biochem Biophys Res Commun, 2016. **473**(2): p. 607-13.
22. Yu, S.N., et al., *Salinomycin induces endoplasmic reticulum stress-mediated autophagy and apoptosis through generation of reactive oxygen species in human glioma U87MG cells.* Oncol Rep, 2017. **37**(6): p. 3321-3328.
23. White, E. and R.S. DiPaola, *The double-edged sword of autophagy modulation in cancer.* Clin Cancer Res, 2009. **15**(17): p. 5308-16.
24. Li, T., et al., *Salinomycin induces cell death with autophagy through activation of endoplasmic reticulum stress in human cancer cells.* Autophagy, 2013. **9**(7): p. 1057-68.
25. Jangamreddy, J.R., et al., *Salinomycin induces activation of autophagy, mitophagy and affects mitochondrial polarity: differences between primary and cancer cells.* Biochim Biophys Acta, 2013. **1833**(9): p. 2057-69.
26. Liu, Y., et al., *Salinomycin induces autophagic cell death in salinomycin-sensitive melanoma cells through inhibition of autophagic flux.* Sci Rep, 2020. **10**(1): p. 18515.
27. Ando, T., et al., *Combined Anticancer Effect of Plasma-Activated Infusion and Salinomycin by Targeting Autophagy and Mitochondrial Morphology.* Front Oncol, 2021. **11**: p. 593127.

28. Zdanowicz, A.I., O.; Ciechanowicz, A.; Chi, H.; Struga, M.; Pyrzynska, B, *Low-Dose Salinomycin Alters Mitochondrial Function and Reprograms Global Metabolism in Burkitt Lymphoma.* International Journal of Molecular Sciences, 2025. **26**.
29. Li, J. and Y. Min, *Pre-clinical evidence that salinomycin is active against retinoblastoma via inducing mitochondrial dysfunction, oxidative damage and AMPK activation.* J Bioenerg Biomembr, 2021. **53**(5): p. 513-523.
30. Cosialls, E., et al., *mTOR inhibition suppresses salinomycin-induced ferroptosis in breast cancer stem cells by ironing out mitochondrial dysfunctions.* Cell Death Dis, 2023. **14**(11): p. 744.
31. Story, P. and A. Doube, *A case of human poisoning by salinomycin, an agricultural antibiotic.* N Z Med J, 2004. **117**(1190): p. U799.
32. Diaz, G.J., Y. Aguillon, and A. Cortes, *Effects on health, performance, and tissue residues of the ionophore antibiotic salinomycin in finishing broilers (21 to 38 d).* Poult Sci, 2018. **97**(6): p. 1922-1928.
33. Hosseini R., H.A., Panahi N., Rajaian H., *A New Insight Into Salinomycin.* Iranian Journal of Veterinary Medicine, 2025. **19**(1): p. 1-10.
34. Boehmerle, W., et al., *Specific targeting of neurotoxic side effects and pharmacological profile of the novel cancer stem cell drug salinomycin in mice.* J Mol Med (Berl), 2014. **92**(8): p. 889-900.
35. Naujokat, C. and R. Steinhart, *Salinomycin as a drug for targeting human cancer stem cells.* J Biomed Biotechnol, 2012. **2012**: p. 950658.
36. Versini, A., et al., *Salinomycin Derivatives Kill Breast Cancer Stem Cells by Lysosomal Iron Targeting.* Chemistry, 2020. **26**(33): p. 7416-7424.
37. Klose, J., et al., *Inhibition of autophagic flux by salinomycin results in anti-cancer effect in hepatocellular carcinoma cells.* PLoS One, 2014. **9**(5): p. e95970.
38. Manago, A., et al., *Early effects of the antineoplastic agent salinomycin on mitochondrial function.* Cell Death Dis, 2015. **6**(10): p. e1930.
39. Korshunov, S.S., V.P. Skulachev, and A.A. Starkov, *High protonic potential actuates a mechanism of production of reactive oxygen species in mitochondria.* FEBS Lett, 1997. **416**(1): p. 15-8.
40. Salaroglio, I.C., et al., *Mitochondrial ROS drive resistance to chemotherapy and immune-killing in hypoxic non-small cell lung cancer.* J Exp Clin Cancer Res, 2022. **41**(1): p. 243.
41. Cheng, C.T., et al., *Arginine starvation kills tumor cells through aspartate exhaustion and mitochondrial dysfunction.* Commun Biol, 2018. **1**: p. 178.

42. Chen, C.L., et al., *Arginine Signaling and Cancer Metabolism.* Cancers (Basel), 2021. **13**(14).